UNIVERSITY OF GHANA

COLLEGE OF BASIC AND APPLIED SCIENCE

GEOPHYSICAL AND HYDROGEOLOGICAL CHARACTERISATION OF THE NASIA BASIN, NORTHERN GHANA

ABDUL-SAMED ALIOU

(10256943)

A THESIS SUBMITTED TO THE UNIVERSITY OF GHANA IN PARTIAL FULFILLMENT OF THE REQUIREMENT FOR THE AWARD OF DOCTOR OF PHILOSOPHY IN EARTH SCIENCE

DEPARTMENT OF EARTH SCIENCE

NOVEMBER 2020

DECLARATION

I hereby declare that this thesis is my own work produced from research under supervision and to the best of my knowledge, it contains no material previously published by another person nor material which has been accepted for the award of any other degree of any institution, except where due acknowledgement has been made.

Abdul-Samed Aliou (Student)	Signature	22/11/2020 Date
Prof. Sandow Mark Yidana (Principal Supervisor)	Signature	26/11/2020 Date
Dr. Larry Pax Chegbeleh (Co- Supervisor)	Signature	26/11/2020 Date.
Dr (Mrs) Yvonne Sena Akosua Loh (Co-Supervisor)	Signature	26/11/2020 Date
Kurt Klitten (Co-Supervisor)	Signature	23/11/2020 Date

ABSTRACT

The development of groundwater resources across the Voltaian Sedimentary Basin (VSB) is constrained by lack of knowledge on the location and suitability of aquifers for borehole construction. The main objective of this study is to evaluate the hydrogeological characteristics of the Nasia Basin to help in delineating suitable locations for groundwater exploration. An integrated geophysical investigation involving resistivity survey using 2D Electrical Resistivity Tomography (ERT), Electromagnetic Survey with EM34-3 and wireline logging of boreholes were employed to determine the resistivity of the different type of lithology occurring in the area and for providing information about the lateral and vertical extent of weathering and fracturing in the subsurface. A total of 58 ERT profiles were run at selected locations and at existing boreholes to obtain information about resistivity in different depth intervals. Majority of the profiles were run across the general strike of rocks of the VSB in the study area with length being either 400 m or 800 m. Five EM-34 ground conductivity profiles of 500-1000 m were conducted on each of two approximately parallel South-North traverses (EM campaign 1) to record the conductivity in the various geological formations and to assess its possible variation related to major geological structures. In addition to the two-parallel profile (EM campaign 1), 12 other EM-34 profiles each 500 m long were carried out at six selected communities in the central part of the study area (EM campaign 2) with the objective of locating areas within the weathered zone capable of storing groundwater for small scale pilot irrigation from dug-wells. The conclusion of the integrated geophysical investigation is that combining

interpretations from various geophysical methods provides an improved characterisation of the hydrogeology. Secondly, hydrogeological investigations were conducted which involved analysis of pumping test results, evaluation of various methods of estimating aquifer transmissivity and assessment of the major factors controlling groundwater occurrence. Using remote sensing and geographical information system (GIS), thematic maps of slope, drainage density and lineament, geological formation were prepared. Other thematic maps such as static water level, regolith thickness, depth, recharge and transmissivity developed from kriging were incorporated into GIS. Finally, multi-criteria analysis and GIS techniques were used to integrate these thematic maps to delineate suitable zones to obtain a comprehensive groundwater potential map of the study area. The results also show that in certain locations such as portions of the Bimbilla formation, probability of obtaining aquifers is very low and therefore the target should be to locate thick regolith for groundwater storage. The results from the hydrogeological investigation indicate that cokriging gives better estimates of spatial aquifer transmissivity and therefore is a better approach considering the paucity of long duration pumping test data. Regression models and variographic analysis conducted confirmed the findings of previous researchers that groundwater within the study area is mainly structurally controlled and not by lithology. The groundwater potential map was classified into five zones that describe the potentiality of each cell in the study area for groundwater exploration. These classes are; very poor, poor, moderate, good and very good groundwater potential areas. It was found that 2% and 18% of the study area was classified as very good and good

potential areas respectively. These are areas found to be concentrated in the Kodjari formation southwest of the Panabako sandstone formation of the study area. About 38% of the study area was classified as moderate potential which is sparsely distributed across the study area and 41% represent poor potential for groundwater exploration occurring mainly in the Bimbilla formation. Less than 1% of the study area was classified as very low potential areas and also concentrated in southeast of the study area. The reliability of the groundwater potential map was tested against successful and dry boreholes and the results showed that generally, the majority of high- and low-yielding boreholes fall in areas predicted by the map. Furthermore, a sensitivity analysis was performed to study the effect of each parameter on the overall groundwater map using the effective weight. It was found that the transmissivity was the most effective among the parameters that have the greatest influence on groundwater occurrence in the study area which is consistent with literature. The integrated geophysical method coupled with the comprehensive groundwater map has provided better information about subsurface geology of the Nasia Basin which is critical for understanding the lithological character in terms of hydrogeological conditions. The general concept of interpreting low resistivity zones as the presence of a sub-vertical fracture zone and therefore regarded as a favorable site has been refuted. A more scientific approach of interpreting geophysical results has been proposed for exploration hydrogeologist in the area and in similar geology. The groundwater potential map further shows that the potential for high yielding boreholes is limited to about 20% of the study area.

Therefore, other strategies to augment for increasing irrigation such as exploring the weathered zone for groundwater storage should be considered.

TABLE OF CONTENTS

LIST OF FIGURES

LIST OF TABLES

DEDICATION

I dedicate this work to the four women who have influenced my life in diverse ways: my lovely wife, Sally Adwoa Afriyie for the love, patience, sacrifice and support through this journey; my daughter, Wendkuuni Nhyira Aliou for being a gift and a blessing in my life; my dear mother, Mamata Mahama for the love, continuous prayer and support and finally my late aunt, Zainab Mahama who I affectionately call mama, for raising me to be the person I am.

ACKNOWLEDGEMENT

My greatest appreciation goes to the Almighty God for His grace and mercy for seeing me through this journey.

I am also grateful to the Danish International Development Agency (DANIDA) for providing the funding (project number 14-P02-GHA) to make this research possible.

My profound gratitude goes to my principal supervisor and coordinator of the project, Prof. Sandow Mark Yidana for first given me the opportunity to be part of the project. I am truly grateful for his immense supervision, constructive criticism and continuous support. To my co-supervisors: Kurt Klitten, I say thank you for the direction, guidance and support; Dr (Mrs) Yvonne S. A. Loh, I appreciate all the encouragement and supervision and to Dr Larry-Pax Chegbeleh, I am most grateful for the guidance especially during the field work.

To my boss Dr Julius Aptidon Awini, Managing Director-Hydronomics Limited, thank you for the patience and support you showed me during my study. God richly bless you.

To my family, I appreciate your endurance and prayers during this period of my study.

I also say a big thank you to Miss Elikplim Abla Dzikunoo for the encouragement, support and assistance.

Richard Mejida Adams and Evans Manu, I cannot forget the support you provided especially during the field campaign. Ben Emunah Aikins and Francis Andorful (RS & GIS Lab-UG), thank you for the time and assistance.

Finally, to Abdul-Rahman Lutuf of Saha Consulting and Services Limited and Rexford A. Ani, I appreciate the words of encouragement. God bless you

CHAPTER ONE

INTRODUCTION

1.1 Background

Groundwater resources are increasingly recognised as a major strategic water resource in the context of a changing climate and human development. In many parts of the world, groundwater has been used as a reliable source of water for numerous purposes such as for irrigation, domestic and industrial uses. For instance, UNESCO (2012) suggests that, over 2.5 billion people worldwide rely on groundwater daily.

In the wake of changing climate coupled with water scarcity, several researchers in the global scene have conducted various investigations in an effort to understand the hydrogeological properties of aquifers for proper management. Hunkeler (2016) for instance has advocated the use of geological method in the form of core sampling using rotary core drilling, augering or sonic vibratory drilling for characterising subsurface of terrains. This approach however has a lot of uncertainties because the information obtained is local and considering the high heterogeneous nature of some terrains, it would not be representative enough.

Geophysical methods are also capable of characterising aquifers to produce good results especially where they are combined with other methods. Ashraf et al. (2018) developed subsurface soil profile based on the combined use of electrical resistivity with well log and pumping test and concluded that, the method was reliable in

identifying potential favorable zones within the area. Danielsen et al. (2007) on the other hand, used transient electromagnetic (TEM) and continuous vertical electrical sounding (CVES) to characterise the hydrogeology of Karoo stratigraphic sequence in Zimbabwe. A more accurate image of the entire subsurface profile was provided using both methods.

Remotely sensed data has been used by Kexiang et al. (2017) for hydrogeological characterisation of the whole Brazil. Their study investigated the relationship between GRACE (Gravity Recovery and Climate Experiment)-derived groundwater changes and geological conditions such as rock properties and aquifer types across Brazil in order to study the groundwater potential. The challenge however with this approach has to do with cost of the analysis especially when measuring or analyzing smaller areas and also it requires a special skill to analyze the images.

Pumping test is widely accepted as the best method for aquifer characterisation according to Fetter (2001). Holland (2011) therefore used pumping test in characterising the hydrogeology of crystalline basement aquifers within the Limpopo Province of South Africa. The study focused on evaluating factors that influence borehole yields and aquifer transmissivities. A limitation with using pumping tests is the fact that it does not provide detailed information about the variability of hydraulic parameter as they are often related to narrow or limited site characterizations, thus, data obtained are only point estimates (Slater, 2002).

Tracer test according to Todd and Mays (2005) have also been used in the determination of aquifer hydraulic parameters though the procedure is simple in practice, results obtained are only approximations due to field limitations. For sparse areas, Yand et al. (2010) have proposed advanced modelling techniques as means of improving characterisation of the complex hydrogeological systems. They used groundwater flow modelling with nonlinear inverse calibration, advective transport, geochemical modelling and isotope study to characterize heterogeneous systems.

In Ghana, besides the Hydrogeological Assessment Project (HAP) which was initiated to provide scientific background for groundwater-based supply projects as well as resource management studies of the Northern Regions of Ghana, studies on characterising the hydrogeology are limited especially for the Voltaian Sedimentary Basin (VSB). This is because most groundwater projects are for rural water supply. There are however a few investigations with various methods of characterising the hydrogeological terrains. Ewusi (2006) assessed the feasibility of various geophysical techniques for groundwater exploration and management in Northern Region. The major limitation of Ewusi (2006) is the reliance on only geophysics to map the groundwater resources even though new insights were presented.

Yidana et al. (2011) characterised the hydrogeological conditions of portions of the Voltaian with pumping test data using regression analysis. The challenge with

this work had to do with the limited data for some of the lithology. Darko (2001) on his part evaluated the groundwater resources in Ghana by classifying the hydrogeologic units on a regional scale. Besides the limited data used for the VSB, the method used in calculating transmissivity was based on different geological environment which can be misleading.

Forkuor et al. (2013) also combined spatial parameters such as recharge rate, regolith thickness, transmissivity, borehole success rate and static water level to assess the groundwater development potential in Northern Ghana. The challenge with this work was the over simplification of the geology of the VSB for instance by generalizing all the rocks as sandstones instead of classifying them in their right geological units.

In recent times, other researchers have used numerical groundwater flow simulations under steady state and transient conditions for hydrogeological studies in the White Volta basin (Attandoh et al. 2013; Darko, 2015; Ofosu-Addo et al. 2008) among others. For a proper groundwater models to be developed, there is the need for a thorough understanding of the hydrogeological setting.

Considering the number of limitations with the various methods stated above, a comprehensive method of characterizing the hydrogeology of the Voltaian supergroup is urgently required. A combined use of geophysics and hydraulic parameters would be adequately to characterise the hydrogeology.

1.2 Problem Statement

The success rates of drilling wet boreholes yielding minimum 10 lpm within the VSB has been reported differently by various researchers to be below 60%. For instance, Dapaah-Siakwan and Gyau-Boakye (2000) reported a success rate of 56% in the VSB while Annon (2000) reported a 38% after evaluating boreholes drilled under the International Development Agency (IDA) funded project. Unihydro (2003) pegged the success rate based on then available data as 25%. In the 2016/2017 financial year of World Vision International, a success rate of 50% was recorded for the Gushiegu and Karaga Districts.

The dry boreholes or low yields recorded within the VSB is partly because of the lack of detailed understanding of the hydrogeology and its relevance for the geophysical data. There appears to be poor understanding of the physical basis of geophysical siting, and in consequence some geophysical techniques are being carried out wrongly and others are not being used to their full potential. Even where techniques are carried out and geophysical data are analysed correctly, they are often not interpreted appropriately. Community members as the ultimate beneficiaries of these boreholes, have their hopes are dashed wherever dry or low yielding boreholes are recorded. Donors also get disappointed about these results and have raised concerns about the huge sums of money that is spent on drilling projects.

Apart from the Hydrogeological Assessment Project (HAP) funded by Canadian International Development Agency between (2005-2011) and the White Volta Basin Monitoring Project (WVBP) funded by Danish International Development Agency (DANIDA) between (2004-2008), which carried out a comprehensive hydrogeological study of the Voltaian supergroup in Ghana, there has not been any hydrogeological studies in the area in recent time.

Although there have been several drilling attempts at various parts of the Voltaian supergroup, most of them have been treated in isolation. This isolated use of site-specific information represents a failure to develop a background understanding, a necessary condition for improving successful groundwater exploration. There has been no or little consensus on what groundwater targets are and no attempt has been made to document the geophysical character of the rocks, such as linking typical geophysical signatures to geological formation or lithology. Most hydrogeological investigations within the study area for groundwater exploration are usually based on just the electrical resistivity method. Further to that, there is little understanding of the probable depth of groundwater within the study area. Forkuor et al. (2013) assert that, little knowledge has been built on groundwater potential through the continuous collection, verification, registration and archival of hydrogeological data from drilled boreholes.

The development of groundwater within this environment is notoriously complicated, with the high number of variable parameters. Detailed

hydrogeological study, which involves combining different geophysical methods and evaluation of hydraulic parameters to develop a comprehensive groundwater potential map is urgently needed. The map will aid groundwater development practitioners in selecting locations for groundwater development. Additionally, it could inform donor and other funding organisations in setting realistic goals and standards for future project success in what is a very difficult terrain to develop groundwater resources.

1.3 Objectives of the Study

The primary objective of this study is to determine the hydrogeological characteristics of the Nasia Basin of the White Volta Basin.

The specific objectives of the study are to:

- evaluate the current conventional methods of interpreting geophysical results in the area;
- develop an appropriate approach for groundwater exploration in the various geological formations and document their electrical resistivities;
- assess the aquifer parameters of the main lithologies and evaluate the factors that control groundwater potential within the area;
- develop a comprehensive groundwater indicator/potential map to aid in groundwater exploration

1.4 Justification

The current approach in exploring groundwater has in general not produced the desired results, especially within the Voltaian terrain, considering the low success rates that has been recorded. Several reasons can be given to the poor results but

key among the reasons is a lack of thorough understanding of the geology and hydrogeology.

This research aims to serve as blue print for the groundwater sector in the quest to enhance success rates of drilling wet boreholes yielding minimum 10 lpm in the area. It comprises several methods of characterising the hydrogeology ranging from remote sensing, geophysical studies, hydrogeology and geostatistics to produce a groundwater potential map. This would go a long way to help achieve goal 6 of the Sustainable Development Goals (SDG) thus achieving universal and equitable access to water.

Secondly the outcome of this research goes to feed into a bigger project funded by DANIDA with the objective of harnessing groundwater for sustainable agriculture as a pilot activity within the project area. Therefore, the results would be used in determining prolific aquifers capable of yielding large volumes of water particularly in the dry season.

This also feeds directly into the government's quest to revolutionise agriculture through the 'planting for food and jobs policy' targeted at employing an estimated number of approximately 770,000 jobs per crop season and about 1.5 million jobs by the end of 2020 (MOFA, 2019). Having access to water can help farmers engage in irrigation especially in the dry season since most of the inhabitants in the study area are farmers and will help provide jobs for the youth and thereby help reduce poverty.

Finally, this research would provide relevant guidelines to all the organizations in the water sector for groundwater development in areas with similar geology.

1.5 The Study Area

1.5.1 Location

The Nasia Basin (Figure 1-1) forms part of the nine sub-catchments of the White Volta Basin and it is located within Northern and North East Regions of Ghana specifically within East Mamprusi, West Mamprusi, Savelugu, Nanton, Karaga and Gushiegu Districts. The study area is bounded between longitude 0° and 1° W and latitude 9° 45° N and 10° 45° N with an area of approximately 5400 km^2. Some of the major towns in the study area are Nalerigu, Gambaga, Walewale, Karaga, Gushiegu and Gbintiri.

1.5.2 Climate and Vegetation

The area lies within the tropical Continental or Interior Savannah Climatic Zone (Dickson and Benneh, 1995). The rainy season starts from May and ends in October with an annual rainfall which ranges between 1005 and 1150 mm, and the heaviest rains occurring in August. The mean monthly temperatures vary from about 36°C in March/April to about 27°C in August. Relative humidity is high during the rainy season (65-85%) but may fall to 20% during the dry season. The area falls within the savannah vegetation zone, which is characterized by tall grasses that grow in tussocks, and widely scattered trees such as baobab and the dawa-dawa trees.

The climate is controlled by circulation patterns of two subtropical air masses; wet maritime monsoonal air from the Gulf of Guinea and Sahara Desert air from the interior of Northern Africa (Lutz et al. 2007). There is significant evapotranspiration mainly due to the warm and dry winds that blow across the Sahara Desert. Evapotranspiration ranges from 650 mm to 1300 mm and varies by season, location, local vegetation type and density (Kwei, 1997).

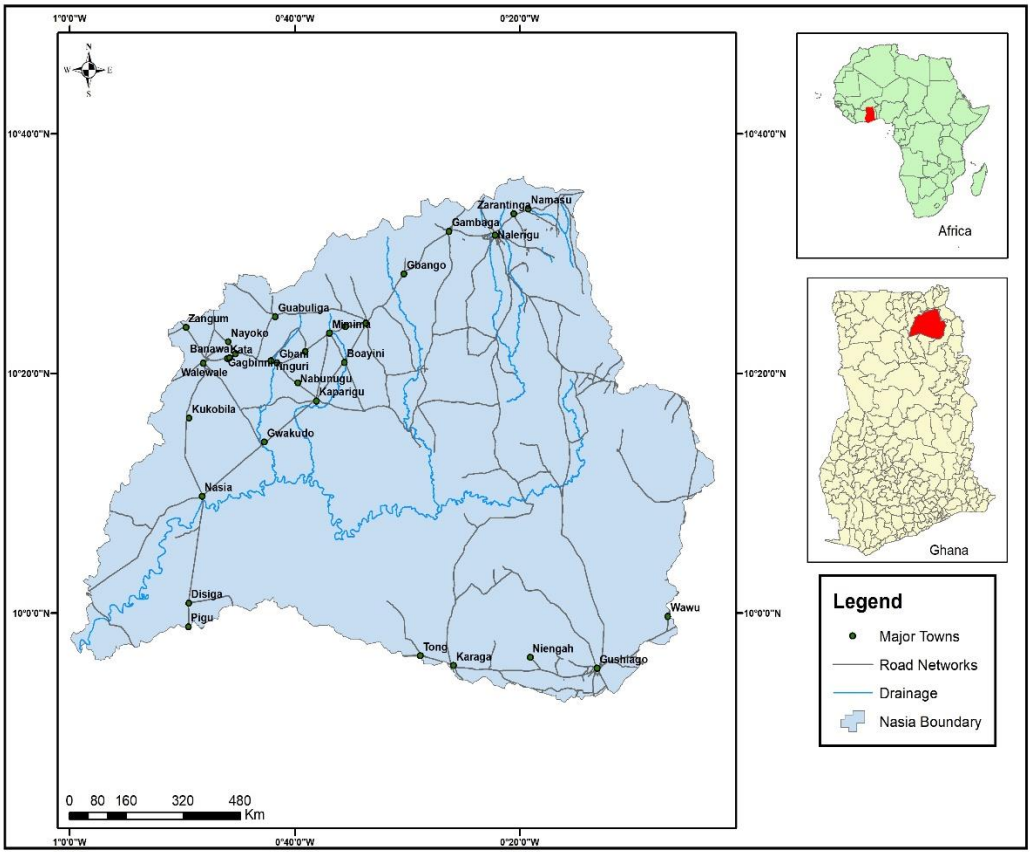

Figure 1 - 1: Map of Nasia Basin of the White Volta Basin

1.5.3 Drainage

The main drainage system in the study area is made up of the Nasia river, which is a tributary to the White Volta. The effect of the drainage system is seen mostly between Savelugu and West Mamprusi District covering the areas between Nabogu and Kukuobilla. These areas are prone to periodic flooding during the wet season, making them suitable for rice cultivation (Ghanadistricts, 2017).

1.5.4 Geology

The area is underlain by rocks belonging to both Oti-Pendjari Group and the Bombouaka Group of the Voltaian supergroup, which covers about 45% of the total landmass of Ghana. Based on a revised lithostratigraphy of the study area, there are four (4) main geological formations, Bimbilla, Kodjari, Panabako Sandstone and Poubogou formations (Carney et al. 2010). Figure 1-2 is a geological map of the study area with the various formations.

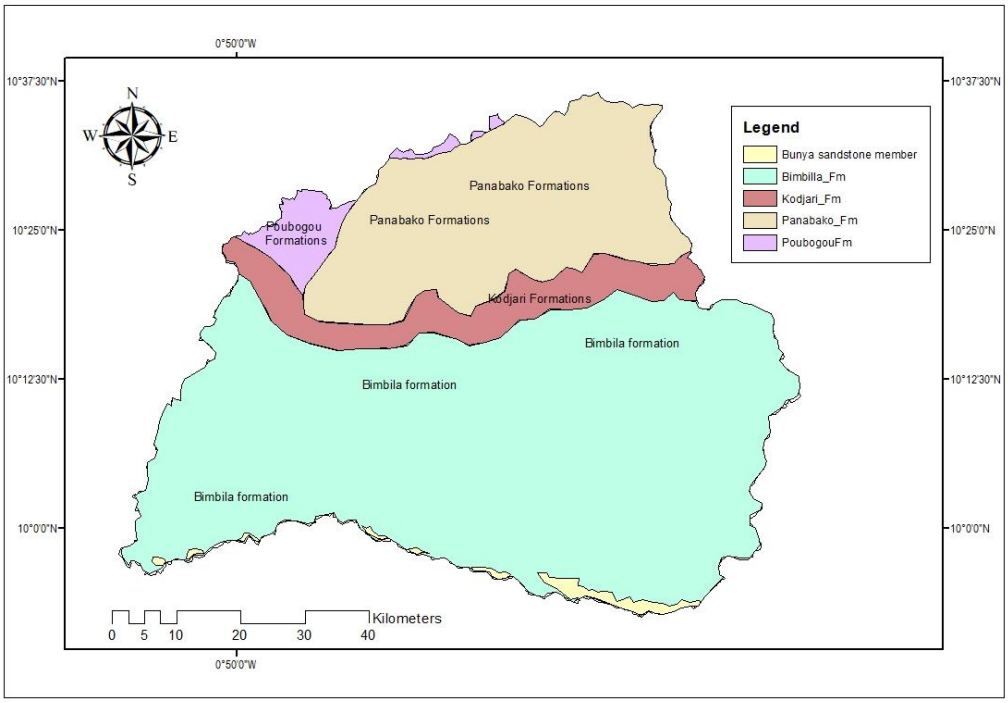

Figure 1 - 2: Geological map of the study area

Carney et al. (2010) indicates that the Bimbila formation consists of green to khaki, micaceous laminated mudstones, siltstones and sandstones which represent a continuation of foreland basin deposition. The siltstones typically occur in thin, tabular beds with wind-rippled tops and low angle cross-bedding. Sandstones are thinly intercalated within the unit and also include the feature-forming, and thus readily mappable Bunya member. The Bunya sandstone member is about 50 m thick and outcrops in the southernmost portions of the study area. It consists of green - grey, medium to thickly-bedded, feldspathic and lithic-rich wacke sandstone. (Jordan et al. 2009).

The formation, Kodjari sometimes referred to as the basal formation of the Oti-Penjari Group. The tillites or tilloids of this group fill an erosional and slightly

angular unconformity of glacial origin. This group stratigraphically overlies the Bombouaka group (Sougy, 1971). Carney et al. (2010) indicate that the distinct triad of lithologies comprise basal tillites, cap-carbonates and laminated tuffs and ash-rich siltstone. Outcrops identified with south of the Gambaga massif, show them as crimson- weathering siliceous tuffaceous siltstones. Barfod et al. (2004) also suggest that it consists mainly of shales and siltstones, and lenses of various facies of sandstones, greywackes, limestones, silexites and tuffs.

The Panaboko sandstone is estimated to be 150-200 m thick, and comprises hard, well-cemented, well sorted, medium-grained, quartzitic sandstones, which are particularly indurated and appear crystalline in the north of the area. Overlying the unit is a typically thin, gravelly laterite, sometimes capped by thin iron oxide cement (Carney et al. 2010; Jordan et al. 2009).

The Poubogou formation of pro-delta mudstones and siltstones outcrops towards north along the Gambaga escarpment and is about 170 m thick and grades into the overlying nearshore-facies quartz arenites of the Panabako sandstone formation (Carney et al. 2010). According to Ayite et al. (2008), the Poubogou formation consists of green-grey micaceous mudstones and siltstones with thin intercalations of fine-grained sandstone.

1.5.5 Hydrogeology

The sedimentary rocks mentioned above are affected by the Pan-African tectonic events and have virtually lost their primary porosity due to cementation and

consolidation (Acheampong and Hess, 2000; Kesse, 1985). Dapaah-Siakwan and Gyau-Boakye (2000) suggest that the beds generally dip gently. Groundwater occurrence is dependent on secondary permeability resulting from fracturing and/or weathering of the rocks. This enhances hydraulic parameters such as storage, transmission and recharge potential (Banoeng-Yakubo et al. 2011). Banoeng-Yakubo et al. (2011) indicate that the weathered zone of the Voltaian is highly variable due to the variability in the clay content. Dapaah-Siakwan and Gyau-Boakye (2000) suggest that the average yield for productive boreholes (minimum yield of 10 lpm) in the area is between 6.2 m^3/hr -8.5 m^3/hr with success rates of less than 60%. Dapaah-Siakwan and Gyau-Boakye (2000) allude that parameters which control groundwater storage appear to be discrete entities of variable spatial extent.

The thickness of the regolith (excluding saprock) according to Carrier et al. (2008) averages around 6 m to 11 m and they have linked that to the relatively stable clay (shale) and quartz (sandstone) composition or by the fine texture or ductile nature of the sedimentary rocks found in the Voltaian. Bannerman (1990) revealed that the most productive fracture zones occur between the depths of 13 m and 80 m with an average of 27 m. Carrier et al. (2008) and Banoeng-Yakubo et al. (2011) indicate the average depth of boreholes is 55 m and it ranges between 45 m and 75 m. The productivity of the aquifers is generally low to moderate with transmissivity range between 0.3 m^2/d to 267 m^2/d and a mean of 11.9 m^2/d.

The evaluation of boreholes by O'Dochartaigh et al. (2011) under the HAP and other projects indicated that depth range of boreholes for the Bunya Sandstone member in the Bimbilla formation is between 30 m to 70 m. They assert that in non-dry boreholes, recorded yields range from 5 l/min to 1000 l/min and concluded that the key groundwater target is likely to be thin fracture zones within the sandstones. For the Bimbilla formation, depth typically ranges between 20 m and 80 m, and it appears to form a moderate to low productivity aquifer. Groundwater targets are the weathered- fracture zones and thin zones at lithological boundaries (O'Dochartaigh et al. 2011). For the Panabako sandstone formation, O'Dochartaigh et al. (2011) indicated that based on their assessment, the depth of boreholes ranged between 30 m and 70 m. The borehole yield ranged between 15 l/min and 35 l/min with groundwater target being the weathered-out fracture zones between 20 m and 30 m. The Formation appears to form a moderate to high productivity aquifer.

Groundwater recharge is reported to range between 1.8 % and 32 % of the annual average precipitation by Yidana and Koffie (2014) while Addai et al. (2016) arrived at a range of 73 mm/yr -110 mm/yr with an average of 94 mm/yr. Afrifa et al,. (2017) on their part, estimated the groundwater recharge in the Gushiegu district in the range of 13.9 mm/y - 218 mm/y, with an average of 89 mm/yr, representing about 1.4%-21.8% (average 8.9%) of the annual precipitation in the area.

1.6 Brief Background of Groundwater Development in the Voltaian

The first assessment of water resources potential was by the Geological survey of Ghana in 1925. Researchers like Annan-Yorke and Cudjoe (1971), Gill (1969), Junner (1946) were among the few who started reporting on groundwater related works within the country and in the Voltaian specifically. Junner (1946) proposed a division of the Voltaian into three layers based on lithology and reported about the presence of large springs along joints and bedding planes at certain locations. Annan Yorke and Cudjoe (1971) conducted their studies on the geology and hydrology of the Voltaian Sedimentary Basin and reported that it consisted of undeformed flat-lying sediments with lots of variation in lithology. Gill (1969) related borehole yields and the quality of water to the various geological formations in the country however with limited data. For instance, in the Northern Region, 36 boreholes were used with an average depth of 105 m and average yield of 4 m^3/h.

Between 1984 and 1995, Water Resources Institute (WRI) of Council for Scientific and Industrial Research conducted an assessment for the entire country using 8000 boreholes. In the Northern, North East and Savana Regions, 150 boreholes were used to arrive at a depth ranging between 35 m -150 m while yield was between 8 l/min - 600 l/min. Nii Consult (1998) also conducted a study of the White Volta Basin using river basins for both surface and groundwater resources and indicated that aquifers with yields varying from 0.6 m^3/hr -18 m^3/hr with a mean of 3.8 m^3/hr were tapped by boreholes drilled to depths between 27 m -91.1 m with a mean of 42.1 m.

Dapaah-Siakwan and Gyau-Boakye (2000) on their part divided the country into three hydrogeological provinces: the Precambrian igneous and metamorphic rocks was described as the Basement Complex comprising 54% landmass, Paleozoic sedimentary basin comprising 45% consisted of the Voltaian Sedimentary Basin and 1% for Cenozoic, Mesozoic, and Paleozoic sedimentary strata along the coast and the Quaternary alluvium along major stream courses. The challenge with these descriptions has to do with lumping of the various geological formations, which could lead to wrong conclusion in terms of hydrogeological potential.

The Canadian International Development Agency (CIDA) funded a Hydrogeological Assessment Project (HAP), which was implemented in conjunction with the Water Resources Commission (WRC) between 2006-2011. The HAP was aimed at improving the knowledge base of the hydrogeological setting in the Northern Ghana by establishing a borehole database with more than 10000 borehole records. Furthermore, by drilling 27 deep monitoring boreholes additional to previously drilled 12 monitoring boreholes funded by DANIDA (White Volta Basin monitoring project), and by conducting geophysical wireline logging in nearly all of them.

The most recent review of the hydrogeology of the Voltaian was conducted by Banoeng-Yakubo et al. (2011). They developed a new hydrogeological map of Ghana, which contained five hydrogeological provinces based on groundwater potential and lithology. The provinces are the Birimian Province, the Crystalline Basement Granitoid Complex Province, the Voltaian Province, the Pan African

Province, and Coastal Sedimentary Province. In their conclusion they indicated that most prolific aquifers were associated with deep weathering and fracturing and suggested that the hydrochemistry is controlled by the weathering of silicate minerals and cation exchange except for unconfined aquifers where anthropogenic activities influence the groundwater hydrochemistry.

CHAPTER TWO

LITERATURE REVIEW

Groundwater management has led to the need for accurate investigation and description of aquifers. A hydrogeological characterization of a specific area can be achieved by estimating the aquifer parameters.

Several methods have been used by different researchers for hydrogeological characterisation, which include geophysical characterisation, aquifer test analysis, tracer test, numerical modelling, remote sensing and Geographical Information System (GIS) techniques.

2.1 Geophysical characterisation of Groundwater Systems

The application of geophysics for groundwater investigations has been extensively presented and reviewed by a lot of researchers (Kearey and Brooks, 1991; Milsom, 2003; Reynolds, 2010; Telford et al. 1976). These applications include mapping the depth and thickness of aquifers (Albouy et al. 2001; Danielsen et al. 2007; Huntley, 1986; Mazac et al. 1985; Robain et al. 1996), locating geological structures such as major fracture systems and fault zones (Batte et al. 2008; Christensen and Sørensen, 1998) and mapping groundwater contamination (Adepelumi et al. 2008; Cimino et al. 2007; Goldman and Kafri, 2006; Kafri et al. 2007; Mills et al. 1988). The commonest among the geophysical methods are the electrical and the electromagnetic (EM) methods which have been reported as the most successful in terms of groundwater resources investigation (Danielsen et al. 2007; Gwaze et al.

2000; MacDonald et al. 2001; Sørensen and Søndergaard, 1999; Soupios et al. 2010).

An illustration of the use of the geophysical technique for a rural water supply in hard rock area in northern Nigeria was shown by Reynolds (1997). The area recorded a failure rate of more than 82% for boreholes prior to the use of geophysics but was dramatically reduced to less than 20% by using an integrated geophysical, geological and photogeological methods.

Danielsen et al. (2007) carried out a geophysical and hydrogeological investigation in Zimbabwe using two geophysical methods; Continuous Vertical Electrical Sounding (CVES) and Transient electromagnetic and concluded that a combination of the geophysical methods is able to provide a substantially better image of the subsurface as compared to one method. By using combined geophysical methods; EM34; Vertical Electrical Sounding (VES) and Magnetic profiling, the main targets for groundwater within a low permeable sedimentary terrain in Nigeria were identified by MacDonald et al. (2001). Another example of using geoelectric method for groundwater exploration is shown by Dahlin and Owen (1998). They used 2D resistivity surveys combined with ground penetrating radar in shallow alluvial aquifers in Zimbabwe. The results were used to develop hydrogeological models of the aquifers for managing a drilling programme. Barker (1990) on his part, used micro-processor-controlled resistivity traversing for siting boreholes in hard rock terrain in Nigeria.

In Sub-Saharan Africa including Ghana the frequent use of the resistivity and EM method in the crystalline basement in particular has resulted in researchers developing specific techniques of interpreting results (Beeson and Jones, 1988; Olayinka and Baker, 1990). These techniques that have been helpful particularly in localizing sub-vertical fractured zones as low resistivity zones within the high resistivity basement rocks have been used by other researchers in other geological terrain and have led to wrong results (MacDonald et al. 2001). This was confirmed by Ó Dochartaigh et al. (2011) in evaluating geophysical practices in Northern Ghana. They concluded that there is a general lack of understanding of geophysical siting techniques among some groundwater practitioners. Like most of the researchers referred to below the different siting techniques was based on low resistivity/high conductivity anomalies as indicators for profitable drilling sites irrespective of the type of geological environment. Furthermore, the direction of the profiles compared to the strike of sedimentary formation is never taken into consideration as being important for the interpretation.

Annon (2000) evaluated the results of eighty (80) boreholes drilled in the Voltaian under the International Development Agency (IDA) funded project and arrived at a 35% to 38% success rate using the conventional four electrode resistivity method while Ewusi, *et al.* (2009) on his part, used the 2-D Multi-Electrode Resistivity Imaging (2-D MERI) technique and recorded a 60% success rate. Though there was an improvement in the success rate, the results would have been far better if other methods were incorporated. Owen (2005) attested to the capability of the MERI by

indicating that it could provide detailed continuous 2D map of the subsurface, identify different lithologies, delineate contact zones and faults, and measure the thickness of the weathered regolith. Mainoo et al. (2019) for instance after a thorough investigation using 2D electrical resistivity tomography to delineate groundwater potential zones in the VSB concluded that a careful application of the method with an in-depth understanding of the geology would significantly improve the success rate of exploring groundwater. MacDonald et al. (2001), however, is of the view that a combined use of different geophysical methods would yield a more favourable outcome than reliance on a single method.

Chegbeleh et al. (2014) developed a method of data interpretation for the sedimentary formation of the Voltaian basin for groundwater exploration using the EM-34 method. Their scheme of interpretation was based on identifying EM highs along parallel traverses of EM profiles presented on one-dimensional (1-D) plots. Though their work is an improvement in the use of the EM-34, the conclusions arrived for the range of conductivity for the area is a challenge considering the heterogeneous nature of the place, the size of the area compared with the number of points used.

Menyeh et al. (2005) used the EM-34 for siting in the Gushiegu-Karaga district which is within the Voltaian sedimentary basin and recorded a 60% success rate out of 100 boreholes that were drilled. They recommended the use of the EM-34 for siting in the area. But considering the complex nature of the VSB, the 60%

success rate is not conclusive enough. Such a terrain requires more than one method to be verified before a conclusion is made for which method is most beneficial.

Klitten and Agyekum (2008) on their part characterised the lithology of the Voltaian sedimentary rocks using geophysical logs in drilled water wells in the Northern Region of Ghana. Klitten and Agyekum (2008), indicate that the lithological sections derived from the geophysical logs provide more information and has led to some revisions of boundaries between lithological sub-units.

2.2 Characterisation of Groundwater Systems Using Hydraulic Parameters

Freeze and Chery (1979) suggest that groundwater exploration relies heavily on investigating the aquifer geometry and understanding hydrogeological parameters for an efficient groundwater management. Hydraulic aquifer parameters are fundamental for groundwater flow modeling. From literature, the main hydraulic parameters commonly used for characterisation include vertical and horizontal hydraulic conductivity, transmissivity and storage capacity. Field estimations of these hydraulic parameters are not always available at sufficient number of data points because of the cost and time in acquiring them and therefore many investigation techniques focus on the estimation of the spatial distribution based on often rather few data points.

There are generally three methods of determining aquifer parameters according to Driscoll (1986): 1) using data collected during pumping tests, 2) analyzing

hydraulic properties of an aquifer material and 3) calculations based on laboratory tests.

2.2.1 Aquifer response curves

Apart from calculating aquifer parameters, the time drawdown diagrams determined from pumping test can provide information on hydrogeological conditions in the aquifer in terms of negative or positive hydraulic boundaries. Several studies (Darko, 2001; Samani et al. 2006; Holland, 2011; Xiao, 2014) have reported the use of time-drawdown graphs in a bid to explain the hydrogeological conditions around pumped boreholes in hard rocks.

Samani et al.(2006) highlighted the strength of drawdown-derivative analysis in ground water evaluation of a heterogeneous aquifer. They integrated conventional time-drawdown analyses, derivative curves and geological information to identify the nature of heterogeneities and assess aquifer response to pumping. Though this approach helps in aquifer interpretation, it is under-utilized due to a lack of published case studies demonstrating its strengths and weaknesses.

Holland (2011) focused on the challenge conducting pumping tests analysis by choosing an appropriate model that best fits the observed drawdown response. He therefore proposed a method for the analysis of pumping test data in weathered-fractured rock aquifers and highlighted the importance of diagnostic plots for the detection of flow regimes and to help in selecting the appropriate theoretical model.

Xiao (2014) followed the approach of Holland (2011) by illustrating the possibility of using derivative pattern for diagnostic analysis of aquifer tests.

In Ghana, Darko (2001) used drawdown curves to identify dominating flow regimes to help in calculation of transmissivity. He illustrated the various components of the aquifer of a borehole in Wenchi located in the VSB using only one borehole for the entire VSB. The limitation with Darko (2001) work is on the use of only one borehole for the assessment.

2.2.2 Aquifer parameters

Specific capacity of a borehole (discharge per hour per m drawdown) has been described by many researchers such as Mace (2001) and Yidana et al. (2011), Yidana et al. (2008) as dependent on factors such as aquifer setting, screen setting and pumping duration and usually calculated using a ratio of well discharge to drawdown after 180 minutes of pumping.

A thorough evaluation of transmissivity estimation has been conducted by Mace (2001) where three main approaches of calculating transmissivity were identified including analytical, empirical and geostatistical method. Mace (2001) indicates that the analytical method involves using mathematical equations that are based on the theory of groundwater flow such as the Cooper- Jacob (1946) method. Jalludin and Razack (2004) used the Cooper-Jacob (1946) method to calculate transmissivity for volcanic and sedimentary aquifer systems in the Republic of Djibouti. This was after the boreholes were pumped for a period ranging between 2 hr to 72 hr to meet the assumptions for this method. Yidana et al. (2011) used the

Copper-Jacob (1946) method to estimate transmissivity for boreholes in some portions of the VSB. The challenges with this method is with the (1) unrealistic assumptions about the aquifer and well hydraulics and (2) limited information on the aquifer or the well.

In many hydrogeological studies, it is not uncommon for specific capacity data to be in abundance compared to data on transmissivity. Various reasons explain this situation such as; high cost associated with carrying out pumping test, time involved in embarking on the exercise and also the availability of the right personnel to conduct the pumping test without compromising on the quality of data.

Empirical methods are therefore developed to relate transmissivity with specific capacity by using paired values of both parameters for a specified pumping time (Mace, 2001). Empirical relationships were first used by Eagon and Iohe (1972) and improved upon and popularized by Razack and Huntley (1991). In Ghana, empirical relations relating transmissivity and specific capacity with limited data was first developed by Acheampong and Hess (2000). Yidana et al. (2008) popularized the method in Ghana using data from the Afram Plains portion of the Voltaian to derive a regression models. The results revealed that transmissivity exists in a non-linear relationship with specific capacity in the area. They concluded that the high regression coefficient showed a high dependence of transmissivity on specific capacity for the area. Aliou *(*2010) also followed the approach of Yidana et al. (2008) and developed a relationship for transmissivity and specific capacity for some portions of the northern part of the Voltaian of Ghana. The relationship obtained did confirm that of previous researchers in other areas though it was based

on a smaller part of the VSB. The duration for the pumping test though was shorter (6 hours) it still showed high coefficient of regression for the estimated transmissivity and specific capacity. Darko and Krásný (2010) and Forkuor et al. (2013) also used an empirical relationship developed by Krásný (1997) to estimate regional transmissivity map for Ghana. Krásný (1997) relationship was too generalized without taking into consideration the difference in geology. HAP (2011) also established a relationship for transmissivity and specific capacity for Northern Ghana based on records of then existing monitoring boreholes. Their relationship however is an amalgamation of all the rocks from both the VSB and the basement complex in the Northern Ghana which makes the model not entirely reliable. Combining parameters derived from different geological setting can introduce too much uncertainty in the model (Mace, 2001).

Using geostatistical techniques such as kriging, kriging with regression and cokriging for estimating aquifer transmissivity and other parameters has been suggested by a number of researchers to be very helpful and has yielded useful results over the years (Aboufirassi and Marino, 1984; Binsariti, 1980; Darling et al. 1994; Delhomme, 1974; 1976; Mace, 2001; Prudic, 1991; Razack and Lasm, 2006), though not from Ghana.

Razack and Lasm (2006) used ordinary kriging to estimate areawise distribution of transmissivity from specific capacity at few locations in a highly fractured aquifer in Western Ivory Coast. The purpose was to compare with other forms of geostatistical estimation of transmissivity. Yidana et al. (2011) developed a spatial

distribution map of transmissivity for portions of the Voltaian basin of Ghana. Carter et al. (2011) also employed ordinary kriging to estimate the spatial distribution of specific capacity of Newark Basin aquifer by using measured values. The challenge with the use of these approaches is with the practicality of having sufficient number of boreholes in a vast field.

Other researchers have also combined kriging with estimated transmissivity from linear regression to produce spatial distribution maps. Examples include Forkuor et al. (2013) who used estimated transmissivity measurements based on Darko and Krásný (2010) relationship to produce interpolated map of transmissivity. Darko (2001) also used kriging with empirical relationship based on Jetel and Krasny (1968) to produce a regionalized transmissivity map of Ghana.

Regression relationships combined with kriging to estimate values of aquifer transmissivity introduce two categories of errors; errors from the regression model and another from the interpolation procedures. These errors affect the quality of the final spatial distribution map produced and therefore renders these techniques inappropriate.

Aboufirassi and Marino (1982) used cokriging to construct a transmissivity map for Yolo Basin, California by employing field measurements of transmissivity and specific capacity. The latter was used in a big scale because there was relatively few transmissivity data available. An important advantage of using cokriging under this circumstance is the ability to still obtain accurate estimations of transmissivity

on the basis of auto and cross-correlation and as well as obtaining estimation variances. Razack and Lasm (2006) used cokriging to estimate transmissivity of aquifers of the Western Ivory Coast. In Ghana, there have been few instances where researchers have estimated transmissivity (Forkuor *et al.* 2013; HAP, 2011; Yidana et al. 2011) based on kriging and kriging with regression but no examples exist on the application of cokriging.

2.2.3 Variographic analysis

A key component of using kriging and cokriging for estimating areawide distribution of transmissivity or other parameters is concerned with spatial variability. Isaak and Srivastava (1989) have elaborated on the assumptions underlying variograms for spatial variability. Researchers such as Razack and Lasm (2006) have also suggested that kriging estimation using variographic analysis is capable of describing the spatial variability of parameters. They allude that variograms are fundamental to characterising complex aquifers. Carter et al. (2011) in predicting specific capacity for Newark basin aquifer system, developed semivariograms to determine whether significant variations had occur and were able to estimate parameters of the modeled variograms such as sill, nugget effect and range for describing spatial correlation. Forkuor et al. (2013) indicates that kriging gives an idea of the precision of estimates by quantifying estimated variance. They experimented with different models and parameters and performed cross-validation to understand the variability of the parameters prior to modeling potential areas of groundwater of Northern Ghana.

2.3 Remote Sensing (RS) and GIS for groundwater mapping

Conventional methods of exploration for characterising groundwater systems are not only tedious but also consume lots of time and money and require skilled manpower. Remote sensing and GIS have been proposed as viable supplementary tools of characterizing groundwater systems. The concept of integrating remote sensing and GIS has proved to be an efficient tool in groundwater studies (Akram and Wani, 2009; Mondal et al. 2009; Narendra et al. 2013; Singh et al. 2013).

Jha et al. (2007) categorized the applications of remote sensing and GIS for groundwater studies into the following (1) exploration and assessment of groundwater resources (2) selection of artificial recharge sites (3) GIS-based subsurface flow and pollution modeling (4) groundwater pollution hazard assessment and protection planning (5) estimation of natural recharge distribution, and (6) hydrogeologic data analysis and process monitoring. Researchers such as Deepika et al. (2013) and Wahyuni et al. (2008) have demonstrated how remote sensing and GIS could be used to detect areas with high potential for groundwater exploration.

Though the use of remote sensing and GIS in groundwater studies has been widely used in many parts of the world, there is limited work in that regard in Ghana. Sander et al. (1996) is among the first researchers who used RS data and GIS to develop a well-siting strategy in the VSB in Ghana. The data used include Landsat Thematic Mapper (TM), SPOT, and infrared aerial photography interpreted for linear vegetation, drainage and bedrock feature that indicate underlying

transmissive fracture zones. The integration of data in a GIS was valuable for effective analyses but also exposed the necessity of accounting for spatial reference and accuracy of data from different sources. The data used covered only the central part of the Voltaian and therefore the conclusions made for the entire area does not apply in all locations. Banoeng-Yakubo (2000) also used remote sensing and data from boreholes in the Upper West Region to identify different rock types and structural conditions favourable for siting high yielding boreholes.

Several attempts have been made to map potential areas for groundwater globally. Forkuor et al. (2013) suggests that the potential maps vary in scale ranging from global assessment, a regional assessment, country-level analyses and basin-level assessment (MacDonald et al. 2001; MacDonald and Davies, 2000; Martin and van de Giesen, 2005; WHYMAP, 2008; Woodford et al. 2006).

A groundwater potential map for Ghana was developed by Gumma and Pavelic (2013) using remote sensing and geographical information system (GIS) techniques. The factors they used are geomorphology, geology, slope, drainage density, annual rainfall, land use/land cover, and soil type. The parameters used however have limited influence on groundwater potential occurrence especially for the study area. The key to identifying groundwater potential is an evaluation of hydraulic parameters, which were absent under this circumstance. Forkuor et al. (2013) combined spatial layers for five critical factors—recharge rate, regolith thickness, transmissivity, borehole success rate and static water level—through a multi-criteria analysis approach to rank groundwater development potential from the viewpoint of groundwater availability and accessibility. The weakness with this

approach concerns the reclassification of the geology of Ghana into two. The Voltaian supergroup was generalized as “sandstones”, while the Precambrian rocks were generalised as “weathered rocks”. This assumption is flawed because there are several rocks within the VSB and not only sandstone. Therefore, the groundwater potential will either be overestimated or underestimated. The most comprehensive groundwater potential map in Ghana prepared recently by Ó Dochartaigh et al. (2011) is an assessment by the British Geological Survey of the groundwater potential in Northern region prior to the implementation of UNICEF Integrated Water and Sanitation (IWASH) project. The map comprised the various geological units in Northern Region, attribute table indicating groundwater development potential and recommendations for appropriate development techniques. The distribution was not uniform because it focused mainly on the selected communities, which benefitted from the IWASH project.

In developing a groundwater potential map using multi-criteria analysis, there are several methods of combining thematic layers. The weighted overlay method used by Saraf and Chowdhury (1998) is recommended as a more robust approach. Forkuor et al. (2013) on their part used the fuzzy approach to standardize all the spatial layers into commensurate scales. While Gumma and Pavelic (2013) and Sander et al. (1996) used overlay method for combining the thematic layers to develop a siting methodology for the VSB. The efficacy of this method is based on the incorporation of human judgement in the analysis. It also takes into consideration the relative importance of each parameter. The most appropriate method for characterising groundwater system would be to combine the various

methods to get a comprehensive map. That approach would help in compensating for the limitations of the individual methods. The Voltaian sedimentary basin known generally to be highly heterogeneous hydrogeologically would require a holistic and comprehensive assessment to characterise the groundwater system as suggested by MacDonald et al. (2001).

Several researchers have employed sensitivity analysis to provide valuable information on the validity of suitability maps that have been developed (Gogu and Dassargues, 2000; Napolitano and Fabbri, 1996; Nwer, 2005). In Ghana, few researches apply sensitivity analysis to determine the reliability of their maps. Most sensitivity analyses carried out are with respect to numeral models that have been developed (Attandoh et al. 2013; Lutz et al. 2007).

CHAPTER THREE

RESEARCH METHODOLOGY

The methodology consists of a desk study, reconnaissance survey and field investigations and analysis of data.

3.1 Sources of Data

The data used in this research were from both primary and secondary sources. The secondary data was acquired from Community Water and Sanitation Agency (CWSA-Tamale), Water Resources Commission, Water Research Institute (WRI)-Accra, Catholic Relief Services, World Vision International, Terahydro Limited and Hydronomics Limited. The data include Geophysical survey reports, Geological logs of boreholes, geophysical wireline logs from a few boreholes, Pumping Test results and hydrochemistry data (for recharge estimate).

3.2 Desk Study

The desk study involved compiling and assessing the following data sets: topographic and geological maps, existing borehole information and previous hydrogeological work in the study area. The borehole data received from the organisations were sorted into usable (233 in Appendix 10 including the 10 project boreholes) and non-usable. For instance, borehole data without geographical coordinates were regarded non-usable and those which did not fall within the study area were discarded. For pumping test results, records of boreholes pumped for 6 hours or more were of prime interest. 67 data set were therefore classified as usable

data (Appendix 7) out of which 16 are primary data set (produced under this study). The purpose of conducting this desk study was to have a detailed overview about the available data and the hydrogeology of the study area. Attention was also on lineament patterns and fractures, the presence of suitable aquifers and their thickness, mean aquifer depth and the expected lithological sequences, among others.

3.3 Reconnaissance Survey

The main purpose of the reconnaissance survey was to locate target areas for geophysical investigations and also to identify existing boreholes for pumping test. It comprised an assessment of topography, geology, stratigraphy, structural features, water points and soil surveys to detect sufficiently permeable strata that by virtue of their relative elevation or depression, geological history and hydrology could be water bearing. Furthermore, social, logistical and accessibility considerations were also taken into account. The reconnaissance survey did also include setting out geophysical traverse lines in the selected target areas. Finally, communities that were earmarked for drilling of the 10 project monitoring boreholes were visited and opinion leaders were made to understand the scope of work to be carried out.

3.4 Field Investigation

This comprised the following activities for providing primary data under this study:

- Geophysical Survey
- Drilling and Construction

- Geophysical logging
- Pumping Test

3.4.1 Geophysical Survey

Geophysical techniques have long been used (since Wenner, 1915) to help in developing groundwater and various successes are recorded (Al-Shaibani, 2008; Chegbeleh et. al. 2014; Danielsen et al. 2007; Ewusi, 2006). However, for areas underlain by low permeability sediments such as the Nasia Basin, a comprehensive approach is required because of the low success rates in finding groundwater. In this study primary as well as secondary data from the three geophysical methods, frequency domain conductivity using Geonics EM34-3XL, Electrical Resistivity Tomography (ERT) and geophysical logging of boreholes were used to assist in the characterising the hydrogeology of the Nasia Basin.

3.4.1.1 Electromagnetic Survey (EM)

The purpose of using this method is 1) to identify structural features; 2) for mapping of the geology; 3) as well as for comparing the results with electrical resistivity. The EM34-3XL frequency domain ground conductivity meter was used for the electromagnetic profiling survey and is shown in Figure 3-1.

Figure 3 - 1: Image of Geonics EM34-3 system (Xia et al. 2001)

The Geonics EM34-3XL conductivity meter consists of a transmitter (Tx) and receiver (Rx) coils, a transmitter and receiver consoles (signal controller and measuring unit), reference cables (10 m, 20 m and 40 m) were used to determine terrain conductivity.

Two field campaigns were undertaken for the conductivity measurements. For the first campaign, profiles were conducted at 10 locations laying on two parallel traverses starting from the North of the study area (Gambaga massif of the Panabako formation and the Poubogou formation) to the south (the Bunya sandstone member), selected using the database of the HAP (EM campaign I). Based on preliminary results obtained from interpretation of geophysical borehole logs, the Bimbilla formation was “loosely” divided into three sub-sections (the upper or elder zone-A, the middle zone-B and the lower or younger zone-C). At

each of those six locations within the Bimbilla formation two parallel profiles with mutual distance of 100 m were conducted and in direction South-North thus perpendicular to the expected strike of the formation. This second EM field campaign (EM campaign II) was focused on areas prone to flooding in order to ensure sufficient water for small scale pilot irrigation schemes. The Electromagnetic equipment provides a direct measurement of apparent conductivity in the region of the measuring coil using the principle of electromagnetic induction. The equipment is operated in the Horizontal dipole (HD=vertical position of the coils by staying on the ground) as well as in the Vertical dipole modes (VD=horizontal position of the coils by staying on the ground). The depth of investigation is approximately 0.75 times coil separation in HD-mode and 1.5 times coil separation in VD-mode.

Accordingly, the depth of investigation (DOI) respectively for the HD-mode and VD-mode for the 3 applied coil separations is seen in Table 3.1.

Table 3.1: Depth of investigation at different coil-separations in HD-mode and VD-mode.

Coil separation:	10 m	20 m	40 m
DOI for HD-mode	7.5 m	15 m	30 m
DOI for VD-mode	15 m	30 m	60 m

Both campaigns were conducted by using the 10 m and the 40 m coil separation, which provides the conductivity of a volume of rock down to four different depth, thus 7.5 – 15 – 30 and 60 m. Some of the collected EM-profiles (secondary data) from other investigations were conducted by using the 20 m and the 40 m coil separation. As seen from Table 3.1 that approach provides only three different

investigation depth because the 20 m VD-mode and the 40 m HD-mode has same investigation depth.

Each of the 10 profiles on the first EM-campaign is 500-1000 m long traversing the various portions of the geological formations within the study area (Figure 3-2a) almost perpendicular to the general strike (E-W) of the formations. The 12 profiles at the 6 locations in the EM campaign II had lengths of 500 m.

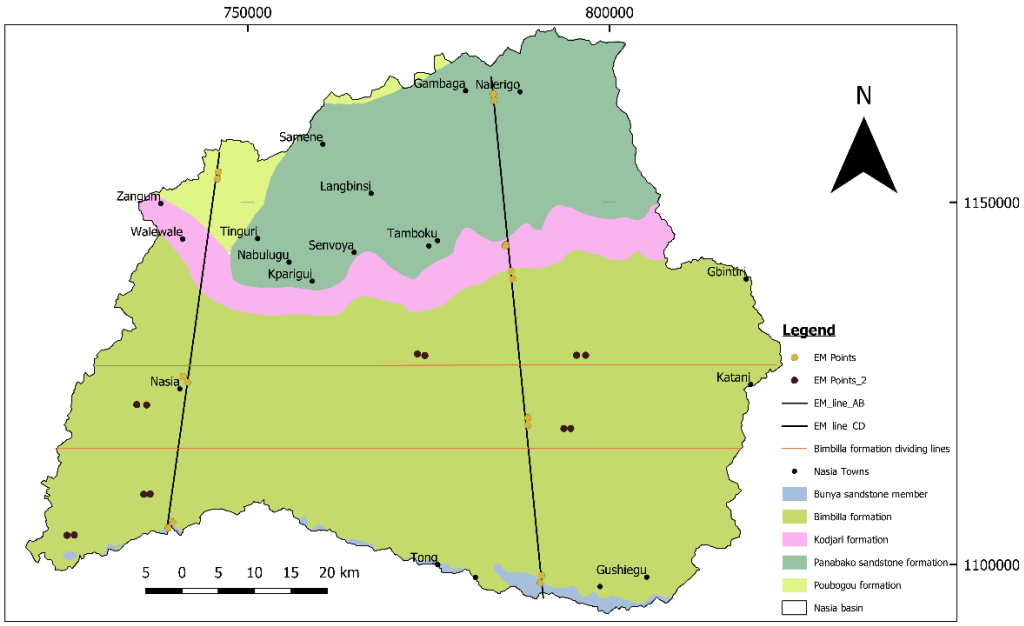

Figure 3 - 2a: A map showing the locations for the EM-points

The eastern traverse runs from the Panabako sandstone in the Gambaga massif into the Kodjari formation and further crossing the Bimbilla and finally ends in the Bunya Sandstone member. The western traverse runs from the Poubogou

Formation into the Kodjari and further through Bimbila and finally ends in the Bunya sandstone member of the Bimbilla formation at Pigu.

For each of the measurements, the transmitter operator stopped at the measurement station; the receiver operator moved the receiver coil backwards or forward until the meter indicated correct inter coil spacing and conductivity was then recorded from the second meter. The equipment was nulled at every site and after changing each cable and occasionally checking the battery level to ensure that the battery indicator was greater than 4.5. For accurate measurement with the EM instrument, alignment of coils is very important during measurement of ground conductivity. McNeil (1980) opines that measurement can be very sensitive to misalignment especially with the vertical mode. Measurements sensitive to human made structures which are conductive such as metallic objects, high electric cable, metallic roofing sheets among were avoided. The coils were also maintained in their respective coplanar modes of operation as much as possible at all times to reduce errors and for accurate measurements.

The processed EM-data from campaign I and II are to be seen in Appendix 1.

3.4.1.2 Electrical Resistivity Tomography (ERT)

The ABEM Terrameter LS which employs the static Lund automatic Electrical Resistivity Imaging (ERI) system was used for the resistivity survey. A number of electrodes were secured into the ground and connected by electrode cables. A switching unit connected to a computer controls the transmission of current into the

ground through two of the electrodes, while potentials are measured over other electrode pairs (Dahlin and Zhou, 2004). The electrode spacing of 20 m was selected and the traverse was between 400 m to 800 m for each selected point.

To drill the monitoring boreholes, 10 locations were selected for conducting the geophysical survey. These locations were deliberately selected on advice from the Danish counterpart GEUS on basis of the preliminary processing and interpretation of the AirTem data, and also with the view of having an even distribution of the boreholes within the study area. In addition to these 10 monitoring boreholes, 60 successful boreholes fitted with hand pumps were identified in the study area, and were calibrated and electrical resistivity measurements recorded. The locations of these ERT points is shown in Figure 3-4b.

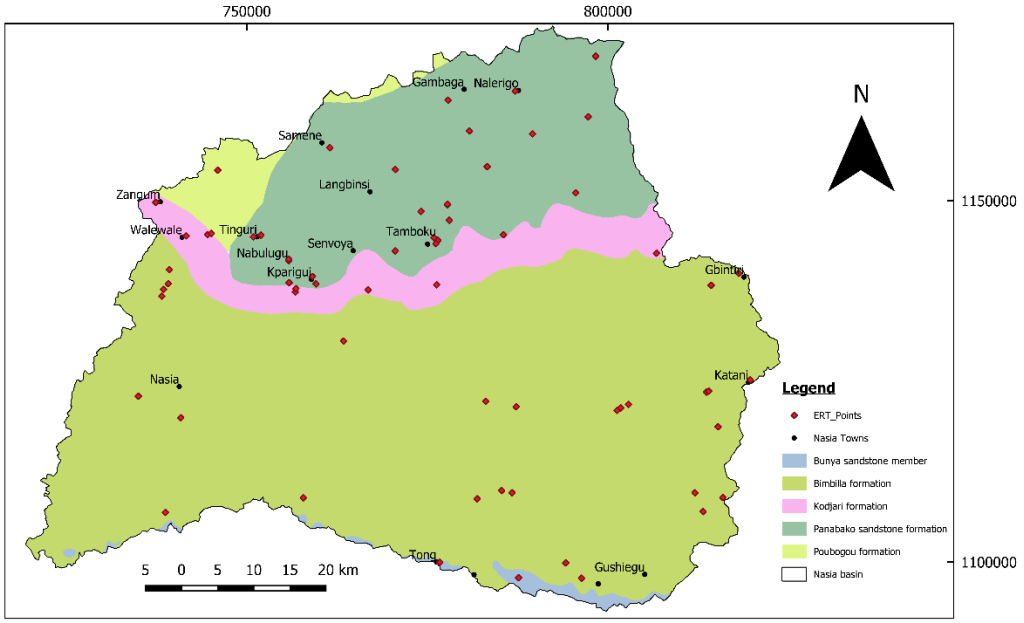

Figure 3-2b: A map showing the locations of the ERT points

The ERT was conducted between the EM-34-3 traverse lines covering a length of 800 m. A multi-method configuration involving Schlumberger, Wenner, Gradient 8 and Dipole-Dipole Array were used. The purpose of combining the different electrode configurations was to: 1) validate the results, 2) establish which configuration was suitable for the prevailing geological framework, 3) provide some level of confidence to support the decision making in selecting suitable drilling points. This is in line with the procedure carried out by Dahlin and Zhou (2004). The ERT-data set are to be seen in Appendix 2.

3.4.2 Drilling and Construction

Hydronomics Ltd, a private drilling company was engaged to drill the 10 boreholes to augment the data in the study area. In addition, 15 shallow wells selected across the study area with a view of having an even distribution were drilled through the weathered zone. The purpose was to determine the thickness as well as collect samples to estimate hydraulic conductivity of the weathered zone. The depth for these 15 shallow wells were up to a maximum of 15 m. The air-flush rotary method with rock-roller bits was used through the weathered zone and for the 10 deep monitoring boreholes the down-the-hole hammer bit was used for penetrating further into the underlying bedrock.

The necessary hydrogeological information such as estimation of the airlift yield, potential fracture zones and water strike zones as well as the lithology were captured during the course of the drilling.

The Drillers report from the 10 deep boreholes as well as from the 15 shallow boreholes are to be seen in Appendix 4. Drilling record of existing boreholes (secondary data-Appendix 4) were used in estimating water strike zones.

3.4.3 Pumping Test

The pumping test was conducted only on six of the 10 monitoring boreholes drilled under this project because the remaining four did not have sufficient yield (dry or nearly dry). In addition to that, 10 existing boreholes fitted with hand pumps were selected and pump tested. These are boreholes that have data on geophysical survey and geological logs. Prior to the pumping test exercise, all pump heads were removed and care was taken not to drop the pump cylinder and riser pipes into the wells. The depth of the boreholes was measured using a calibrated rope tied to a heavy metal. The discharge rate was estimated during the pumping test.

The duration of pumping for the boreholes varied from 6 hrs to 24 hrs for the constant discharge and between 3 to 6 hrs for recovery test. The procedure for conducting both the constant discharge and recovery test were in line with the steps recommended by ICRC (2011) and MacDonald et al. (2005).

3.4.4 Geophysical logging

Wireline-logging was done after drilling of the 10 project monitoring wells in order to obtain a detailed lithological profile at each borehole, and to establish knowledge on the resistivity of the different formations. Furthermore, to validate the results and the interpretation of the respective ERT-profile. Wireline logging data from additional 7 boreholes previously drilled and used for monitoring by Water

Resources Commission under the Hydrogeological Assessment Project were made available and included in this study. All the geophysical borehole logging was conducted by WRI using Robertson Geo wireline logging equipment and processed with Viewlog 4.0 from EarthFX (Klitten and Agyekum, 2019).

In conducting the geophysical logging, Klitten and Agyekum (2019) indicated that the accessible depth section of each borehole was logged at 1 cm intervals using a set of five digital geologging tools (probes), Robertson's (RG) Micrologger, a Winch, and a Computer. The logging tools used are: 1) Focused Guard (GLOG) tool to control the casing and screen setting and obtain information about the formation resistivity within the close vicinity of open-constructed borehole sections, 2). Dual Induction (DUIN) tool was undertaken to obtain information on formation conductivity, which is transformed into formation resistivity, even through plastic lined casings where the GLOG tool does not provide valid data, 3) Fluid Temperature and Conductivity (TCGS) logging tool conducted under static water condition to determine the log profile of groundwater salinity and temperature and 4) finally, High Resolution Impeller flowmeter (HRFM) logging tool to determine inflow rates in boreholes with yields higher than 20 lpm. The methodology used is in line with Klitten & Agyekum (2008), Agyekum & Klitten (2008), Agyekum (2009), and Agyekum et al. (2013) , all with reference to work on the Voltaian sedimentary rocks.

The processed wireline logging data from each of the 17 boreholes and the belonging interpretation are presented as comprehensive logging-sheets in Appendix 3.

3.5 Data Processing and Analysis

Prior to analysis, the data was manually inspected for quality assurance.

3.5.1 Geophysical survey (EM34, ERT and borehole wireline logging)

The interpretation of EM34 data is generally qualitative although their inversions can be done for layered models using some commercial programs (Inman, 1975). For this study, the results of the measured apparent conductivity in both horizontal dipole (HD) and vertical dipole (VD) modes were plotted on Microsoft Excel program against the station distance to give the measured conductivity. The response curves from both dipole modes were compared to determine anomalous regions. The criteria used for interpretation are in line with Chegbeleh et al. (2014) which is identifying possible gradual crossover and a gradual peak. Therefore, areas of interest for the interpretation were the crossovers which are locations where the VD response values exceeded the HD response values and also gradual peaks and sinks. These regions were used in mapping the geology based on the corresponding apparent conductivity.

The resistivity data (ERT-profiles) at the 10 DWVP boreholes were processed with the RES2DINV version 3.5 (Loke, 2001), the raw data (the *dat*-file) is read into the software and edited by using the option 'change first electrode location' to

reposition the first electrode at starting zero (0) mark of the profile line. The elevation information was also entered for each of the profile line in the inversion files and saved while the text files *.txt* were saved for documentation. The approaches described by Loke and Dahlin (2002) and Loke et al. (2003) were used. The inversion method works by reducing the difference between the measured resistivities and the calculated response of the estimated model through a number of iterations, until satisfactory agreement between model response and field data is reached or no further improvement is possible (Dahlin 2001). This is usually represented in the value of the root mean square (RMS) error. The computer program automatically subdivides the subsurface into a number of blocks, and then uses a least-squares inversion scheme to determine the appropriate resistivity value for each block. The underlying model is a two-dimensional finite element model that accounts for topography.

For all the 70 ERT-profiles, the processing was later repeated under study stay in Denmark by using the software "Aarhus Workbench" (AWB) version 5.8.0.8 (Auken et al. 2009), which is a dedicated program package for management, processing, inversion, and visualization of geophysical data and models in a fully-featured GIS environment. The dat-file was downloaded from the console of the ERT set-up into the AWB software. The dat-file is the main data file containing the measured DC and in order to ensure that the profile lines are correctly positioned on the GIS, an *ewp* file containing the coordinates was also created to help specify a coordinate system. A file was also created to supply the topography. It has a processing feature which shows the data points at each focus depth along with

pseudo section and electrode positions. The smooth method of inversion was carried out, and a priori information such as resistivity and layer thickness from geophysical logging of some of the boreholes was used to constrain the inversion. Compared with other 2D software which usually truncates the data around the start and end portion of the profile, this software is rather able to show the entire probing depth of the profile. The resulting resistivity 2D-profiles from the AWB-processing are shown in Appendix 2, however only 50 data-set were validated as being acceptable for AWB-processing.

The hydrogeological interpretation of the geophysical data as presented in Chapter 4 was based on the resultant 2D modeled images. The geophysical signatures were estimated from the resistivity values and the depths of penetration detected from the various profiles supported by knowledge about the lithological setting of the place from the borehole records. Priority was given to the AWB-processed images (profiles).

For the geophysical logging, the software used for processing the data and presentation of the results is ViewLog 4.0 from EarthFX (Klitten & Agyekum, 2019). It is a program designed for presentation of geophysical log data with geological logs and interpretations primarily for use in the non-petroleum sectors. The program was used to display conductivity log, resistivity log, gamma log, flow log and fluid conductivity & temperature logs. Detailed studies of the natural gamma enabled the correlation of the geophysical logs with the lithostratigraphic units within the study area. Analysis of the results from geophysical logging has in

this study focused on extracting resistivity of the encountered geological formations and comparing these with the ERT results and geologic logs.

The general geophysical parameters of the various geological formation of the rocks was determined for the Nasia Basin based on comparison of the responses recorded from the three geophysical methods.

3.5.2 Analysis of pumping test results

In analysing pumping test data for aquifer parameters such as transmissivity, the Theis (1935) analytical model is the most common method that is used with specific assumptions (Kruseman and de Ridder, 1971). The Cooper-Jacob (1946) model has been suggested by Halford et al. (2006) to be the most convenient for single well tests. Acheampong and Hess (1998) for instance used this method in estimating aquifer parameters for the southern Voltaian Sedimentary Basin of Ghana. According to Todd (1959) and Acheampong and Hess (1998), the method was originally derived for isotropic porous media but aquifers with secondary permeability such as the study area exhibit homogeneous characteristics when sufficiently large volumes of water are considered and as such the Cooper-Jacob (1946) method could be used. Researchers such as Yidana et al. (2011) suggest that results from such tests produce reasonable hydraulic characteristics of aquifers for basin characterization.

Halford et al. (2006) indicate that the Cooper-Jacob (1946) method requires that pumping should be done for a reasonable length of time at a sustained rate for transient conditions to be induced. Since the pumping test was conducted without

an observation borehole, only drawdown data from the pumped well is available. Drawdown is not only caused by the aquifer conditions, but also caused by "well loss" such as turbulent water flow which results in additional drawdown of the water level. To minimise the effect of such "well loss", the early portions (1st log cycle) of the drawdown-time curve data is not used for the analysis (Acheampong and Hess, 1998; Darko, 2001).

For this study, out of 67 pumping test data-set available, 41 boreholes were pumped at six (6) hours with three (3) hour recovery. These 41 data-set could not be used for the transmissivity calculation because of the short duration of pumping but were used for calculating specific capacity. The remaining test data from 26 boreholes were pumped between 12 hrs-24 hrs with a few pumped for 9 hrs and this pumping duration was considered to be significant enough to induce transient conditions as such have met the Cooper-Jacob (1946) method assumptions.

The data from the pumping test was presented in Micosoft Excel and the drawdown and residual drawdown were estimated by subtracting the static water level from the dynamic water level. Semi-logarithmic graphs were constructed by plotting drawdown on the vertical axis against time in minutes on horizontal logarithmic axis representing the constant discharge curve for each data-set. The recovery data were similarly constructed by plotting the residual drawdown against logarithm of time in minutes after pump stop.

Transmissivity (T) was therefore estimated on drawdown data as well as on recovery data for the 26 boreholes based on the Cooper-Jacob (1946) method as shown in equation 3.1

$$T = \frac{0.183Q}{\triangle S} \quad 3.1$$

$\triangle$S is the drawdown per log cycle in m, Q is discharge rate in m^3/d and T in m^2/d

Since the pumping duration for all the 67 data-set was at least 6 hours, the **Specific Capacity (SC)** was calculated from drawdown after 360 minutes of pumping using equation 3.2.

$$SC = Q/S \quad 3.2$$

where Q is the discharge rate in m^3/d and S is the drawdown after 360 minutes of pumping.

3.5.3 Estimation of Recharge

Recharge is an essential parameter in determining groundwater potential as suggested by several researchers (Forkuor et al. 2013; Macdonald et al. 2016; MacDonald et al. 2001). Recharge estimates at 72 water points were obtained from Addai et al. (2016) and shown in Appendix 8. They are based on Chloride Mass Balance method, thus the recharge Rg = (Clpr /Clgw)*Pr – where Clpr is the Chloride content in precipitation, Clgw is te Chloride content in groundwater, and Pr is the precipitation. This method was used due to its apparent conservative nature based on an assumption that, the only source of chloride in groundwater system comes from precipitation and that chloride does not react or decay in the process of reaching the groundwater system (Yidana and Koffie, 2013). Researchers such as Carrier et al. (2008) have used this method due to its simplicity in design.

3.5.4 Geostatistical Analysis

For the present study, the available transmissivity estimates from 26 boreholes is not sufficient to characterise the hydrogeology of the area. Therefore, two geostatistical methods were used to estimate the transmissivity from specific capacity and the best approach was adopted. First and foremost, an empirical relationship in the form of regression analysis between transmissivity and specific capacity was established for two scenarios; a relationship between transmissivity for the entire Nasia Basin (based on the 26 boreholes) and another which is formation-specific (thus based on a rather low number of boreholes within each formation). Based on the results of the regression analysis, a comparison was then made between these two scenarios to determine the major factors that control groundwater within this highly heterogeneous environment. Even though the data for transmissivity is limited and would affect the purpose of the comparison, this approach could be built upon by future researchers with abundant data to characterise aquifers. The software used for the regression analysis is IBM SPSS Statistics version 20 (IBM Corp. 2011).

Secondly because of the abundance of specific capacity data, transmissivity was estimated using cokriging as recommended by Aboufirassi and Mariño (1984). The software used is GS^+ version 10 (Robertson, 2008). 222 specific capacity data were used as secondary variate and 26 transmissivity estimated using Cooper-Jacob (1946) method as the primary variate. Structural analysis using variograms was conducted prior to kriging and cokriging for all the parameters following procedure

adopted by (Aboufirassi and Mariño, 1984; Isaaks and Srivastava, 1989; Razack and Lasm, 2006).

Interpolated maps using kriging were developed to estimate spatial distribution of depth, specific capacity, yield, static water level, regolith thickness, recharge and hydraulic conductivity at unsampled locations in the study area. The maps of the respective parameters were produced using GS+ version 10 (Robertson, 2008).

Graphical representations of the dataset (histograms and box and whiskers) were constructed using SPSS for easy examination of parameters. The histogram was also used to check both the skewness and kurtosis of the dataset. Descriptive statistics such as central tendencies (mean, median and mode) and standard deviation were also estimated using the IBM SPSS Statistics software. Normal distribution and homoscedasticity are key requirements of optimal multivariate statistical analyses. All the parameters in the dataset did not meet the requirement for normal distribution which is very common for most earth science data, therefore they were transformed and also back transformed using the function within the GS+ version 10 (Robertson, 2008) to obtain a normal distribution since this is an essential requirement for optimal geostatistical modeling (Salifu et al. 2013; Yidana et al. 2011). This was followed by construction of experimental variograms and cross-variogram for the selection of an appropriate theoretical model. The sill, nugget and range were determined to help in explaining the variability of the parameters. The final step was validating the model and creation of an interpolated map of the respective parameters.

3.6 Remote Sensing and Geographical Information System

3.6.1 Satellite Imagery and Digital Elevation Model (DEM)

Two satellite data, Advanced Spaceborne Thermal Emission and Reflection Radiometer (ASTER) Digital Elevation Model (DEM) were obtained from United States Geological Survey (USGS) Earth Explorer website (earthexplorer.usgs.gov). Figure 3-4 is the model builder using ArcGIS 10.6 (ESRI, 2011) for the estimation of slope and drainage density layers.

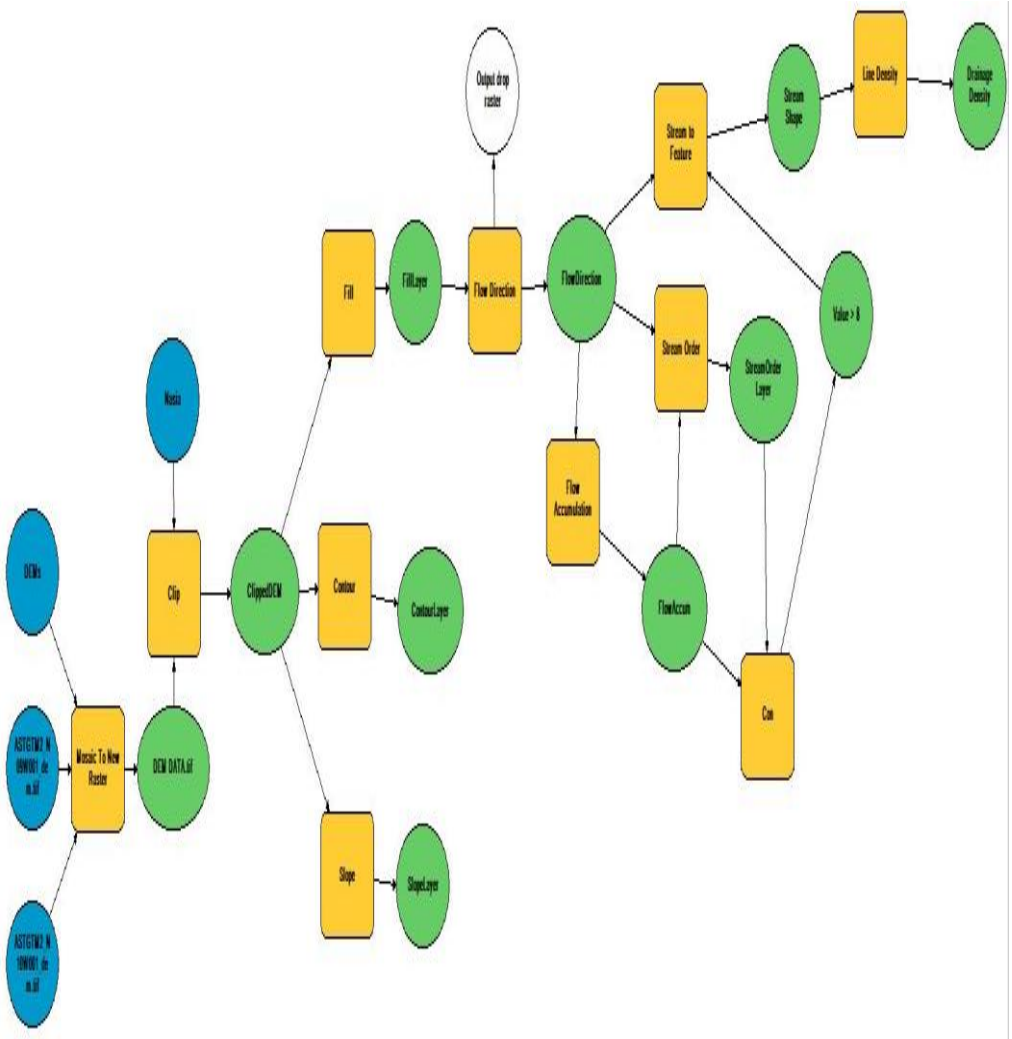

Figure 3 - 3: Model builder for remote sensing

3.6.2 *Slope and Drainage Density*

The slope was also derived from the DEM image using the slope tool in the spatial analyst tool in ArcGIS 10.6 (ESRI, 2011).

Drainage density is the total length of all the streams and rivers in a drainage basin divided by the total area of the drainage basin (Pradhan and Youssef, 2010). The drainage analysis involves various steps to arrive at drainage density for the study area. The methodology used by Seidu (2017) was adopted for the analysis by filling in all sinks in the DEM of the Nasia Basin using the fill tool in ArcGIS 10.6 (ESRI, 2011). The flow direction tool was used to create a raster data from the DEM to show all the direction that water flows on the surface. Other tools used are the stream to feature, stream order together with the conditional tool to create line density and subsequently the drainage density. These steps are illustrated in Figure 3.4.

3.6.3 *Lineament density*

The lineaments are linear features on the Earth's surface that reflect a general surface expression of underground fractures (Pradhan and Youssef, 2010). The lineament data for the study area was acquired from Water Resources Commission under the Hydrogeological Assessment Project (HAP) funded by the Canadian International Development Agency (CIDA) and also from a digitized map from the Ghana National Petroleum Commission. These two lineament files were converted into shapefiles and merged in ArcGIS 10.6 (ESRI, 2011). The merged lineament shapefile was then converted to a raster image to be used for multi criteria analysis.

3.7 Groundwater Potential Map

Several researchers (Forkuor et al. 2013; Chandra et al. 2019; Gumma and Pavelic, 2013) have integrated Remote Sensing (RS) and Geographical Information System (GIS) to produce groundwater potential map in an effort to manage groundwater resources.

For the Nasia Basin, the files of the parameters used for the potential map were exported from GS+ to ArcGIS 10.6. The eight parameters are well depth, depth to static water level, regolith thickness, recharge, transmissivity, terrain slope, drainage density and lineament density. The next step was to mask these parameters with the shapefile of the Nasia Basin. After masking the parameters, they were converted to raster images for standardization. The raster images for each of the parameters were reclassified due to their disparate scales to make any combination meaningful (Forkuor et al. 2013).

3.7.1 Weighted Overlay Analysis

This is a combined analysis of multiclass maps and has the advantage of integrating human judgment based on experience about the local environment. No standard scale is required and it considers the relative importance of each parameter and the classes it belongs to (Saraf and Choudhury, 1998).

Weights were assigned to the various parameters based on a probably subjective valuation of their contribution and influence on groundwater potential within the study. Studies by Forkuor et al. 2013; Gumma and Pavelic, 2013; and Nsiah et al. (2018) served as a guide in assigning the weights to the parameters. The thematic

maps were overlaid using the overlay tool in Arc GIS 10.6 to produce a comprehensive groundwater potential map. Figure 3.5 is a flowchart illustrating the steps followed in producing the groundwater potential map for the Nasia Basin.

3.7.2 Classification of Groundwater Potential Map

The groundwater potential was classified into five zones. This classification is based on the probability of each zone having a high yielding to low yielding potential based on the combination of the various thematic layers. The zones are as follows: (a) very poor (b) poor (c) moderate (d) good, and (e) very good.

3.7.3 Validation of Groundwater Potential Map

The reliability of the groundwater potential map was tested against measured borehole yields and also locations of dry boreholes. A number of researchers have used yield as an independent parameter in validating potential maps that have been developed (Forkuor et al. 2013; Gumma and Pavelic 2013).

3.7.4 Sensitivity Analysis

Sensitivity analysis is used to determine the influence of different criteria weights on the spatial pattern of a suitability map (Nwer, 2005). For this research, two scenarios to test the influence of the weights assigned to the individual parameters on the final groundwater potential map was performed. The approach used by Napolitano and Fabbri (1996) was employed to test the sensitivity of the map.

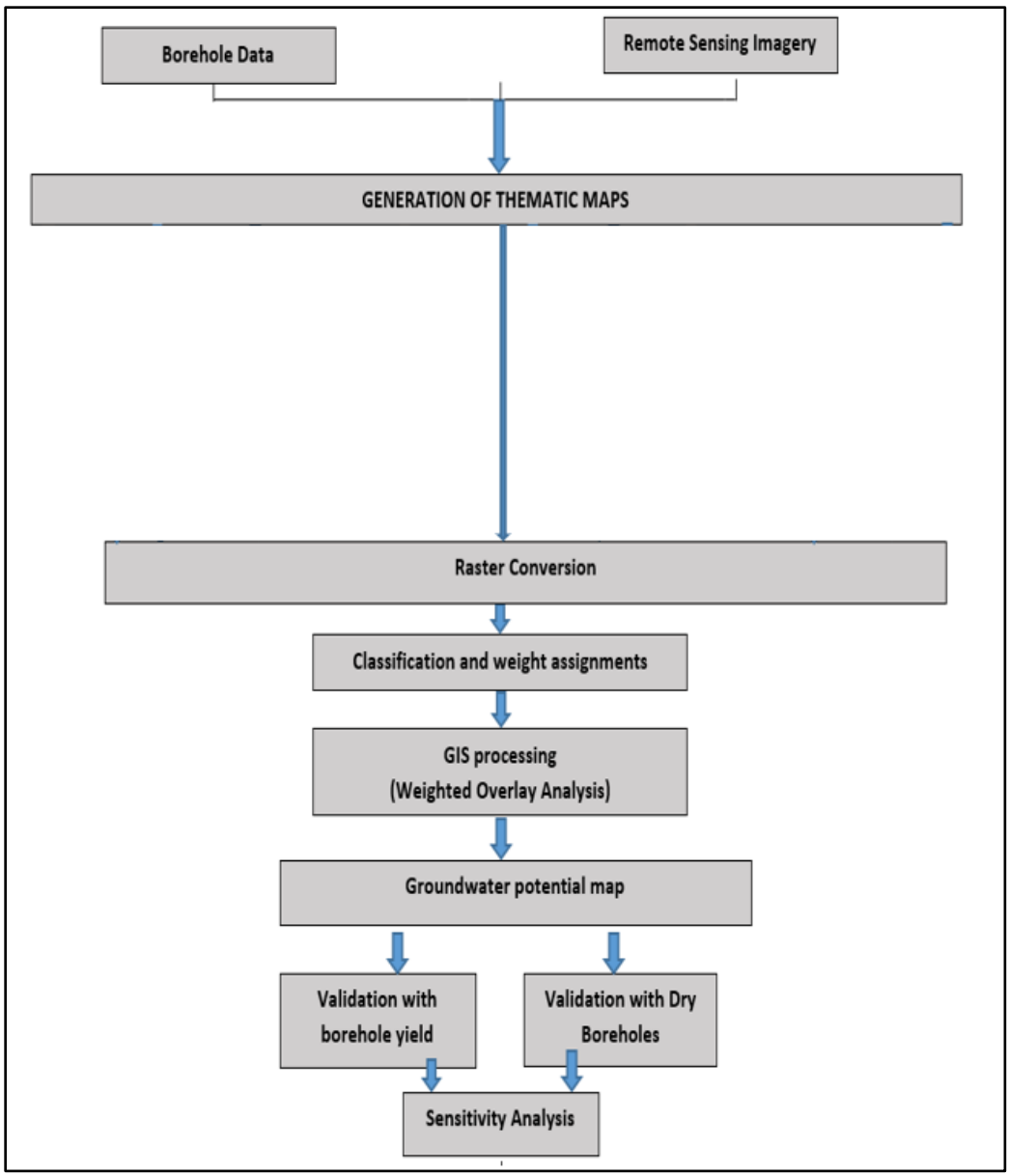

Figure 3 - 4: Flow chart for developing groundwater potential map

CHAPTER FOUR

RESULTS AND DISCUSSION

4.1 Geophysical Investigations

The results of geophysical investigations are discussed based on two broad categories. The first approach evaluates the current method used by hydrogeologists in interpreting geophysical results within the Nasia Basin. The second approach seeks to determine the most appropriate method for groundwater exploration in view of the challenges faced with groundwater development in the study area. It must be noted that not all the geophysical results in the communities are presented in this chapter but selected results in each of the geological formations. Results of all primary as well as most of the secondary geophysical investigations using the electromagnetic method, electrical resistivity tomography (ERT) and geophysical wireline logging are included as Appendices 1, 2 and 3 respectively.

4.1.1 Evaluation of current hydrogeological interpretation method of geophysical investigations

The electrical resistivity method is the most widely used method for groundwater prospecting in Ghana and has produced good results mainly for the crystalline basement. Within the VSB however, the results have been appalling for many reasons, example wrong interpretation of geophysical results. Figure 4.1a shows the electrical resistivity imaging (ERT-profile) at borehole DWVP09 and with traverse length of 800 m. Figure 4.1a illustrates an instance where wrong interpretation has resulted in a dry borehole. The ERT results from Figure 4.1a

indicates that station 370 with the pointed arrow was the point selected for drilling. The profile at the drilling point essentially shows a three-layer structure. A 20 m thick high resistivity top layer (>3500 Ωm) overlies a 40 m conductive layer (20 Ωm), which in turn overlies a moderately resistive layer (80 Ωm). The root mean squared (RMS) error of electrical resistivity from the profile is 41.7%. Borehole DWVP09 is situated within the Panabako sandstone formation with the upper portion of the profile interpreted as laterite and dry weathered sandstone accounting for the high resistivity recorded. The second layer at point 370 m was interpreted as a possible wet fractured/saturated sandstone layer because the resistivity was very low, approximately 20 Ωm.

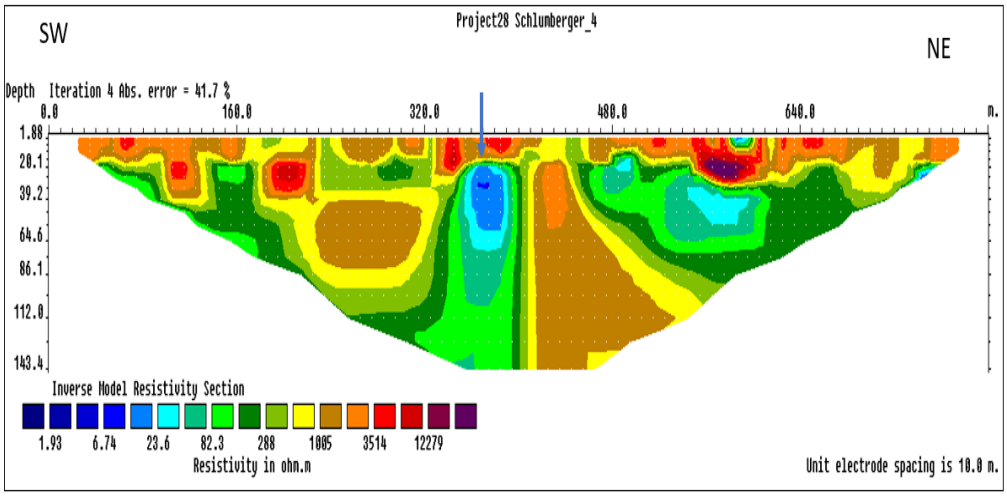

Figure 4 - 1a: ERT-profile (RES2DINV processed) at DWVP09 Samene, drilled at station 370.

This interpretation is consistent with the observations of Ewusi et al. (2009) who indicate that within the sandstone formation, resistivities below 70 Ωm should be

targeted. Despite the low resistivity interpreted as fractures within the bedrock, the drilling was unsuccessful with borehole yield of 4 lpm which is below the minimum required yield of 10 lpm for even a hand pump. This indicates that the geological environment is complex as such the groundwater exploration must be based on a sound understanding of the geology and proper interpretation of the geophysical results (Mainoo et al. 2019).

Another instance that explains the wrong interpretation of geophysical results is illustrated by the reliance on the root mean squared (RMS) error after iterations. The RMS error is the difference between the calculated and measured apparent resistivity values as a result of adjustment made to the resistivity of the model blocks subject to the smoothness constraints used. The aim is to obtain a model with the lowest possible RMS error. However, that model can sometimes show large and unrealistic variations in the resistivity values thereby not being the most probable model from a geological perspective. Figure 4.1b shows a 2 D electrical resistivity profile at borehole DWVP02 similarly located within the Panabako sandstone of the Voltaian supergroup. The borehole was drilled at station 410 m (with the pointed arrow) and the root mean squared error of electrical resistivity values is 42.8%. The results show three sections, a 10 m thin upper layer with very high resistivity (>2000 Ωm) overlying a low resistivity layer (<64 Ωm) but only to 55 m depth followed by high resistivity (>5000 Ωm). The upper layer was interpreted as dry weathered sandstone followed by wet fractured layer with low resistivity and the high resistive layer beyond 55 m as the fresh sandstone bedrock.

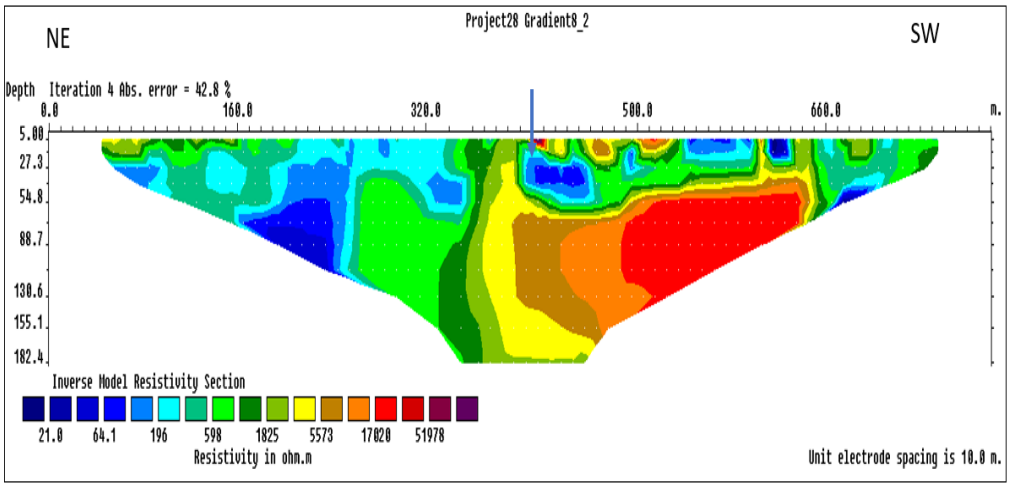

Figure 4 - 1b: ERT-profile (RES2DINV processed) at DWVP02 Tamboku, drilled at station 410.

Considering the high value of RMS error for this profile, (42.8%), researchers such Ashraf et al. (2018) and Loke, et. al. (2003) have advocated for a rejection of the model if RMS error exceeds a threshold of 5% because according to them it indicates an unacceptable fit. This means the model badly represents the measured apparent resistivities. However, after the drilling and pumping for 24 hrs, a yield of 132 lpm was recorded and with a final drawdown of 6 m only. It is noticeable on the wireline flow-log seen on Figure 4-1c, that both the two water bearing fractures are located in the boundary between a low resistivity and a high resistivity bed which is the boundary between two different lithological units. Irrespective of the high RMS of the processed ERT-profile, there is a relatively good fit to the actual resistivities and their variation towards depth on the wireline logs seen on Figure 4-1c.

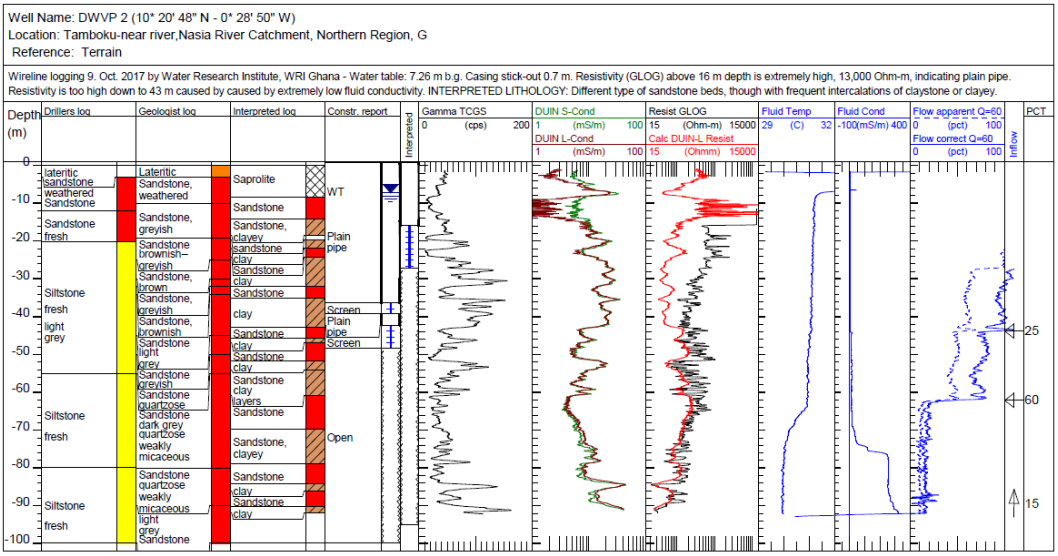

Figure 4-1c: Geophysical wireline logs of borehole DWVP 02 Tamboku, drilled at ERT station 410.

The shifts from high resistivity (>2000 Ωm) to low resistivity (<64 Ωm) at 10 m depth followed by again high resistivity (>5000 Ωm) on the ERT-profile are seen on the Calc. Resistivity-log at respectively 14 m and 44 m depth. Furthermore, the resistivity level on the latter fits very well to the level of the two upper layers on the ERT-profile, whereas the resistivity below 44 m depth on the wireline-log is 100-500 Ωm, thus far much lower than the high resistivity (>5000 Ωm) at greater depth on the ERT-profile.

This outcome of the ERT-profile at borehole DWVP02 contradicts that of Figure 4.1a because both ERT-profiles have high values for RMS error, both boreholes were drilled in a low resistivity zone and in the same geological formation. This result clearly indicates the complex nature of the hydrogeology and implies there

are other controlling factors that should be considered when exploring for groundwater.

4.1.2 Development of a more appropriate groundwater exploration method within the various geological formations

Researchers such as Chegbeleh et al. (2014), Ewusi et al. (2009) and Menyeh et al. (2005) have provided techniques of improving the location of targets for water drilling in Ghana or provided methods of interpreting geophysical results for groundwater exploration. Though few successes have been recorded from some of these approaches, a lot needs to be done in a more holistic and scientific manner. For instance, Chegbeleh et al. (2014) talks about the ability of the EM equipment to detect fractured zones and for delineation of geological features, and also incorporating knowledge about local geology and other hydrogeological factors in interpretation. Comte et al. (2012), Khalil et al. (2012) and Van Dam (2010) have indicated that using more than one geophysical method enhances data interpretation and better results are obtained.

The results of the geophysical investigations are discussed with respect to the geological formations within the two main geological groups (Bombouaka and Oti/Pendjari) in the study area. An integrated approach is applied to characterise the aquifers for the respective formations. The results of the processing of an ERT-profile in terms of vertical distribution of resistivity like in the previous section (4.1.1) has been validated by comparison to the wireline resistivity log in the borehole drilled on basis of interpretation of the ERT-profile. In situations where

there are EM34-profiles at the same location or in close proximity, it has been included in the comparison.

The ERT is expected to be useful for hydrogeological investigations as it is sensitive to the aquifer lithology (clay mineral content), the pore-water content and pore-water mineralization; it allows the spatial distribution of these important hydrogeological features to be characterized (Fetter 1988). However, differentiating among these features is difficult on the basis of the ERT results alone. Knowledge from wireline logs on resistivity of the actual geological formation aids in the processing and interpretation of ERT-data and EM34-data. Therefore, through coupling ERT with other methods of investigation or datasets this difficulty is resolved.

4.1.2.1 Bombouaka Group

There are two geological formations that fall within the Bombouaka group in the Nasia Basin, the Poubogou formation and the Panabako sandstone formation as seen in Figure 4.2 and in addition, the locations of boreholes in the Bombouaka Group with the respective geophysical data discussed in this chapter are shown.

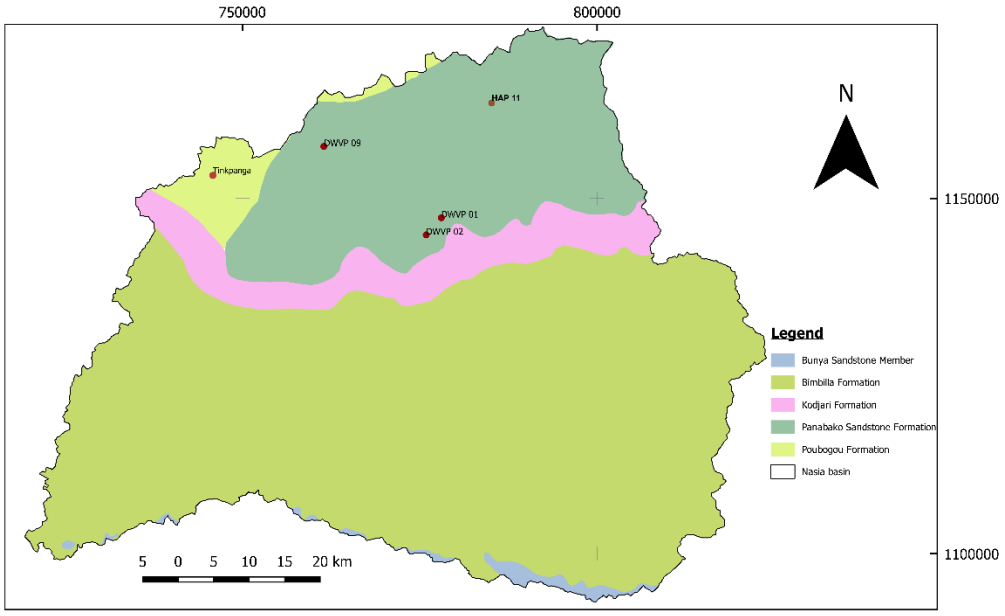

Figure 4.2: A geological map showing the locations of DWVP09-DWVP02-Tenkpanga-DWVP01-HAP11

4.1.2.1.1 Poubogou Formation

The Poubogou Formation forms a small portion of the basin and is made up of green-grey, micaceous mudstones and siltstones with intercalations of arenaceous and argillaceous material (Carney et al. 2010).

The thin intercalations of siltstone and fine-grained sandstone according to Ayite et al. (2008), are typically planar bedded, with sharp top-surfaces and undulatory, slightly channelized bases which in places show spectacular ball-and-pillow load structures.

Figure 4.2a shows results from the electromagnetic (EM) profiling measurements located at Tenkpanga (from campaign I) in both horizontal dipole (HD) and vertical dipole (VD) modes plotted against station distance. The conductivity measurements

in both modes are conducted by using the 20 m and 40 m coil separation, thus obtaining depth of investigation 15 m and 30 m as well as 30 m and 60 m respectively. Two sections of contrasting conductivity are visible; from SSW a high conductivity is recorded on both the 20 m and 40 m coils (0 to about st. 600 m) towards NNE is juxtaposed to a relatively low conductivity between 600 m and 1000 m with a stream flowing from NW towards SE. This stream is interpreted as a normal fracture network. Field observation confirms the presence of few sandstone outcrops towards north eastern part of the traverse. The high conductivity (unstable) between 0 and 600 m is probably associated with Poubogou mudstones and siltstones while the low conductivity towards NNE indicates presence of Panabako sandstone overlaying Poubogou formation.

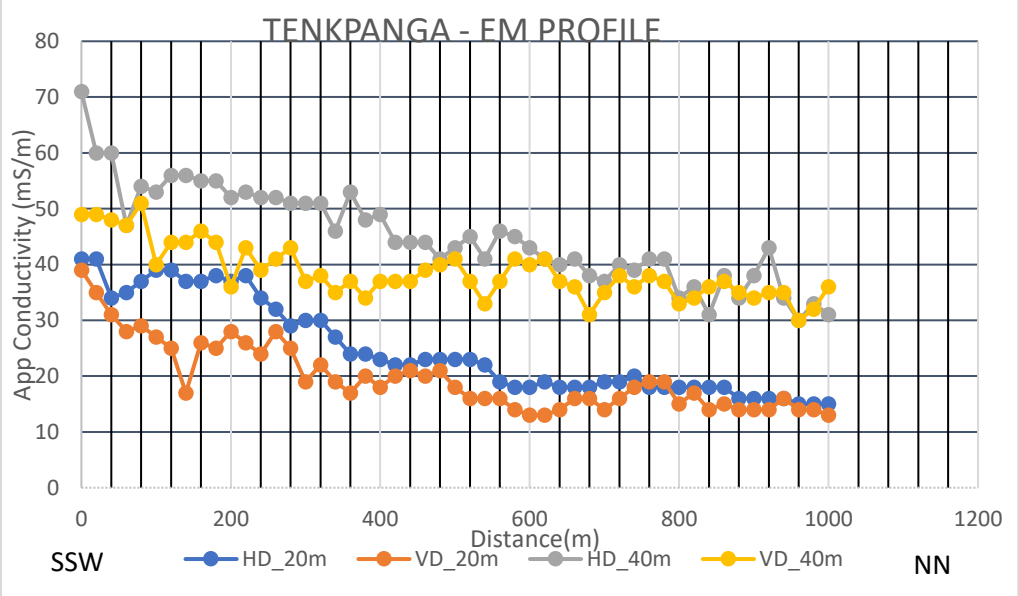

Figure 4 - 2 a: EM-34 profile of Tenkpanga in the Poubogou formation

Validation of the interpretation of the EM results was provided by an 800 m ERT profile undertaken along the same traverse. Figure 4-2b with the ERT profile after

AWB processing shows a general dip of layers towards NNE with increasing resistivity. The topmost layer (about 10 m) shows high resistivity which could represent the hard-lateritic cover and dry weathered materials. That fits well with the lower conductivity at 20 m coil separation compared to 40 m coil separation on the EM-34 profile, Figure 4-2a. Two contrasting resistivities are also observed below the 10 m depth confirming the conductivity variation along the EM profile. A relatively low resistivity is recorded from the SSW direction towards a higher resistivity in the NNE direction. Even though the two methods show similar resistivity/conductivity variation along the traverse and with depth, it is worth to notice that the ERT-resistivity in general seems far too high compared to the resistivity elaborated from the EM-34 irrespective of the coil separation and HD/VD mode. The ERT-resistivity is higher than 1000 Ωm in the uppermost 20 m compared to EM-conductivity of 15-40 mS/m equal to 60-25 Ωm for coil 20 m separation and in both modes. For both modes but with 40 m coil separation the EM-conductivity 30-60 mS/m equal to 30-15 Ωm, thus similarly much lower that the ERT-resistivities below 20 m depth.

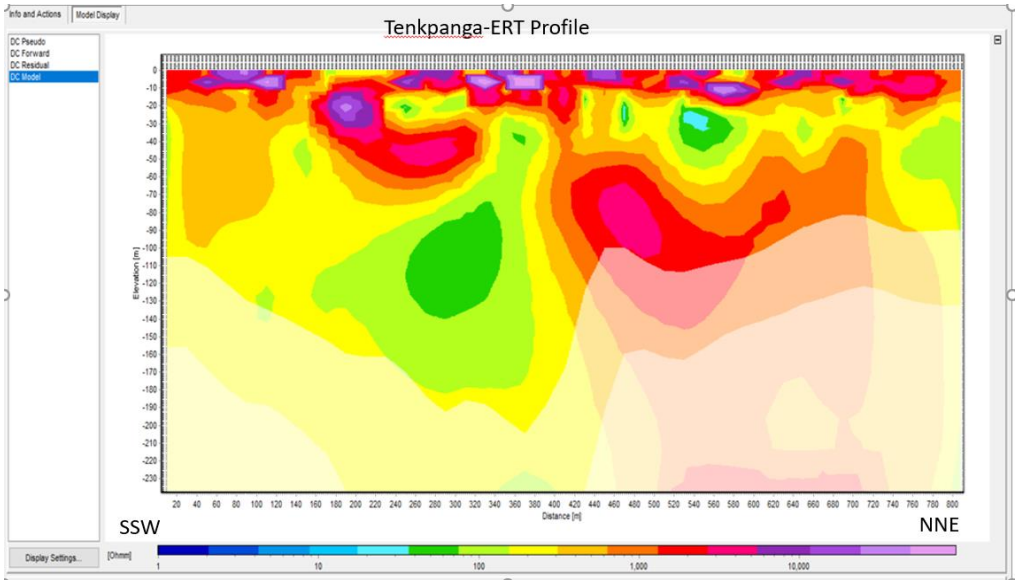

Figure 4 - 2 b: ERT profile of Tenkpanga in the Poubogou formation (AWB processed).

From the geophysical results for the Poubogou formation, it is evident that the traditional approach of interpreting geophysical results is inappropriate and may have contributed to the high number of unsuccessful boreholes within the VSB (Akudago et al. 2009).

When prospecting for groundwater within the Poubogou formation, the main factor to be considered is most probably the contact between the Poubogou mudstone/siltstones and the occasionally overlaying Panabako sandstones which is reflected on ERT-profiles by the contrasting resistivity and by contrasting conductivities on EM-profiles in deep exploration modes (HV-40 and VD-40). Groundwater targets are not necessarily the low resistivity or high resistivity units in the profile. Secondly, the direction of the profiles compared to the expected strike

of the formation, as well as of the dip and the trend of the resistivity distribution should also be considered.

4.1.2.1.2 Panabako Sandstone Formation

This formation is mainly made up of fine-to medium-grained sparsely feldspathic quartz-arenites and it covers the north-north eastern portion of the Nasia basin. Results from ERT, geophysical borehole logging and Electromagnetic profiling at two more locations within the Panabako sandstone formation have been used to analyse the option for characterising the aquifers for groundwater exploration within this formation. Figure 4.2 c and Figure 4.2 d show the ERT-profile (also included in Appendix 2) and geophysical wireline logs of DWVP01 located at Tamboku. The AWB-processed 800 m long ERT-profile (Figure 4.2 c) shows three layers, with the upper 10-15 m thick layer having from SW towards NE two contrasting resistivities- a high resistivity from SW (>500 Ωm), station 0 to 340 m then a relatively low resistivity (100-200) Ωm from station 340-m to 800-m. The upper layer overlies a 20-30 m thick relatively low resistive layer (60-100) Ωm which is followed by a high resistive bedrock (>500 Ωm). A subvertical structure (located approximately between st.340-420m) indicated by two contrasting resistivity from the upper layer to the bedrock is observed. The high resistivity at the upper layer is interpreted as dry weathered sandstone (or laterite) whereas the second layer with low resistivity is characteristic of fractured or intercalations of siltstone/clay.

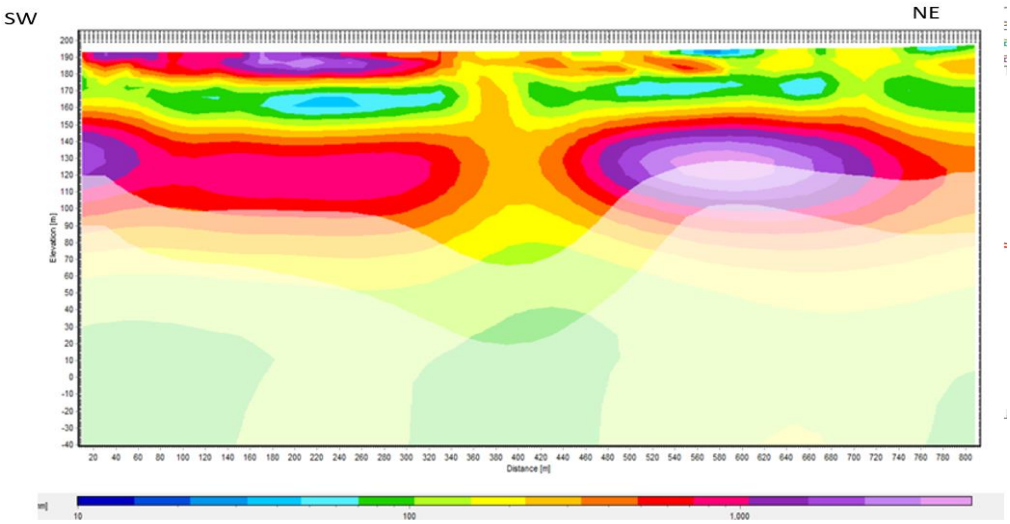

Figure 4 - 2 c: 800 m long ERT profile (AWB processed) at DWVP01, Tamboku (drilled at station 420) in the Panabako sandstone formation.

Since primary permeability within this geological environment is virtually non-existent, interpretation of geophysical survey results should be targeted at sections that could indicate secondary permeability (Yidana et al. 2020). Figure 4.2 c for instance, shows a subvertical structure as mentioned above between stations 340 m to 420 m. Station 420 m was therefore selected for drilling which resulted in a yield of 22 lpm after 24 hr pumping test (specific capacity after 6 hours was 0.33 lpm/m). This geophysical result of the AWB-processing of the ERT-profile is much better corroborated with the result of the geophysical wireline-logging in borehole DWVP01 at station 420 m (Figure 4.2 d) than the comparison with the RES2DINV result as seen in Appendix 5A.

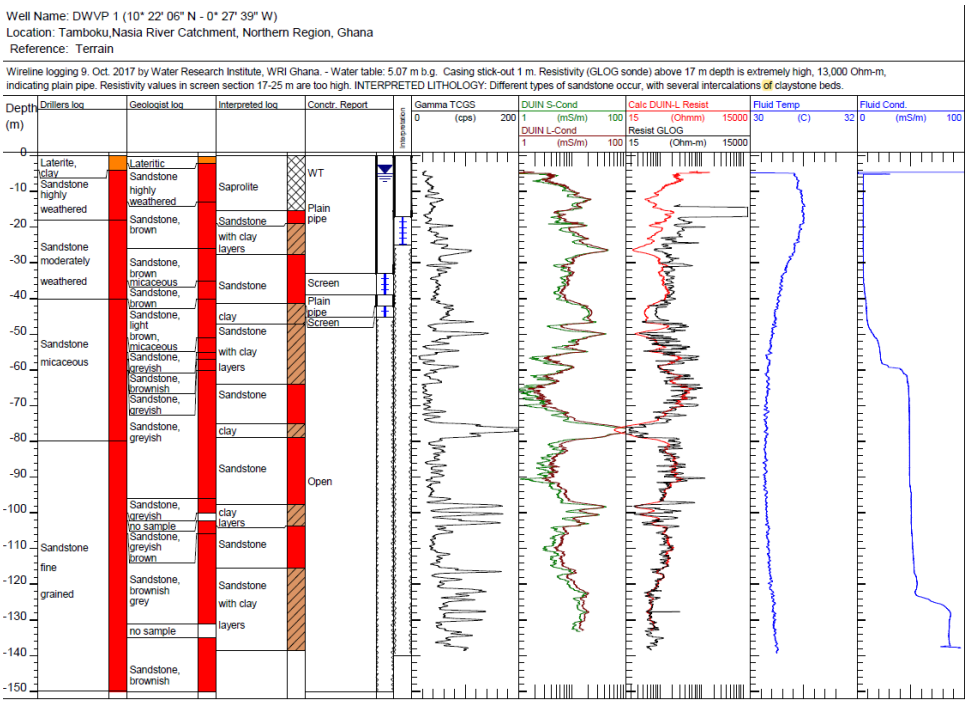

Figure 4 - 2 d: Geophysical wireline logs of borehole DWVP01(drilled at ERT st. 420) in Panabako sandstone.

Furthermore, several portions of the wireline logs (Gamma-, Conductivity- and Resistivity-log on Figure 4-2 d) show values interpreted as intercalation of mudstones/clay layers within the sandstone as suggested by Ayite et al. (2008), but neither seen on the drillers log nor on the log of the geologist. Notice also, that the resistivity log (Figure 4.2d) calculated from the conductivity-log shows 10 m upper layer with high resistivity followed by 30-40 m shifting but in average lower resistivity over shifting but in average high resistivity layers to 115 m depth, i.e. generally a three-layer situation with mutual resistivity proportion similar to the ERT-profile as it is described above.

One more case with analysis of different geophysical methods applied at same borehole in the Panabako formation is from borehole HAP 11 at Nalerigu SHS. (secondary data) with conductivity measurements from 20 m and 40 m coil separation over a traverse of 400 m. Comparison of the response curves from both the horizontal and vertical dipole modes with 40 m coil separation (deep exploration depth) shows three distinct peak anomalies at the stations C70, C175 and C 265. These anomalies are thought associated with subvertical fracture zones in the bedrock. Therefore, station C265 on the EM-34 profile was selected for drilling and it yielded 24 lpm.

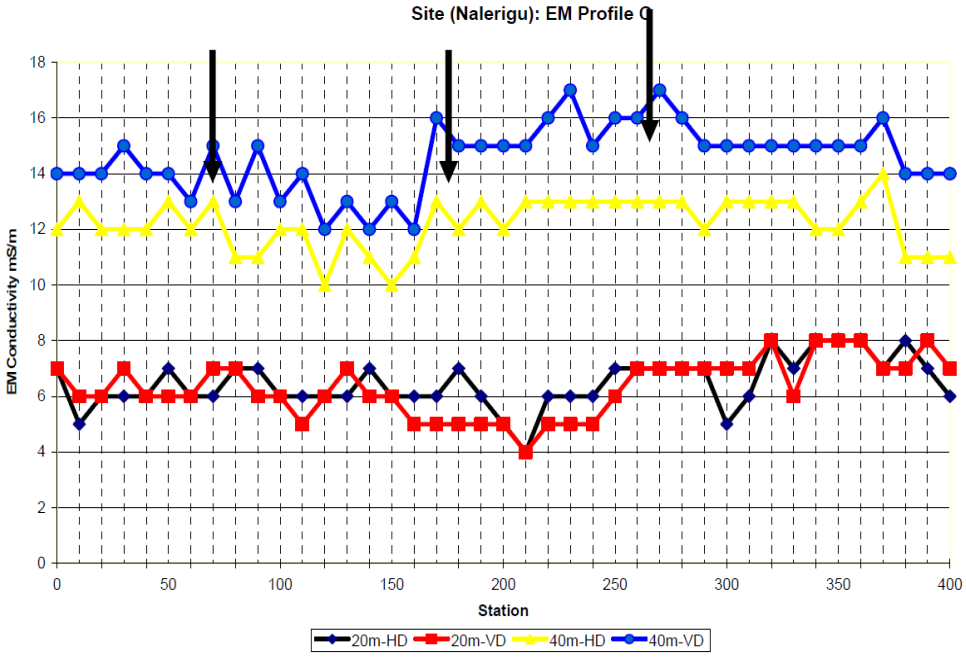

Figure 4 – 2 e: EM profile at HAP 11 (Nalerigu SHS at st.265) in the Panabako sandstone formation

The ERT-profile (secondary data) along the same traverse as the EM-profile and in the same direction is shown on Figure 4-2f. It shows a two layered situation, a high resistivity, ≥1800 Ωm at the upper layer and gradually decreasing downwards to below 460 Ωm between 20 m to 30 m depth suggesting a possible change in lithology. The high resistivity is interpreted as lateritic cover and dry weathered sandstone, and the lower resistivity is interpreted as wet fractured sandstone or sandstone with intercalations of mudstone.

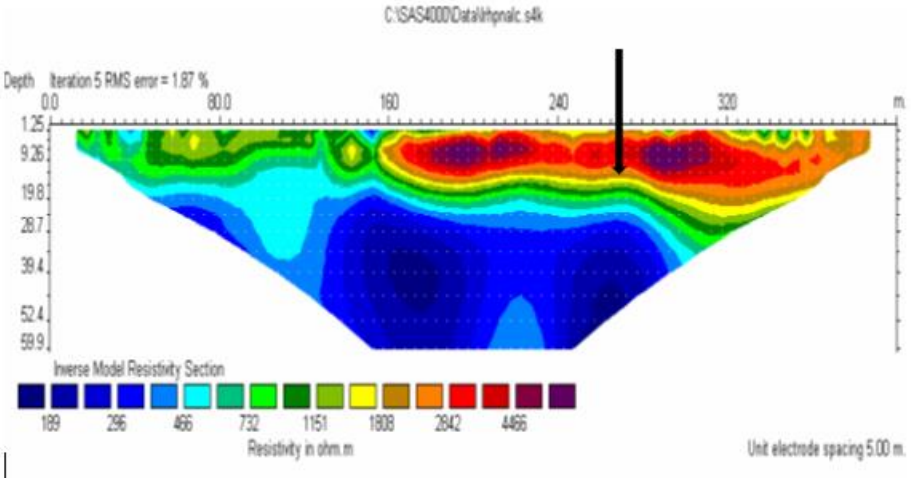

Figure 4 – 2 f: ERT profile (RES2DINV processed) at borehole HAP 11, Nalerigu SHS (drilled at st. 265).

When comparing the ERT-profile with the EM-profile there are significant differences and some similarities: The lower resistivity from st. 0 to st. 180 of the uppermost 20-40 m thick layer compared to the resistivity on the remaining section of the ERT-profile is not reflected by corresponding contrary conductivity variation on the EM-20 m coil-separation profile irrespective of the modes HD or VD. There is hardly any variation seen on the EM-20 m coil profile. The generally lower

resistivity below 20-40 m depth on the ERT-profile is confirmed by the generally higher conductivity on the EM-40 m coil separation profile compared to the EM-20 m coil separation profile. Similarly, the conductivity variation along the EM-40 m profile showing lower conductivity from st. 0 to st. 180 compared to the remaining section fits well to the higher resistivity below 30-40 m from st. 0 to st. 180 on the ERT-profile compared to the remaining section on the ERT-profile.

Summarizing the ERT-profile shows a two-layer situation, an extremely high resistivity (>1000Ωm) to 20 m depth followed by a somehow lower resistivity (<500 Ωm) to at least 60 m depth. Oppositely, the wireline logs (Gamma- and Calculated Resistivity-log on Figure 4-2g) unambiguously show the occurrence of 6 different lithologies within the same depth of 60 m, and with following resistivities: 500-1000/ <40/ 250/ 75/ 1500/ 250 Ωm corresponding to sandstone/ claystone/ sandstone/ claystone/ sandstone quartsitic/ sandstone and with the following thicknesses: 10/ 4/ 17/ 2/ 11/ 20 m. Below the depth of 64 m, the resistivity gradually decreases to 100 Ωm at 83 m depth. Below this depth a completely different rock occurs with frequently varying resistivity below 100 Ωm as well as frequently varying but rather high gamma-radiation, a mudstone with frequent intercalations of siltstone and fine-grained sandstone, thus most probably the Poubogou Formation.

Obviously, neither the ERT-profile nor the EM-profile with four investigation depth can reflect the details of a complex lithological profile as the one in borehole HAP 11 documented by the geophysical wireline logging, Figure 4-2g. Both methods do reflect, that the resistivity of a top layer is higher than the average

resistivity below. However, the magnitude of the resistivities on the ERT-profile seems generally too high compared to the resistivity-log (calculated from the Induction conductivity-log), whereas the EM-conductivities of the 20 m as well as of the 40 m coil separation in both modes correspond reasonable well to the conductivities on the Induction-log (Long coil distance = DUIN L.Cond).

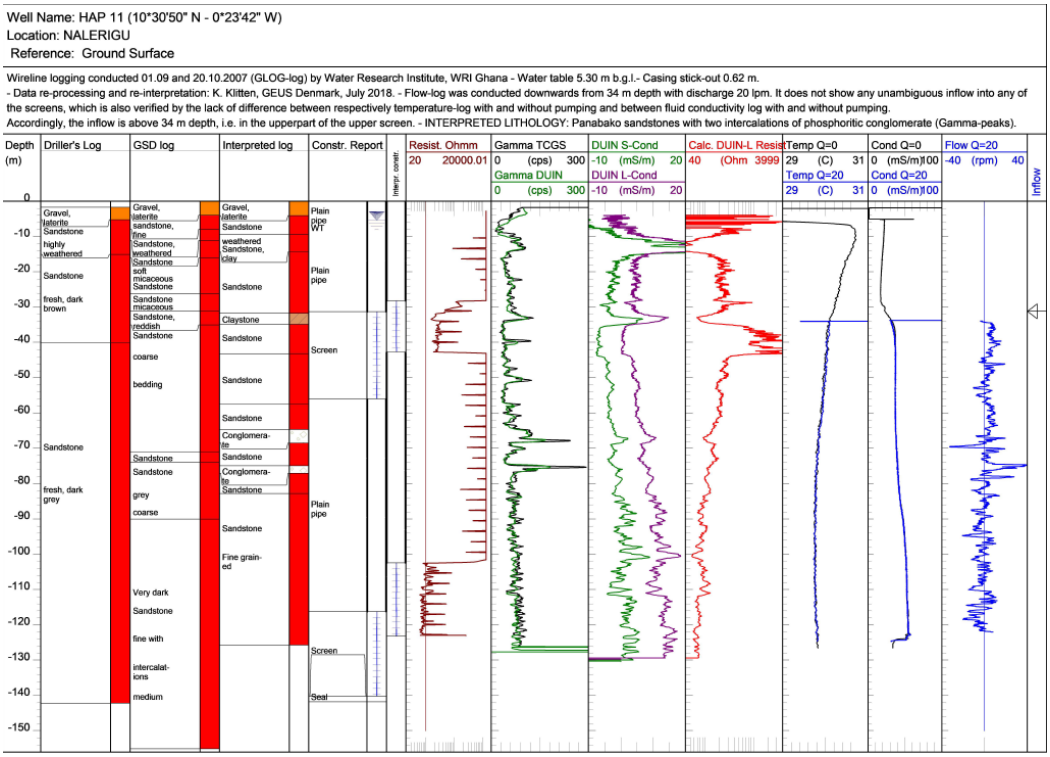

Figure 4 - 2 g: Geophysical wireline logs of HAP 11 at Nalerigu SHS

In summary, within the Panabako sandstone formation water-bearing sub-horizontal fractures if any are often related to distinct distinct lithological boundaries (like in DWVP 02 mentioned earlier) and occurrence of several significant intercalations of claystone in a sandstone are therefore good indicators for groundwater availability. Where there were intercalations of the different units,

the layers of each individual rock materials are easily distinguished by differences in gamma radiation and in resistivity on geophysical wireline logs in a borehole. Unfortunately, none of the two surface geophysical methods, ERT and EM, can provide such detailed information but only rough indication of the very general lithological profile and furthermore identification of eventual sub-vertical boundaries between significant different lithologies. Though, if the two methods are indicating that a certain depth section of the sandstone has lower resistivity than otherwise normal for that type of sandstone, it can be an indication of claystone intercalations thus being a positive indication on possibility for sub-horizontal water-bearing fractures along the boundary between the sandstone and the claystone intercalations. Therefore, the recommendation given by Ewusi et al. (2009), that within the sandstone formation, resistivities below 70 Ωm should be targeted, needs to be evaluated in terms of whether a low resistivity is a horizontal anomaly on a profile thus indication of a sub-vertical fracture zone – or an anomalous low resistivity at a certain depth thus indicating a section in the sandstone with claystone intercalations.

4.1.2.2 Oti/Pendjari Group

This group is made up of the Kodjari and the Bimbila formations within the study area as seen on the map below, Figure 4.3, where also the locations with boreholes and with geophysical data discussed in this section are shown.

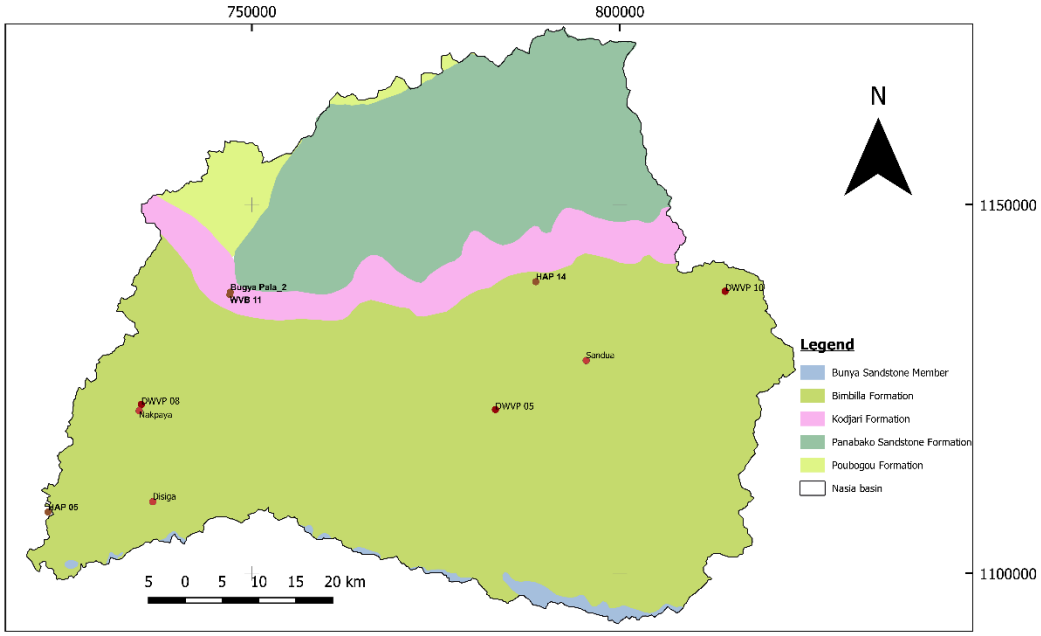

Figure 4.3a: A geological map showing DWVP 10 & Sandua – DWVP 05 - DWVP 08 & Nakpaya – HAP 05 and Disiga – HAP 14 – Bugya Pala (WVB 11 & B2).

4.1.2.2.1 Bimbilla Formation

This formation constitutes about two-thirds of the study area comprises green to khaki, micaceous laminated mudstones, siltstones and tabular, sharp-based sandstones. The Bunya Sandstone Member forms the top of this Formation, with few outcrops in the southernmost portions of the study area (Carney et al. 2010; Jordan et al. 2009). The four locations (DWVP 10, DWVP 05 & DWVP 08, and HAP 05) within this formation selected for discussion are expected to represent respectively elder-, middle- and younger part of the formation.

The first case within the Bimbila formation selected for discussion is the 100 m deep borehole DWVP 10 at Sakpa representing the eldest part of the Bimbila

formation since the Kodjari formation is encountered at 73 m depth, Figure 4.3c. The 400 m ERT-profile at borehole DWVP 10 (Figure 4.3b) shows a 30-40 m top layer with low resistivity (25-50 Ωm) along most of the profile, though being above 100 Ωm from st. 280. Below the top layer seems the resistivity gradually to increase towards greater depth and surprisingly to be more than 1000 Ωm below about 60 m depth. The lateral variation of the resistivity indicates slightly dipping layers, but without indication of any significant resistivity anomaly.

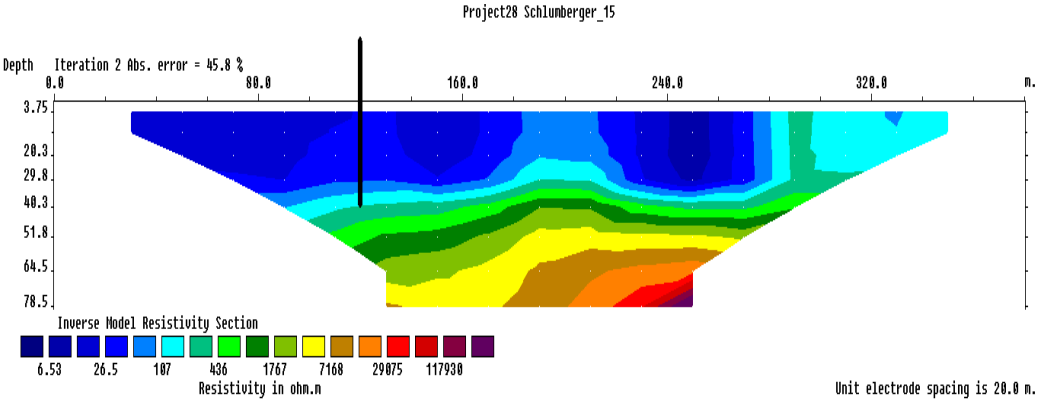

Figure 4 - 3b.: 400 m long ERT-profile (RES2DINV processed) at borehole DWVP 10 Sakpa (at st. 120) located within "Bimbila old" underlain by the Kodjari formation.

Comparison of the ERT profile and the wireline resistivity log in the 100 m deep borehole DWVP 10 (Figure 4.3c) shows a generally bad fit. Because the resistivity log shows in the uppermost 20 m only 15-20 Ωm, and below 20 m depth follows an almost uniform siltstone with resistivity of 20-30 Ωm to 85 m depth after which the resistivity is increasing to 50 Ωm only. Thus the significantly increasing

resistivity from being 50 Ωm at 30-40 m on the ERT-profile to much higher than 1000 Ωm below 60 m depth does not tally at all with the wireline resistivity log.

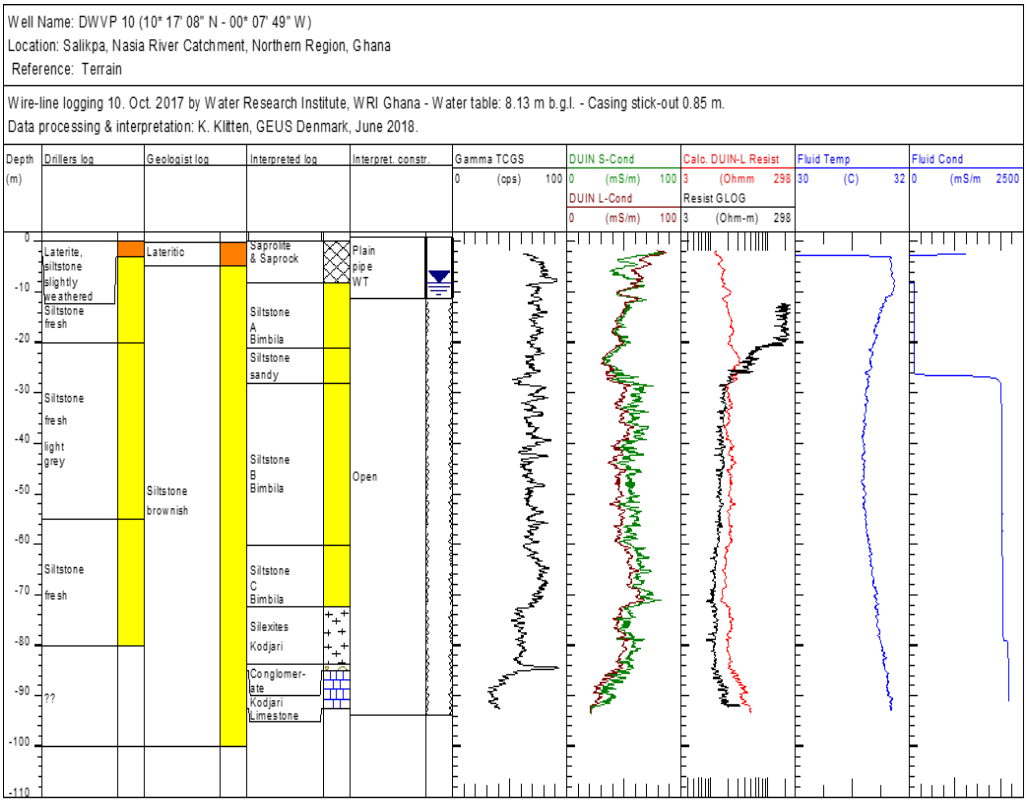

Figure 4 – 3c: Geophysical wireline logs of borehole DWVP10 Sakpa (drilled at st. 120 on ERT-profile) showing Bimbila formation underlain from 73 m by Kodjari formation.

Opposite to what was not seen on any of the previous shown resistivity logs in boreholes in the Panabako formation, the resistivity of the uppermost 10-20 m of the Bimbila formation has always a lower resistivity than seen in the bedrock below, thus reflecting the weathering of the latter (Saprolite + Saprock).

This is confirmed by the results of conductivity measurement from the electromagnetic profile in Figure 4.3d located at Sandua some 20 km WSW of

borehole DWVP 10, and also expected to represent the elder part of the Bimbilla formation. The EM profile-A is one of two parallel 500 m long and SSE-NNW directed profiles conducted in campaign II with the purpose of localizing a feasible site for dug-well construction in order to exploit groundwater from areas with as thick Saprolite & Saprock as possible. The dry borehole DWVP 08 is located about 400 m NNE of the northern end of the EM profiles and was already drilled, when the EM survey was conducted.

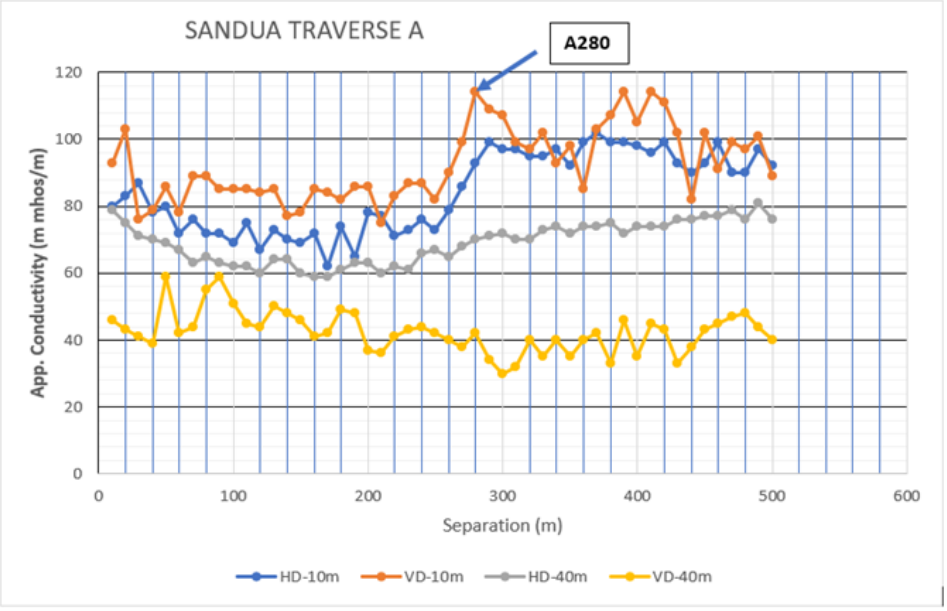

Figure 4 – 3 d: EM Profile-A as one of two parallel SE-NW profiles at Sandua ("Bimbila old" formation).

The conductivity on the 10 m coil separation profile for both dipole modes is significantly higher than on the 40 m coil separation profiles. The VD-40 profile indicates a rather uniform bedrock with resistivity of 20-25 Ωm, whereas the three more shallow profiles, VD-10, HD-10 and HD-40 indicate thicker and more clayey

low resistivity (10 Ωm) overburden on the right section compared to the left section of the profile (the northern section compared to the southern). Accordingly, this northern section on the profile with thicker and more clayey overburden is considered to provide good groundwater storage thus a dug well was suggested to be constructed at st. 280 as shown on Figure 4.3d above.

The second case within the Bimbilla Formation selected for discussion is the 100 m deep borehole DWVP 05 at Kpodu (Pobbul), which is expected to represent the middle part of the Bimbila formation. Figure 4.3e and Figure 4.3f show respectively the ERT-profile and the geophysical wireline logs of borehole DWVP05 (Kpodu). The 400 m long ERT profile shows a very low resistivity (<15 Ωm) in the 30 m top layer along the first 180 m against a generally higher but varying resistivity in the 30 m thick top layer along the last 220 m profile. The borehole DWVP 05 was suggested drilled at st. 200 being a relative resistivity-high anomaly (40 Ωm) in the top layer to 40m depth followed by an increase to more than 100 Ωm at 60 m, though even to much higher resistivity after st. 200. The lateral variation of the resistivity below 40 m depth does indicate a vertical sub-structure like a fault at st. 200, and that was why the borehole was drilled there. However, the rock encountered was not particularly fractured, and the yield obtained was only 13 lpm and with 28.5 m after 6 hours pumping.

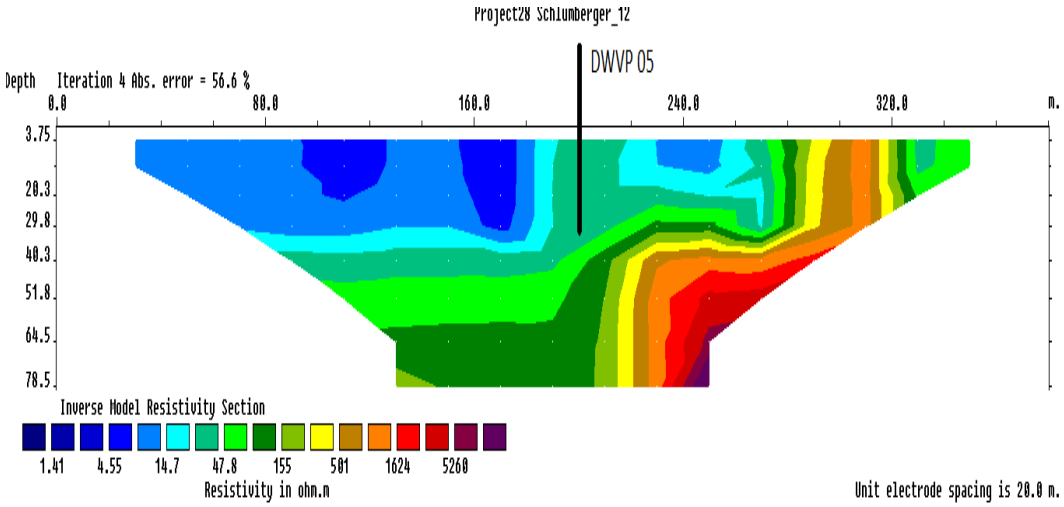

Figure 4-3e: 400 m long ERT-profile (RES2DINV processed) at borehole DWVP 05 Kpodu (drilled at st.200) within "Bimbila middle" formation.

Comparison of the ERT-profile and the resistivity log (calculated from the DUIN-long log) in the 100 m deep borehole DWVP 05 (Figure 4-3f) gives a generally bad fit. Because the ERT-profile shows too high resistivities and does not reflect the very constant resistivity of 15-20 Ωm in the obviously homogeneous bedrock of siltstone seen on the resistivity log the whole way to the bottom of the borehole, though with even lower resistivity in the uppermost 20 m reflecting the Saprolite and Saprock.

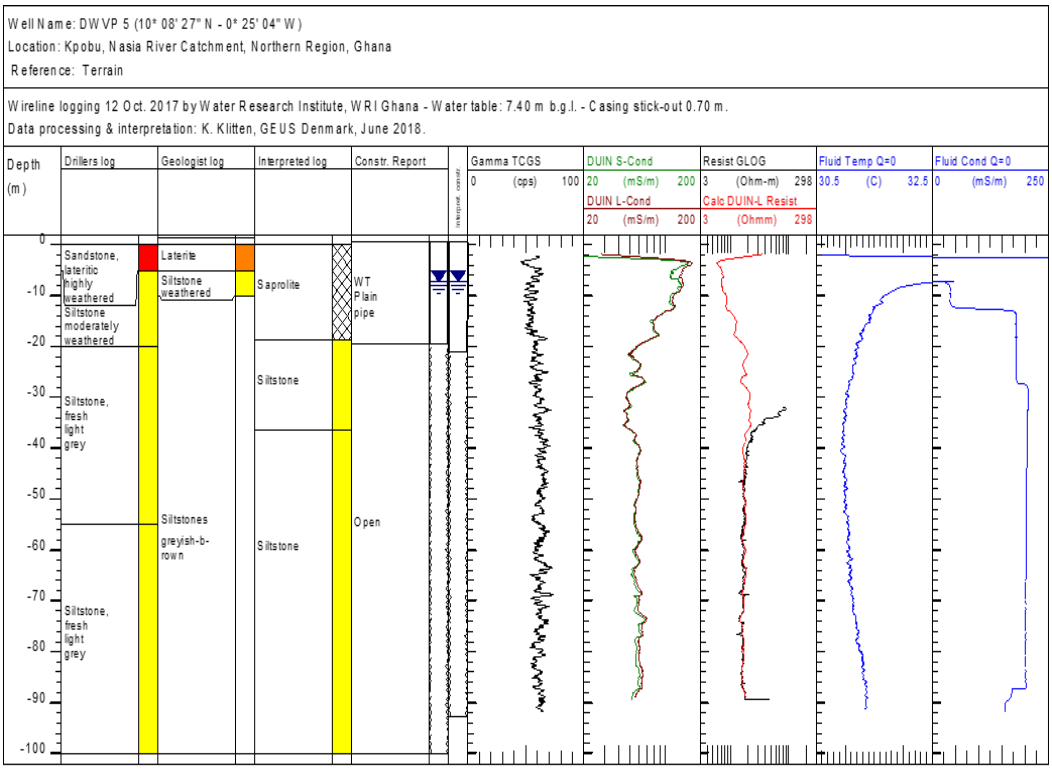

Figure 4 – 3 f: Geophysical wireline logs at borehole DWVP05 at (Kpobu) ("Bimbila middle" formation).

The third case within the Bimbila formation selected for discussion is the 100 m deep borehole DWVP08 at Nakpaya, which is also expected to represent the middle part of the Bimbila formation, though with a different lithology compared to DWVP 05 as seen on Figure 4-3g below by having several intercalations of sandy beds in the siltstone. The sandy beds are indicated by peaks with low gamma-radiation and low conductivity. The thickness and resistivity of the Saprolite + Saprock is respectively 10 m and 5-15 Ωm. The resistivity of the bedrock from 10 m depth is varying between 10 and 70 Ωm, thus with the generally highest in the section from 16 m to 32 m (having an average of 50 Ωm) and the generally lowest from 32 m to 66 m (having an average of 15 Ωm).

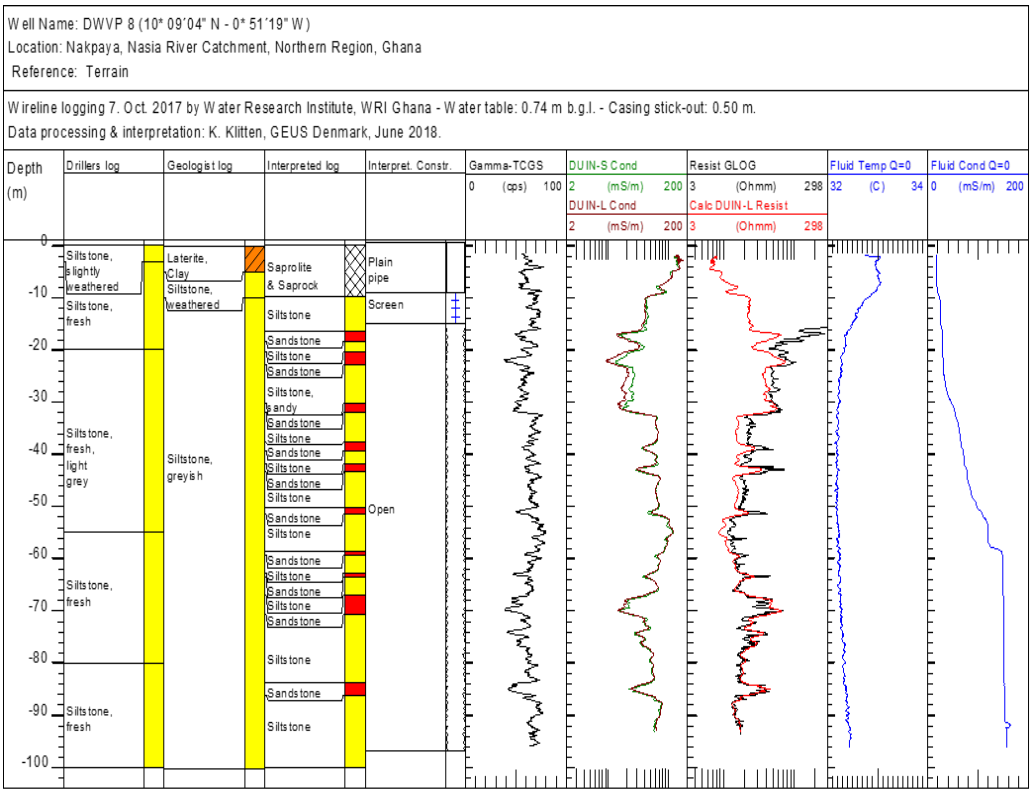

Figure 4 – 3g: Geophysical wireline logs of borehole DWVP08 at Nakpaya ("Bimbila middle" formation).

The ERT profile of DWVP 08 (Nakpaya), Figure 4.3h, generally shows a 15-20 m thick top layer with low but varying resistivity (10 Ωm -25 Ωm) along the 400 m profile, and interpreted as being Saprolite & Saprock. The bedrock below the top layer seems to have a resistivity of 75 Ωm, though with an 80 m wide sub-vertical structure in the central part of the profile with a resistivity of 40 Ωm only, which therefore could be a wide fractured and weathered zone. Accordingly, the borehole site was selected at st. 160, thus within this structure and also within a low resistivity anomaly (<20 Ωm) of the top layer. Irrespective of these indications on a prospective drilling site, the outcome was a dry borehole.

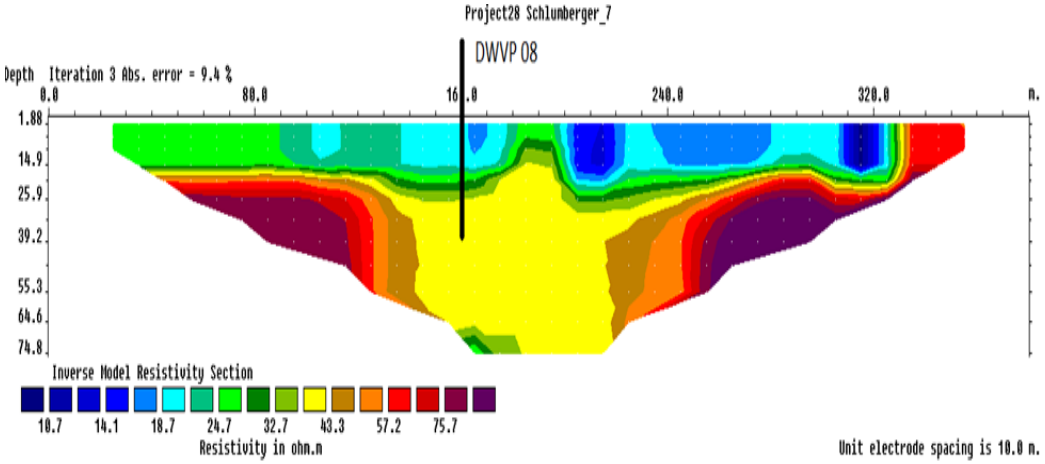

Figure 4 – 3h: 400 m ERT-profile (RES2DINV processed) at borehole DWVP08, Nakpaya (drilled at st. 160) within "Bimbila middle" formation.

When comparing the ERT-profile and the resistivity log (calculated from the DUIN-long log) in the 100 m deep borehole DWVP 08 (Figure 4-3g) a fairly good fit is obtained for the uppermost low-resistivity layer and its thickness as well as on the average resistivity of 40 Ωm of the bedrock (siltstone with intercalations of sandstone). Though, the ERT-profile does not reflect the lithological variation of the siltstone as it is illustrated by the geophysical wireline logs, an example is by the varying resistivity from 20 m depth the whole way down to the bottom of the borehole.

The EM profile at Nakpaya in Figure 4-3i is one of two parallel and 500 m long and SSW-NNE directed profiles conducted in campaign II with the purpose of localizing a feasible site for dug-well construction in order to exploit groundwater from areas with thick Saprolite & Saprock. The dry borehole DWVP 08 is located

about 400 m NNE of the northern end of the EM profiles and was already drilled, when the EM survey was conducted.

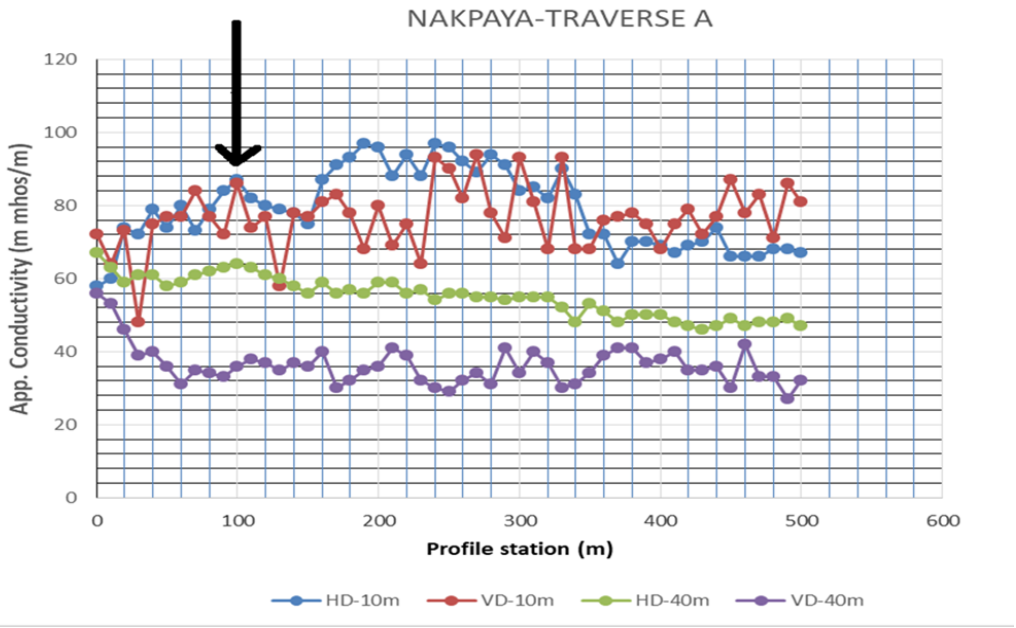

Figure 4 -– 3i: 500 m long EM profile-A in SSW-NNE direction at Nakpaya ("Bimbila middle" formation).

The VD-40 profile indicates a rather uniform bedrock along the profile with conductivity of 35-40 mS/m corresponding to resistivity of 25-30 Ωm of the bedrock, whereas the two more shallow profiles, VD-10 and HD-10 shows much higher and more varying conductivity reflecting much lower resistivity (10-15 Ωm) and varying thickness of the clayey overburden, thus maximum thickness expected from st. 100 to st. 340. Accordingly, this section on the profile with thicker and more clayey overburden is considered to provide good groundwater storage thus a dug well was suggested to be constructed at st. 100 as shown on Figure 4-3i.

As being representative for the younger part of the Bimbilla Formation HAP05 (Janga) is selected as an example. The 2D ERT-profile shows at the borehole site st. 220 two layers (Figure 4.3j), thus an upper rather thin zone (<5m) with resistivity surprisingly higher than 100 Ωm and underlain by quite low resistivity 15-25 Ωm to 55 m depth.

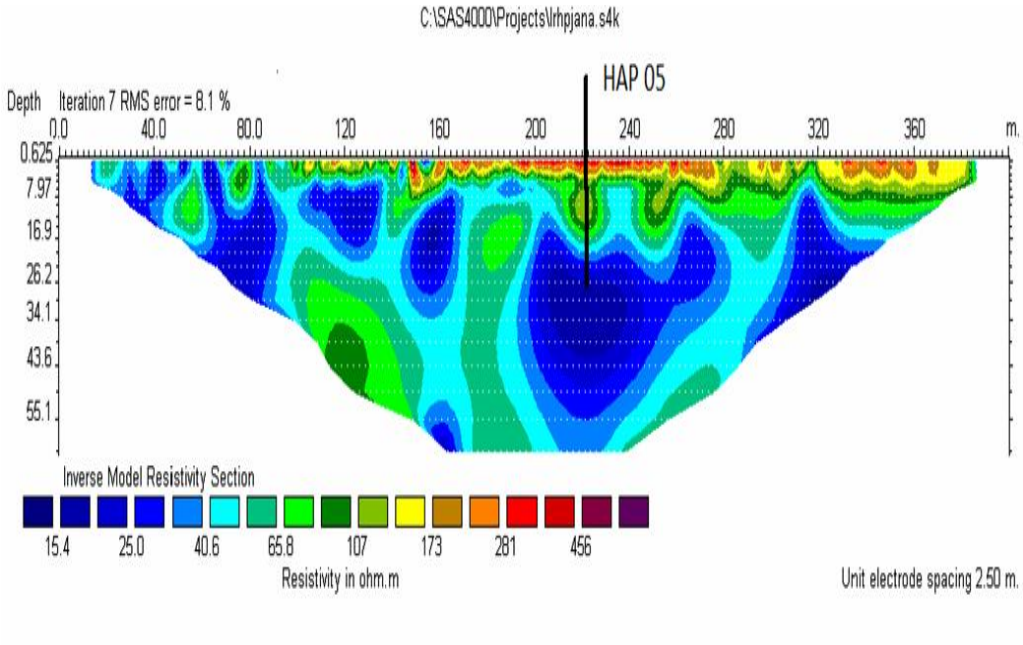

Figure 4 -– 3j: ERT profile at borehole HAP 05 (Janga) at st.220 (younger part of Bimbila formation) after RES2DINV processing.

The borehole HAP 05 was drilled to a depth of 166 m, and the drillers log as well as the geologist log, Figure 4-3k, describe the whole penetrated section as being a homogeneous mudstone without any indications on fractures from a depth of 22 m, above which the rock was completely weathered (Saprolite). The resistivity wireline log (calculated from DUIN-long, in Figure 4-3k) shows that most of the 22 m thick weathered zone has a much lower resistivity, 10 Ωm, than the top layer

seen on the ERT profile. The resistivity log as well as the Gamma-log further confirmed the occurrence of a very homogenous bedrock with a resistivity of 15-22 Ωm and a Gamma-radiation of 60-70 cps (counts per second) the whole way down to 120 m. An obstacle at that depth made it impossible to continue wireline logging further downwards. Thus, the resistivity of the bedrock seen on the ERT profile was actually verified by the wireline logs. The comparison between the ERT profile at borehole HAP 05 (Janga) and the geophysical wireline resistivity log is also included in Appendix 5B.

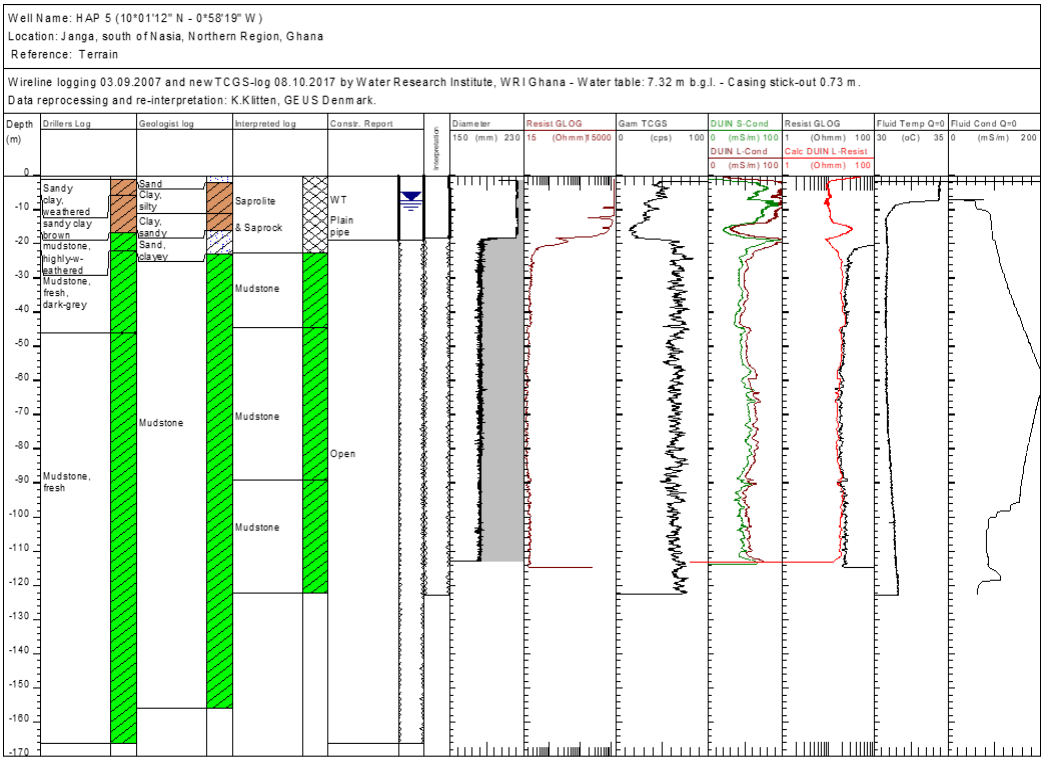

Figure 4 – 3k: Geophysical wireline logs in borehole HAP 5 Janga (younger part of Bimbila formation).

The yield after drilling was 5 lpm which is below the minimum required yield for hand pump (10 lpm). Since the bedrock had no fractures, it implies that the recorded

yield of 5 lpm is a result of contribution from only the quite thick and clayey overburden (22 m) verified by the geophysical wireline logs. Figure 4.3l shows results of apparent conductivity measurement using EM 34 at Disiga located some 13 km ENE of borehole HAP 05, but still expected to represent the younger part of Bimbilla Formation. Even though the results are from a different area far away from HAP 05, the trend is consistent with the observations from results of HAP5. Thus, the high apparent conductivity (>100 mS/m and >60mS/m) for the two shallow profiles, HD-10 and VD-10 compared to the more uniform and much lower conductivity (40mS/m) on the deep profile VD-40 indicates a rather thick weathered zone (>10<20 m depth) above a homogeneous mudstone with a resistivity of 25 Ωm, which is quite similar to the observations in borehole HAP 05.

It was concluded from the EM-34 profile (Figure 4-3l) that the target for groundwater exploitation by dug-well construction should be the thicker weathered zone in the right section of the profile, thus towards the southwestern end of EM-profile A. However, due to risk for frequent flooding of that area the dug-well was actually constructed at st. 90 shown on the profile. But even so, the dug-well is expected to benefit from the groundwater storage potential not being far away.

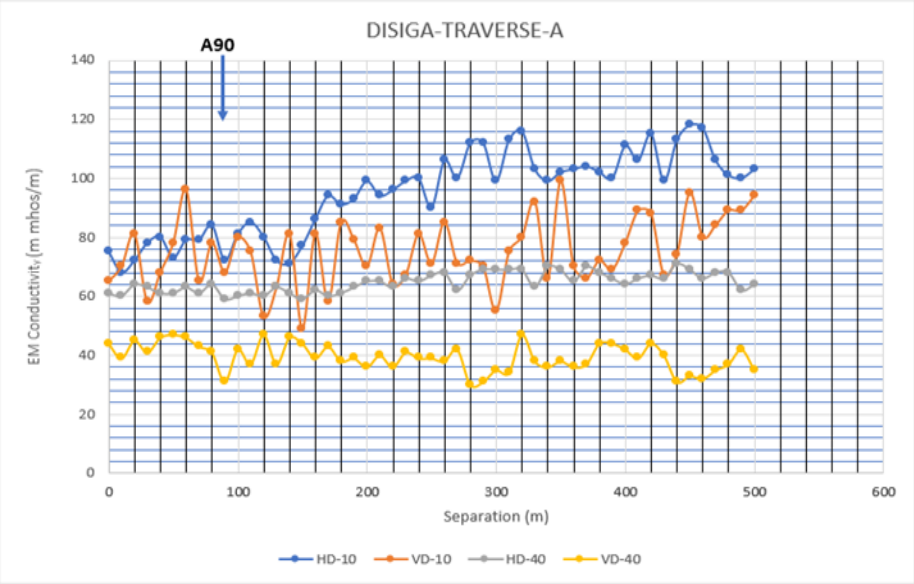

Figure 4 – 3l: EM profile-A as one of two parallel NE-SW profiles at for selection of feasible site for dug-well construction (within Bimbila young formation).

Finally, the Bunya sandstone member, which forms the top of the Bimbilla formation, seems to have high potential for groundwater exploitation. Jordan et al. (2009) reports that the Bunya Sandstone occurs in the Karaga area as a series of disconnected outliers which are the evidence for the continuation of the synclinal structure (Dakar Syncline). This structural feature might have caused a higher secondary permeability and therefore could serve as good targets for groundwater exploration. Field observation and data from CWSA and World Vision show that several high yielding boreholes (see Appendix 10) used for small town and mechanized system in Karaga and Tong townships were completed in the Bunya sandstone member. Unfortunately, there do not exist any geophysical wireline

logging data from boreholes in the Bunya sandstone in the Nasia Basin. Therefore, validation of the evaluated resistivities from possible ERT-profiles and EM-profiles from locations within this sandstone could not be conducted.

4.1.2.2.2 Kodjari Formation

The first location to discuss in this section is the geophysical wireline logs of borehole HAP 14 at Tuuni (secondary data), which was thought to represent the elder part of the Bimbilla Formation, and is shown in Figure 4-4a below. However, the interpretation of the geophysical wireline logs has disclosed that the uppermost 80 m of the 120 m deep borehole HAP 14 consist of the three sub-units of the Kodjari formation, thus the silexites, the limestone and the tillite, underlain by Panabako sandstone from 80 m depth.

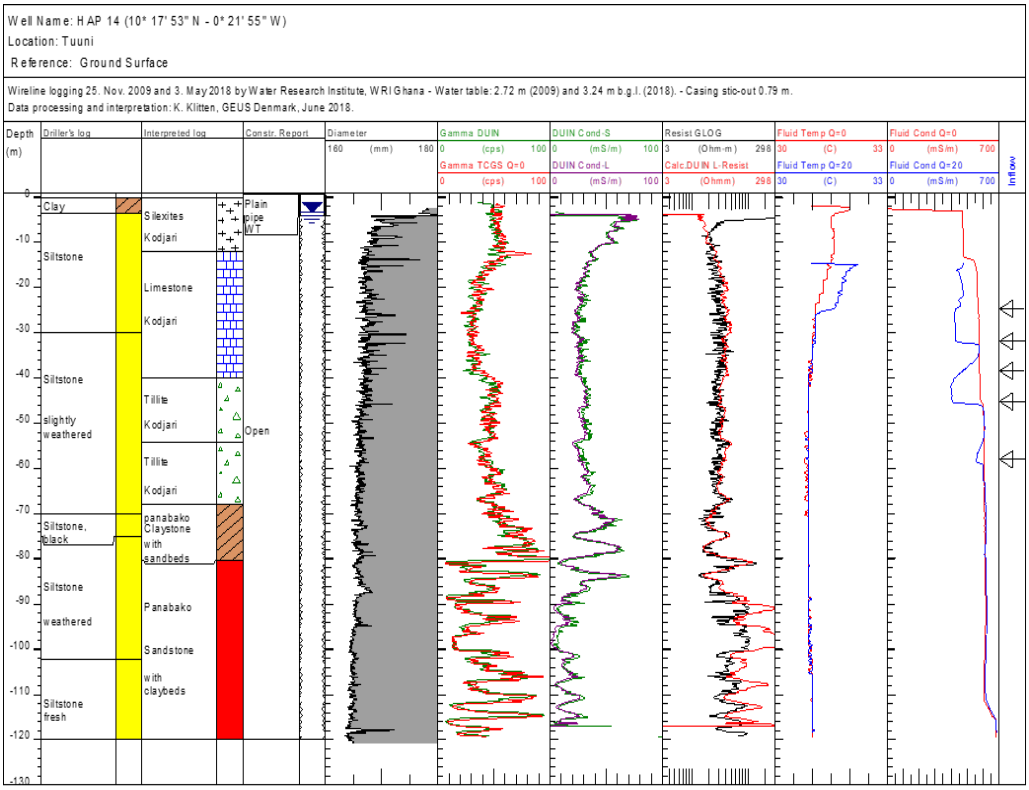

Figure 4-4a: Geophysical wireline logs of borehole HAP 14 Tuuni (at st. 120 on ERT-profile) in Kodjari formation underlain by Panabako sandstone.

The borehole HAP 14 was drilled at station 120 on the ERT profile shown in Figure 4-4b below. The 400 m ERT-profile (processed by RES2DINV) shows a 10-15 m top layer with low resistivity (22 -38 Ωm) below which the resistivity is gradually increasing to more than 138 Ωm at about 60 m depth, thus without any indication of any significant lithology boundary. Furthermore, there is hardly any lateral variation in the resistivity along the profile, thus indicating the absence of any geological anomaly or structure.

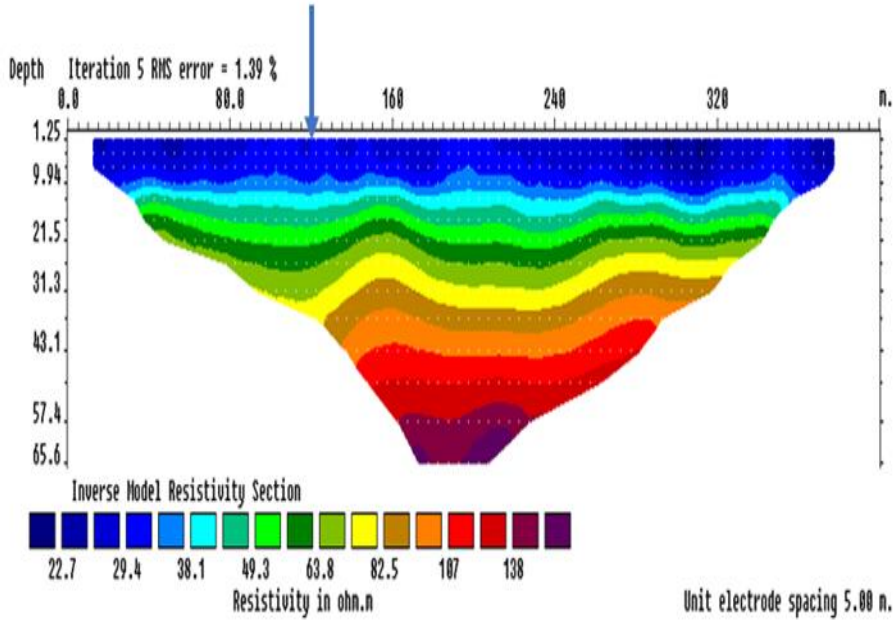

Figure 4 - 4b: The ERT-profile at borehole HAP 14 Tuuni (at st. 120) located within the Kodjari formation.

Comparison of the ERT profile and the wireline resistivity log of borehole HAP 14 fits relatively well for the upper portion of the latter showing a 12 m top layer with resistivity of 15-25 Ωm followed by an almost uniform resistivity of 25-40 Ωm to 80 m. Then followed by an erratic but in average higher resistivity (50-300 Ωm) after 80 m indicating sandstone with clay intercalations, the latter seen as low resistivity peaks and corresponding high gamma-radiation peaks, which is typical for certain sections of the Panabako formation (as an example see logs in DWVP 02 on Figure 4-1d). This suggests that in areas underlain by the Kodjari formation, drilling deeper is encouraged if sufficient yield is not obtained, because it has the possibility of encountering water bearing Panabako sandstone. Though, the

groundwater in Panabako sandstone below Kodjari can be too saline like in this borehole HAP 14 where the fluid conductivity log shows values higher than 600 mS/m, Figure 4-4a.

In addition, Figure 4-4c illustrates two profiles A and B for HAP 14, Tuuni as reported by WRI in 2009. Profile A was conducted from south towards north – and profile B from west towards east. The difference in the variation of the conductivity for both dipole modes between the two profiles is noticeable, because it most probably reflects whether the profile is perpendicular (profile A) or parallel (profile B) to dip of the sedimentary layer sequence.

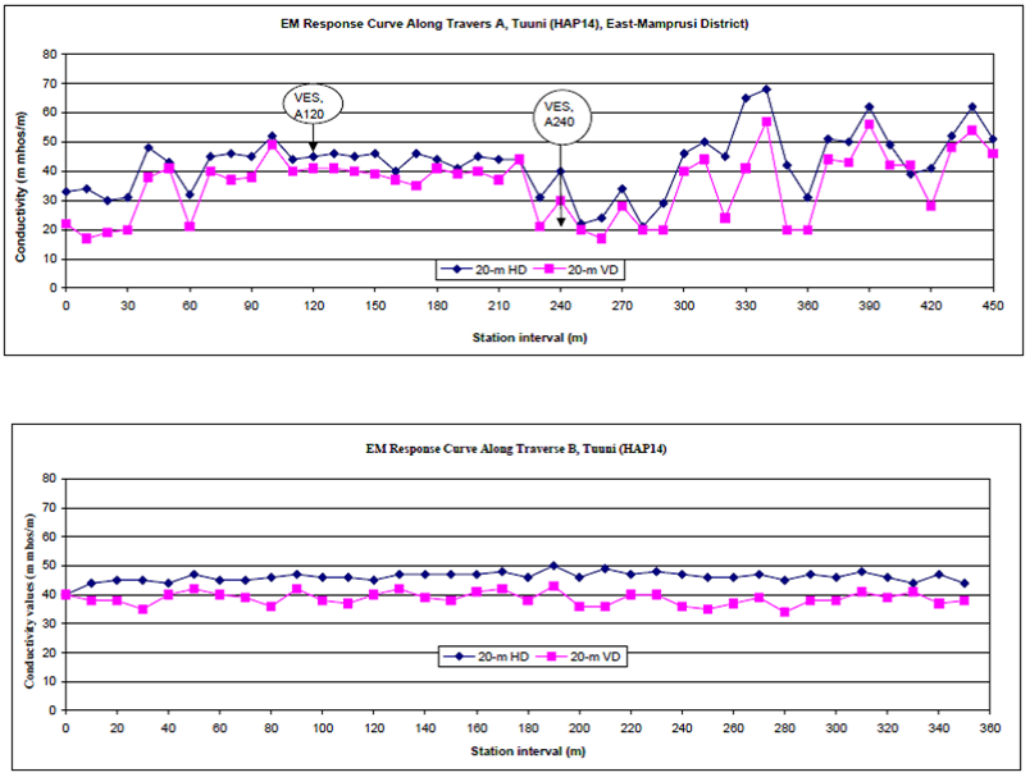

Figure 4-4c: EM-34 response curves along traverses A and B, Tuuni (HAP 14).

Another case of geophysical data from Kodjari area are the geophysical wireline logs of the two boreholes WVB11-Bugya Pala 1 and Bugya Pala 2, location seen on the geological map, Figure 4.3a. The geophysical logs are shown in Figure 4.4d and Figure 4.4e respectively. A high conductivity is recorded for the upper layer to a depth of about 20 m in both boreholes, and it was originally interpreted as the weathered zone. However, weathering is normally decreasing downwards thus being reflected by a gradually increasing resistivity towards depth. Obviously, this is not the case in any of the two boreholes, where the shift in conductivity thus resistivity at about 20 m depth is quite abrupt. It is worth noting that the extreme high conductivity in this upper zone particularly in borehole Bugya-Pala 2 most probably is caused by high content of conductive minerals other than clay since the gamma-radiation is not particular high. It might be magnetite rich Kodjari ashes or iron and manganese rich Kodjari limestone. Further studies of the near-surface layer at Bugya-Pala 2 borehole is necessary to confirm the observed unusual high conductivity and to determine the reason for it. The difference in gamma radiation for the two boreholes accounts for the difference in lithology, which is recorded by the driller only in the 56 m deep borehole WVB 11. Mudstone at bottom is here overlain by two types of bedded sandstones, where the upper one is having higher gamma-radiation and much lower resistivity than the lower one, and therefore re-interpreted as Kodjari tillite. The lower one from 20 to 50 m depth in WVB 11 is re-interpreted as being Panabako sandstone based on the level and pattern of the gamma-log as well as of the resistivity-log. The mudstone at bottom might be the Poubogou formation.

The 40 m deep borehole Bugya-Pala 2 is located only 400 m north of WVB 11, and is without any information on lithology. Re-interpretation of the lithology based on the gamma-log and the resistivity-log (calculated from DUIN-Long conductivity log) concludes that a sandstone, possible Panabako, occurs at the lowermost 5 m at bottom overlain by 13 m mudstone, possible Kodjari tillite, and then the uppermost 22 m highly conductive layer of Kodjari ashes or Kodjari limestone as mentioned above. The very different resulting lithology of boreholes with a mutual distance of only 400 m indicates a highly heterogeneous geological environment which might be explained by the Kodjari formation laying unconform on an uneven erosion surface of the Panabako formation. This requires a combination of various interpretation and observation when exploring for groundwater. It was observed for during the data collection period, in Bugya Pala for instance, the hand dug wells were uniquely located along a straight line and they had water throughout the year. This observation and interpretation of the geophysical logs means the thick weathered zone are good indicators for groundwater within this formation. Furthermore, the study has exposed a need for improvement of the geological description of the samples from drilling boreholes for groundwater exploitation.

Jordan et al. (2009) indicates that ‘tillite-like conglomerate’ consisting of various rock fragments enclosed within an unsorted, quartzitic to feldspathic sandy matrix was identified in a borehole beyond 60 m depth in the Kodjari. This presupposes that drilling deeper boreholes within this formation has a possibility of encountering good fractures. However, as mentioned above under discussion of the borehole

HAP 14 there seems to be a risk for encountering too saline groundwater below the Kodjari formation.

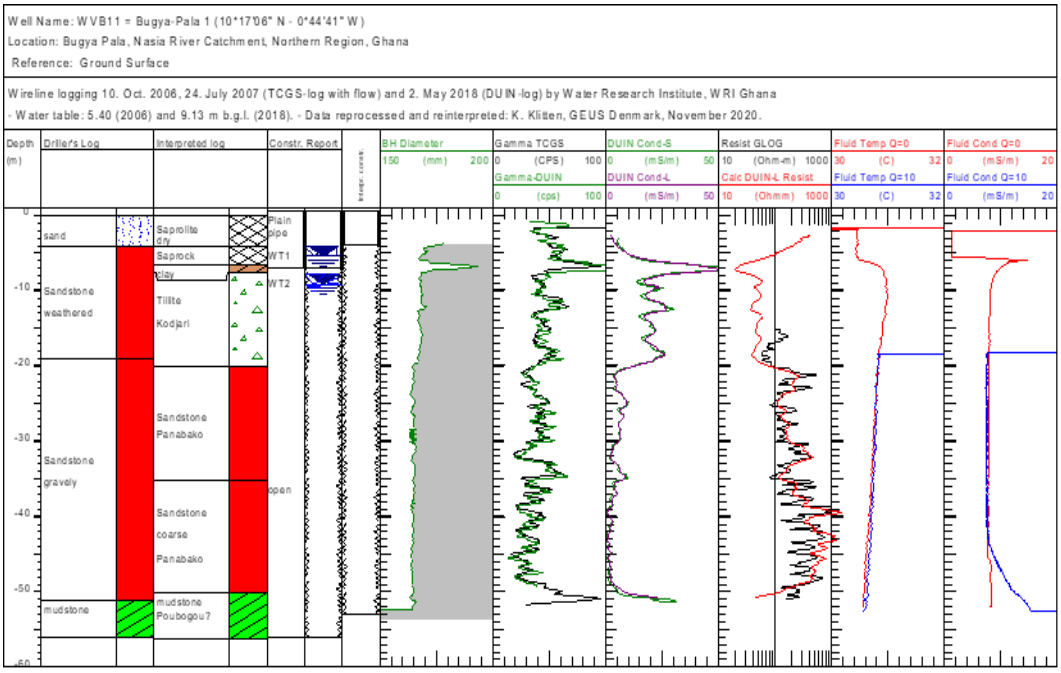

Figure 4 – 4d: Geophysical wireline logs from WVB 11(Bugya Pala)

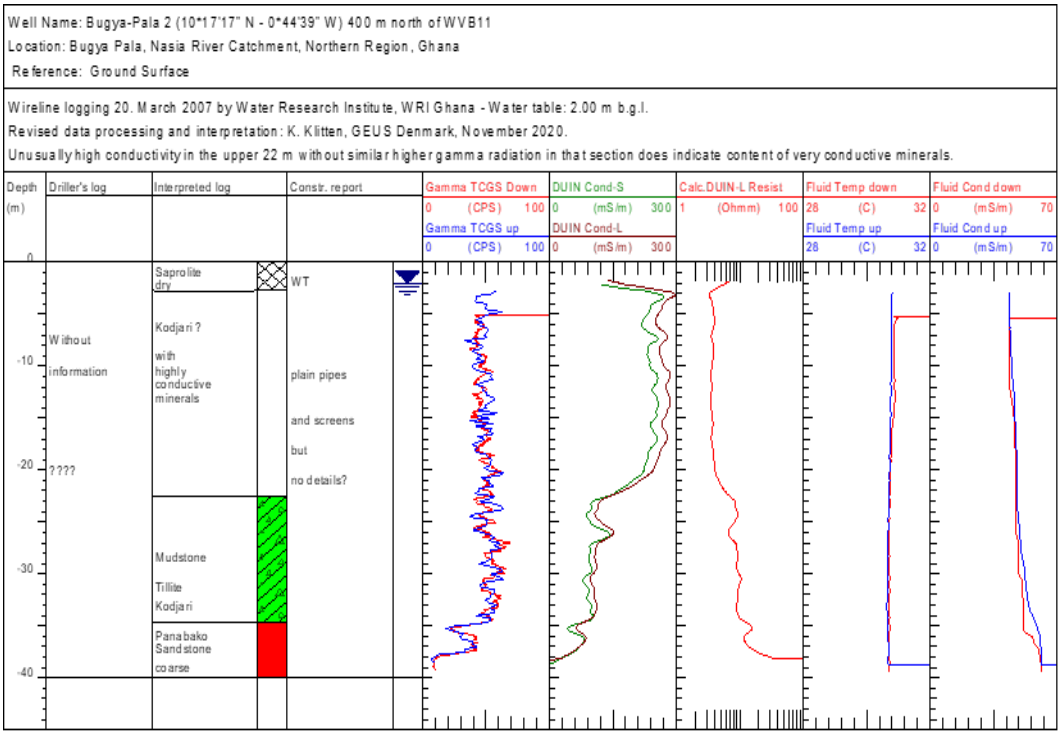

Figure 4 - 4e: Geophysical wireline logs from CWSA borehole Bugya Pala-2.

The extreme low and very uniform resistivity of Figure 4-4e of the uppermost 20 m indicates a highly conductive rock type, because weathering (Saprolite) will normally decrease towards depth thus be reflected by a gradually increasing resistivity towards depth.

4.1.3 Geophysical characteristics of rocks

A general characteristic of the Voltaian sedimentary rocks obviously seems not sufficient for groundwater governance institutions and researches to make economical feasible development of the groundwater resources. Improvement of

the knowledge on the lithostratigraphy within the different formations of the VSB and on their respective geophysical and hydrogeological characteristics seems needed.

In the UK for instance, Beamish (2013) used conductivity information from airborne electromagnetic survey to classify rock lithologies. His study has provided new information on the conductivity characteristics for many geological formations. New empirical map of the bedrock conductivity of the UK has also been developed.

There are currently only some few researchers who have made documentation of resistivity of the different rock types in Ghana (Ewusi, 2006; Awini, 2008; Agyekum, 2009), however not related in details to the individual formations in the VSB. Having such information would be a good step for groundwater development especially for the Voltaian supergroup.

Results from the electromagnetic profiles (Appendix 1) of some of the locations, electrical resistivity profiles (Appendix 2) at some boreholes and geologic logs in Appendix 4 were used to characterise the geophysical signature (resistivity) of the various geological formations. In some limited cases, geophysical logs from monitoring boreholes (Appendix 3) were used to validate the interpretation. The Appendix 5 consists of a summary of the interpretation from the combined geophysical methods. Similar combined use of different methods for characterising rocks has been used by other researchers (Comte et al. 2012; Danielsen et al. 2007; Sonkamble et al. 2014).

Figure 4-4f is an illustration of how the resistivity for HAP14 (Tuuni) was interpreted by combining various geophysical methods and geological log. The geological borehole description was matched with the electrical resistivity image (ERT-profile) at the drilled location. The resistivity was extracted and compared with the results from the geophysical logs (wireline) for confirmation. The case is presented in details in the previous section 4.1.2.2.2 Kodjari Formation.

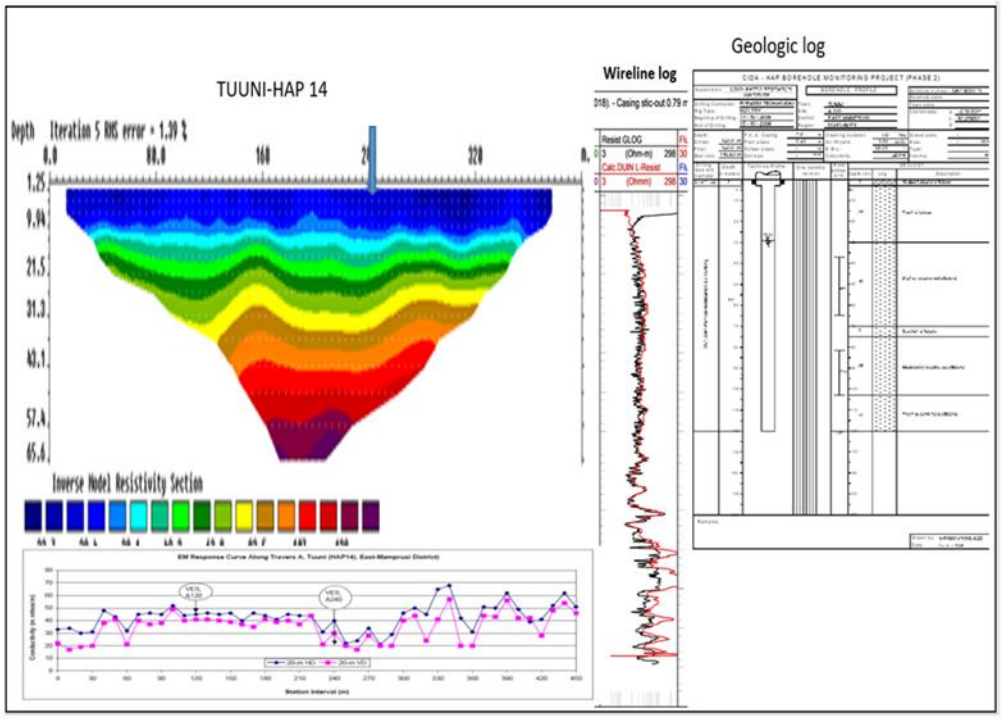

Figure 4 – 4f: An illustration of how resistivity is compared using different methods.

The ERT-profile in Figure 4-4f illustrates an example where neither reflect the magnitude nor the variation with depth of the resistivity of the bedrock compared to the actual observation of the same on the wireline resistivity log. Furthermore, that the EM profiles HD-20 (blue) and VD-20 (red) provides information on the resistivity of the overburden, which fits quite well with the wireline resistivity log.

Table 4.1 summarizes the resistivity obtained of the weathered zone (Saprolite + Saprock) as well as of the bedrock by the three different methods, ERT-profiling, EM-34 profiling and wireline resistivity log, at each of the cases discussed in this Chapter 4.1. The wireline resistivity is read from the DUIN-long conductivity log after being transferred to Calculated DUIN-L resistivity. This because the Focussed Guard resistivity probe provides trustworthy resistivity only of open sections of boreholes (without casing and screen), and first from 10 m below the water table in the borehole. Therefore, the Guard resistivity probe does not provide information on resistivity of the weathered zone.

The resistivity values from the ERT-profile and from the EM-34 profiles are read at the location on the profile of the borehole with wireline logs. The conductivity read in mS/m from the EM-34 profile is transferred to resistivity in Ωm by 1000/conductivity. For EM-34 readings for the weathered zone is the HD-10 profile applied, though if not available then the HD-20 profile. EM-34 readings for the bedrock is the VD-40 profile. For ERT readings for the weathered zone is the average to 10-15 m depth applied, and for bedrock the dominating resistivity further down is applied. The readings of the resistivity of the respective weathered zone and the bedrock from the wireline log are determined by the pattern of the resistivity variation towards depth.

Table 4-1a: Resistivity of weathered zone and of bedrock from cases discussed

Location	**Figure no.**	**Formation**	**Saprolite + Saprock**			**Bedrock**		
			EM HD-10 or 20	ERT	Calc.Res. log	EM VD-40	ERT	Calc.Res. log
DWVP 09	4.1a and 4.1b	Panabako	-	3500	100-1000	-	20 & 80	300 & 100
DWVP 02	4.1c and 4.1d	Panabako	-	>2000	100-1000	-	60 & >5000	60 & 100-500
Tenkpanga	4.2a and 4.2b	Poubogou	25-60	>1000	-	15-30	50-500	-
DWVP 01	4.2c and 4.2d	Panabako	-	200-500	100-1000	-	60-100 & >500	50-100 & 100-400
HAP 11	4.2e, 4.2f and 4.2g	Panabako above Poubogou	125-200 -	>1800 -	100-1000 -	60-100 -	200-500 -	100-250 80-100
DWVP 10	4.3b and 4.3c	Bimbila old above Kodjari	-	20-30	15-20	-	>500	20-30
Sandua EM**	4.3d	Bimbila old	10-15	-	-	15-25	-	-
DWVP 05	4.3e and 4.3f	Bimbila middle	-	30-40	5-15	-	>100	15-20
DWVP 08 Nakpaya EM**	4.3g and 4.3h 4.3i	Bimbila middle Bimbila middle	- 10-15	10-25 -	5-15	- 25-30	40-75 -	10-70 -
HAP 05 incl. EM	4.3j and4.3k Not shown	Bimbila middle	45	100-300	10	30	15-25	15-22
Disiga EM**	4.3l	Bimbila young	8-15	-	-	20-30	-	-
HAP 14	4.4a, 4.4b, 4.4c (and 4.4f)	Kodjari above Panabako	22 -	20-40 -	10-20 -	25* -	40-140 -	20-40 50-300
WVB 11 = Bugya Pala 1	4.4d	Kodjari tillite Panabako Poubogou	- - -	- - -	100-300 - -	- - -	- - -	50 100-1000 <100
Bugya Pala 2	4.4e	Kodjari Kodjari tillite Panabako	- - -	- - -	5-10 - -	- - -	- - -	4 10 >10

As described in the discussion of the different cases and seen in the table there are in general a bad fit between the resistivity from the ERT-profile of the weathered zone as well as of the bedrock compared to the factual resistivity on the wireline log. Most often is the resistivity from the ERT-profile far too high compared to the wireline resistivity log. Oppositely, the resistivity values evaluated from EM profiles corresponds quite well to the factual resistivity on the wireline log.

Accordingly, values from the latter two methods are given higher priority in the following Table 4.1b, in which the range of resistivity for the various geological formations in the study area is summarized. The Panabako Sandstone Formation from the Table 4.1b has the highest resistivity for bedrock and weathered zone. This is expected since the rocks are according to Jordan et al. (2009) very hard and well cemented. Kesse (1985) also indicated that these rocks are generally well consolidated and are inherently impermeable. The resistivity of the weathered zone is quite often showing higher resistivity than the bedrock, which is opposite to what is seen for Bimbilla formation as well as for the Poubogou Formation.

When it comes to the bedrock the resistivity of Bimbila seems relatively lower compared with that of the Poubogou Formation though both are composed of similar rocks (mudstone, siltstone with thin beds of sandstone). Telford et al. (1990) suggest that resistivity of some rock types varies with age and lithology. The Poubogou formation which belongs to the Bombouaka Group according to Jordan et. al. (2009) was deposited earlier than the Bimbilla Formation (Oti/ Pendjari

Group) and therefore could possibly be the explanation for why the fresh bedrock of Poubogou is having slightly higher resistivity than the fresh bedrock of Bimbila. The lower resistivity in the Bimbilla Formation is most probably caused by higher clay content.

The Kodjari has a similarly low resistivity as the Bimbila, which could be as a result of its composition, basal tillites, a cap-carbonate limestone and laminated tuffs and ash rich siltstones (Carney et al. 2010). In certain cases, it can even be extremely low caused by content of conductive minerals other than clay.

There is a high variability of the resistivity generally in the area which supports the assertion by many researchers about the complex nature of the geology. Extreme caution such as including the direction of a geophysical EM or ERT profile and comparing them with the expected strike and dip of the sediments in the interpretation of such profiles, is needed when exploring for groundwater. Finally, it seems needed also to give more attention to the electrode contact to the terrain when conducting the ERT-profiling, because the insufficient electrode contact to terrain might be the reason for the generally too high resistivities obtained from this method.

Table 4.1b: Resistivity of the geological formations of the Nasia Basin

Geologic Formation	**Saprolite+Saprock**	**Bedrock**
	Resistivity (Ohm-m)	Resistivity (Ohm-m)
POUBOGOU	25-60	80-100
PANABAKO SANDSTONE	100-1000	50-1000
KODJARI KODJARI mineralized	10-300 5-10	10-50 4
BIMBILLA	5-20	15-70

Based on the above discussion of the geophysical results, it is evident that there is a need to rethink with the concept of interpreting such results. The best approach would be to place much emphasis on the geology of the VSB, direction of their dip and strike, their trend of the resistivity. The purpose of geophysics is to gain better understanding of the geology which will then increase the knowledge on how to exploit the groundwater.

4.2 Evaluation of Groundwater Characteristics

The groundwater characteristics (depth, regolith-the entire weathered zone, static water level, depth of water strike and yield) in the study area has been grouped under the main geological formations. Tables 4.2a to 4.2d provide descriptive statistics of these parameters in the various geological formations.

From the descriptive statistics table, despite the difference in the total number of boreholes sampled in each formation, the minimum depth of borehole is 31 m in all the formations except the Kodjari which has 21 m. The maximum depth of drilling however varied with the deepest in the Bimbilla formation (166 m), Poubogou formation having 92 m, Panabako sandstone (155 m) and 80 m for the Kodjari formation. The average depth of boreholes in all the formations ranged between 50 – 60 m which is in consonance with that of Carrier et al. (2008). The low standard error for depth in each of the formations (2.05-3.01) m is an indication of the reliability of the mean. The high standard deviations for depth indicate the degree of variability and only few boreholes account for the high values. The high depth in Bimbilla formation (166 m) and Panabako sandstone formation (155 m) are

boreholes drilled under the HAP project for research as such do not represent the general depth of drilling in the area. The skewness and kurtosis indicate the high variability of depth for all the formations and show non normal distribution of the dataset.

The thickness of regolith for all the formations in Table 4.2 ranges between 2 m-19 m with an average between 7.2 m-8.55 m and the least is recorded in the Poubogou formation. The low value recorded for the Poubogou formation could be from the small number of boreholes in the dataset. The average thickness of regolith obtained for all the formation generally agrees with the findings of previous researchers (Banoeng-Yakubo et al. 2011; Carrier et al. 2008; Dapaah-Siakwan and Gyau-Boakye, 2000). The reliability of the mean in each of the geological formations is indicated by the low values obtained for both the standard error and the standard deviation. The skewness indicates that the data on thickness of regolith is normally distributed and a kurtosis of shows that there are fewer datasets at the tails of the distribution in each of the formations.

The yield in all the formations in Table 4.2a-4.2d ranges from 5 m^3/day to 720 m^3/day with mean ranging between 56 m^3/d to 107 m^3/d. The standard error and standard deviations are relatively high in all the formations indicating that the yield is spread out over large range. It is also observed that standard deviation is greater than the mean in all the formations which indicates a high variation between the values, and an abnormal distribution of the dataset. Yidana et al. (2020) suggests

that high variability in the borehole yield is indicative of a significant spatial variability in the aquifer hydraulic properties. The skewness indicates that the yield is not normally distributed. This is because most of the boreholes are designed for hand pump use (with minimum required yield of 10 lpm equal 14 m^3/d) and therefore the target is not to drill further to obtain higher yields if sufficient yield is completed.

Table 4.2a: Summary of Groundwater Characteristics in Bimbilla Formation

	N	Range	Min	Max	Mean		Std. Deviation	Variance	Skewness		Kurtosis	
	Statistic	Statistic	Statistic	Statistic	Statistic	Std. Error	Statistic	Statistic	Statistic	Std. Error	Statistic	Std. Error
Depth (m)	92	135	31	166	59.80	2.26	21.69	470.56	1.83	0.25	5.62	0.50
Thickness of Regolith	92	15	3	18	7.60	0.33	3.21	10.29	0.57	0.25	0.18	0.50
Yield (m3/d)	92	570	6	576	85.32	12.45	119.57	14296.17	2.51	0.25	6.41	0.50
SWL (m)	92	34	2	36	8.82	0.62	5.96	35.56	2.70	0.25	8.86	0.50
Depth of water strike (m)	37	60	15	75	30.73	2.51	15.25	232.54	1.61	0.39	2.39	0.76

Table 4.2b: Summary of Groundwater Characteristics in Poubogou Formation

	N	Range	Min	Max	Mean		Std. Deviation	Variance	Skewness		Kurtosis	
	Statistic	Statistic	Statistic	Statistic	Statistic	Std. Error	Statistic	Statistic	Statistic	Std.	Statistic	Std.
Depth (m)	21	61	31	92	50.38	3.01	13.80	190.45	1.44	0.50	3.16	0.97
Thickness of Regolith	21	9	3	12	7.29	0.57	2.59	6.71	-0.10	0.50	-1.07	0.97
Yield (m3/d)	21	260	14	274	56.92	16.62	76.15	5798.48	2.50	0.50	5.49	0.97
SWL (m)	21	14	2	16	5.95	0.66	3.01	9.05	1.84	0.50	5.52	0.97
Depth of water strike (m)	3	11	25	36	31.00	3.22	35.57	31.00	-0.78	1.23		

Table 4.2c: Summary of Groundwater Characteristics in Kodjari Formation

	N	Range	Min	Max	Mean		Std. Deviation	Variance	Skewness		Kurtosis	
	Statistic	Statistic	Statistic	Statistic	Statistic	Std. Error	Statistic	Statistic	Statistic	Std.	Statistic	Std.
Depth (m)	39	59	21	80	52.59	2.11	12.824	164.46	0.18	0.38	-0.13	0.74
Thickness of Regolith	39	17	2	19	7.49	0.45	3.433	11.78	0.91	0.38	2.28	0.74
Yield (m3/d)	39	710	10	720	107.51	14.53	163.677	26790.15	2.43	0.38	5.71	0.74
SWL (m)	39	18	1	19	5.77	1.16	4.055	16.45	1.32	0.38	2.03	0.74
Depth of water strike (m)	18	35	18	53	25.61	1.24	8.354	69.78	2.34	0.54	6.45	1.04

Table 4.2d: Summary of Groundwater Characteristics in Panabako Sandstone

	N	Range	Min	Max	Mean		Std. Deviation	Variance	Skewness		Kurtosis	
	Statistic	Statistic	Statistic	Statistic	Statistic	Std. Error	Statistic	Statistic	Statistic	Std. Error	Statistic	Std. Error
Depth (m)	82	124	31	155	58.13	2.77	25.07	628.54	2.04	0.27	4.67	0.53
Thickness of Regolith	82	14	2	16	8.55	.374	3.39	11.49	0.10	0.27	-0.31	0.53
Yield (m3/d)	82	426.24	5.76	432.00	70.52	8.77	79.44	6311.22	2.07	0.27	4.97	0.53
SWL (m)	82	16	0.5	16	7.02	0.40	3.64	13.26	0.327	0.27	-0.72	0.53
Depth of water strike (m)	38	65	10	75	27.66	1.97	12.14	147.47	1.88	0.38	5.11	0.75

From Tables 4.2a-4.2d, the range of SWL is 0.5 m-19 m and the average SWL for the geological formations is in the range of 5.77 m -8.82 m. The low standard error (<1 m) and standard deviations (<6 m) of SWL represent a high reliability of the mean. The Bimbilla formation which had a maximum drilling depth in the study area also had the highest SWL. The composition this formation, mudstone/siltstones with thin beds of sandstones (Jordan et al. 2009) could be the reason for this high SWL since these rocks generally are considered to have poor groundwater potential (Carrier et al. 2008).

An evaluation of the depth of water strike to determine the probable depth of encountering water within each of the formation is illustrated in Table 4.2 (a-d).

The average depth of striking water ranges between 25 m -31 m for all the formations. This is similar to the observations made by Bannerman (1990) who reported that the average depth for most productive fractures is 27 m. The results in Table 4.2a to 4.2d also point to the fact that, apart from the Poubogou formation, the average depth of water strikes over the study area exceeds the average thickness of regolith (weathering depth) suggesting that productive yields are mainly derived from water-bearing fractures struck at depth. This agrees with conclusions of researchers like Carrier et al. (2008) and Ewusi et al. (2009). Nsiah et al. (2018) in determining the groundwater potential zone of the Nabogo in the Northern Region of Ghana revealed that groundwater strike in the basin is at depths ranging from 3.5 m - 68.98 m with a mean depth of 24.4 m. The map they generated showed that, for a high potential zone water could be intercepted at a depth of about 30 m to 43 m during drilling. This conclusion even though is not within the study area, however falls within the broader VSB therefore can generally be said to compare with the findings of this work

To explore the distribution of the groundwater parameters for the entire study area, statistical methods such as Box plots and Histograms were used as shown in Figure 4.5a-4.5d and Figure 4.6a-4.6d respectively.

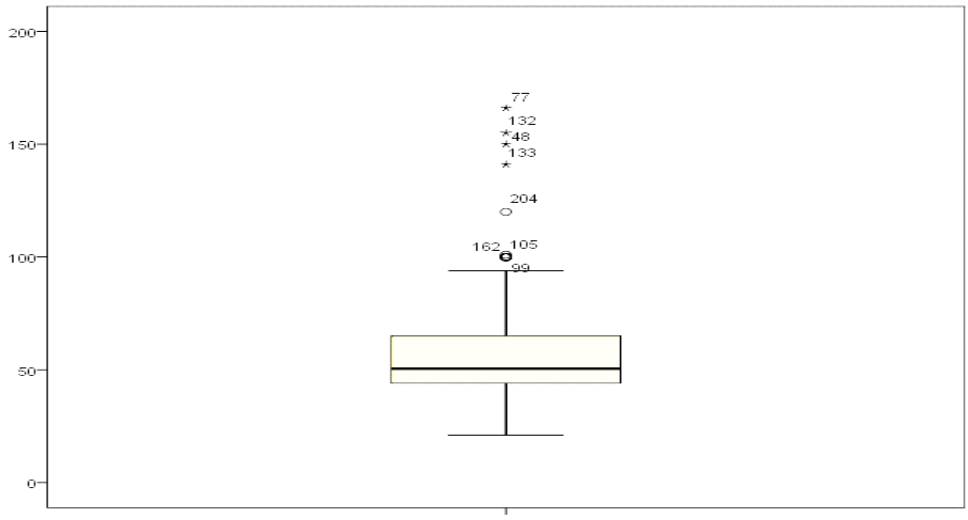

Figure 4 - 5a: Box Plot for Depth (m) for the Nasia basin

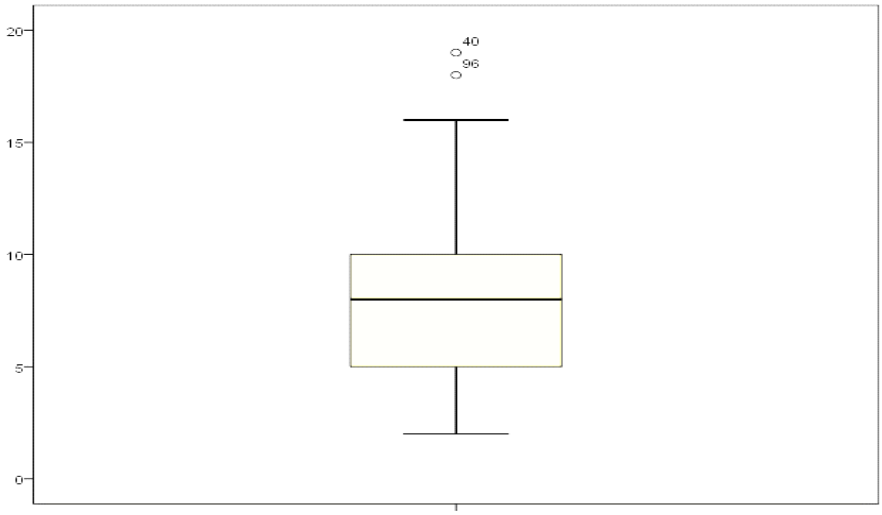

Figure 4 - 5b: Box Plot for Thickness of Regolith (m) for the Nasia basin

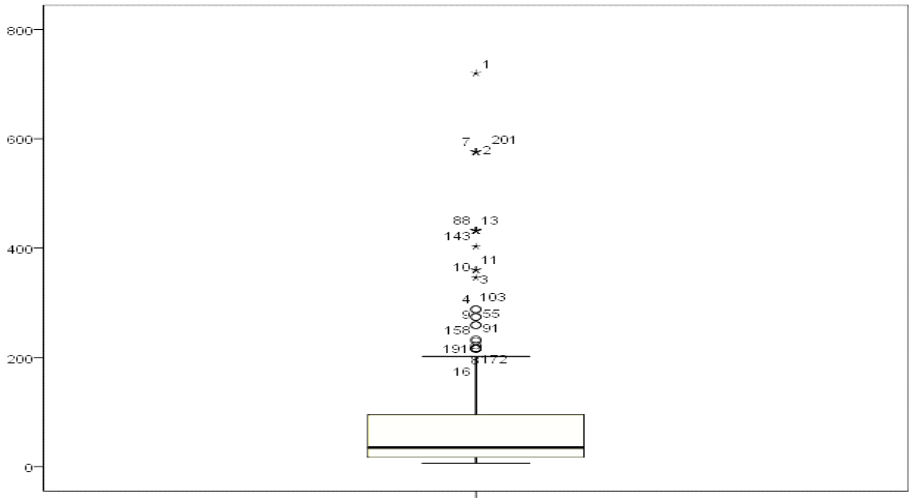

Figure 4 - 5c: Box Plot for Yield (m^3/d) for the Nasia basin

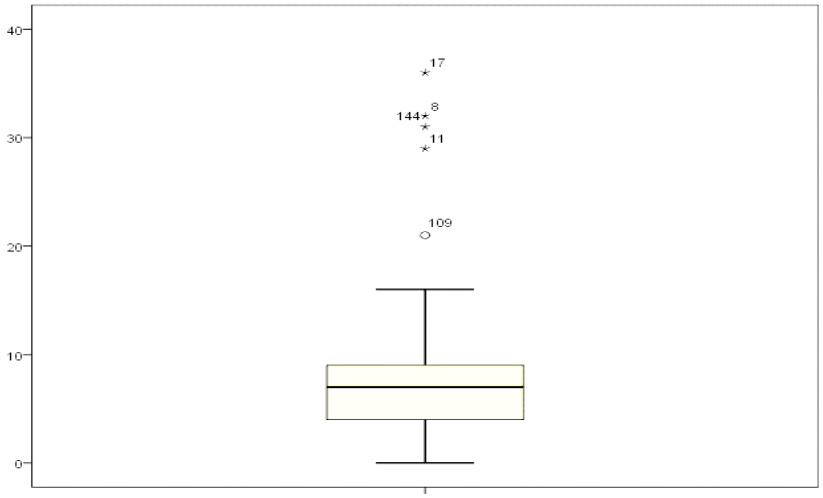

Figure 4 - 5d: Box Plot for SWL (m) for the Nasia basin

Figures 4.5a to 4.5d clearly show extreme variabilities which suggest that a lot of processes influence these parameters in the study area. For instance, the minimum and maximum values for parameters such as depth and yield for the entire study area in Tables 4.2a to 4.2d are 21m -166 m and 5 m^3/d - 720 m^3/d respectively. These extreme variation is an indication of the complexity of the hydrogeology of

the study area and suggest that the parameters are controlled possibly by discrete entities created due to weathering or fracturing (Yidana et al. 2011).

Besides that, depth is mainly influenced by the ability to encounter water as such drilling is stopped once sufficient yield is encountered. In certain situation also, financial considerations influence the depth to which drilling is completed. In order to make savings from these projects, most of the boreholes are completed before at depths not exceeding between 50 m -100 m even when the yields are low.

The data showed in Tables 4.2 (a-d) and Appendix 6, high degree of skewness is displayed which is very common for geoscience data. However multivariate statistical analyses require both normal distribution and homoscedasticity, therefore, all the data were log-transformed as illustrated in Figures 4.6 (a-d) for the entire study area. Even though the transformed parameters do not depict perfect normal distribution, they are however an improvement over the raw data.

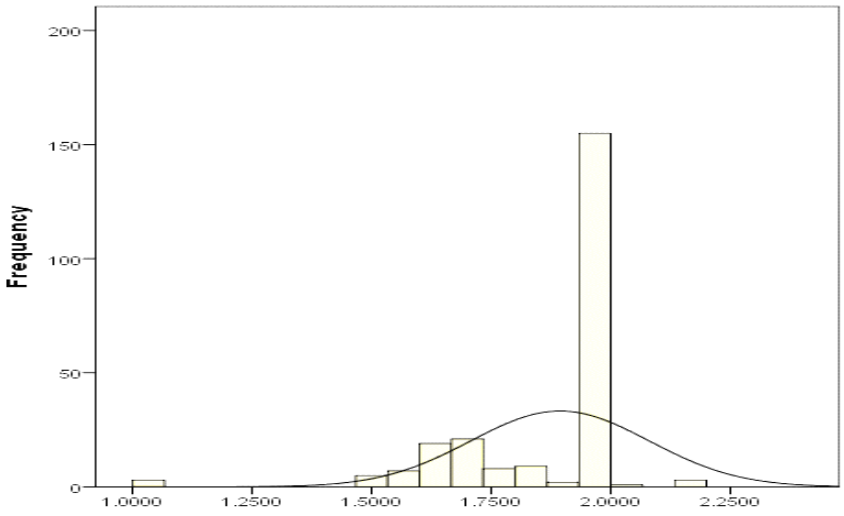

Figure 4 - 6a: Histogram of Log-Transformed Depth (m) for the entire Nasia basin

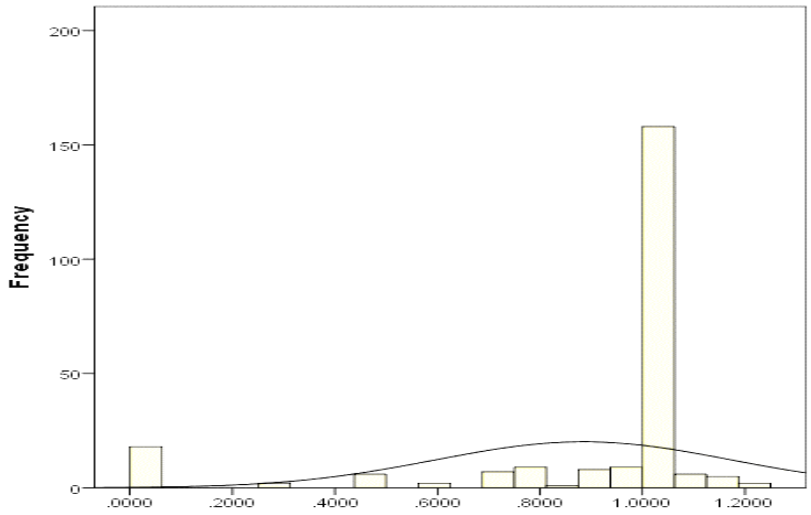

Figure 4 - 6b: Histogram of Log-Transformed Thickness of Regolith (m)

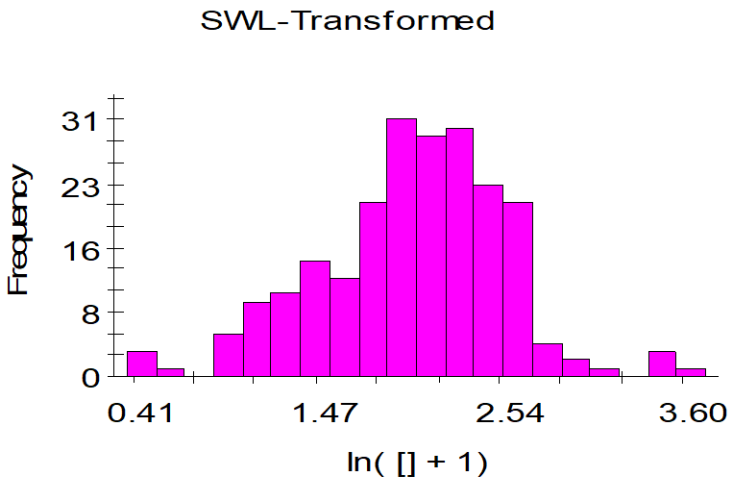

Figure 4 - 6c: Histogram of Log-Transformed SWL (m)

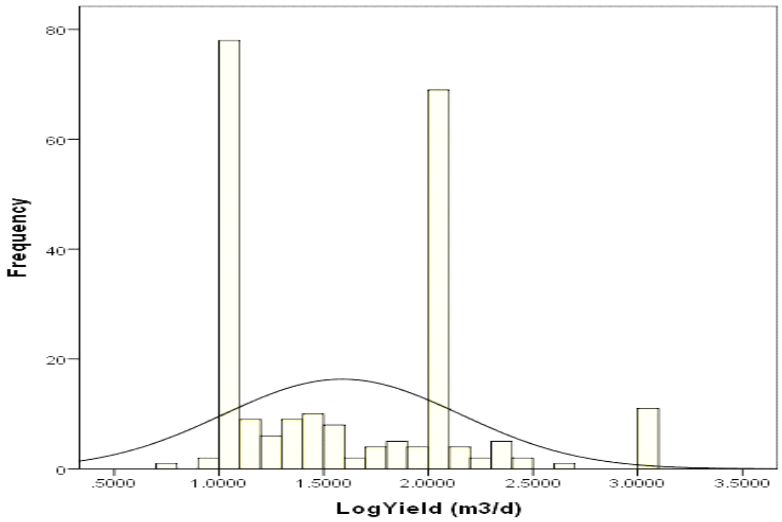

Figure 4 - 6d: Histogram of Log-Transformed Yield for the entire Nasia basin

4.3 Analysis of aquifer response

A total of 67 boreholes pump tested at different duration (6-48 hours) of constant discharge and 3 -12 hours recovery is presented in Appendix 7.

Various geologic and hydrogeologic conditions such as recharge, fracture, groundwater storage in the vicinity of the well can result in a number of different types of drawdown curves.

Figures 4.7a and 4.7b are graphs of drawdown against time which illustrate different aquifer response within the study area.

Figure 4.7a is a graph of constant discharge for a borehole in Daboya No.2 in the West Mamprusi District with drawdown against time. It is observed from the graph that, the curve steeps after 200 minutes which indicates an aquifer limited by boundary of some kind. Calculation of aquifer parameters according to Driscoll (1980) should not be made in any part of the slope of the curve reflecting a boundary. The borehole is situated within the Bimbilla formation and the geologic

log (Appendix 4) shows intercalations of mudstone and siltstone between 18 m – 31 m. Mudstone/Siltstone generally do not produce good aquifers therefore are interpreted as low permeable aquitard under this circumstance and could possibly be the cause of the steepening in Figure 4.7a.

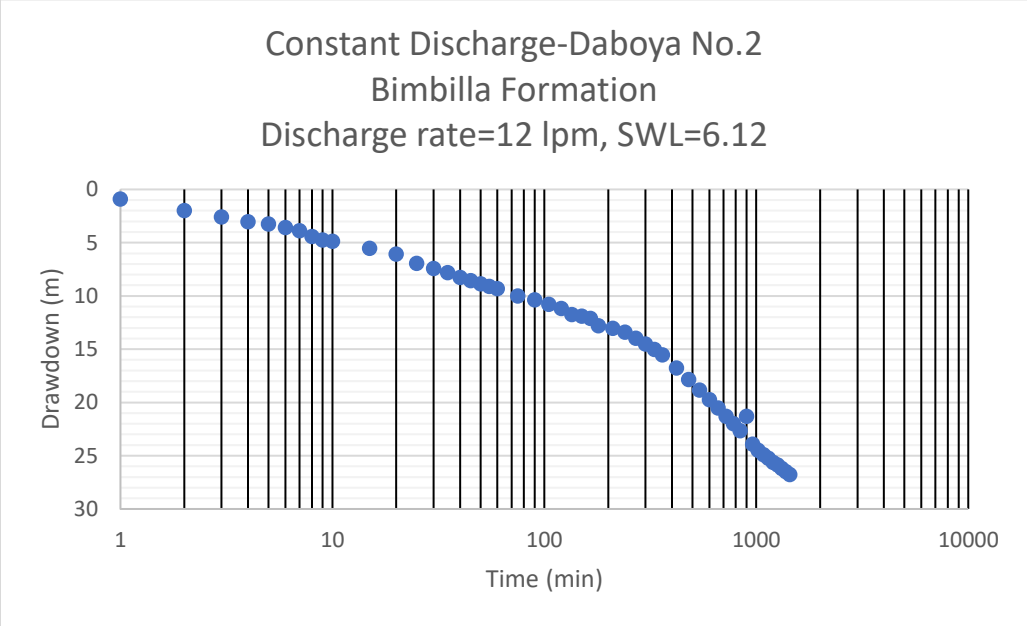

Figure 4 - 7a: A graph of drawdown (m) against Time (min) for Daboya No.2(illustrating boundary condition)

The graph in Figure 4.7b also illustrates a case of well loss for the first 5 minutes with a significant drop in drawdown followed by a good aquifer indicated by the quick response in recovery. This compares well with the observations made by Acheampong and Hess (1998). Within the study area, the Kodjari is known to produce high yielding boreholes and could have accounted for the rapid recovery in yield as seen in the curve. The composition of the Kodjari formation, thus having a distinctive triad of lithologies; basal tillites and diamictons overlain by cap-carbonate and laminated tuffs and ash-rich siltstones. These comprise among

others, matrix-supported conglomeratic lenticles with small pebble size clasts of quartz and various metamorphic lithologies (Carney et al. 2010). These materials have the ability of enhancing secondary permeability and thereby increasing the groundwater potential.

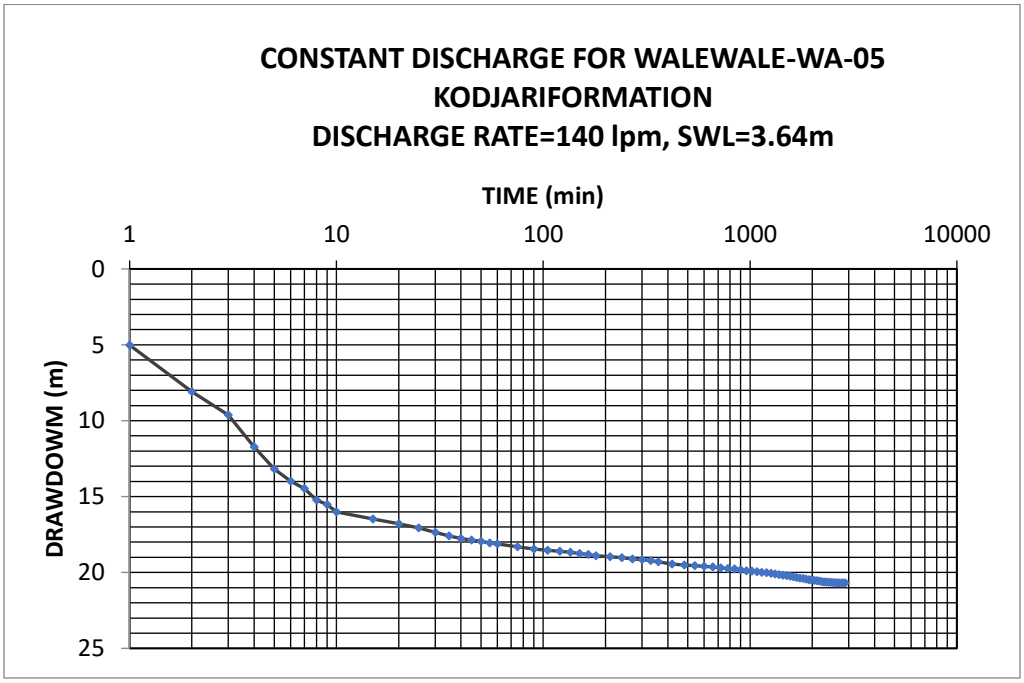

Figure 4 - 7b: Graph of Drawdown (m) against Time (min) for Walewale -WA-05(illustrating well loss and a high yielding aquifer conditions)

4.4 Estimation of hydraulic parameters

Evaluation of the yielding potential of aquifers require fairly an accurate determination of hydraulic characteristics. Several methods are used in estimating these parameters and they include laboratory and pumping test analysis.

4.4.1 Specific Capacity (SC)

Results of specific capacity for the study area are shown in Appendix 9 based on 220 boreholes. The SC was estimated from drawdown after 360 minutes of pumping. The purpose of selecting drawdown after 360 minutes as indicated earlier was to make use of the large secondary data with final drawdown after 6 hours. The specific capacity for the study area ranges between 0.12 m^3/d/m to 960 m^3/d/m with an average of 17.00 m^3/d/m. The specific capacity values are skewed more towards boreholes in the Bunya sandstone member of the Bimbilla formation and the Kodjari formation. The skewness of the specific capacity values is associated with the high yields that have been obtained within these formations. The high mean specific capacity of the boreholes implies they have intercepted either numerous small open fractures or a single fracture (Acheampong and Hess, 1998; Rushton, 1987). The specific capacity values generally are comparable with those of Yidana et al. (2011) except for two boreholes that are located in the Kodjari (Walewale-WA-01 and Walewale 1-Norst). Several other factors such as well setting, pumping duration and aquifer setting (aquifer type) can influence specific capacity (Mace, 2001). Well setting is linked to factors such as the radius (which is inversely proportional to specific capacity) and degree of penetration of the aquifer.

4.4.2 Transmissivity

Various methods were used in estimating transmissivity and they include empirical and geostatistics.

4.4.2.1 Analytical Method of estimating Transmissivity

Transmissivity estimated using the Cooper Jacob (1946) model for single-well test for 26 boreholes with pumping duration varying between 9 hrs and 48 hrs is shown in Appendix 9. The transmissivity in the area varies significantly with a minimum value 0.25 m^2/day and a maximum of 263 m^2/day and an average value of 32 m^2/day. From Appendix 9, it can be deduced that only two borehole had high transmissivity (Walewale-WA-01 and Walewale 1-Norst). Aside these two boreholes, the values of transmissivity compares generally well with the findings of Yidana et al. (2011) and Darko and Krásný (2010) with their transmissivity estimates been below 50 m^2/day. The two boreholes with the high transmissivity values were drilled in the Kodjari formation whilst the boreholes used by (Yidana et al. 2011) were within the Bimbilla formation. The Bimbilla formation beside the Bunya sandstone member are dominated by mudstone/siltstone and generally have low yields. The Kodjari formation on the other hand, is comprised of matrix-supported conglomeratic lenticles with small pebble size clasts of quartz and various metamorphic lithologies (Carney et al. 2010) which are capable of enhancing its permeability. The major limitation with approach of estimating transmissivity has to do with the limited number of boreholes for the entire study area.

4.4.2.2 Empirical Method of estimating Transmissivity

Empirical methods using regression models have been used by (Acheampong and Hess, 1998; Yidana et al. 2011; Yidana et al. 2008) to help in predicting transmissivity in areas with only specific capacity data. The specific capacity and

transmissivity data were log transformed to meet the requirement of normality (Figure 4.8 and Figure 4.9 respectively) prior to being used for the regression model. Though the figures do not represent a perfect normal distribution but are a significant improvement from the raw data. Two categories of regression relationships were conducted, the first involved transmissivity estimates for the entire 26 study area with the corresponding specific capacity. The second regression relationship developed was based on data specific to the geologic formation. LogT was used as the dependent variable and Log SC, the independent variable.

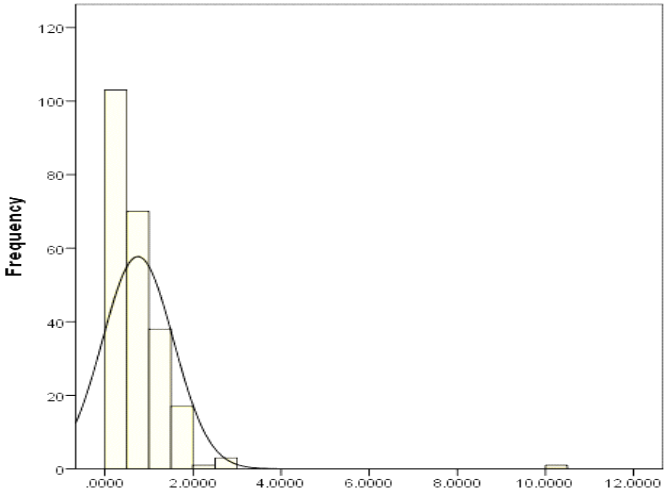

Figure 4 - 8: Log-Transformed Specific Capacity for the Study area

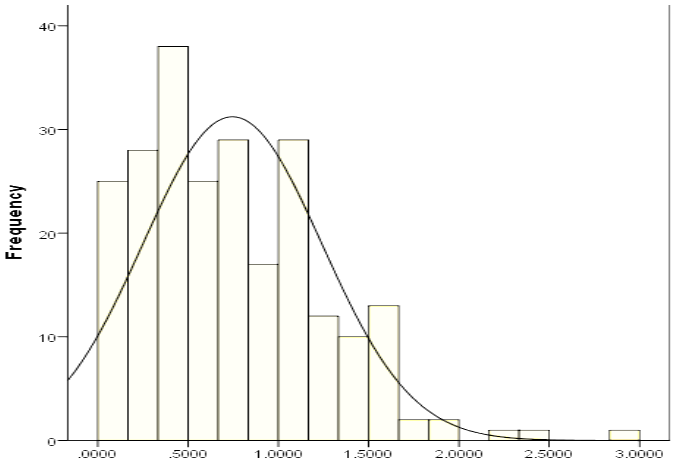

Figure 4 - 9: Log-Transformed Transmissivity for the entire study area

Equation 4.1 and 4.2 illustrate the relationship between 26 transmissivity and corresponding specific capacity data sets for the entire study area.

$$LogT = 0.970\ LogSC + 0.020 \quad (4.1)$$

$$T = 1.047\ SC^{0.970} \quad (4.2)$$

$$R^2 = 0.954$$

The coefficient of determination, R^2, implies that 95 % of the transmissivity in the area is due to the specific capacity data. This value generally implies that the sample size model is good enough to render the model applicable within the Nasia basin. Acheampong and Hess (1998) however indicate that considering the small sample size, the applicability of such a model to the rest of the basin is unclear.

The value of the coefficient of determination suggests high dependence of transmissivity on specific capacity. Researchers like Acheampong and Hess (1988),

Yidana et al (2008) have developed similar relationship but for the Southern part of the Voltaian but this is an improvement similar to Yidana et al. (2011) relationship for a portion of the Northern Voltaian. The coefficient of regression compares well with that of Yidana et al. (2011).

The second regression model (formation-specific) based on data from the Bimbilla, Kodjari and Panabako Sandstone formations. It must be acknowledged that the regression relationship for the formation specific is based on limited data. Most of the pumping test results did not meet a critical assumption in the Cooper-Jacob (1946) method, the requirement for long duration pumping (Kruseman & de Ridder, 1971). They were pumped for less than 6 hours and therefore could not be used for the analysis. The Bimbilla formation had 10 boreholes, the Panabako Sandstone formation 9 boreholes and the Kodjari formation had only 7 boreholes.

The regression relationship for Bimbilla formation is illustrated in equation 4.3 and 4.4, that for the Kodjari is equation 4.5 and 4.6. The Panabako sandstone is represented by equation 4.7 and 4.8.

$$LogT = 0.919\ LogSC + 0.086 \quad (4.3)$$

$$T = 1.219\ SC^{0.919} \quad (4.4)$$

$$R^2 = 0.895$$

The coefficient of determination, R^2, for the rocks within Bimbilla formation is 89.5% which means that the about 90% of the transmissivity in the study area can be predicted by specific capacity.

$$LogT = 0.992\ LogSC + 0.004 \quad (4.5)$$

$$T = 1.009\ SC^{0.992} \quad (4.6)$$

$$R^2 = 0.949$$

From equations 4.5 and 4.6, the coefficient of determination, R^2, suggests that there is a large dependence (over 94%) of aquifer transmissivity on specific capacity within rocks of the Kodjari formation.

$$LogT = 0.942\ LogSC + 0.23 \quad (4.7)$$

$$T = 1.698\ SC^{0.942} \quad (4.8)$$

$$R^2 = 0.976$$

Within the Panabako sandstone formation, a coefficient of determination, R^2, of 97.6% is obtained implying that about 98% of the aquifer transmissivity is influenced by the specific capacity. This value agrees with the model for sandstones estimated by Yidana et al. 2011 for the Northern part of the Voltaian.

The coefficients of determination in all the three formations shown above indicate a strong dependence of transmissivity on specific capacity. Yidana et al. (2011)

indicates that the significance of these models gives credence to the complexity of the Voltaian aquifers significant variations in aquifer properties in space. Thus formation-specific model would yield better optimal results than one relationship that applies to the larger Voltaian.

Though all the coefficient of regression from the equations above suggest a strong relationship, the representativeness and accuracy of the original data used is unclear based on the limited sample size (Acheampong and Hess, 1998; Yidana et al. 2011).

The results of transmissivity calculated from these regression models (equation 4.1 to 4.8) is presented in Appendix 10. A comparison between the transmissivity estimates for the entire study area and that of formation-specific shows a relatively small difference, less than 1.5 m^2/day with most of the values below 0.6 m^2/day. Since the difference between the two set of transmissivity values is not significant, it means that groundwater within the Nasia sub-basin is structurally controlled and not by lithology. In appendix 11 for instance, the thickness of the regolith in all the boreholes is thin and this means, the storage ability of the aquifer would be low and therefore would not be able to contribute to groundwater potential as suggested by Carrier et al. (2008) and Ewusi et al. (2009). The structural control of groundwater in the area is confirmed by researchers such as Yidana et al. (2008) by suggesting that horizontal fractures and joints resulting from secondary fracturing are the main determinants of both transmissivity and specific capacity. Acheampong and Hess (1998) have also indicated that the nature, aperture and degree of interconnection between joints determine the hydrogeological fortunes of the rocks in the area.

4.4.2.3 Geostatistical Method of estimating Transmissivity

To improve on the accuracy of predicting transmissivity with less error based on limited data, cokriging was used by combining 26 transmissivity records and 222 specific capacity data. This approach has been used by researchers such as Aboufirassi and Mariño (1984), Lance et al. (1996) and fairly recently by Razack and Lasm (2006).

To depict the structural character of transmissivity and specific capacity for the terrain, variographic analysis was conducted on these parameters. Experimental variograms of transmissivity (lnT) and specific capacity (ln SC) were determined as shown in Figure 4.12 and 4.13 respectively. Prior to that, the data for transmissivity and specific capacity were transformed from their skewed raw form as shown in Figures 4.10 (a and b) into Figures 4.11 (a and b).

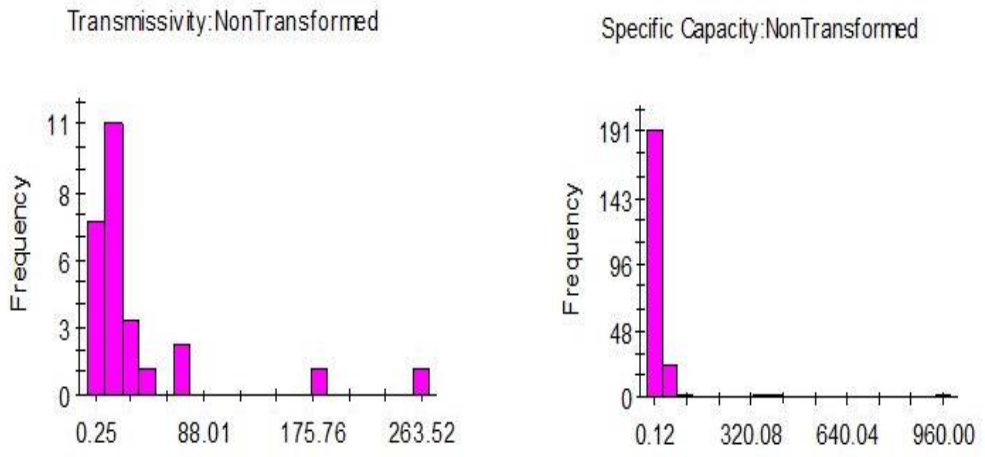

Figure 4 - 10 (a): Untransformed Transmissivity and (b) Specific Capacity

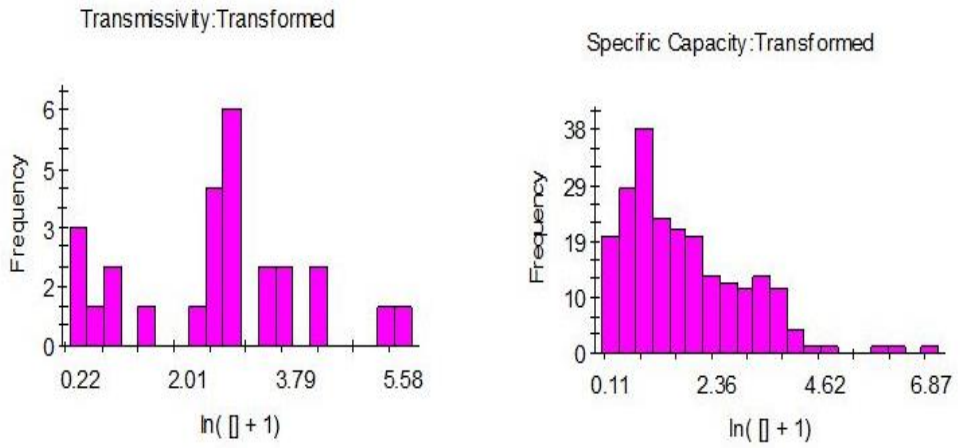

Figure 4 - 11: (a)Transformed Transmissivity and (b) Specific Capacity

The experimental variogram is presented in Figures 4.12 and Figure 4.13 for transmissivity and specific capacity respectively. Both variograms are fitted with a spherical model and their cross variogram is presented in Figures 4.14. Appendix 11 contains cross validated results of the transmissivity and specific capacity which were used in selecting the appropriate model.

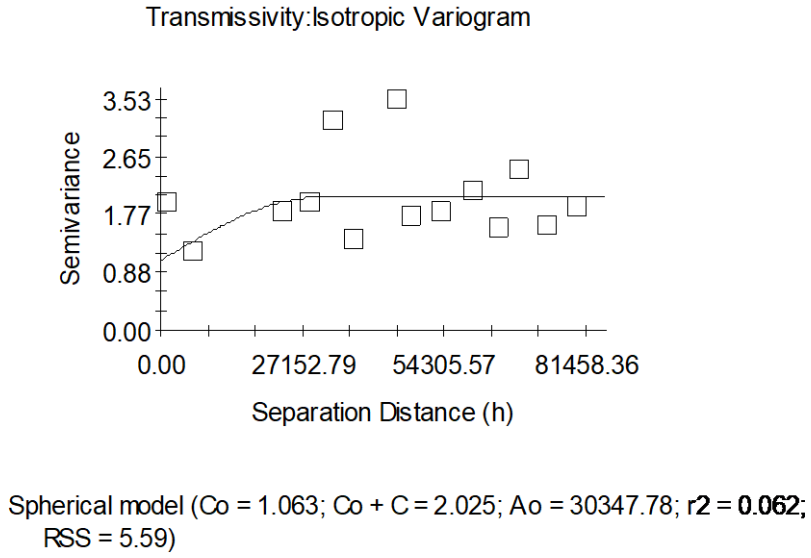

Figure 4 - 12. Experimental variogram and fitted model for Transmissivity

The variogram of Transmissivity displayed in Figure 4.12, has a nugget effect of 1.06 m^4/d^2. The nugget effect indicates that aquifer transmissivity within the terrain is highly variable and significantly controlled by distance. Researchers such as Isaaks and Srivastava (1989) and Razack and Lasm (2006) have associated the occurrence of the nugget effect to either sample errors or subtle variability in the data of the parameter. Several factors account for this variability in aquifer transmissivity in the study area. Yidana et al. (2011) for instance suggest that the variation in thickness of the weathered zone can influence the variability in transmissivity. They associated the variation to the low-grade metamorphism during the Pan-African tectonic event coupled with high temperature and pressure which has reduced the primary permeability of the rocks. Their conclusion was that, hydrogeological properties in the terrain are based on the degree of secondary permeability which varies significantly in the study area. This assertion is supported by Jalludin and Razack (2004) who reported that transmissivity is decreased by the effects such as weathering, hydrothermal and volcanic activities whereas tectonics activities rather enhance transmissivity.

Aside the nugget effect, the variogram has a sill of 2.025 m^4/d^2 which indicates the total variance and it also has a range of 30348 m which indicates the distance between the sampling points at which the sill is reached. The presence of the sill and range indicate that distance has control over transmissivity in the study area. Beyond this range, the variance measured between the data points is independent from the respective data points and therefore correlation does not exist. Other

factors that are likely to contribute to the high degree of variability of transmissivity in the area could be to proximity to stream network, proximity to lineament among others. Rainfall in the study area is erratic as such its contribution to stream network would be seasonal which would lead to a variable transmissivity. Pradhan (2009) suggest that the stream network indirectly influences the groundwater potential of an area due to its relation to surface runoff and permeability.

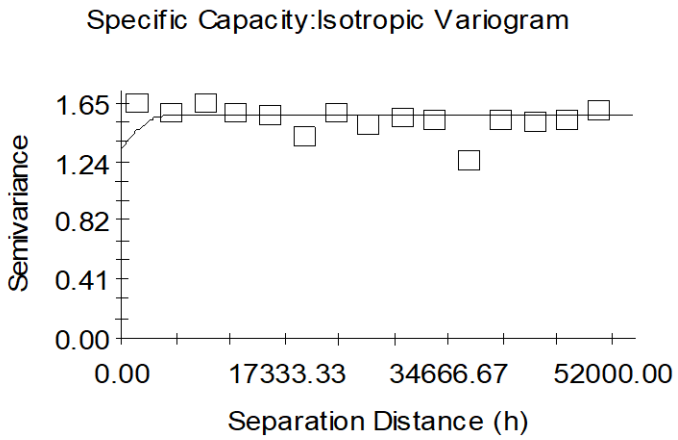

Figure 4 - 13. Experimental variogram and fitted model for Specific Capacity

Specific capacity and transmissivity are closely related and such similar factors would contribute to their distribution in the basin. Figure 4.13 shows that the experimental variogram is fitted with spherical model with a nugget effect of 1.339 $m^6/d^2/m^2$. This means that the parameter under consideration is highly variable and it is controlled by distance. The sill and range of specific capacity from Figure 4.13 are 1.560 $m^6/d^2/m^2$ and 4661m respectively. Specific capacity is related to aquifer setting, well setting and pumping duration (Mace, 2001; and Yidana et al. 2011).

Transmissivity is one of the attributes of aquifer setting and since aquifer transmissivity is highly variable within the terrain, it presupposes that factors that contribute to the variability in transmissivity also affect specific capacity.

A cross variogram of transmissivity and specific capacity is illustrated in Figure 4.14 which has a nugget effect of 1.084 indicating the level of variability of the parameter, a sill of 2.185 that shows the total variance and a range of 3055 which shows the distance at which the variance measured between data points to be independent from the respective data points. Thus, correlation ceases to exist between the points beyond the range.

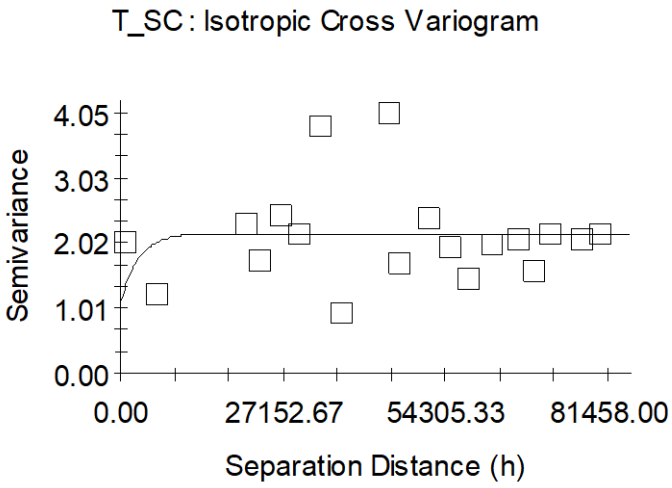

Figure 4 - 14: Cross variogram for transmissivity and specific capacity

4.5. Variographic analysis of hydrogeological parameters

4.5.1 Yield

In order to develop a good kriged map of borehole yield in the study area, 220 boreholes were used to develop a good variogram. The yield data was first transformed from the skewed nature (Figure 4.15 a) to normalized form as shown in Figure 4.15 (b) before being used for the variograms.

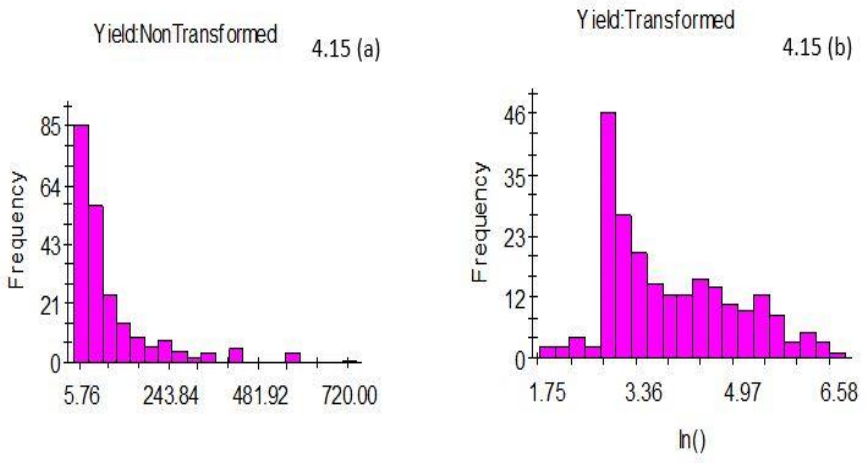

Figure 4 - 15. Histograms of borehole Yield

The transformed yield data shown in Figure 4.15 does not show a perfect normal distribution but rather an improvement over the raw data. The experimental variogram for the borehole yield is presented in Figure 4.16.

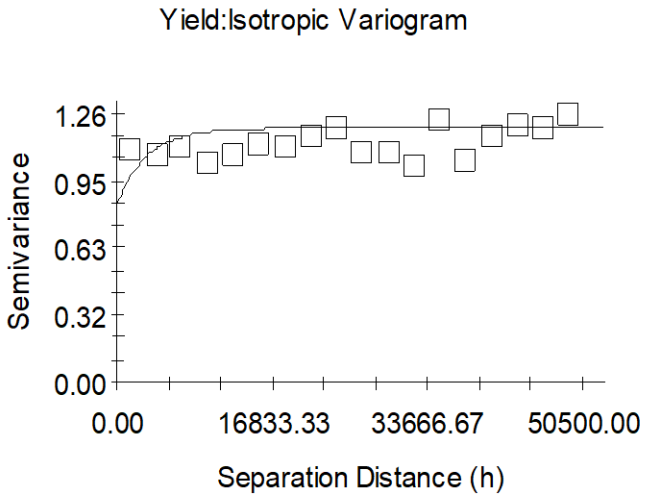

Figure 4 - 16: Variogram of Yield fitted with an exponential model

The variogram of yield shown in Figure 4.16 is fitted with an exponential theoretical model with a nugget effect of 0.843 m^6/d^2, a sill of 1.195 m^6/d^2 and a range of 3253 m. The nugget effect describes the level of variability that is characterized by the study area. This means that borehole yield is significantly controlled by distance. Yield has been reported by many researchers to be influenced by various factors. Nsiah et al. (2018) for instance reports that yield within the Nabogo basin is related to fracturing of the rocks and poor fracture network would contribute to the variability of borehole yield. Acheampong and Hess (1998) as reported by Yidana et al. (2011) that the large variations are controlled by discrete entities created in the wake of weathering and/or fracturing of the primary rock. Darko and Krásný (2010) attribute the variability of yields to the impervious nature of the rocks though they contain structures that enhance

percolation of water to form limited groundwater reservoirs that are structurally dependent and discontinuous in occurrence. Other factors such as slope, proximity of boreholes to stream, the extent of well development, the construction materials used and the appropriateness of the drilling method all have a play in the variability of yield. Inadequate well development and the choice of inappropriate screen for the material of the aquifer zone may also affect the distribution of well yield. The sill and range give an indication of the influence of distance on the yield. The presence of these two attributes of the variogram clearly suggest that distance has control over yield within the study area. The results of cross validation of the yield prior to selection of the appropriate theoretical model is shown in Appendix 13. The purpose of this cross-validation technique is to compare estimated and true values using only yield information available in the sample data set.

4.5.2 Depth

The depth data used for the variographic analysis was first transformed as a requirement for geostatistical measure as shown in Figure 4.17. A total of 220 boreholes with record on depth were used for this analysis. The variogram for the depth of boreholes is displayed in Figure 4.18 which was fitted with an exponential theoretical model.

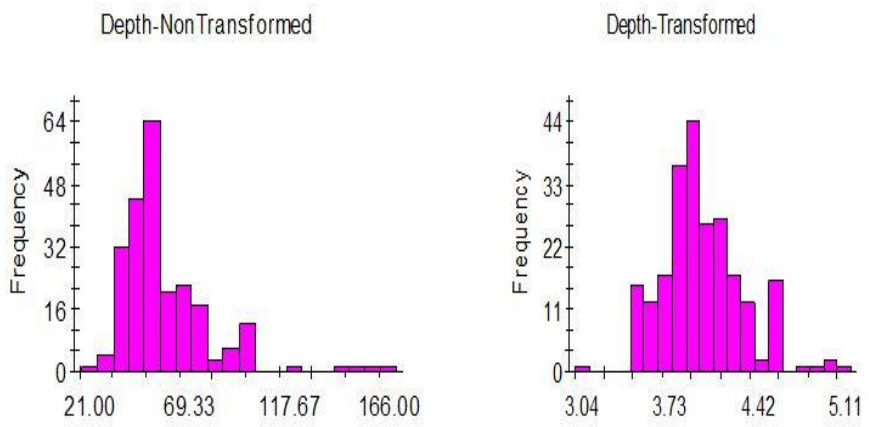

Figure 4 - 17: Histograms showing Depth data

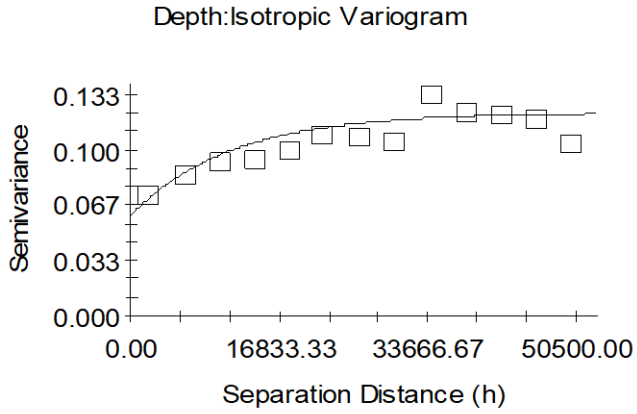

Figure 4 - 18: Variogram of borehole depth fitted with an exponential model

The variogram of depth displayed in figure 4.18 above has a nugget effect which shows the level of variability of depth within the study area. The nugget effect from the above variogram is 0.0607 m^2. The sill and the range for the depth from the variogram are 0.1224 m^2 and 11431m. Appendix 13 contains the cross validated figure of variogram for depth which was used in selecting the appropriate theoretical model. The variability can be associated to the fact that boreholes

generally within the study area are need base. As such the focus has always been to obtain water at a minimum yield of 10 l/min rather than any other reason. Therefore, drilling stops immediately sufficient yield is attained and this does not take in consideration the general depth of drilling in the study. A lot of researchers have attempted to relate borehole yields with depth but no concrete scientific conclusion has been reached so far. Within the Voltaian for instance, Asare and Klitten (2008) evaluated the results of five borehole drilled beyond 100 m. All the boreholes were highly productive however the results contradict that from the HAP monitoring boreholes. Depths beyond 150 m could not even yield up to 10 l/min which refutes any conclusion that would have been made by Asare and Klitten (2008).

4.5.3 Static Water Level (SWL)

Results of the distribution of SWL are shown in Figure 4.19 with raw data (non-transformed) of SWL as well as normalized SWL (transformed).

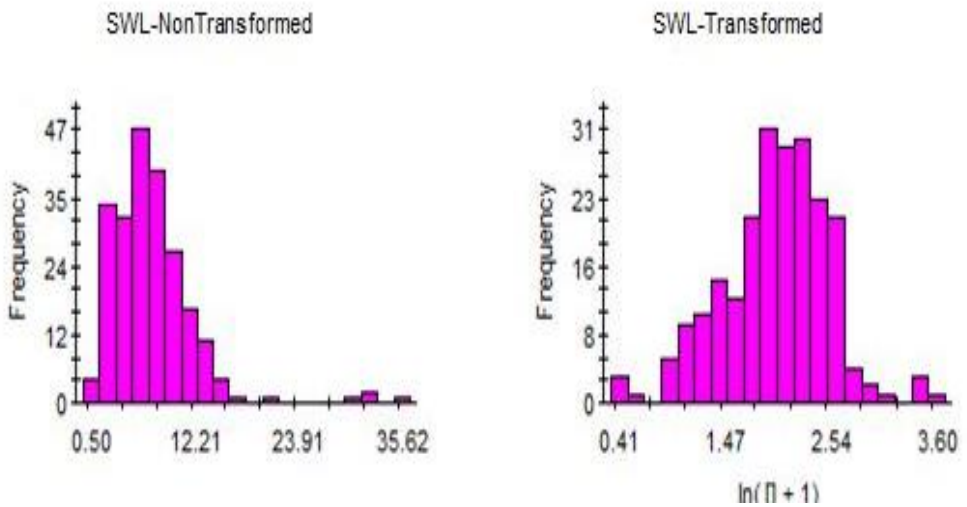

Figure 4 - 19: Histograms showing SWL distribution

The variogram for SWL is shown in figure 4.20 fitted on an exponential theoretical model. The variogram contains a nugget effect with a value of 0.1986 m^2, a sill and a range of 0.2818 m^2 and 423.5 m respectively. Cross validation of the variogram is presented in Appendix 11.

Ayamsegna and Amoateng-Mensah (2002) suggest that, the variation in SWL of boreholes in the terrain is mainly due to excessive usage. Aside that, they also indicated that high temperatures and extended dry seasons are to blame for the early drying up of surface water sources, which could recharge the groundwater system. Forkuor et al. (2013) have confirmed the conclusions of Ayamsegna and Amoateng-Mensah (2002) by suggesting that SWL fluctuates within a range from season to season due to variations in recharge rate and pumpage.

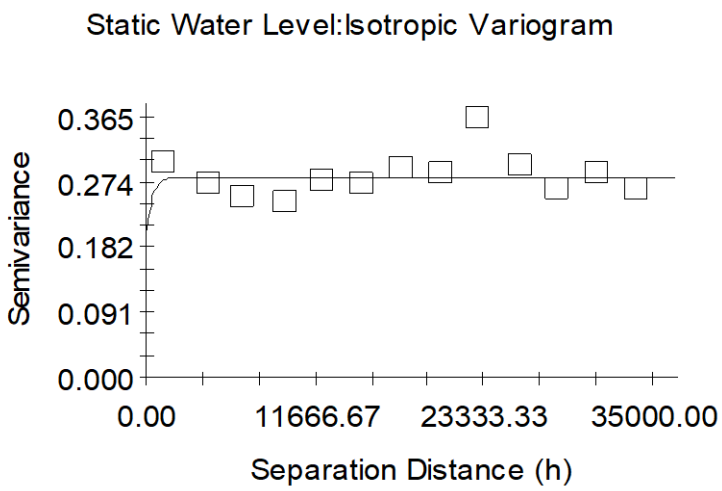

Figure 4 - 20: Variogram of SWL fitted with a variogram

4.5.4 *Regolith*

Regolith has been defined by Eggleton (2001) as the entire unconsolidated or secondarily re-cemented cover that overlies more coherent bedrock that has been formed by weathering, erosion, transport and/or deposition of the older material

The regolith for this study area was determined from geological logs of successful boreholes totaling 220. Figure 4.21 is an illustration of a raw data without transformation (left) and also the transformed data (right). This was necessary since the raw data is skewed and would require being normalized for geostatistical analysis.

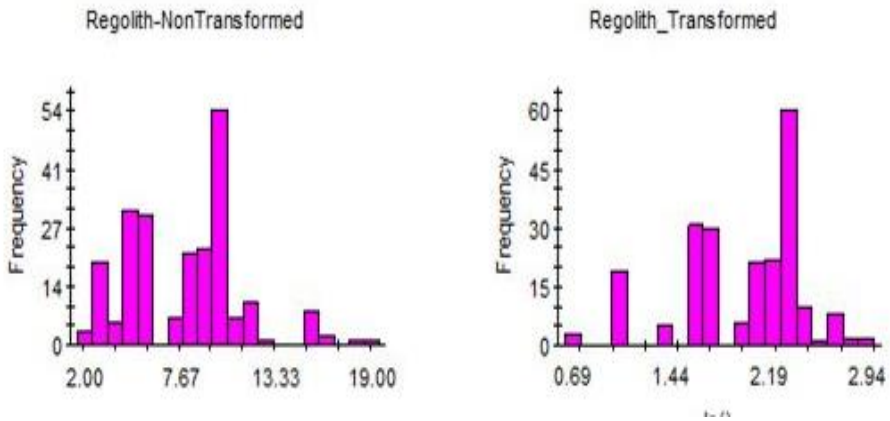

Figure 4 - 21. Histogram showing distribution of raw and transformed Regolith

The variogram for the regolith is shown in Figure 4.22, fitted with an exponential theoretical model. The nugget effect of is 0.1304 m^2/y^2, the sill and the range are 0.2207 m^2/y^2 and 3327 m respectively. The results for the cross validation of the regolith is presented in Appendix 11. Even though the regolith is relatively thin, the level of variability is significant as seen in the nugget effect. MacDonald et al. (2001) and Carrier et al. (2008) suggest that the relatively thin regolith may be as a

result of the presence of stable clay or the presence of quartz in sandstones, which are resistant to weathering.

The regolith can also significantly be affected by topography. Generally, locations with high topography such as the Gambaga areas under the Panabako sandstone formation are exposed more to weathering than low topographic areas due to gradient. Larger surface areas of the high topographic area are available for the breakdown of the geologic materials.

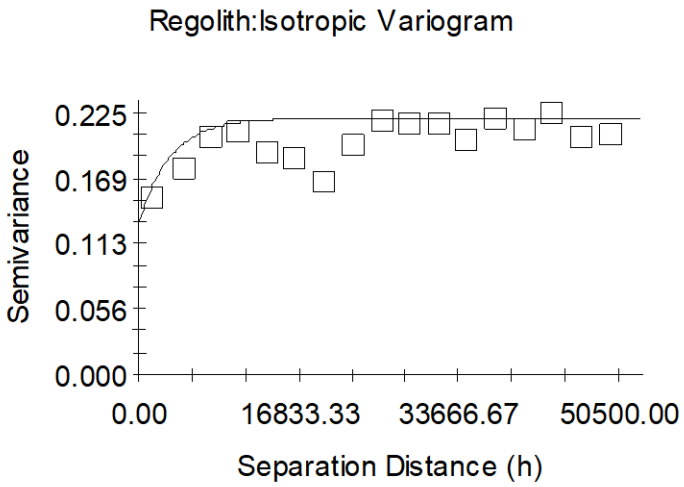

Figure 4 - 22: Variogram of Regolith fitted with an exponential model

4.5.5 Recharge

A total of 73 data points was used in performing this analysis. The recharge for this study are based on values quoted by Addai et al. (2016) using the Chloride Mass Balance method (Appendix 8).

The data was transformed from its raw skewed nature for normal distribution as shown in Figure 4.23.

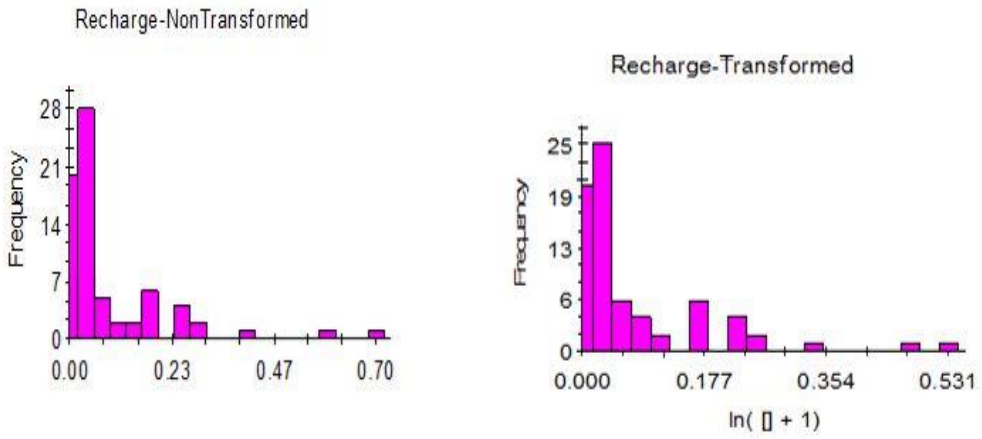

Figure 4 - 23: Histograms showing the distribution of Recharge

The variogram for the recharge is displayed in Figure 4.24 and it is fitted with an exponential theoretical model. The model has a nugget effect of 0.00667 m^2/yr^2, a sill and a range of 0.01251 m^2/yr^2 and 8364 m respectively. Appendix 11 contains the results of the cross validation of recharge.

Recharge in the study area is prominent during the wet season when meteoric water goes beyond the permeable portions of the lateritic and sandy soils through the weathered zone into the fractured aquifer, particularly in places where there is hydraulic continuity between the weathered zone and the underlying fissures.

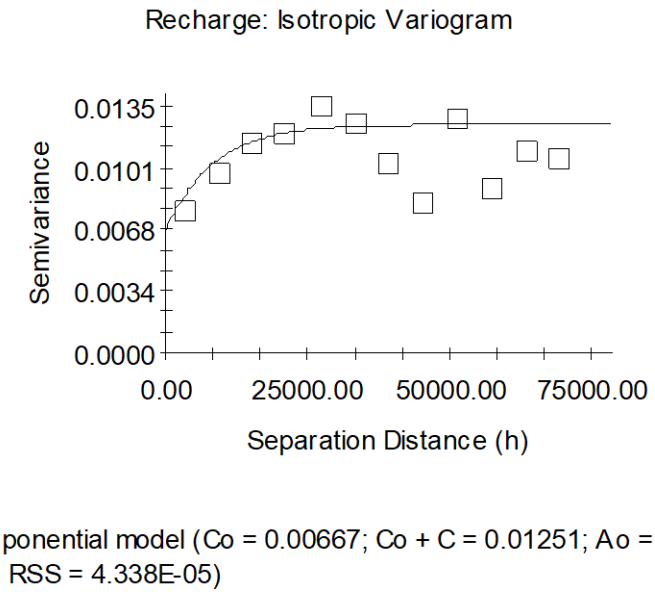

Figure 4 - 24: Variogram for Recharge fitted with an exponential model

The nugget effect implies that recharge in the area is highly variable and as Carrier et al. (2008) indicates that, the spatial variability is related to the nature of the material of the unsaturated zone and the variability in rainfall patterns. Apambire (2000) suggest that recharge is variable and based his estimates on a function of lithology and total annual rainfall. According to Forkuor et al. (2013), factors such as geology, rainfall (intensity and distribution), land use, and soil type have been quoted by Sandwidi (2007) and Obuobie (2008) as the cause of variability to recharge.

4.6 Groundwater Potential Map

The groundwater potential map was developed from Remote Sensing and Geographic Information System using multi criteria analysis (weighted overlay technique). The procedures used by Gumma and Pavelic (2013) were implemented in developing the groundwater potential map.

4.6.1 Thematic/Interpolation Maps

Interpolation maps were developed for all the hydrogeological parameters that influence groundwater potential within the study area. Kriging and cokriging geostatistical techniques of interpolation were used based on the results of the variograms for each of the hydrogeological parameter.

4.6.1.1 Aquifer Transmissivity

Figure 4.27 shows the results of cokriging to estimate aquifer transmissivity for the study area. The aquifer transmissivity appears to be low/moderate from the NE direction and increases towards the middle part of the study area. Then finally reduces towards the SW around Janga. The high transmissivity zone observed in the middle portion is associated with the Kodjari formation which according to Ó Dochartaigh (2011) is the most productive in the terrain in terms of groundwater potential. High transmissivity also noticed around the south west portion of the study area. These are associated with the Bunya sandstone members within the Bimbilla formation. It is observed that the locations showing high transmissivity are also having high values for yield.

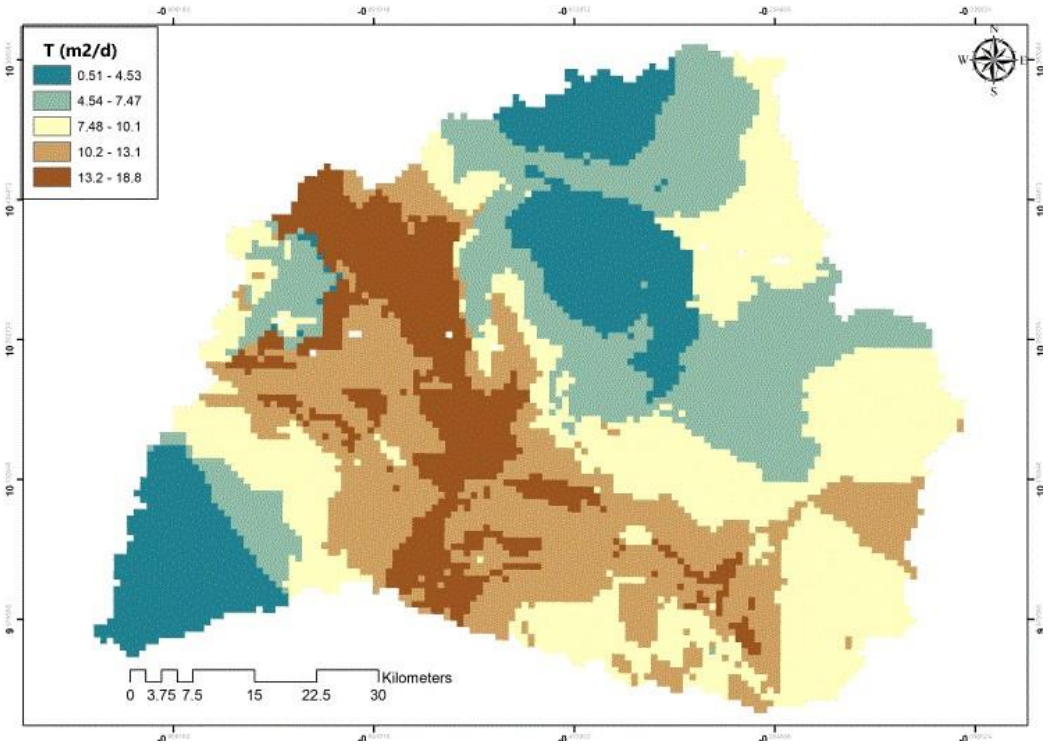

Figure 4 - 27: 2-D Spatial distribution of aquifer transmissivity from cokriging for the study area

4.6.1.2 Specific Capacity

Spatial distribution map of specific capacity based on variograms developed in the study area is presented in Figure 4.28. The specific capacity map follows the same pattern as the transmissivity map. From the two maps shown in Figure 4.28 below, it is obvious that about two thirds of the study fall within the low specific capacity zone with values below 5 m^3/d/m. Comparing this specific capacity map with the geological map of the study area clearly shows that the low values are associated with rocks of the Panabako sandstone formation possibly places without fractures. The Poubogou and the Bimbilla formations also show indication of low values which maybe because of the dominant impermeable mudstone-siltstone rock type

with very low potential for groundwater. The middle part of the study area corresponds to the Kodjari formation and the lower part of the study area is within the Bunya Sandstone member of the Bimbilla formation. These two locations show indications of medium to high specific capacity. There are few spots within the Panabako Sandstone that show high values of specific capacity. The results from the map follows the trend observed by Ó Dochartaigh et al. (2011)

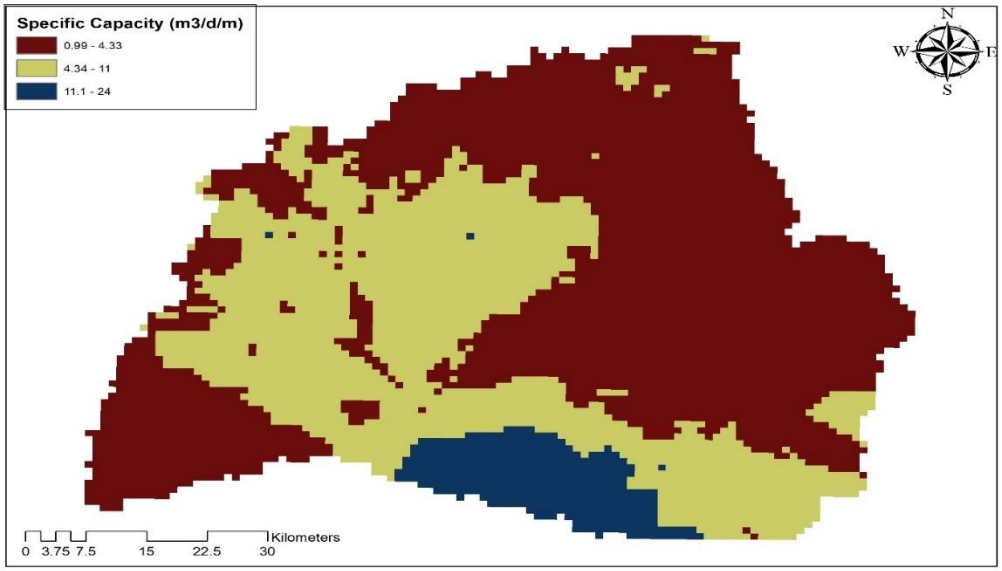

Figure 4 - 28: Spatial distribution of Specific Capacity in the study area

4.6.1.3 Depth

The spatial distribution of depth in the study area is shown in the kriged map presented in Figure 2.29. The map shows that most of the boreholes in the study area are drilled to depth less than 60m with few boreholes beyond 60m. The variability of depth is mainly because most boreholes are based on community need as such drilling ends as soon as an appreciable yield is obtained.

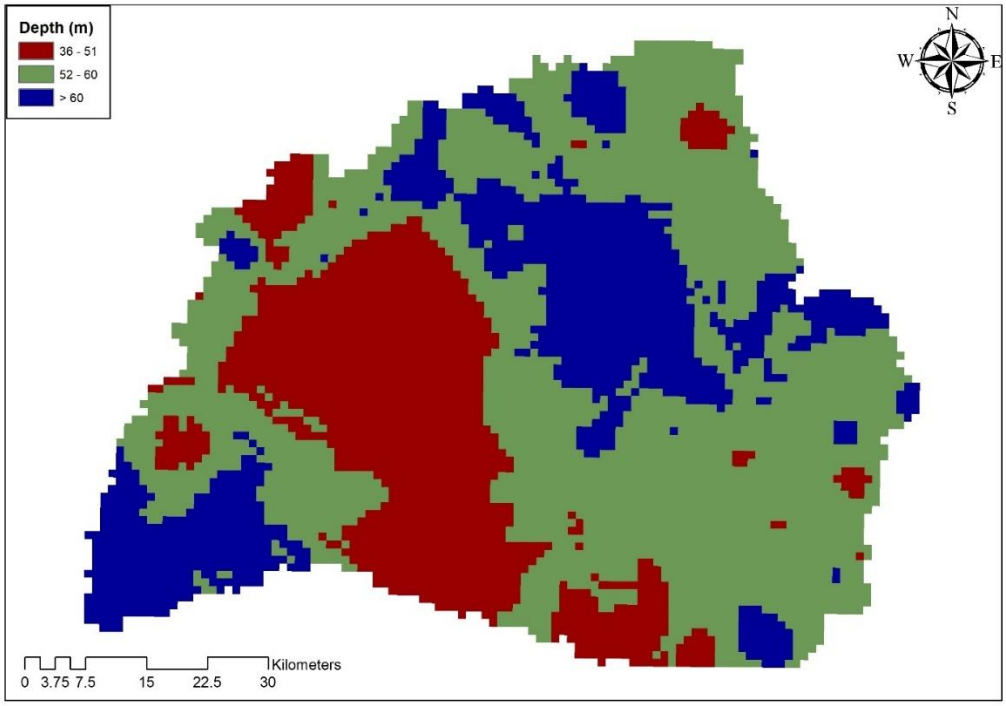

Figure 4 - 29: Spatial distribution of Depth of productive boreholes in the study area.

4.6.1.4 Thickness of Regolith

The spatial distribution of the thickness of the weathered zone in the study area is depicted in the kriged image of Figure 4.30. Generally, there is a thin thickness of the regolith in the study area. This compares with the conclusions made by Carrier et al. (2008) for the entire Voltaian basin. It can be observed that most of the boreholes covering about two-thirds of the study area have a thickness of approximately 7m. There are however pockets of relatively thicker weathered zones, more than 10m scattered about the study area. The north eastern and south western part of the study area have slightly higher weathered zone thickness.

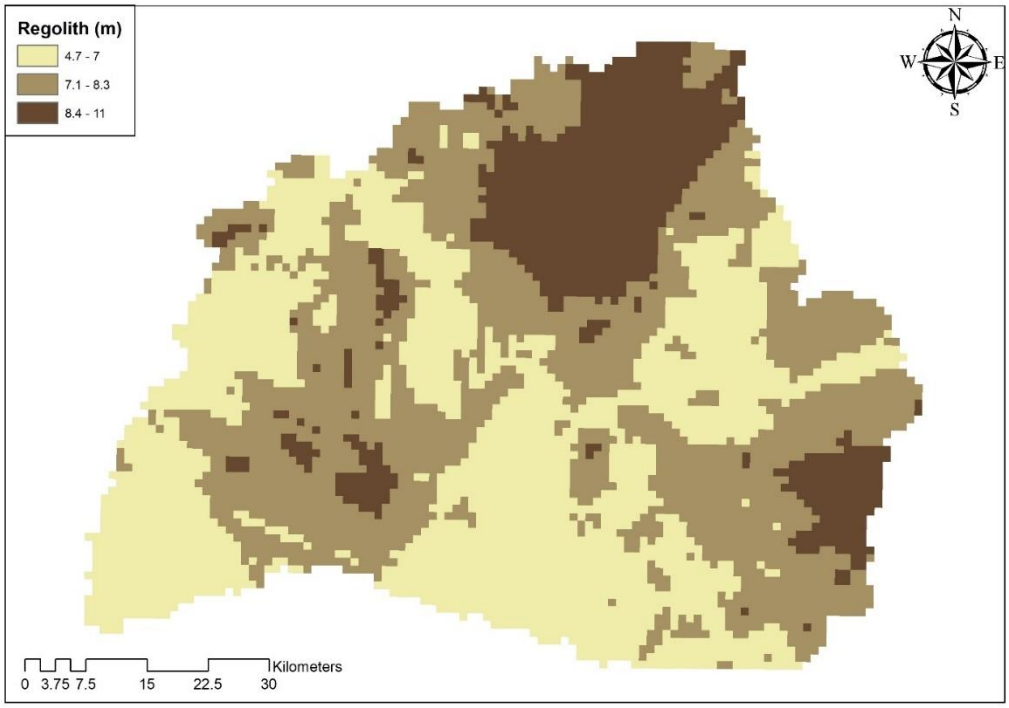

Figure 4 - 30: 2-D Spatial distribution of Regolith in the study area

4.6.1.5 Static Water Level (SWL)

Figure 4.31 shows a kriged 2-D spatial distribution of static water level in the study area. It is observed that, the middle portion towards the eastern part of the study have low SWL below 6m. These areas are underlain by rocks of the Kodjari and Panabako sandstone formations and similar trend is also observed in the spatial distribution of specific capacity and transmissivity of the study area. High SWL is recorded for boreholes located within the Bimbilla formation and a small part of the Panabako Sandstone formation (North of the study area). SWL may fluctuate within a range partly due to variation in recharge and demand from pumpage (Forkuor et al. 2013). The high values of SWL indicate that access to groundwater is a challenge and the vice versa for low SWL. The Bimbilla formation is generally

considered to have low groundwater due to the impermeable mudstone/siltstone rocks that dominate the formation.

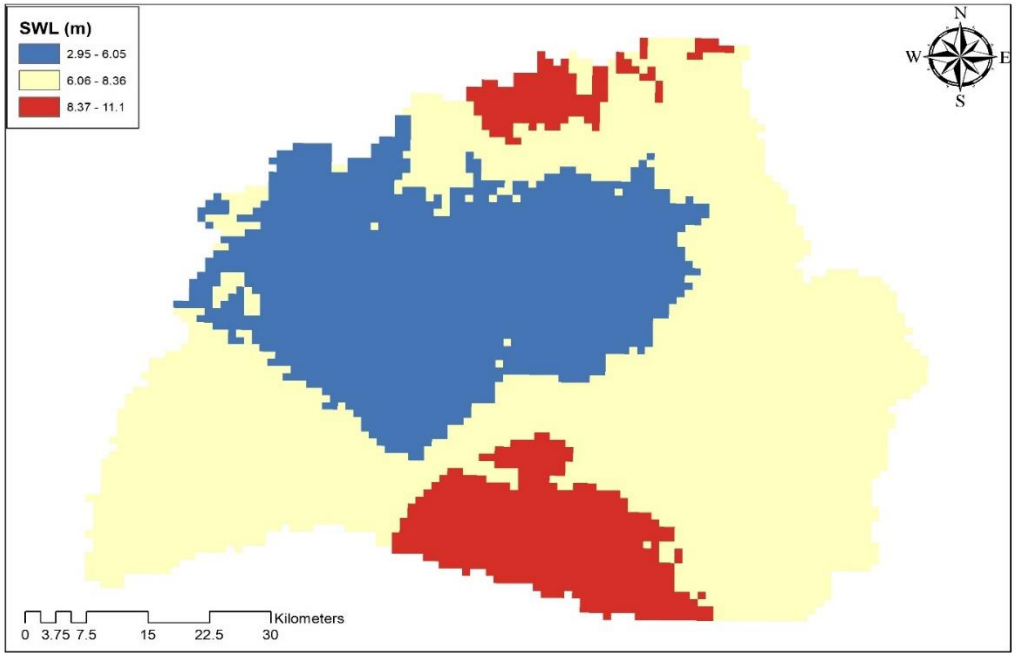

Figure 4 - 31: 2-D Spatial distribution of SWL in the study area

4.6.1.6 Yield

The kriged yield map of the study area is shown in Figure 4.32. The map shows a general feature of low yield across the study area with some level of variability which can be attributed to the fact that the entities considered as water bearing structures are discrete (Acheampong and Hess, 1988). The variability of yield in the study area supports the assertion that groundwater occurrence is mainly due to secondary permeability. The high yielding boreholes are located in the southern part of the study area which is within the Bunya sandstone member and few spots

within the central part of the study area (Kodjari formation). The potential of the Bunya sandstone member has been stated by Ó Dochartaigh *et al.* (2011) as very favourable for groundwater occurrence.

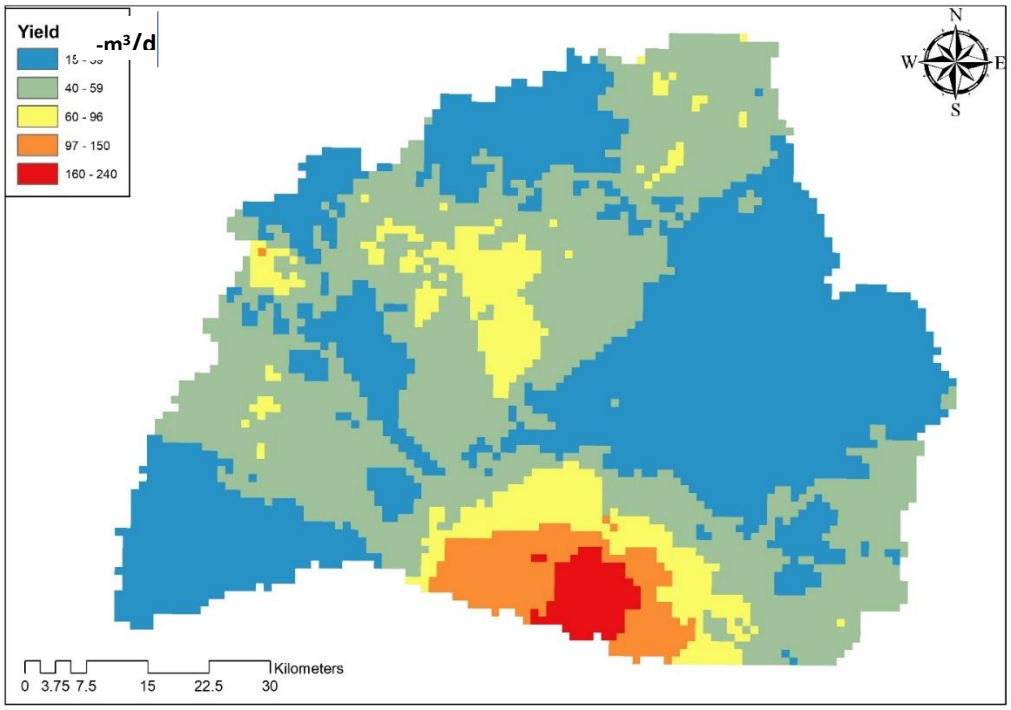

Figure 4 - 32: Spatial distribution of Yield in the study area

4.6.1.7 Drainage density

The drainage density for the study area is shown in Figure 4.34. The drainage mimics the major river (River Nasia). The flow is from the east and terminates at the south west. Overall, higher drainage densities are noted in the south east and south west parts (Bimbilla formation) than in the northern side (Kodjari and Panabako sandstone formations) of the study area.

High drainage density implies that a large proportion of the precipitation goes as surface runoff which explains why the Bimbilla formation has low groundwater

potential. Low drainage density suggests that, rainfall infiltrates the ground and few channels are required to carry the runoff.

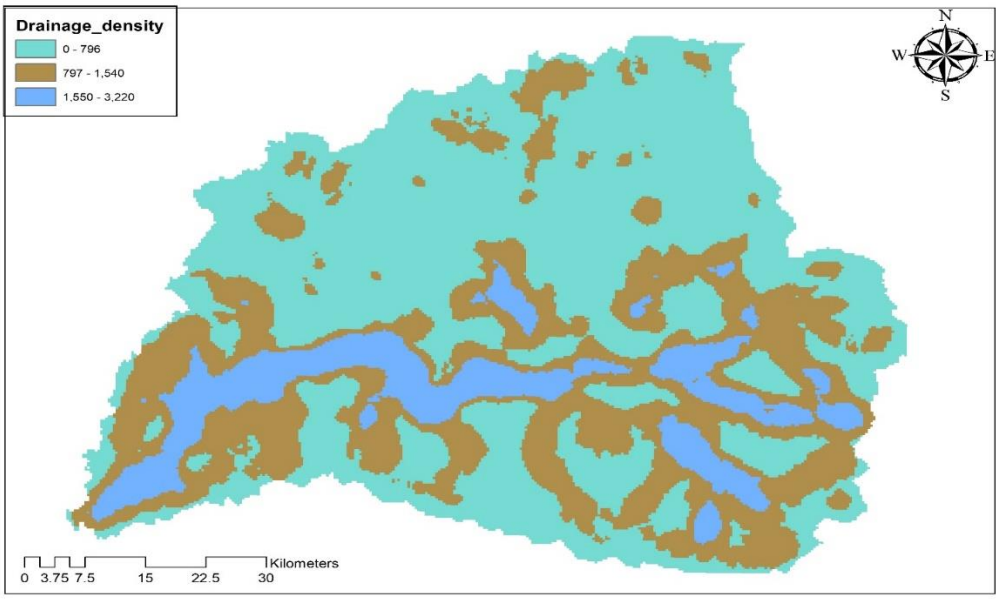

Figure 4 - 33: Drainage Density in the study area

4.6.1.8 Recharge

Figure 4.34 shows the spatial distribution of recharge in the study area. Groundwater recharge potential can be considered to be relatively high in the central part and low in the rest of the study area. It is observed that the recharge follows the pattern of the drainage density. This could mean that groundwater is recharged mainly from drainage system which is as a result of infiltration from rainfall. The low recharge is attributed to the significant clay content in the

overburden which tends to impede vertical infiltration and percolation (Attandoh et al. 2013).

4.6.1.9 Slope

The slope of the study area is presented in Figure 4.35. Areas with steep slopes such as the Northern part of the area which has the Gambaga escarpment will have more run off occurring leading to reduced infiltration. Magesh et al. (2011) suggests that this will reduce recharge which eventually will affect groundwater potential. As infiltration is inversely related to slope, a gentle slope promotes an appreciable groundwater infiltration.

From the slope map it can be seen that the central part of the study area has nearly level and gentle slopes which means these areas are more likely to have higher infiltration and therefore higher recharge. It is observed that the slope and drainage density share similar patterns, thus higher values towards lower portion of north west (Janga community). Nearly level slope and gentle slope are favourable for groundwater accumulation since the resident time for rainwater is longer compared to steeply sloping surfaces (Arnous, 2016; Waikar and Nilawar, 2014).

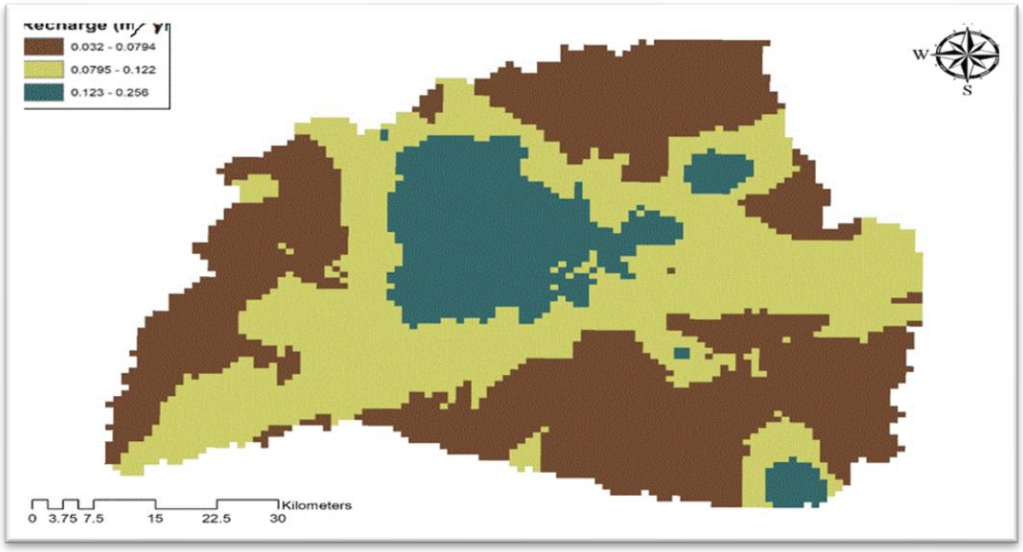

Figure 4 - 34: Spatial distribution of Recharge in the study area

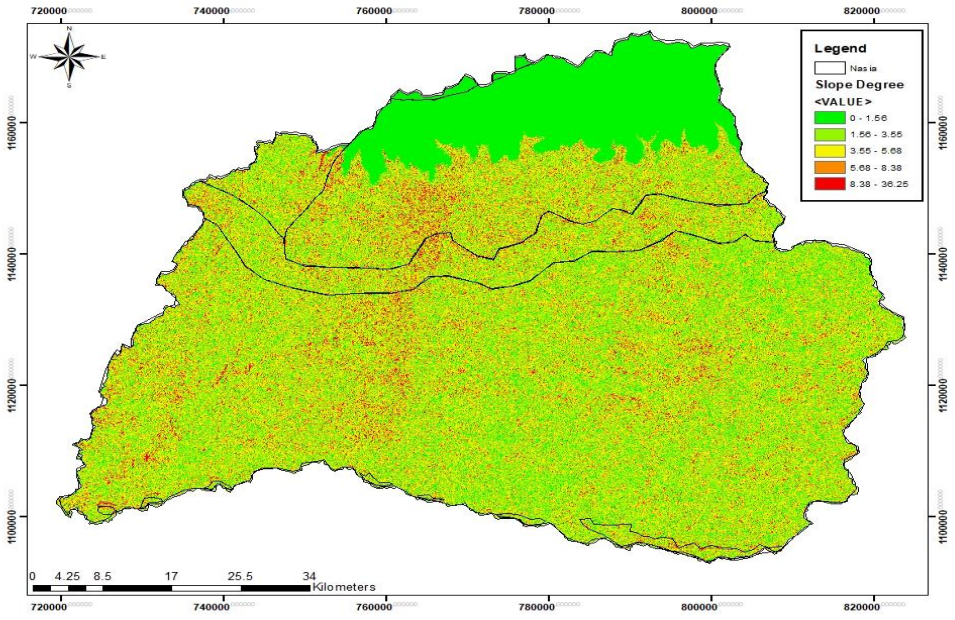

Figure 4 - 35: Slope in the study area

4.6.1.10 Lineament

The general pattern of lineament in Figure 4.37 is E-W direction with a few in the NW-SE direction. The presence of the lineaments can be attributed to both geologic

and geomorphic processes like fractures or linear valleys which contribute in accumulation of groundwater in the subsurface. More lineament features are observed in the middle and upper portion of the study which could explain the relative high groundwater in those areas.

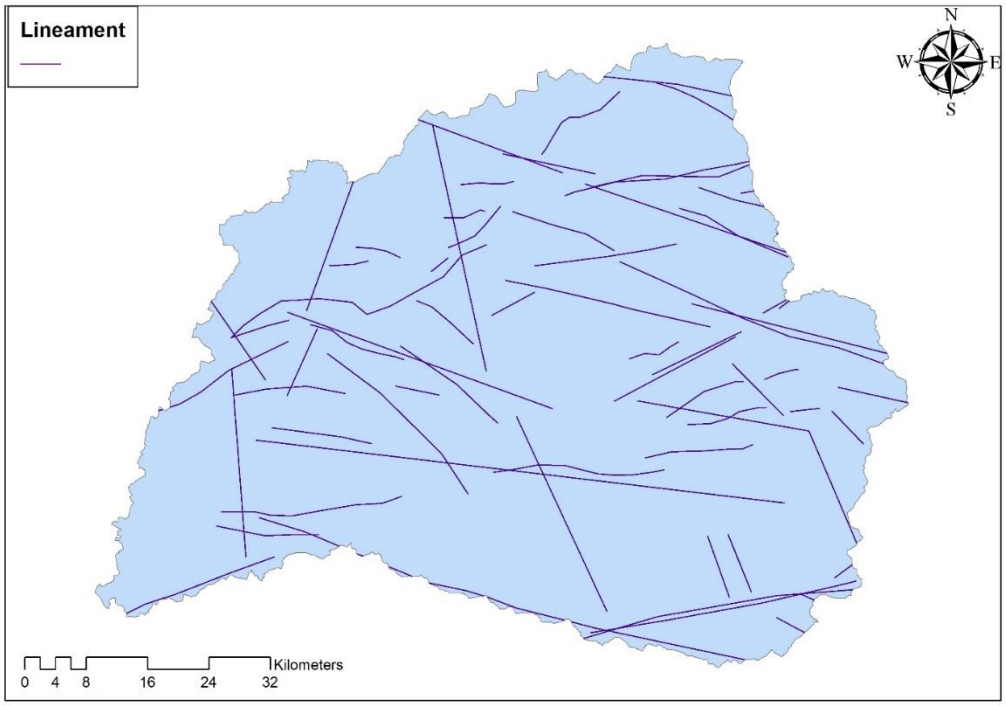

Figure 4 - 36: Lineament map of the study area

4.6.2 Multi Criteria Analysis (Weighted Overlay Technique)

4.6.2.1 Reclassification of parameters

All the thematic layers for the various parameters were reclassified as a requirement for the multicriteria analysis. The values for the reclassification ranged between 1 and 5 depending on the variability of the parameter. The borehole depth was reclassified into three categories based on the available data, a thorough evaluation

of borehole records and knowledge from experience in drilling boreholes in the study area. The acceptable depth of borehole by Community Water and Sanitation Agency (CWSA) is 40 m, but most boreholes drilled averaged around 60m and maximum of 100m. Therefore, the manual function in Arc GIS 10.6 classification criteria was used to classify depth into three (3) categories. Figure 4.38 is an illustration of how the rescaling of depth for the area was performed. The SWL layer was zoned into three using natural breaks of values (Figure 4.39). Low values were interpreted to have high potential for groundwater because some of those boreholes are very productive even in the dry season compared with boreholes where the SWLs are high. Further to that, the shallower depths indicates the groundwater is easily accessible (Martin & van de Giesen, 2005). Transmissivity was divided into 5 classes using the natural break function of classification in Arc GIS 10.6. The purpose of using the natural break function is to cater for the heterogeneous nature of the terrain. Figure 4.40 is an illustration of how the reclassification was performed.

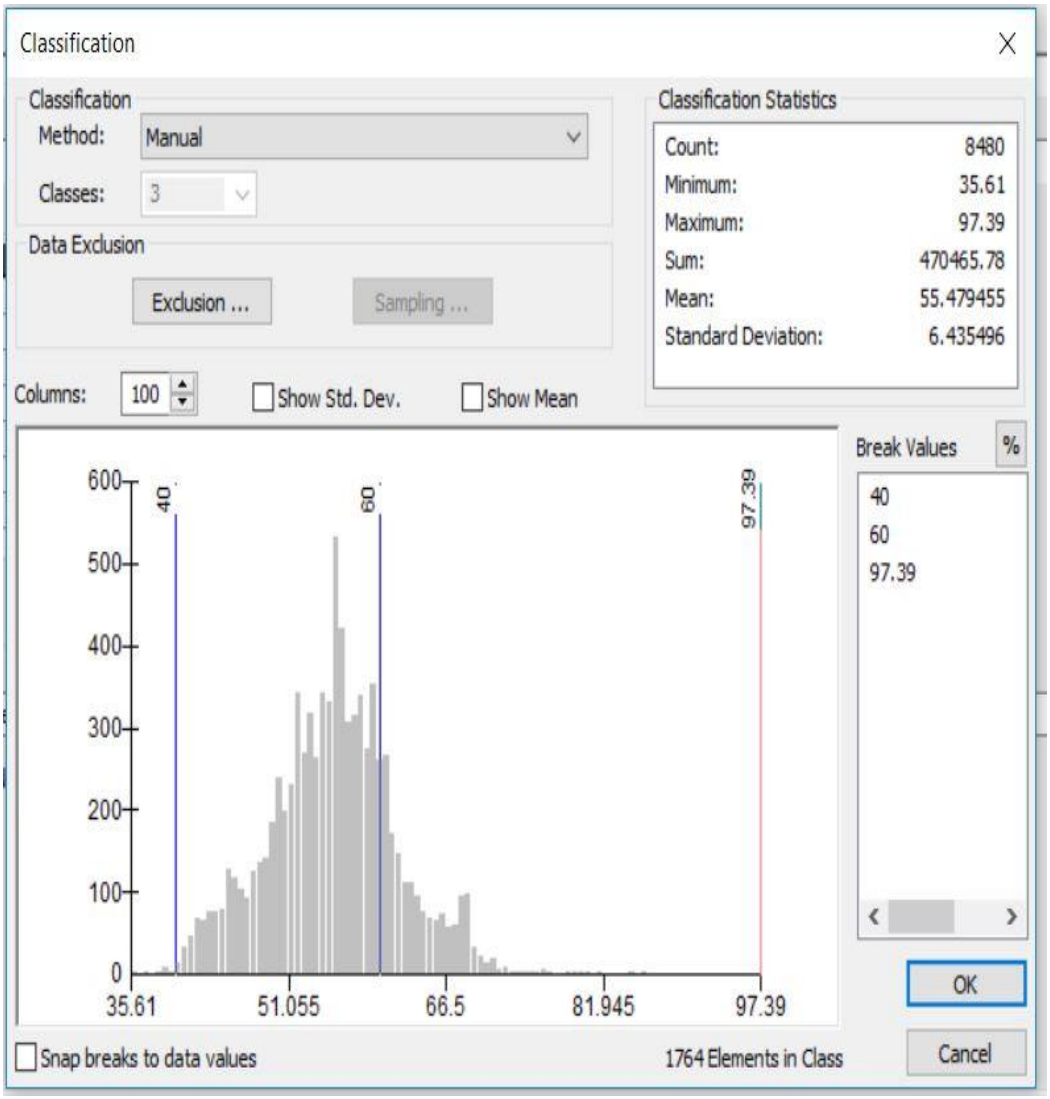

Figure 4 - 37: Reclassification of Depth of borehole

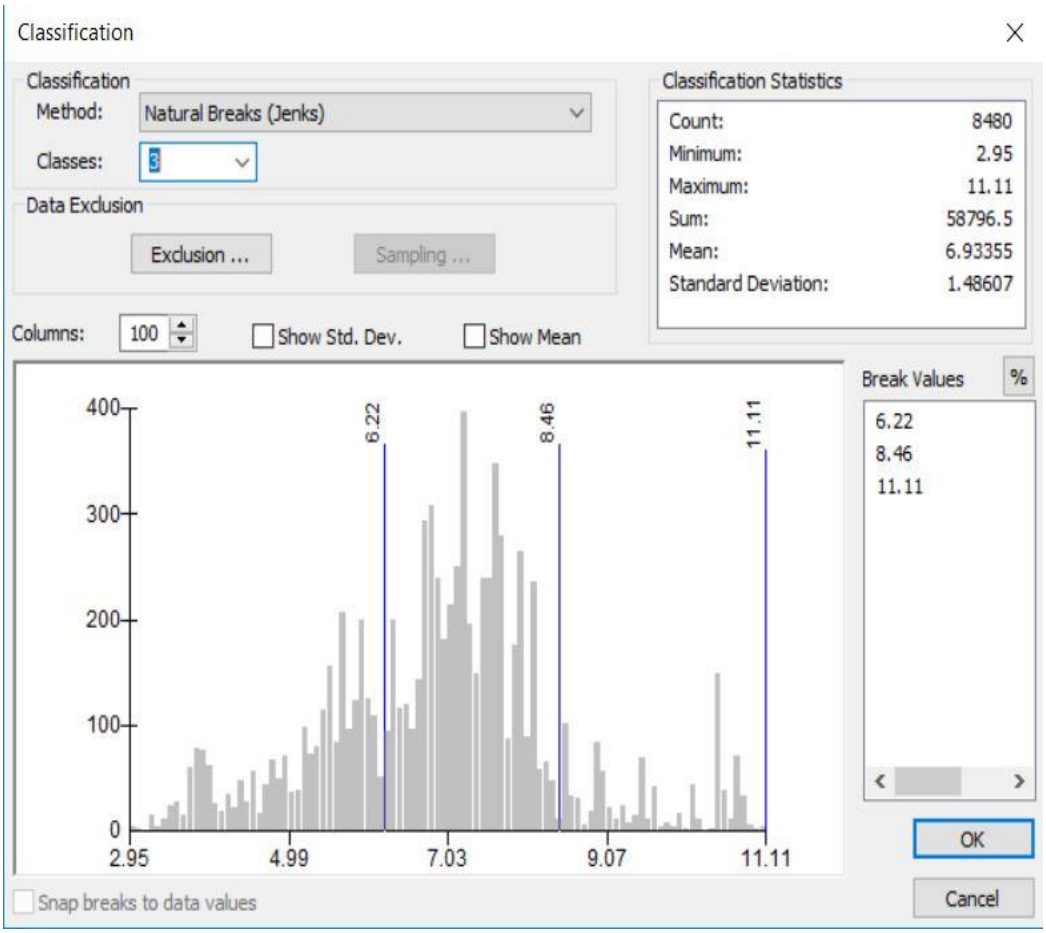

Figure 4 - 38: Reclassification of SWL

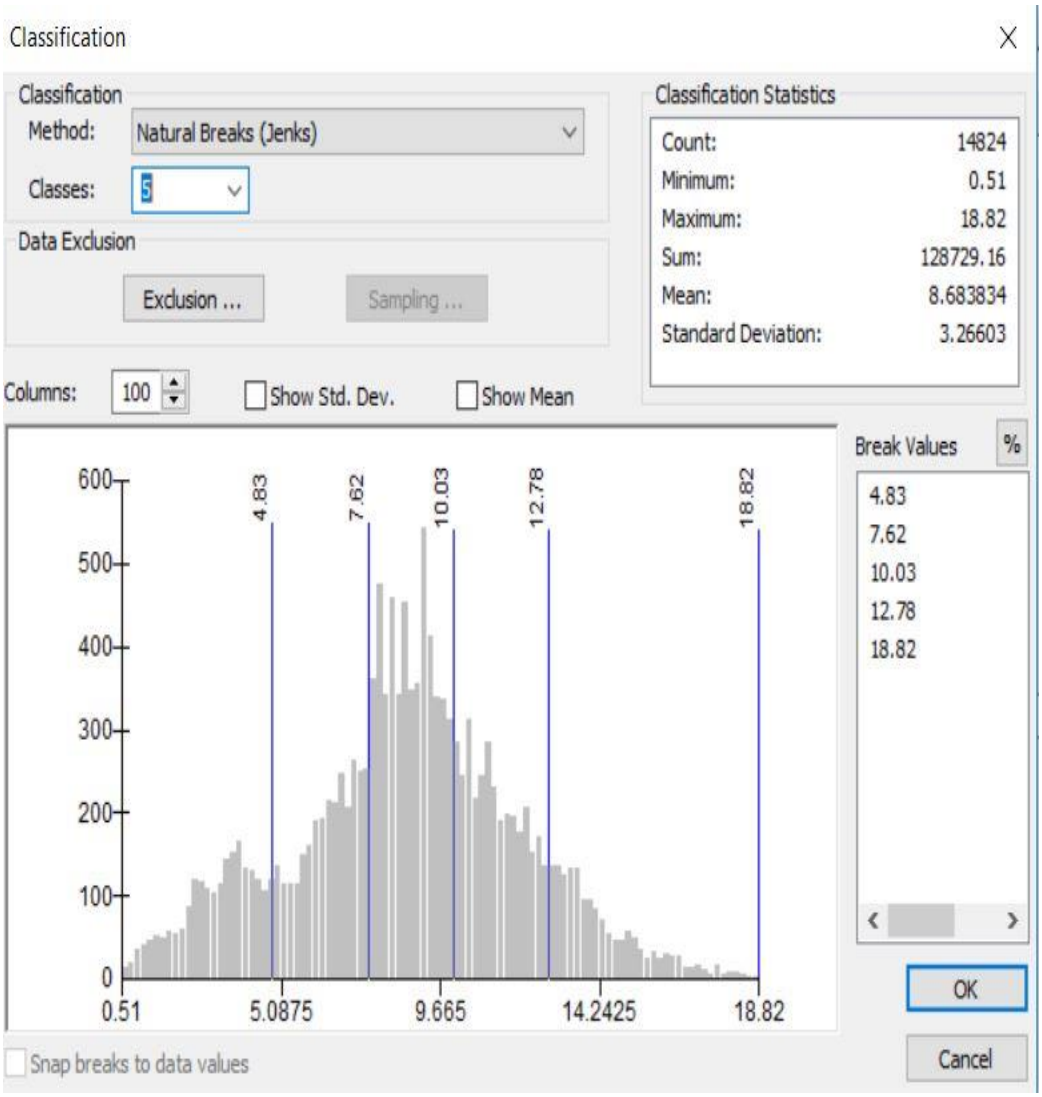

Figure 4 - 39: Reclassification of aquifer Transmissivity

The illustration of the remaining parameters (lineament, density, Recharge, Regolith and Drainage density) is presented in Appendix 12. The classification for these parameters was based on the natural breaks function in Arc GIS 10.6. This was to cater for the variability of each parameters. New maps were developed from the reclassified parameters and are presented in Appendix 13.

4.6.2.2 Assignment of score factors and weight

The strength of the weighted overlay technique according to Gumma and Pavelic (2013) is based on the fact that human judgment/expert opinion including previous literature can be incorporated into the analysis. Table 4.4 shows the scaled values and weights assigned to the different classes and parameters. The attributes of the reclassified features were assigned scores based on their influence on groundwater potential. A scale factor ranging 1 to 5 was adopted where 1,2,3,4 and 5 represent very low, low, moderate, high and very high. Secondly, weights (% of influence) totaling 100% were assigned to the various parameters taking account of their likely importance for groundwater occurrence and replenishment. The higher the percentage weight, the more influence a particular parameter will have in the groundwater potential.

Based on literature, expert knowledge on drilling and data on depth in the study area the same value of scale factor was assigned to the reclassified depth range. There is no direct relationship about the influence of depth to groundwater potential in the study area. Therefore, a value of 2 representing low influence was assigned for all the classes of depth with a 5% influence weight. Slope gradient influences the infiltration of rainfall in that steeper slopes generate less recharge because water runs rapidly off the surface during rainfall, allowing less time for infiltration and recharge. Therefore, high scores were assigned to the plain region with lower slope because low runoff is usually a good recharge zone. A weight of 10% was assigned to slope representing its contribution to groundwater in the study area.

Lineaments connote presence of secondary permeability. The occurrence of groundwater in the study area according to Banoeng-Yakubo et al. (2011) is characterised by the presence of secondary porosity. Therefore, distance close to lineaments would offer good opportunities for groundwater development and for that matter a weight of 15% has been assigned to lineament layer (Murthy and Mamo, 2009). Regolith is a good indicator of an aquifer's storativity implying that high regolith thickness is an indication of higher storage. The study area generally has thin regolith as suggested by Carrier et al. (2008) and also from the current data. Therefore, a weight of 5% was assigned to regolith thickness.

Groundwater recharge is associated to the characteristics of the drainage system. Generally, the denser the drainage system, the lower is the recharge rate. For that matter, a higher scale factor was assigned to less dense drainage areas and vice versa. Singh et al. (2013) indicates that low drainage density implies greater groundwater percolation and accumulation. Therefore, recharge rate will also be high. A weight of 10% was assigned to both drainage density and groundwater recharge since they are interconnected in terms of their influence on groundwater potential.

Likewise, information on SWLs implies availability of water in terms of accessibility. Thus, based on the classes of SWL layer, high potential is associated with shallower depths whereas high values of SWL connotes low potential (Forkuor et al. 2013; Nsiah et al. 2018). A weight of 10 % was assigned to the SWL layer as its overall contribution to groundwater in the area. Other factors such

evapotranspiration was considered in assigning the weight to SWL. The geology of the study area was reclassified into the formations and was rated according to the influence of each formation on the groundwater potential. Different scale factors were assigned to the formations based on the lithological descriptions, geophysical interpretation and the inherent hydraulic characteristics of the rocks in the various formations. Table 4.4 shows the scale factor and the weight (10% influence) that was assigned to geology as its contribution to the groundwater potential of the study area. Transmissivity according to Krásný (1997) has been accepted as the best hydraulic parameter to express groundwater abstraction possibilities and to be represented in hydrogeological maps. Holland (2012) indicates that the magnitude of transmissivity helps in understanding the water-bearing characteristics of hydrogeological bodies and is a decisive factor for groundwater-abstraction possibilities. In view of the above assertions, a weight of 25% representing the highest weight was assigned to transmissivity. High scale factors also represent high transmissivity and vice versa.

These approach of assigning scores and weight follows the procedure adopted by Forkuor et al. (2013), Gumma and Pavelic (2013) and Nsiah et al. (2018) who applied similar method to produce groundwater potential map for Northern region, Ghana and Gushiegu district respectively.

Table 4.3 Scaled values and weights assigned to the different classes and parameters.

Parameter	Reclassified	Scale Value/Factor score	Potential of Score	Weight (% Influence)
Depth	1	2	Low	5
	2	2	Low	
	3	2	Low	
Regolith	1	3	Moderate	5
	2	4	High	
	3	5	Very High	
Recharge	1	1	Very Low	10
	2	2	Low	
	3	3	Moderate	
	4	4	High	
	5	5	Very High	
SWL	1	5	Very High	10
	2	4	High	
	3	3	Moderate	
Aquifer Transmissivity	1	1	Very Low	25
	2	2	Low	
	3	3	Moderate	
	4	4	High	
	5	5	Very High	
Geological formation	Bimbilla	2	Low	10
	Poubogou	2	Low	
	Panabako Sandstone	3	Moderate	
	Kodjari	4	High	
Lineament	1	5	Very High	15
	2	4	High	
	3	3	Moderate	
Drainage Density	1	5	Very High	10
	2	4	High	
	3	3	Moderate	
Slope	1	5	Very High	10
	2	4	High	
	3	3	Moderate	
TOTAL SCORE				100

4.6.2.3 Groundwater Potential Map

The overlay tool in Arc GIS 10.6 was used to produce the comprehensive groundwater potential map in Figure 4.41. The groundwater potential map has been divided into five classes: (a) very poor (b) poor (c) moderate (d) good, and (e) very good across.

It indicates that places with moderate groundwater potential covers an area of 2010 km^2 and it is widely distributed across most parts of the study area. This area corresponds with most part of the Bimbilla, Poubogou and some portion of the Panabako Sandstone formation. This outcome is in sync with results from other researchers who have also indicated that the groundwater potential of the Bimbilla is low (Ewusi et. al. 2009). The portion of Bimbilla that has a moderate groundwater potential is associated with the Bunya sandstone member at the lower part of the Bimbilla formation and also the central part of Bimbilla formation. Carney et al. (2010) suggests that the Bunya sandstone member is very young and with a reasonable high porosity compared to the other units within the Voltaian. Field observation indicates that the central part of the Bimbilla formation in most places is covered by ephemeral streams which could have contributed to the moderate groundwater potential. About 2205 km^2 of the map represent areas with poor groundwater potential which is dominated by the Bimbilla formation with few places in the Poubogou formation. These areas are comprised of mudstones and siltstone which are considered highly impermeable. The total area that falls under the category of good groundwater potential covers 985 km^2 and 104 km^2 also

represents the category of very good groundwater potential. Most of the very good to good groundwater potential falls within the Kodjari formation and southwest of the Panabako sandstone formation.

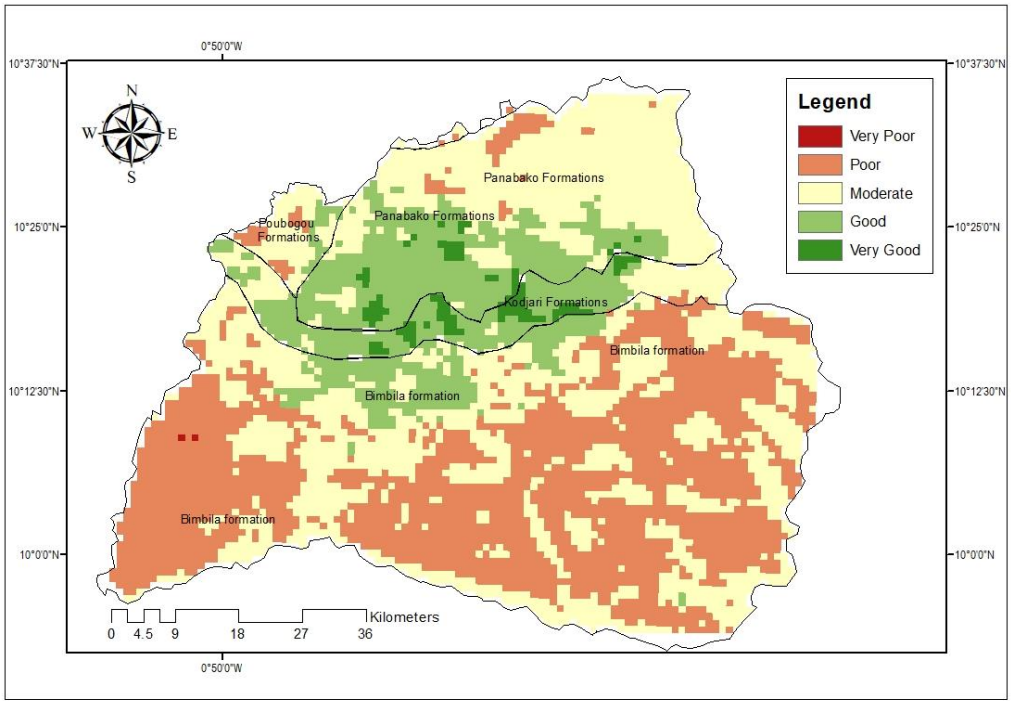

Figure 4 - 40: Groundwater Potential Map of the study area

The Kodjari Formation is considered the most prolific unit within the study area based on an evaluation of drilling records in the Voltaian basin (Ó Dochartaigh et al. 2011). Where there are fractures or intercalation of other units within the Panabako sandstone formation, high yielding aquifers are recorded.

The very poor groundwater potential covers an area of 22 km^2 which is within the mudstone siltstone areas of the Bimbilla formation. The Bimbilla formation is

known to be generally of poor groundwater potential. The very poor groundwater potential of the Bimbilla formation is evident in the outcome of the low yields that have been recorded under the Hydrogeological Assessment Project-HAP (1 dry well and HAP05 at Janga and HAP 14) as wells as poor yields under the Danida White Volta Basin Project -DWVP 04, DWVP06 and DWVP08, DWVP10 (Appendix 7).

4.6.3 Validation of Groundwater Potential Map

The reliability of the potential map in predicting probability of obtaining groundwater was tested using both yield and dry boreholes. The yield map was superimposed on the groundwater potential map to identify the trend of distribution and it is as shown in Figure 4.42.

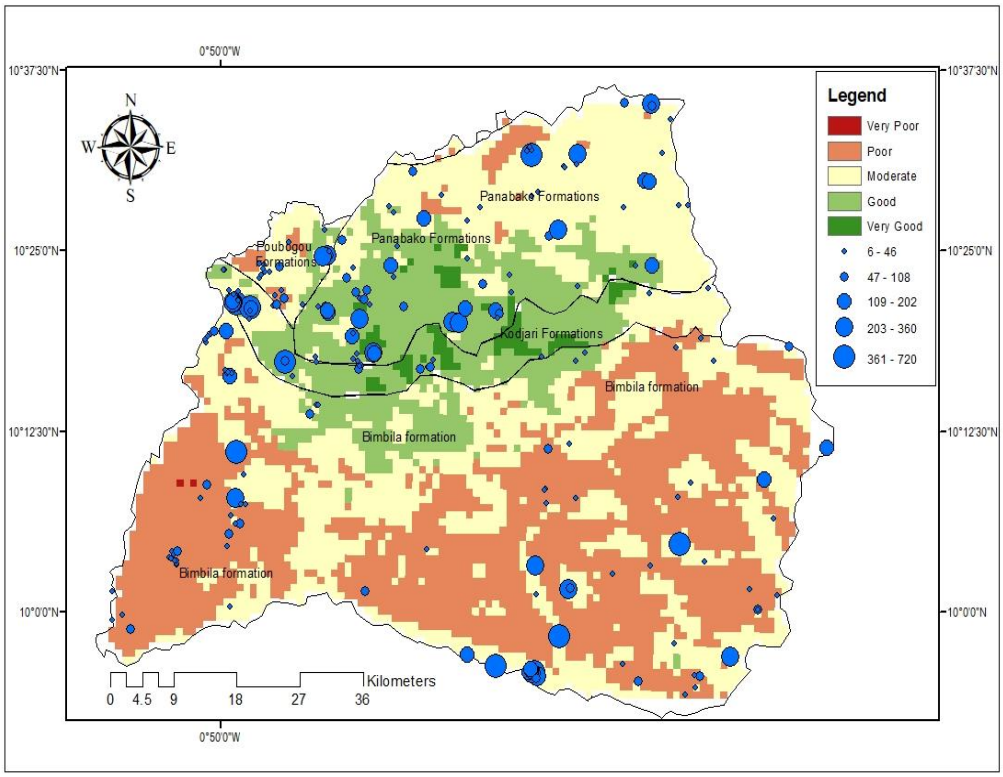

Figure 4 - 41: Groundwater potential map with reported yield (m^3/d) of productive boreholes

Figure 4.42 shows that the distribution of boreholes with high yields generally follow the same pattern as the very good to good groundwater potential zones. Similarly, the poor groundwater potential also follows the pattern as the low yielding boreholes. There are however few instances where high yielding boreholes are located in the low groundwater potential zones or vice versa. This is expected considering the level of heterogeneity of the study area with high variability in almost all the hydrogeological parameters.

Furthermore, 117 dry boreholes extracted from the HAP database were used in validating the groundwater potential map. These dry boreholes were superimposed

on the groundwater potential map as shown in Figure 4.43. The distribution of the dry boreholes follows the pattern of groundwater potential zones of the study area. Few dry boreholes happen to fall within the zones with good groundwater potential which is expected when dealing with a highly heterogeneous environment

Based on the results of validation obtained from these maps (Figure 4.42 and 4.43), the groundwater potential map developed can be regarded as reliable in predicting the groundwater potential of the study area.

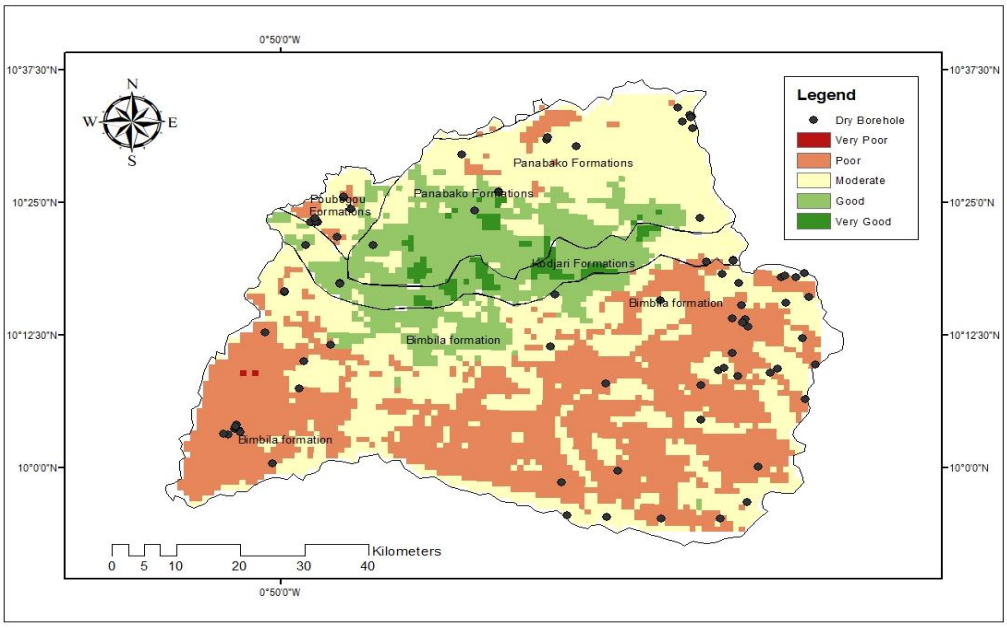

Figure 4 - 42: Groundwater potential map with dry boreholes of study area

4.6.4 Sensitivity Analysis

The purpose of sensitivity is to determine the influence of different criteria weights on the spatial pattern of a suitability map (Nwer, 2005). For this study, two scenarios were used to determine the sensitivity of the groundwater potential map

to slight changes in the weights assigned to the parameters following the approach by (Atandoh et al. 2013; Gogu and Dassargues 2000; Napolitano and Fabbri, 1996;). Several scenarios have been tried to determine the sensitivity of the groundwater potential map, the most suitable illustrations are in Appendix 14.

Figure 4.44 is the first scenario for the sensitivity analysis and it involved tweaking the weight of transmissivity and geological formation while maintaining the rest of the parameters. The result (Figure 4.44) though slightly similar to the trend of the groundwater potential map, a significant variation is observed. High yielding boreholes are located in the poor and moderate zones of the Bimbilla formation. This map implies that transmissivity has a greater influence in groundwater potential of the study area. Therefore the groundwater in the area is structurally controlled and not by lithology (Acheampong and Hess, 1998; Banoeng-Yakubo et al. 2011; Yidana et al. 2011).

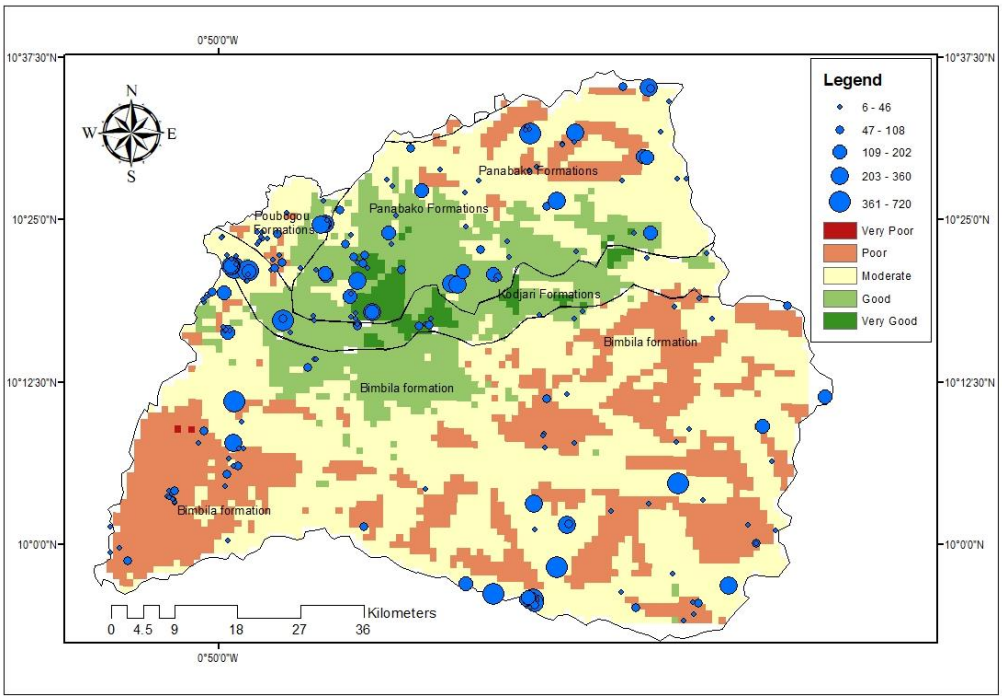

Figure 4 - 43: Sensitivity Analysis 1

The second scenario involved slight increment in the weight of lineament with a corresponding decrease in transmissivity. This was informed by the significant number of features on the lineament map in Figure 4.37. The results of the sensitivity analysis 2 suggest that a greater proportion of the Bimbilla formation has good groundwater potential but interestingly, the high yielding boreholes do not follow that trend. This is also at variance with what pertains on the ground and from literature. It therefore means that though lineament has an influence on the potential of groundwater, the influence should not be over-estimated, transmissivity remains the single most important parameter that has a higher influence on groundwater potential. As Krásný (1997) stipulates, "transmissivity has been

accepted as the best hydraulic parameter to express groundwater abstraction possibilities and to be represented in hydrogeological maps".

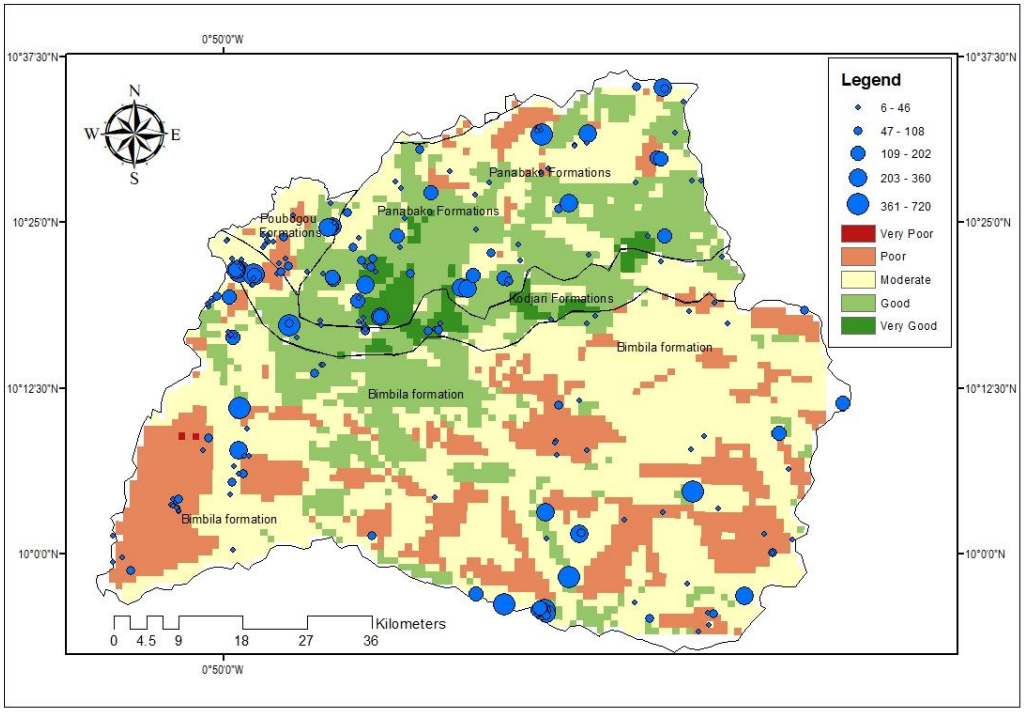

Figure 4 - 44: Sensitivity Analysis 2

CHAPTER FIVE

CONCLUSIONS AND RECOMMENDATIONS

5.1 Conclusions

The study is the first attempt in characterising the hydrogeology of the Nasia basin with comprehensive data ranging from geophysical to hydrogeological and to produce a groundwater potential map. The research has demonstrated that the current conventional methods of exploring for groundwater by interpreting low resistive layers or zones from geophysical survey as suitable locations are inappropriate and has contributed to the significant number of low yielding and dry boreholes that is recorded in the Nasia Basin and the Voltaian Supergroup at large.

Based on an integration of various geophysical methods, the geophysical characteristics of the rocks within the geological formations in the study area have been established to guide future groundwater endeavors. The results indicate that the regolith resistivity for the Panabako sandstone formation is between is 100 Ωm to 1000 Ωm and the bedrock is from 50 Ωm to 1000 Ωm. The Bimbilla formation has a regolith resistivity from 5 Ωm to 20 Ωm and a bedrock of 15 Ωm to 70 Ωm. The Kodjari and Poubogou formations have regolith resistivity ranging from 10 Ωm to 300 Ωm and 25 Ωm to 60 Ωm respectively. The bedrock resistivity for the Kodjari formation ranges between 10 Ωm to 50 Ωm while that for the Poubogou formation is from 80 Ωm to 100 Ωm. When interpreting geophysical results, the focus should be on understanding the geology from the direction of the profiles compared to the expected strike of the formation as well as of the dip and the

trend/pattern of distribution of resistivity. The contact from these features are targets worth exploring. The results also show that in places such as the Bimbilla formation, not all locations are worth exploring but rather the weathered zone could hold significant water that can be tapped.

Results of the hydraulic properties indicate that the average depth of striking water in the Nasia Basin exceeds the thickness of the regolith suggesting that productive yields are mainly derived from water bearing structures. Further to that, structural analysis conducted using variograms and regression models indicate that the groundwater in the study area is mainly structurally controlled. This corroborates the findings of research conducted in the Southern part of the Voltaian Supergroup in Ghana. Based on the limited data from the pumping test, geostatistical methods were employed to determine aquifer transmissivity of under sampled, using regression models and cokriging technique. Cokriging using specific capacity as the secondary parameter has proven very reliable and useful in providing better spatial estimation of transmissivity of the Nasia Basin. Cokriging is reliable because it considers the spatial auto-correlation of transmissivity and the spatial cross-correlation between transmissivity and specific capacity due to its abundance.

A comprehensive groundwater potential map is developed based on wide range of parameters which influence the occurrence of groundwater in the study area. The study demonstrates that geospatial and multi-criteria analysis techniques in combination with reliable field data could be used for assessment of groundwater potential zones. Based on the map, an area of 104 km^2 is classified as having very good groundwater potential and about 985 km^2 is considered having good potential.

These are areas that fall within the Kodjari formation and southwest of the Panabako sandstone formation. About 2205 km^2 represent areas with poor groundwater potential dominated by the Bimbilla formation with few places in the Poubogou formation and are comprised of mudstones and siltstone which are considered highly impermeable. The map indicates that places with moderate groundwater potential cover an area of 2010 km^2 and they are widely distributed across most parts of the study area. South west of the Nasia basin with an area of 22 km^2 is considered to have poor groundwater potential. This is made up of siltstones and mudstone belonging to the Bimbilla formation.

An assessment of the results of the groundwater potential map indicates that only about 20% of the study area is capable of yielding high boreholes thus fall within the good to very good potential zones. Therefore, other strategies to augment for increasing irrigation such as exploring the weathered zone for groundwater storage should be considered. The reliability of the groundwater potential map was tested against successful and dry boreholes and the results from sensitivity analysis shows high degree of confidence in the prediction.

Exploration hydrogeologist in the area could use the groundwater potential map as well as the methodology for interpreting geophysical results as a guide when selecting areas for hydrogeological studies especially when high yielding boreholes are required for mechanized systems.

5.2 Recommendations

- The geophysical studies conducted under this research was based on only successful boreholes, it is recommended that further studies be conducted on dry boreholes and the results interpreted along with the respective geologic logs. This would give a proper understanding of the geology of the area.
- Few boreholes were used within the Poubogou formation and therefore it is recommended that further studies targeted at obtaining detailed hydrogeological data within the Poubogou formation be undertaken.
- The Kodjari formation should be explored further especially within Bugya Pala where two monitoring boreholes produced contrasting results. In addition, during the recognisance survey, it was observed that hand dug wells in the community were situated along a straight line and they never run out of water even in the dry seasons.
- It is further recommended that, apparent conductivity measurement using EM-34 method be undertaken on a wider area and incorporated into a GIS environment. This will help to present and analyze the data in contour form instead of as individual lines so that an overall picture of the variation of electrical conductivity (resistivity) of the area can be understood. Superimposing the depth, yield, static water level data on the contoured map can result in establishing the interesting relationship between the parameters.

- The Bimbilla formation which most part of it falls under the very low, low to moderate groundwater potential should be investigated further. The groundwater dynamics of the regolith should be studied in detail to help ascertain its viability for storing groundwater in a sustainable manner as proposed from this study.
- Further geophysical studies using geophysical logging should be conducted on more existing boreholes to help in providing more information that would help in the interpretation of the subsurface lithology.
- In addition, extensive pumping test for a minimum duration of 24 hrs should be conducted on existing boreholes in the individual geological formations to help in determining the aquifer parameters and compare with the findings from this study.
- The groundwater potential map should be developed for the individual geological formations using the same approach in this study then compared with the results from this research. This will enhance the understanding of both aquifer behaviour and the occurrence of groundwater which will lead to better understanding of the hydraulic connection between the regolith and the underlying fractured bedrock.

REFERENCES

ABEM Instrument, AB. (2016). ABEM 33 3000 95 Terrameter LS Instruction Manual.

Aboufirassi, M. & Mariño, M. A. (1984). Cokriging of aquifer transmissivities from field measurements of transmissivity and specific capacity. *Journal of the International Association for Mathematical Geology*, *16*(1), 19–35. https://doi.org/10.1007/BF01036238

Acheampong, S. Y. & Hess, J. W. (1998). *Hydrogeologic and hydrochemical framework of the shallow groundwater system in the southern Voltaian Sedimentary Basin , Ghana*. 527–537.

Addai, M. O. Yidana, S. M. Chegbeleh, L. P. Adomako, D. & Banoeng-Yakubo, B. (2016). Groundwater recharge processes in the Nasia sub-catchment of the White Volta Basin: Analysis of porewater characteristics in the unsaturated zone. *Journal of African Earth Sciences*, *122*, 4–14. https://doi.org/10.1016/j.jafrearsci.2015.04.006

Adepelumi, A.A. Ako B.D. Ajayi T.R. Afolabi O. & Omotoso E.J. (2008). Delineation of saltwater intrusion into the freshwater aquifer of Lekki Penisula, Lagos, Nigeria. *Environ Geol 56(5):927–933*

Afrifa, G.Y. Sakyi, P.A, Chegbeleh, L.P. (2017). Estimation of groundwater recharge in sedimentary rock aquifer systems in the Oti basin of Gushiegu District, Northern Ghana. *Journal of African Earth Sciences* 131 (2017) 272e283

Agyekum, W. Klitten, K. Armah, T. Banoeng-yakubo, B. & Amartey, E. O. (2013).

Geophysical borehole logging for control of driller ' s records : hydrogeological case study from Voltaian sedimentary rocks in northern Ghana. *Appl Water Sci*, *3*, 491–500. https://doi.org/10.1007/s13201-013-0097-y

Agyekum, A.W. (2009). Application of geophysical borehole logging for hydrological studies in Northern Ghana. PhD Thesis, Department of Geology, University of Ghana

Ahmed, S. & De Marsily, G. (1987). Comparison of Geostatistical Methods for Estimating Transmissivity Using Data on Transmissivity and Specific Capacity. *Water Resources Research* 23 (9): 1717–37. https://doi.org/10.1029/WR023i009p01717.

Akudago, J. A. Chegbeleh, L.P. Nishigaki M. Nanedo, N.A. Ewusi, A. & Kankam-Yeboah, K. (2009). Borehole Drying: A Review of the Situation in the Voltaian Hydrogeological System in Ghana. *Journal of Water Resource and Protection* 01 (03): 153–63. https://doi.org/10.4236/jwarp.2009.13020

Akram, J. and Wani, M.H. (2009) Delineation of groundwater potential zones in Kakund watershed, Eastern Rajastan, using remote sensing and Gis techniques. *Journ Geol. Soc. India, v.73, pp.229–236*

Albouy, Y. Aundireux, P. Rakotondrasoa, G. Ritz M. Descloitres, M. Join, J.L. & Rasolomanana, E. (2001). Mapping coastal aquifers byJoing inversion of DC and TEM sounding-three case histories. *Groundwater 39(1):87–97*

Aliou, A-S. (2010). Evaluation of physical and chemical characteristics of groundwater in Norther Ghana-A case of Savelugu-Nanton District.

Unpublished Thesis (MPhil), University of Ghana, Environmental Science Programme

Allison, G.B. Gee, G.W. & Tyler, S.W. (1994). Vadose-zone techniques for estimating groundwater recharge in arid and semiarid regions. *Soil Science Society of America J. 58: 6-14.*

Alyamani, M. S. & Sen, Z. (1993). Determination of Hydraulic Conductivity from Grain-Size Distribution Curves. *Ground Water, 31,551-555.*

Annan-Yorke, R. & Cudjoe, J. E. (1971). Geology of the Voltaian Basin; Ghana Geol. *Survey*

Dept. Special Bull. 29, 5p

Anomohanran, O. (2013). Evaluation of Aquifer Characteristics in Echi, Delta State, Nigeria Using Well Logging and Pumping Test Method. *American Journal of Applied Sciences 10 (10): 1263–69.* https://doi.org/10.3844/ajassp.2013.1263.1269

Al-Shaibani, A. M. (2008). Hydrogeology and hydrochemistry of a shallow alluvial aquifer, western Saudi Arabia. *Hydrogeology Journal*, *16*(1), 155–165. https://doi.org/10.1007/s10040-007-0220-y

Alyamani, M.S. & Sen, Z. (1993). Determination of hydraulic conductivity from complete grain-size distribution curves. *Ground Water 31*(4):551-555

Anon (2000). Unpublished technical report, International Development Agency (IDA) funded 80 borehole drilling program, 150 pp.

Arnous, M. O. (2016). Groundwater Potentiality Mapping of hard rock terrain in arid regions using geospatial modelling: example from Wadi Feiran basin,

South Sinai, Egypt. *Hydrogeology Journal, Vol. 24, pp. 1375-1392.*

Asare, E. & Klitten, K. (2008). Water productivity from five 100–150 m deep exploratory boreholes in middle and upper Voltaian sediments in the Afram Plains, Ghana. *The Voltaian Basin, Ghana Workshop and Excursion*, March 10-17. Pp 61-63.

Ashraf, M. A. M. Yusoh, R. Sazalil, M. A. & Abidin, M. H. Z. (2018). Aquifer Characterization and Groundwater Potential Evaluation in Sedimentary Rock Formation. *Journal of Physics: Conference Series*, *995*(1). https://doi.org/10.1088/1742-6596/995/1/012106

Attandoh, N. Yidana, S. M. Abdul-Samed, A. Sakyi, P. A. Banoeng-Yakubo, B. & Nude, P. M. (2013). Conceptualization of the hydrogeological system of some sedimentary aquifers in Savelugu-Nanton and surrounding areas, Northern Ghana. *Hydrological Processes*, *27*(11), 1664–1676. https://doi.org/10.1002/hyp.9308

Auken, E. Viezzoli, A. & Christiansen, A.V. (2009). A single software for processing, inversion, and presentation of AEM data of different systems: The AarhusWorkbench. *In Proceedings of the International Geophysical Conference and Exhibition, Adelaide, SA, Australia, 22–25 February 2009; pp. 1–5*

Augustine, N.V. 2015. Estimating Specific Storage and Matrix Compressibility from Barometric Efficiency in the Southern Alberta Paskapoo Aquifer System. *University of Calgary. Master Science Degree, Thesis* .

Auken, E. Pellerin, L. Christensen, N.B. & Sørensen, K. (2006). A survey of current

trends in near-surface electrical and electromagnetic methods. *Geophysics*, Vol. 71, No. 5 September-October 2006_; P. G249–G260, 8 Figs. 10.1190/1.2335575

Award, H.S. Al-Bassam, A.M. (2001). HYDCOND: A computer program to calculate hydraulic conductivity from grain size data in Saudi Arabia. *Water Res. Dev. 17*(2), *237-246.*

Awini, J.A. & Klitten, K. (2008). Resistivity of Voltaian sedimentary rocks evaluated from geophysical borehole logs. *The Voltaian Basin, Ghana Workshop and Excursion*, March 10-17. Pp 65-68

Ayamsegna, J. A. & Amoateng-Mensah, P. (2002). Well monitoring : World Vision 's experience in Ghana. *Sustainable Environmental Sanitation and Water Services*, 1–4.

Ayite, A. Awua, F. & Kalvig, P. (2008). Lithostratigraphy of the Gambaga massif. In:Kalsbeek, F. (Ed.), The Voltaian Basin, Ghana. Workshop and Excursion, March 10–17, 2008. Geological Survey of Denmark and Greenland(GEUS), Copenhagen,pp. 41–44. Abstract Volume.

Batte, A. Muwanga, A. Sigrist, P.W. & Owor, M. (2008). VES as an exploration technique to improve on the certainty of groundwater yield in the fractured crystalline basement of eastern Uganda. *Hydrogeol J, 16*(8),1683–1693

Banoeng-Yakubo, B. Yidana, S.M. Ajayi, J.O. Loh, Y. Asiedu, D.K. (2011). Hydrogeology and groundwater resources of Ghana: a review of the hydrogeology and groundwater hydrochemistry of Ghana. *In: McMann, J.M. (Ed.), Potable Water and Sanitation. Nova Science Publishers.*

Bannerman, R. R. (1990). Appraisal of hydrogeological conditions and analysis of boreholes in the Nanumba and Western Gonja Districts – Northern Region, Ghana: Assessment of groundwater potential for hand dug wells. *Final Report for Rural Action NORRIP/GTZ*

Barfod, G.H. Vervoort J.D. Montanez I.P. & Riebold, S. (2004) Lu-Hf geochronology of phosphorites in ancient sediments. *In: 13th Goldschmidt Conf. Copenhagen, June 5-11, Geochemica Cosmochemica Acta, Abstract vol. 68, C15, A336.*

Bredehoeft, J.D. (2002). The water budget myth revisited: why hydrogeologists model, *Ground Water, 40*(4), 340-345, 2002

Beamish, D. (2013). The bedrock electrical conductivity map of the UK. *Journal of Applied Geophysics*, *96*, 87–97. https://doi.org/10.1016/j.jappgeo.2013.06.001

Bazuhair, A.S. & Wood, W.W. (1996). Chloride mass-balance method for estimating ground water recharge in arid areas: example from westernSaudi Arabia. *Journal of Hydrology 186: 153–159.*

Beeson, S. & Jones, C.R.C. (1988). The combined EMT/VES geophysical method for siting boreholes. *Groundwater* 26, 54-63

Biswajeet Pradhan, Ahmed M. Youssef, (2010). Manifestation of remote sensing data and GIS on landslide hazard analysis using spatial-based statistical models. *Arabian Journal of Geosciences 3(3):319-326*

Boadu, F.K. Gyamfi, J. & Owusu. E. (2005). Determining subsurface fracture characteristics from azimuthal resistivity surveys: A case study at Nsawam, Ghana. *Geophysics,* Vol.70 (5), pp. B35 – B42

Bockgård, N. (2000). Recharge of groundwater in crystalline rocks – a review. Uppsala Universitet. *Inst. för geovetenskaper. Report Series A, nr 55*.

Bourdet, D. Whittle, T. Douglas, A.A. Pirard Y.M. (1983). A new set of type curves simplifies well test analysis. *World Oil* 196(6): 95–106.

Boüwer, H. (1978). Groundwater hydrology. *McGraw-Hill Book*, New York, 480 pp.

Carney, J. N. Jordan, C. J. Thomas, C. W. Condon, D. J. Kemp, S. J. & Duodo, J. A. (2010). Lithostratigraphy, sedimentation and evolution of the Volta Basin in Ghana. *Precambrian Research* (183), 701–724.

Carman, P. C. (1937). Fluid Flow through Granular Beds. *Trans.Inst.Chem. Eng.* 15,150.

Carman, P.C. (1956). *Flow of Gases through Porous Media*. Butterworths Scientific Publications, London.

Carrier, M. Lefebvre, R. Racicot, J. & Asare, E. B. (2008). Access to Sanitation and Safe Water : Northern Ghana hydrogeological assessment project. *33rd WEDC International Conference, Accra* (33rd WEDC International Conference), 353–361.

Chandra, S. Auken, E. Maurya, P. K. Ahmed, S. & Verma, S. K. (2019). Large Scale Mapping of Fractures and Groundwater Pathways in Crystalline Hardrock By AEM. *Scientific Reports*, *9*(1), 1–11.

https://doi.org/10.1038/s41598-018-36153-1

Chegbeleh, L. P. Akudago, J. A. Nshigaki, M. & Edusei, S. N. K. (2014). Electromagnetic Geophysical Survey for The Electronic Journal of the International Association for Environmental Hydrology. *Hydrology, Environmental*, *17*(April 2009).

Christensen, N.B. & Sørensen, K.I. (1998). Surface and borehole electric and electromagnetic methods for hydrogeophysical investigations. *Euro J Environ Eng Geophys* 3(1):75–90

Cimino, A, Cosentino, C. Oieni, A. Tranchina, L. (2007). A geophysical and geochemical approach fro seawater intrusion assessment in the Acquedolci coastal aquifer (Northern Sicily). *Environ Geol* 55:1473–1482

Cooper, H. H. Jr. &. Jacob, C. E. (1946). A generalized graphical method for evaluating formation constants and summarizing well-field history. *American Geophysical Unio, Transactions 27*(4): 526-534.

Cooper, G.G. Oates, F & D. P. McGregor 1931. Report on water supply of the coastal area of the eastern province of the Gold Coast Colony: Dept. of Geol. Survey 27, 19p.

Cobbing, A.J.E. & Davies, J. (2004). Understanding problems of low recharge and low yield in boreholes: an example from Ghana, pp. 87 - 96. *In Water Resources of Arid Areas - Stephenson, Shemang & Chaoka(eds)*.

Corriols, M. Bjelm, L. & Dahlin, T. (2000). Resistivity surveying applied to groundwater studies in the Leon-Chinandega Plains, Nicaragua, Central America. *In: Proceedings for the EEGS-ES, annual meeting, Bochum,*

Germany

Comte, J. C. Cassidy, R. Nitsche, J. Ofterdinger, U. Pilatova, K. & Flynn, R. (2012). The typology of Irish hard-rock aquifers based on an integrated hydrogeological and geophysical approach. *Hydrogeology Journal*, *20*(8), 1569–1588. https://doi.org/10.1007/s10040-012-0884-9

Danielsen, J. E. Dahlin, T. Owen, R. Mangeya, P. & Auken, E. (2007). Geophysical and hydrogeologic investigation of groundwater in the Karoo stratigraphic sequence at Sawmills in northern Matabeleland, Zimbabwe: A case history. *Hydrogeology Journal*, *15*(5), 945–960. https://doi.org/10.1007/s10040-007-0191-z

Dahlin, T. (2001). The Development of DC Resistivity Imaging Techniques. *Computers & Geoscience* 27 (July 1999): 1019–29.

Dahlin, T. & Zhou, B. (2004). A numerical comparison of 2D resistivity imaging with 10 electrode arrays. *Geophys Prospect* 52:379–398

Dapaah-Siakwan, S. & Gyau-Boakye, P. (2000). Hydrogeologic framework and borehole yields in Ghana. *Hydrogeology Journal*, *8*(4), 405–416. https://doi.org/10.1007/PL00010976

Darko, E. (2015). Hydrogeological Characterization of the White Volta River Basin of Ghana MPhil Thesis (*University of Ghana)*. https://doi.org/10.1038/253004b0

Darko, P. & Krásný, J. (2010). Regional transmissivity distribution and groundwater potential in hard rock of Ghana. *Groundwater in Fractured Rocks*, pp. 109–119. https://doi.org/10.1201/9780203945650.ch6

Darko P. K. (2001). *Quantitative aspects of hard rocks aquifers: Regional evaluation of groundwater resources in Ghana*. A thesis submitted for the degree of a Doctor of Philosophy (Ph.D). Charles University, Praque. PhD Thesis

Deepika, B. Kumar, A. & Jayappa, K.S. (2013). Integration of hydrological factors and demarcation of groundwater prospect zones: insights from remote sensing and GIS techniques. *Environ. Earth Sci*. v.70(3), pp.1319–1338.

Delhomme, J. P. (1974). La cartographie d'une grandeur physique a partir de donnees de differentes qualit6s, *in Proceedings, International Association of Hydrogeologists, Memoir* 10, v. 1, p. 185-194. 1976,

Delhomme, J. P. (1976). Application de la theorie des variables regionalisees dans les sciences de l'eau: Fontainebleau, France, Ecole des Mines de Paris, *PhD. dissertation*.

De Marsily, G. (1986). Quantitative hydrogeology. Academic Press, London, 440 pp

Dobrin, M.B. (1976). Introduction to geophysical prospecting. *McGraw- Hill*, New York

Douwe, J.J. & Meulenkamp, E. (2006). Neogene supradetachment basin development on Crete (Greece) during exhumation of the South Aegean core complex. *Basin Res* 18:103–124

Domenico, P. & Schwartz, F. (1998) Physical and chemical hydrogeology, 2nd edn edn. *Wiley*, New York.

Dickson, K..B. & Benneh, G. (1995). A New Geography of Ghana, 3rd revised edition. *Longman*, Malaysia.

Driscol, F. G. (1986). Groundwater and Wells-Second Edition. *Johnson Systems Inc*. St. Paul, Minnesota 55112

Eggleton, R.A. ed. (2001). The regolith glossary. Perth: CRC LEME.

ESRI (2011). ArcGIS Desktop: Release 10. Redlands, CA: Environmental Systems Research Institute.

Ewusi, A. (2006). Groundwater Exploration and Management using Geophysics : Northern Region of Ghana. Unpublished PhD thesis: Brandenburg Technical University, Chair of Environmental Geology, Germany, 171 pp.

Ewusi, A. Kuma, J. S. & Voigt, H. J. (2009). Utility of the 2-D multi-electrode resistivity imaging technique in groundwater exploration in the Voltaian Sedimentary Basin, Northern Ghana. *Natural Resources Research*, *18*(4), 267–275. https://doi.org/10.1007/s11053-009-9102-4

Fetter, C. W. (2001). Applied Hydrogeology (4th ed.). Prentice Hall, New Jersey: Merrill Publishing Company

Forkuor, G. Pavelic, P. Asare, E. & Obuobie, E. (2013). Modelling potential areas of groundwater development for agriculture in northern Ghana using GIS/RS. *Hydrological Sciences Journal*, *58*(2), 437–451. https://doi.org/10.1080/02626667.2012.754101

Freeze, R.A. & Cherry, J.A. (1979). *Groundwater*. Prentice Hall, New Jersey

Carter, G.P. Miskewitz, R.J. Isukapalli, S. Mun, Y. Vyas, V. Yoon, S. Georgeopoulos, P. & Uchrin, C.G. (2011). Comparison of kriging and

cokriging for the geostatistical estimation of specific capacity in the Newark Basin (NJ) aquifer system, *Journal of Environmental Science and Health* Part A, 46:4, 371-377, DOI: 10.1080/10934529.2011.542373

Ghana Districts. (2017). http://www.ghanadistricts.com Cited 2017, September 24; 10.00am).

Ghana Government. (2017). http://www.ghana.gov.gh/index.php/media-center/features/1620-ensuring-reliable-water-supply-for-agriculture-what-options cited on 30/08/2017 at 6:38am

Gill, H. E. (1969). A ground-water reconnaissance of the Republic of Ghana, with a description of geohydrologic provinces. *US Geological Survey Water Supply Paper* 1757-K.

Goldman, M. Arad, A. Kafri, U. Gilad, D. & Melloul, A. (1988) Detection of freshwater/seawater interface by the time domain electromagnetic (TDEM) method in Israel. Naturwet Tijdsehr70:339–344

Gogu, R. Dassargues, A. (2000). Current trends and future challenges in groundwater vulnerability assessment using overlay and index methods.Environ. Geol. 39, 549–559, http://dx.doi.org/10.1007/s002540050466.

Gumma, M. K. & Pavelic, P. (2013). Mapping of groundwater potential zones across Ghana using remote sensing , geographic information systems and spatial modeling. *Environ Monit Assess.* 3561–3579. https://doi.org/10.1007/s10661-012-2810-y

Gwaze P. Dahlin, T. Owen, R. Gwavava, O. Danielsen, J. (2000). Geophysical investigations of the Karoo Aquifer at Nyamandhlovu, Zimbabwe. I*n: Proceedings for the EEGS-ES, annual meeting*, Bochum, Germany

Hiscock, K.M. Rivett, M.O. & Davison, R.M. (2002). Sustainable groundwater development Geological Society, London, *Special Publications*, 193, 1-14, 1 January 2002, https://doi.org/10.1144/GSL.SP.2002.193.01.01

Holland, M. (2011). Hydrogeological characterisation of crystalline basement aquifers within the Limpopo Province , South Africa by. *University of Pretoria* (February), 1–148.

Holland, M. (2012). Evaluation of factors influencing transmissivity in fractured hard-rock aquifers of the Limpopo province. *Water SA*, *38*(3), 379–390. https://doi.org/10.4314/wsa.v38i3.3

Hunkeler, D. (2016). Geological and Hydrogeological Characterization of Subsurface. *Hydrocarbon and Lipid Microbiology Protocols*, 27–44. https://doi.org/10.1007/8623_2016_211

Huntley, D. Nommensen, R. & Steffey, D. (1992). The Use of Specific Capacity to Assess Transmissivity in Fractured-Rock Aquifers. *Ground Water* 30 (3): 396–402.

Hydrogeological Assessment Project of Northern Ghana. (2011). Final Technical Report Volume I-CIDA Ref: 7038883-SNC-Lavalin Ref: 604138-INRS Ref:R1325-ISBN: 978-2-89146-708-7 Report. For CSIR Water Research Institute, Ghana

IBM Corp. Released (2011). IBM SPSS Statistics for Windows, Version20.0.

Amrmonk, NY: IBM Corp.

Inman, J.R. (1975). Resistivity inversion with ridge regression. *Geophysics* 40, 798–817

Isaaks, H. E. & Srivastava, R. M. (1989). Applied geostatistics. New York: *Oxford University Press.*

Jacob, C. E. and Lohman, S. W. (1952). Nonsteady flow to a well of constant drawdown in an Extensive aquifer: *American Geophysical Union Transactions*, v. 33, no. 4, p. 559-569.

Jalludin, M. & Razack, M. (2004). Assessment of hydraulic properties of sedimentary and volcanic aquifer systems under arid conditions in the Republic of Djibouti (Horn of Africa). *Hydrogeology Journal*, *12*(2), 159–170. https://doi.org/10.1007/s10040-003-0312-2

Jetel, J. & Krasny, J. (1968). Approximate aquifer characteristics in regional hydrogeological study. *Vest. Ustr. Ust 360 geol. Praha* 43(5), 459-461

Jha, M.K. Chowdhury, A. Chowdary, V.M. & Peiffer, S. (2007). Groundwater management and development by integrated remote sensing and geographic information systems: prospects and constraints *Water Resour. Manage*. 21 (2007), pp. 427-467, 10.1007/s11269-006-9024-4

Jordan, C. J. Carney, J. N. Thomas, C. W. & McDonnell, P. (2009). Ghana Airborne Geophysics Project in the Volta and Keta Basin: *BGS Final Report*. (8), 325.

Junner, N.R. & Hirst, T. (1946). The Geology and Hydrogeology of the Voltaian Basin. *Gold Coast Geological Survey Memoir* **8**, 51p

Karasaki, K.J. Long, C.S. Witherspoon, P.A. (1988). Analytical models of slug

tests. *Water Resources Research* 24(1): 115–126.

Kafri, U. Goldman, M. Levi, E. (2007). The relationship between the saline groundwater within the Arava Right Valley in Israel and the present and ancient base levels as detected by deep geoelectromagnetic soundings. *Environ Geol* 54:1435–1445

Kanta, A. Soupios P. Barsukov, P. Kouli, M. & Vallianatos F. (2013). Aquifer characterization using shallow geophysics in the Keritis Basin of Western Crete, Greece. Environ Earth Sci. DOI 10.1007/s12665-013-2503-z

Kearey, P. Brooks, M. & Hill, I. (2002). An Introduction to Geophysical Exploration. *TJ International, Padstow, Cornwal.* THird. https://doi.org/10.1108/eb003648.

Keith, J. Halford, Willis, D.W. & Schreiber, R.P. (2006). Interpretation of Transmissivity Estimates from Single-Well Pumping Aquifer Tests Technical Note. *Ground Water* 44, no. 3: 467–471

Kesse, G.O. (1985). The Mineral and Rocks Resources of Ghana. *A.A. Balkema Publishers.* Netherlands-Rotterdam 39-50.

Kexiang H. Awange J.L. Khandu, E.F. Goncalves, R.M. & Fleming, K. (2017). Hydrogeological characterisation of groundwater over Brazil using remotely sensed and model products. *Science of the Total Environment* 599–600 (2017) 372–386

Khalil, M.A. Abbas, A.M. Santos, F.M. Masoud, U. & Salah, H. (2012). Application of VES and TDEM techniques to investigate sea water intrusion in Sidi Abdel Rahman area, northwestern coast of Egypt. *Arab J Geosci* 1–9

(in press).

Klitten, K. & Agyekum, W. (2019). Geophysical Wire-line Logging of Boreholes in Nasia River Catchment Basin - Groundwater Development and Sustainable Agriculture in Nasia River Basin of Ghana - Danida Project ID 14-P02-GHA, *GEUS report 2019*, Copenhagen, Denmark

Kirsch, Reinhard, Hanna-Maria Rumpel, Wolfgang Scheer, and Helga Wiederhold. 2006. Groundwater Resources in Buried Valleys. A Challenge for Geosciences. Edited by Reinhard

Kirsch, H.R. Scheer, W. & Wiederhold, H. (2006) Groundwater Resources in Buried Valleys. A Challenge for Geosciences. Edited by Reinhard Leibniz Institute forApplied Geosciences (GGA-Institut).

Krásný, J. (1997). Transmissivity and permeability distribution in hard rock environment: a regional approach. *Hard Rock Hydrosystems, Proceedings of Rabat Symposium* (241).

Kruseman, G.P. & de Ridder, N.A. (1971). Analysis and evaluation of pumping test data. In *ILRI Publication 47* (second, Vol. 12). https://doi.org/10.1016/0022-1694(71)90015-1

Kwei, C.A. 1997. Evaluation of groundwater potential in the Northern Region of Ghana.

International Development Agency (CIDA) Accra, Ghana.

Lance, H. & Huntley, D.M.R. (1996). Cokriging Limited Transmissivity Data Using Widely Sampled Specific Capacity. *Groundwater*, *34*(1), 12–18.

Lapointe, P. Morris, W. A. & Harding, K. L. (1986). Interpretation of magnetic susceptibility: a new approach to geophysical evaluation of the degree of rock

alteration. *Canadian Journal of Earth Sciences*, *23*(3), 393–401. https://doi.org/10.1139/e86-041

Loke, M. H. Acworth, I. & Dahlin, T. (2003). A comparison of smooth and blocky inversion methods in 2D electrical imaging surveys. *Exploration Geophysics*, *34*(3), 182–187. https://doi.org/10.1071/EG03182

Lloyd, J.W. (1999). Water Resources of Hard Rock Aquifers in Arid and Semi Arid Zones.Pdf. -4020-6540-8_2.

Lutz, A. Thomas J. M. Pohll, G. & McKay W. A. (2002). Groundwater resource sustainability in the Nabogo Basin of Ghana. *J African Earth Sci.* Vol. 49, pp. 61–70, 2007

Macdonald, A. M. & Davies, J. (2000). A brief review of groundwater for rural water supply in sub-Saharan Africa. In *BGS Technical Report WC/00/33* (Vol. 1). https://doi.org/10.13140/RG.2.2.21914.64964

MacDonald, A. M. Davies, J. & Peart, R. J. (2001). Geophysical methods for locating groundwater in low permeability sedimentary rocks: Examples from southeast Nigeria. *Journal of African Earth Sciences*, *32*(1), 115–131. https://doi.org/10.1016/S0899-5362(01)90022-3

Mace, R. E. (2001). Estimating Transmissivity Using Specific-Capacity Data. *Bureau of Economic Geology*, 2011 (In Press)

McNeill, J. (1980). Electromagnetic Terrain Conductivity measurement at Low induction Number, Ontario, Canada. Available at: http://www.geonics.com/pdfs/technicalnotes/tn6.pdf.

Meju, M. (2005). Simple relative space–time scaling of electrical and

electromagnetic depth sounding arrays: implications for electrical static shift removal and joint DC TEM data inversion with the most-squares criterion. *Geophys. Prospect*. 53,1–17

Magesh, N.S. Chandrasekar, N. Soundranayagam, J.P. (2011). Morphometric evaluation of Papanasam and Manimuthar watersheds, parts of WesternGhats, Tirunelveli district, Tamil Nadu India: a GIS approach. Environ. *Earth Sci*. 64, 373–381, http://dx.doi.org/10.1007/s12665-010-0860-4

Mainoo, P.A. Manu, E. Yidana, S.M. Agyekum, W.A. Stigter, T. Duah, A.A. & Preko, K. (2019). Application of 2D-Electrical resistivity tomography in delineating groundwater potential zones: Case study from the voltaian super group of Ghana. *Journal of African Sciences* 160 (2019)103618. https://doi.org/10.1016/j.jafrearsci.2019.103618

Manap, M.A. Sulaiman, W.N.A. Ramli, M.F. Pradhan, B. & Surip, N. (2011). A knowledge-driven GIS modeling technique for groundwater potential mapping at the Upper Langat Basin, Malaysia. *Arab J Geosci.* DOI 10.1007/s12517-011-0469-2

Martin, N. & van de Giesen, N. (2005). Spatial distribution of groundwater production and development potential in the volta river basin of Ghana and burkina faso. *Water International*, *30*(2), 239–249. https://doi.org/10.1080/02508060508691852

Mazac, O. Kelly W.E. & Landa, I. (1985). A hydrogeophysical model for relations between electrical and hydraulic properties of aquifers. *J Hydrol 79*(1–2), 1–19.

Mendoza, A. Bjelm, L. & Dahlin, T (2000). Resistivity imaging as a tool for groundwater studies at Santo Domingo, Central Nicaragua. *In: Proceedings for the EEGS-ES,* annual meeting, Bochum,Germany

Menyeh, A. Noye, R. M. & Danuor, S. K. (2005). Prospecting for groundwater using the electromagnetic method in the voltaian sedimentary basin in the northern region of Ghana_ a case study of the Gushegu-Karaga district. *Jounal of Science and Technology*, *25*(2), 53–65.

Milsom, J. (2003). *Field geophysics, the geological field guide series*. 3rd edition. Wiley

Ministry of Food and Agriculture.(2017). http://mofa.gov.gh/site/wpcontent/uploads/2018/03/PFJ%20document%20New%20New.pdf[accessed on 20th June, 2019 at 17:41]

Mondal, M.S. Pandey, A.C. & Garg, R.D. (2009). Groundwater prospects evaluation based on hydrogeomorphological mapping using high resolution satellite images: A case study in Uttarakhand. *Jour. Indian Soc. Remote Sensing*, v.36(1), pp.69–76.

Morris, B.L, Lawrence, A. R.L, Chilton, P. J. C. Adams, B. Calow R. C. and Klinck, B. A. (2003). Groundwater and its Susceptibility to Degradation: A Global Assessment of the Problem and Options for Management. *Early Warning and Assessment Report Series*, RS. 03-3. United Nations Environment Programme, Nairobi, Kenya.

Murthy, K.S.R. & Mamo, A.G. (2009). Multi-criteria decision evaluation in groundwater zones identification in Moyale–Teltele subbasin, South Ethiopia. *Int. J. Remote Sens.* 30, 2729–2740.

Napolitano, P. Fabbri, A.G. 1996. Single-parameter sensitivity analysis for aquifer vulnerability assessment using DRASTIC and SINTACS.Application of Geographic Information Systems in Hydrology and Water Resources Management (Proceedings of the Vienna Conference, April1996). IAHS Publ. no. 235 April 1996, 559–566

Narendra, K. Rao, K.N. & Latha, P.S. (2013). Integrating Remote Sensing and Gis for Identification of Groundwater Prospective Zones in the Narava Basin, Visakhapatnam Region, Andhra Pradesh. *Jour. Geol. Soc.* India, v.81, pp.248–260.

Nii Consult (1998). Information building Block. Ghana Water Management Study. *Unpublished Consultancy Report for the Ministry of Works and Housing*, Ghana/Danida/WorldBank

Nsiah, E. Appiah-Adjei, E. K. & Adjei, K. A. (2018). Hydrogeological delineation of groundwater potential zones in the Nabogo basin, Ghana. *Journal of African Earth Sciences*, Vol. 143, pp. 1–9. https://doi.org/10.1016/j.jafrearsci.2018.03.016

Nwer, B.A.B. (2005). The application of land evaluation technique in the north-east of Libya, National Soil Resources Institute, Faculty of Environment, Cranfield

Obuobie, E. (2008). Estimation of groundwater recharge in the context of future

climate change in the White Volta River Basin, West Africa. GLOWA Volta Project, *Ecology and Development Series* No. 62. Available from: http://www.glowa-volta.de/publ_theses.html [Accessed 10 Feb 2020].

Ó Dochartaigh B.É. Davies. J. Beamish, D. & MacDonald, A.M. (2011). BGS Consultancy: UNICEF IWASH Project, Northern Region, Ghana. *Final Report British Geological Survey Open Report, OR/11/.67pp.*

Odong, J. (2008). Evaluation of Empirical Formulae for Determination of Hydraulic Conductivity based on Grain-Size Analysis, *The Journal of American Science*, 4, 1–6, 2008

Ofosu-Addo, D. Jianmei, C. & Dong, S. (2008). Groundwater Development and Evaluation of the White Volta Basin (Ghana) using numerical Simulation. *The Journal of American Science*, *4*(4), 64–71.

Olayinka, A. & Barker, R. (1990). Borehole siting in crystalline basement areas of Nigeria with a microprocessor controlled resistivity traversing system. *Groundwater* 28, 178-183.

Olofsson, B. (1994) Flow of groundwater from soil to crystalline rock. *Applied Hydrogeology*, vol 2, nr 3, pp. 71−83.

Olsson, T. (2000) Projekt Utredning Hallandsås – PUH. Bedömning av grundvattenpåverkan. Resultat av genomförda utredningar. *Banverket. Report* 2000-10-23

Owen, R.J. Gwavava, O. & Gwaze, P. (2005). Multi-electrode resistivity survey for groundwater exploration in the Harare greenstone belt, Zimbabwe. *Hydrogeology Journal* 14: 244–252

Prudic, D.E. (1991). Estimates of hydraulic conductivity from aquifer-test analyses and specific-capacity data, Gulf Coast regional aquifer systems, south-central United States: *U.S. Geological Survey, Water-Resources Investigations,* WRI 90-4121,38 p.

Pelig-Ba, J.B. (2004). Estimation of water balance in the Northern Region of Ghana. *Ghana Journal of Development Studies* 1 (2), 118-141

Pradhan, B. (2009). Groundwater potential zonation for basaltic watersheds using satellite remote sensing data and GIS techniques. *Cent. Eur. J. Geosci.* 1, 120–129.

Quist, L.G. (1976). A preliminary report on groundwater assessment of the Accra Plains. *WRI/CSIR*, Accra, Ghana

Razack, M. & Lasm, T. (2006). Geostatistical estimation of the transmissivity in a highly fractured metamorphic and crystalline aquifer (Man-Danane Region, Western Ivory Coast). *Journal of Hydrology*, *325*(1–4), 164–178. https://doi.org/10.1016/j.jhydrol.2005.10.014

Robertson, G.P. (2008). GS+: Geostatistics for the Environmental Sciences. *Gamma Design Software, Plainwell*, Michigan USA.

Reynolds J.M. (2010). An introduction to applied and environmental geophysics. *Willey, New York (in preparation)*. ISBN-13: 9780471485353

Reynolds, J.M. (1997). An introduction to applied and environmental geophysics, *John Wiley & Son*, Chichester, 796 pg.

Salifu, M. Yidana, S.M. Osae, S. & Armah, Y.S.J. (2013). The Influence of the

Unsaturated Zone on the High Fluoride Contents in Groundwater in the Middle Voltaian Aquifers- The Gushegu District, Northern Region of Ghana. *Hydrogeol Hydrol Eng* 2013, 2:2 http://dx.doi.org/10.4172/2325-9647.1000107

Samani, N. Pasandi, M. & Barry, D. A. (2006). pumping and recovery test data. *Journal of Geological Society of Iran* (1), 29–41.

Sander, P. Chesley, M.M. & Minor, T.B. (1996). Groundwater assessment using remote sensing and GIS in a rural groundwater project in Ghana: lessons learned. *Hydrogeology Journal* **4** (3) 40-49

Sandwidi, W.J.P. (2007). Groundwater potential to supply population demand within the Kompienga Dam basin in Burkina Faso. Bonn, Germany: Zentrum für Entwicklungsforschung – Center for Development Research University of Bonn, *Ecology and Development Series*, No. 55. Available from: http://www.zef. de/1400.html [Accessed 10 May 2019].

Saraf A.K. & Chowdhury, P.R. (1998). Integrated remote sensing and GIS for ground water exploration and identification of artificial recharge sites. *International Journal of Remote Sensing,* 19(10): 1825-1841.

Scanlon, B.R. Keese, K.E. Flint, A.L. Flint, L.E. Gaye, C.B. Edmunds, W.M. & Simmers, I. (2006). Global synthesis of groundwater recharge in semiarid and arid regions. *Hydrol. Processes* 20 (15): 3335-3370

Seidu, J. (2017). Integration of geological and geophysical data to delineate groundwater potential zones using GIS –A case study of Tarkwa. MPhil Thesis-University of Mines and Technology, Ghana

Slater, L. (2002). Electrical-hydraulic relationships observed for unconsolidated sediments. *Water Resources Research*, 38(10), 1–13. http://doi.org/10.1029/2001WR001075

Singh, P. Thakur, J. K. & Kumar, S. (2013). Delineating groundwater potential zones in a hard-rock terrain using geospatial tool. *Hydrological Sciences Journal*, *58*(1), 213–223. https://doi.org/10.1080/02626667.2012.745644

Sonkamble, S. Chandra, S. Nagaiah, E. Dar, F. A. Somvanshi, V. K. & Ahmed, S. (2014). Geophysical signatures resolving hydrogeological complexities over hard rock terrain-a study from Southern India. *Arabian Journal of Geosciences*, *7*(6), 2249–2256. https://doi.org/10.1007/s12517-013-0931-4

Sougy J. (1971) Remarquessur la stratigraphie du Protérozoïquesupérieur du bassinvoltaïen: influence de la paléosurfaced'érosionglaciaire de la base du groupe de l'Otisur le tracésinueux des Volta et de certainsaffluents. *Comptes Rendus Académie des Sciences* Paris 272, 800–803

Sørensen, K.I. & Søndergaard, V.H. (1999). Large-scale geophysical mapping and its application for groundwater protection in urban areas. *In: Proceedings for SAGEEP*, Oakland, CA,pp 481–486

Soupios, P. Kalisperi, D. Kanta, A. Kouli, M. Barsukov, P. & Vallianatos, F. (2010). Coastal aquifer assessment based on geological and geophysical survey, North Western Crete, Greece. *Environ earth* Sci 61(1):63–77

Spane, J.F. & Wurstner, S. (1993). DERIV: A computer program for calculating pressure derivatives for use in hydraulic test analysis. *Groundwater* 31(5): 814–822.

Stewart, M.T. (1982). Evaluation of electromagnetic methods for rapid mapping of salt water interfaces in coastal aquifers. *J. Ground Water* 20, 538–545.

Telford, W.M. Geldart, L.P. & Sheriff, R.E. (1990). Telford - Applied Geophysics (Second edition). *Cambridge University Press.*

Theis (1963). Estimating the transmissivity of a water-table aquifer from the specific capacity of a well, in U.S. *Geological Survey Water-Supply Paper*, 1536-1, p. 332-336.

Tiab, D. & Kumar, A. (1980). Detection and Location of Two Parallel Silling Faults around a Well. *Journal of Petroleum Technology*, 20, 1701-1708.

Thomasson, H. J. Olmstead, F. H. & LeRoux, E. R. (1960). Geology, water resources, and usable groundwater storage capacity of part of Solano County, CA: U.S. *Geological Survey Water Supply Paper*, No. 1464,693 p.

Teeuw, R. M. (1995). Groundwater exploration using remote sensing and a low-cost geographical information system. *Hydrogeology Journal* 3 (3)

Todd, D.K. & Mays, L.W. (2005). Groundwater Hydrology (3rd ed.). *John Wiley and Sons, Inc*.

Tod, J. (1981). Ground water resources in the Northern Region of Ghana. *NORRIP Sectoral Report* UNESCO (1984). Groundwater in hard rocks, *In Studies and Reports in Hydrology*, 33. UNESCO Paris.

Unihydro Limited (2003). Unpublished Technical report on rural water supply and sanitation project in the Northern Region

United Nation Development Program.(2019).

http://www.gh.undp.org/content/ghana/en/home/sustainable-development-goals/goal-6-clean-water-and-sanitation.html. [Accessed on 23/04/19 at 12:03pm].

United Nations Educational Scientific Cultural Organisation.(2012). *World's groundwater resources are suffering from poor governance, experts say* http://www.unesco.org/new/en/media-services/single-view/news/worlds_groundwater_resources_are_suffering_from_poor_gove/

Viljoen, J.H.A. Gyapong, W. Le Berre, W. Reddering, J.S.V. Thomas, E. Atta-Ntim, K. (2008). Geology of Sheet 10010 South of Gambaga. Jn; Kalsbeek, F. (Ed.). *The Voltaian Basin, Ghana. Workshop and Excursion*, March 10-17, 2008, Abstract Volume. Geological

Survey of Denmark and Greenland (GEUS). Copenhagen, pp. 39-40.

Van Dam R.L. (2010). Landform characterization using geophysics—recent advances, applications, and emerging tools. *Geomorphology*. doi:10.1016/j.geomorph.2010.09.005

Van Overmeeren, R. (1989). Aquifer boundaries explored by geoelectrical measurements in the coastal plain of Yemen. A case of equivalence. *Geophysics* 54, 38–48

Wahyuni, S. Oishi, S. & Sunada, K. (2008). The estimation of the groundwater storage and its distribution in Uzbekistan. Annual Jour. *Hydraulic Engg*. v.52, pp.31–36

Waikar, M.L. & Nilawar, A.P. (2014). Identification of Groundwater Potential

Zone using Remote Sensing and GIS Technique. *International Journal of Innovative Research in Science, Engineering and Technology*, Vol. 3, pp. 12163-12174.

Xiao, L. (2014). Evaluation of groundwater flow theories and aquifer parameters estimation. *PhD Thesis-University of the Western Cape*.

Yang, Y.S.A.A. Cronin, T. E. & Kalin, R.M.(2010). Characterizing a heterogeneous hydrogeological system using groundwater flow and geochemical modelling. *Journal of Hydraulic Research 42* (sup1),147–55. https://doi.org/10.1080/00221680409500058

Yidana, S.M. & Koffie, E. (2014). The groundwater recharge regime of some slightly metamorphosed neoproterozoic sedimentary rocks: an application of natural environmental tracers. *Hydrol. Process*. http://dx.doi.org/10.1002/hyp.9859

Yidana, S. M. Aliou, A.S. Banoeng-Yakubo, B. & Nude, P. M. (2011). Characterization of the Hydrogeological Conditions of Some Portions of the Neoproterozoic Voltaian Supergroup in Northern Ghana. *Journal of Water Resource and Protection*, *03*(12), 861–875. https://doi.org/10.4236/jwarp.2011.312096

Yidana, S. M. Dzikunoo, E. A. Aliou, A. S. Adams, R. M. Chagbeleh, L. P. & Anani, C. (2020). The geological and hydrogeological framework of the Panabako, Kodjari, and Bimbilla formations of the Voltaian supergroup – Revelations from groundwater hydrochemical data. *Applied Geochemistry*, *115*(February), 104533. https://doi.org/10.1016/j.apgeochem.2020.104533

Yidana, S. M. Ophori, D. & Banoeng-Yakubo, B. (2008). Hydrogeological and hydrochemical characterization of the Voltaian Basin: The Afram Plains area, Ghana. *Environmental Geology*, *53*(6), 1213–1223. https://doi.org/10.1007/s00254-007-0710-1

APPENDICES

APPENDIX 1-EM-34 PROFILES

BANAWA-KODJARI FORMATION-SAMPLE OF INTERPRETATION

BANAWA			GEOLOGY	KODJARI FORMATION
Bearing		Profile Length	700 m	
Profile No.	A	Date:		
	10-m Separation		40m COIL SEPEARTION	
STATIO	HD-10	VD-10	HD-40	VD-40
0	56	38	37	28
20	64	47	35	38
40	66	27	38	48
60	67	40	36	42
80	72	41	43	49
100	78	43	39	45
120	92	44	43	36
140	84	51	56	42
160	74	42	50	48
180	93	41	50	42
200	87	50	50	37
220	91	56	46	48
240	80	58	47	35
260	79	66	50	38
280	64	56	55	37
300	58	58	54	43
320	69	57	51	40
340	56	59	51	33
360	62	53	54	41
380	57	65	54	40
400	54	67	61	33
420	44	68	60	43
440	69	77	63	49
460	56	66	61	41
480	59	81	70	38
500	54	80	61	32
520	46	82	60	34
540	43	73	65	27
560	51	81	57	44
580	39	84	58	38
600	37	54	58	32
620	54	63	54	40
640	44	73	51	33
660	29	64	51	44
680	27	70	54	40
700	37	56	52	41

Areas marked yello on the graph show a normal trend where the shallow formation has a higher conductivity than the deeper formation.

Areas marked green show a switch in the trend probably due to structural geological changes where the shallow formation has a lower conductivity than the deeper formation.

Areas marked red on the graph and data sheets show contact regions of structural changes, or anomalous zones, probably fractures or folds. These are usually areas of high groudwater potential.

Location: Gambaga – Nalerigu

10m Coil Separation

Bearing		Profile Length:	800 m
Profile No.	A	Date:	10/5/2017
STATION	10-m Separation		Remarks
	HD	VD	
0	29	18	
20	24	16	
40	7	6	
60	24	28	
80	29	21	
100	28	26	
120	37	26	
140	33	18	
160	28	20	
180	38	29	
200	40	33	
220	31	26	
240	30	23	
260	38	30	
280	37	24	
300	32	11	
320	17	12	
340	16	10	
360	35	35	
380	39	23	
400	14	34	
420	37	17	
440	35	26	
460	30	21	
480	38	33	
500	25	21	
520	24	13	
540	23	20	
560	19	9	
580	34	26	
600	31	24	
620	34	21	
640	33	20	
660	33	17	
680	37	24	
700	31	26	
720	34	28	
740	38	34	
760	18	13	
780	16	21	
800	26	20	
820	42	38	
840	17	15	
860	41	26	

40m Coil Separation

GAMBAGA			
Bearing		Profile Length:	800 m
Profile No.	A	Date:	10/5/2017
STATION	40-m Separation		Remarks
	HD	VD	
0	22	24	
20	24	26	
40	18	21	
60	21	23	
80	18	22	
100	27	32	
120	16	21	
140	22	21	
160	22	23	
180	19	21	
200	20	27	
220	19	23	
240	21	24	
260	22	16	
280	22	17	
300	17	15	
320	15	14	
340	15	17	
360	15	10	under pylons
380	15	14	
400	32	19	
420	22	16	
440	26		
460	21		
480	20		

10m Coil Separation

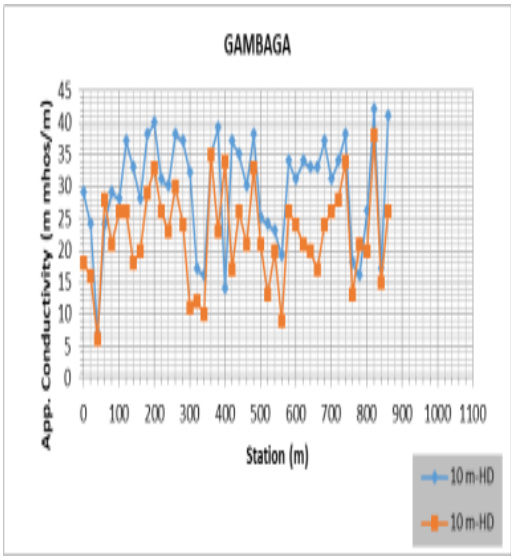

40m Coil Separation

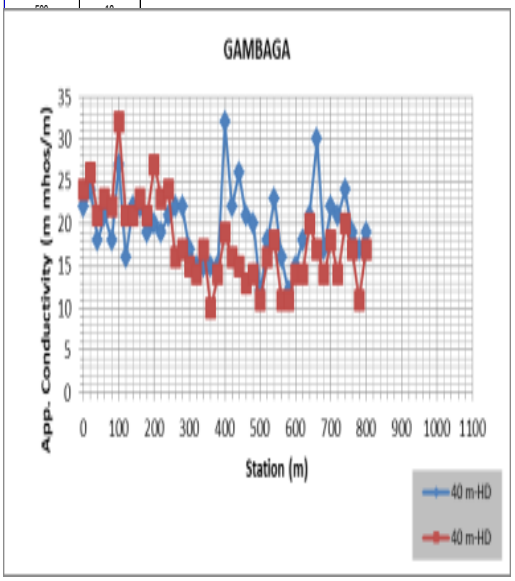

Location: Kpalvaka

10m Coil Separation

KPALVAKA			
Bearing		Profile Length:	800 m
Profile No.	A	Date:	10/6/2017
STATION	10-m Separation		Remarks
	HD	VD	
0	52	47	
20	33	34	
40	56	44	
60	49	44	
80	41	45	
100	45	33	
120	43	40	
140	45	37	
160	45	31	
180	34	17	
200	45	44	
220	46	42	
240	48	47	
260	51	41	
280	44	38	
300	46	36	
320	39	41	
340	31	26	
360	46	28	
380	42	30	
400	33	30	
420	43	44	
440	50	42	
460	34	44	
480	54	37	
500	48	50	
520	34	43	
540	19	42	
560	53	42	
580	47	21	
600	40	48	
620	39	48	

40m Coil Separation

KPALVAKA			
Bearing		Profile Length:	800 m
Profile No.	A	Date:	10/6/2017
STATION	40-m Separation		Remarks
	HD	VD	
0	41	33	
20	37	30	
40	38	37	
60	38	37	
80	41	38	
100	40	31	
120	38	38	
140	42	40	
160	44	40	
180	33	40	
200	39	38	
220	42	33	
240	50	38	
260	37	44	
280	36	36	
300	41	31	
320	34	38	
340	35	38	
360	40	32	
380	34	38	
400	47	36	
420	39	36	
440	28	36	
460	38	33	
480	34	37	
500	40	33	
520	40	36	
540	33	31	
560	32	35	
580	40	34	
600	38	44	
620	39	21	
640	40	37	
660	44	42	
680	38	38	
700	40	34	
720	42	36	
740	40	35	
760	44	32	
780	38	38	
800	32	32	
820	33	28	

10m Coil Separation

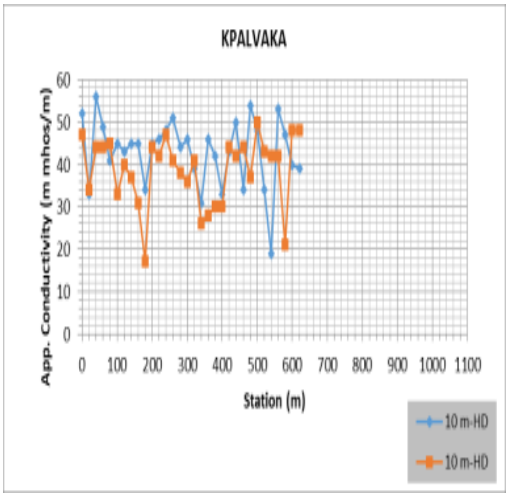

40m Coil Separation

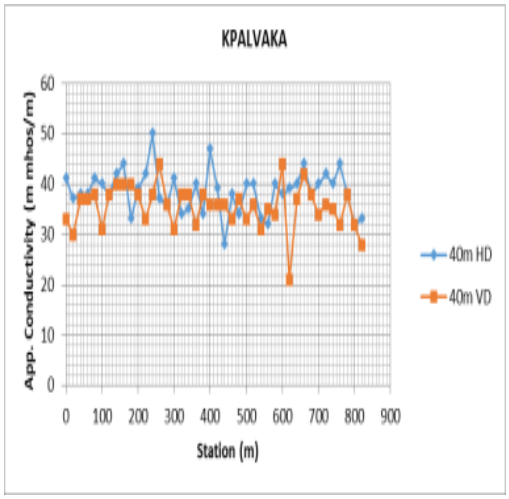

Location: Nasia

10m Coil Separation

NASIA			
Bearing		Profile Length:	1000 m
Profile No.	A	Date:	10/8/2017
STATION	10-m Separation		Remarks
	HD	VD	
0	46	58	
20	76	68	
40	73	70	
60	62	54	
80	92	77	
100	91	88	
120	96	88	water (rice farm)
140	94	79	
160	141	102	
180	110	93	
200	142	98	
220	116	101	
240	94	89	
260	91	64	
280	105	95	water
300	91	93	
320	102	98	
340	136	106	
360	110	101	
380	95	98	
400	111	85	
420	97	87	
440	105	93	
460	112	100	
480	107	88	
500	94	84	
520	97	81	
540	98	89	
560	98	77	
580	85	66	
600	98	76	
620	96	69	
640	97	78	
660	96	66	
680	96	79	
700	88	81	
720	85	68	
740	70	52	
760	71	71	
780	86	71	
800	90	78	
820	78	76	
840	61	50	
860	89	72	
880	69	57	
900	77	76	
920	58	56	
940	58	48	
960	58	48	
980	58	56	
1000	51	74	

40m Coil Separation

NASIA			
Bearing		Profile Length:	1000 m
Profile No.	A	Date:	10/8/2017
STATION	40-m Separation		Remarks
	HD	VD	
0	53	42	
20	55	46	
40	62	47	
60	65	44	
80	67	41	
100	67	41	
120	64	34	
140	66	47	
160	65	44	
180	69	44	
200	67	48	
220	70	51	
240	69	50	
260	70	51	
280	69	41	
300	73	51	
320	75	52	
340	70	48	
360	74	50	
380	73	54	
400	67	53	
420	70	53	
440	72	57	
460	72	60	
480	72	57	
500	77	51	
520	70	50	
540	74	65	muddy water
560	74	56	
580	76	57	
600	74	55	
620	68	53	
640	69	54	
660	68	59	
680	70	55	
700	70	61	
720	71	44	
740	81	57	
760	72	51	
780	75	58	Rice farm (muddy water)
800	75	54	
820	70	46	
840	68	54	
860	69	51	
880	60	49	
900	62	44	
920	67	48	
940	59	55	
960	56	54	
980	64	49	
1000	56	48	

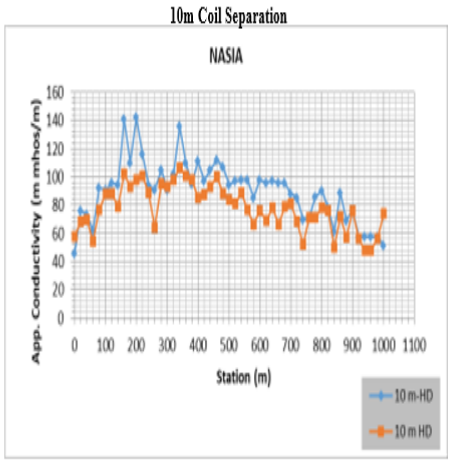

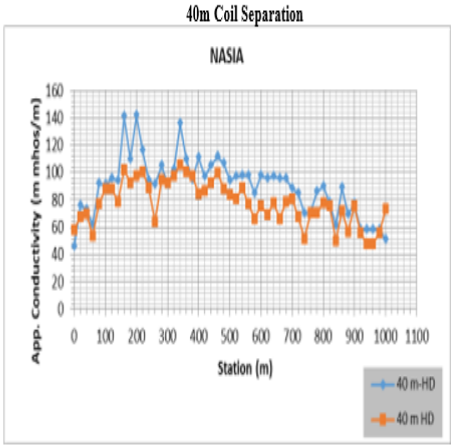

Location: Pigu

10m Coil Separation

PIGU			
Bearing		Profile Length	1000 m
Profile No.	A	Date:	6/10/2017
STATION	10-m Separation		Remarks
	HD	VD	
0	77	54	
20	67	51	
40	55	60	
60	72	71	
80	45	54	
100	53	40	
120	98	42	
140	41	52	
160	63	54	
180	65	51	
200	62	50	
220	55	38	
240	34	23	
260	50	44	
280	48	37	
300	69	47	
320	48	31	
340	49	51	
360	51	47	
380	36	33	
400	54	47	
420	62	41	
440	43	29	
460	57	42	
480	68	58	
500	84	44	
520	46	23	
540	48	34	
560	43	44	
580	62	51	
600	56	43	
620	51	46	
640	52	31	
660	49	45	
680	54	61	
700	58	42	
720	49	30	
740	47	34	
760	35	52	
780	51	30	
800	18	14	
820	22	12	
840	15	22	
860	45	10	
880	51	30	
900	43	40	
920	41	34	
940	52	41	
960	64	51	
980	55	44	
1000	58	31	

40m Coil Separation

			PIGU
Bearing		Profile Length:	1000 m
Profile No.	A	Date:	10/6/2017
STATION	40-m Separation		Remarks
	HD	VD	
0	64	51	
20	61	53	
40	72	64	
60	72	74	
80	67	68	
100	68	66	
120	66	61	
140	71	61	
160	70	69	
180	71	65	
200	73	58	
220	60	63	
240	61	68	
260	75	63	
280	70	61	
300	70	62	
320	64	60	
340	74	65	
360	68	59	
380	64	59	
400	61	66	
420	67	64	
440	61	57	
460	67	61	
480	68	64	
500	67	61	
520	67	62	
540	66	57	
560	60	61	
580	67	59	
600	63	66	
620	66	58	
640	63	60	
660	61	63	
680	74	61	
700	71	63	
720	66	66	
740	70	62	
760	67	61	
780	72	60	
800	78	63	
820	66	70	
840	71	61	
860	69	59	
880	66	57	
900	61	62	
920	65	60	
940	64	59	
960	66	64	
980	67	62	
1000	70	64	

10m Coil Separation

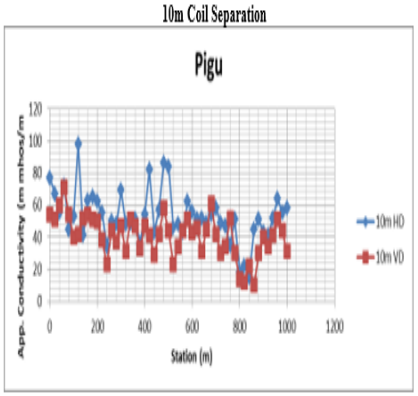

40m Coil Separation

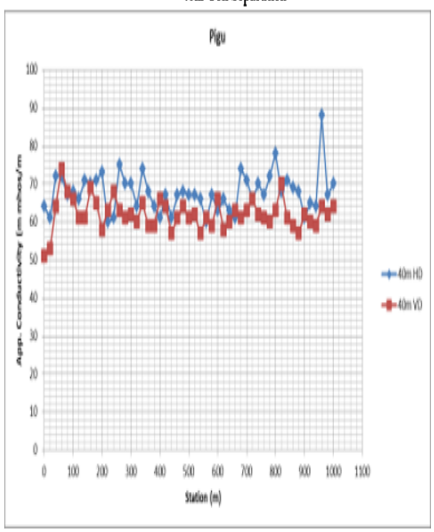

Location: Shelayilli

10m Coil Separation

			Shelayilli
Bearing		Profile Length:	1000 m
Profile No.	A	Date:	10/8/2017
STATION	10-m Separation		Remarks
	HD	VD	
0	63	41	
20	61	55	
40	41	21	
60	58	37	
80	66	61	
100	73	56	
120	55	47	
140	33	27	
160	66	50	
180	50	51	
200	39	33	
220	52	48	
240	73	55	
260	58	46	
280	39	42	
300	48	35	
320	44	30	
340	51	54	
360	47	42	
380	55	51	
400	51	52	
420	39	28	
440	50	40	
460	46	21	
480	68	51	
500	68	46	
520	14	22	
540	34	11	
560	16	11	
580	35	21	
600	57	42	
620	46	37	
640	48	44	
660	25	24	
680	14	12	
700	40	34	
720	44	40	
740	47	37	
760	56	60	
780	49	41	
800	80	49	
820	40	34	
840	33	34	
860	29	35	
880	17	31	
900	28	32	
920	58	82	
940	58	80	
960	46	54	
980	33	46	
1000	52	58	

40m Coil Separation

			Shelayili
Bearing		Profile Length:	1000 m
Profile No.	A	Date:	10/8/2017
STATION	40-m Separation		Remarks
	HD	VD	
0	53	48	
20	54	51	
40	58	57	
60	54	52	
80	58	53	
100	55	56	
120	58	59	
140	61	58	
160	61	65	
180	63	72	
200	58	70	
220	58	65	
240	59	67	
260	58	62	
280	49	56	
300	58	61	
320	53	61	
340	60	59	
360	84	54	
380	53	52	
400	55	56	
420	61	58	
440	57	61	
460	55	48	
480	55	43	
500	55	58	
520	65	42	
540	55	53	
560	61	49	
580	86	53	
600	58	51	
620	61	80	
640	59	43	
660	49	53	
680	61	48	
700	53	52	
720	59	42	
740	54	49	
760	59	51	
780	52	57	
800	70	39	
820	59	46	
840	65	38	
860	58	48	
880	53	58	
900	63	56	
920	64	41	
940	45	29	
960	59	63	
980	66	45	
1000	49	48	

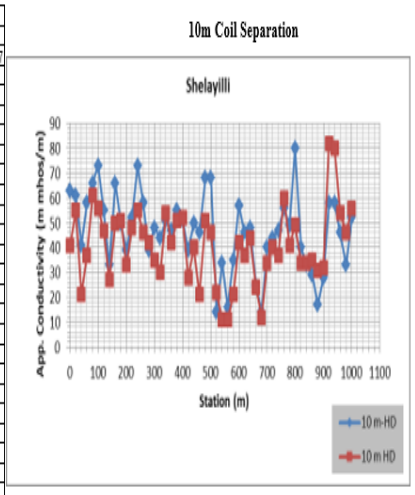

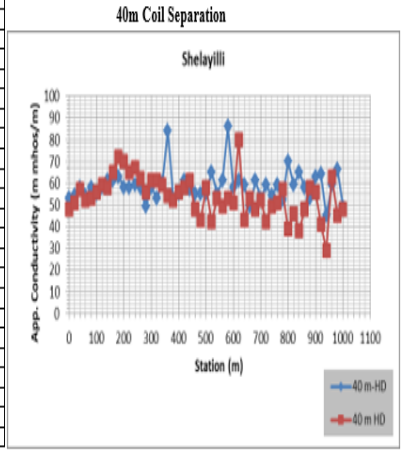

Location: Tinkpanga

20m Coil Separation

		Tinkpanga	
Bearing		Profile Length:	1000 m
Profile No.	A	Date:	10/4/2017
STATION	20-m Separation		Remarks
	HD	VD	
0	41	39	
20	41	35	
40	34	31	
60	35	28	
80	37	29	
100	39	27	
120	39	25	
140	37	17	
160	37	26	
180	38	25	
200	37	28	
220	38	26	
240	34	24	
260	32	28	
280	29	25	
300	30	19	
320	30	22	
340	27	19	
360	24	17	
380	24	20	
400	23	18	
420	22	20	
440	22	21	
460	23	20	
480	23	21	
500	23	18	
520	23	16	
540	22	16	
560	19	16	
580	18	14	
600	18	13	
620	19	13	
640	18	14	
660	18	16	
680	18	16	
700	19	14	
720	19	16	
740	20	18	
760	18	19	
780	18	19	
800	18	15	
820	18	17	
840	18	14	
860	18	15	
880	16	14	
900	16	14	
920	16	14	
940	16	16	
960	15	14	
980	15	14	
1000	15	13	

40m Coil Separation

		Tinkpanga (745847, 1153212) (745989, 1154183)	
Bearing		Profile Length:	1000 m
Profile No.	A	Date:	10/4/2017
STATION	40-m Separation		Remarks
	HD	VD	
0	31	36	
20	33	32	
40	30	30	
60	34	35	
80	43	35	
100	38	34	
120	34	35	
140	38	37	
160	31	36	
180	36	34	
200	34	33	
220	41	37	Starting point of ERT cable
240	41	38	
260	39	36	
280	40	38	
300	37	35	
320	38	31	
340	41	36	
360	40	37	
380	41	41	
400	43	40	
420	45	41	
440	46	37	
460	41	33	
480	45	37	
500	43	41	
520	41	40	
540	44	39	
560	44	37	
580	44	37	
600	49	37	
620	48	34	
640	53	37	Contact between Damango and Kodjari
660	46	35	
680	51	38	
700	51	37	
720	51	43	
740	52	41	
760	52	39	
780	53	43	
800	52	36	
820	55	44	
840	55	46	
860	56	44	
880	56	44	
900	53	40	
920	54	51	
940	47	47	
960	60	48	Stream
980	60	49	
1000	71	49	

20m Coil Separation

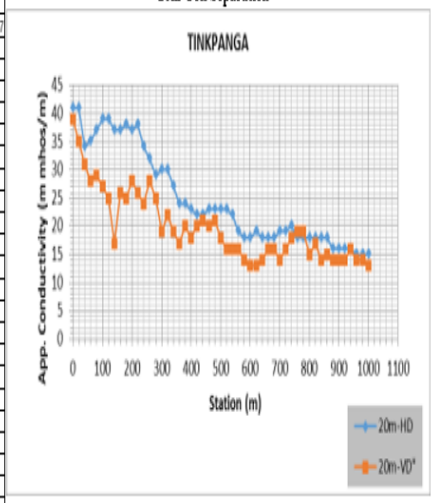

40m Coil Separation

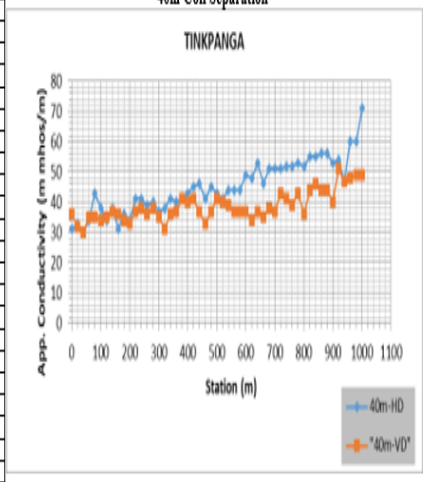

Location: Disiga A

10m Coil Separation

			Disga
Bearing		Profile Length:	500m
Profile No.	A	Date:	1/28/2019
STATION	10-m Separation		Remarks
	HD	VD	
0	75	85	
10	88	70	
20	72	81	
30	78	58	
40	80	88	
50	73	78	
60	79	98	
70	79	85	
80	84	78	
90	72	88	
100	81	80	
110	85	75	
120	80	53	
130	72	83	
140	71	81	
150	77	49	
160	88	81	
170	94	58	
180	91	85	
190	93	79	
200	99	70	
210	94	83	
220	96	84	
230	99	87	
240	100	81	
250	90	71	
260	106	85	
270	100	71	
280	112	72	
290	112	70	
300	99	55	
310	113	75	
320	116	80	
330	103	92	
340	99	66	
350	102	99	
360	103	70	
370	104	66	
380	102	72	
390	100	89	
400	111	78	
410	106	89	
420	115	88	
430	99	87	
440	113	74	
450	118	95	
460	117	80	
470	106	84	
480	101	89	
490	100	89	
500	103	94	

40m Coil Separation

			Disga
Bearing		Profile Length:	500m
Profile No.	A	Date:	1/28/2019
STATION	40-m Separation		Remarks
	HD	VD	
0	61	44	
10	60	39	
20	64	45	
30	63	41	
40	61	46	
50	61	47	
60	63	46	
70	61	43	
80	64	41	
90	59	31	
100	60	42	
110	61	37	
120	60	47	
130	63	37	
140	61	46	
150	59	44	
160	62	39	
170	60	43	
180	61	38	
190	63	39	
200	65	38	
210	65	40	
220	63	38	
230	66	41	
240	65	39	
250	67	39	
260	68	38	
270	62	42	
280	67	30	
290	69	31	
300	69	35	
310	69	34	
320	69	47	
330	63	38	
340	70	38	
350	69	38	
360	65	36	
370	70	37	
380	68	44	
390	66	44	
400	64	42	
410	66	39	
420	67	44	
430	66	40	
440	71	31	
450	69	33	
460	66	32	
470	68	35	
480	68	37	
490	62	42	
500	64	35	

10m Coil Separation

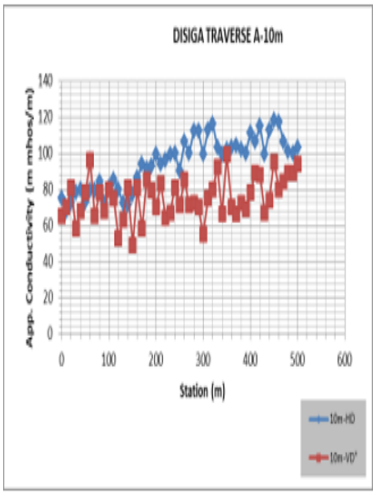

40m Coil Separation

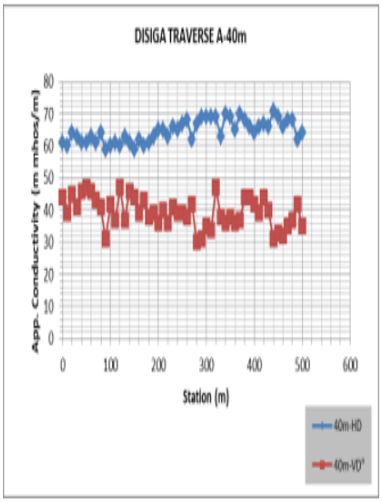

Location: Disiga B

10m Coil Separation

			Disiga
Bearing		Profile Length:	500m
Profile No.	B	Date:	1/28/2019
STATION	10-m Separation		Remarks
	HD	VD	
0	109	95	
10	98	79	
20	98	92	
30	105	87	
40	98	84	
50	100	96	
60	102	83	
70	108	101	
80	102	83	
90	111	80	
100	104	86	
110	101	93	
120	107	81	
130	105	89	
140	103	93	
150	100	85	
160	101	84	
170	108	96	
180	115	97	
190	107	88	
200	104	92	
210	109	88	
220	105	81	
230	109	81	
240	107	83	
250	108	92	
260	109	80	
270	108	93	
280	107	81	
290	111	83	
300	107	88	
310	109	86	
320	112	88	
330	105	98	
340	108	86	
350	101	83	
360	112	75	
370	114	70	
380	127	84	
390	115	78	
400	115	84	
410	119	96	
420	119	88	
430	118	80	
440	118	80	
450	123	87	
460	117	86	
470	114	81	
480	112	70	
490	119	77	
500	132	85	

40m Coil Separation

			Disiga
Bearing		Profile Length:	500m
Profile No.	B	Date:	1/28/2019
STATION	40-m Separation		Remarks
	HD	VD	
0	65	43	
10	63	35	
20	64	40	
30	63	37	
40	62	47	
50	60	41	
60	64	43	
70	60	45	
80	64	38	
90	38	38	
100	65	40	
110	63	35	
120	64	43	
130	64	39	
140	64	42	
150	65	40	
160	66	48	
170	66	39	
180	66	46	
190	66	37	
200	66	26	
210	67	45	
220	65	34	
230	66	41	
240	66	36	
250	62	35	
260	67	44	
270	67	34	
280	66	43	
290	66	45	
300	67	42	
310	66	50	
320	65	31	
330	65	42	
340	66	37	
350	67	40	
360	68	46	
370	68	47	
380	63	31	
390	69	36	
400	69	40	
410	70	40	
420	70	41	
430	70	38	
440	69	42	
450	68	37	
460	70	45	
470	67	41	
480	68	37	
490	71	44	
500	80	40	

10m Coil Separation

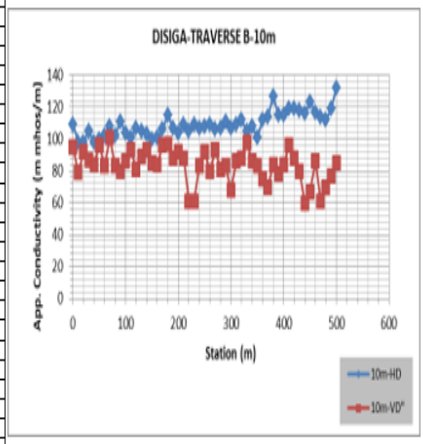

40m Coil Separation

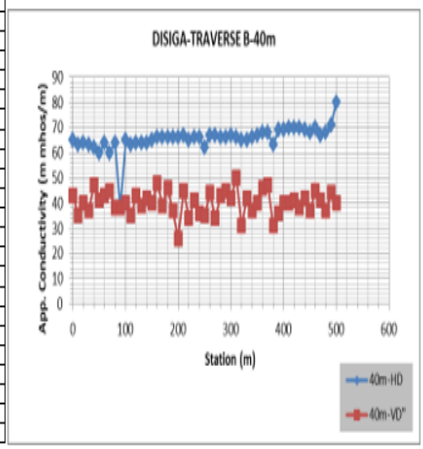

Location: Kaptun A

10m Coil Separation

			Kaptun
Bearing		Profile Length:	500m
Profile No.	A	Date:	1/25/2019
STATION	10-m Separation		Remarks
	HD	VD	
0	88	89	
10	70	77	
20	70	75	
30	78	79	
40	81	89	
50	79	73	
60	81	78	
70	89	81	
80	85	80	
90	88	84	
100	89	75	
110	93	77	
120	96	86	
130	98	77	
140	99	85	
150	99	95	
160	94	78	
170	98	84	
180	98	89	
190	94	99	
200	97	92	
210	97	82	
220	100	73	
230	97	89	
240	94	79	
250	91	88	
260	96	84	
270	97	78	
280	97	81	
290	99	73	
300	92	70	
310	99	78	
320	98	84	
330	103	70	
340	105	78	
350	108	91	
360	106	78	
370	104	82	
380	105	88	
390	104	81	
400	105	77	
410	109	90	
420	109	80	
430	103	85	
440	109	82	
450	105	90	
460	107	72	
470	107	83	
480	106	89	
490	107	97	
500	114	105	

40m Coil Separation

			Kaptun
Bearing		Profile Length:	500m
Profile No.	A	Date:	1/25/2019
STATION	40-m Separation		Remarks
	HD	VD	
0	71	48	
10	65	58	
20	69	42	
30	67	35	
40	68	35	
50	70	34	
60	68	42	
70	64	36	
80	69	38	
90	72	37	
100	70	32	
110	72	45	
120	73	30	
130	70	39	
140	71	40	
150	73	41	
160	70	47	
170	72	30	
180	74	39	
190	72	47	
200	70	29	
210	72	50	
220	67	38	
230	73	32	
240	73	37	
250	73	50	
260	70	39	
270	69	49	
280	71	40	
290	72	40	
300	72	40	
310	72	40	
320	73	42	
330	72	33	
340	74	50	
350	74	49	
360	78	46	
370	79	45	
380	74	42	
390	74	30	
400	72	39	
410	72	38	
420	79	42	
430	75	45	
440	78	38	
450	74	49	
460	78	37	
470	77	38	
480	73	50	
490	73	33	
500	77	49	

10m Coil Separation

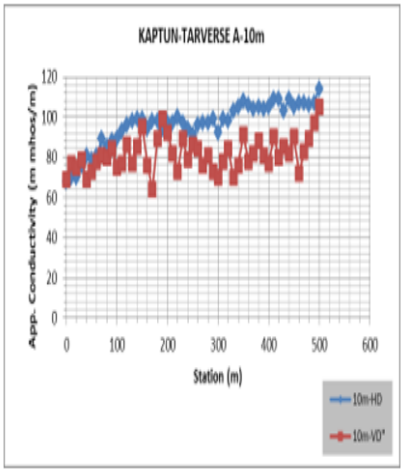

40m Coil Separation

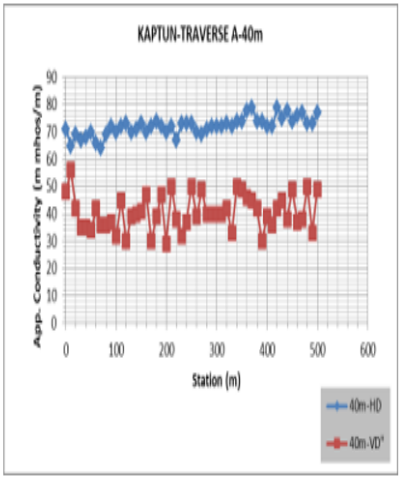

Location: Kaptun B

10m Coil Separation

			Kaptun
Bearing		Profile Length:	500m
Profile No.	B	Date:	1/25/2013
STATION	10-m Separation		Remarks
	HD	VD	
0	98	107	
10	116	111	
20	112	95	
30	112	90	
40	109	88	
50	105	87	
60	104	85	
70	97	92	
80	112	98	
90	114	98	
100	103	83	
110	98	87	
120	122	88	
130	115	77	
140	117	98	
150	108	88	
160	115	85	
170	84	88	
180	115	88	
190	121	108	
200	118	95	
210	108	88	
220	118	95	
230	118	82	
240	108	72	
250	117	89	
260	102	82	
270	113	72	
280	119	88	
290	124	88	
300	108	80	
310	104	83	
320	99	85	
330	91	78	
340	95	88	
350	95	88	
360	95	80	
370	104	77	
380	108	91	
390	104	80	
400	102	89	
410	103	84	
420	104	81	
430	100	89	
440	102	93	
450	108	74	
460	95	87	
470	104	87	
480	99	89	
490	110	70	
500	103	80	

40m Coil Separation

			Kaptun
Bearing		Profile Length:	500m
Profile No.	B	Date:	1/25/2013
STATION	40-m Separation		Remarks
	HD	VD	
0	78	57	
10	82	47	
20	73	41	
30	73	45	
40	70	40	
50	72	54	
60	70	46	
70	70	52	
80	69	44	
90	69	38	
100	71	40	
110	73	39	
120	73	41	
130	73	41	
140	74	46	
150	74	46	
160	74	39	
170	70	42	
180	73	42	
190	75	45	
200	74	42	
210	72	41	
220	73	47	
230	72	42	
240	70	38	
250	70	49	
260	72	41	
270	73	47	
280	70	44	
290	72	44	
300	69	52	
310	71	47	
320	67	46	
330	61	50	
340	62	49	
350	66	46	
360	65	41	
370	64	41	
380	63	44	
390	64	46	
400	67	50	
410	63	44	
420	69	44	
430	69	45	
440	70	39	
450	73	35	
460	74	37	
470	73	43	
480	70	38	
490	67	52	
500	67	55	

10m Coil Separation

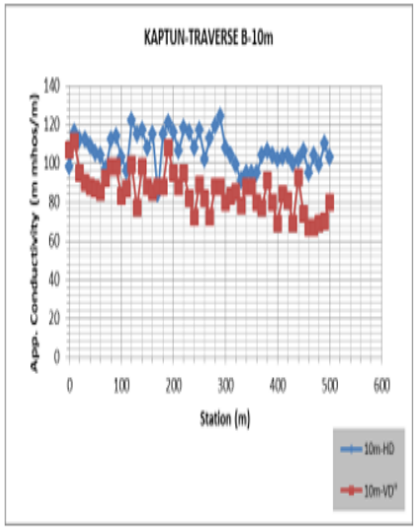

40m Coil Separation

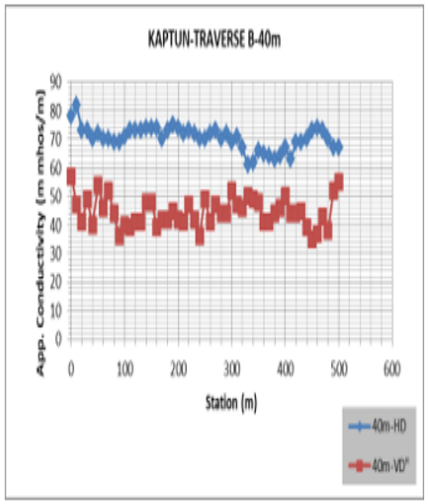

Location: Nakpaya A

10m Coil Separation

			Nakpaya
Bearing		Profile Length:	500m
Profile No.	A	Date:	1/27/2019
STATION	10-m Separation		Remarks
	HD	VD	
0	58	72	
10	60	64	
20	74	73	
30	72	48	
40	79	75	
50	74	77	
60	80	77	
70	73	84	
80	79	77	
90	84	72	
100	87	86	
110	82	74	
120	80	77	
130	79	58	
140	78	78	
150	75	77	
160	87	81	
170	91	83	
180	93	78	
190	97	68	
200	96	80	
210	88	69	
220	94	75	
230	88	84	
240	97	93	
250	98	90	
260	92	82	
270	89	94	
280	94	78	
290	91	71	
300	84	93	
310	85	81	
320	82	68	
330	90	93	
340	83	68	
350	72	68	
360	72	76	
370	64	77	
380	70	78	
390	70	75	
400	69	68	
410	67	75	
420	69	79	
430	70	72	
440	74	77	
450	66	87	
460	66	78	
470	66	83	
480	68	71	
490	66	86	
500	67	81	

40m Coil Separation

			Nakpaya
Bearing		Profile Length:	500m
Profile No.	A	Date:	1/27/2019
STATION	40-m Separation		Remarks
	HD	VD	
0	67	56	
10	63	53	
20	59	46	
30	61	39	
40	61	40	
50	58	36	
60	59	31	
70	61	35	
80	62	34	
90	63	33	
100	64	36	
110	63	36	
120	61	37	
130	60	35	
140	58	37	
150	56	36	
160	59	40	
170	56	30	
180	57	32	
190	56	35	
200	59	36	
210	59	41	
220	56	39	
230	57	32	
240	54	30	
250	56	29	
260	56	32	
270	55	34	
280	55	31	
290	54	41	
300	55	34	
310	55	40	
320	55	37	
330	52	30	
340	48	31	
350	53	34	
360	51	39	
370	48	41	
380	50	41	
390	50	37	
400	50	38	
410	48	40	
420	47	35	
430	46	35	
440	47	38	
450	49	30	
460	47	42	
470	48	33	
480	48	33	
490	49	27	
500	47	32	

10m Coil Separation

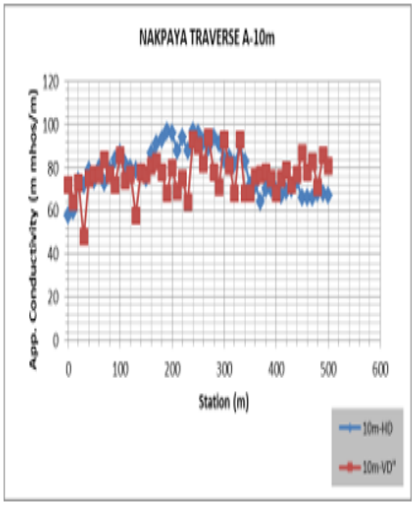

40m Coil Separation

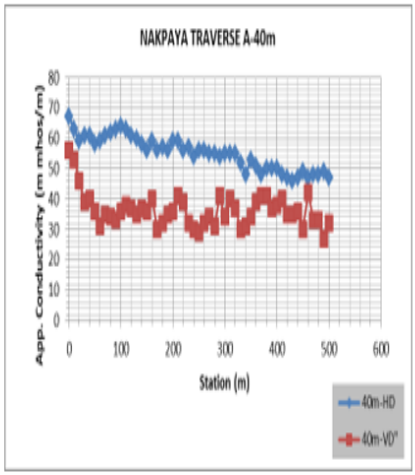

Location: Nakpaya B

10m Coil Separation

			Nakpaya
Bearing		Profile Length:	500m
Profile No.	B	Date:	1/27/2019
STATION	10-m Separation		Remarks
	HD	VD	
0	66	71	
10	86	78	
20	85	94	
30	91	84	
40	99	102	
50	101	98	
60	107	100	
70	111	85	
80	109	96	
90	117	113	
100	121	98	
110	123	101	
120	114	92	
130	111	107	
140	114	115	
150	110	94	
160	114	87	
170	109	107	
180	98	113	
190	101	75	
200	91	88	
210	96	99	
220	91	90	
230	84	92	
240	85	87	
250	65	97	
260	82	89	
270	79	84	
280	79	85	
290	74	73	
300	83	78	
310	86	96	
320	74	89	
330	84	83	
340	103	77	
350	94	98	
360	85	94	
370	94	90	
380	88	91	
390	79	94	
400	77	90	
410	90	99	
420	83	88	
430	79	82	
440	79	97	
450	73	81	
460	83	100	
470	73	78	
480	87	91	
490	81	85	
500	80	98	

40m Coil Separation

			Nakpaya
Bearing		Profile Length:	500m
Profile No.	B	Date:	1/27/2019
STATION	40-m Separation		Remarks
	HD	VD	
0	70	47	
10	67	48	
20	73	42	
30	77	38	
40	78	52	
50	78	45	
60	78	47	
70	78	45	
80	80	41	
90	79	40	
100	80	38	
110	82	49	
120	83	47	
130	80	41	
140	78	55	
150	75	48	
160	78	53	
170	75	46	
180	74	44	
190	71	50	
200	70	40	
210	68	43	
220	64	46	
230	66	41	
240	67	44	
250	63	46	
260	64	45	
270	66	44	
280	64	40	
290	60	40	
300	61	43	
310	62	42	
320	62	42	
330	61	41	
340	61	42	
350	62	43	
360	65	40	
370	62	44	
380	60	44	
390	62	40	
400	61	39	
410	62	42	
420	60	43	
430	61	41	
440	60	43	
450	62	39	
460	60	42	
470	60	39	
480	60	39	
490	58	40	
500	59	39	

10m Coil Separation

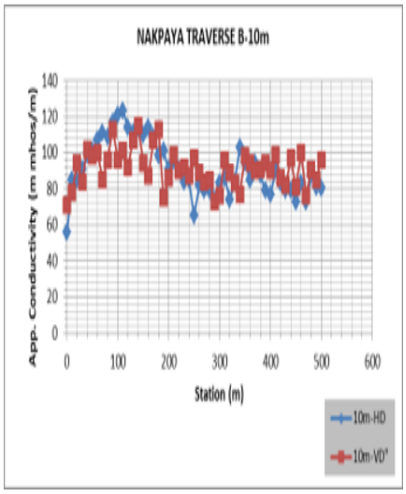

40m Coil Separation

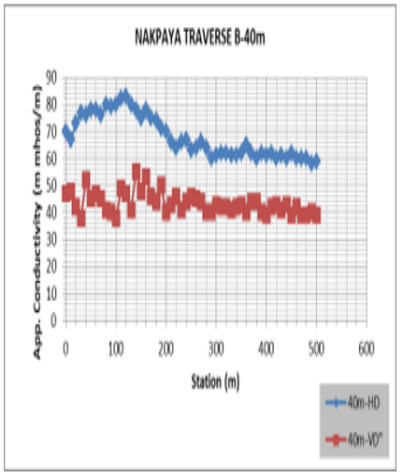

Location: Safam A

	10m Coil Separation				40m Coil Separation		
			Safam				Safam
Bearing		Profile Length:	500m	Bearing		Profile Length:	500m
Profile No.	A	Date:	1/29/2019	Profile No.	A	Date:	1/29/2019
STATION	10-m Separation		Remarks	STATION	40-m Separation		Remarks
	HD	VD			HD	VD	
0	47	43		0	45	38	
10	52	61		10	43	36	
20	47	50		20	42	39	
30	56	53		30	43	36	
40	53	52		40	43	34	
50	54	59		50	41	33	
60	59	55		60	43	34	
70	48	65		70	44	34	
80	51	60		80	44	42	
90	53	59		90	45	39	
100	58	58		100	45	33	
110	69	65		110	45	30	
120	70	59		120	47	29	
130	68	62		130	45	36	
140	61	59		140	47	35	
150	64	67		150	48	34	
160	67	55		160	48	34	
170	70	62		170	43	34	
180	77	66		180	46	28	
190	66	59		190	49	35	
200	68	55		200	49	32	
210	70	73		210	46	30	
220	61	65		220	50	33	
230	68	58		230	50	28	
240	78	73		240	50	31	
250	74	69		250	51	30	
260	77	60		260	49	32	
270	69	78		270	49	30	
280	78	75		280	47	32	
290	77	63		290	46	31	
300	72	67		300	49	30	
310	71	78		310	49	35	
320	65	71		320	47	34	
330	55	68		330	46	33	
340	60	63		340	48	35	
350	66	64		350	47	39	
360	72	70		360	47	40	
370	63	67		370	48	35	
380	72	61		380	50	29	
390	76	63		390	47	31	
400	80	62		400	48	29	
410	76	66		410	50	32	
420	68	71		420	53	31	
430	67	74		430	51	40	
440	75	68		440	52	38	
450	79	73		450	49	32	
460	83	77		460	51	38	
470	76	80		470	51	32	
480	84	82		480	56	38	
490	75	83		490	49	40	
500	80	78		500	50	31	

10m Coil Separation

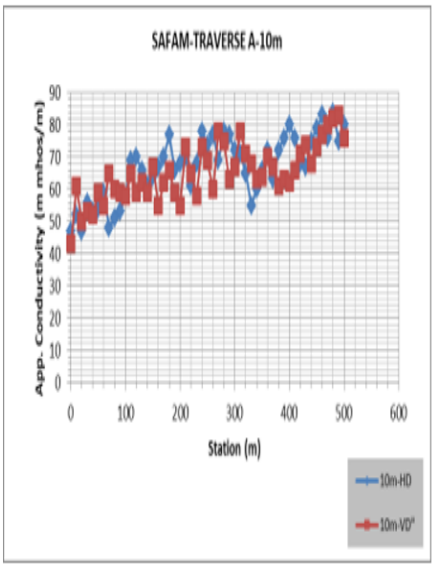

40m Coil Separation

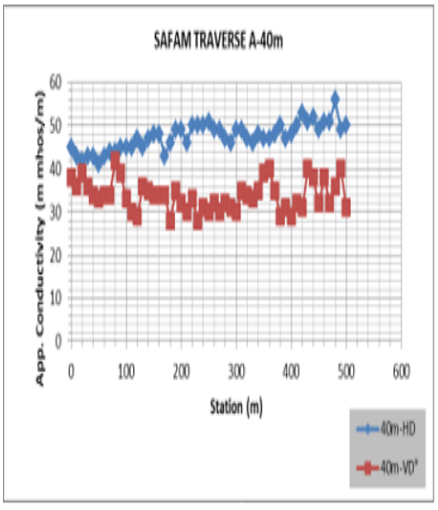

Location: Safam B

10m Coil Separation

			Safam
Bearing		Profile Length:	500m
Profile No.	B	Date:	1/29/2019
			Remarks
STATION	HD-10m	VD-10m	
0	77	68	
10	87	72	
20	82	73	
30	93	75	
40	93	75	
50	84	81	
60	84	75	
70	80	78	
80	78	68	
90	78	72	
100	80	79	
110	77	68	
120	88	86	
130	88	77	
140	85	92	
150	84	77	
160	96	79	
170	98	73	
180	99	81	
190	94	91	
200	101	99	
210	101	87	
220	103	93	
230	102	83	
240	104	92	
250	111	89	
260	106	73	
270	100	95	
280	102	98	
290	106	89	
300	110	86	
310	100	94	
320	106	99	
330	102	88	
340	97	91	
350	98	100	
360	95	92	
370	104	95	
380	99	94	
390	97	88	
400	97	87	
410	94	84	
420	93	73	
430	91	88	
440	91	89	
450	93	61	
460	102	101	
470	109	84	
480	117	82	
490	108	125	
500	102	84	

40m Coil Separation

			Safam
Bearing		Profile Length:	500m
Profile No.	B	Date:	1/29/2019
STATION	40-m Separation		Remarks
	HD	VD	
0	47	35	
10	49	38	
20	52	34	
30	50	32	
40	49	29	
50	49	31	
60	49	34	
70	48	38	
80			
90	50	41	
100	48	37	
110	50	34	
120	49	39	
130	46	35	
140	51	36	
150	52	42	
160	50	38	
170	50	36	
180	53	34	
190	52	34	
200	53	30	
210	53	34	
220	54	35	
230	53	35	
240	56	40	
250	56	33	
260	56	36	
270	55	32	
280	58	35	
290	58	35	
300	56	33	
310	53	35	
320	54	29	
330	55	35	
340	53	33	
350	53	37	
360	53	36	
370	53	33	
380	53	34	
390	50	35	
400	54	38	
410	55	39	
420	54	42	
430	55	41	
440	55	41	
450	58	36	
460	60	39	
470	62	24	
480	62	23	
490	63	25	
500	60	30	
510	59	38	

10m Coil Separation

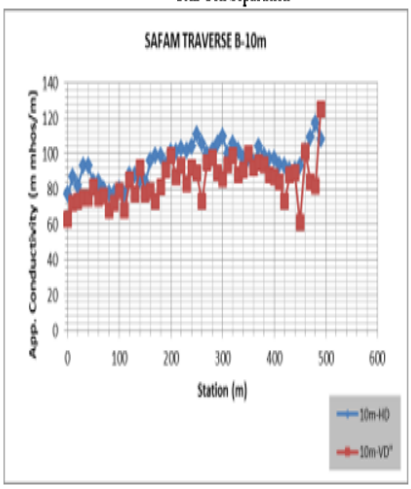

40m Coil Separation

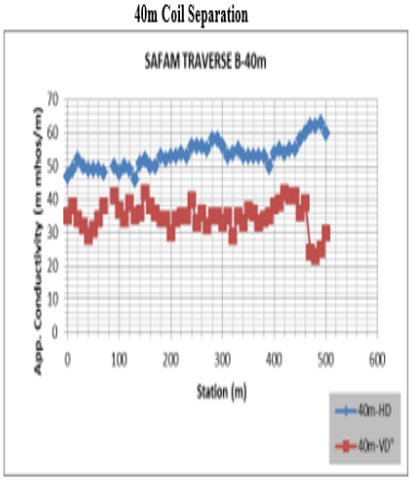

Location: Sandua A

10m Coil Separation

			Sandua
Bearing		Profile Length:	500m
Profile No.	A	Date:	1/24/2019
STATION	10-m Separation		Remarks
	HD	VD	
0			
10	80	93	
20	83	103	
30	87	78	
40	78	79	
50	80	88	
60	72	78	
70	76	89	
80	72	89	
90	72	85	
100	69	85	
110	75	85	
120	67	84	
130	73	85	
140	70	77	
150	69	78	
160	72	85	
170	62	84	
180	74	82	
190	85	86	
200	78	86	
210	77	75	
220	71	83	
230	73	87	
240	76	87	
250	73	82	
260	79	90	
270	86	99	
280	93	114	
290	99	109	
300	97	107	
310	97	99	
320	95	97	
330	95	102	
340	97	93	
350	92	98	
360	99	85	
370	102	103	
380	99	107	
390	99	114	
400	98	105	
410	96	114	
420	99	111	
430	93	102	
440	90	82	
450	93	102	
460	99	91	
470	90	99	
480	90	97	
490	97	101	
500	92	89	

40m Coil Separation

			Sandua
Bearing		Profile Length:	500m
Profile No.	A	Date:	1/23/2019
STATION	40-m Separation		Remarks
	HD	VD	
0	78	58	
10	79	46	
20	75	43	
30	71	41	
40	70	39	
50	69	59	
60	67	42	
70	63	44	
80	65	55	
90	63	59	
100	62	51	
110	62	45	
120	60	44	
130	64	50	
140	64	48	
150	60	46	
160	59	41	
170	59	42	
180	61	49	
190	63	48	
200	63	37	
210	60	38	
220	62	41	
230	61	43	
240	66	44	
250	67	42	
260	65	40	
270	68	38	
280	70	42	
290	71	34	
300	72	30	
310	70	32	
320	70	40	
330	73	35	
340	74	40	
350	72	35	
360	74	40	
370	74	42	
380	75	33	
390	72	46	
400	74	35	
410	74	45	
420	74	43	
430	76	33	
440	76	38	
450	77	43	
460	77	45	
470	79	47	
480	76	48	
490	81	44	
500	76	40	

10m Coil Separation

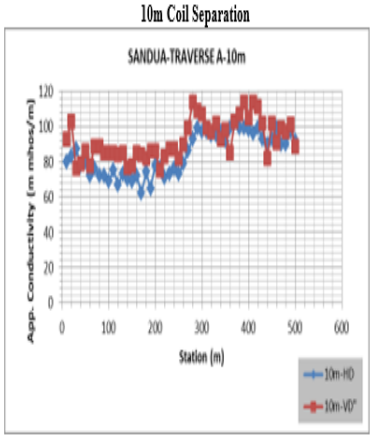

40m Coil Separation

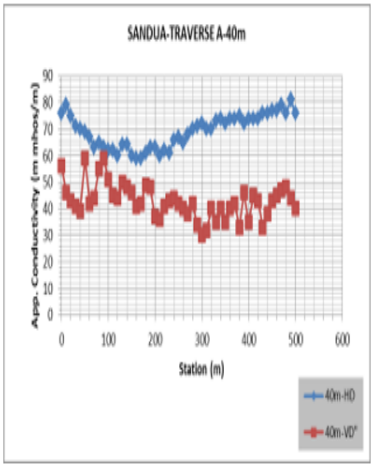

Location: Sandua B

10m Coil Separation

			Sandua
Bearing		Profile Length:	500m
Profile No.	B	Date:	1/24/2019
STATION	10-m Separation		Remarks
	HD	VD	
0			
10	58	68	
20	56	66	
30	55	75	
40	58	71	
50	59	67	
60	58	72	
70	59	71	
80	58	68	
90	63	70	
100	67	61	
110	66	73	
120	64	80	
130	67	80	
140	72	77	
150	72	81	
160	74	82	
170	66	80	
180	63	64	
190	62	78	
200	61	72	
210	58	76	
220	60	79	
230	66	78	
240	66	80	
250	63	75	
260	66	81	
270	66	79	
280	66	89	
290	70	83	
300	73	91	
310	71	90	
320	77	87	
330	85	88	
340	88	97	
350	97	70	
360	88	104	
370	88	103	
380	85	100	
390	88	95	
400	88	105	
410	94	97	
420	95	98	
430	92	95	
440	93	106	
450	91	98	
460	97	100	
470	101	105	
480	109	103	
490	105	102	
500	109	106	

40m Coil Separation

			Sandua
Bearing		Profile Length:	500m
Profile No.	B	Date:	1/24/2019
STATION	40-m Separation		Remarks
	HD	VD	
0			
10	74	51	
20	70	47	
30	69	55	
40	70	48	
50	69	59	
60	69	63	
70	68	59	
80	66	55	
90	66	55	
100	65	46	
110	69	47	
120	71	55	
130	72	55	
140	71	50	
150	71	38	
160	70	41	
170	70	44	
180	69	55	
190	69	55	
200	68	62	
210	70	59	
220	66	55	
230	67	44	
240	72	48	
250	70	41	
260	70	49	
270	68	55	
280	69	45	
290	69	47	
300	66	51	
310	67	49	
320	71	45	
330	70	47	
340	73	48	
350	73	41	
360	76	50	
370	77	46	
380	74	52	
390	75	56	
400	75	51	
410	72	44	
420	76	56	
430	77	50	
440	79	57	
450	78	53	
460	80	55	
470	82	49	
480	82	52	
490	84	44	
500	84	35	

10m Coil Separation

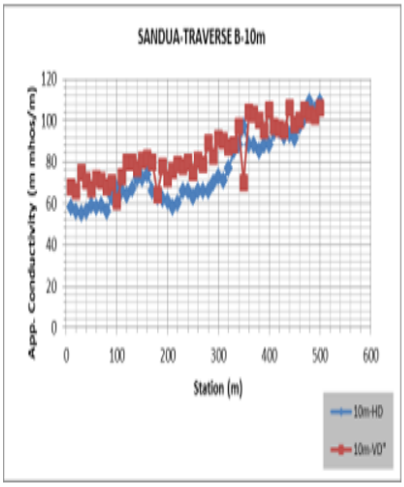

40m Coil Separation

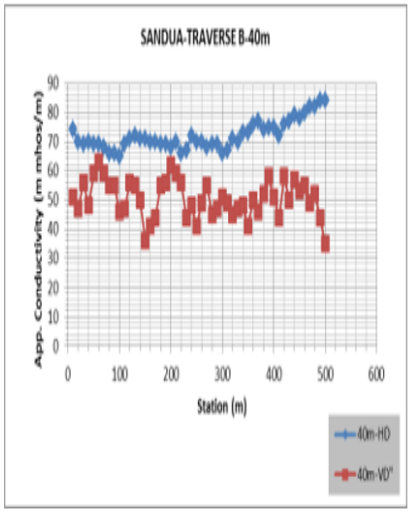

Location: Takalgu A

10m Coil Separation

			Takalgu
Bearing		Profile Length:	500m
Profile No.	A	Date:	1/28/2019
STATION	10-m Separation		Remarks
	HD	VD	
0	73	88	
10	80	72	
20	85	82	
30	72	83	
40	71	72	
50	71	67	
60	84	70	
70	70	62	
80	65	70	
90	74	68	
100	78	67	
110	74	70	
120	73	81	
130	88	67	
140	81	88	
150	78	72	
160	94	111	
170	94	90	
180	95	82	
190	100	91	
200	88	86	
210	98	108	
220	97	80	
230	100	77	
240	95	97	
250	85	79	
260	92	89	
270	98	77	
280	98	79	
290	100	89	
300	97	84	
310	90	92	
320	87	80	
330	90	91	
340	100	93	
350	92	87	
360	104	110	
370	107	94	
380	101	86	
390	86	71	
400	98	100	
410	90	84	
420	83	76	
430	85	84	
440	83	75	
450	93	83	
460	94	99	
470	112	81	
480	107	96	
490	100	83	
500	108	102	

40m Coil Separation

			Takalgu
Bearing		Profile Length:	500m
Profile No.	A	Date:	1/28/2019
STATION	40-m Separation		Remarks
	HD	VD	
0	88	67	
10	84	50	
20	78	46	
30	79	50	
40	75	55	
50	74	67	
60	75	59	
70	74	62	
80	75	57	
90	75	85	
100	77	59	
110	78	66	
120	77	65	
130	75	60	
140	78	67	
150	80	54	
160	80	54	
170	82	59	
180	89	82	
190	91	44	
200	87	55	
210	81	43	
220	87	67	
230	85	59	
240	82	66	
250	82	61	
260	79	68	
270	78	54	
280	78	60	
290	80	53	
300	80	61	
310	78	69	
320	81	58	
330	82	44	
340	81	46	
350	81	51	
360	84	53	
370	85	45	
380	81	55	
390	80	63	
400	81	54	
410	79	43	
420	77	62	
430	83	56	
440	80	57	
450	81	52	
460	83	44	
470	82	52	
480	83	48	
490	77	43	
500	81	52	

10m Coil Separation

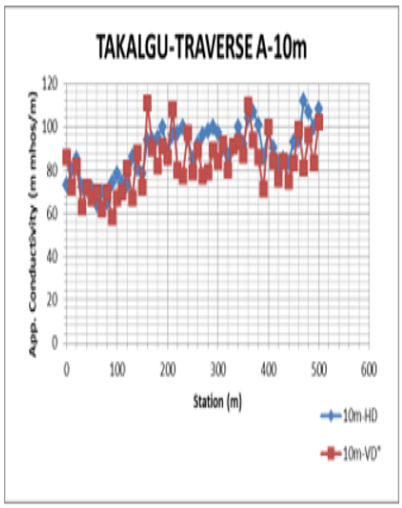

40m Coil Separation

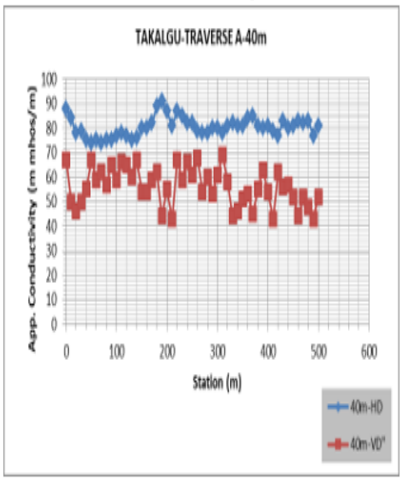

Location: Takalgu B

10m Coil Separation

			TAKALGU
Bearing		Profile Length:	500m
Profile No.	B	Date:	1/28/2019
			Remarks
STATION	HD-10m	VD-10M	
0	129	92	
10	104	87	
20	95	83	
30	88	79	
40	90	80	
50	100	83	
60	105	98	
70	109	85	
80	102	87	
90	91	73	
100	95	85	
110	101	78	
120	105	89	
130	84	82	
140	109	91	
150	102	78	
160	119	89	
170	99	88	
180	103	90	
190	95	82	
200	107	83	
210	97	82	
220	91	90	
230	94	77	
240	95	80	
250	95	85	
260	103	77	
270	88	74	
280	104	78	
290	105	84	
300	100	85	
310	109	84	
320	118	79	
330	97	82	
340	102	77	
350	110	93	
360	105	82	
370	108	88	
380	108	90	
390	112	93	
400	101	107	
410	101	81	
420	104	94	
430	102	75	
440	110	97	
450	110	75	
460	111	82	
470	106	88	
480	111	94	
490	112	102	
500	98	90	

40m Coil Separation

			Takalgu
Bearing		Profile Length:	500m
Profile No.	B	Date:	1/28/2019
STATION	40-m Separation		Remarks
	HD	VD	
0	78	44	
10	80	50	
20	79	51	
30	80	52	
40	81	51	
50	80	51	
60	79	56	
70	79	55	
80	78	48	
90	77	48	
100	78	57	
110	79	58	
120	73	50	
130	82	51	
140	79	54	
150	74	35	
160	80	43	
170	80	62	
180	79	53	
190	80	54	
200	80	49	
210	79	40	
220	79	50	
230	78	50	
240	82	52	
250	79	70	
280	79	54	
270	77	57	
280	81	60	
290	84	58	
300	82	58	
310	81	52	
320	79	41	
330	79	52	
340	79	47	
350	78	55	
360	79	58	
370	80	52	
380	80	54	
390	80	48	
400	82	51	
410	78	42	
420	81	54	
430	78	52	
440	83	47	
450	79	53	
460	83	48	
470	83	43	
480	83	44	
490	83	45	
500	77	50	

10m Coil Separation

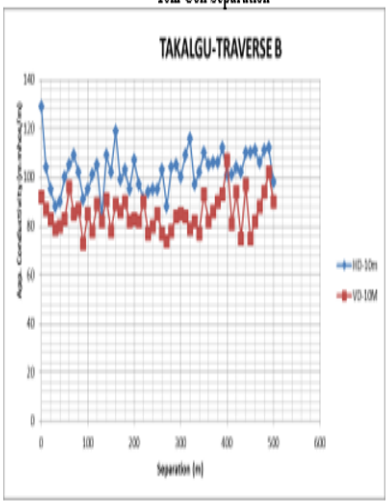

40m Coil Separation

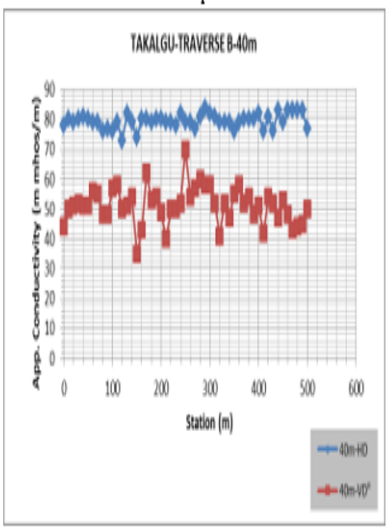

APPENDIX 2-ERT PROFILES

1. DWVP01

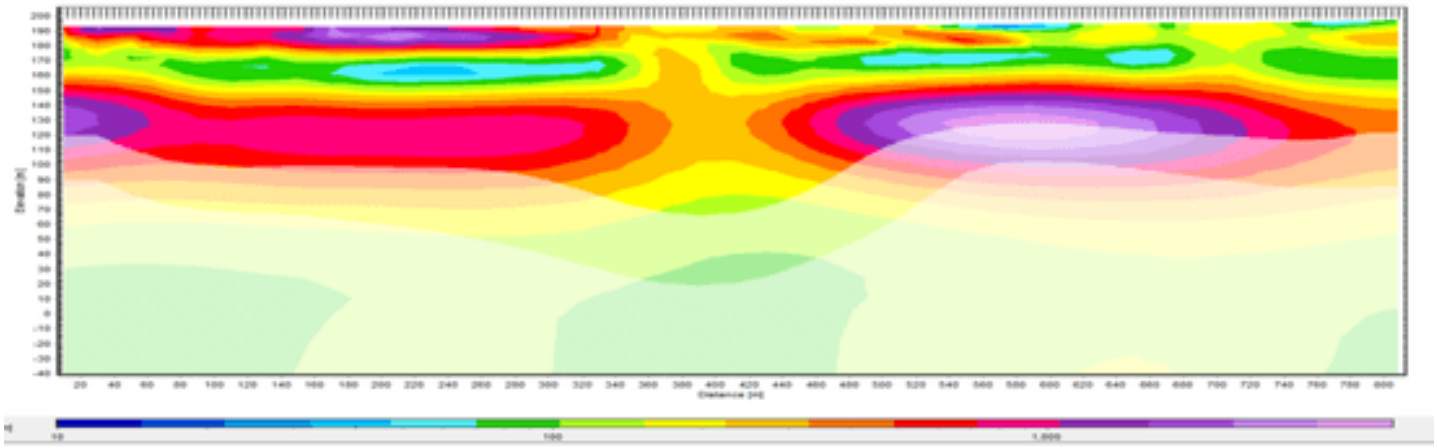

2. DWVPO2

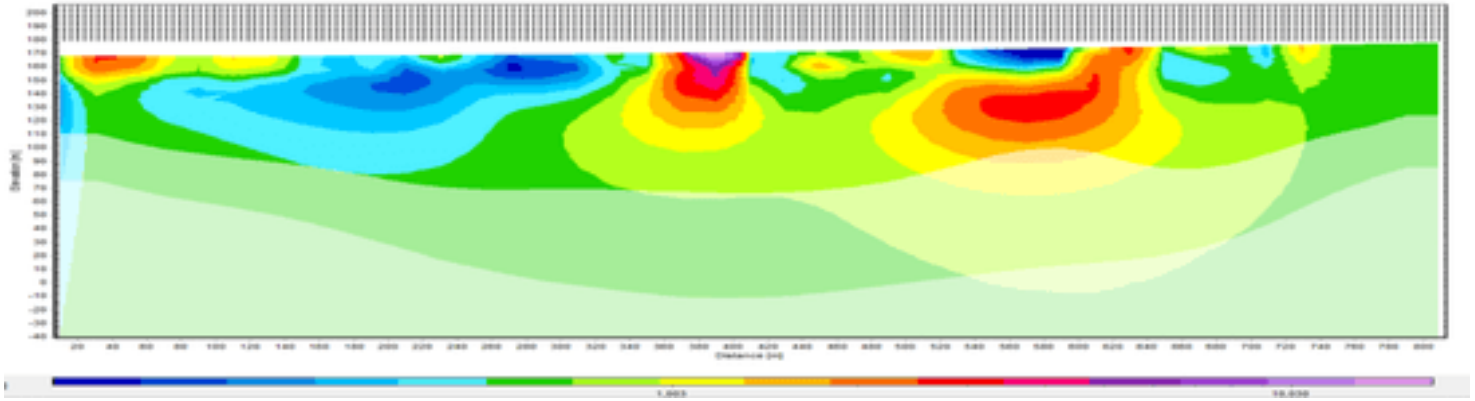

3. DWVP06

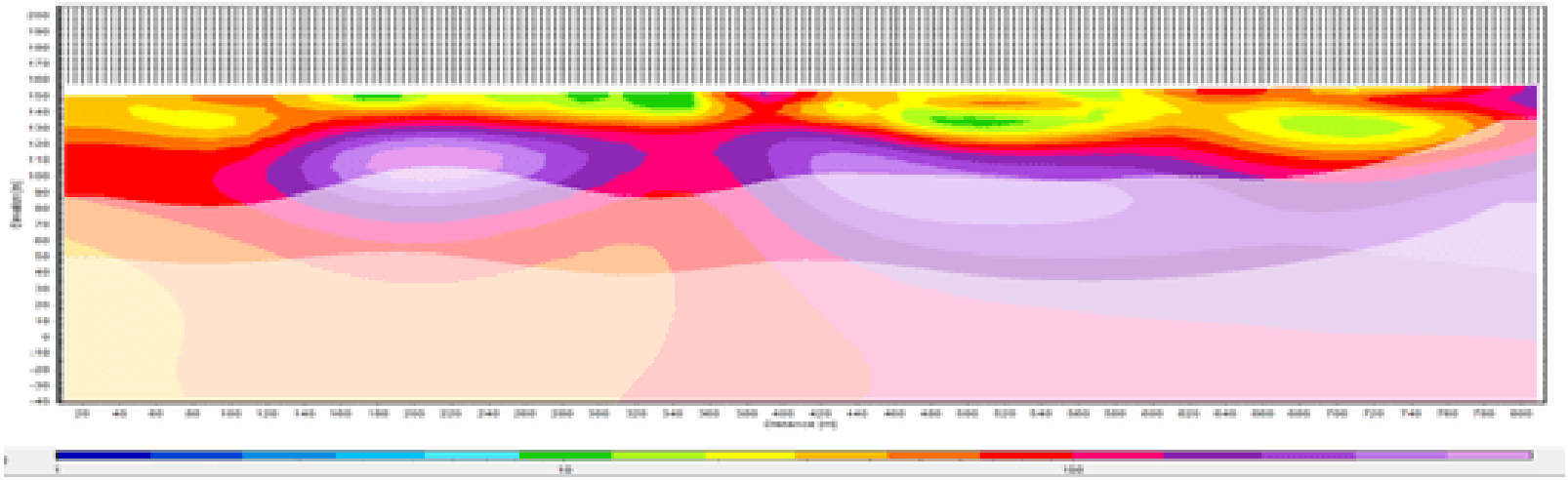

4. DWVP07

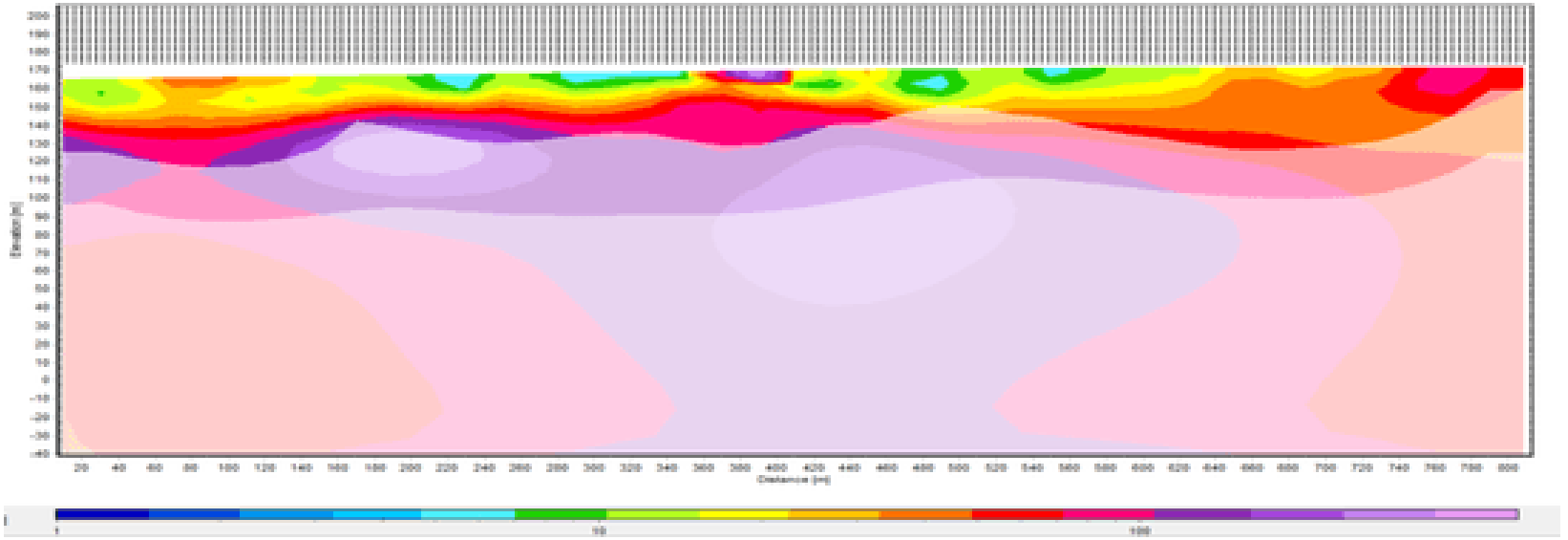

5. BANAWA 1

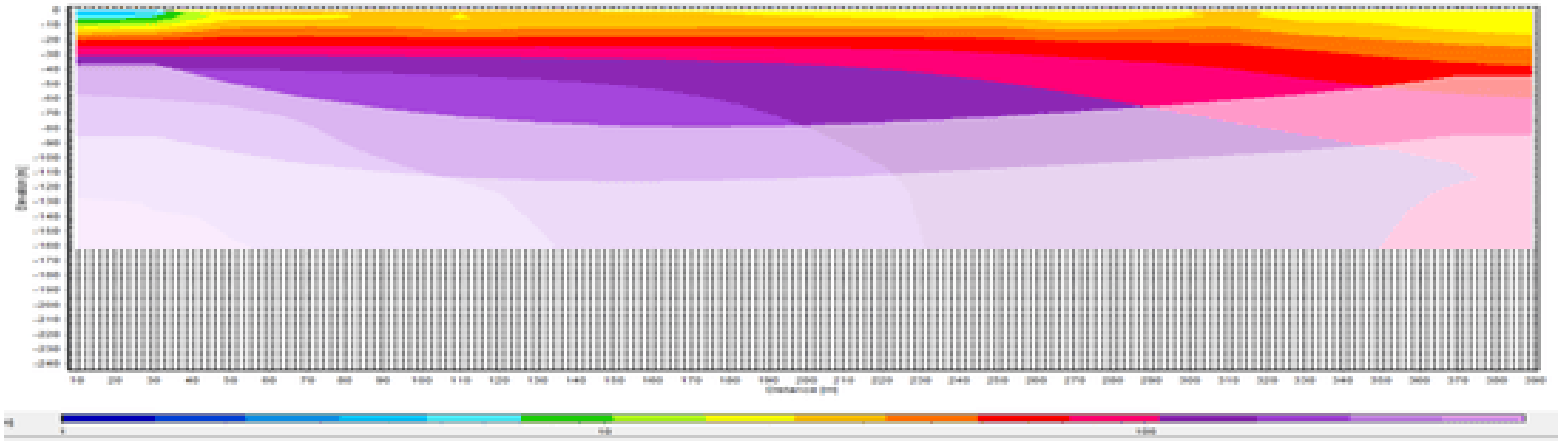

6. DIDOGLL

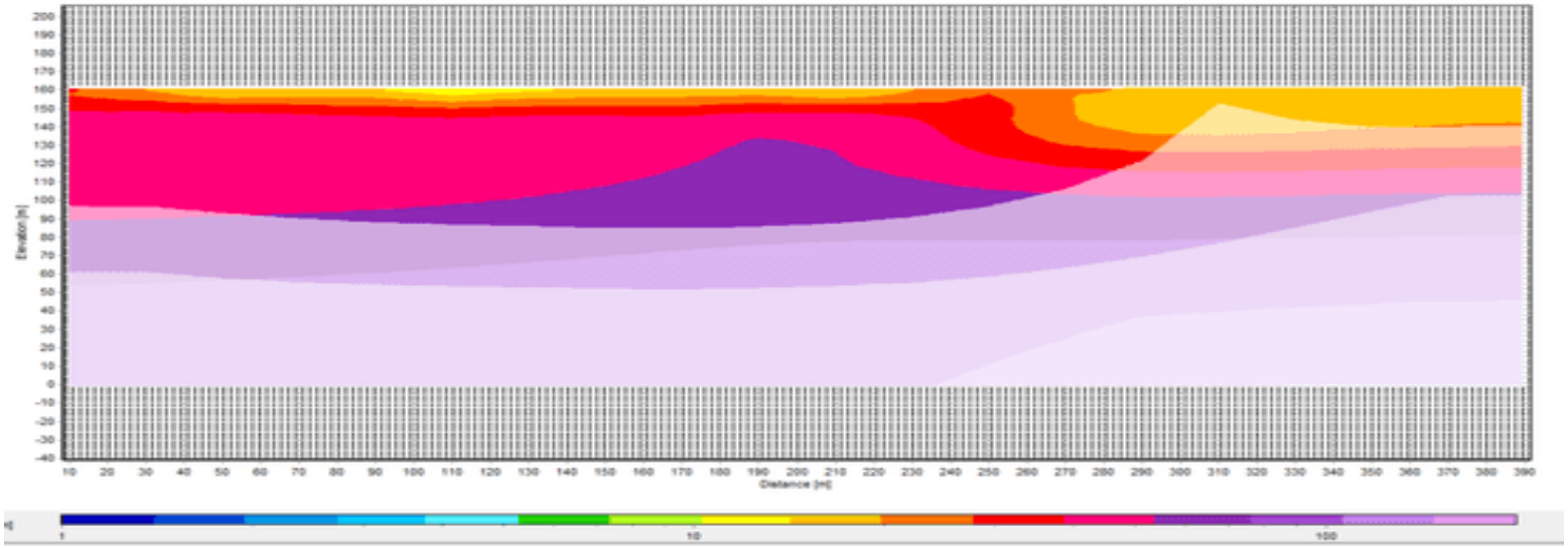

7. DINDANE DRY

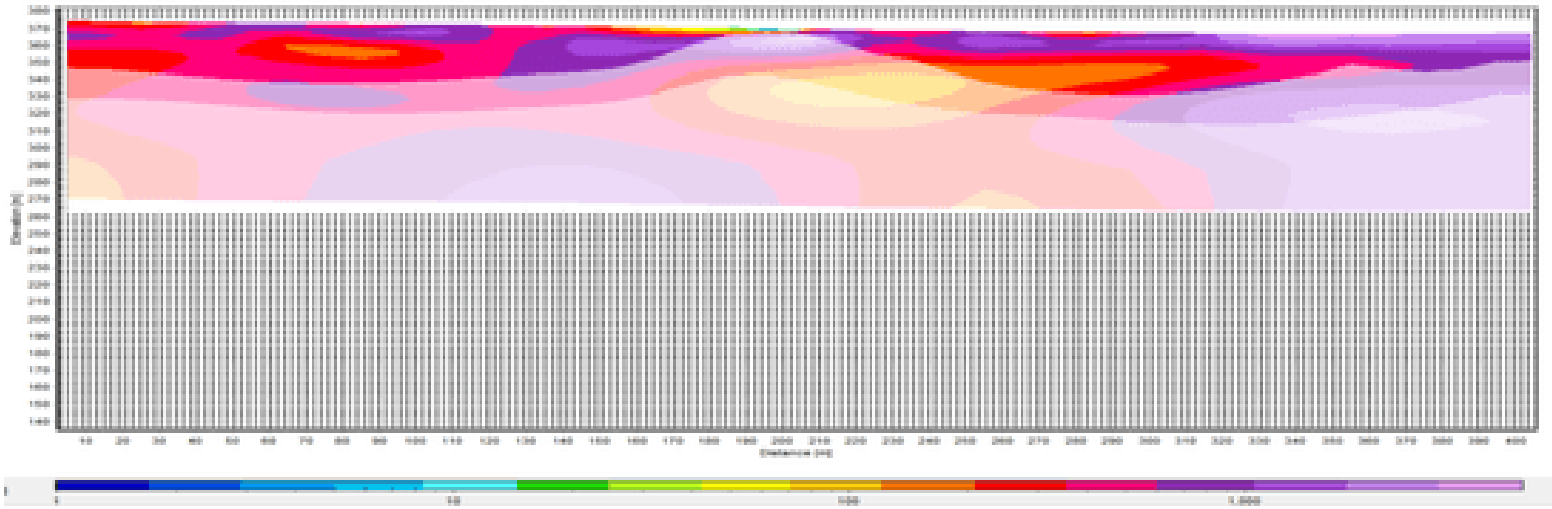

8. JEMAKA

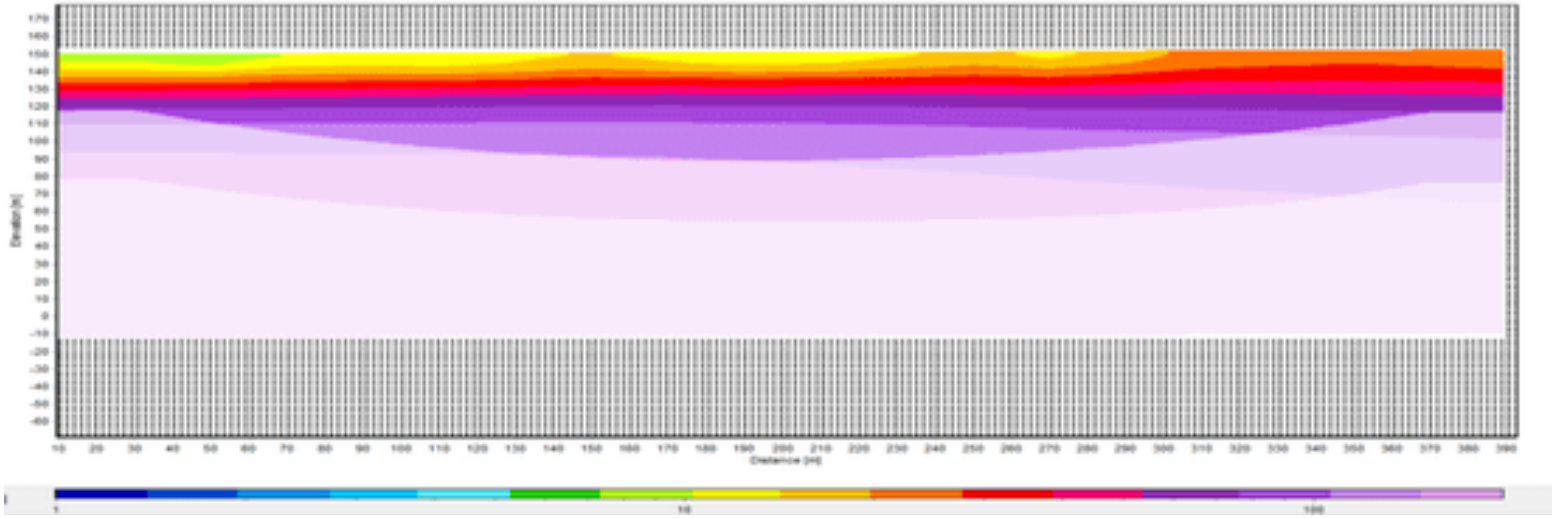

9. BANAWA 2

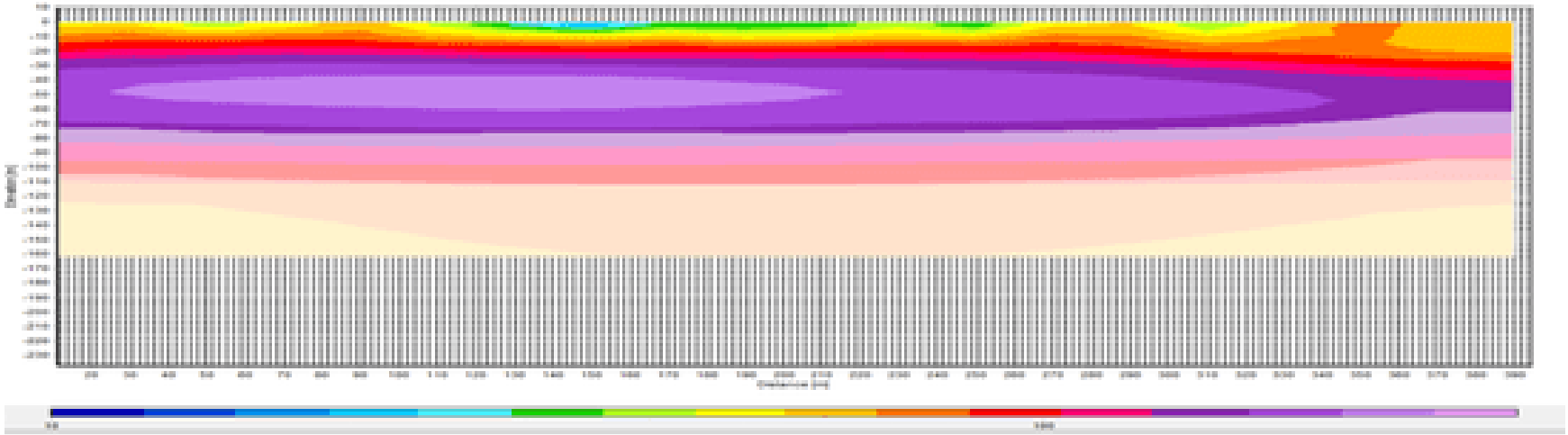

10. BOAMASA BH1

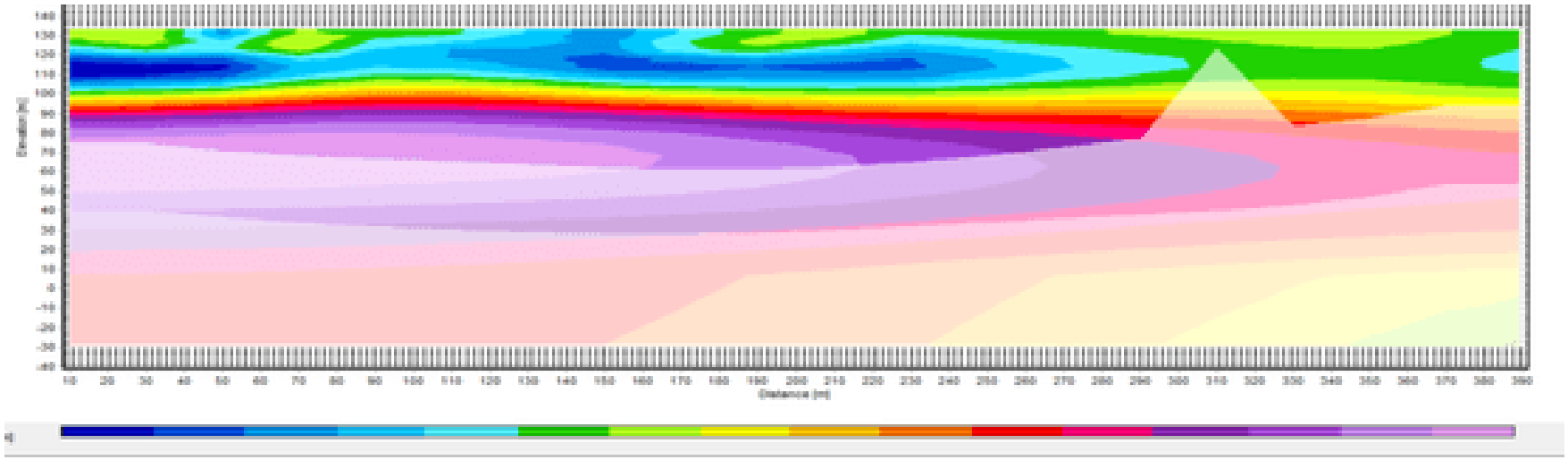

11. BOAMASA BH 2

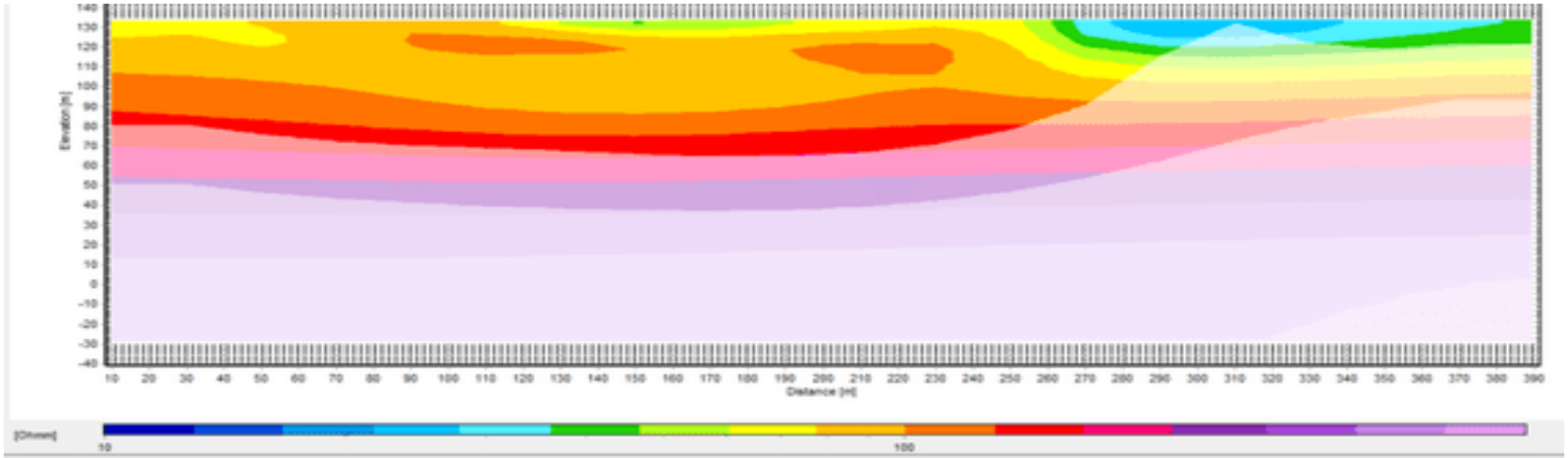

12. DAGBIRIBORE BH1

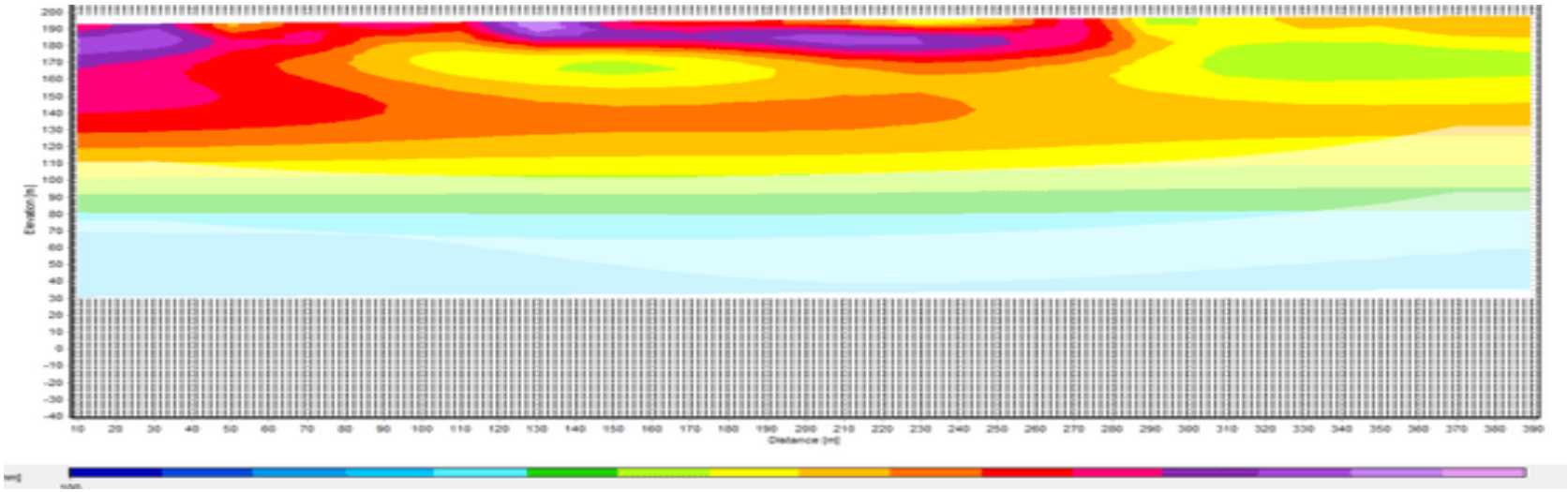

13. DAGBIRIBORE BH2

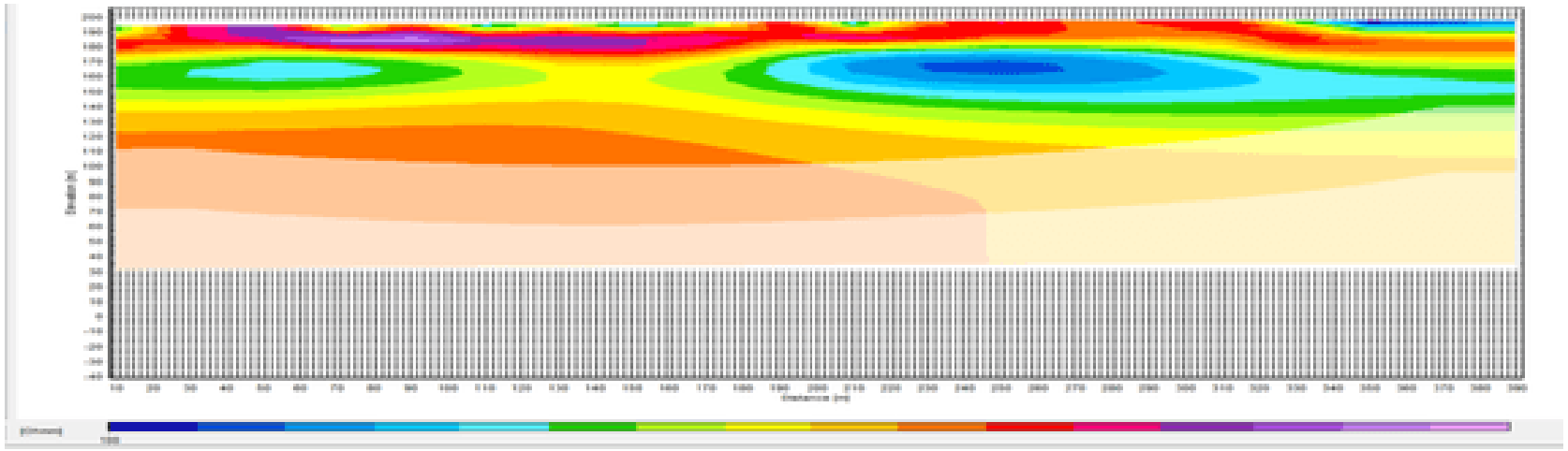

14. DISIGA

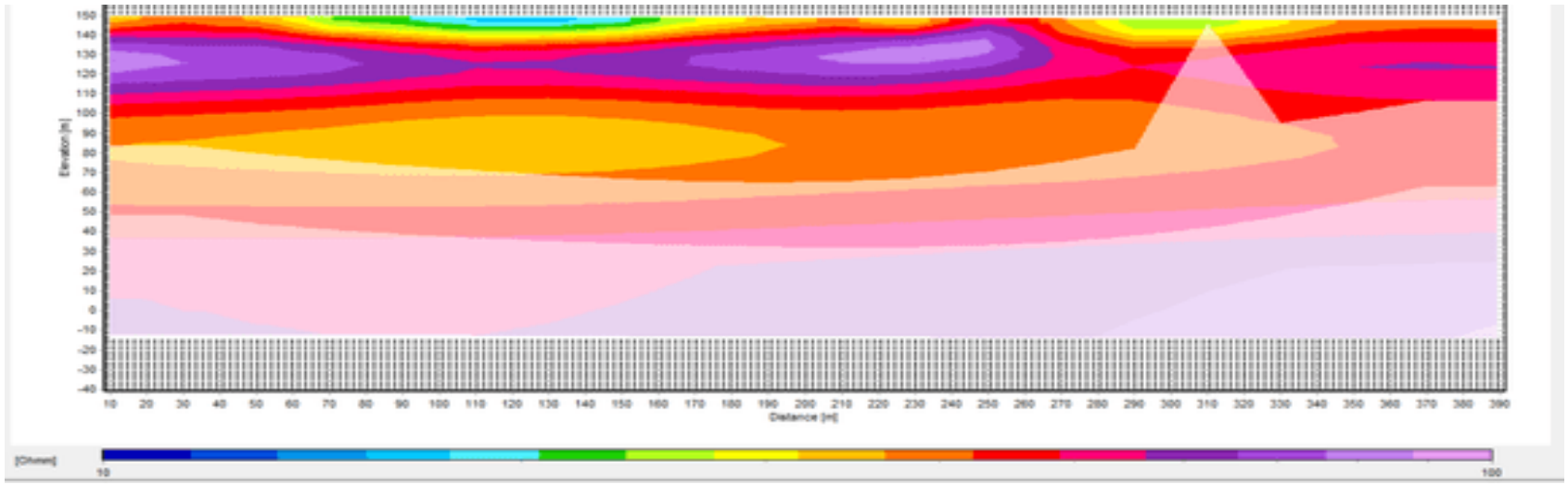

15. GBALIGA

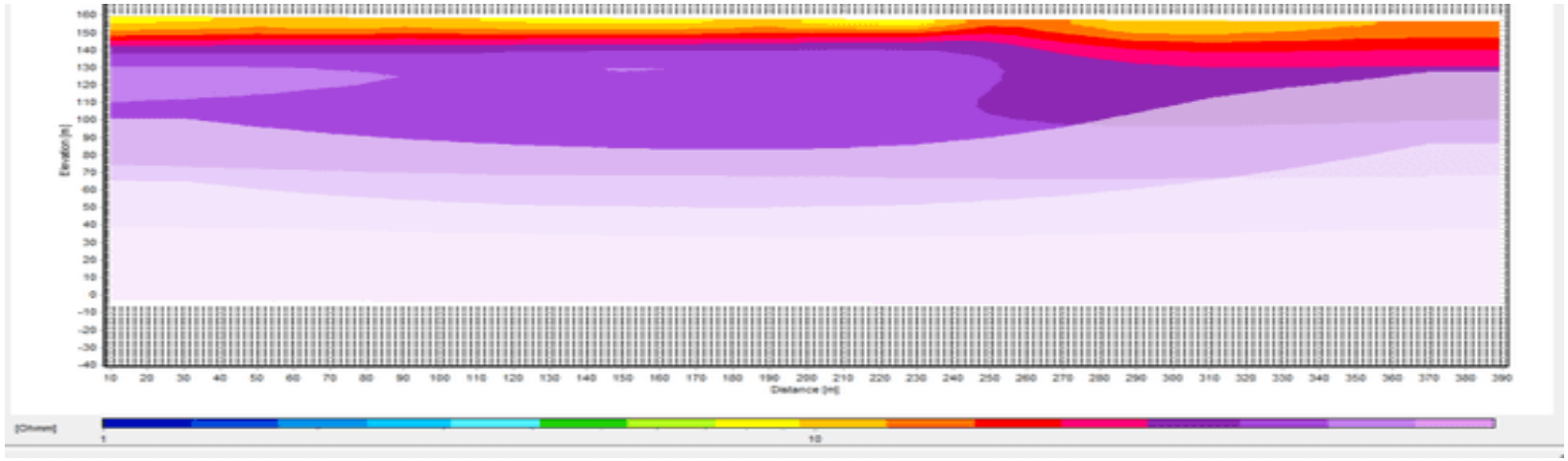

16. JEMAKA 2

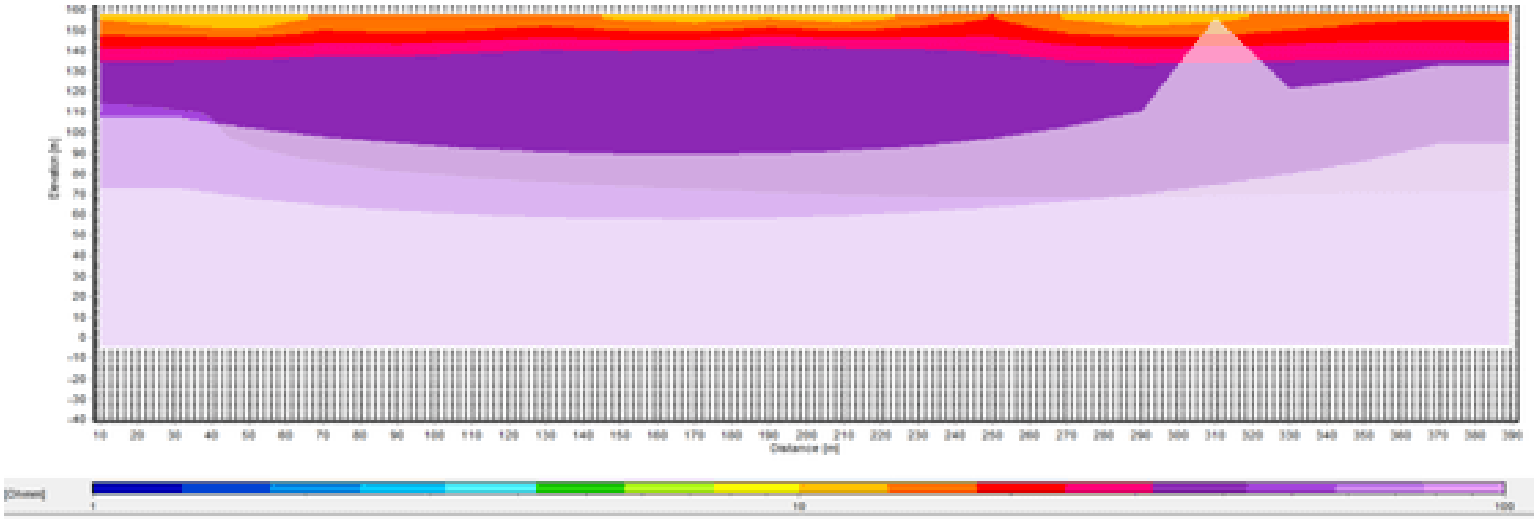

17. KATANI

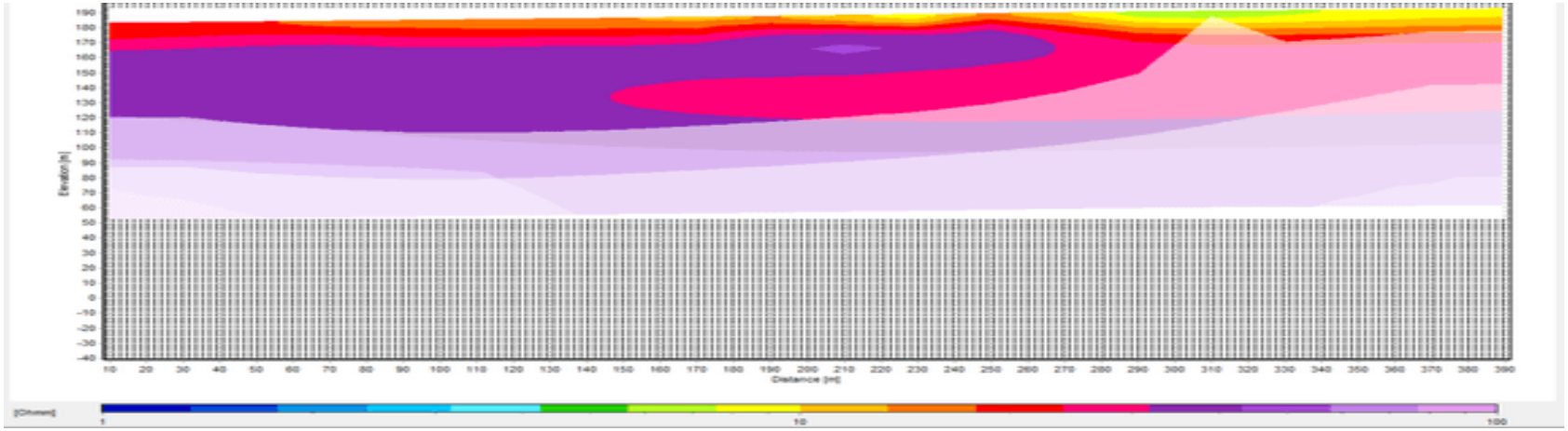

18. KOLINVA

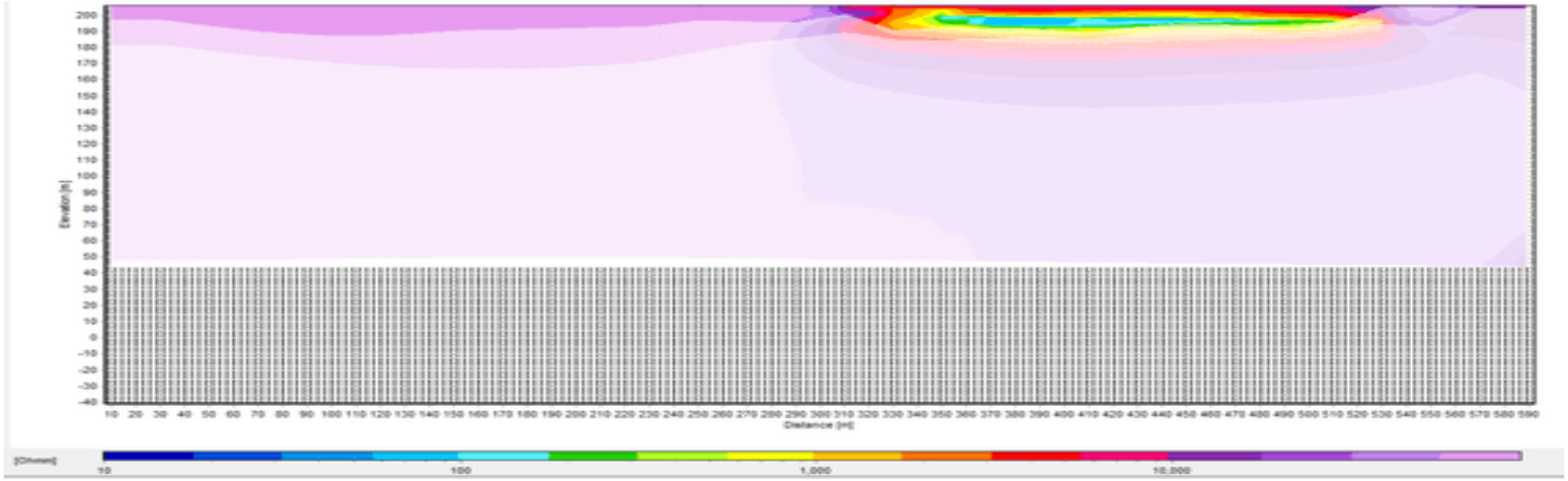

19. NABULUGU BH 2

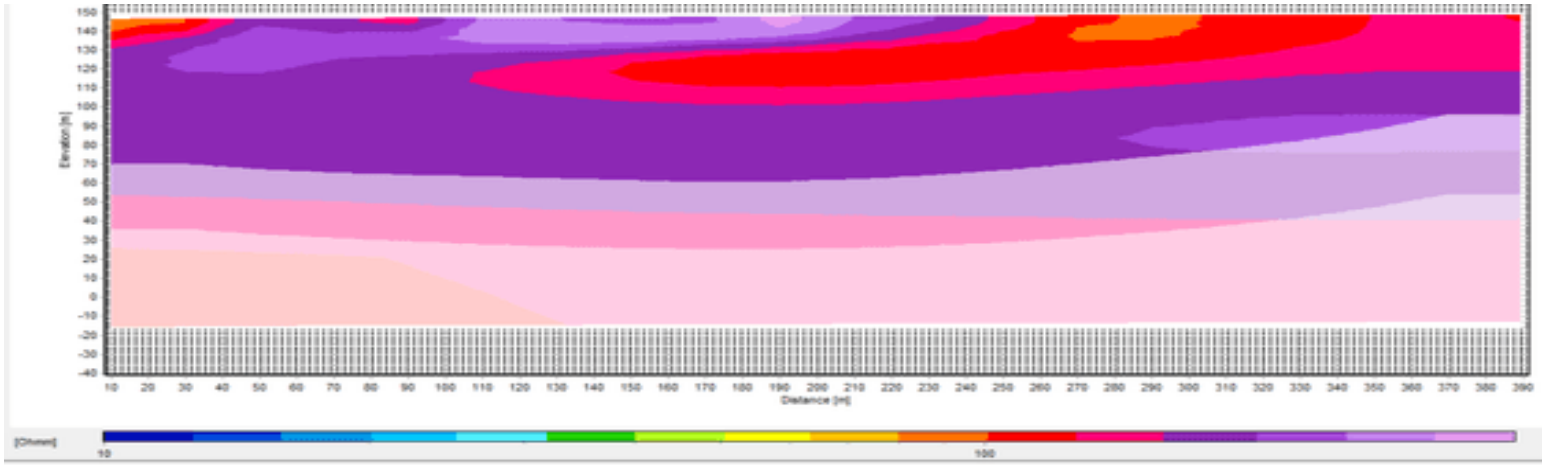

20. KPALVOKO

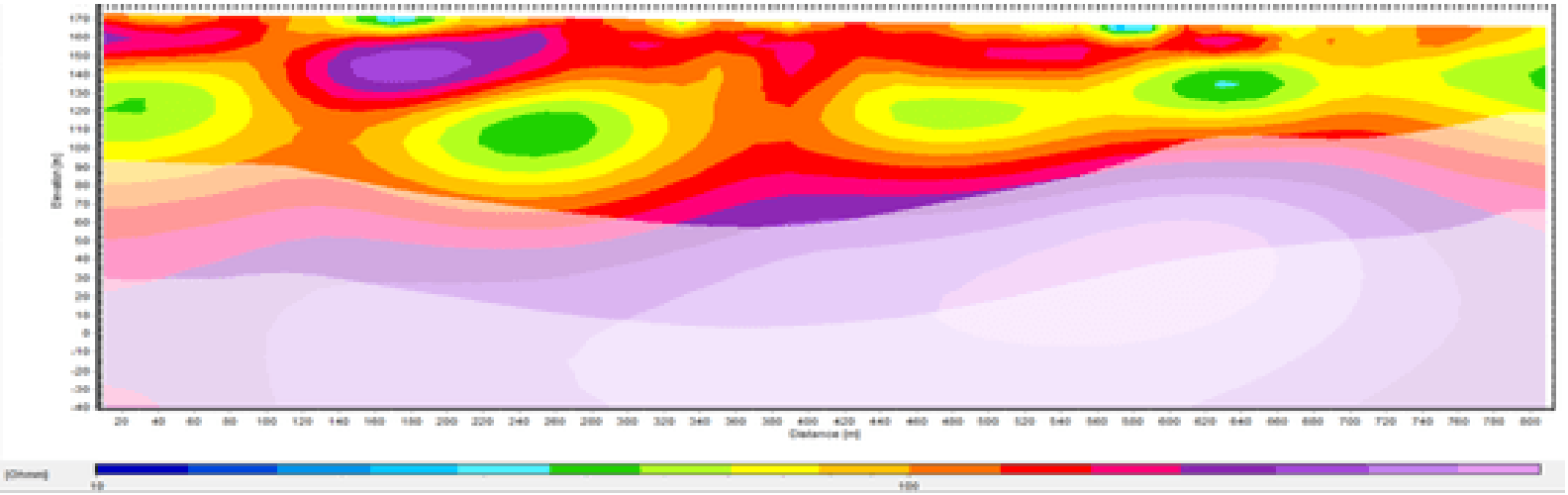

21. LOAGRI

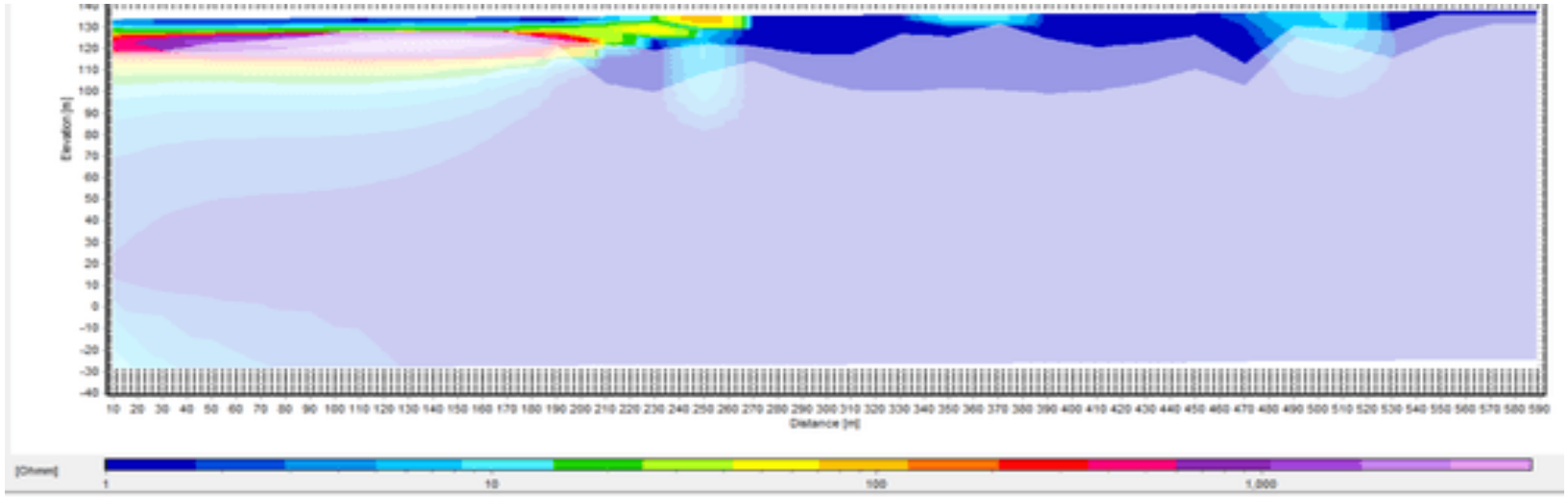

22. MANCHUGU

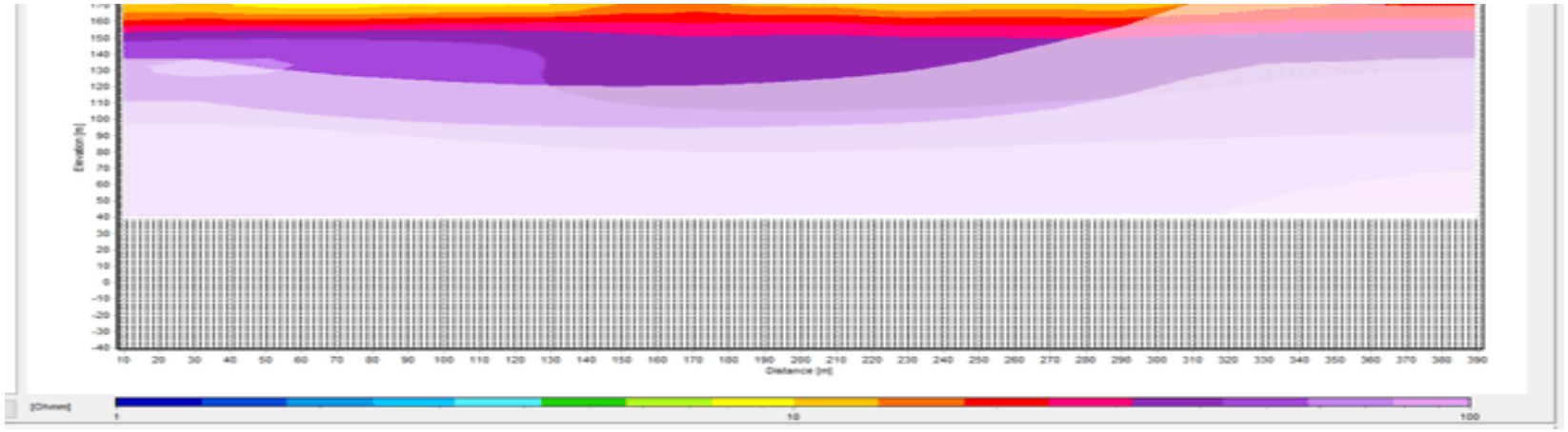

23. MOATANKURA

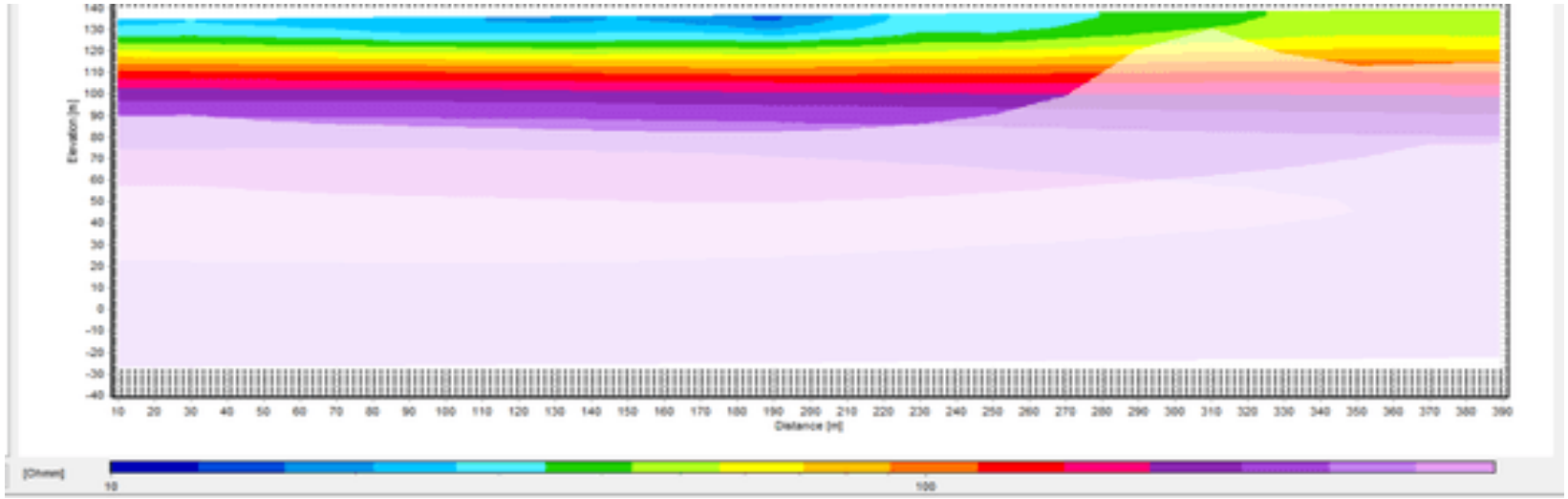

24. NAMBRUGU

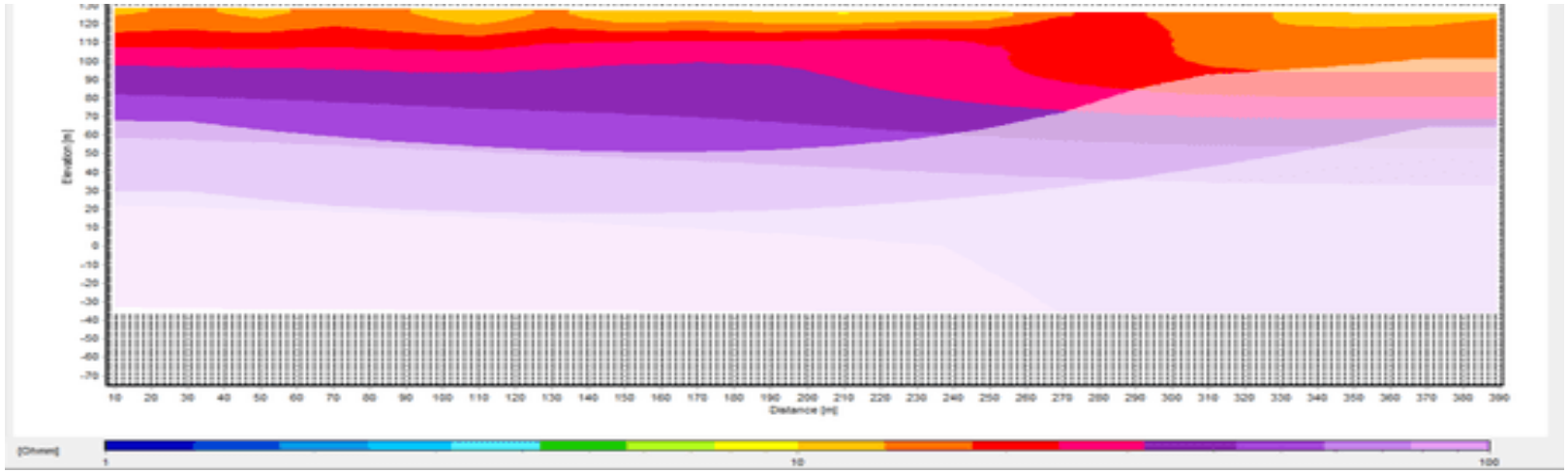

25. NALERIGU

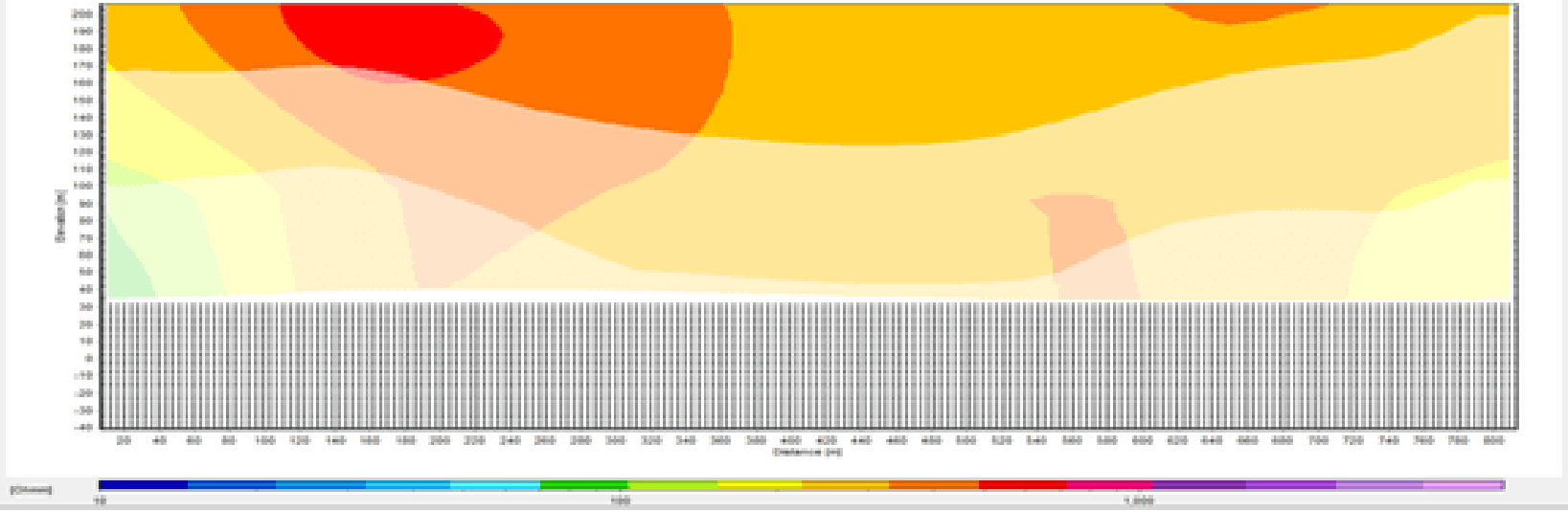

26. NASIA

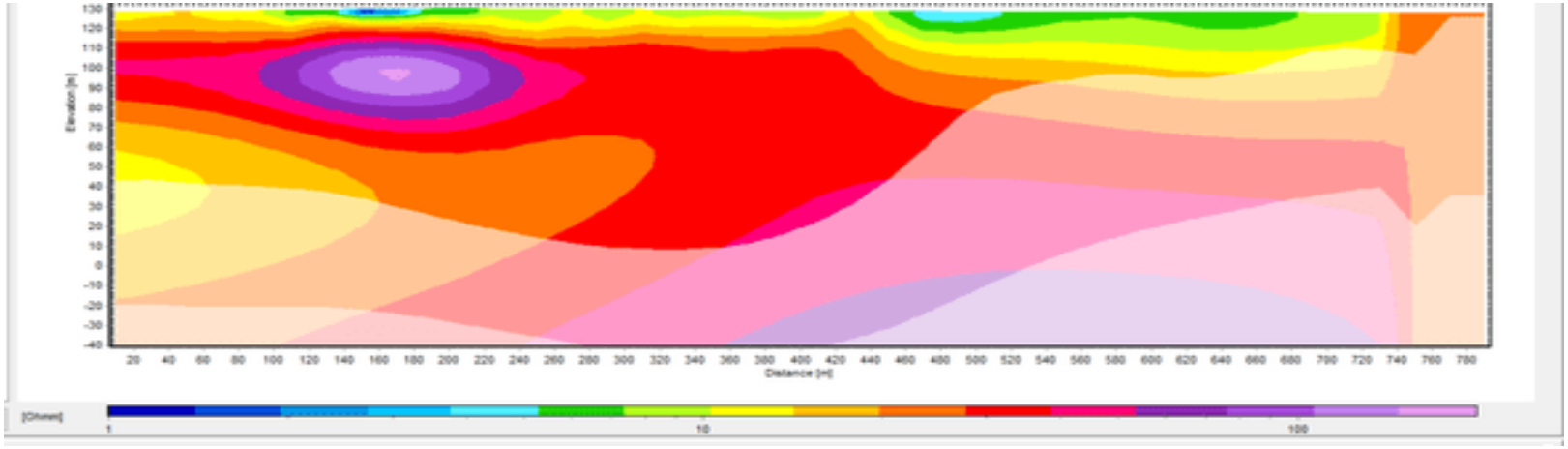

27. KUKUA-ARTESIAN

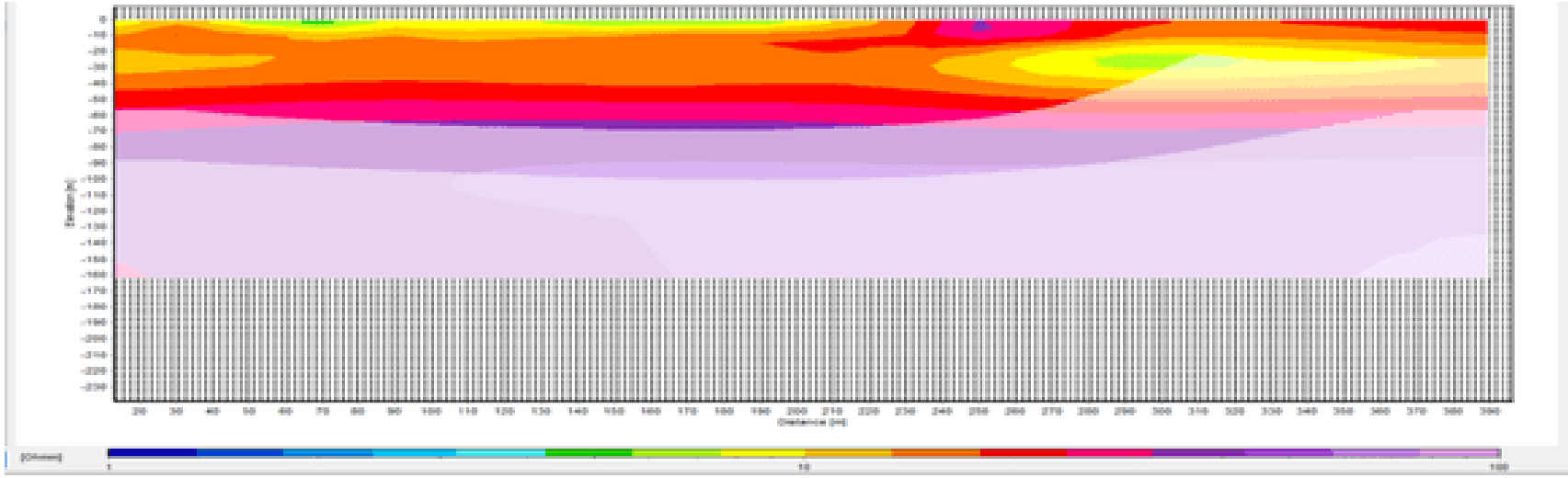

28. LATARE

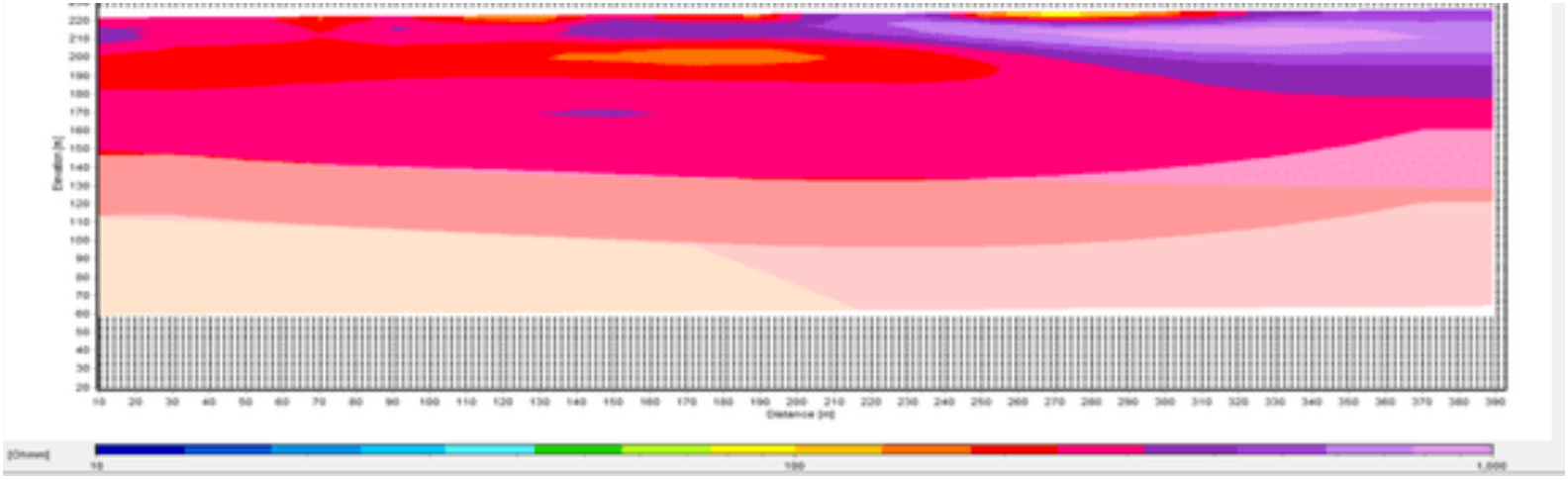

29. NAGBOO

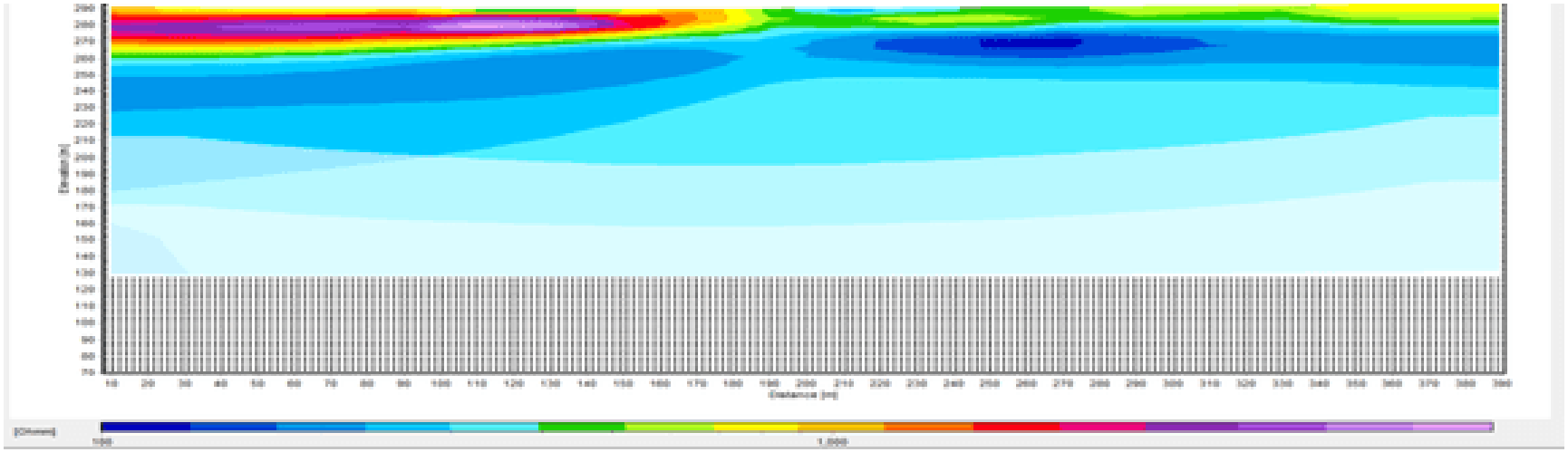

30. MANIE

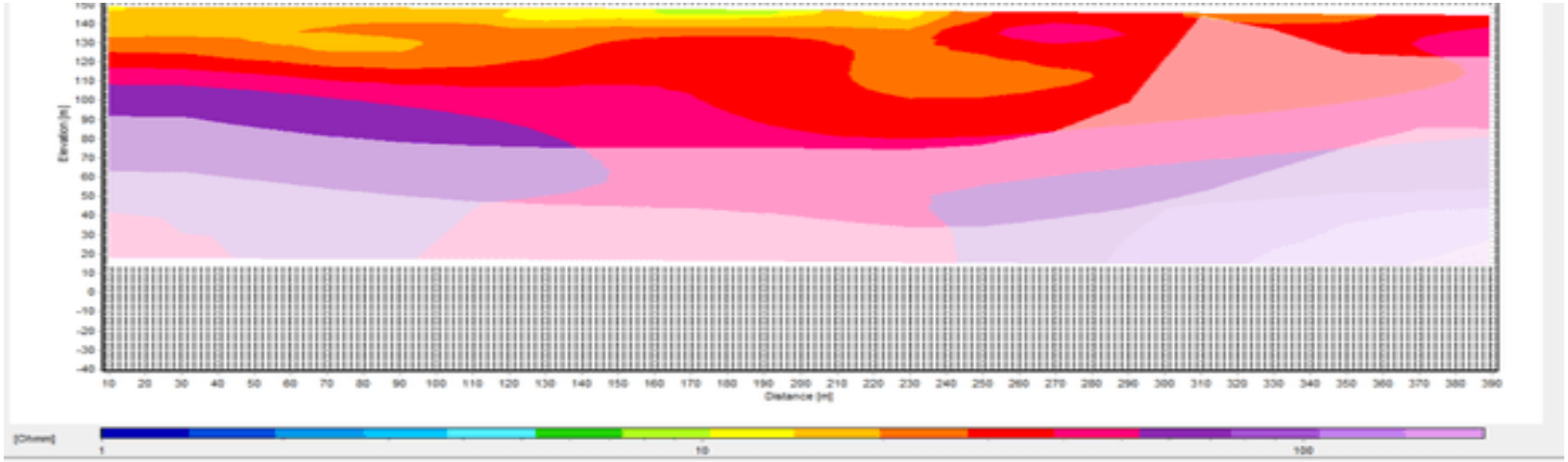

31. TICHIRIGATABA

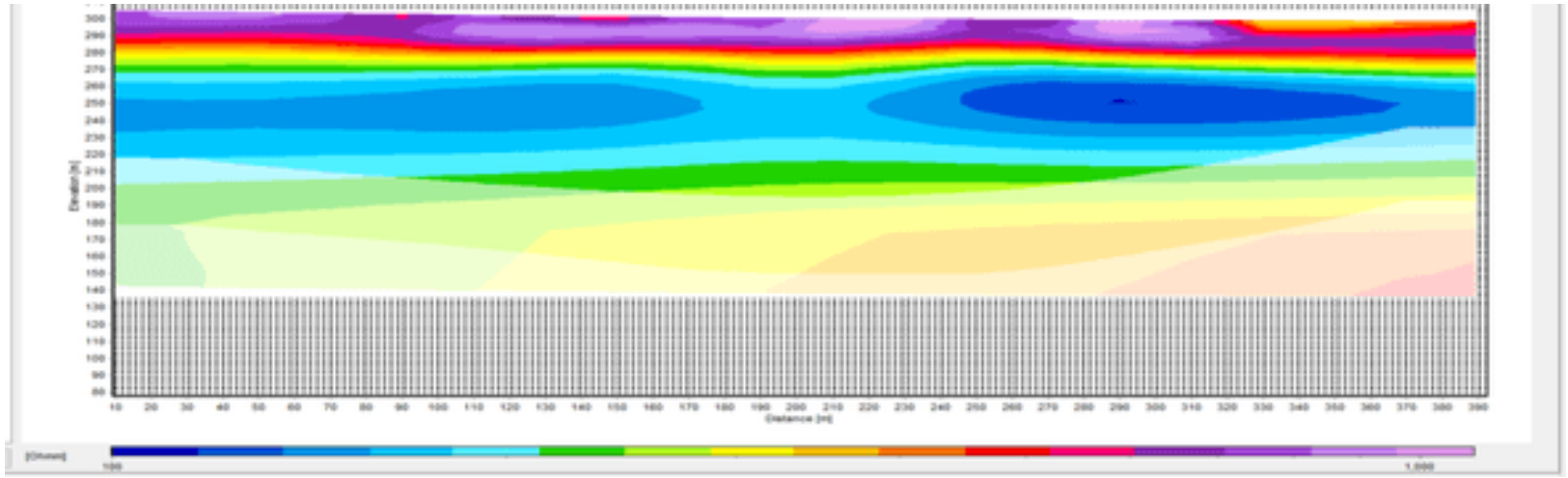

32. NANORI

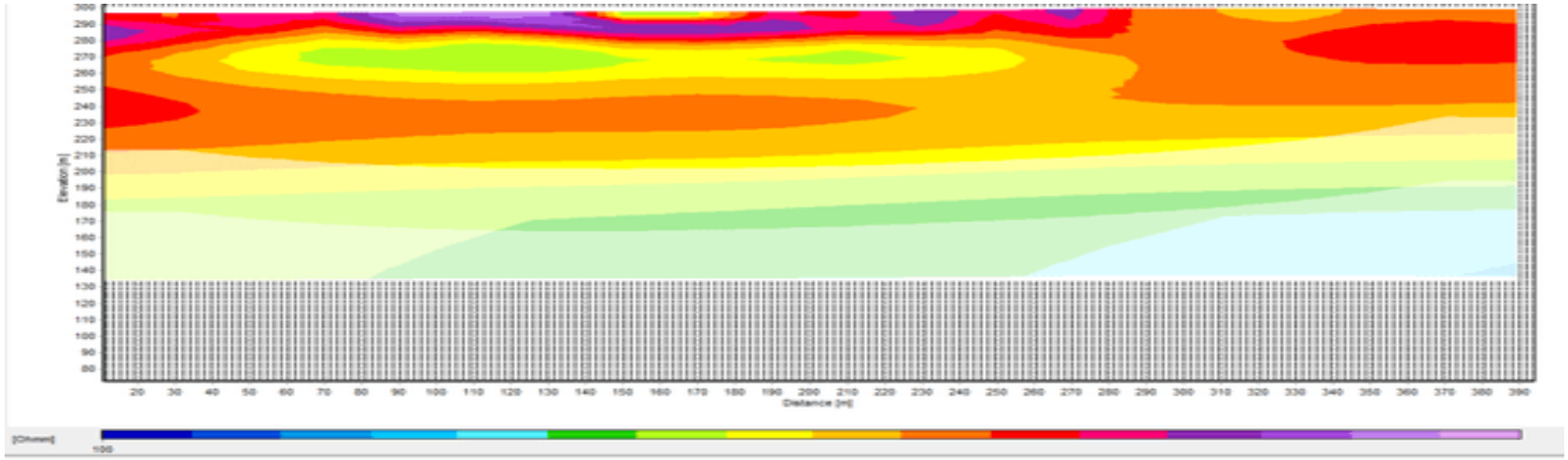

33. NYANSON

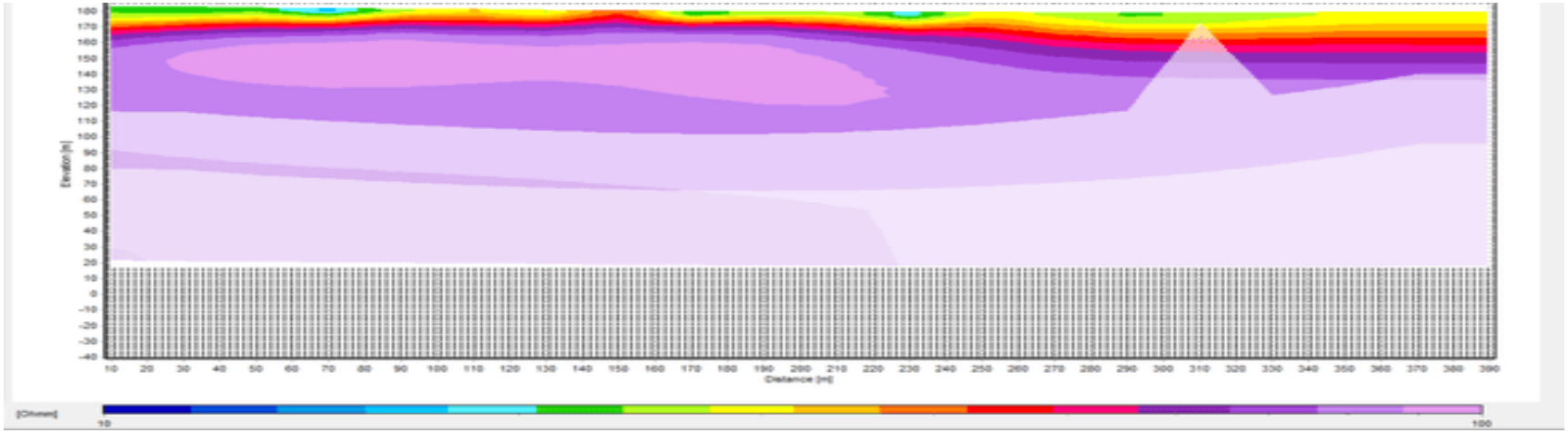

34. NYINGALE

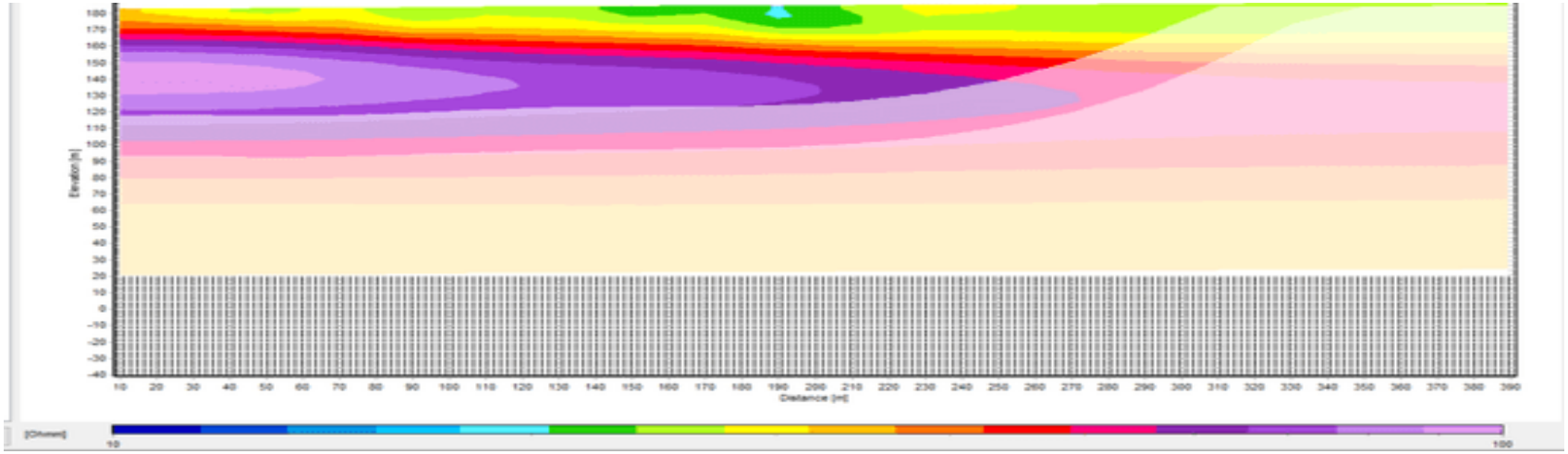

35. POMO

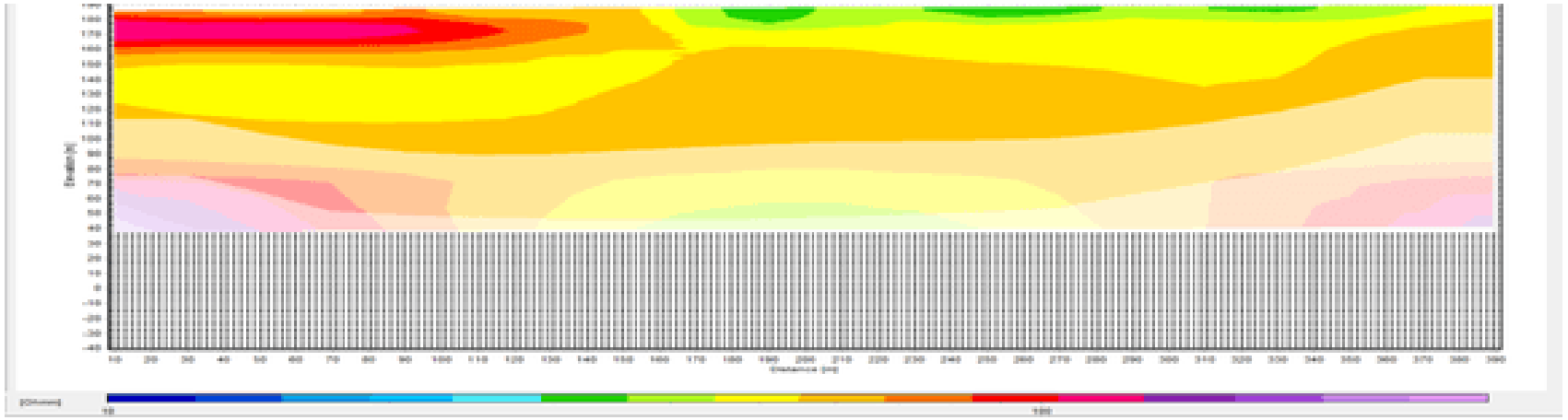

36. SHEVOYA-CHIEF HOUSE

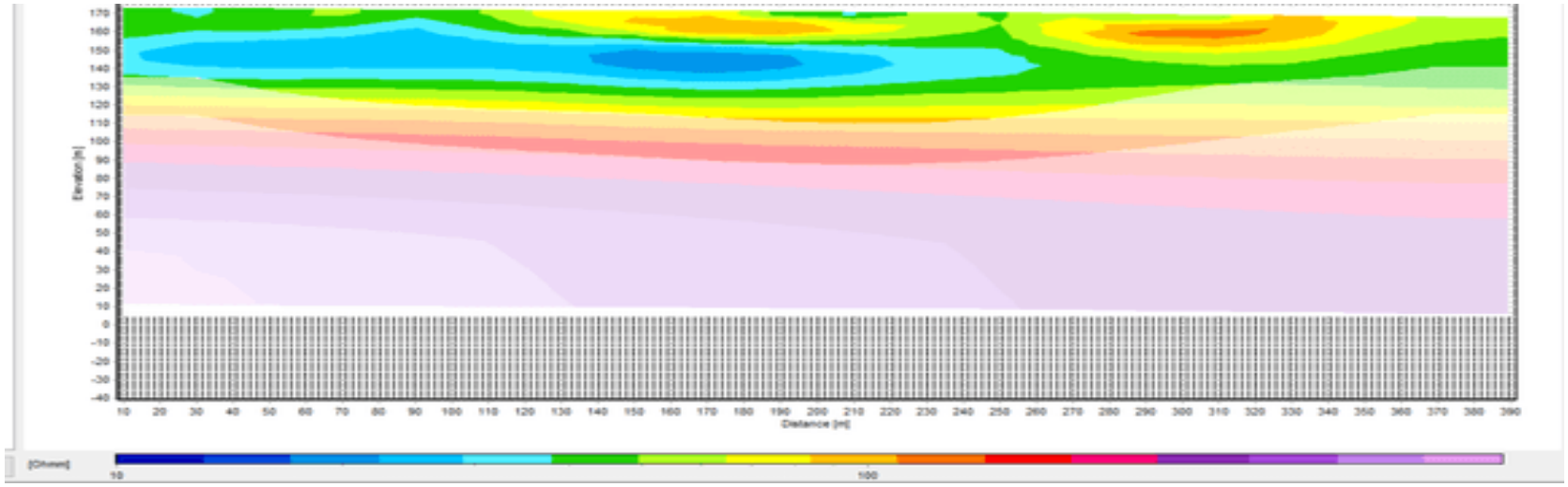

37. SURUGU

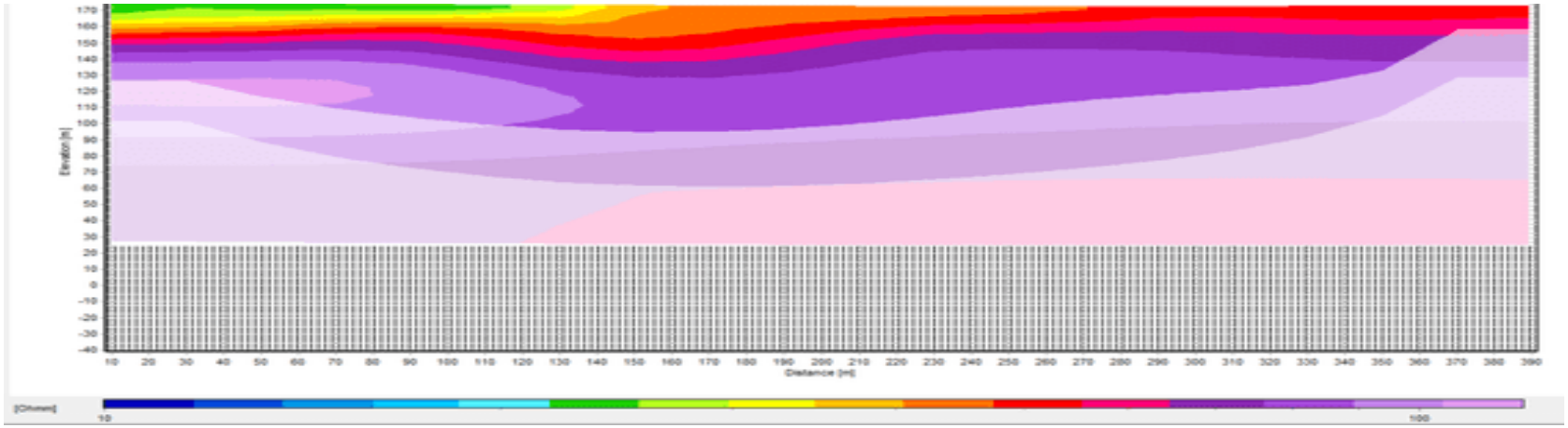

38. TAMBOKO

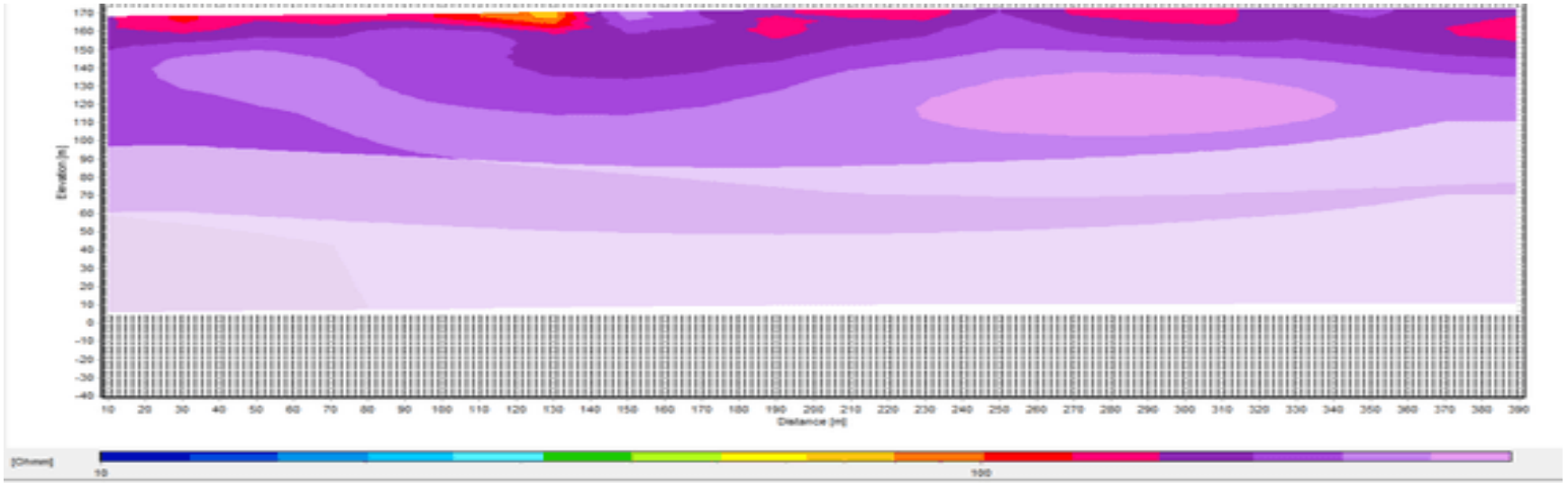

39. TINGURI 1

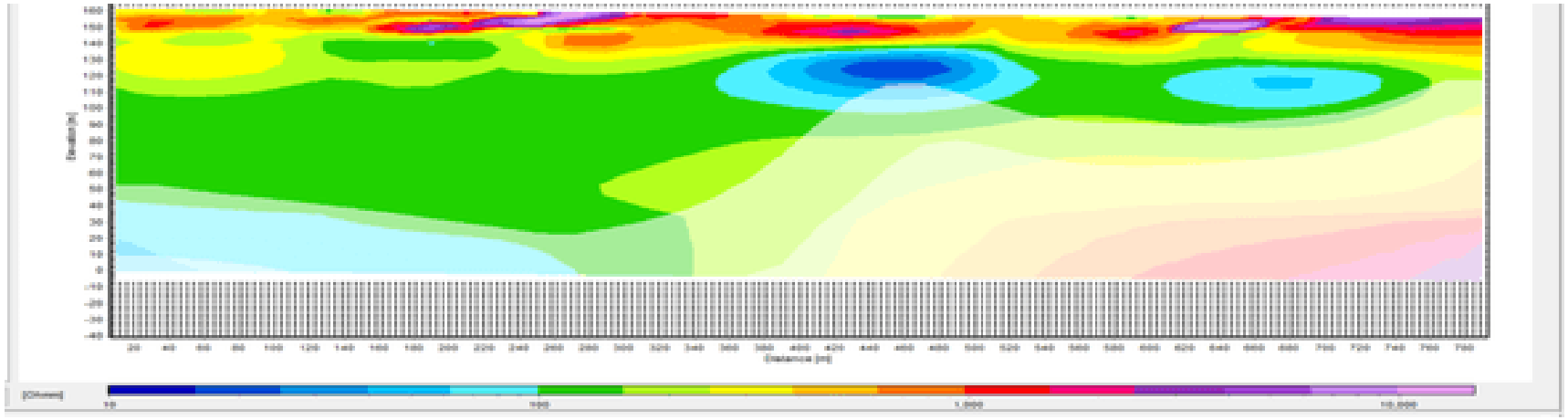

40. TINGURI 2

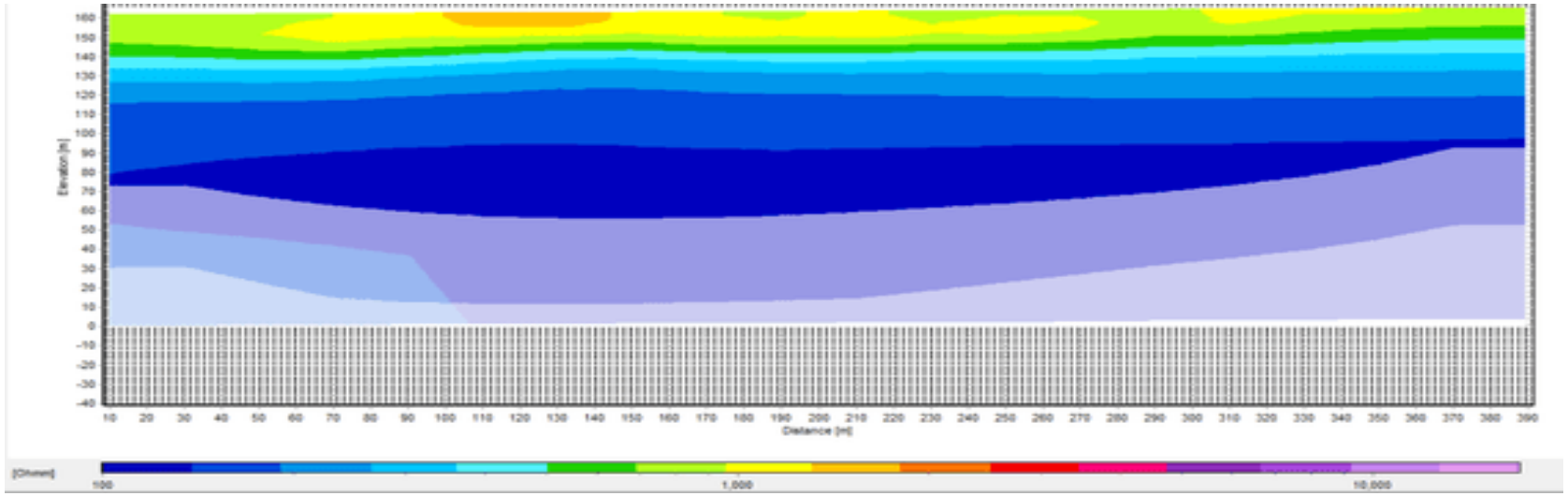

41. TINGURI 3

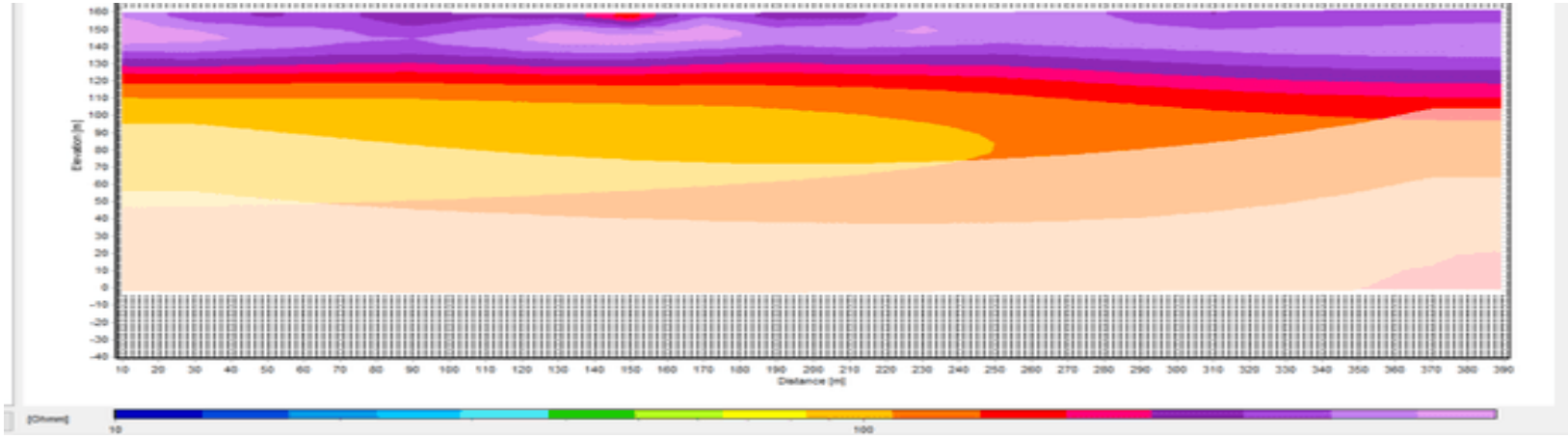

42. TINKAYA

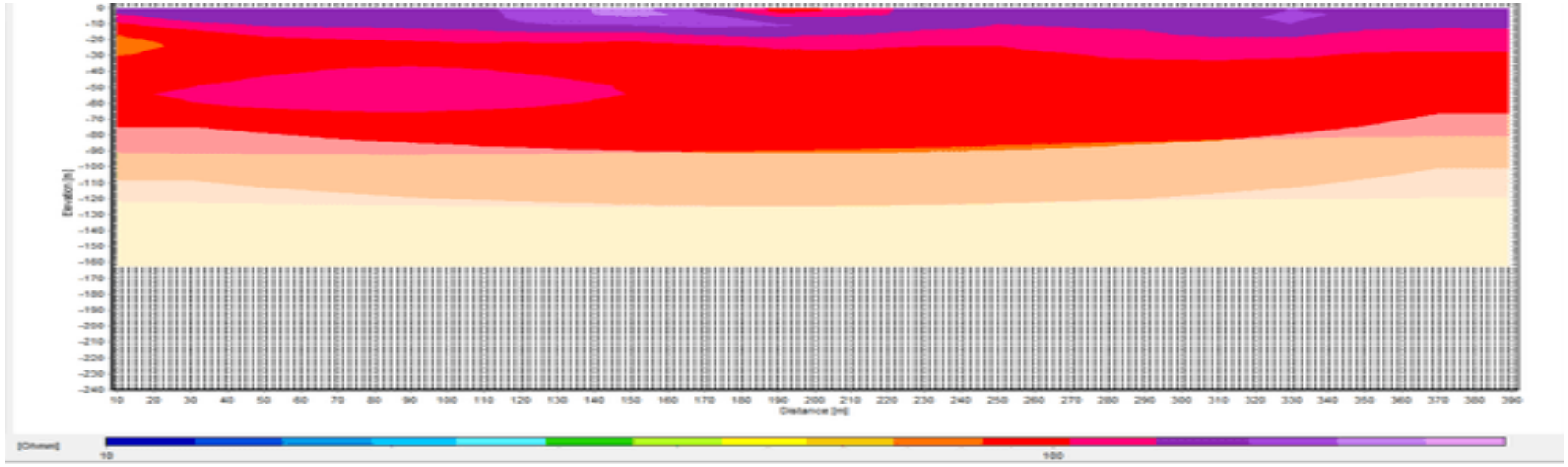

43. TUGBANG

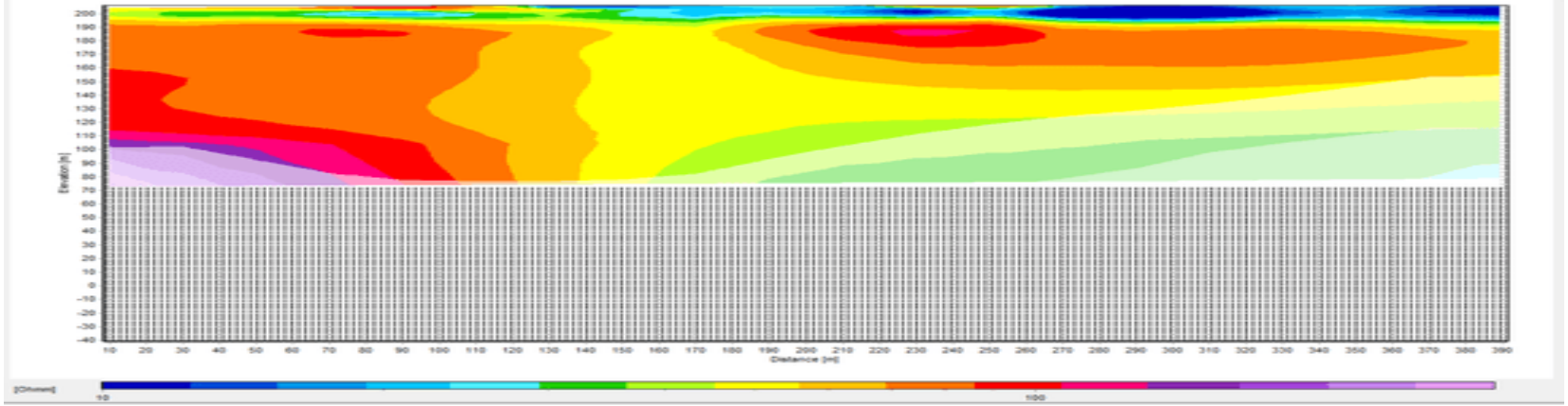

44. YIBEE

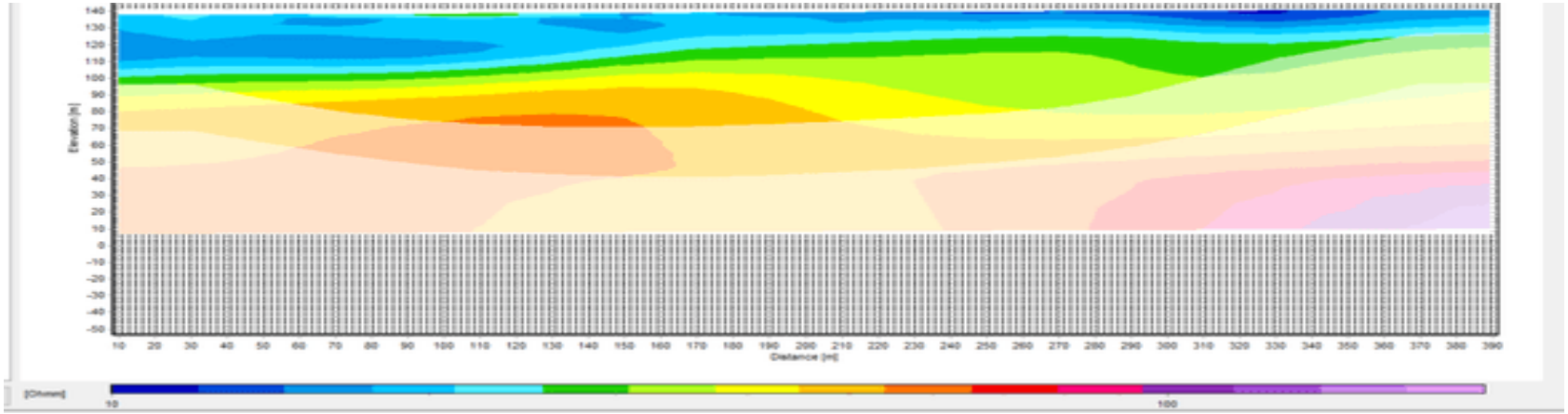

45. NASIA ERT/EM

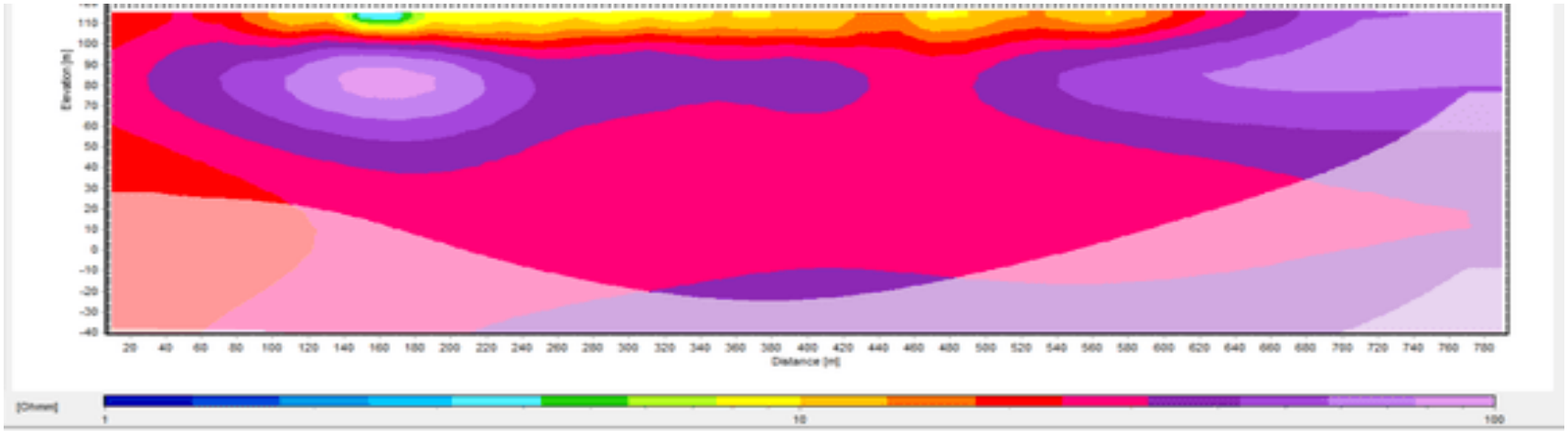

46. PIGU

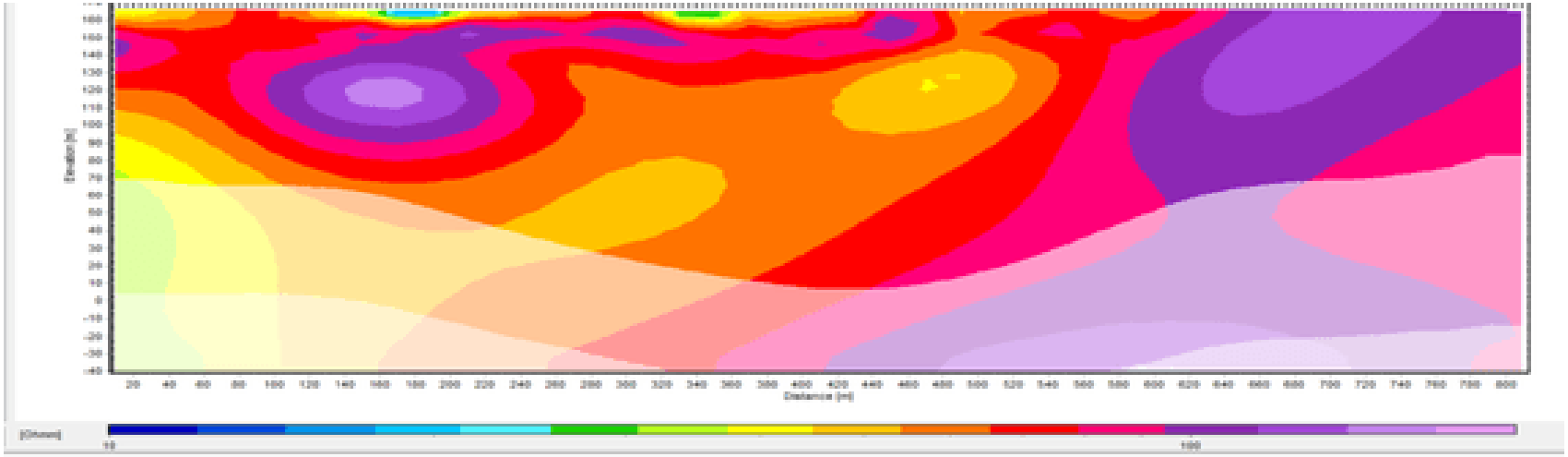

47. BANAWA ER/EM

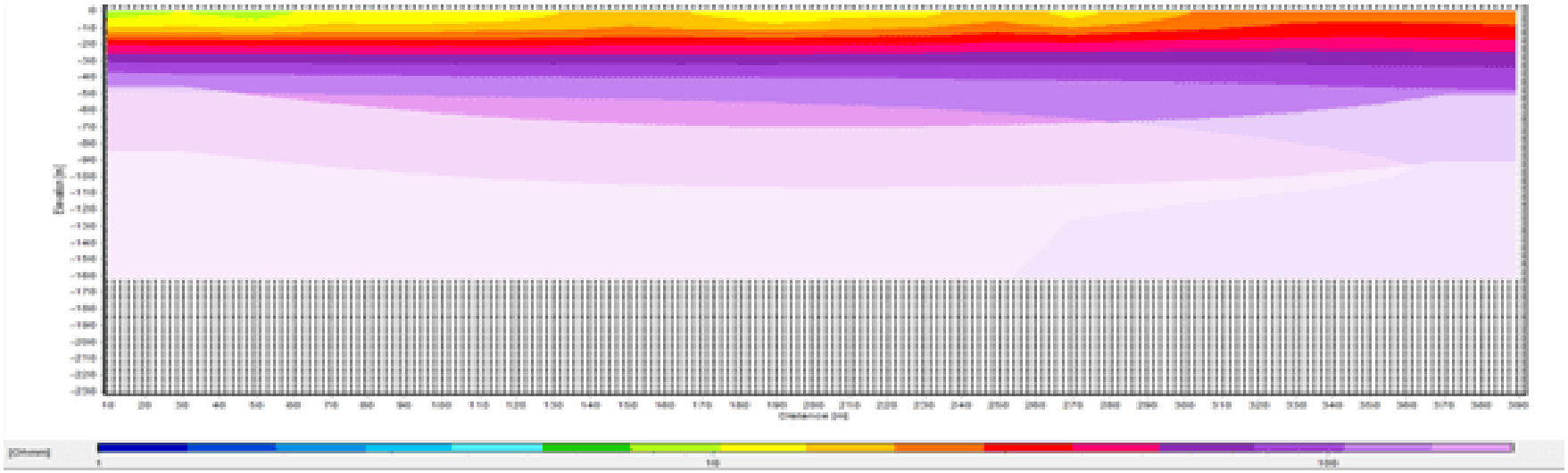

48. WUNDUA

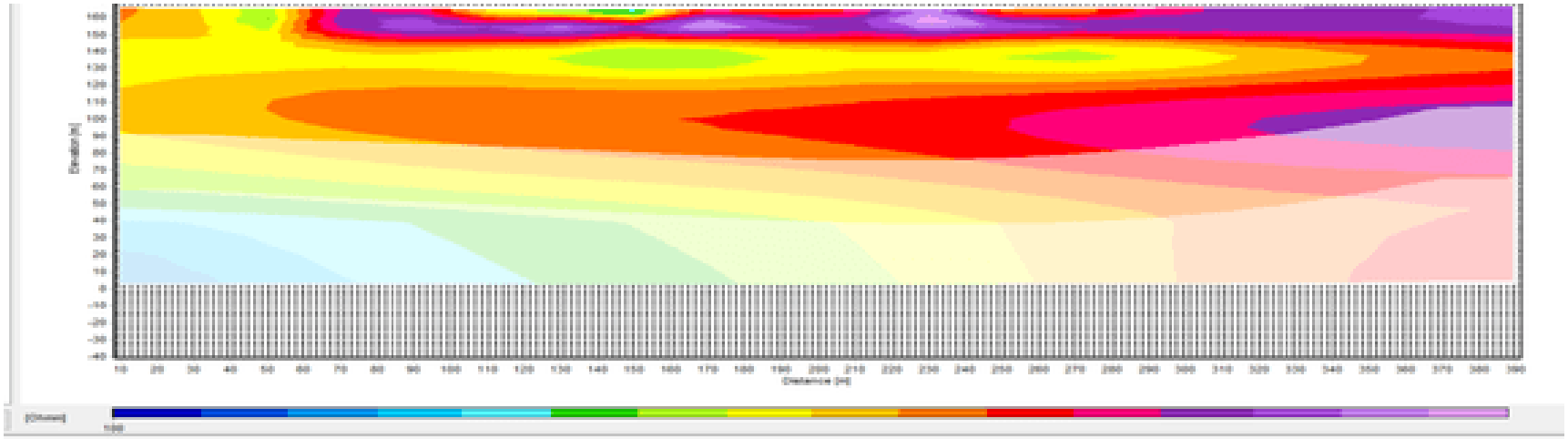

49. DWVP04

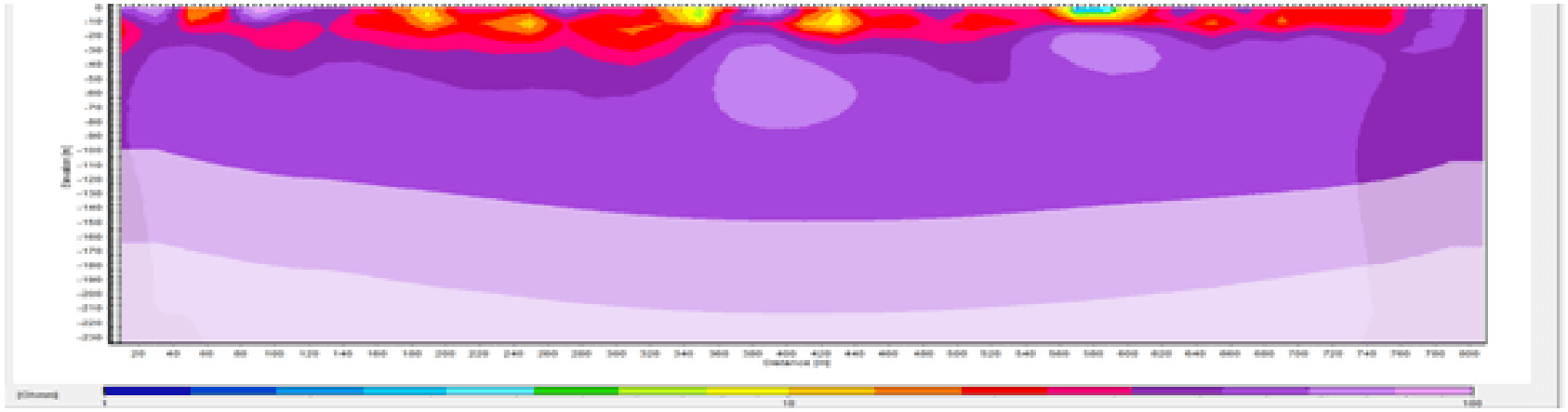

50. DWVP9

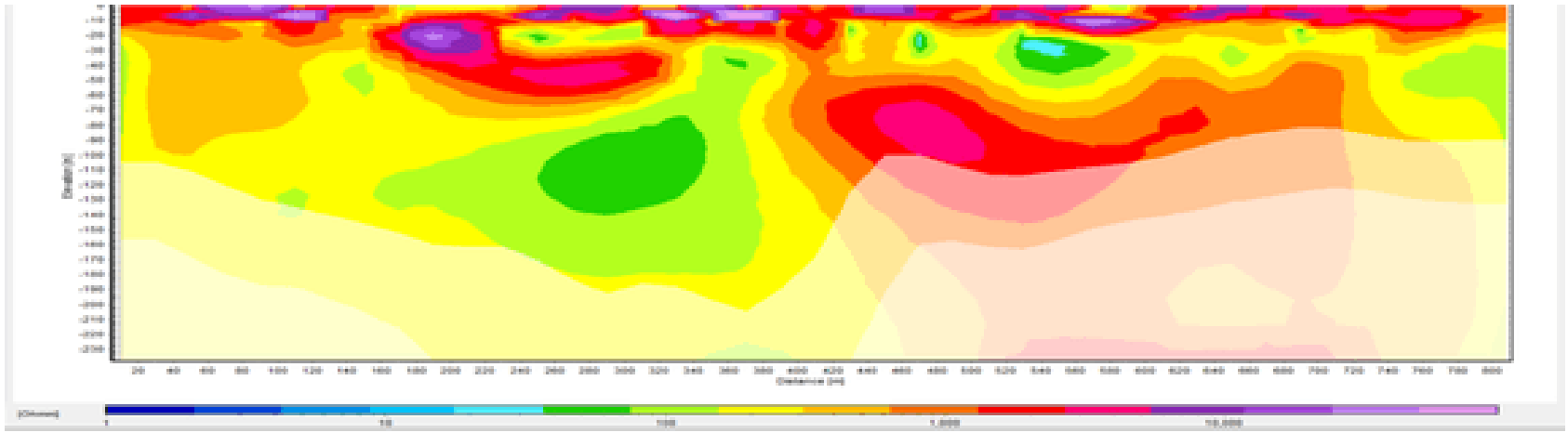

51. DWVP03

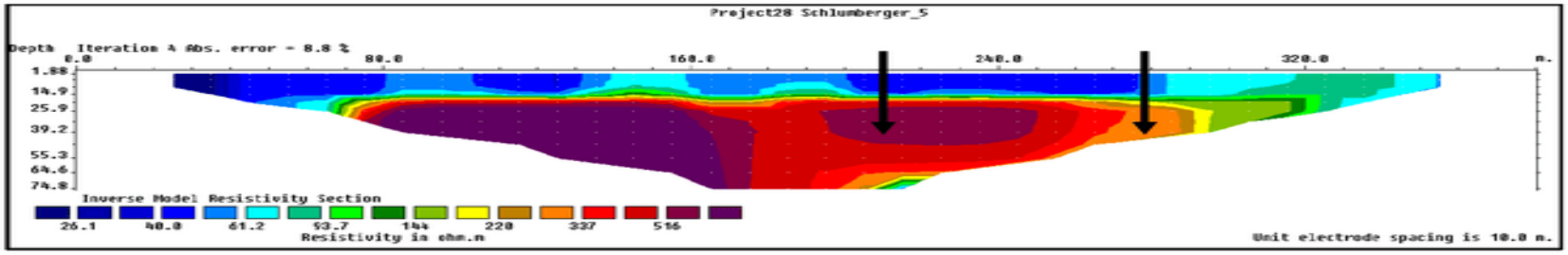

52. DWVP05

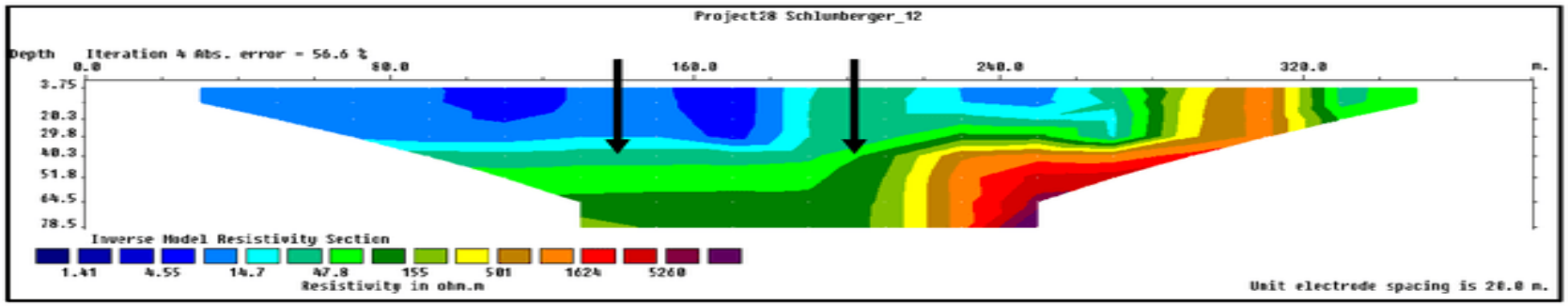

53. DVWP08

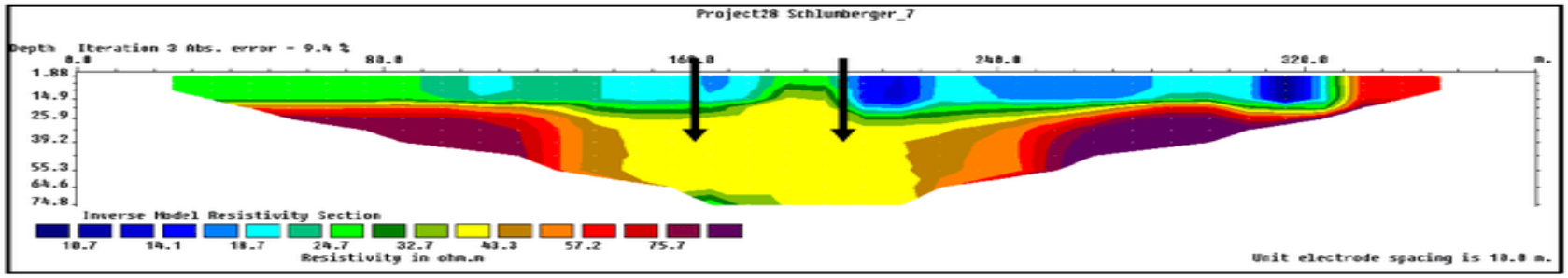

54. DWVP10

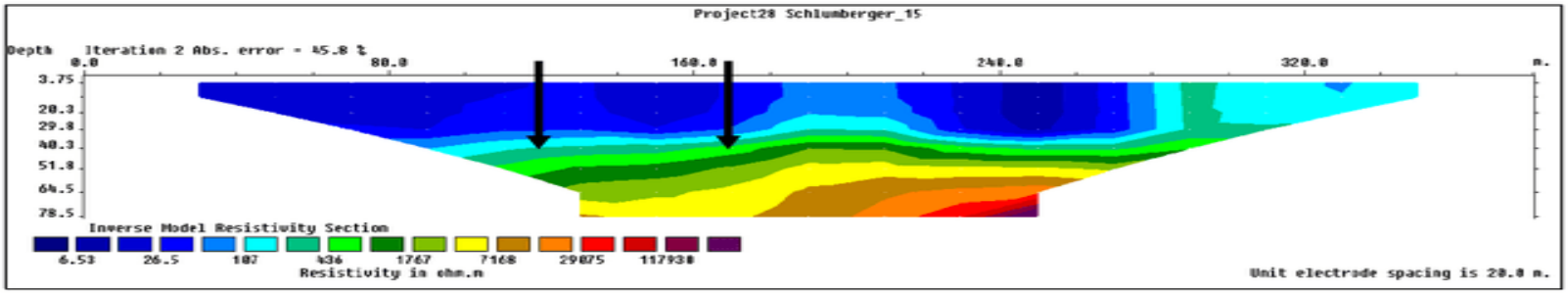

55. Gbimsi

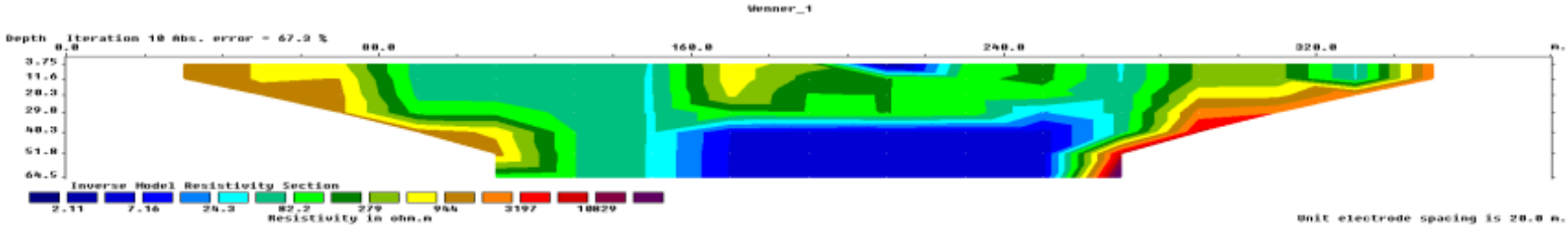

56. Guabulga

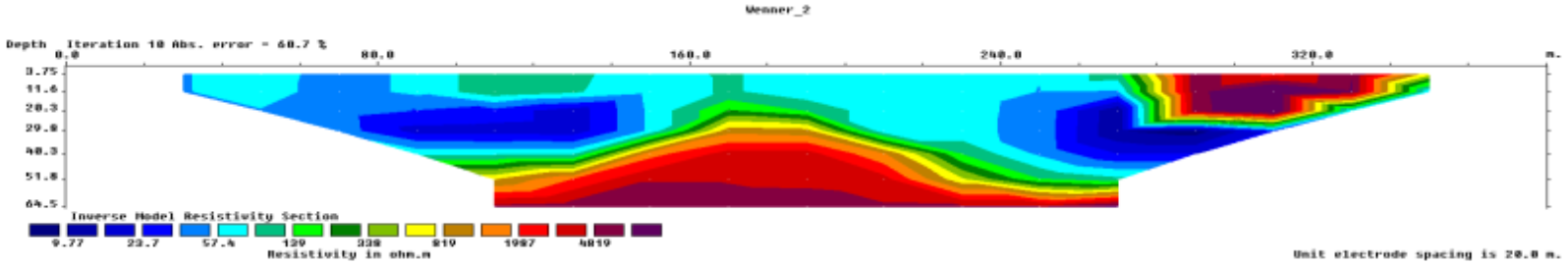

57. Mishio

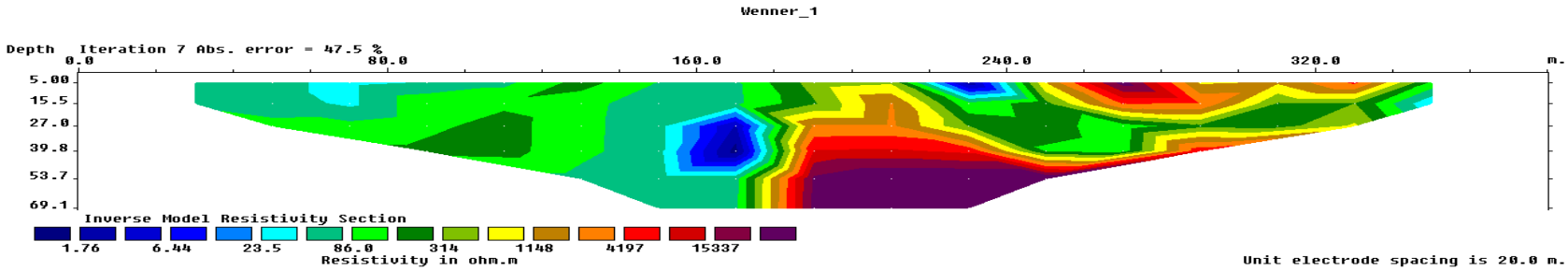

58. Daboya No. 2 Chps Compound

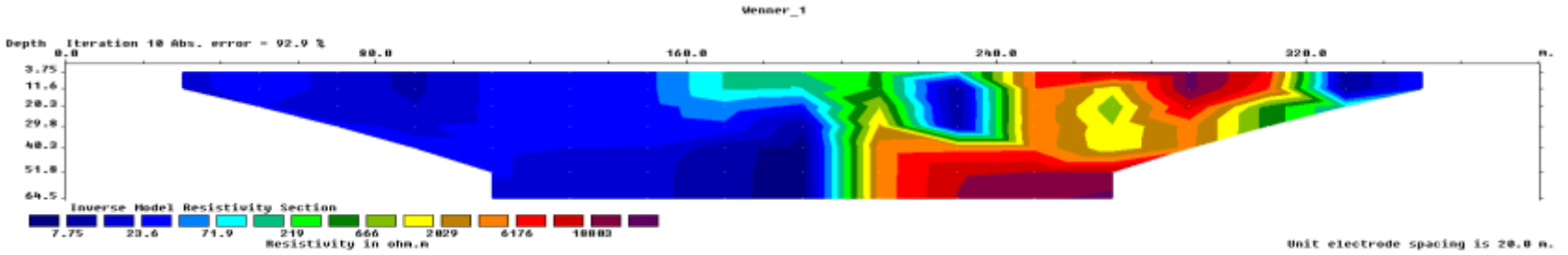

59.Sooba Community

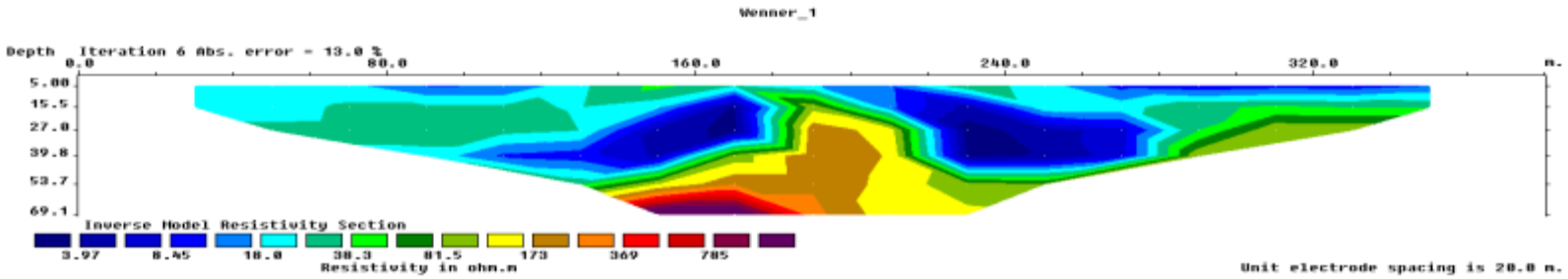

60. Sooba Primary School

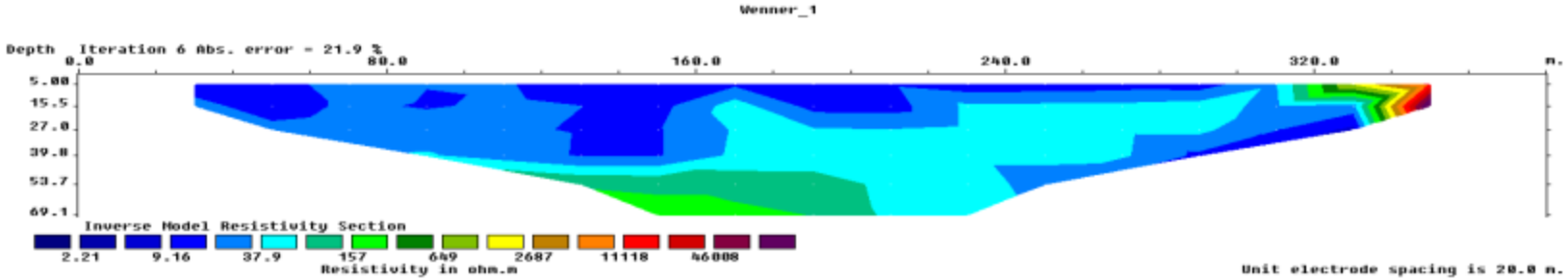

61.Tinguri Pope John RC

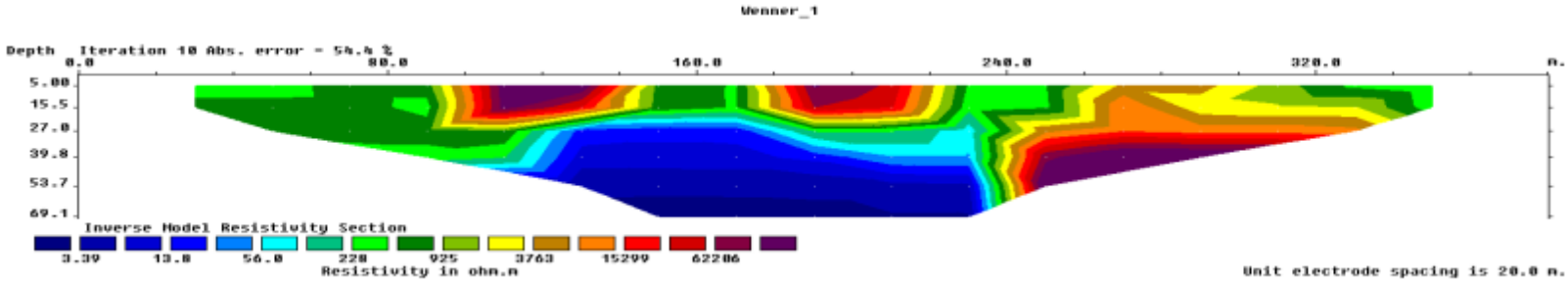

62. Shelinyoya

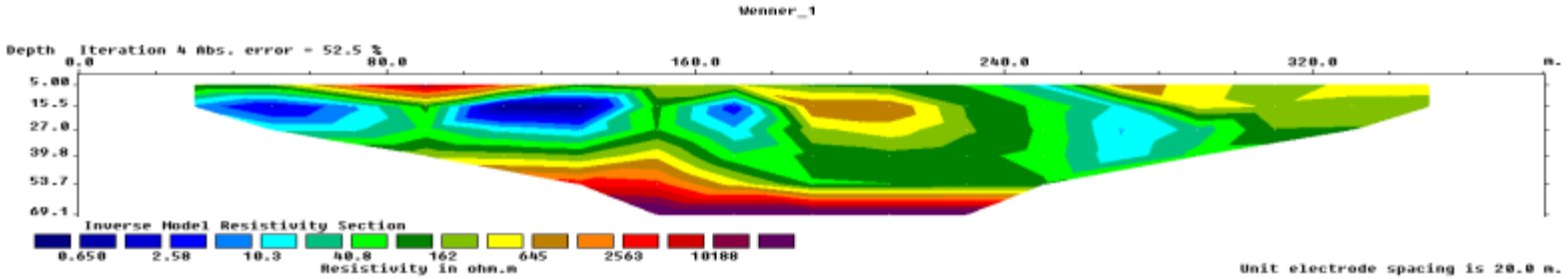

63. Zanguya

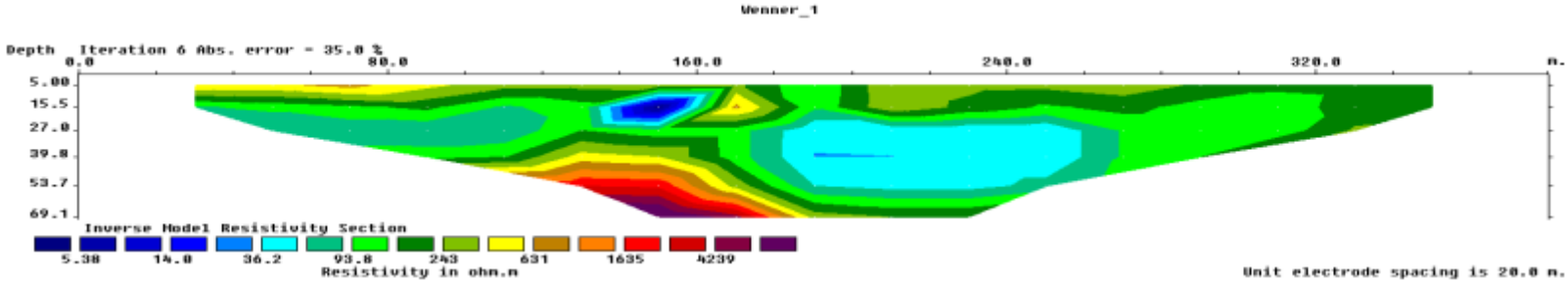

64.Nasia Chps Compound

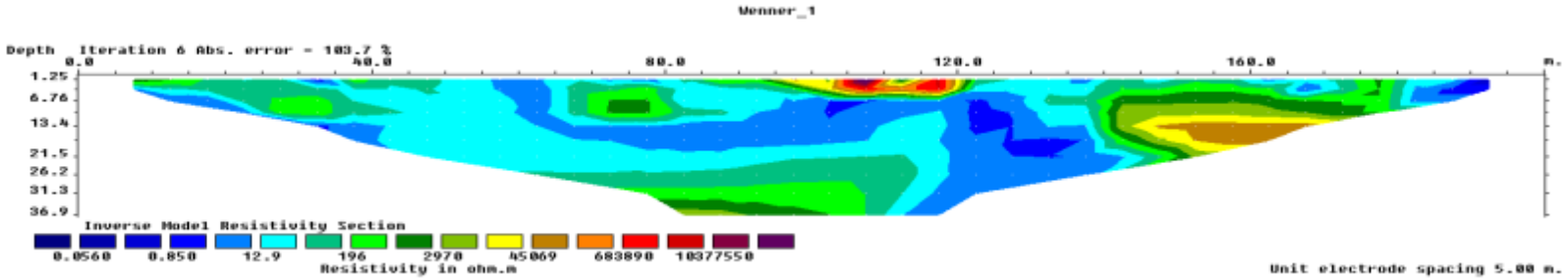

65. Loagri Primary

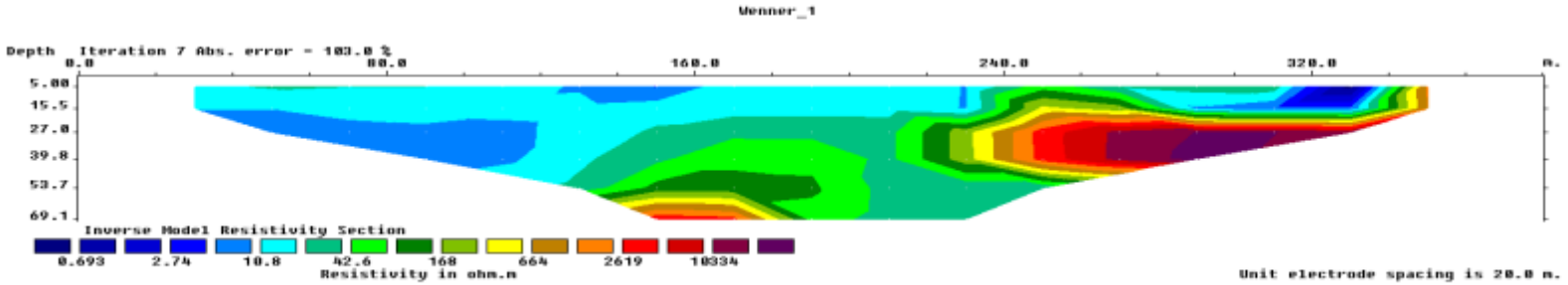

66.Loagri Community

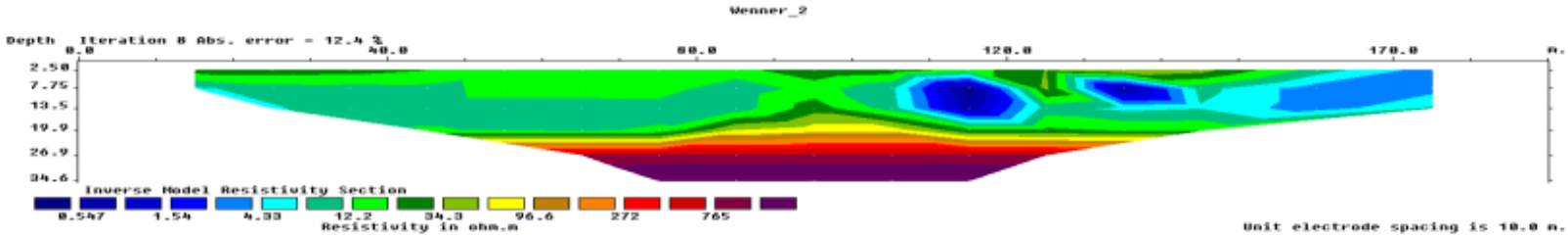

67. Kparigu

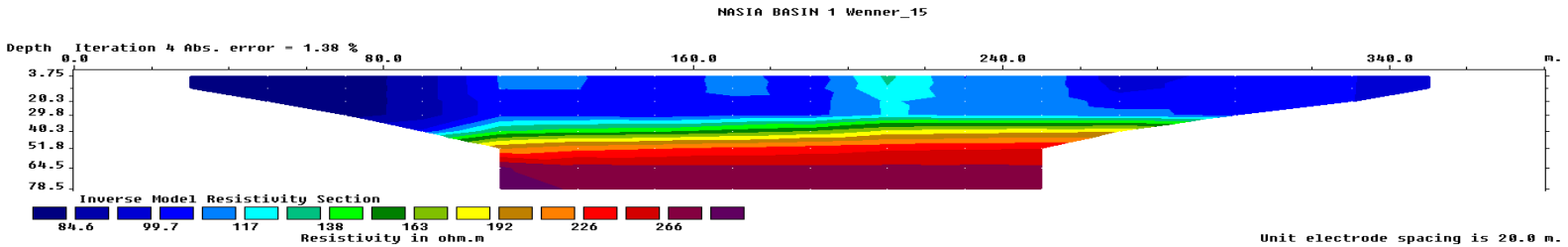

68.Kukua

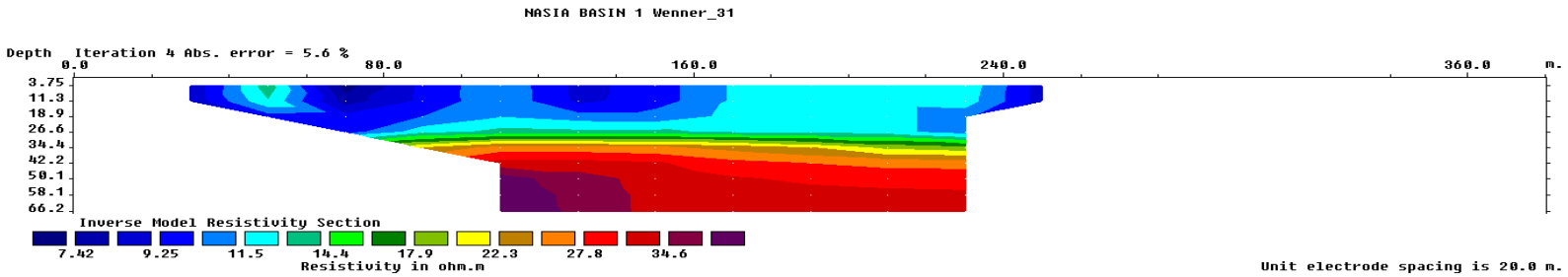

69.Kolinva

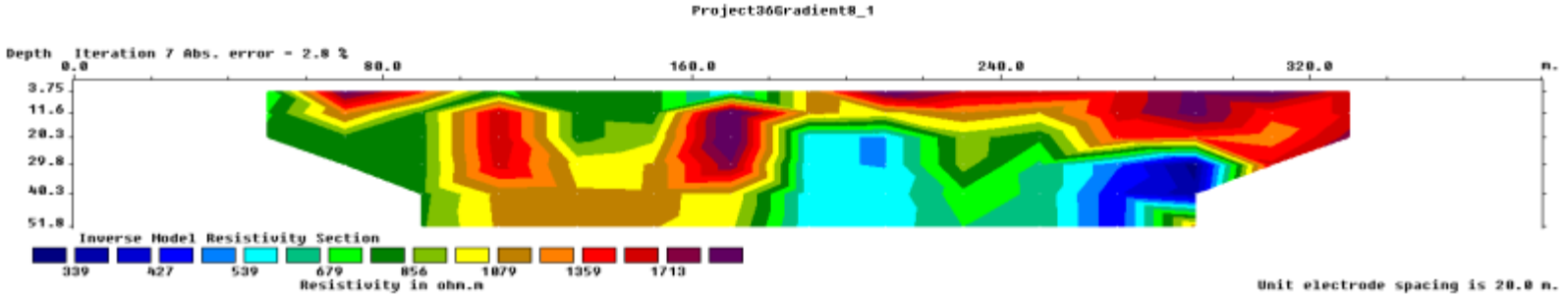

70. Takorayili

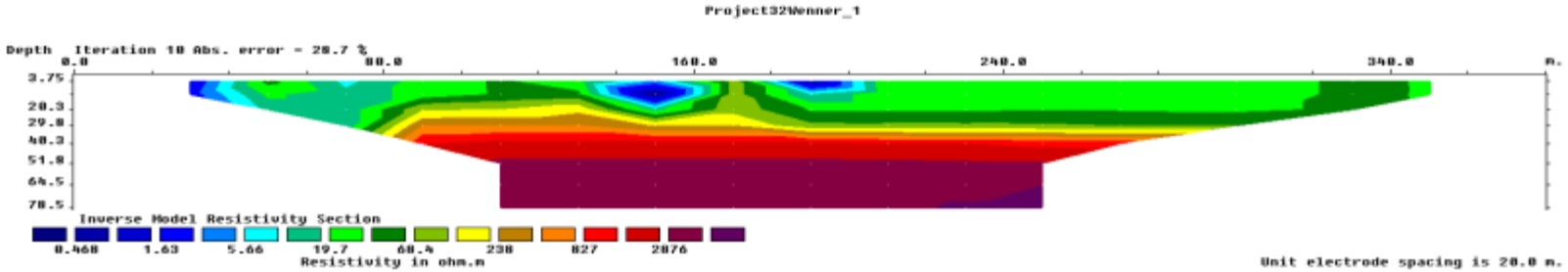

APPENDIX 3- GEOPHYSICAL WIRELINE LOGS

1. DWVP 01

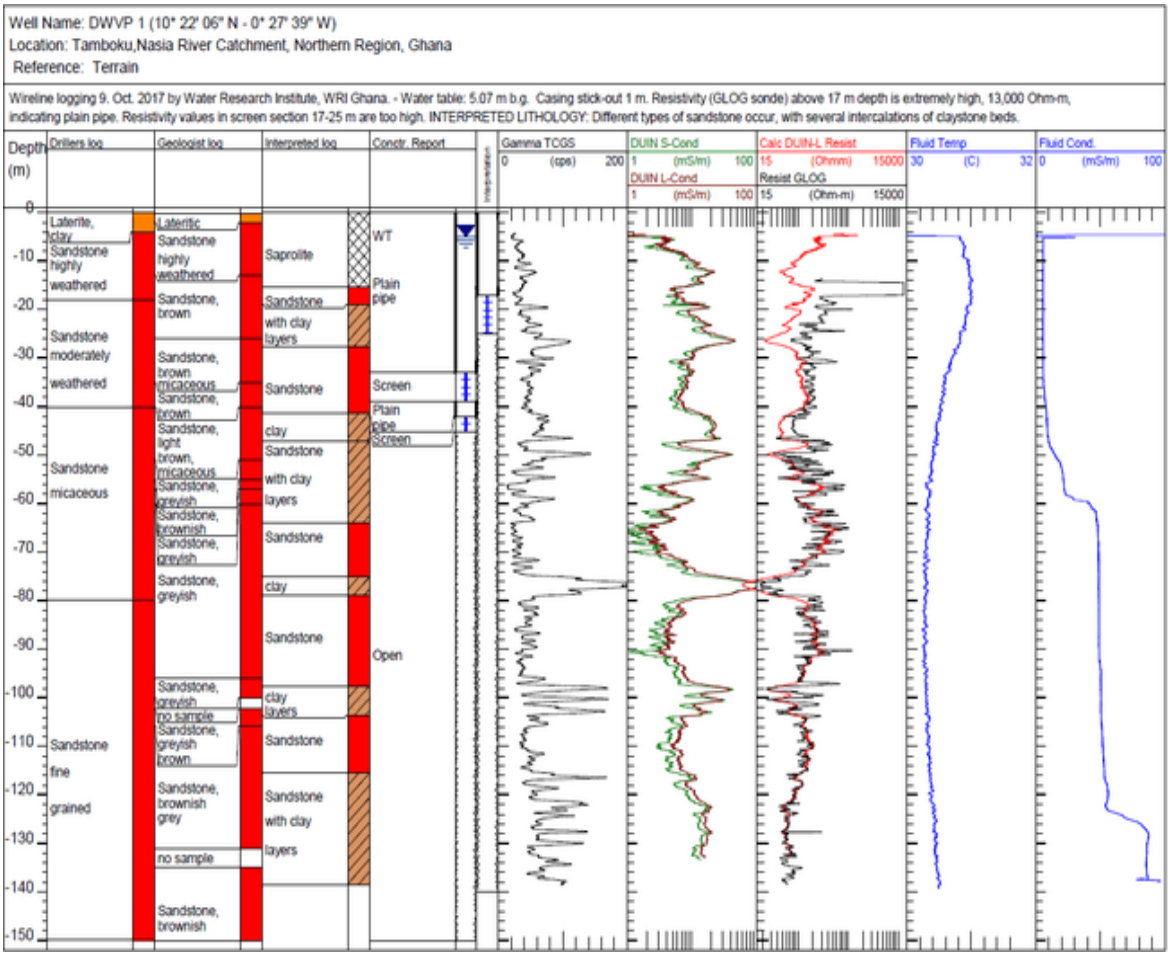

2. DWVP02

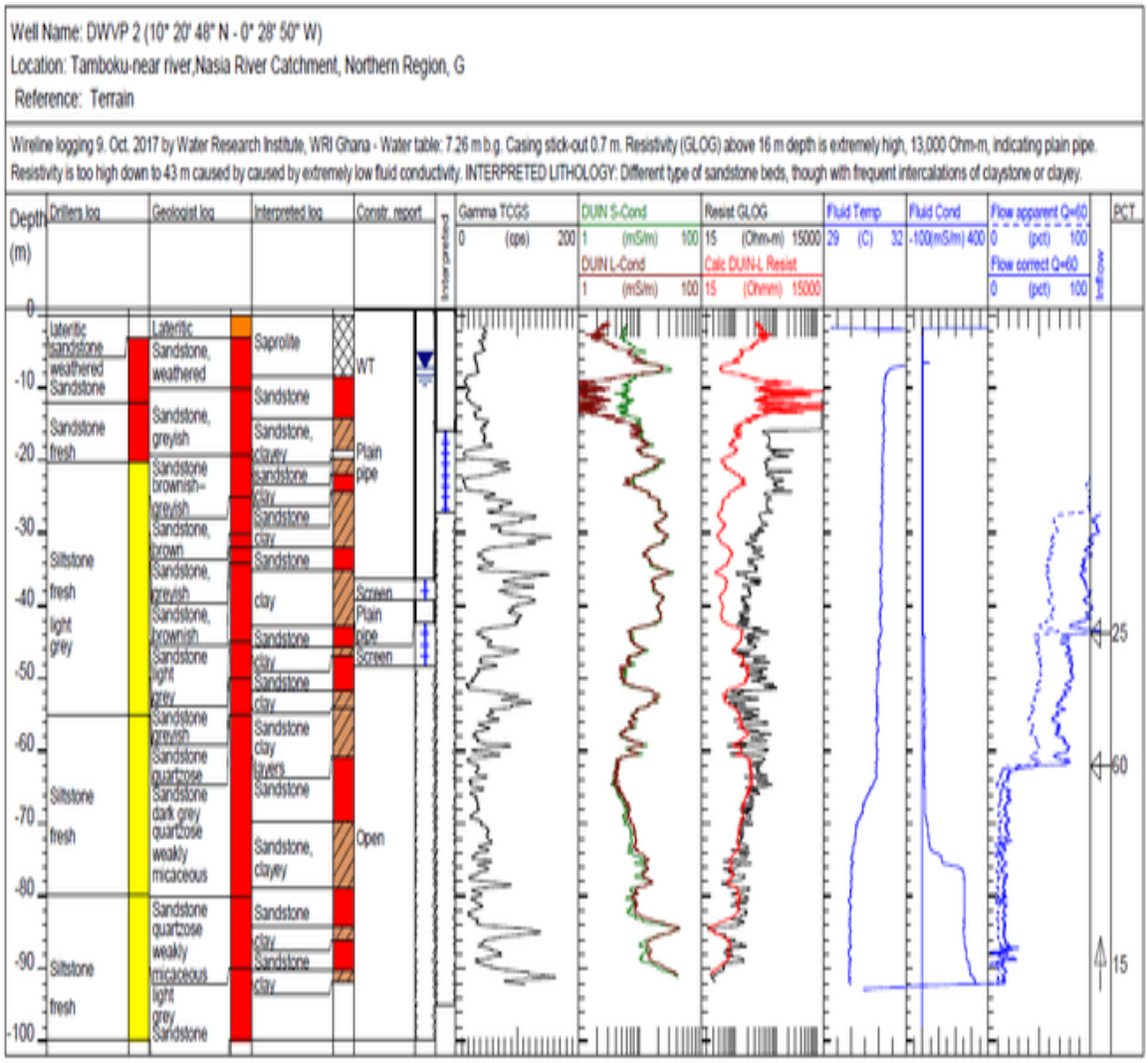

3. DWVP03

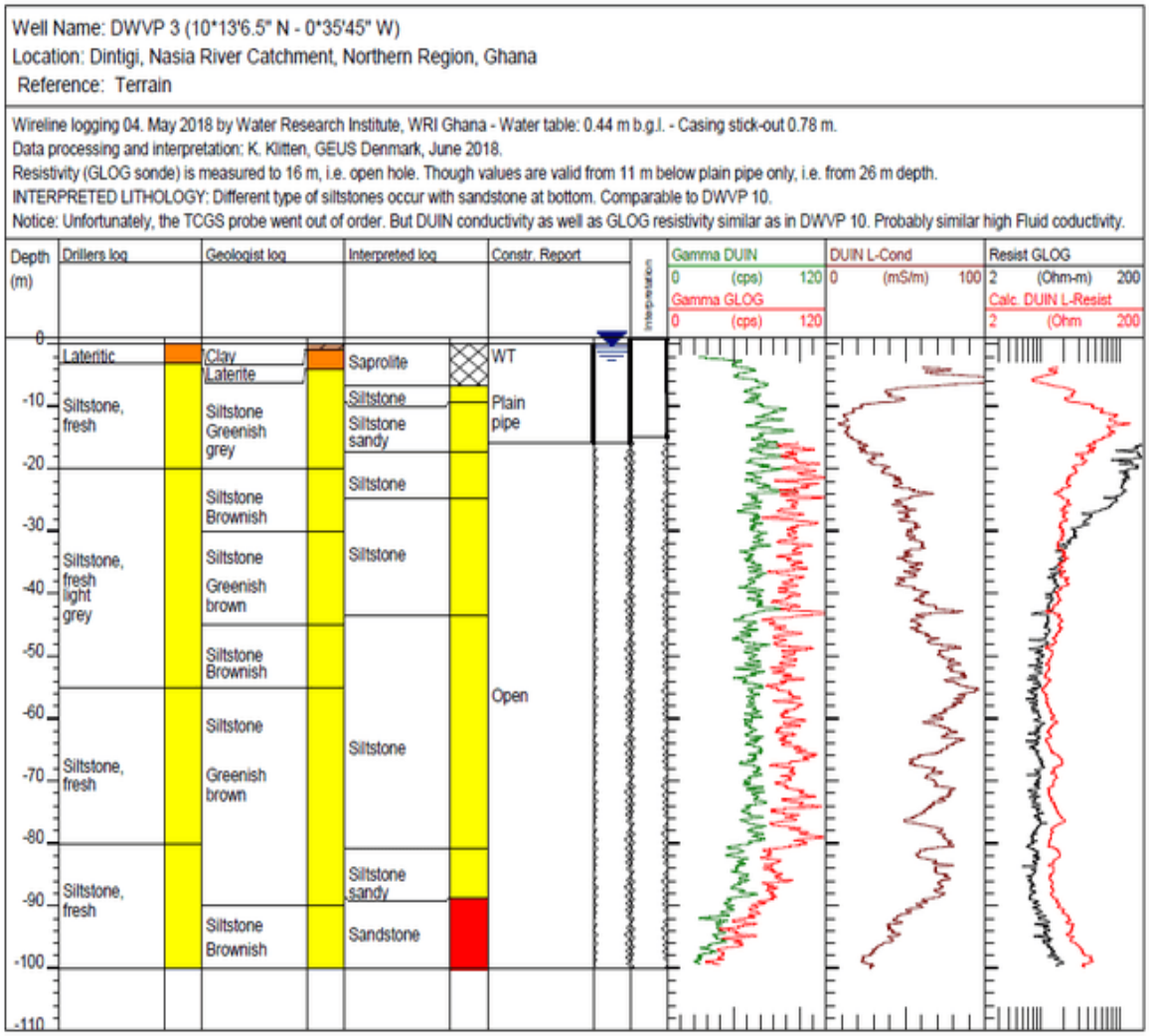

4. DWVP04

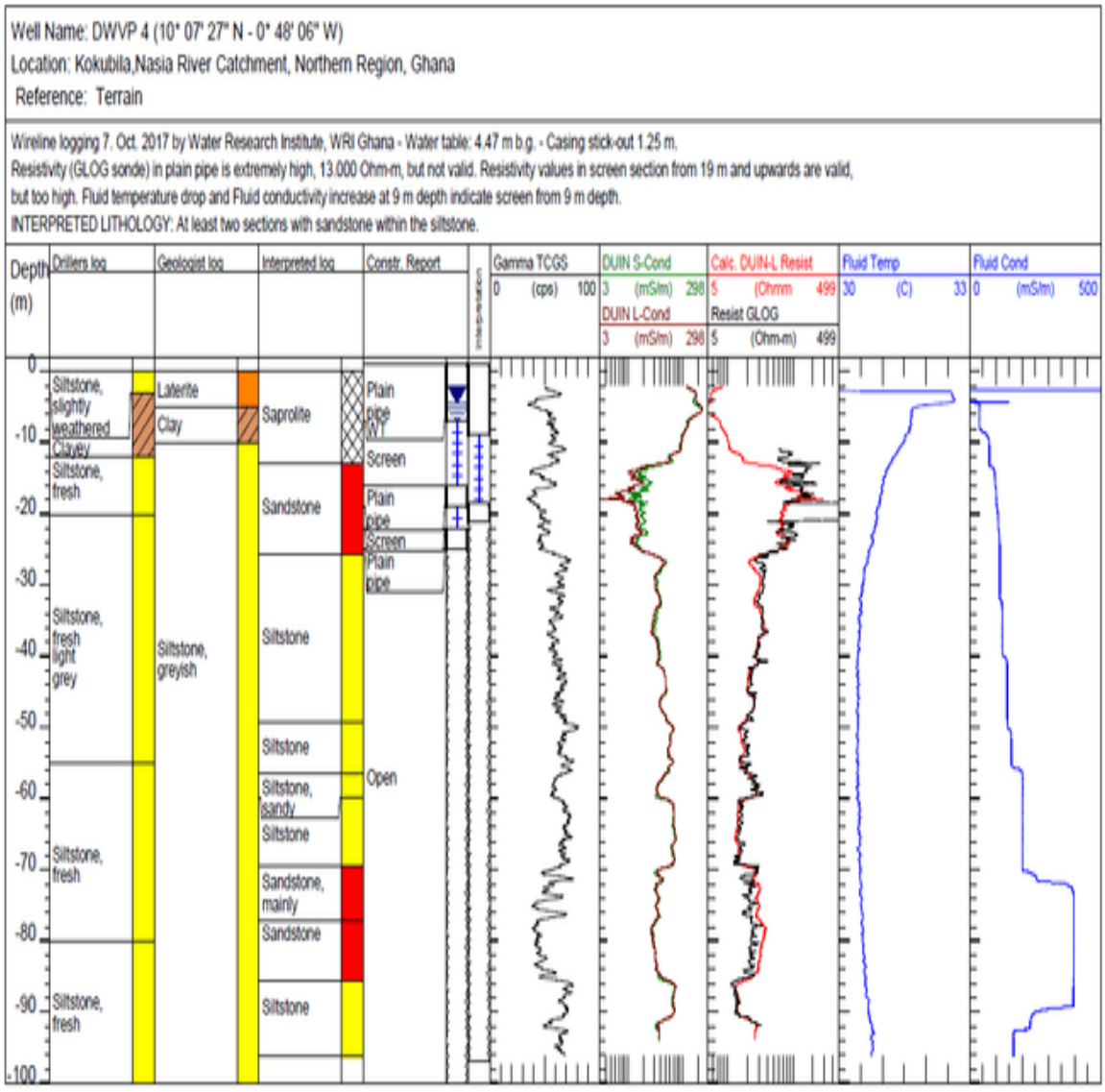

5. DWVP05

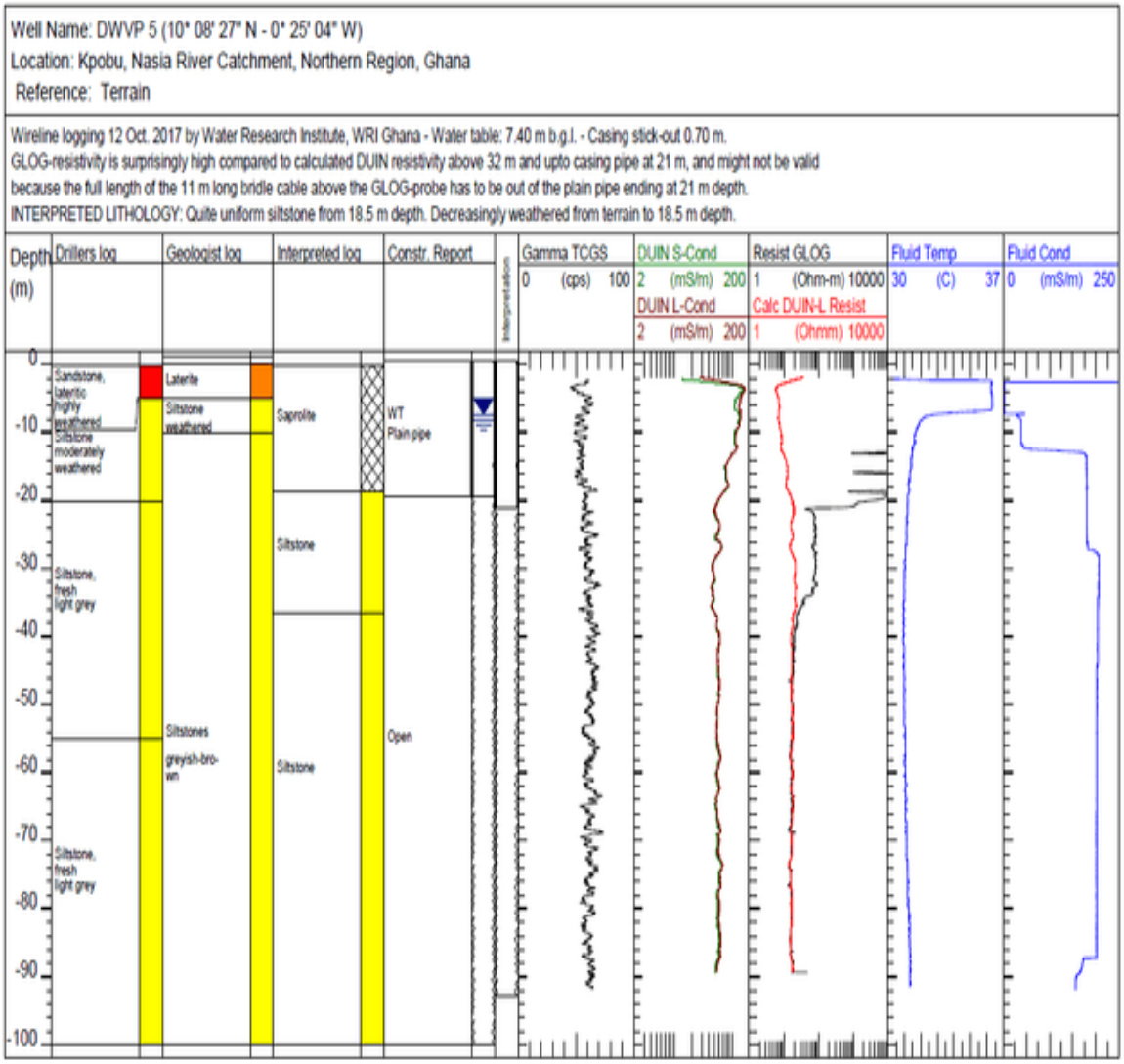

6. DWVP06

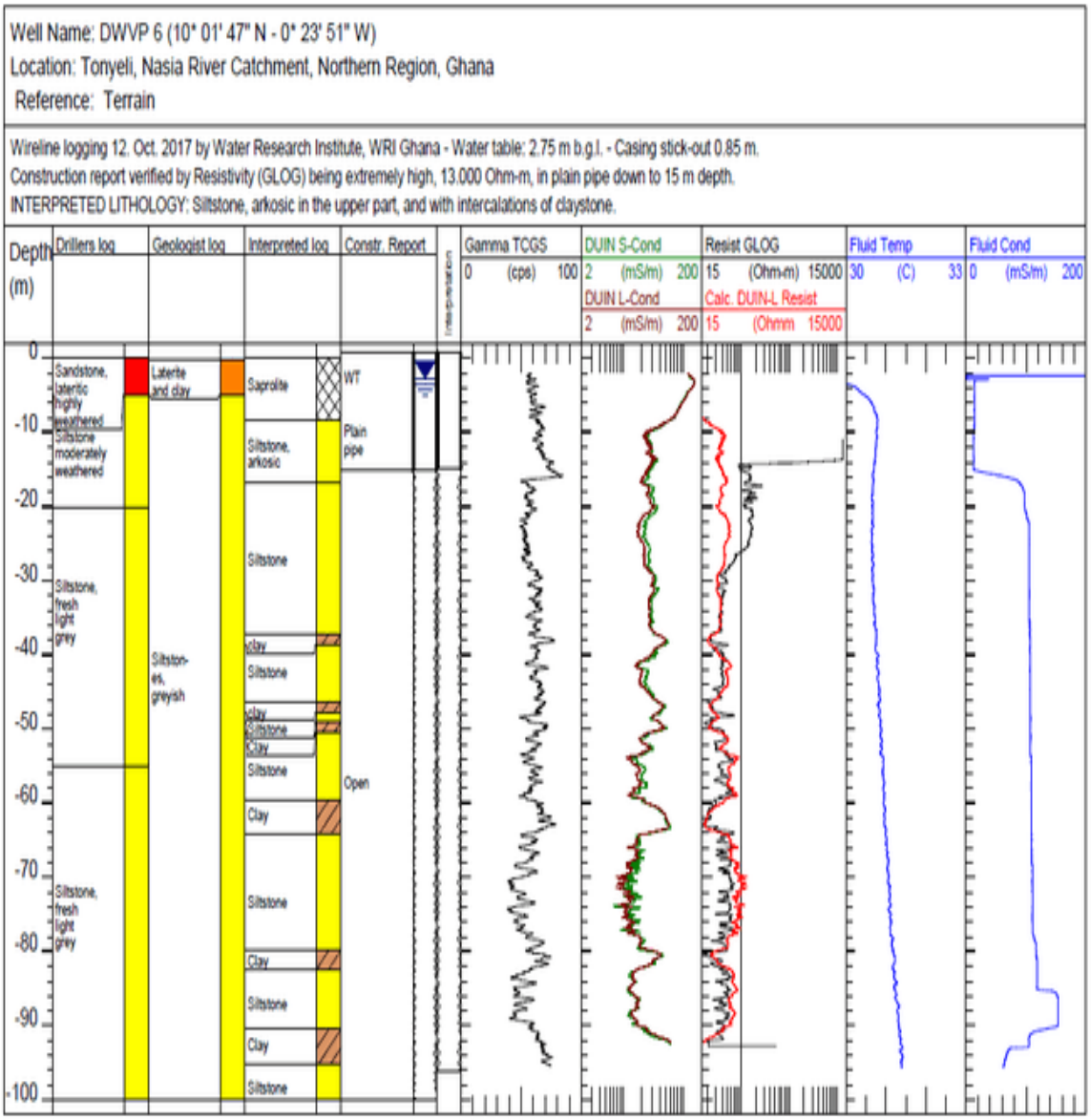

7. DWVP07

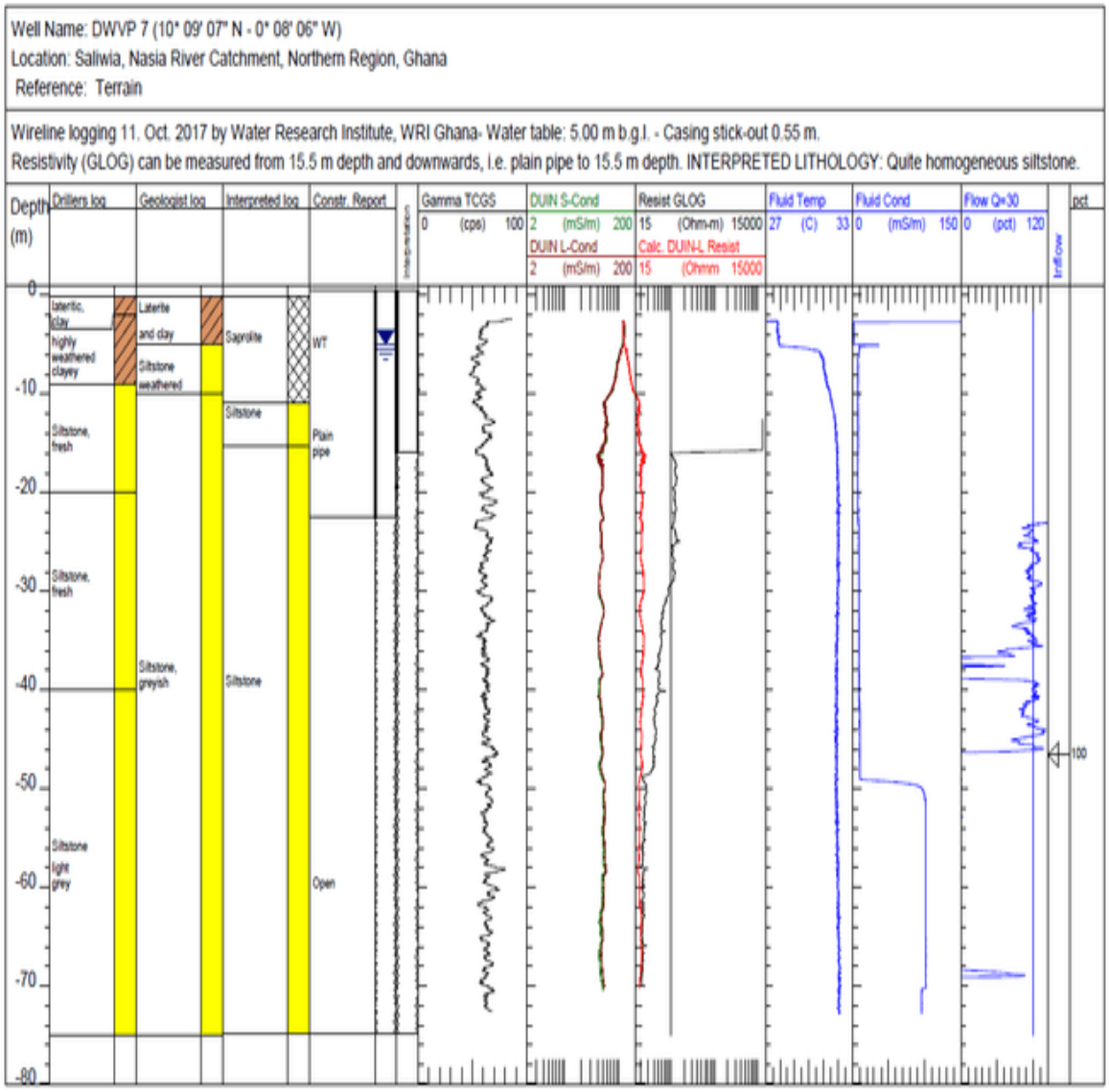

8. DWVP08

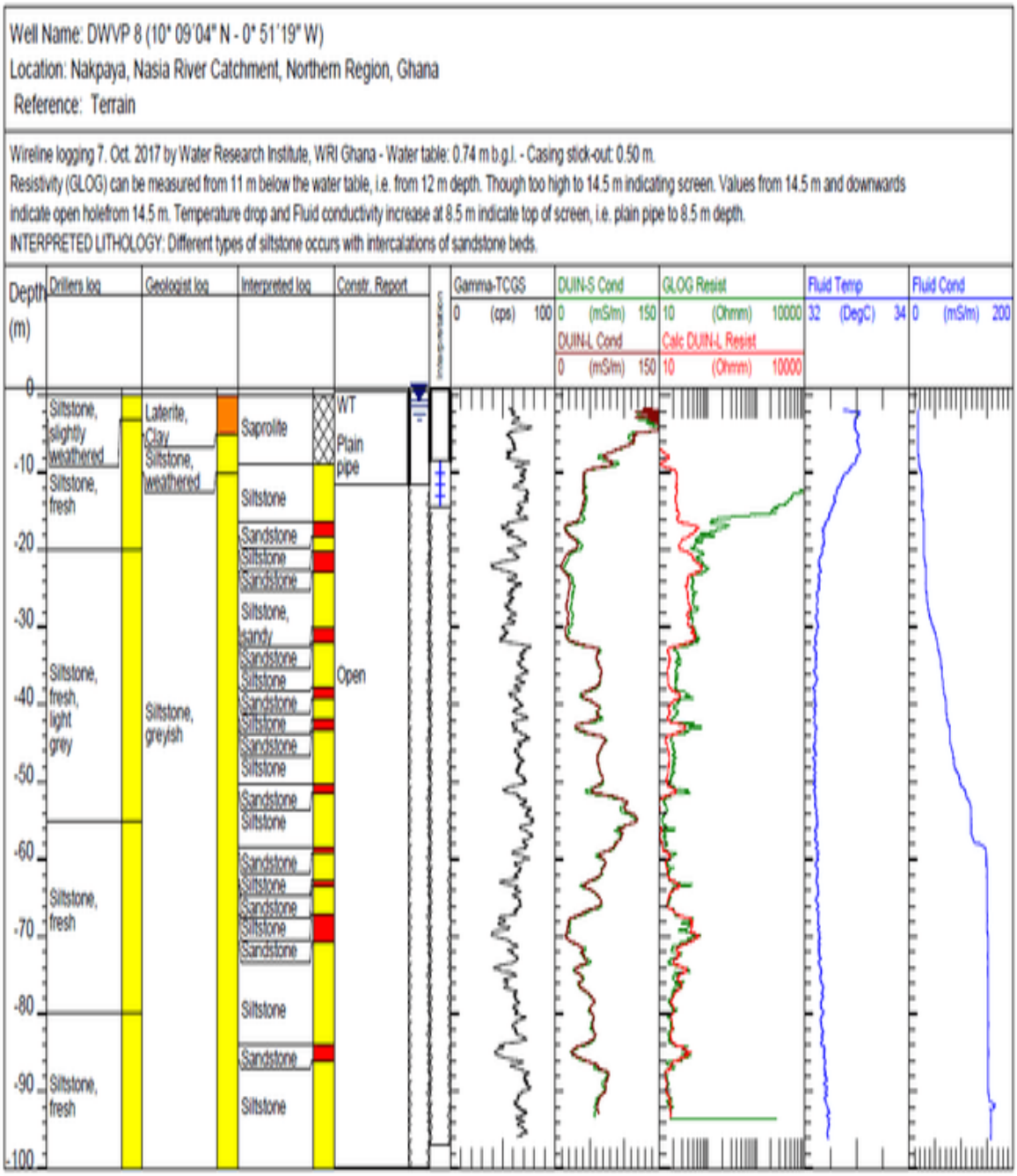

9. DWVP09

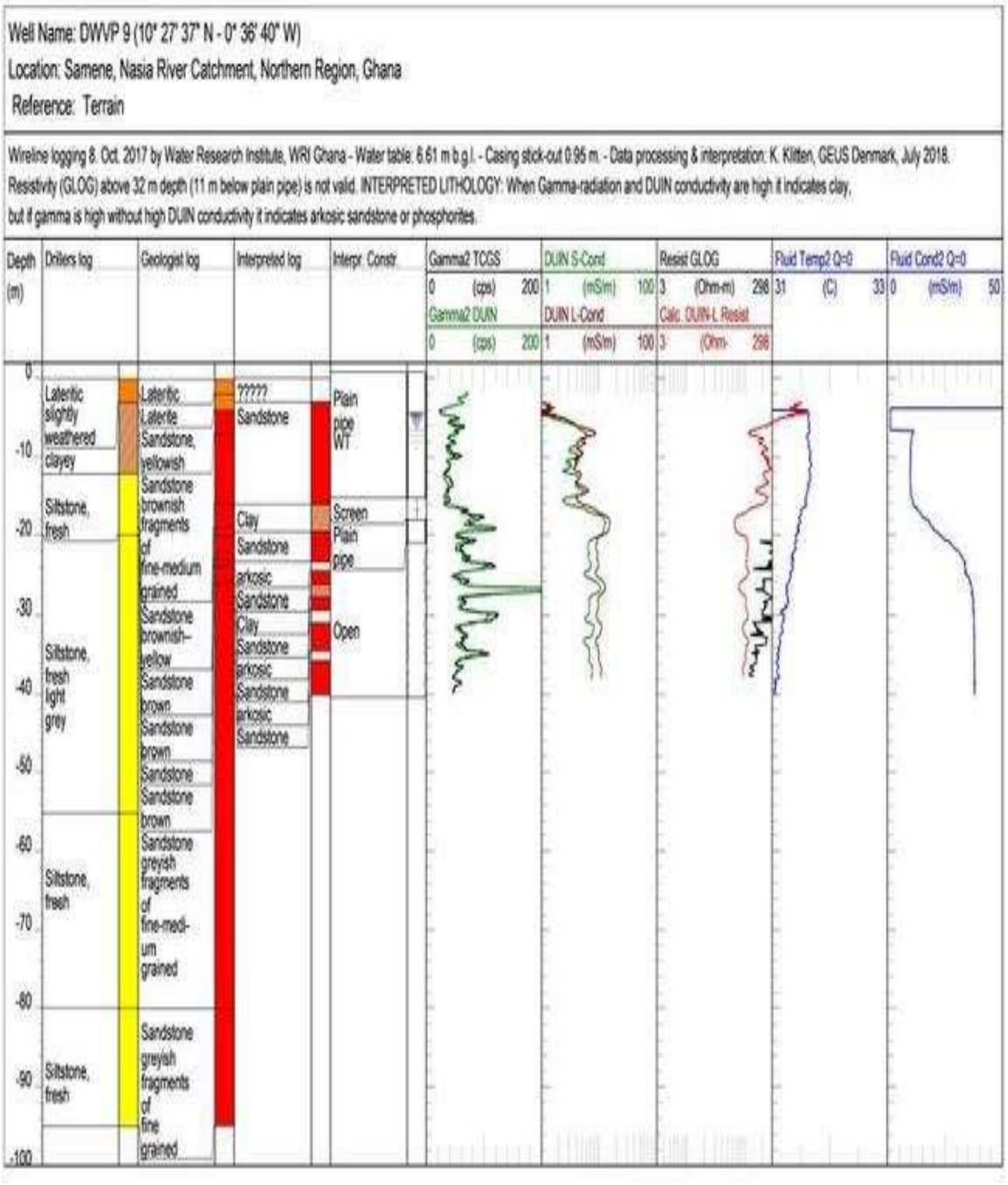

10. DWVP10

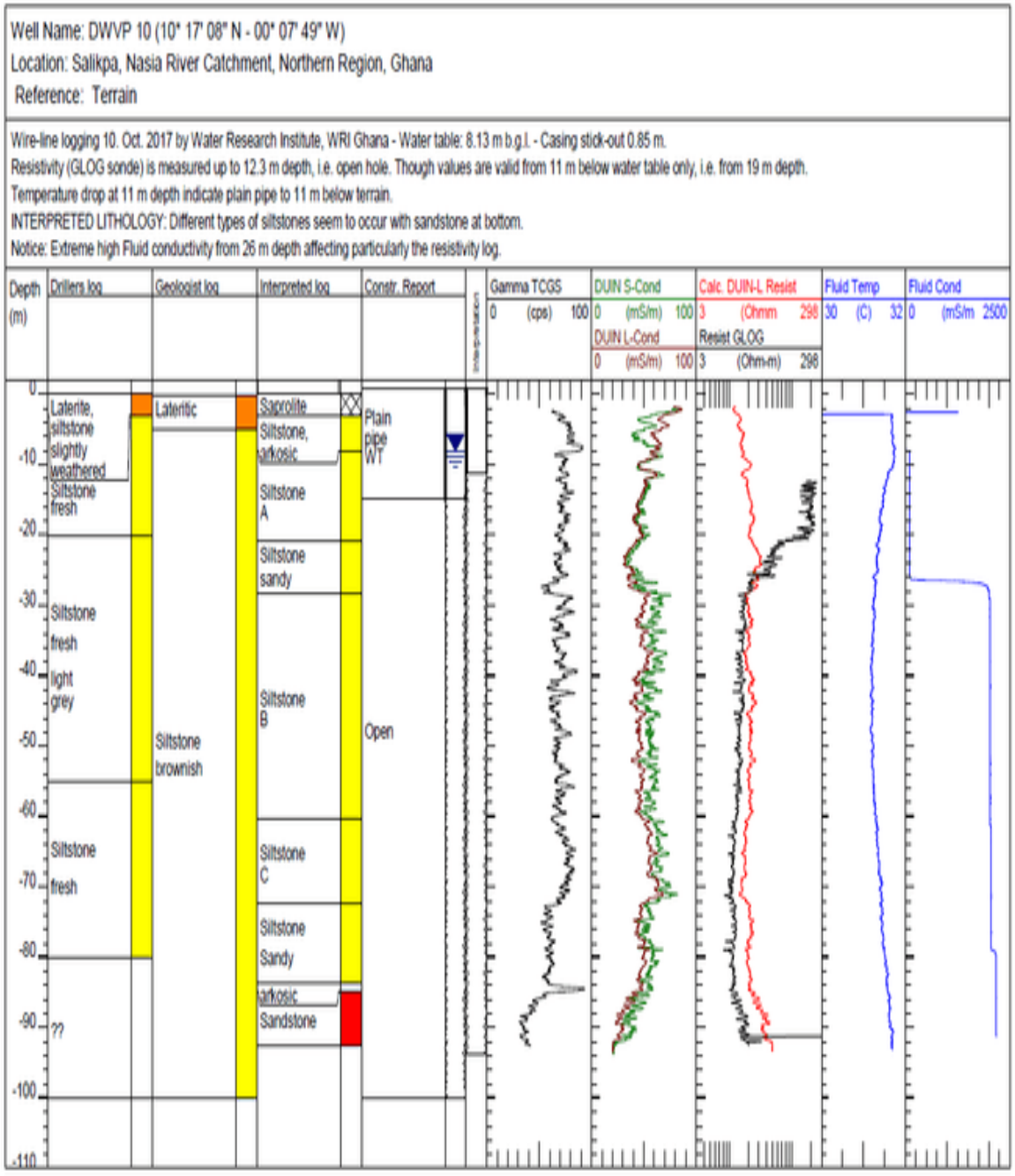

11. HAP05

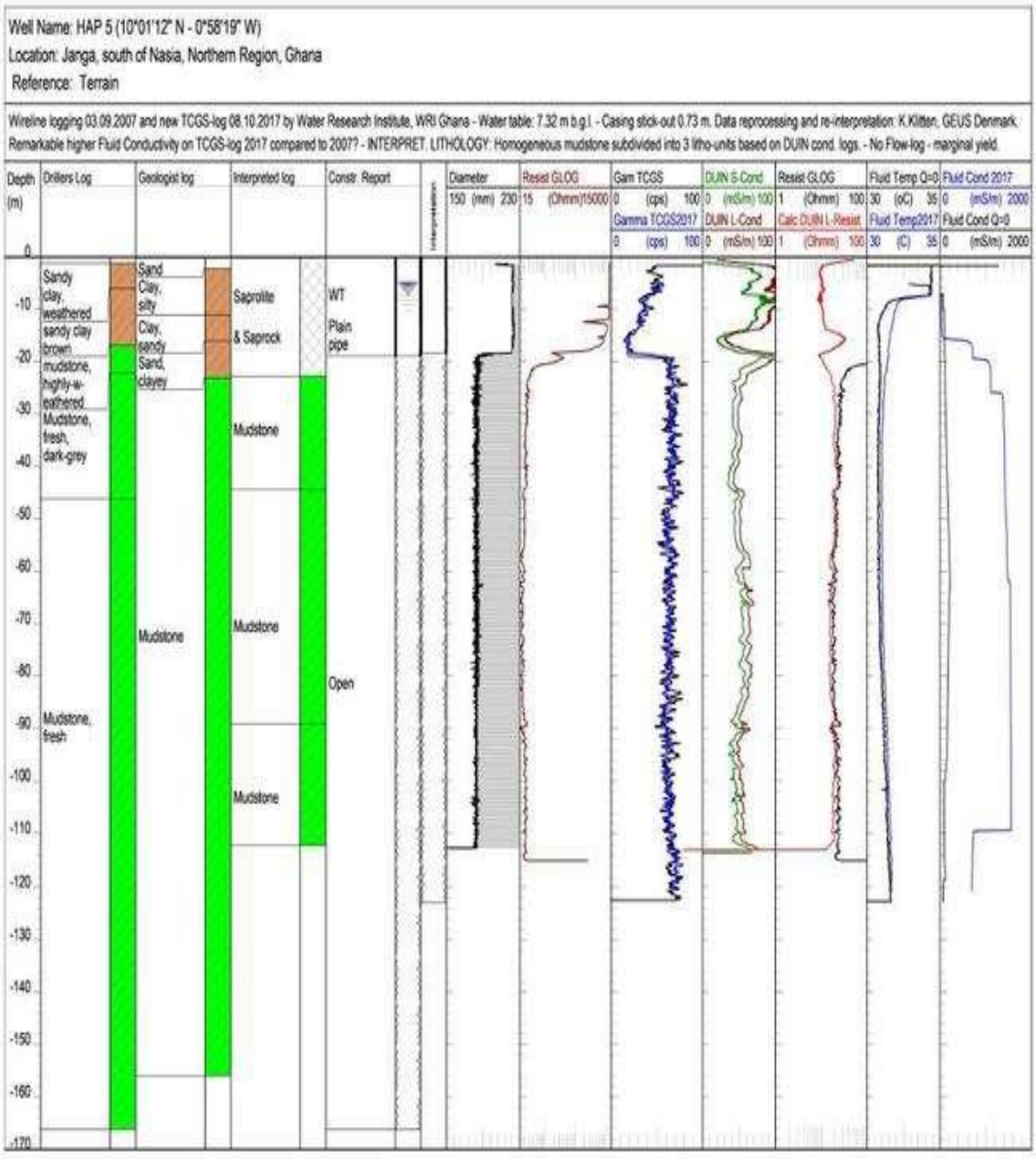

12. BUGYA PALA-2

Well Name: Bugya-Pala 2 (10°17'17" N - 0°44'39" W) 400 m north of WVB11
Location: Bugya Pala, Nasia River Catchment, Northern Region, Ghana
Reference: Ground Surface

Wireline logging 20. March 2007 by Water Research Institute, WRI Ghana - Water table: 2.00 m b.g.l. - Data processing and interpretation: K. Klitten, GEUS Denmark, July 2018.
INTERPRETED LITHOLOGY: Unusually high conductivity in the upper 22 m without similar high gamma- is interpreted as Saprolite & Saprock like in WVB11 (Bugya Pala 1) located 400 m more south. The 10 times higher conductivity in the Saprolite+Saprock in Bugya Pala 2 compared to Bugya Pala 1 can only partly be explained by a 6 times higher Fluid conductivity. A more conductive mineralogy in BP2 lithology might also be the explanation for the higher formation conductivity. The Gamma radiation is only slightly higher in Bugya Pala 2 than compared to Bugya Pala 1, i.e. in average 50 cps compared to 35 cps thus also indicating different lithology in the two boreholes. No flow-log was conducted.
The difference between the downwards Fluid conductivity log and the upwards is caused by the water being forced upwards by the downwards running probe in the 5" borehole.

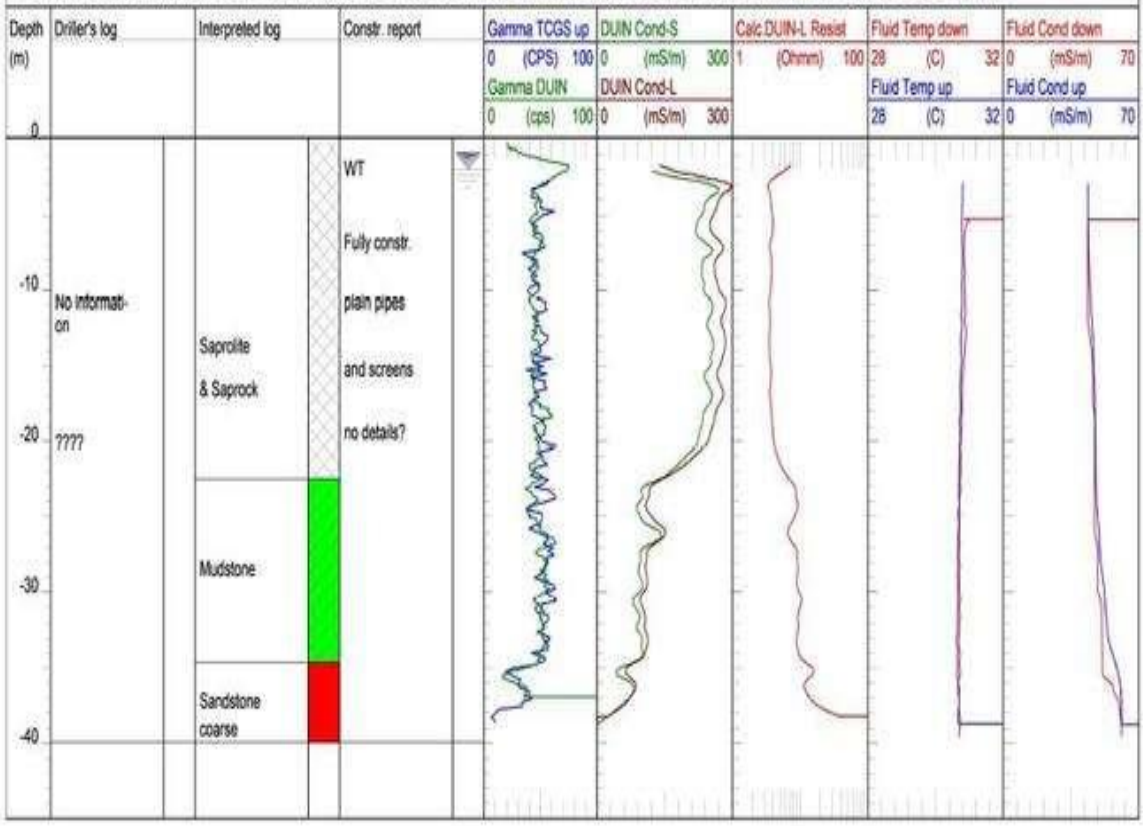

13. WVB-11

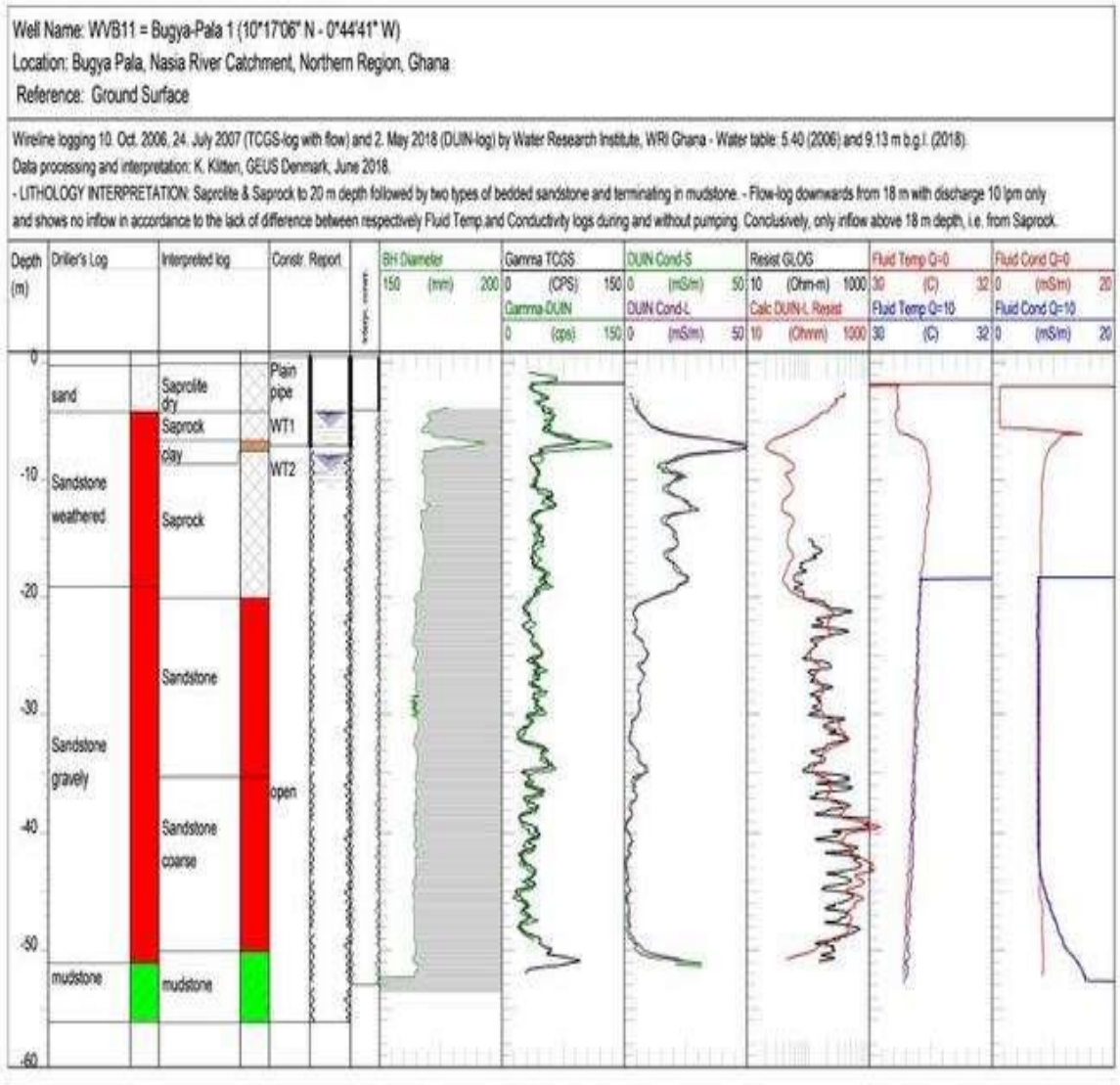

14. WVB12

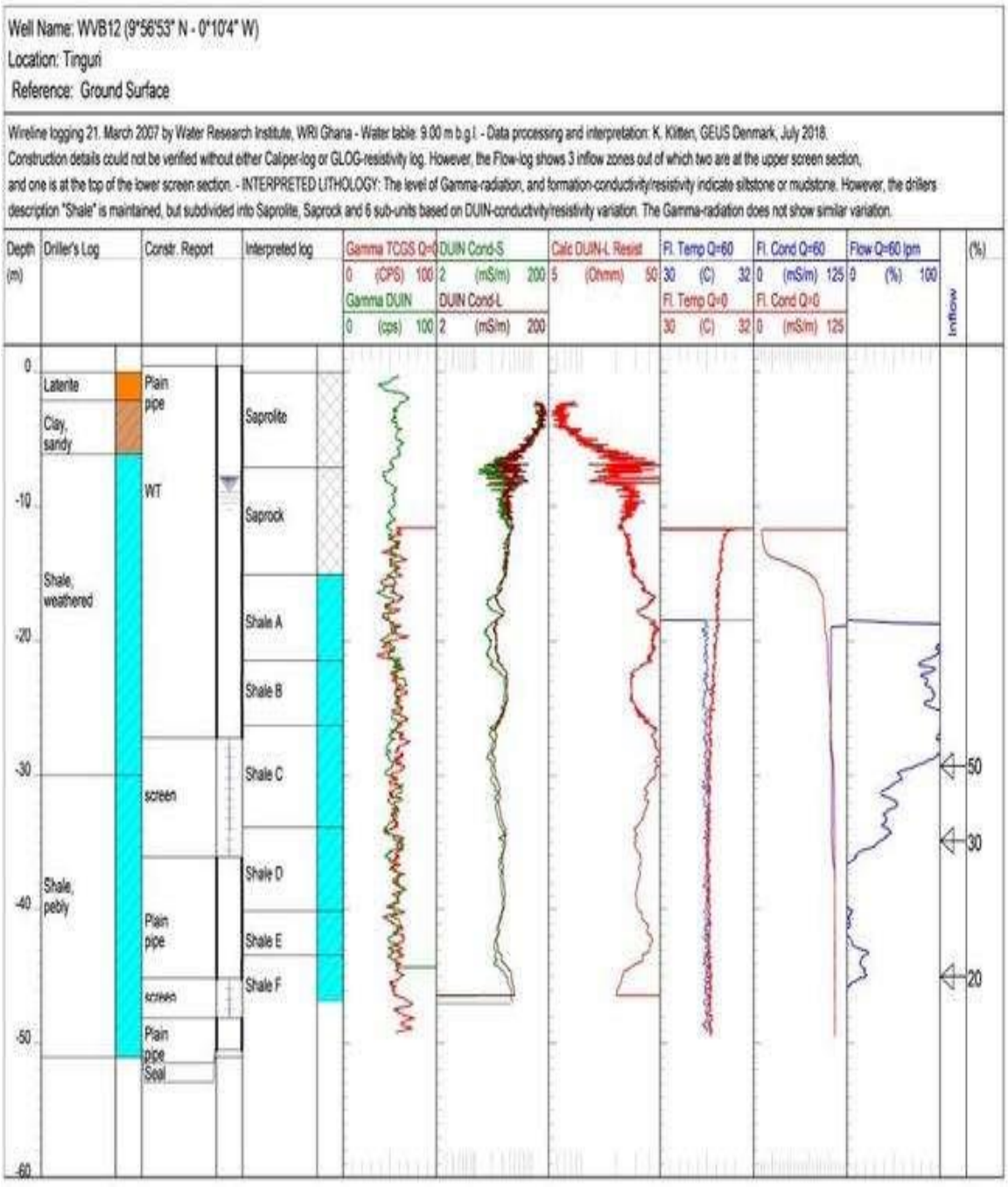

15. HAP 11

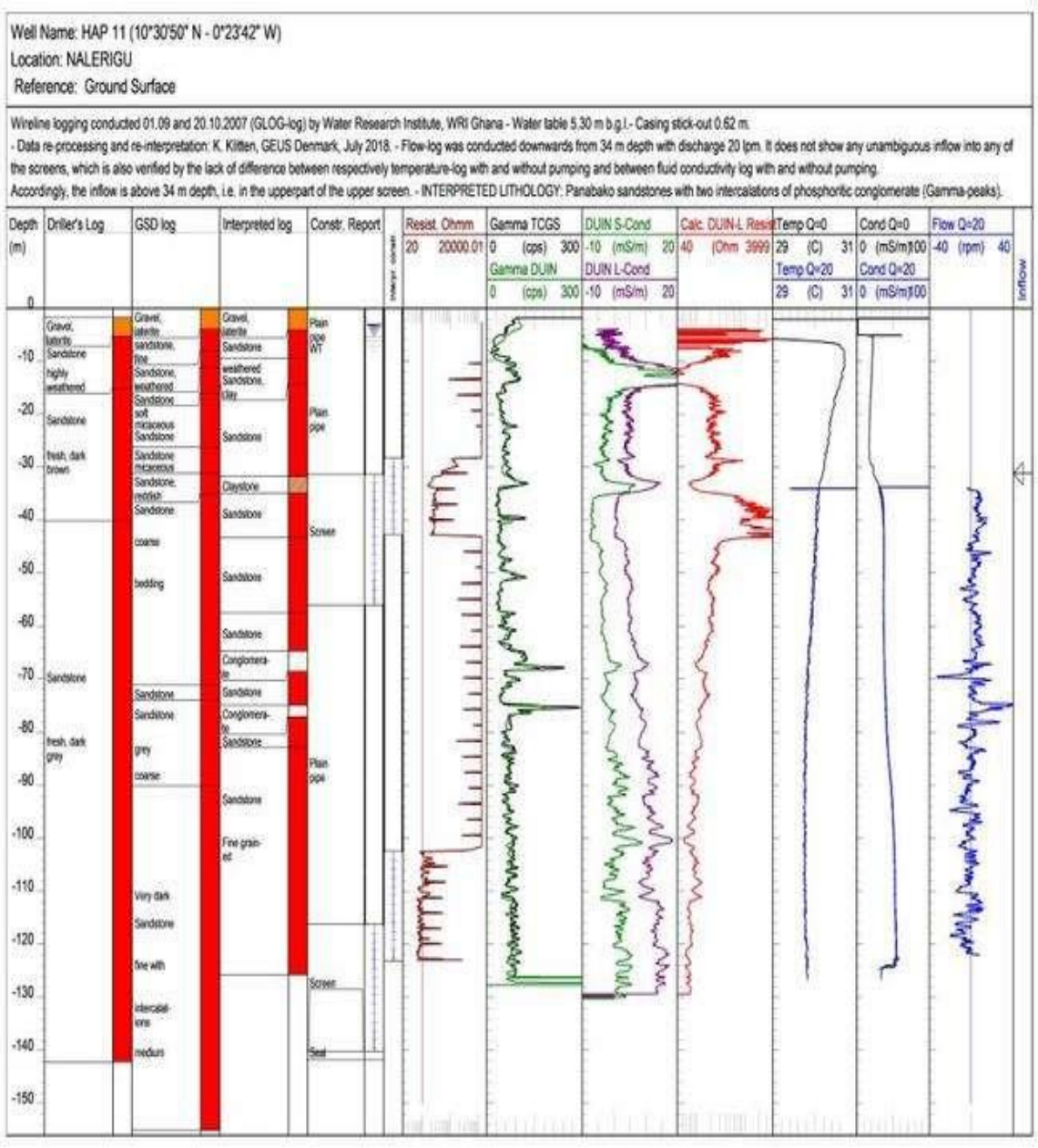

16. HAP 14

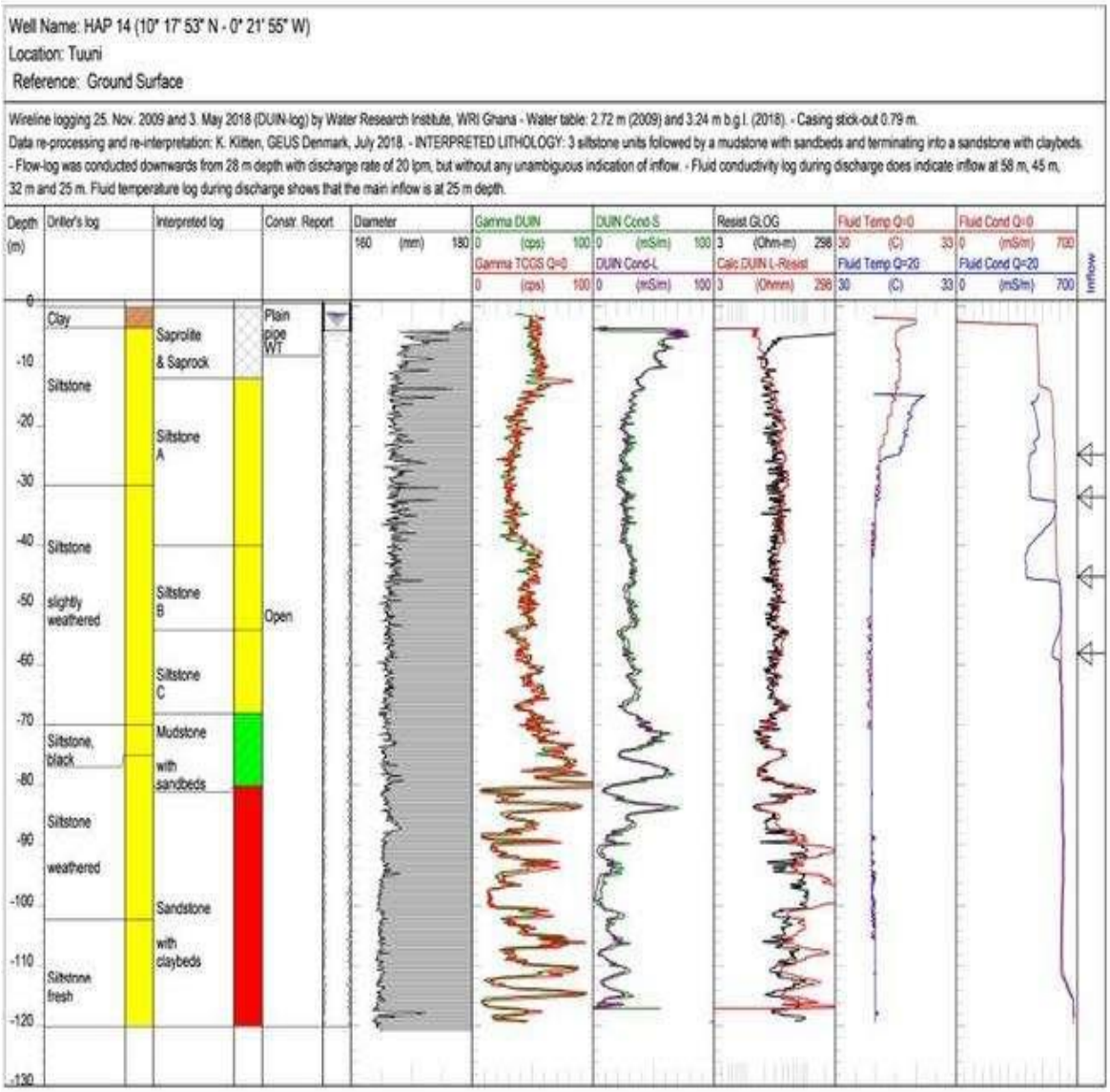

17. HAP 12

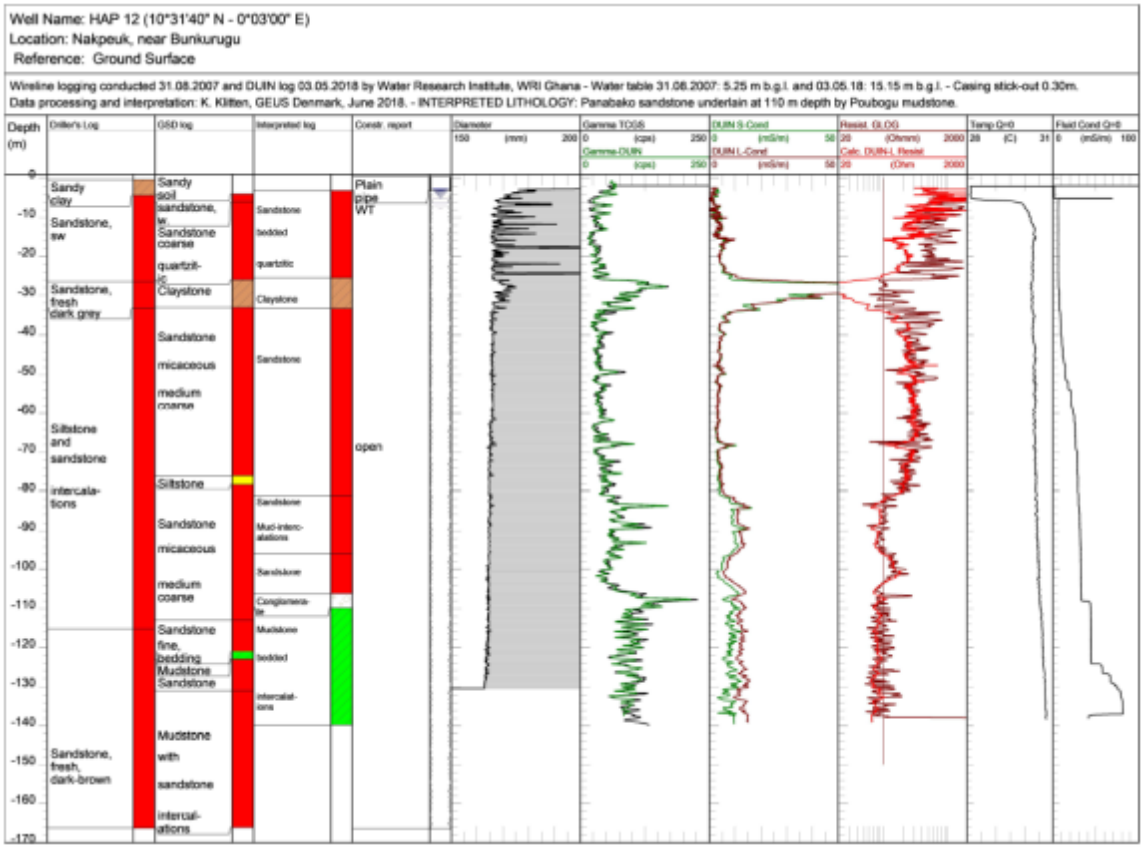

APPENDIX 4- GEOLOGICAL LOGS

1. DWVP01

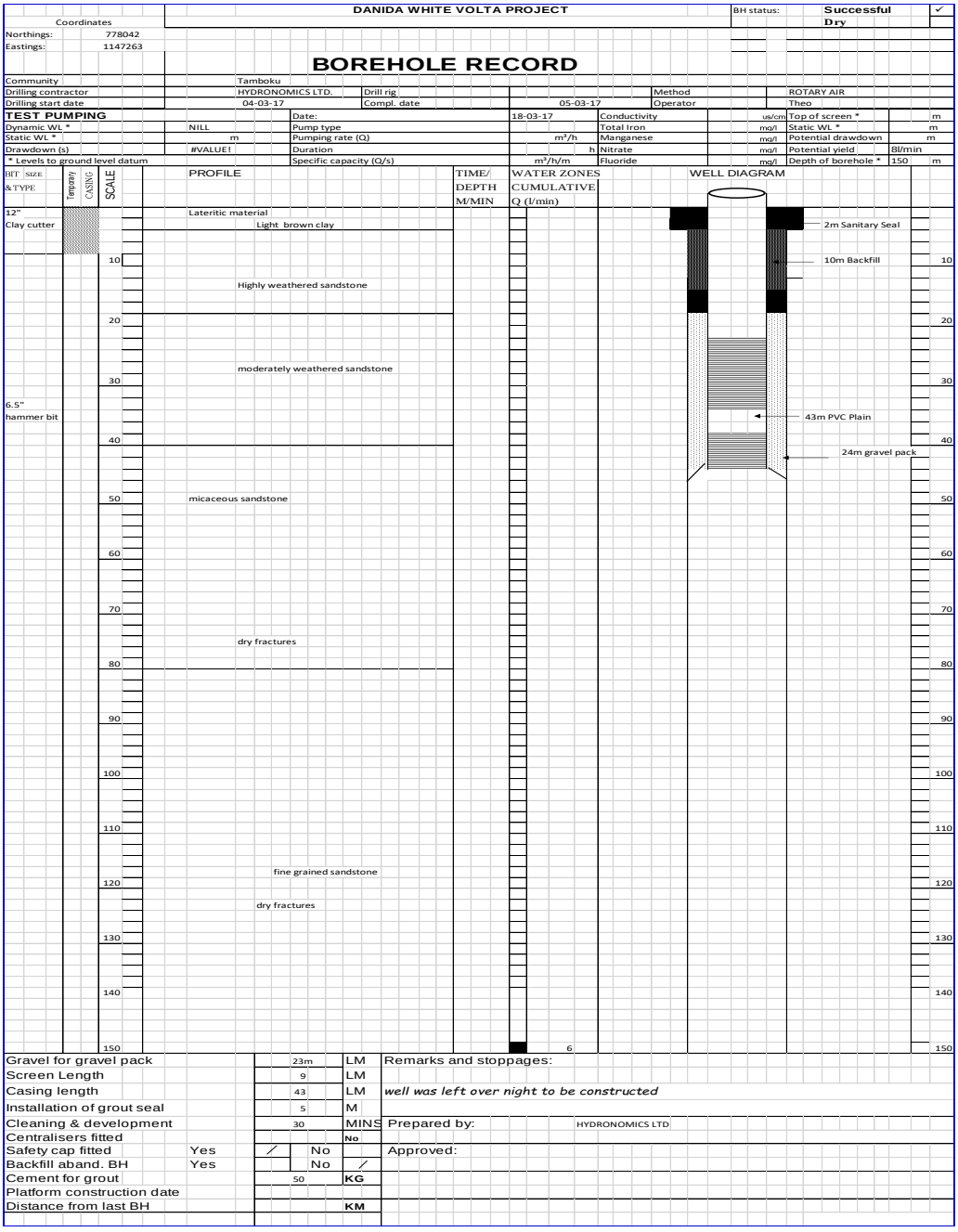

DANIDA WHITE VOLTA PROJECT

BH status: Successful ✓ / Dry

Coordinates
Northings: 778042
Eastings: 1147263

BOREHOLE RECORD

Community	Tamboku				
Drilling contractor	HYDRONOMICS LTD.	Drill rig		Method	ROTARY AIR
Drilling start date	04-03-17	Compl. date	05-03-17	Operator	Theo

TEST PUMPING		Date:	18-03-17	Conductivity	us/cm	Top of screen *	m
Dynamic WL *	NILL	Pump type		Total Iron	mg/l	Static WL *	m
Static WL *	m	Pumping rate (Q)	m^3/h	Manganese	mg/l	Potential drawdown	m
Drawdown (s)	#VALUE!	Duration	h	Nitrate	mg/l	Potential yield	l/s/min
* Levels to ground level datum		Specific capacity (Q/s)	$m^3/h/m$	Fluoride	mg/l	Depth of borehole *	150 m

BIT SIZE & TYPE	Temporary CASING	SCALE	PROFILE	TIME/ DEPTH M/MIN	WATER ZONES CUMULATIVE Q (l/min)
12" Clay cutter		10	Lateritic material		
			Light brown clay		
		20	Highly weathered sandstone		
		30	moderately weathered sandstone		
6.5" hammer bit		40			
		50	micaceous sandstone		
		60			
		70			
		80	dry fractures		
		90			
		100			
		110			
		120	fine grained sandstone		
		130	dry fractures		
		140			
		150			6

WELL DIAGRAM

Gravel for gravel pack		23m	LM	Remarks and stoppages:	
Screen Length		9	LM		
Casing length		43	LM	*well was left over night to be constructed*	
Installation of grout seal		5	M		
Cleaning & development		30	MINS	Prepared by:	HYDRONOMICS LTD
Centralisers fitted			No		
Safety cap fitted	Yes ✓		No	Approved:	
Backfill aband. BH	Yes		No ✓		
Cement for grout		50	KG		
Platform construction date					
Distance from last BH			KM		

2. DWVP02

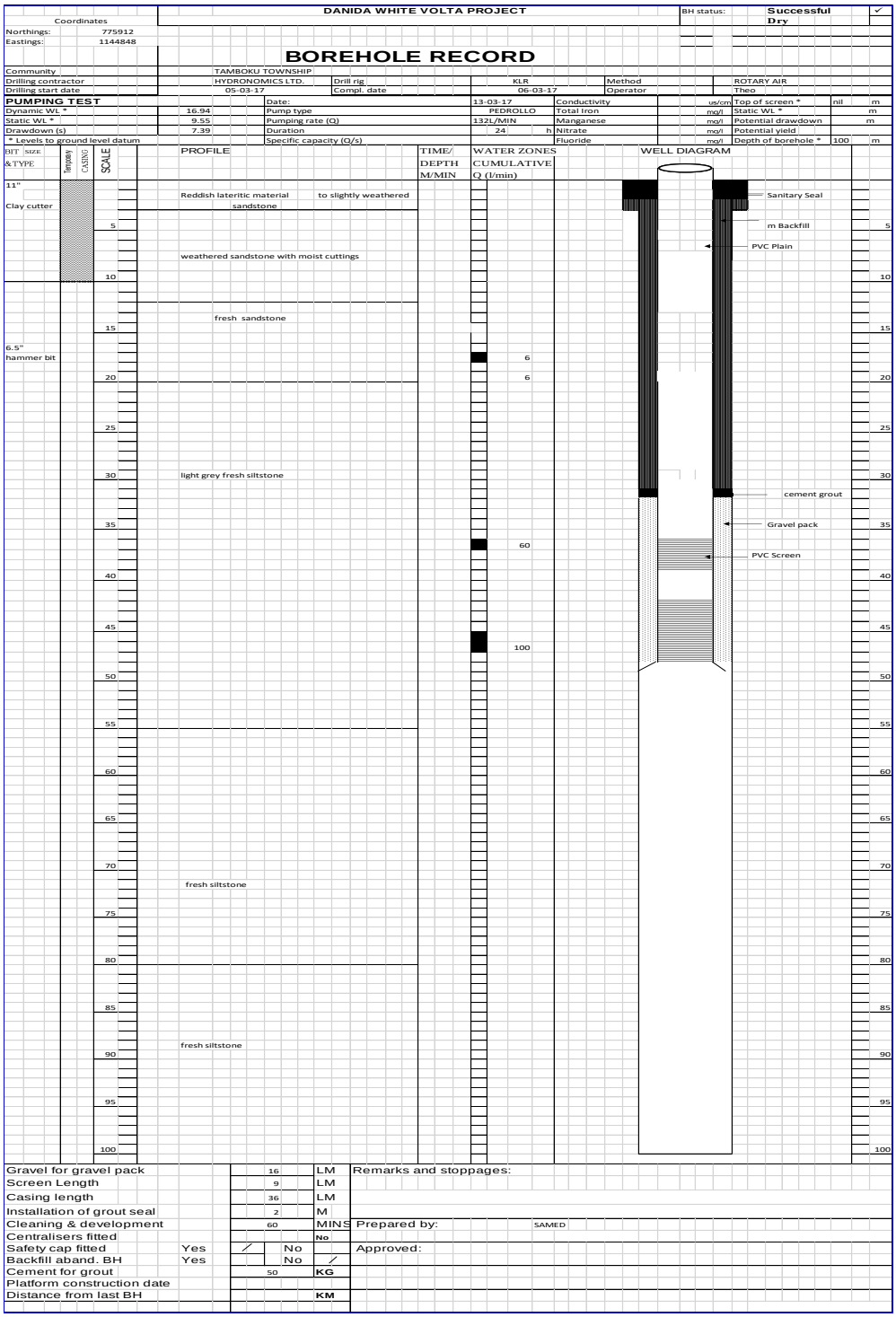

DANIDA WHITE VOLTA PROJECT

BH status: Successful / Dry ✓

Coordinates
Northings: 775912
Eastings: 1144848

BOREHOLE RECORD

Community	TAMBOKU TOWNSHIP						
Drilling contractor	HYDRONOMICS LTD.	Drill rig	KLR	Method	ROTARY AIR		
Drilling start date	05-03-17	Compl. date	06-03-17	Operator	Theo		

PUMPING TEST		Date:	13-03-17	Conductivity	us/cm	Top of screen *	nil	m
Dynamic WL *	16.94	Pump type	PEDROLLO	Total Iron	mg/l	Static WL *		m
Static WL *	9.55	Pumping rate (Q)	132L/MIN	Manganese	mg/l	Potential drawdown		m
Drawdown (s)	7.39	Duration	24 h	Nitrate	mg/l	Potential yield		
* Levels to ground level datum		Specific capacity (Q/s)		Fluoride	mg/l	Depth of borehole *	100	m

BIT SIZE & TYPE	Temporary CASING	SCALE	PROFILE	TIME/ DEPTH M/MIN	WATER ZONES CUMULATIVE Q (l/min)	WELL DIAGRAM
11" Clay cutter		0	Reddish lateritic material to slightly weathered sandstone			Sanitary Seal
		5				m Backfill
		10	weathered sandstone with moist cuttings			PVC Plain
		15	fresh sandstone			
6.5" hammer bit		20		6	6	
		25				
		30	light grey fresh siltstone			cement grout
		35				Gravel pack
		40		60		PVC Screen
		45				
		50		100		
		55				
		60				
		65				
		70				
		75	fresh siltstone			
		80				
		85				
		90	fresh siltstone			
		95				
		100				

Gravel for gravel pack		16	LM	Remarks and stoppages:
Screen Length		9	LM	
Casing length		36	LM	
Installation of grout seal		2	M	
Cleaning & development		60	MINS	Prepared by: SAMED
Centralisers fitted			No	
Safety cap fitted	Yes /	No		Approved:
Backfill aband. BH	Yes	No /		
Cement for grout		50	KG	
Platform construction date				
Distance from last BH			KM	

3. DWVP03

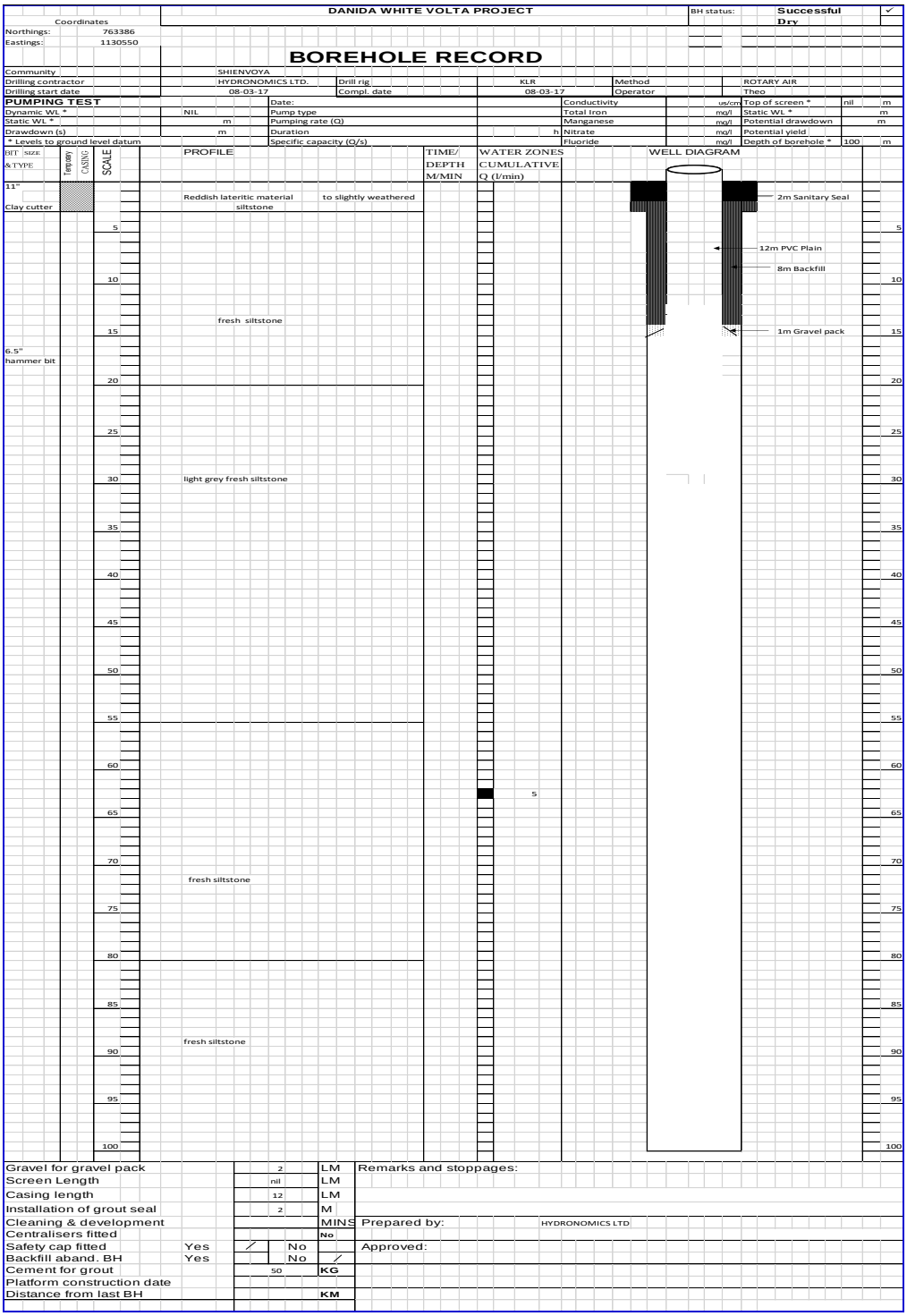

DANIDA WHITE VOLTA PROJECT

BH status: Successful ✓ Dry

Coordinates
Northings: 763386
Eastings: 1130550

BOREHOLE RECORD

Community	SHIENVOYA						
Drilling contractor	HYDRONOMICS LTD.	Drill rig	KLR	Method	ROTARY AIR		
Drilling start date	08-03-17	Compl. date	08-03-17	Operator	Theo		

PUMPING TEST		Date:		Conductivity	us/cm	Top of screen *	nil	m
Dynamic WL *	NIL	Pump type		Total Iron	mg/l	Static WL *		m
Static WL *	m	Pumping rate (Q)		Manganese	mg/l	Potential drawdown		m
Drawdown (s)	m	Duration	h	Nitrate	mg/l	Potential yield		
* Levels to ground level datum		Specific capacity (Q/s)		Fluoride	mg/l	Depth of borehole *	100	m

BIT SIZE & TYPE	CASING (temporary)	SCALE	PROFILE	TIME/ DEPTH M/MIN	WATER ZONES CUMULATIVE Q (l/min)	WELL DIAGRAM
11" Clay cutter		0–5	Reddish lateritic material to slightly weathered siltstone			2m Sanitary Seal
		5–10				12m PVC Plain; 8m Backfill
		10–15	fresh siltstone			
6.5" hammer bit		15–20				1m Gravel pack
		20–25				
		25–30	light grey fresh siltstone			
		30–35				
		35–40				
		40–45				
		45–50				
		50–55				
		55–60				
		60–65			5	
		65–70				
		70–75	fresh siltstone			
		75–80				
		80–85				
		85–90	fresh siltstone			
		90–95				
		95–100				

Gravel for gravel pack	2	LM	Remarks and stoppages:	
Screen Length	nil	LM		
Casing length	12	LM		
Installation of grout seal	2	M		
Cleaning & development		MINS	Prepared by:	HYDRONOMICS LTD
Centralisers fitted		No		
Safety cap fitted	Yes ✓	No	Approved:	
Backfill aband. BH	Yes	No ✓		
Cement for grout	50	KG		
Platform construction date				
Distance from last BH		KM		

4. DWVP04

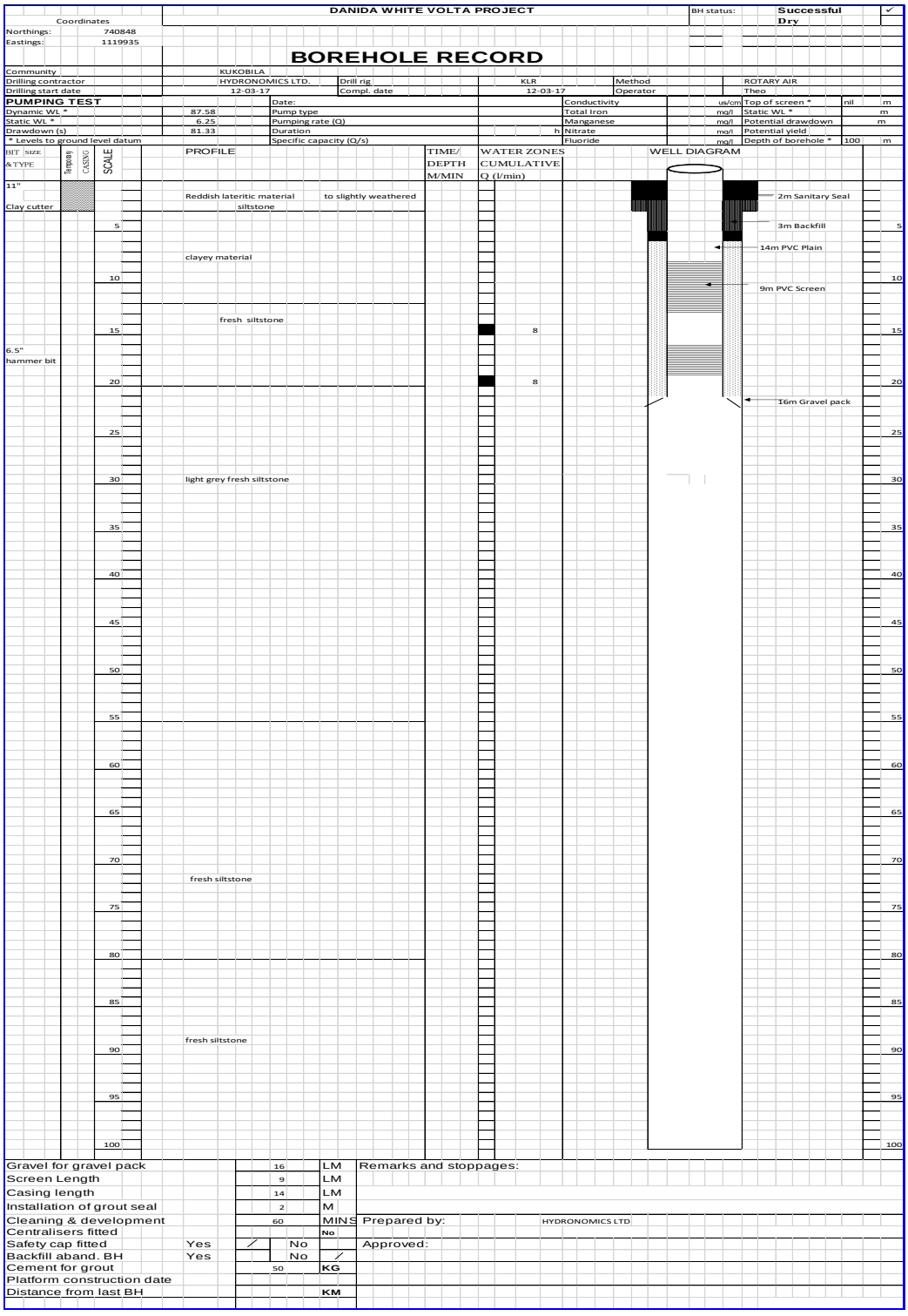

DANIDA WHITE VOLTA PROJECT

BH status: Successful / Dry

Coordinates
Northings: 740848
Eastings: 1119935

BOREHOLE RECORD

Community	KUKOBILA						
Drilling contractor	HYDRONOMICS LTD.	Drill rig	KLR	Method	ROTARY AIR		
Drilling start date	12-03-17	Compl. date	12-03-17	Operator	Theo		

PUMPING TEST								
Dynamic WL *	87.58	Date:		Conductivity	us/cm	Top of screen *	nil	m
Static WL *	6.25	Pump type		Total Iron	mg/l	Static WL *		m
Drawdown (s)	81.33	Pumping rate (Q)		Manganese	mg/l	Potential drawdown		m
* Levels to ground level datum		Duration	h	Nitrate	mg/l	Potential yield		
		Specific capacity (Q/s)		Fluoride	mg/l	Depth of borehole *	100	m

BIT SIZE & TYPE | Temporary | CASING | SCALE | PROFILE | TIME/ DEPTH M/MIN | WATER ZONES CUMULATIVE Q (l/min) | WELL DIAGRAM

11" Clay cutter

Reddish lateritic material to slightly weathered siltstone

clayey material

fresh siltstone

8

6.5" hammer bit

8

light grey fresh siltstone

fresh siltstone

fresh siltstone

2m Sanitary Seal
3m Backfill
14m PVC Plain
9m PVC Screen
16m Gravel pack

Gravel for gravel pack		16	LM	Remarks and stoppages:
Screen Length		9	LM	
Casing length		14	LM	
Installation of grout seal		2	M	
Cleaning & development		60	MINS	Prepared by: HYDRONOMICS LTD
Centralisers fitted			No	
Safety cap fitted	Yes ✓		No	Approved:
Backfill aband. BH	Yes		No ✓	
Cement for grout		50	KG	
Platform construction date				
Distance from last BH			KM	

5. DWVP05

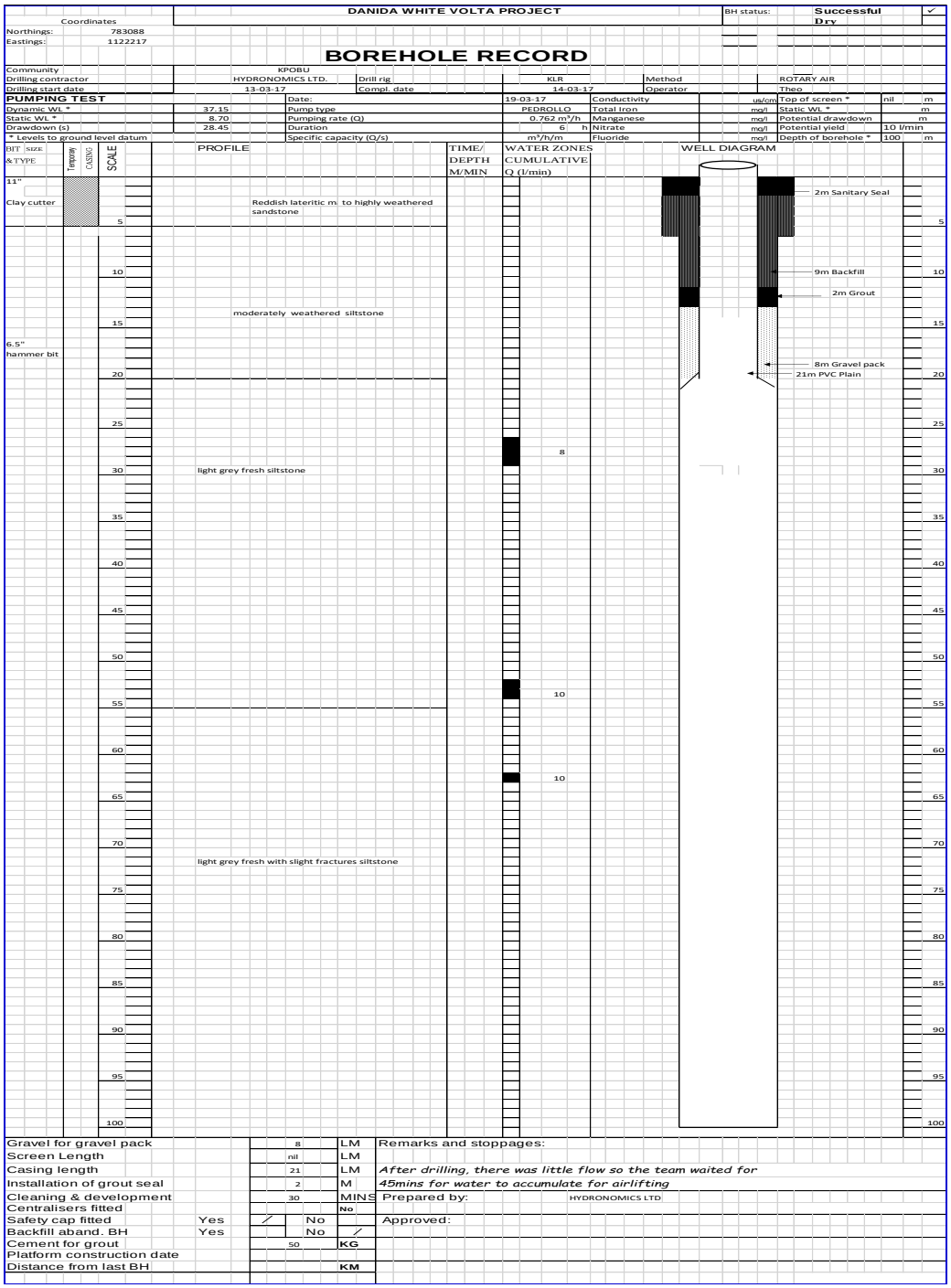

DANIDA WHITE VOLTA PROJECT

BH status: Successful / Dry

Coordinates
Northings: 783088
Eastings: 1122217

BOREHOLE RECORD

Community	KPOBU						
Drilling contractor	HYDRONOMICS LTD.	Drill rig	KLR	Method	ROTARY AIR		
Drilling start date	13-03-17	Compl. date	14-03-17	Operator	Theo		
PUMPING TEST		Date:	19-03-17	Conductivity	us/cm	Top of screen *	nil m
Dynamic WL *	37.15	Pump type	PEDROLLO	Total Iron	mg/l	Static WL *	m
Static WL *	8.70	Pumping rate (Q)	0.762 m³/h	Manganese	mg/l	Potential drawdown	m
Drawdown (s)	28.45	Duration	6 h	Nitrate	mg/l	Potential yield	10 l/min
* Levels to ground level datum		Specific capacity (Q/s)	m³/h/m	Fluoride	mg/l	Depth of borehole *	100 m

BIT SIZE & TYPE: 11" Clay cutter; 6.5" hammer bit

Tamping; CASING; SCALE

PROFILE:
- Reddish lateritic m to highly weathered sandstone
- moderately weathered siltstone
- light grey fresh siltstone
- light grey fresh with slight fractures siltstone

TIME/DEPTH M/MIN

WATER ZONES CUMULATIVE Q (l/min): 8; 10; 10

WELL DIAGRAM:
- 2m Sanitary Seal
- 9m Backfill
- 2m Grout
- 8m Gravel pack
- 21m PVC Plain

Gravel for gravel pack		8	LM	Remarks and stoppages:
Screen Length		nil	LM	
Casing length		21	LM	*After drilling, there was little flow so the team waited for*
Installation of grout seal		2	M	*45mins for water to accumulate for airlifting*
Cleaning & development		30	MINS	Prepared by: HYDRONOMICS LTD.
Centralisers fitted			No	
Safety cap fitted	Yes /	No		Approved:
Backfill aband. BH	Yes	No /		
Cement for grout		50	KG	
Platform construction date				
Distance from last BH			KM	

6. DWVP06

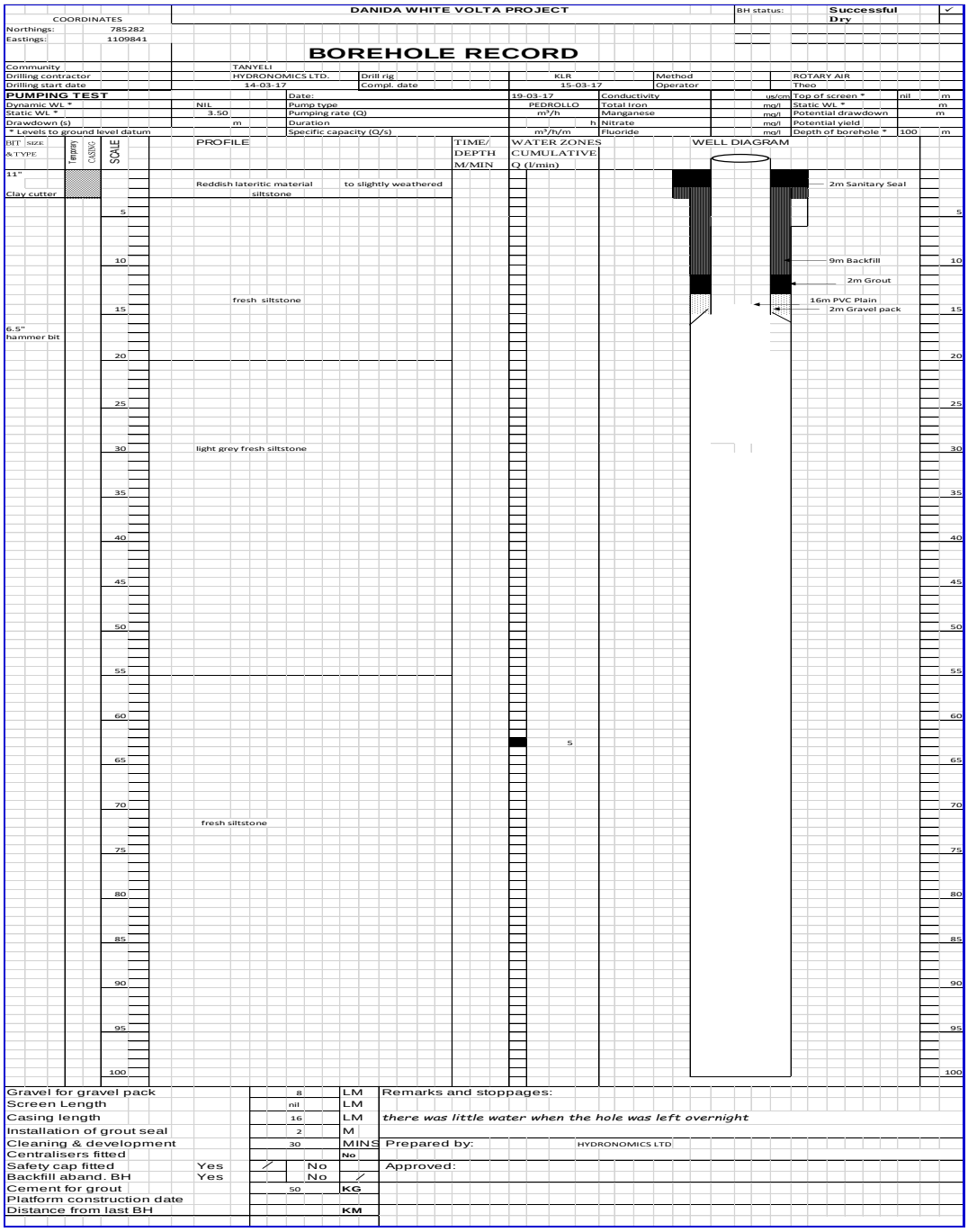

DANIDA WHITE VOLTA PROJECT

BH status: Successful / Dry

COORDINATES
Northings: 785282
Eastings: 1109841

BOREHOLE RECORD

Community	TANYELI						
Drilling contractor	HYDRONOMICS LTD.	Drill rig	KLR	Method	ROTARY AIR		
Drilling start date	14-03-17	Compl. date	15-03-17	Operator	Theo		

PUMPING TEST								
Dynamic WL *	NIL	Date:	19-03-17	Conductivity	us/cm	Top of screen *	nil	m
Static WL *	3.50	Pump type	PEDROLLO	Total Iron	mg/l	Static WL *		m
Drawdown (s)	m	Pumping rate (Q)	m^3/h	Manganese	mg/l	Potential drawdown		m
* Levels to ground level datum		Duration	h	Nitrate	mg/l	Potential yield		
		Specific capacity (Q/s)	$m^3/h/m$	Fluoride	mg/l	Depth of borehole *	100	m

BIT SIZE & TYPE	Tamping	CASING	SCALE	PROFILE	TIME/ DEPTH M/MIN	WATER ZONES CUMULATIVE Q (l/min)
11" Clay cutter			0	Reddish lateritic material to slightly weathered siltstone		
			5			
			10			
			15	fresh siltstone		
6.5" hammer bit			20			
			25			
			30	light grey fresh siltstone		
			35			
			40			
			45			
			50			
			55			
			60			
			65			5
			70	fresh siltstone		
			75			
			80			
			85			
			90			
			95			
			100			

WELL DIAGRAM

Gravel for gravel pack		8	LM	Remarks and stoppages:
Screen Length		nil	LM	
Casing length		16	LM	*there was little water when the hole was left overnight*
Installation of grout seal		2	M	
Cleaning & development		30	MINS	Prepared by: HYDRONOMICS LTD
Centralisers fitted			No	
Safety cap fitted	Yes / No			Approved:
Backfill aband. BH	Yes No /			
Cement for grout		50	KG	
Platform construction date				
Distance from last BH			KM	

7. DWVP07

DANIDA WHITE VOLTA PROJECT

BH status: **Successful** ✓ / **Dry**

Coordinates
Northings: 813968
Eastings: 1123607

BOREHOLE RECORD

Community	SALIWIA						
Drilling contractor	HYDRONOMICS LTD.	Drill rig		Method	ROTARY AIR		
Drilling start date	16-03-17	Compl. date	16-03-17	Operator	Theo		

TEST PUMPING		Date:	18-03-17	Conductivity	us/cm	Top of screen *	m
Dynamic WL *	51.2	Pump type		Total Iron	mg/l	Static WL *	m
Static WL *	5.25	Pumping rate (Q)	m^3/h	Manganese	mg/l	Potential drawdown	m
Drawdown (s)	45.91	Duration	h	Nitrate	mg/l	Potential yield	45l/min
* Levels to ground level datum		Specific capacity (Q/s)	$m^3/h/m$	Fluoride	mg/l	Depth of borehole *	75 m

BIT SIZE & TYPE	Temporary CASING	SCALE	PROFILE	TIME/ DEPTH M/MIN	WATER ZONES CUMULATIVE Q (l/min)
12" Clay cutter		0	Lateritic material		
			Light brown clay		
		5			
			Highly weathered light brown clay mixed		
		10			
			fresh siltstone		
		15			
6.5" hammer bit					
		20			
		25	fresh siltstone		
		30			
		35			
		40			
		45			
		50			
		55			
		60	Light grey siltstone		134
		65			
		70			45
		75			45

WELL DIAGRAM

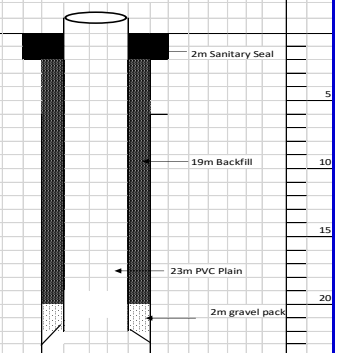

Gravel for gravel pack	19m	LM	Remarks and stoppages:	
Screen Length	nil	LM		
Casing length	23	LM	*well was drilled closed to a valley. Two wells in the community are uphill and have low*	
Installation of grout seal	5	M	*yield.There have been several unsuccessful attempts in the community*	
Cleaning & development	30	MINS	Prepared by:	HYDRONOMICS LTD
Centralisers fitted		No		
Safety cap fitted	Yes /	No	Approved:	
Backfill aband. BH	Yes	No /		
Cement for grout	50	KG		
Platform construction date				
Distance from last BH	13	KM		

8. DWVP08

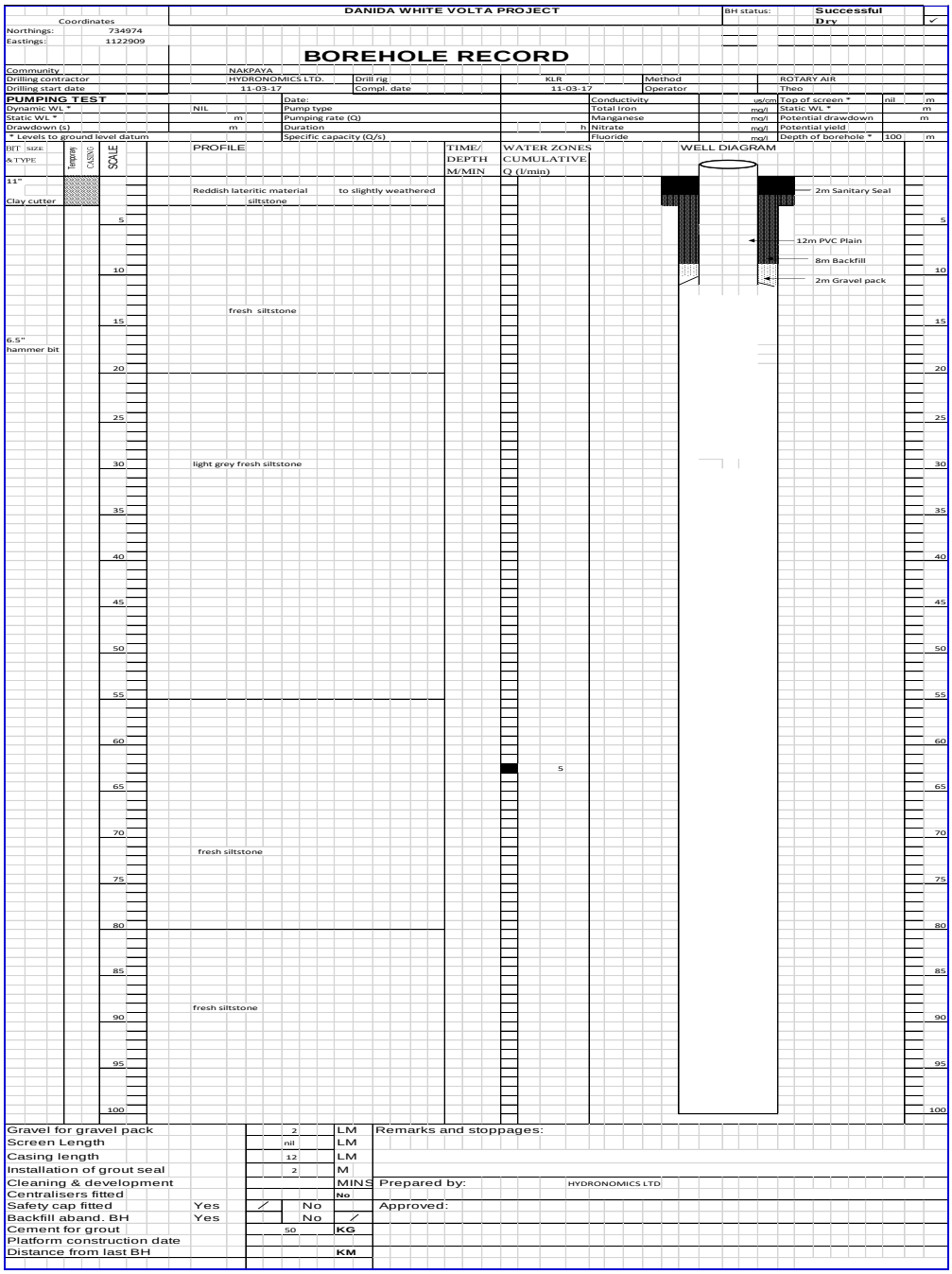

DANIDA WHITE VOLTA PROJECT

BH status: Successful ✓ Dry

Coordinates
Northings: 734974
Eastings: 1122909

BOREHOLE RECORD

Community	NAKPAYA						
Drilling contractor	HYDRONOMICS LTD.	Drill rig	KLR	Method	ROTARY AIR		
Drilling start date	11-03-17	Compl. date	11-03-17	Operator	Theo		

PUMPING TEST								
Dynamic WL *	NIL	Pump type		Conductivity	us/cm	Top of screen *	nil	m
Static WL *	m	Pumping rate (Q)		Total Iron	mg/l	Static WL *		m
Drawdown (s)	m	Duration	h	Manganese	mg/l	Potential drawdown		m
* Levels to ground level datum		Specific capacity (Q/s)		Nitrate	mg/l	Potential yield		
				Fluoride	mg/l	Depth of borehole *	100	m

BIT SIZE & TYPE: 11" Clay cutter; 6.5" hammer bit

PROFILE:
- Reddish lateritic material to slightly weathered siltstone
- fresh siltstone
- light grey fresh siltstone
- fresh siltstone
- fresh siltstone

TIME/DEPTH M/MIN

WATER ZONES CUMULATIVE Q (l/min): 5

WELL DIAGRAM:
- 2m Sanitary Seal
- 12m PVC Plain
- 8m Backfill
- 2m Gravel pack

Gravel for gravel pack		2	LM	Remarks and stoppages:
Screen Length		nil	LM	
Casing length		12	LM	
Installation of grout seal		2	M	
Cleaning & development			MINS	Prepared by: HYDRONOMICS LTD
Centralisers fitted			No	
Safety cap fitted	Yes ✓	No		Approved:
Backfill aband. BH	Yes	No ✓		
Cement for grout		50	KG	
Platform construction date				
Distance from last BH			KM	

9. DWVP09

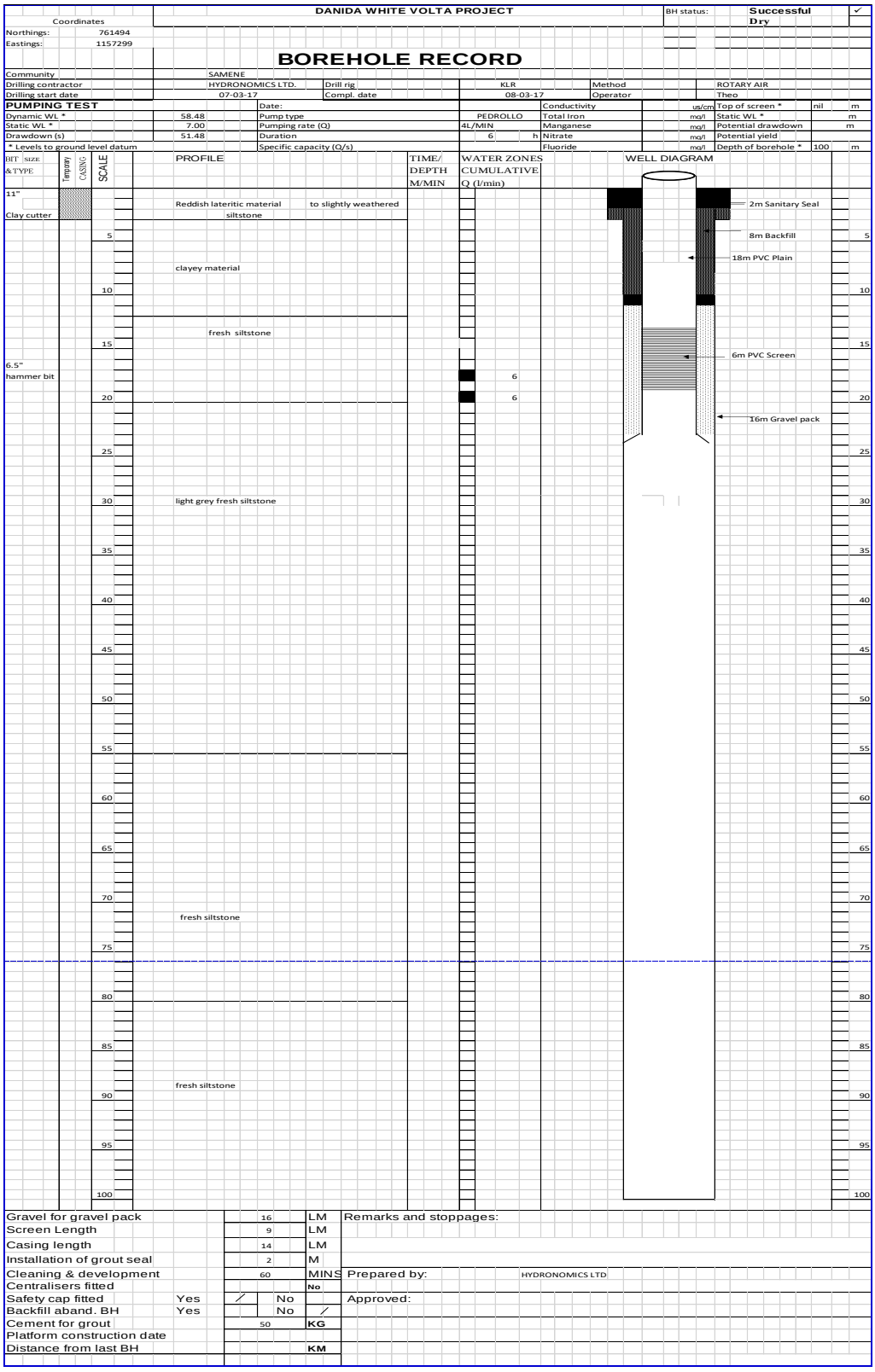

DANIDA WHITE VOLTA PROJECT

BH status: Successful ✓ Dry

Coordinates
Northings: 761494
Eastings: 1157299

BOREHOLE RECORD

Community	SAMENE						
Drilling contractor	HYDRONOMICS LTD.	Drill rig	KLR	Method	ROTARY AIR		
Drilling start date	07-03-17	Compl. date	08-03-17	Operator	Theo		

PUMPING TEST								
Dynamic WL *	58.48	Date:		Conductivity		us/cm	Top of screen *	nil m
Static WL *	7.00	Pump type	PEDROLLO	Total Iron		mg/l	Static WL *	m
Drawdown (s)	51.48	Pumping rate (Q)	4L/MIN	Manganese		mg/l	Potential drawdown	m
* Levels to ground level datum		Duration	6 h	Nitrate		mg/l	Potential yield	
		Specific capacity (Q/s)		Fluoride		mg/l	Depth of borehole *	100 m

BIT SIZE & TYPE	Temporary CASING	SCALE	PROFILE	TIME/ DEPTH M/MIN	WATER ZONES CUMULATIVE Q (l/min)
11" Clay cutter		0	Reddish lateritic material to slightly weathered siltstone		
		5			
		10	clayey material		
		15	fresh siltstone		
6.5" hammer bit					6
		20			6
		25			
		30	light grey fresh siltstone		
		35			
		40			
		45			
		50			
		55			
		60			
		65			
		70			
		75	fresh siltstone		
		80			
		85			
		90	fresh siltstone		
		95			
		100			

WELL DIAGRAM

2m Sanitary Seal
8m Backfill
18m PVC Plain
6m PVC Screen
16m Gravel pack

Gravel for gravel pack		16	LM	Remarks and stoppages:	
Screen Length		9	LM		
Casing length		14	LM		
Installation of grout seal		2	M		
Cleaning & development		60	MINS	Prepared by:	HYDRONOMICS LTD
Centralisers fitted			No		
Safety cap fitted	Yes ✓	No		Approved:	
Backfill aband. BH	Yes	No ✓			
Cement for grout		50	KG		
Platform construction date					
Distance from last BH			KM		

10. DWVP10

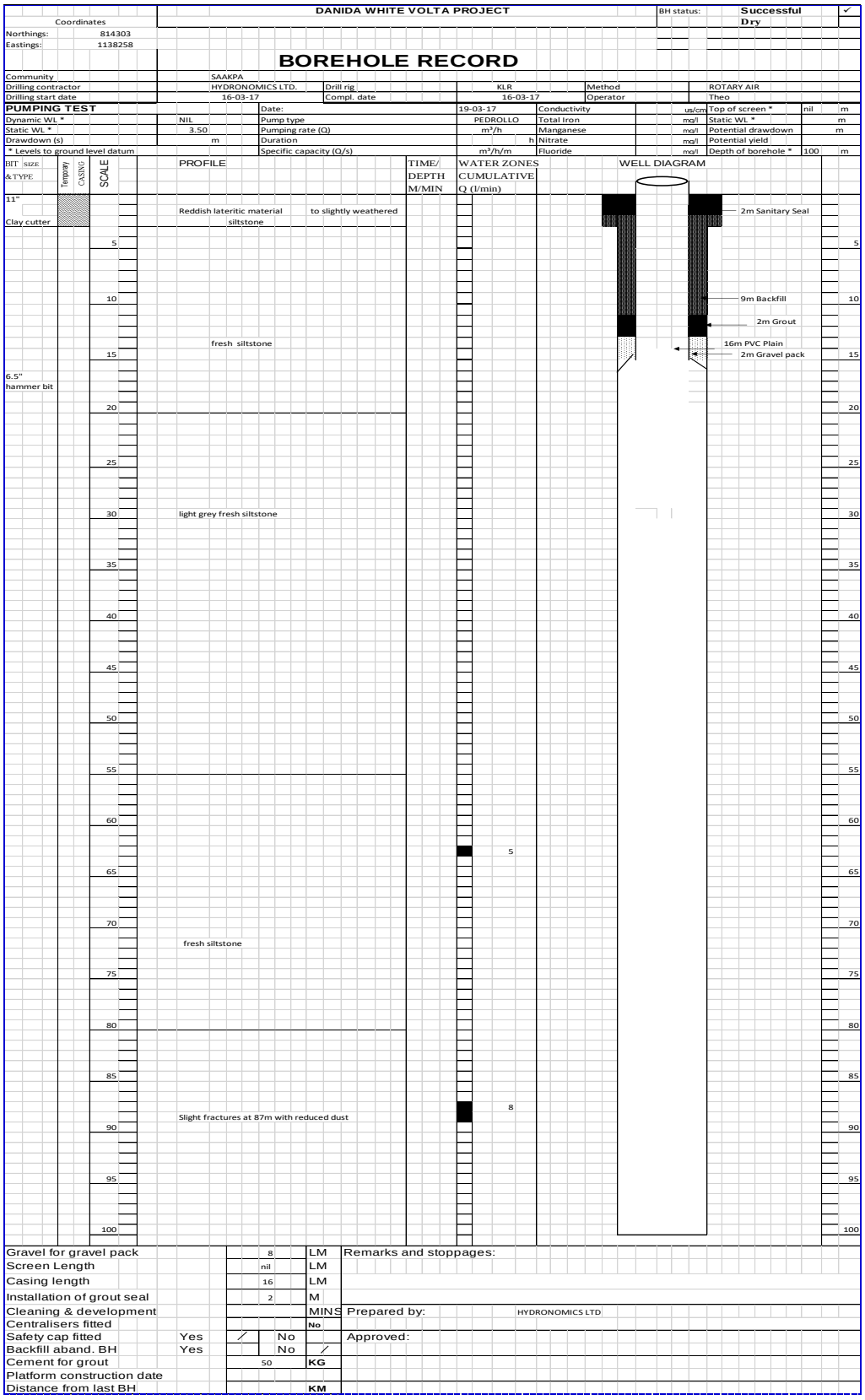

DANIDA WHITE VOLTA PROJECT

BH status: Successful ✓ Dry

Coordinates
Northings: 814303
Eastings: 1138258

BOREHOLE RECORD

Community	SAAKPA						
Drilling contractor	HYDRONOMICS LTD.	Drill rig	KLR	Method		ROTARY AIR	
Drilling start date	16-03-17	Compl. date	16-03-17	Operator		Theo	

PUMPING TEST		Date:	19-03-17	Conductivity	us/cm	Top of screen *	nil m
Dynamic WL *	NIL	Pump type	PEDROLLO	Total Iron	mg/l	Static WL *	m
Static WL *	3.50	Pumping rate (Q)	m^3/h	Manganese	mg/l	Potential drawdown	m
Drawdown (s)	m	Duration	h	Nitrate	mg/l	Potential yield	
* Levels to ground level datum		Specific capacity (Q/s)	$m^3/h/m$	Fluoride	mg/l	Depth of borehole *	100 m

BIT SIZE & TYPE	Temporary CASING	SCALE	PROFILE	TIME/ DEPTH M/MIN	WATER ZONES CUMULATIVE Q (l/min)
11" Clay cutter		0	Reddish lateritic material to slightly weathered siltstone		
		5			
		10			
		15	fresh siltstone		
6.5" hammer bit		20			
		25			
		30	light grey fresh siltstone		
		35			
		40			
		45			
		50			
		55			
		60			5
		65			
		70	fresh siltstone		
		75			
		80			
		85			8
		90	Slight fractures at 87m with reduced dust		
		95			
		100			

WELL DIAGRAM: 2m Sanitary Seal; 9m Backfill; 2m Grout; 16m PVC Plain; 2m Gravel pack

Gravel for gravel pack	8	LM	Remarks and stoppages:
Screen Length	nil	LM	
Casing length	16	LM	
Installation of grout seal	2	M	
Cleaning & development		MINS	Prepared by: HYDRONOMICS LTD
Centralisers fitted		No	
Safety cap fitted	Yes ✓	No	Approved:
Backfill aband. BH	Yes	No ✓	
Cement for grout	50	KG	
Platform construction date			
Distance from last BH		KM	

APPENDIX 5A- ERT-PROFILES COMPARED TO WIRELINE LOGS FOR DWVP BOREHOLES

COMPARISON OF RESISTIVITIES ON ERT-PROFILES AT DWVP DRILLING POINTS WITH WIRELINE RESISTIVITY LOGS

ERT-profile at DWVP borewell Resistivity order: Blue<Green<Red<Purple	ERT resistivities (Ωm) at drilling point	Wireline resistivity at drill-point (Ωm)	Conclusion on comparison
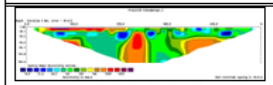 **DWVP 01** Tamboku (Dabgriboari) at st.420 – ERT-profile length 800 m from southwest towards northeast. – Geology: Panabako formation–Drilling depth: 150m - Pumping test: 22 lpm/65.8m/6h.	Suggested and drilled at st.420 being a resistivity-low anomaly (<60 Ωm) to depth of 40m followed by 100- 142 Ωm.	0-15m/ 300-40 15-26m/ 20 to 200 26-40m/ 100 to 200 40-50m/ 20 to 150 50-70m/ 100 to 400 70-80m/ 10 to 100 80-96m/ 100 to 300 96-104m/ 25 to 100 104-115m/ 100 to 150 115-140m/ 50 to 100	Relative bad fit - Example, the upper 50 m having varied but an average of 100 Ωm, the next 50 m around 200 Ωm then having around 100 Ωm to 200 m.
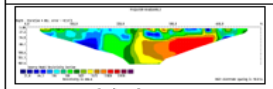 **DWVP 02** Tamboku River at st.410 – ERT-profile length 800 m from southwest towards northeast. – Geology: Panabako formation – Drilling depth: 100m – Pumping test: 132 lpm/5.8m/6h.	Suggested at st.230 being a resistivity-low anomaly (<64 Ωm) to great depth. Changed to st.410 due to difficult accessibility at st.230, but still being a resistivity-low anomaly (<64 Ωm) but only to 55m depth followed by very high resistivity >5000 Ωm.	0-8m/ 700-40 8-14m/ 1000 14-42m/ 40 to 60 42-83m/100 to 300 83-92m/ 20-70	Relatively good fit – Example, the 25 m low resistivity layer and the underlying high-resistivity layer verified by Res-log, but the high resistivity is exaggerated. The ERT indicates the low-resist layer is dipping towards southwest.
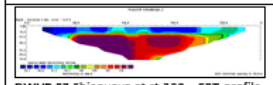 **DWVP 03** Shienvya at st.280 – ERT-profile length 400 m from southwest towards northeast. – Geology: Bimbila old – Drilling depth: 100m – Nearly dry!	Suggested and drilled at st.280 without being a resistivity-low anomaly because resistivity is generally low (<40 Ωm) to 15m followed by about 500 Ωm.	0-7m/ 20-7 7-20m/ 20-100 20-39m/ 20-30 39-88m/ 15-20 88-100m/ 20-45	Generally bad fit - ERT provides far too high resistivity in the Regolith as well as in the host rock, Bimbila old.
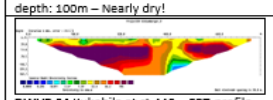 **DWVP 04** Kukobila at st.440 – ERT-profile length 800 m. – Geology: Bimbila young – Drilling depth: 100m - Pumping test: 12 lpm/81.3m/6h.	Suggested and drilled at st.440 being a Resistivity-low anomaly (<20 Ωm) and further decreasing below 80m towards 10 Ωm.	0-13m/ 4-20 13-25m/ 70-200 25-70m/ 15-30 70-86m/ 30 86-92m/ 12 >92m/ 25	Generally bad fit – ERT provides too high resistivities and does not reflect the vertical variation seen on the Res-log.
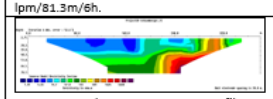 **DWVP 05** Kpobu at st. 200 – ERT-profile length 400 m. – Geology: Bimbila middle – Drilling depth: 100m - Pumping test: 13 lpm/28.5m/6h.	Suggested and drilled at st.200 being a relative resistivity-high anomaly (50 Ωm) to 40m depth followed by increase to 150 Ωm.	0-21m/ 6-12 21-36m/ 20-22 36-90m/ 16	Generally bad fit – ERT provides too high resistivities and does not reflect the vertical variation seen on the Res-log.
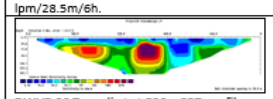 **DWVP 06** Tanveli at st.520 – ERT-profile length 800 m. – Geology: Bimbila young – Drilling depth: 100m - Dry!	Suggested and drilled at st. 520 being a resistivity-low anomaly (25 Ωm) to 80m depth followed by slight increase to 35 Ωm.	0-10m/ 6-30 10-40m/ 40-60 40-92m/ 20-70	Generally bad fit – ERT provides too low resistivities and does not reflect the vertical variation seen on the Res-log.

ERT-profile at DWVP borewell Resistivity order: Blue<Green<Red<Purple	ERT resistivities (Ωm) at drilling point	Wireline resistivity at drill-point (Ωm)	Conclusion on comparison
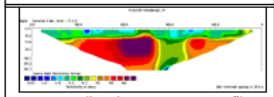 **DWVP 07** Salinwei at st.300 – ERT-profile length 800 m. – Geology: Bimbila middle – Drilling depth: 75m - Pumping test: 80 lpm/45.9m/6h.	Suggested at st. 460 being a significant resistivity-low anomaly with less than 20 Ωm to 40 m depth followed by resistivity of 50 Ωm to greater depth. Drilling changed to st. 300 due to terrain evaluation, and characterized by a resistivity-low anomaly (<10 Ωm) to 20m, however underlain by surprisingly high resistivity (>800 Ωm) at 50m depth.	0-11m/ 7-20 11-70m/ 20-22	Generally bad fit – ERT provides too thick top layer with low resistivity, and far too high resistivity in the underlying host rock. It does not reflect the vertical variation seen on the Res-log.
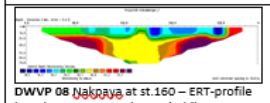 **DWVP 08** Nakpaya at st.160 – ERT-profile length 400 m. – Geology: Bimbila young – Drilling depth: 100m - Dry!	Suggested and drilled at st. 160 being a resistivity-low anomaly (<20 Ωm) to 15m depth followed by an increase to 40 Ωm.	0-10m/ 6-15 10-32m/ 22-100 32-67m/ 10-20 67-96m/ 15-60	Fairly good fit for the uppermost low-resistivity layer, but ERT does not reflect the vertical variation further below by showing only an average value of 40 Ωm which seems quite realistic.
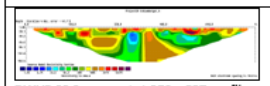 **DWVP 09** Samene at st.370 – ERT-profile length 800 m. – Geology: Panabako – Drilling depth: 95m - Pumping test: 4 lpm/47.5m/6h.	Suggested and drilled at st. 370 being a resistivity-low anomaly (<20 Ωm) from 20m depth to 60m followed by resistivity of about 80 Ωm to greater depth, but covered by a 20 m thick high-resistivity top-layer (>3500 Ωm).	0-5m/ 600-1000 5-16m/ 100-250 16-38m/ 60-100	Generally bad fit – ERT provides too thick top layer with high resistivity, and far too low resistivity in the underlying host rock. It does not reflect the vertical variation on the Res-log to 38m depth.
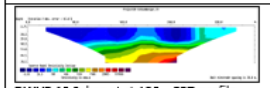 **DWVP 10** Sakpa at st.120 – ERT-profile length 400 m. – Geology: Bimbila old – Drilling depth: 100m - Nearly dry!	Suggested and drilled at st. 120 without being a resistivity-low anomaly because resistivity is generally low (<30 Ωm) to 30m depth along most of the profile followed by surprisingly high resistivity (>500 Ωm) at greater depth.	0-12m/ 12-20 12-28m/ 20-30 28-71m/ 15-20 71-84m/ 20 84-92m/ 20-50	Relatively good fit for the uppermost 30 m, but ERT provides far too high resistivity in the underlying host rock.

APPENDIX 5B- ERT-PROFILES COMPARED TO WIRELINE LOGS FOR DWVP BOREHOLES

COMPARISON OF RESISTIVITIES ON ERT-PROFILES AT OTHER DRILLING POINTS WITH WIRELINE RESISTIVITY LOGS

ERT-profile at HAP&WVB borewell Resistivity order: Blue<Green<Red<Purple	**ERT resistivities (Ωm) at drilling point**	**Wireline resistivity at drill-point (Ωm)**	**Conclusion on comparison**
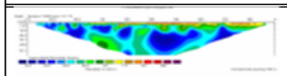 **HAP 05** Janga at st. A220 – ERT-profile length 400 m. Geology: Bimbila formation– Drilling depth: 166m - Pumping test: 5 lpm.	Suggested and drilled at st. A220 being a place with low resistivity (15-25 Ohmm) between 7m-55m after a drop from a moderate resistive regolith.	0-15m/10-30 15-19m/30-8 19-45/8-25 45-100/25-15	Relatively good fit and same resistivity range is recorded in the bedrock though the ERT does not show up to 100m depth.
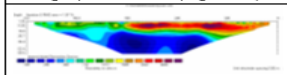 **HAP 11** Nalerigu at st. C265 – ERT-profile length 400 m. – Geology: Panabako Sandstone – Drilling depth: 141m – Pumping test: 24lpm.	Suggested and drilled at st. C265 being a low resistive zone (180-300 Ohmm) between 20-60m below the high resistive (1800-3000) upper layer. This low resistivity is interpreted as possible fracture.	0-11m/900-40 11-28m/40-1000 28-32m/1000-70 32-45m/70-4000 45-64m/4000-100 64-72m/100-150 72-100m/150-50 100-140m/50-60	Relative bad fit. Trend of resistivity corresponds because there is an upper portion with very high resistivity and a gradual decline on both ERT and wireline. However, the depths do not fit possibly because ERT depth of penetration is 60m.
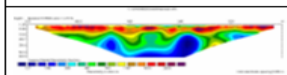 **HAP 12** Nakpeuk at st. B240 – ERT-profile length 400 m. Geology: Panabako Sandstone – Drilling depth:166m – Pumping test: 6lpm.	Suggested and drilled at st. B240 being a low resistive area ranging from 127-300 Ohmm at 20m and beyond, indicative of a weak zone within the bedrock	0-15m/2000-100 15-26m/100-20 30-40m/20-200 40-48m/200-700 48-50m/700-200 50-62m/200-500 62-68m/500-100 68-70m/100-400 80-94m/250-70 94-102m/70-200 102-136m/200-70	Fits at the upper portion and also ERT falls within the range of wireline resistivity readings. However wireline resistivity shows varying values at depth which indicates an intercalation different rocks but cannot be seen in ERT.
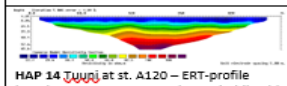 **HAP 14** Tuuni at st. A120 – ERT-profile length 400 m. From – Geology: Bimbila old – Drilling depth: 120m - Pumping test: 10 lpm	Suggested and drilled at st. A120. Generally having a top low resistive layer (22-38 Ohmm) which is typical of the place, possibly weathered material at about 12m followed by a moderate resistive bedrock (49-83 Ohmm).	0-10m/15-20 10-20m/20-40 20-30m/40-50 30-41m/50-30 41-50m/30-40 50-56m/40-50 56-70m/50-15 70-78m/50-15 78-82m/15-150 82-84m/150-15 84-86m/15-40 86-90m/40-100 90-92m/100-298 92-94m/298-60 94-100m/60-298 100-102m/298-40 102-104m/40-100 104-106m/100-40 106-108m/40-250 108-110m/250-30 110-113m/30-190 113-115m/190-40 115-116m/40-190 116-120m/190-298	Relatively good fit for the upper portion with almost uniform resistivity but erratic after 70m. Possibly intercalations with high resistivity at various sections which is contrary to what is expected of the rock types within that formation.

ERT-profile at HAP&WVB borewell Resistivity order: Blue<Green<Red<Purple	**ERT resistivities (Ωm) at drilling point**	**Wireline resistivity at drill-point (Ωm)**	**Conclusion on comparison**
WVB 11 Bugya Pala. Geology: Kodjari – Drilling depth: 56m – Pumping test: 9lpm	NA	0-7m/300-20 7-18m/20-60 28-22m/60-200 22-25m/200-100 25-32m/100-400 32-35m/400-100 35-40m/100-1000 40-41m/1000-300 41-44m/300-1000 44-48m/1000-400 48-51m/400-40	Results indicate a low resistive upper portion which is probably due to weathering then a gradual increase into the bedrock and a sudden decrease which could be fracture beyond
WVB 12 Tinguri : Geology: Bimbila young – Drilling depth: 51m - Pumping test: 120lpm	NA	0-7m/5-50 7-12m/50-25 12-17m/25-40 17-18m/40-30 18-19m/30-50 19-25m/50-25 25-30m/25-50 30-35m/50-30 35-43m/30-40 43-46m/40-20	The resistivity of the entire area fluctuates slightly with just a few variation that ranges averagely between 25-50 Ohmm. With few uniform upper portion (weathered area) varies slightly higher. A gradual variation in resistivity but limited between range of 40-20 Ohmm.

APPENDIX 6- HISTOGRAMS OF 7 PARAMETERS

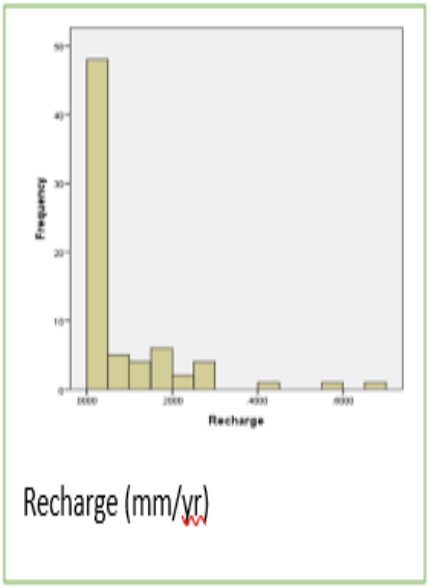

Recharge (mm/yr)

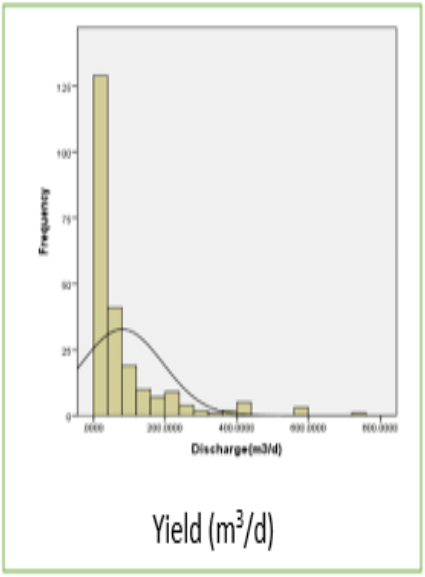

Yield (m^3/d)

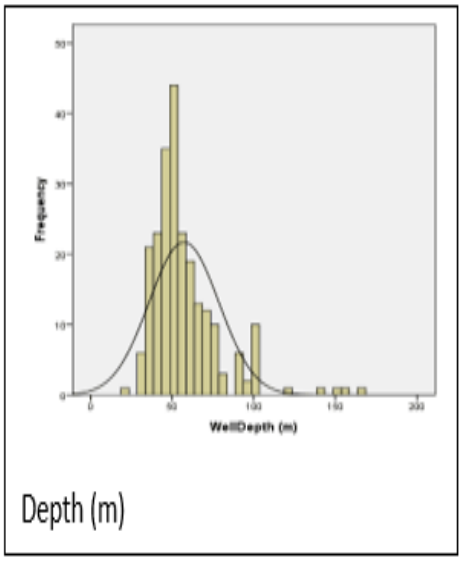

Depth (m)

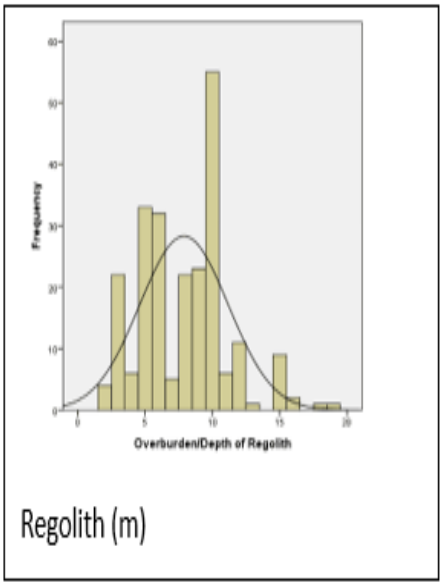

Regolith (m)

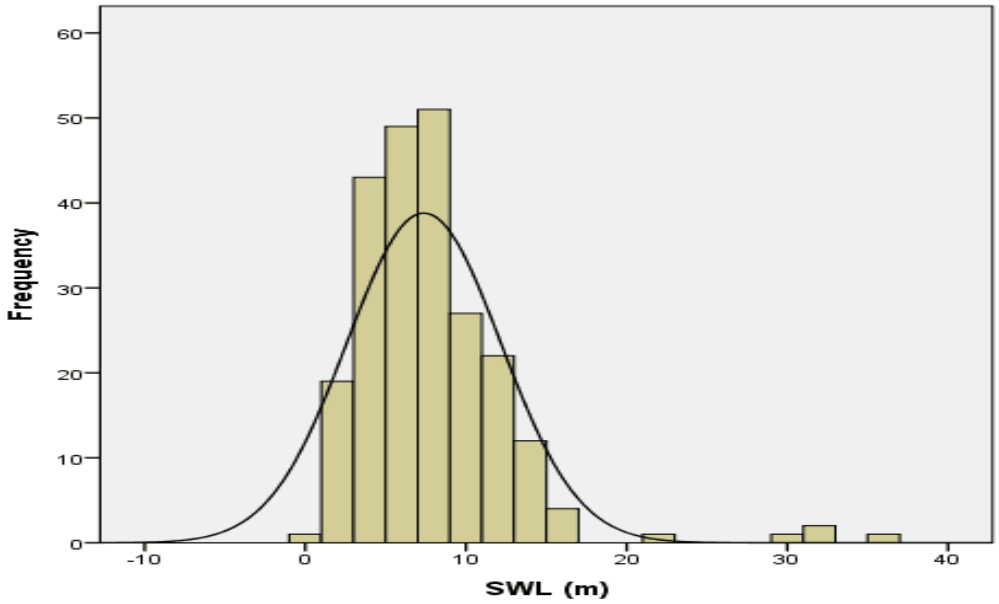

Static Water Level (m)

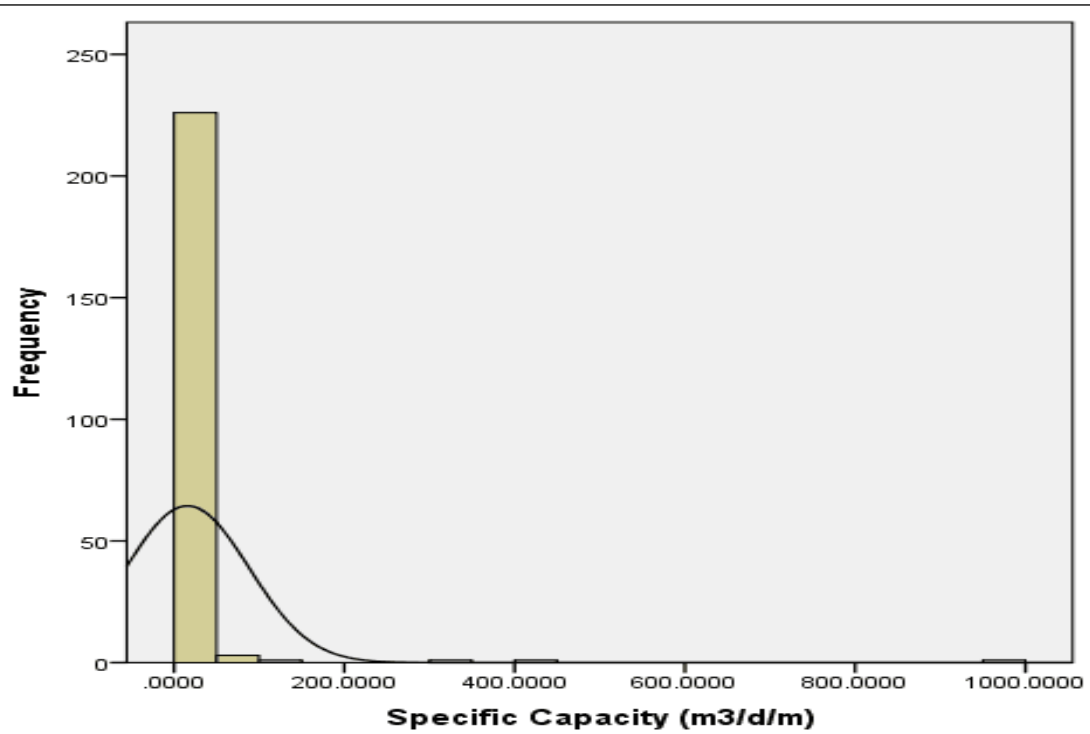

Specific Capacity ($m^3/d/m$)

APPENDIX 7- DRAWDOWN AND RECOVERY GRAPHS OF 26 PUMPING TEST RESULTS > 6 HRS

Location: Daboya No. 2

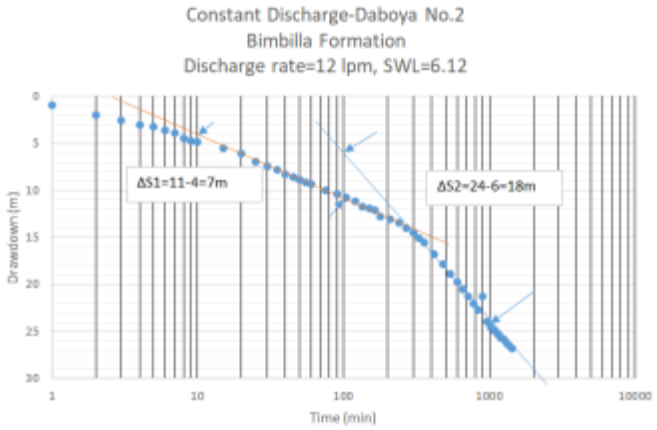

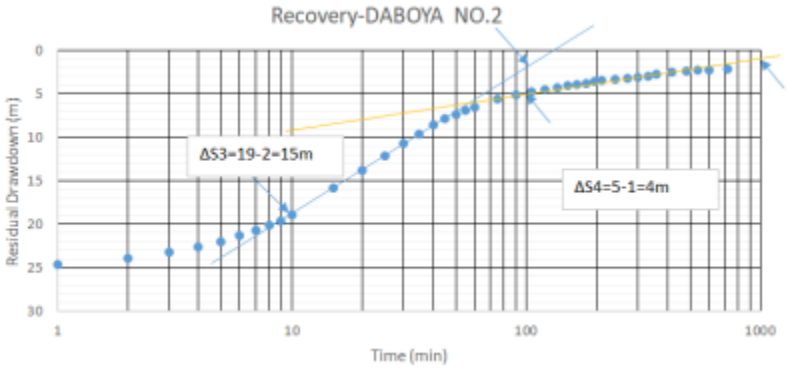

Location: Karaga 1

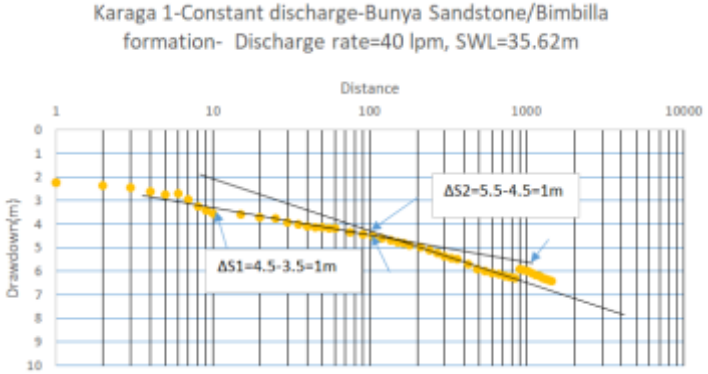

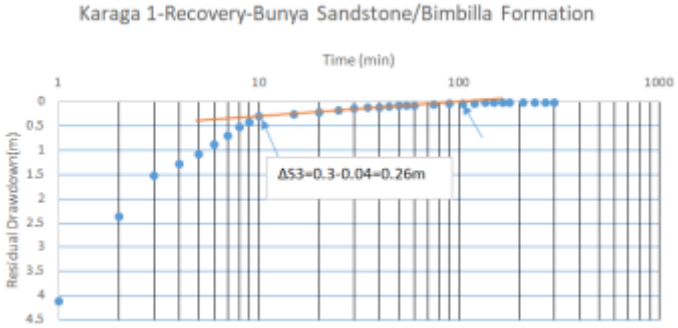

Location: Karaga 2

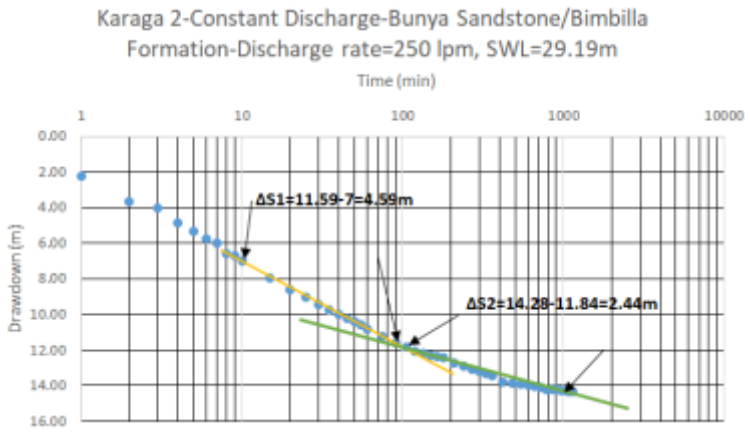

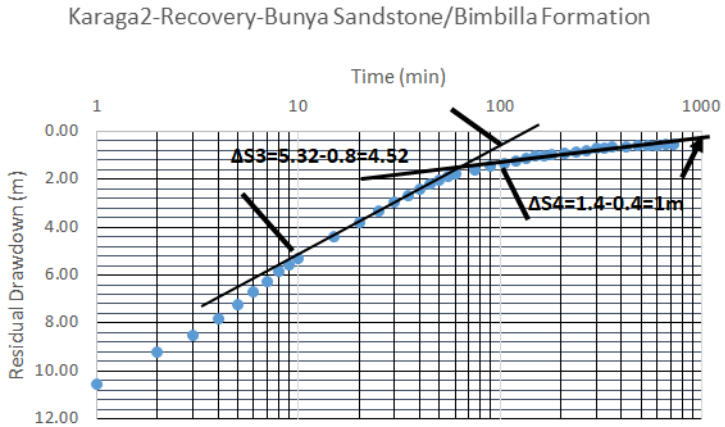

Location: Karaga 3

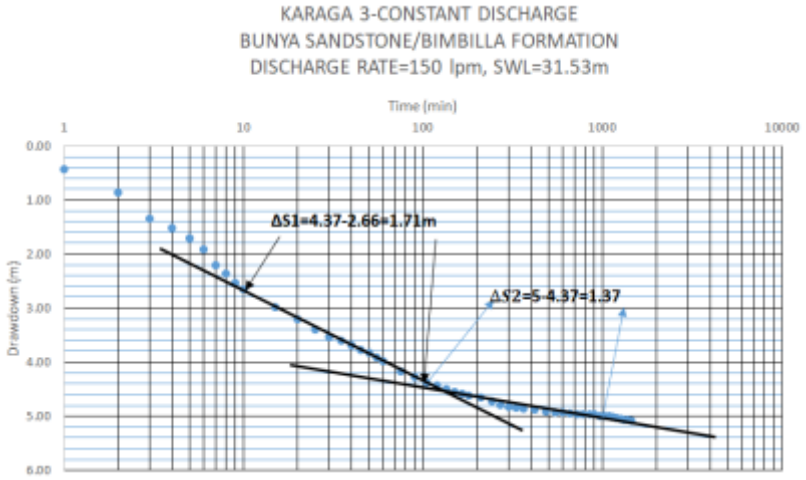

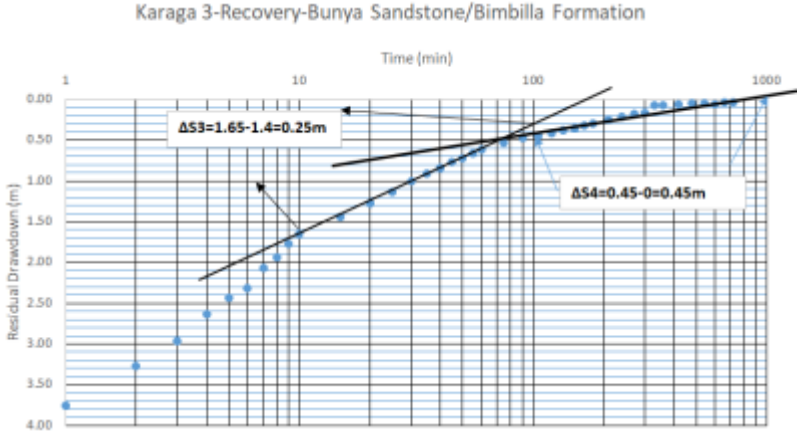

Location: Karaga 4

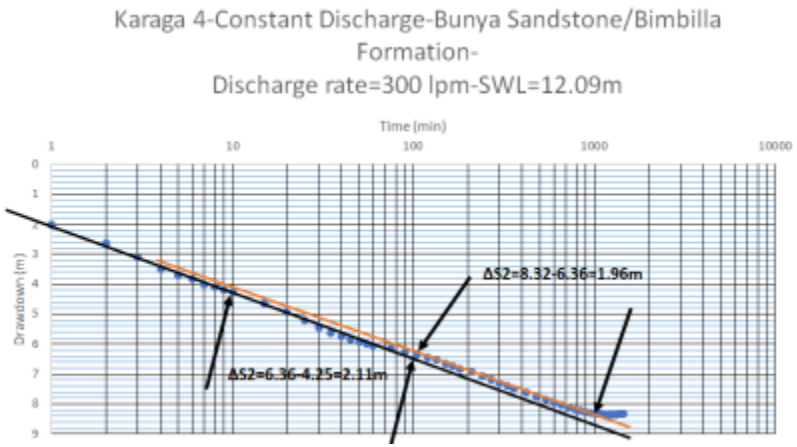

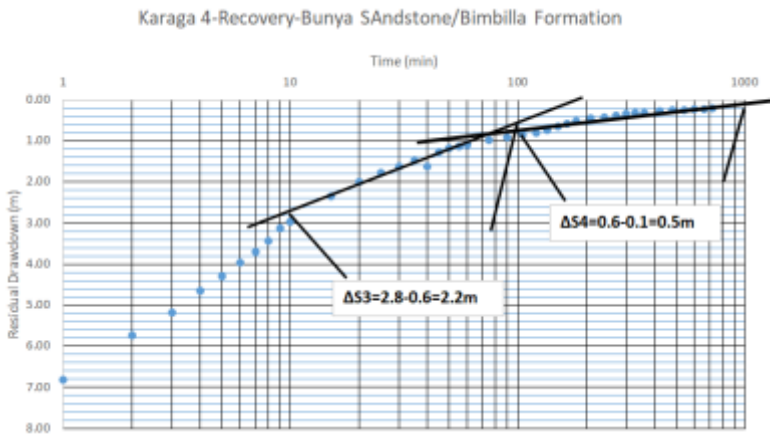

Location: Gambaga SHS 1

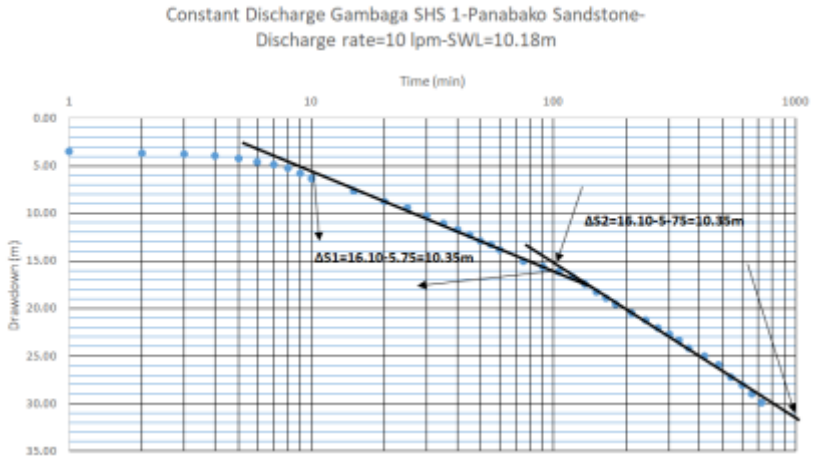

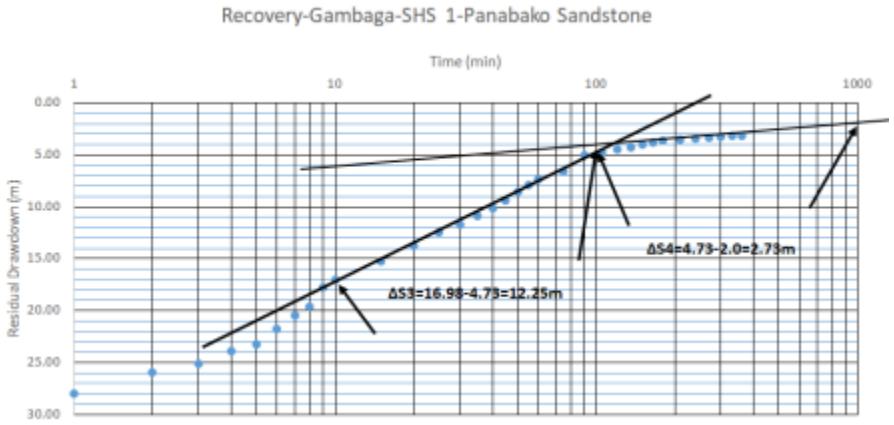

Location: Gambaga SHS 2

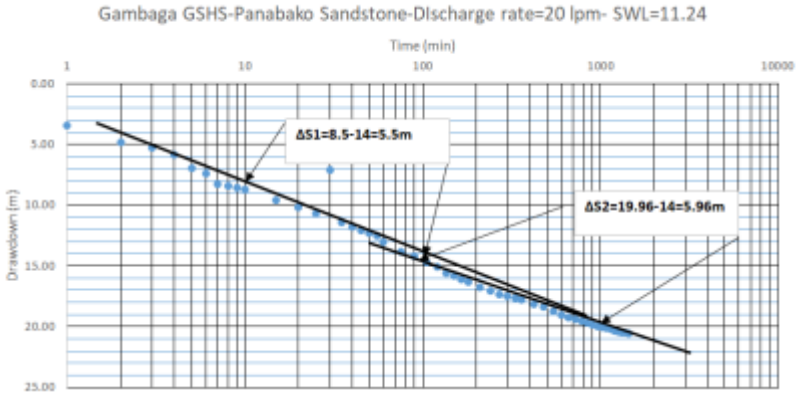

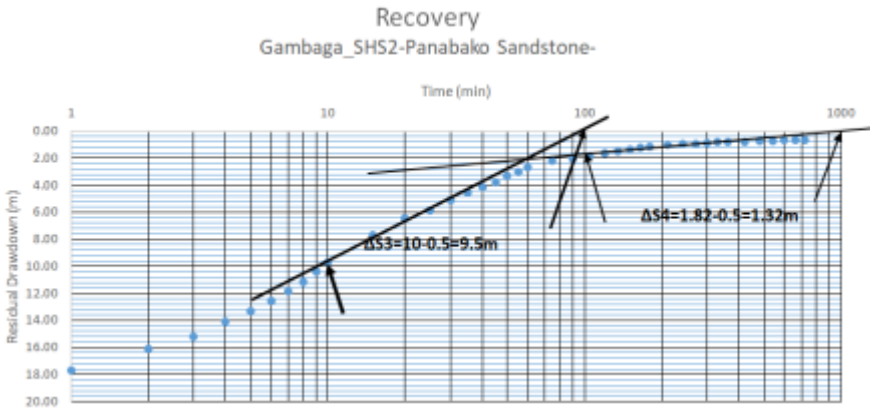

Location: Gambaga SHS 3

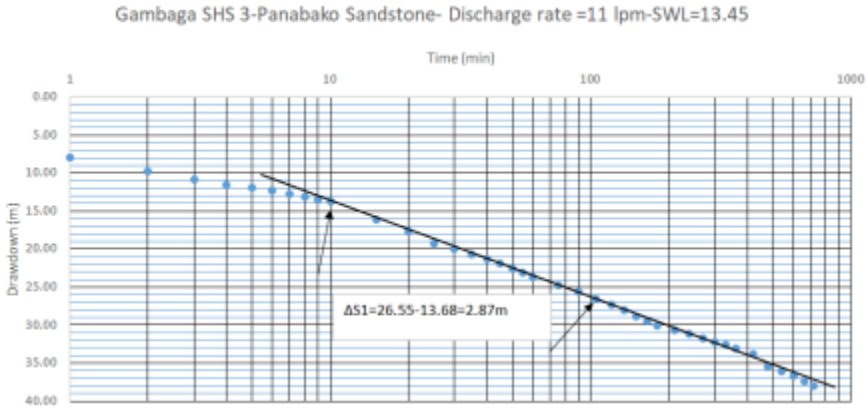

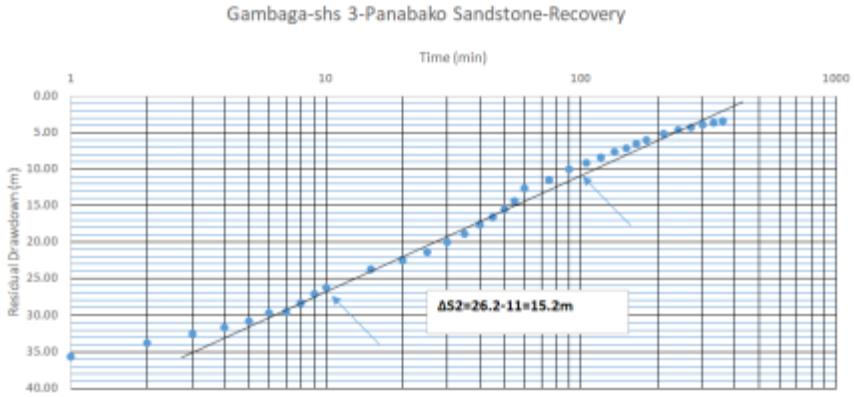

Location: Gambaga SHS 4

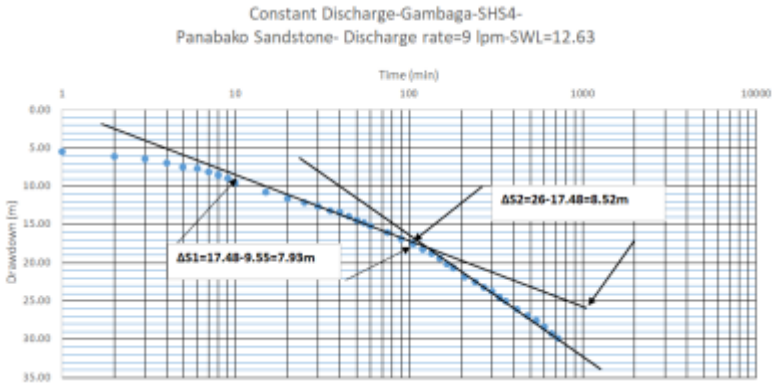

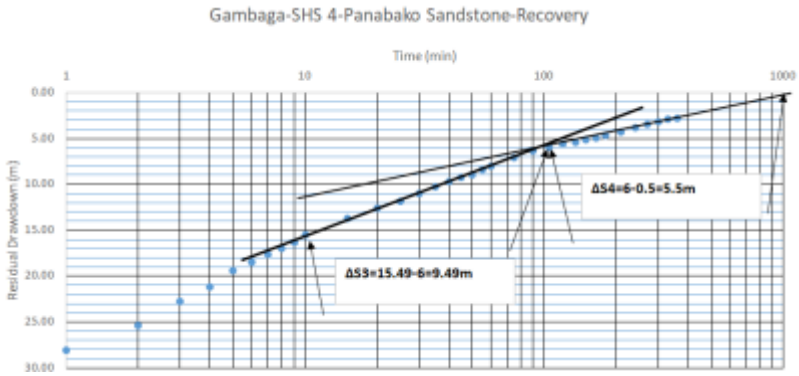

Location: Gambaga GB-01

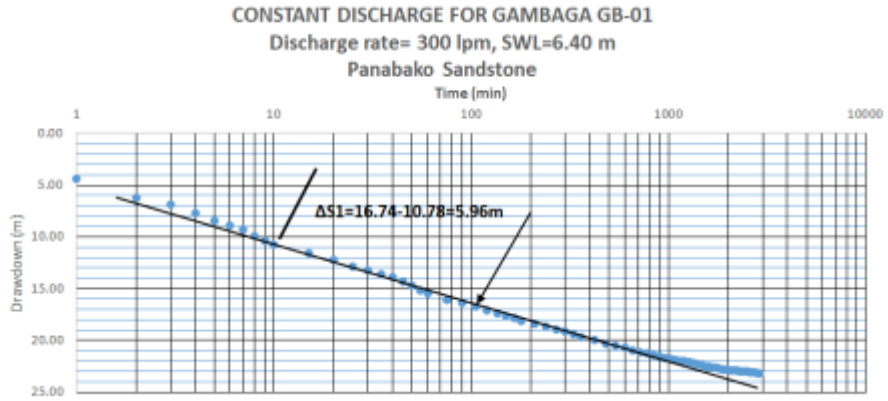

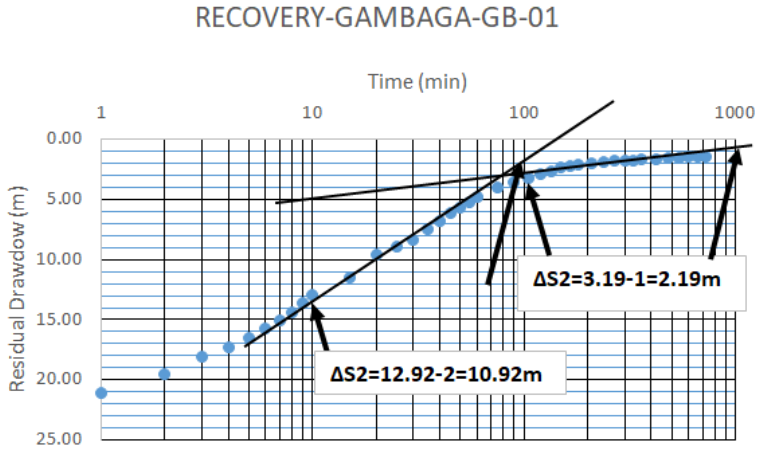

Location: Nalerigu NA-01

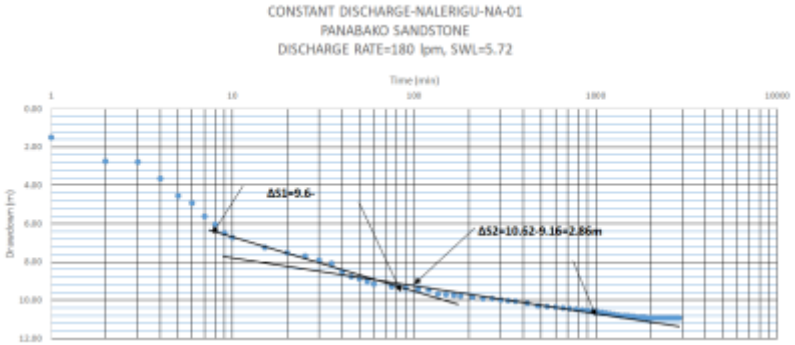

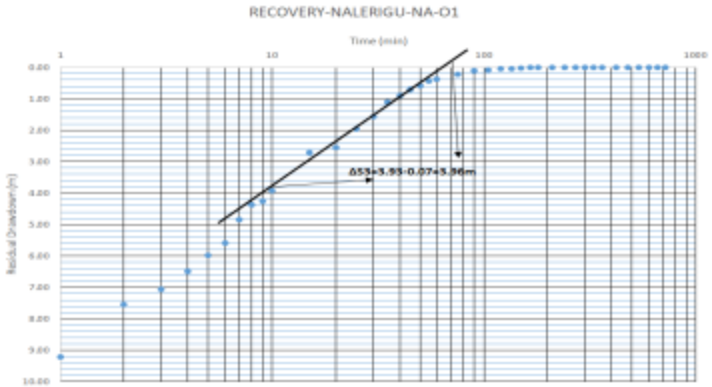

Location: Karaga Yepala

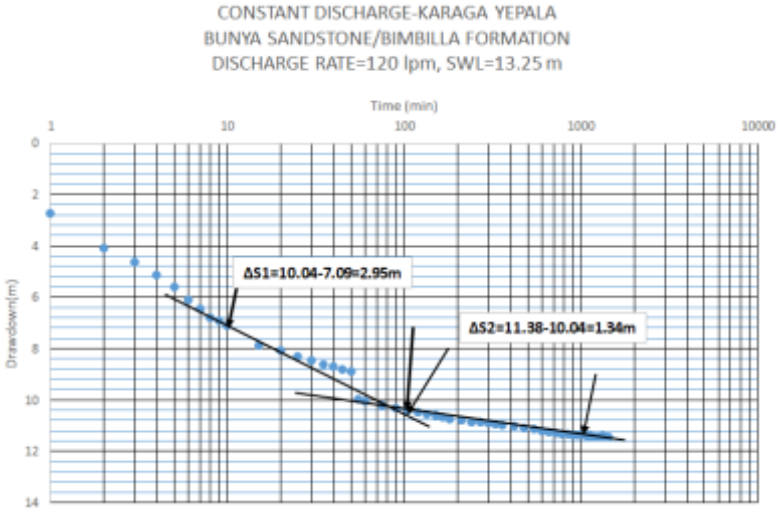

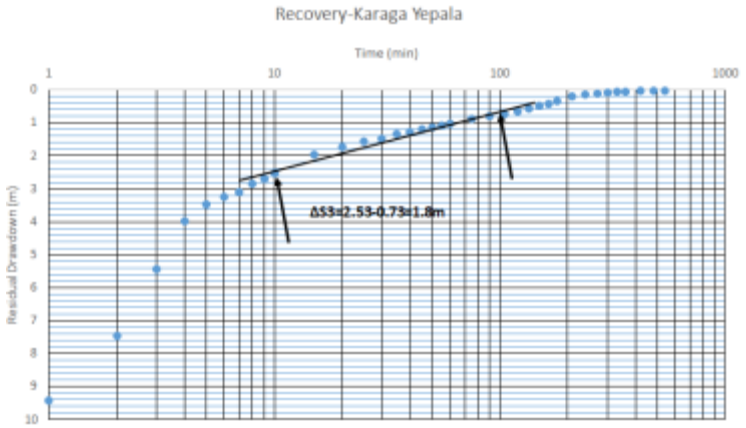

Location: Karaga

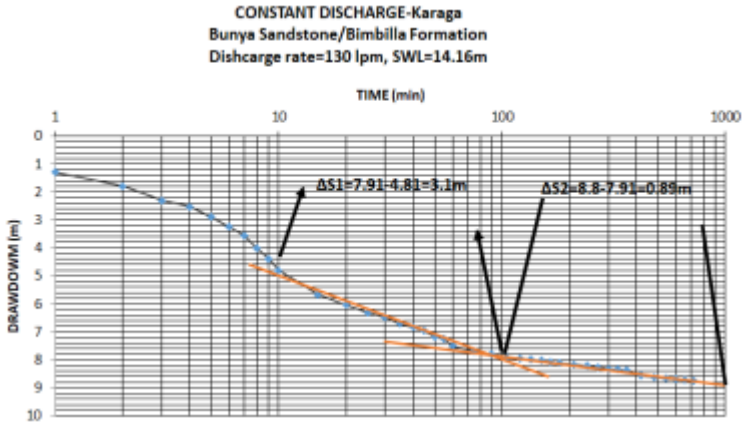

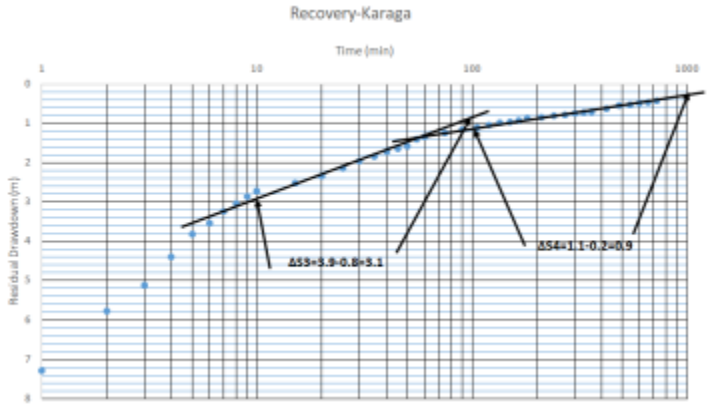

Location: Walewale-WA-05

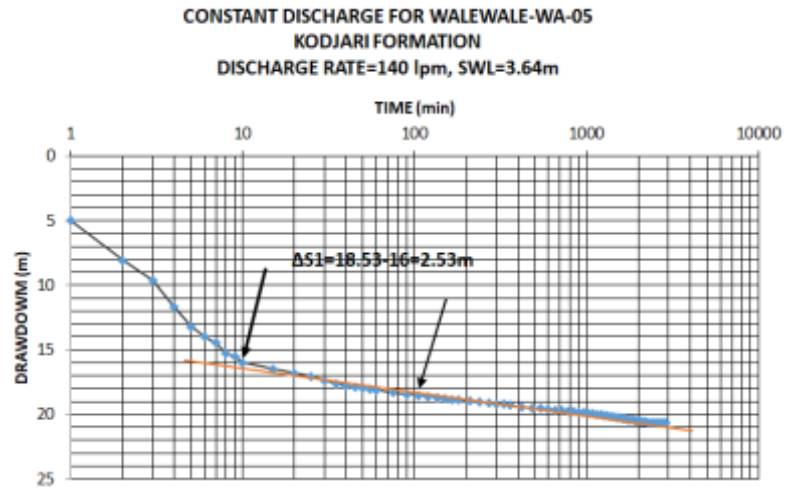

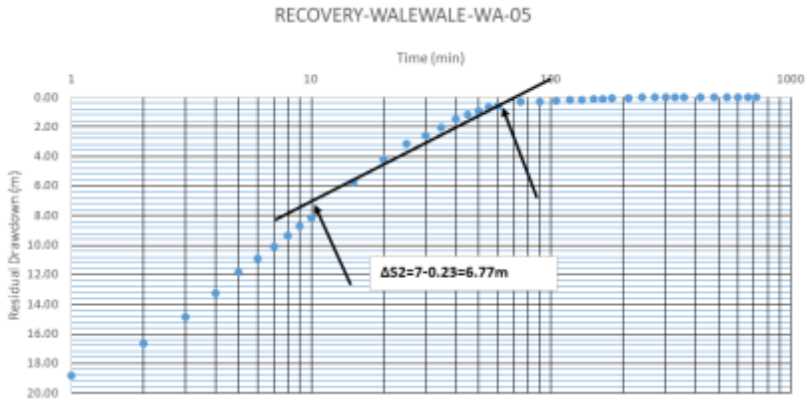

Location: Walewale-WA-01

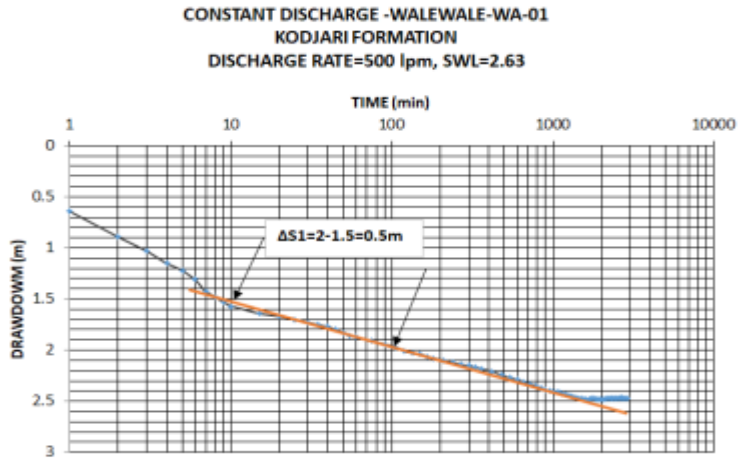

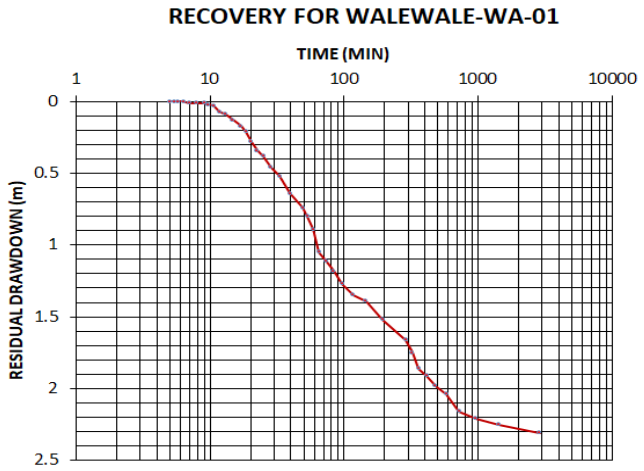

Location: Walewale-WA-02

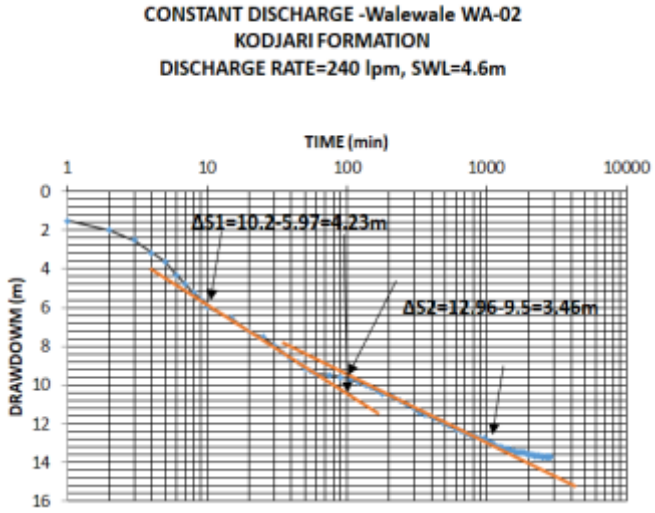

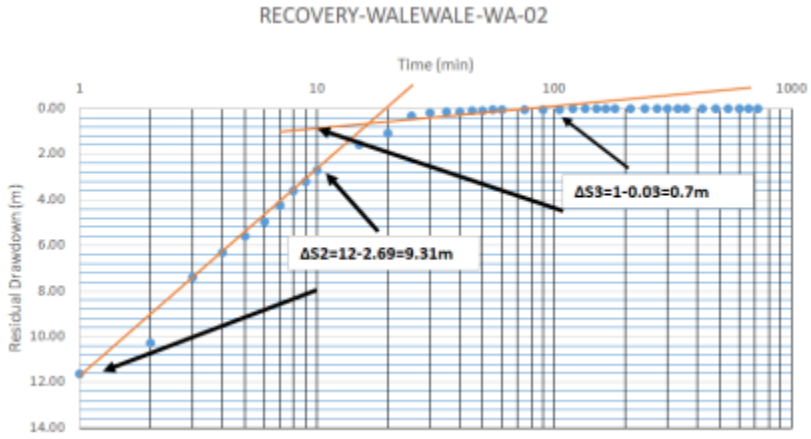

Location: Walewale-WA-03

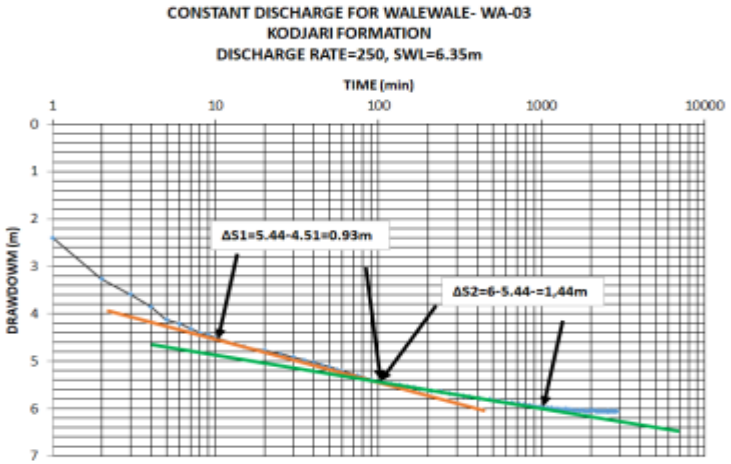

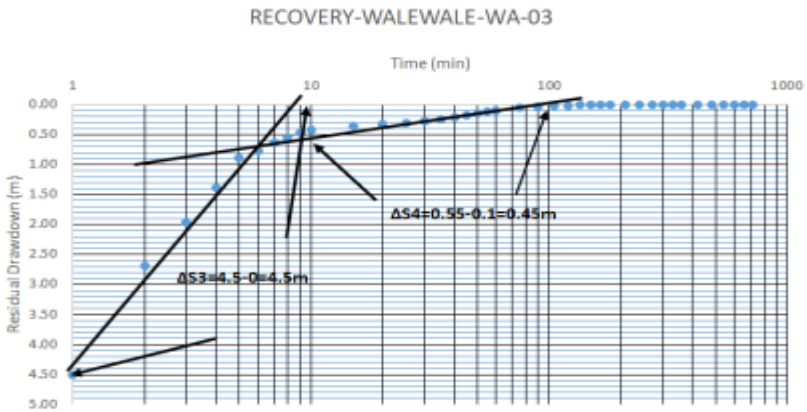

Location: Tong

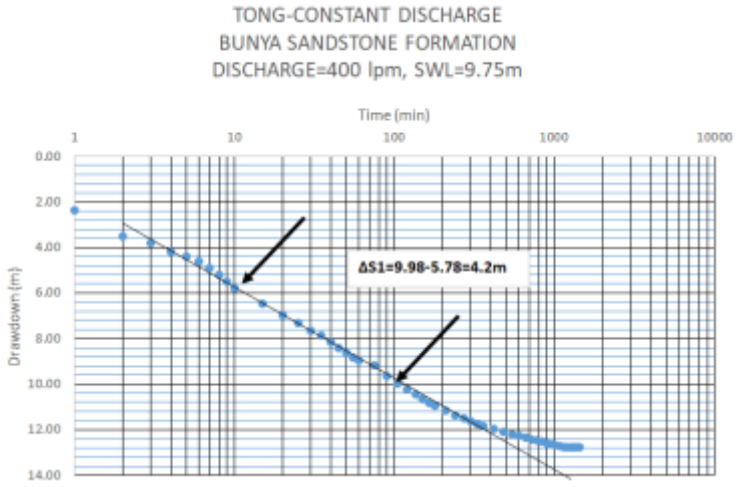

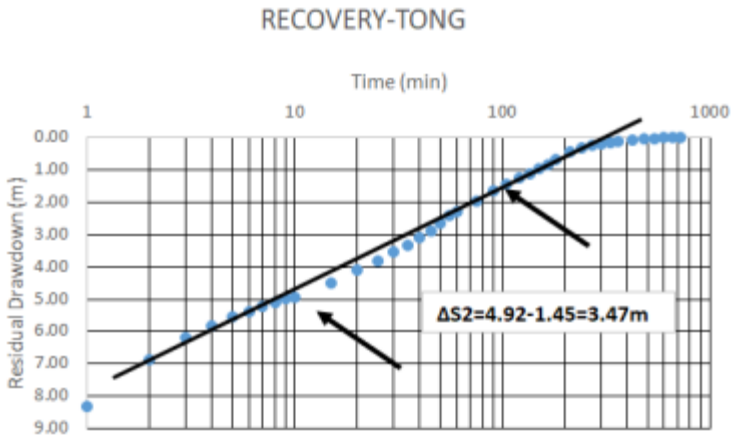

Location: DWVP 02

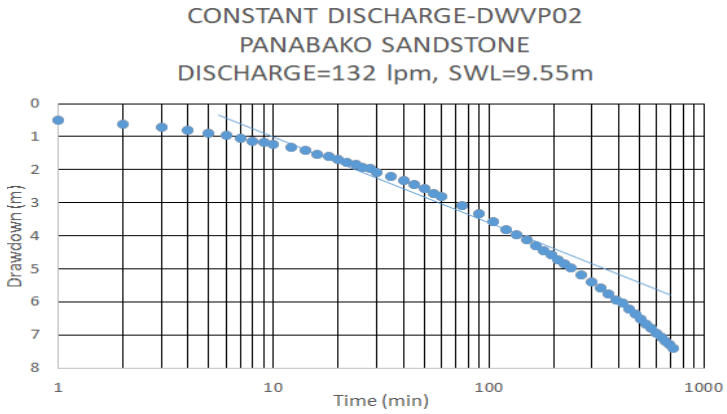

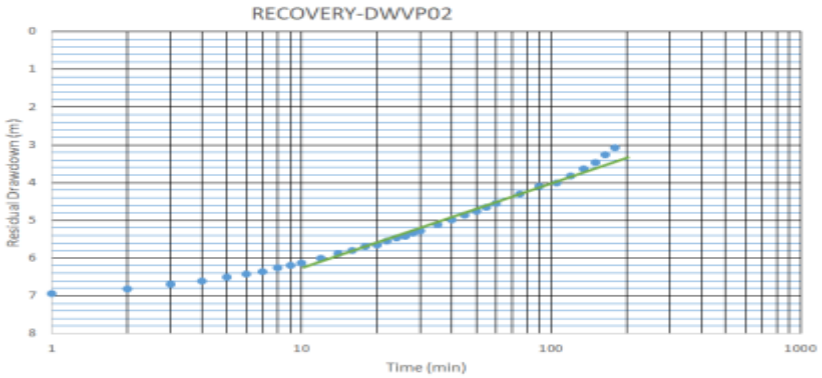

Location: Walewale – 1 – NORST

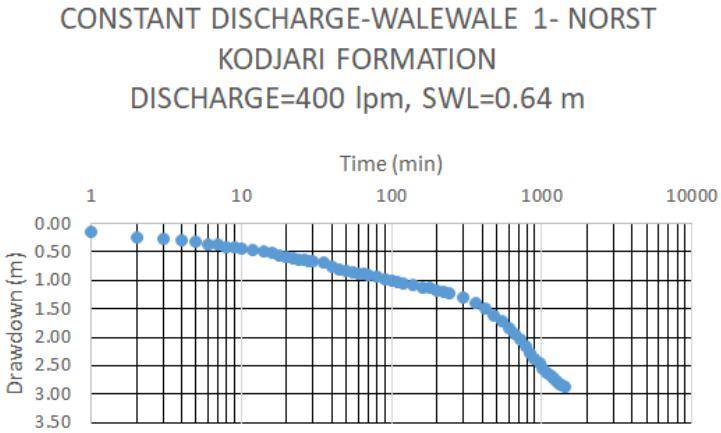

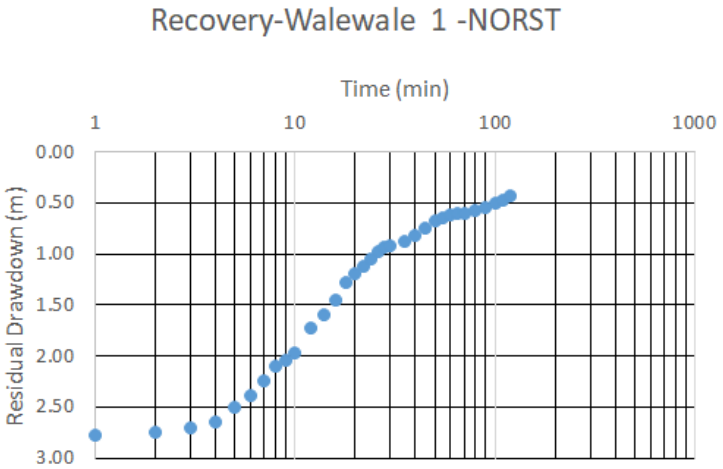

Location: Walewale – 2 – NORST

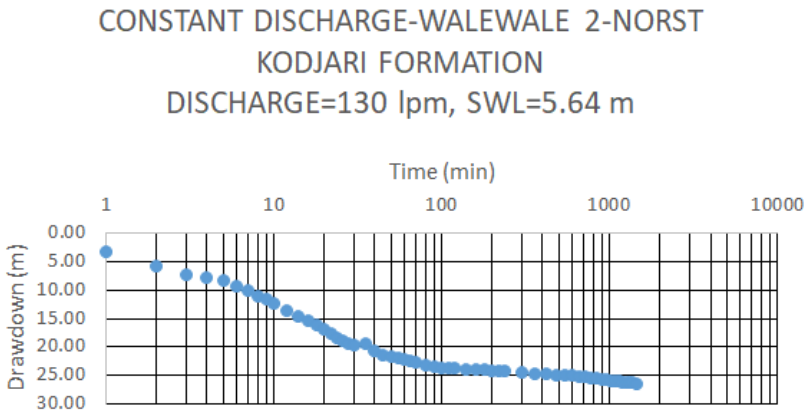

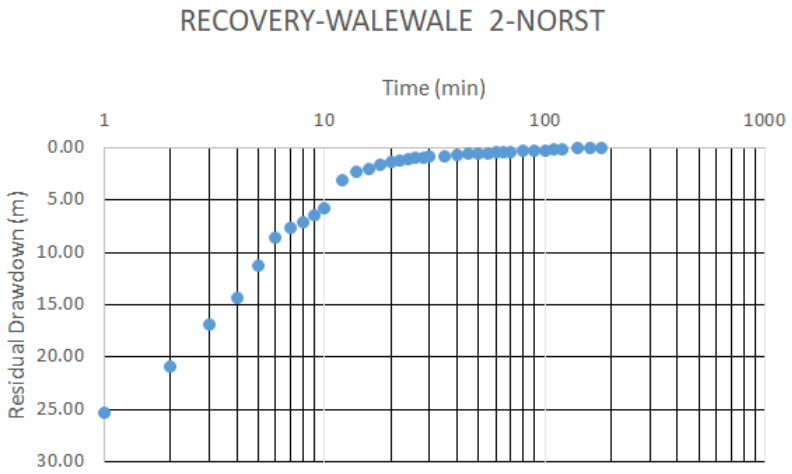

Location: Walewale – 3 – NORST

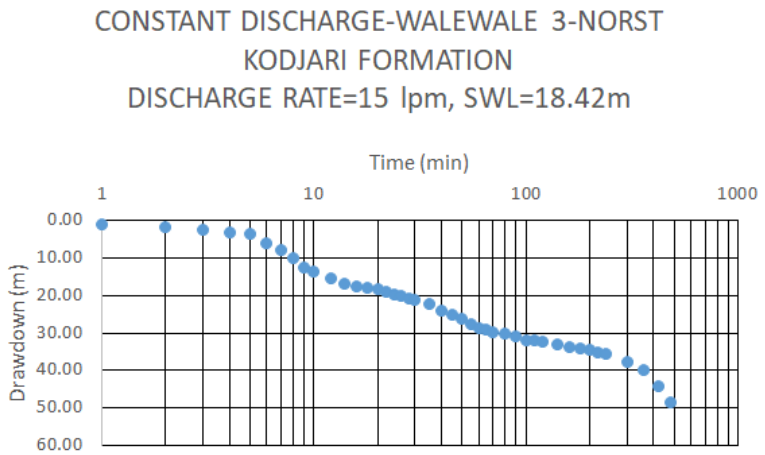

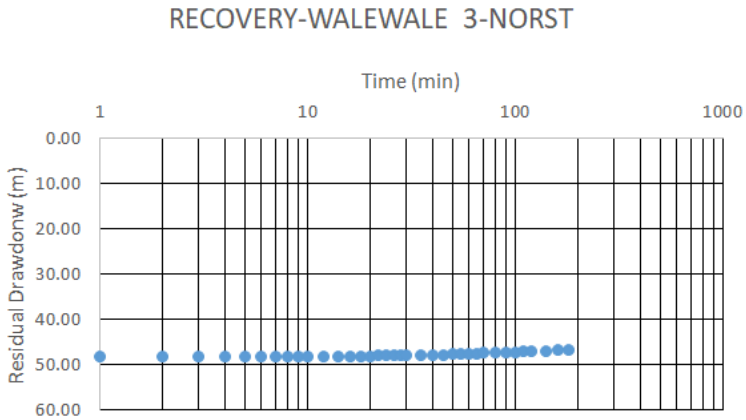

Location: Wundua 1

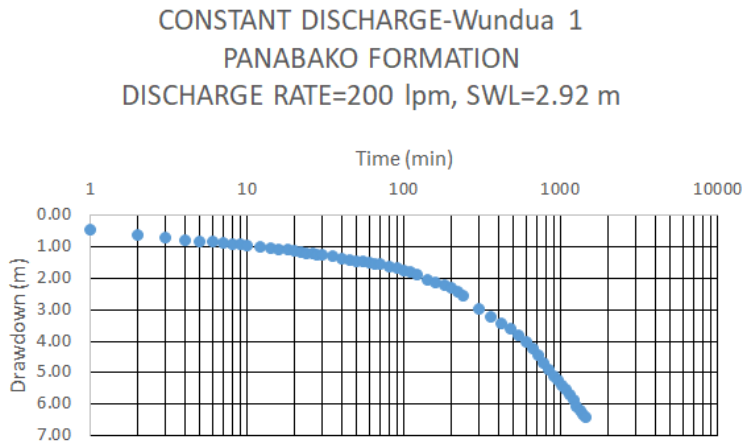

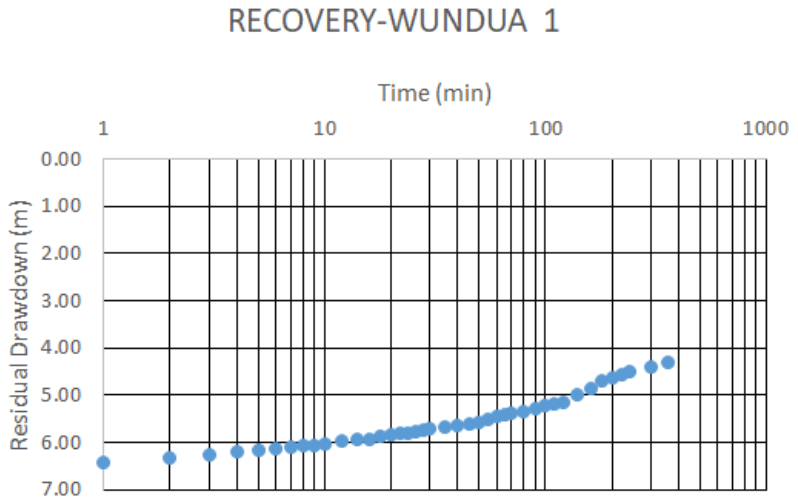

Location: Wundua 2

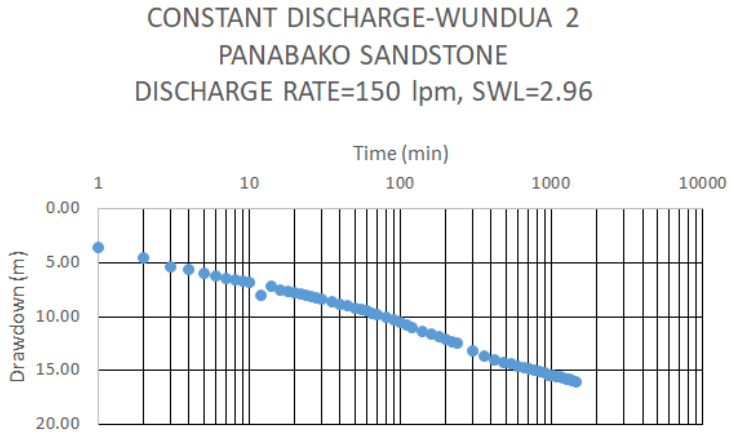

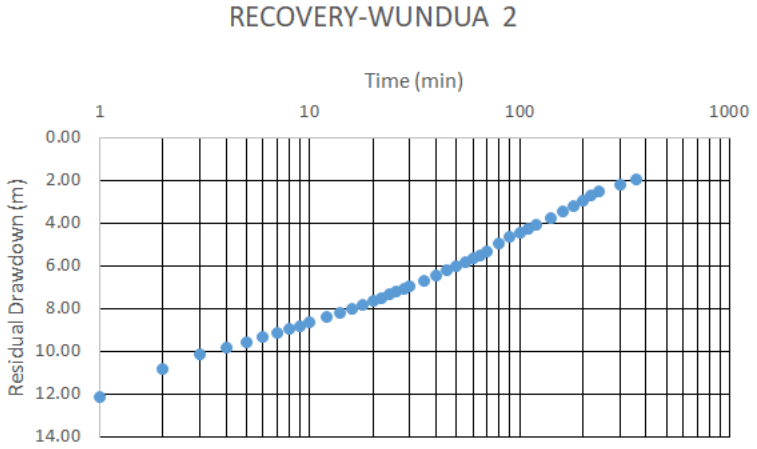

Location: Gushegu S-7

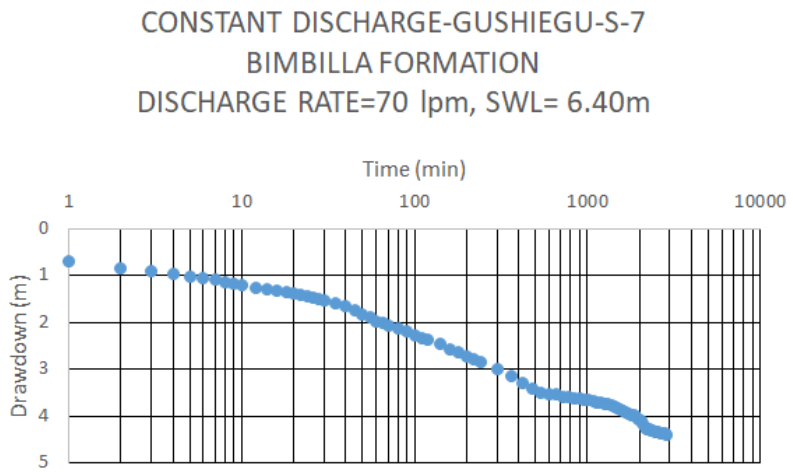

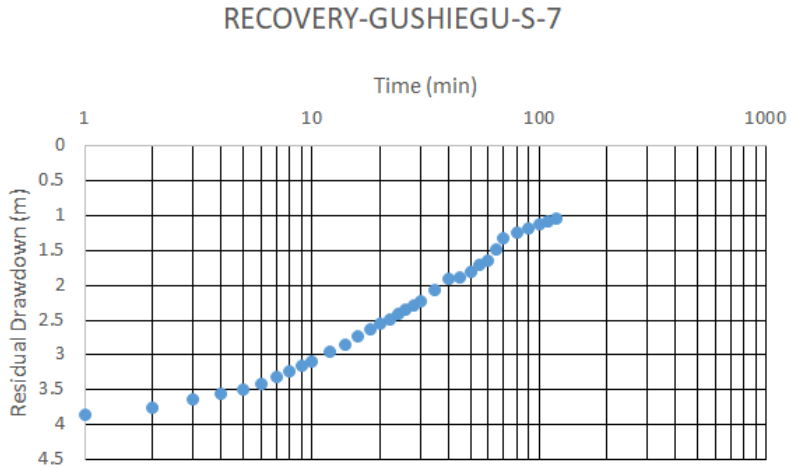

Location: Gushegu H-25-02

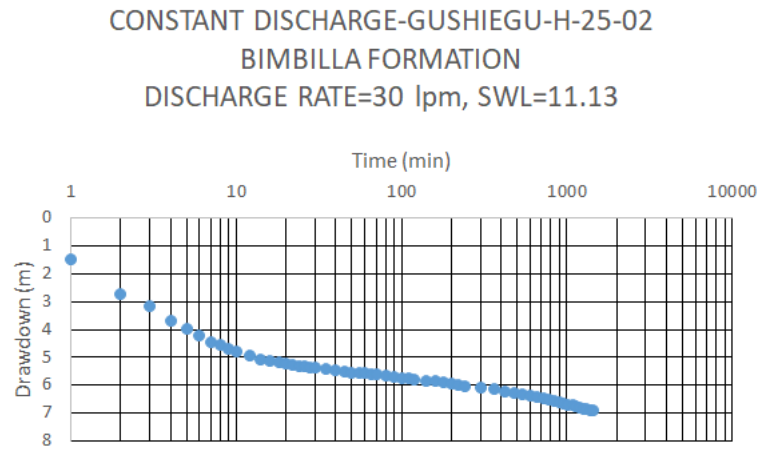

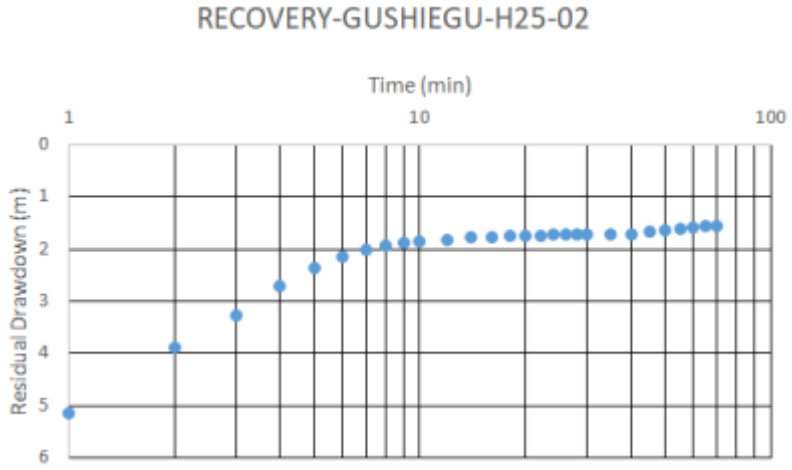

APPENDIX 8- RECHARGE ESTIMATES BASED ON CHLORIDE MASS BALANCE METHOD AT 60 BOREHOLES

ID	EASTINGS	NORTHINGS	Cl_Concentration in Groundwater (mg/L)	Cl_Concentration in precipitation (mg/L)	Precipitation (m/yr)	Recharge-Rg (m/yr)	%Rg
GW001	788676	1138932	5.06	1.31	1.1	0.285	28.50
GW003	788491	1135548	657.86	1.31	1.1	0.002	0.22
GW004	788455	1147997	8.37	1.31	1.1	0.172	17.25
GW005	787922	1148355	144.31	1.31	1.1	0.010	1.00
GW006	788320	1150174	164.14	1.31	1.1	0.009	0.88
GW007	795566	1152185	94.56	1.31	1.1	0.015	1.53
GW008	795318	1150418	2.07	1.31	1.1	0.696	69.59
GW009	789863	1158668	82.96	1.31	1.1	0.017	1.74
GW010	788681	1164391	248.28	1.31	1.1	0.006	0.58
GW011	797847	1170387	47.55	1.31	1.1	0.030	3.04
GW015	778224	1154314	37.68	1.31	1.1	0.038	3.83
GW016	780823	1159615	64.12	1.31	1.1	0.023	2.25
GW017	780054	1164851	61.28	1.31	1.1	0.024	2.35
GW018	780140	1165276	39.06	1.31	1.1	0.037	3.69
GW019	778162	1163815	33.45	1.31	1.1	0.043	4.31
GW020	773080	1158983	48.25	1.31	1.1	0.030	2.99
GW021	770662	1154159	7.95	1.31	1.1	0.182	18.16
GW022	760580	1157946	44.08	1.31	1.1	0.033	3.27
GW023	761556	1153446	7.68	1.31	1.1	0.188	18.79
GW024	766280	1151079	10.77	1.31	1.1	0.134	13.40
GW025	740625	1146125	5.12	1.31	1.1	0.282	28.20
GW026	742355	1149687	46.29	1.31	1.1	0.031	3.12
GW027	744714	1145441	54.87	1.31	1.1	0.026	2.63
GW028	745750	1146207	18.93	1.31	1.1	0.076	7.62
GW029	748714	1145545	31.97	1.31	1.1	0.045	4.51
GW030	755458	1142101	21.57	1.31	1.1	0.067	6.69
GW031	759007	1139515	49.40	1.31	1.1	0.029	2.92
GW032	764343	1129821	5.72	1.31	1.1	0.252	25.24
GW033	766851	1137447	6.11	1.31	1.1	0.236	23.60
GW034	756705	1137331	30.40	1.31	1.1	0.047	4.75
GW035	750921	1132636	34.64	1.31	1.1	0.042	4.17
GW036	747004	1137902	61.68	1.31	1.1	0.023	2.34
GW037	722076	1109007	33.93	1.31	1.1	0.043	4.25
GW038	735303	1122376	39.32	1.31	1.1	0.037	3.67
GW039	740305	1119629	253.91	1.31	1.1	0.006	0.57

ID	EASTINGS	NORTHINGS	Cl_Concentration in Groundwater (mg/L)	Cl_Concentration in precipitation (mg/L)	Precipitation (m/yr)	Recharge-Rg (m/yr)	%Rg
GW040	781433	1094718	101.31	1.31	1.1	0.014	1.42
GW041	783023	1122017	206.50	1.31	1.1	0.007	0.70
GW042	787438	1121223	10.77	1.31	1.1	0.134	13.40
GW045	790748	1118809	8.21	1.31	1.1	0.176	17.58
GW046	783072	1115950	229.55	1.31	1.1	0.006	0.63
GW047	781558	1113424	232.68	1.31	1.1	0.006	0.62
GW048	782309	1111850	28.95	1.31	1.1	0.050	4.99
GW049	781902	1108714	41.92	1.31	1.1	0.034	3.44
GW050	784456	1111204	39.47	1.31	1.1	0.037	3.66
GW051	780799	1103998	142.02	1.31	1.1	0.010	1.02
GW052	781025	1100930	202.43	1.31	1.1	0.007	0.71
GW053	787415	1097843	125.27	1.31	1.1	0.012	1.15
GW054	791144	1097675	186.39	1.31	1.1	0.008	0.77
GW055	796316	1097722	121.09	1.31	1.1	0.012	1.19
GW056	809345	1101161	204.97	1.31	1.1	0.007	0.70
GW057	813502	1102172	189.34	1.31	1.1	0.008	0.76
GW058	816360	1106532	198.04	1.31	1.1	0.007	0.73
GW059	819613	1113513	35.95	1.31	1.1	0.040	4.01
GW060	819225	1118333	52.56	1.31	1.1	0.027	2.75
GW061	817330	1124857	16.65	1.31	1.1	0.087	8.67
GW062	819609	1125200	215.97	1.31	1.1	0.007	0.67
GW063	818450	1139704	14.14	1.31	1.1	0.102	10.21
GW064	807585	1142444	205.04	1.31	1.1	0.007	0.70
GW065	798912	1144860	201.67	1.31	1.1	0.007	0.72
GW066	779330	1164579	25.08	1.31	1.1	0.058	5.75
	742559	1149527	60.00	1.31	1.1	0.024	2.41
	737585	1149844	34.50	1.31	1.1	0.042	4.18
	740379	1124007	7.65	1.31	1.1	0.189	18.87
	780342	1166037	13.81	1.31	1.1	0.105	10.45
	804970	1098155	2.42	1.31	1.1	0.597	59.69
	755894	1141695	7.67	1.31	1.1	0.188	18.81
	759069	1138944	3.55	1.31	1.1	0.407	40.65
	766584	1137462	5.70	1.31	1.1	0.253	25.32
	761186	1149104	6.00	1.31	1.1	0.241	24.05
	760551	1157994	26.00	1.31	1.1	0.056	5.55
	740654	1144976	54.00	1.31	1.1	0.027	2.67
	741607	1144659	38.00	1.31	1.1	0.038	3.80

APPENDIX 9- DESCRIPTIVE STATISTICS OF PARAMTERS

	Total No.	Range	Minimum	Maximum	Mean		Std. Deviation	Variance	Skewness		Kurtosis	
						Std. Error				Std. Error		Std. Error
Well Depth (m)	222	145	21.0	166	57.43	1.46	21.75	473.06	2.01	0.16	5.81	0.33
Thickness of Regolith (m)	222	17	2.0	19	7.98	0.22	3.23	10.43	0.44	0.16	0.25	0.33
Yield (m^3/d)	222	714	6.0	720	84.24	7.76	115.67	13378.79	2.70	0.16	8.35	0.33
SWL (m)	222	36	0.5	36	7.38	0.33	4.87	23.72	2.53	0.16	10.82	0.33
Transmissivity (m^2/d)	26	264	0.25	264	32.46	11.72	59.75	3570.57	3.12	0.46	9.96	0.89
Specific Capacity ($m^3/d/m$)	222	960	0.12	960	16.45	4.95	73.80	5446.61	10.60	0.16	126.51	0.33

APPENDIX 10- MASTER TABLE WITH 233 BOREHOLES

Community	BH ID	Formation	Northing	Easting	Depth (m)	LogD(m)	Thickness of Regolith	LogRegolith (m)	Discharge (l/min)	Discharge (m3/d)	LogYield (m3/d)	SWL (m)	LogSWL (m)	water strik	Drawdown (m) at 360mins	Specific Capacity (l/min/m)	Specific Capacity (m3/d/m)	LogSC(m3/d/m)	Transmissivity (m2/d)-sormation-specific	Transmissivity-Entire Nsia (m2/d)
Karaga 1	DWVP220	BIMBILLA	1098267	781857	50	1.7	8	0.9	40	57.6	1.76	35.62	1.55		5.49	7.29	10.49	1.06	10.54	10.54
Karaga 2	DWVP221	BIMBILLA	1098648	781359	52	1.72	3	0.48	250	360	2.56	29.19	1.47		13.41	18.64	26.85	1.44	14.35	14.35
Karaga 3	DWVP222	BIMBILLA	1098172	782058	40	1.6	7	0.85	150	216	2.33	31.53	1.5		4.86	30.86	44.44	1.66	23.12	23.12
Karaga 4	DWVP223	BIMBILLA	1098712	781772	40	1.6	6	0.78	300	432	2.64	12.09	1.08		7.48	40.11	57.75	1.77	37.47	37.47
Karaga Yepala	DWVP230	BIMBILLA	1098871	781296	50	1.7	5	0.7	120	172.8	2.24	13.25	1.12		10.96	10.95	15.77	1.22	10.72	10.72
Karaga	DWVP231	BIMBILLA	1098680	780915	55	1.74	3	0.48	130	187.2	2.27	14.45	1.16		8.38	15.51	22.34	1.37	11.05	11.05
Tong	DWVP236	BIMBILLA	1099506	776216	65	1.81	5	0.7	400	576	2.76	9.75	0.99		11.84	33.78	48.65	1.70	25.1	25.10
GUSHIEGU-S-7	DWVP242	BIMBILLA	1098426	805150	93	1.97	5	0.7	70	100.8	2	6.4	0.81		3.13	22.36	32.20	1.52	34.16	34.16
GUSHIEGU-H-25-02	DWVP243	BIMBILLA	1098553	804261	93	1.97	6	0.78	30	43.2	1.64	11.13	1.05		6.15	4.88	7.02	0.90	8.69	8.69
DABOYA C150	DWVP50	BIMBILLA	1113018	730148	52	1.72	10	1	12	17.28	1.24	6.12	0.79	20	15.54	0.77	1.11	0.32	0.45	0.45
TUUNI	HAP 14	BIMBILLA	1139654	788493	120	2.08	12	1.08	10	14.4	1.16	3.42	0.53	35	31.42	0.32	0.46	0.16	0.60	0.49
JANGA	HAP 05	BIMBILLA	1108645	722136	166	2.22	15	1.18	5	7.2	0.86	7.65	0.88	16	26.43	0.19	0.27	0.10	0.37	0.29
TINGURI	WVB12	BIMBILLA	1100980	809369	51	1.71	12	1.08	150	216	2.33	8.94	0.95	27	4.91	30.55	43.99	1.65	39.47	41.11
KUKOBILA	DWVP4	BIMBILLA	1119935	740848	100	2	12	1.08	12	17.28	1.24	6.25	0.8	15	81.33	0.15	0.21	0.08	0.29	0.23
KPOBU	DWVP5	BIMBILLA	1122217	783088	100	2	18	1.26	13	18.72	1.27	8.7	0.94	27	28.45	0.46	0.66	0.22	0.83	0.70
SALINWIA	DWVP7	BIMBILLA	1123607	813968	75	1.88	10	1	80	115.2	2.06	5.25	0.72	63	45.91	0.13	0.19	0.08	0.26	0.21
NYANSON	DWVP11	BIMBILLA	1097722	796354	34	1.53	4	0.6	41	59.04	1.77	6.4	0.81	20	5.21	7.87	11.33	1.09	11.35	11.03
NYINGALE	DWVP12	BIMBILLA	1099834	794165	58	1.76	9	0.95	10	14.4	1.16	4.2	0.62	32	8.12	1.23	1.77	0.44	2.06	1.82
DIDOGLL	DWVP13	BIMBILLA	1108845	757832	31	1.49	7	0.85	43	61.92	1.79	5	0.7	20	5.5	7.82	11.26	1.09	11.28	10.96
GBALIGA	DWVP14	BIMBILLA	1109553	786728	53	1.72	5	0.7	70	100.8	2	3.21	0.51	22	4.26	16.43	23.66	1.39	22.32	22.53
JAMAGA	DWVP15	BIMBILLA	1108713	781901	55	1.74	4	0.6	30	43.2	1.64	10.64	1.03	32	29.09	1.03	1.49	0.40	1.76	1.54
LOARI	DWVP16	BIMBILLA	1136756	738217	46	1.66	5	0.7	25	36	1.56	8.06	0.91	26	13.08	1.91	2.75	0.57	3.09	2.79
DISIGA	DWVP17	BIMBILLA	1106822	738717	55	1.74	5	0.7	15	21.6	1.33	10.45	1.02	32	6.5	2.31	3.32	0.64	3.67	3.35
NAMBURUGU	DWVP18	BIMBILLA	1138624	787296	50	1.7	5	0.7	30	43.2	1.64	4.43	0.65	22	8.1	3.70	5.33	0.80	5.67	5.31
NASIA CHIPS	DWVP41	BIMBILLA	1123690	740519	75	1.88	6	0.78	10	14.4	1.16	31.29	1.5	46	38	0.26	0.38	0.14	0.50	0.41
LOAGRI PRIM.	DWVP42	BIMBILLA	1137100	737852	75	1.88	5	0.7	10	14.4	1.16	10.56	1.02	22	58.7	0.17	0.25	0.10	0.34	0.27
LOAGRI COMM.	DWVP43	BIMBILLA	1136616	738087	75	1.88	6	0.78	10	14.4	1.16	8.52	0.93	41	60.64	0.16	0.24	0.09	0.33	0.26
SOOBA COMM.	DWVP44	BIMBILLA	1112634	731113	75	1.88	5	0.7	10	14.4	1.16	9.1	0.96	17	64.51	0.16	0.22	0.09	0.30	0.24
SOOBA PRIM.	DWVP45	BIMBILLA	1112654	730866	75	1.88	3	0.48	10	14.4	1.16	9.4	0.97	27	63.09	0.16	0.23	0.09	0.32	0.25
DABOYA CHIPS	DWVP46	BIMBILLA	1113758	730454	75	1.88	3	0.48	10	14.4	1.16	8.42	0.93	18	62.11	0.16	0.23	0.09	0.32	0.25
SAKULO	DWVP47	BIMBILLA	1111415	792672	50	1.7	4	0.6	10	14.4	1.16	6.99	0.84	36	58.89	0.17	0.24	0.09	0.33	0.26
NAMBURUGU	DWVP48	BIMBILLA	1121067	787370	60	1.78	3	0.48	10	14.4	1.16	6.24	0.8	42	47.54	0.21	0.30	0.11	0.40	0.33
KOFIYIRI A170	DWVP49	BIMBILLA	1105606	723505	52	1.72	3	0.48	10	14.4	1.16	9.1	0.96	15	35.08	0.29	0.41	0.15	0.54	0.44
SOOBA A-0	DWVP51	BIMBILLA	1112147	731209	70	1.85	5	0.7	5	7.2	0.86	7.2	0.86		52.6	0.10	0.14	0.06	0.20	0.16
SOOBA A50	DWVP52	BIMBILLA	1112189	731202	94	1.97	3	0.48	4	5.76	0.76	7.8	0.89		48.14	0.08	0.12	0.05	0.17	0.13
JANGA	DWVP59	BIMBILLA	1105056	722110	100	2	6	0.78	20	28.8	1.46	8.3	0.92	75	19.11	1.05	1.51	0.40	1.78	1.56
SAFAM	DWVP60	BIMBILLA	1103887	724651	50	1.7	8	0.9	40	57.6	1.76	4.28	0.63	19	22.57	1.77	2.55	0.55	2.88	2.60
KUKOBILA -BH30	DWVP61	BIMBILLA	1117418	740053	60	1.78	8	0.9	50	72	1.86	3.31	0.52	25	20.86	2.40	3.45	0.65	3.80	3.48
KUKOBILA-BH31	DWVP62	BIMBILLA	1118433	738768	100	2	9	0.95	20	28.8	1.46	5.78	0.76	75	25.44	0.79	1.13	0.33	1.36	1.18
KUKOBILA-BH32	DWVP63	BIMBILLA	1117410	739444	80	1.9	5	0.7	11	15.84	1.2	6.12	0.79	42	13.69	0.80	1.16	0.33	1.40	1.21
KUKOBILA-BH33	DWVP64	BIMBILLA	1114466	738328	100	2	8	0.9	20	28.8	1.46	11.68	1.07	27	18.44	1.08	1.56	0.41	1.83	1.61
KUKOBILA-BH 34	DWVP65	BIMBILLA	1116160	738508	50	1.7	9	0.95	65	93.6	1.97	5.05	0.7	45	5.24	12.40	17.86	1.28	17.24	17.15
YIBEE	DWVP70	BIMBILLA	1121288	801782	40	1.6	12	1.08	14	20.16	1.3	12.6	1.1	19	8.3	1.69	2.43	0.54	2.76	2.48
Nakpaya Sch.	DWVP71	BIMBILLA	1122375	735306	34	1.53	10	1	47	67.68	1.83	5.62	0.75	21	8.09	5.81	8.37	0.97	8.59	8.22
MANCHUGU	DWVP72	BIMBILLA	1118672	815267	34	1.53	10	1	24	34.56	1.54	5.31	0.73	24	7.4	3.24	4.67	0.75	5.02	4.67
Pomo	DWVP73	BIMBILLA	1106940	813190	72	1.86	6	0.78	12	17.28	1.24	7.5	0.88	47	42.11	0.28	0.41	0.15	0.54	0.44
Surugu	DWVP75	BIMBILLA	1109553	812054	44	1.64	6	0.78	15	21.6	1.33	3.3	0.52	22		1.13	1.63	0.42	1.91	1.68
Tugban	DWVP78	BIMBILLA	1108880	815915	43	1.63	10	1	12	17.28	1.24	2.39	0.38	23		1.04	1.50	0.40	1.77	1.55
Komoayili-05	DWVP119	BIMBILLA	1103400	785127	50	1.7	10	1	300	432	2.64	7.31	0.86		4.24	70.75	101.89	2.01	85.40	92.86
kamoayili-04	DWVP120	BIMBILLA	1103413	785123	55	1.74	6	0.78	120	172.8	2.24	9.5	0.98		8.36	14.35	20.67	1.34	19.72	19.76
Tong	DWVP121	BIMBILLA	1115314	802064	65	1.81	6	0.78	400	576	2.76	9.75	0.99		12.75	31.37	45.18	1.66	40.45	42.19
Achinayili	DWVP122	BIMBILLA	1115508	802102	70	1.85	6	0.78	10	14.4	1.16	5.4	0.73		34.87	0.29	0.41	0.15	0.54	0.44
Duna	DWVP123	BIMBILLA	1112294	781788	45	1.65	10	1	180	259.2	2.41	8.48	0.93		7.44	24.19	34.84	1.55	31.85	32.79
Talole	DWVP124	BIMBILLA	1112421	797937	52	1.72	11	1.04	13	18.72	1.27	6.32	0.8		13.86	0.94	1.35	0.37	1.61	1.40
Gbankoni	DWVP126	BIMBILLA	1141642	804855	68	1.83	8	0.9	30	43.2	1.64	12	1.08		26.2	1.15	1.65	0.42	1.93	1.70
Dimia	DWVP127	BIMBILLA	1145168	771642	70	1.85	6	0.78	85	122.4	2.09	11.7	1.07			26.73	38.49	1.60	34.91	36.12
Loagri #1	DWVP142	BIMBILLA	1136623	738765	63	1.8	5	0.7	20	28.8	1.46	8.81	0.94		9.6	2.08	3.00	0.60	3.35	3.04

Community	BH ID	Formation	Northing	Easting	Depth (m)	LogD(m)	Thickness of Regolith	LogRegolith (m)	Discharge (l/min)	Discharge (m3/d)	LogYield (m3/d)	SWL (m)	LogSWL (m)	water strik	Drawdown (m) at 360mins	Specific Capacity (l/min/m)	Specific Capacity (m3/d/m)	LogSC(m3/d/m)	Transmissivity (m2/d)-sormation-specific	Transmissivity-Entire Nsia (m2/d)
Nakpaya	DWVP145	BIMBILLA	1120620	734510	44	1.64	3	0.48	16	23.04	1.36	6.11	0.79		10.36	1.54	2.22	0.51	2.54	2.27
Wungu 1	DWVP154	BIMBILLA	1141576	735749	44	1.64	10	1	10	14.4	1.16	5.55	0.74		31.24	0.32	0.46	0.16	0.60	0.49
Wungu 2	DWVP155	BIMBILLA	1141004	734987	50	1.7	10	1	30	43.2	1.64	1.5	0.18		16.95	1.77	2.55	0.55	2.88	2.60
Wungu 3	DWVP156	BIMBILLA	1141808	736288	61	1.79	6	0.78	25	36	1.56	10.13	1.01		22.02	1.14	1.63	0.42	1.91	1.68
Wungu 4	DWVP157	BIMBILLA	1141322	735368	51	1.71	8	0.9	10	14.4	1.16	2.64	0.42		22.46	0.45	0.64	0.21	0.81	0.68
Wungu Nab	DWVP158	BIMBILLA	1142020	736320	50	1.7	8	0.9	40	57.6	1.76	8.83	0.95		8.15	4.91	7.07	0.91	7.36	6.98
Nasia	DWVP160	BIMBILLA	1126568	739463	50	1.7	5	0.7	280	403.2	2.61	8.39	0.92		15.04	18.62	26.81	1.44	25.04	25.43
Loagri	DWVP161	BIMBILLA	1136305	738511	50	1.7	8	0.9	100	144	2.16	6.71	0.83		13.2	7.58	10.91	1.08	10.96	10.63
Najong	DWVP164	BIMBILLA	1140734	817320	90	1.95	9	0.95	55	79.2	1.9	13.14	1.12		17.72	3.10	4.47	0.74	4.83	4.47
Nanyiri	DWVP165	BIMBILLA	1127796	822717	75	1.88	15	1.18	90	129.6	2.11	6.86	0.84		5.43	16.57	23.87	1.40	22.50	22.72
Kukobila bh1	DWVP166	BIMBILLA	1120514	739645	45	1.65	10	1	50	72	1.86	4.35	0.64		7.09	7.05	10.16	1.05	10.26	9.92
Kukobila bh3	DWVP168	BIMBILLA	1120529	739636	42	1.62	12	1.08	75	108	2.03	4.75	0.68		3.27	22.94	33.03	1.53	30.33	31.14
Kukobila bh4	DWVP169	BIMBILLA	1120681	739349	54	1.73	10	1	200	288	2.46	3.14	0.5		5.98	33.44	48.16	1.69	42.89	44.89
Karaga BH1	DWVP173	BIMBILLA	1098178	781783	33	1.52	6	0.78	21	30.24	1.48	1.7	0.23		26.48	0.79	1.14	0.33	1.37	1.19
Karaga BH2	DWVP174	BIMBILLA	1097924	782037	36	1.56	10	1	66	95.04	1.98	4.47	0.65		5.04	13.10	18.86	1.30	18.12	18.08
Karaga BH3	DWVP175	BIMBILLA	1099067	781148	33	1.52	11	1.04	110	158.4	2.2	5.06	0.7		19.52	5.64	8.11	0.96	8.34	7.97
Tiya I	DWVP179	BIMBILLA	1113418	730729	34	1.53	5	0.7	16	23.04	1.36	7.7	0.89		6.34	2.52	3.63	0.67	3.99	3.66
Tiya II	DWVP180	BIMBILLA	1113799	731237	36	1.56	10	1	64	92.16	1.96	6.35	0.8		17.89	3.58	5.15	0.79	5.50	5.13
Tiya III	DWVP181	BIMBILLA	1112910	730348	54	1.73	10	1	10	14.4	1.16	7	0.85		8.88	1.13	1.62	0.42	1.90	1.67
Wungu	DWVP182	BIMBILLA	1140596	735174	46	1.66	5	0.7	10	14.4	1.16	9.76	0.99		13.85	0.72	1.04	0.31	1.26	1.09
Gbitugu	DWVP186	BIMBILLA	1100905	772284	55.58	1.74	3	0.48	120	172.8	2.24	16.2	1.21			27.78	40.00	1.61	36.17	37.49
Kanshegu	DWVP188	BIMBILLA	1095968	802991	56	1.75	3	0.48	20	28.8	1.46	8.11	0.91			0.96	1.38	0.38	1.64	1.43
Kpubo	DWVP190	BIMBILLA	1122017	783027	46	1.66	10	1	10	14.4	1.16	8.31	0.92			0.38	0.54	0.19	0.69	0.58
Kpugi	DWVP191	BIMBILLA	1102549	801440	65	1.81	15	1.18	28	40.32	1.61	11.48	1.06			7.33	10.55	1.06	10.63	10.29
Kunaayili	DWVP192	BIMBILLA	1096890	804478	61	1.79	10	1	32	46.08	1.66	6.82	0.83			3.10	4.47	0.74	4.83	4.47
Kunkundanyili	DWVP193	BIMBILLA	1119883	740221	48	1.68	10	1	25	36	1.56	21.24	1.33			8.20	11.80	1.11	11.78	11.47
Nalogu	DWVP198	BIMBILLA	1113101	805679	42	1.62	5	0.7	10.11	14.56	1.16	6.93	0.84			0.77	1.11	0.32	1.34	1.16
Namborigu	DWVP199	BIMBILLA	1138777	806700	55	1.74	8	0.9	10	14.4	1.16	9.2	0.96			0.54	0.78	0.25	0.97	0.82
Manie	DWVP201	BIMBILLA	1123083	803547	62.1	1.79	10	1	12	17.28	1.24	10.41	1.02			0.53	0.76	0.25	0.95	0.80
Yilang	DWVP210	BIMBILLA	1127927	786384	65	1.81	6	0.78	13	18.72	1.27	10.98	1.04			0.38	0.55	0.19	0.70	0.59
Yizegu	DWVP211	BIMBILLA	1120296	783287	61.9	1.79	10	1	13	18.72	1.27	10.6	1.03			0.42	0.60	0.20	0.76	0.64
Zagsilari	DWVP212	BIMBILLA	1131456	749858	44	1.64	11	1.04	38	54.72	1.74	7.29	0.86			3.21	4.62	0.75	4.98	4.62
Bonglna	DWVP216	BIMBILLA	1127245	783467	59.9	1.78	5	0.7	36	51.84	1.71	10.54	1.02			3.09	4.45	0.74	4.81	4.46
Sedugo	DWVP217	BIMBILLA	1114339	766456	34.9	1.54	10	1	15	21.6	1.33	7.97	0.9			1.97	2.83	0.58	3.17	2.87
Baliga	DWVP218	BIMBILLA	1109374	786487	61.6	1.79	10	1	151	217.44	2.34	7.08	0.85			7.74	11.14	1.08	11.17	10.85
TINKAYA	DWVP36	Poubugou	1145542	748719	65	1.81	10	1	28	40.32	1.61	4.2	0.62	32	19.22	1.46	2.10	0.49	2.41	2.15
GUABULINGA	DWVP40	Poubugou	1152283	752445	92	1.96	6	0.78	10	14.4	1.16	9.21	0.96	36	51.01	0.20	0.28	0.11	0.38	0.30
Zasilari	DWVP82	Poubugou	1150291	745461	44	1.64	5	0.7	38	54.72	1.74	7.29	0.86	25	11.85	3.21	4.62	0.75	4.98	4.62
Tenkpanga	DWVP131	Poubugou	1153416	746636	46	1.66	5	0.7	15	21.6	1.33	6.7	0.83		1.92	7.81	11.25	1.09	11.27	10.95
Gbimsi 1	DWVP136	Poubugou	1150642	742552	40	1.6	10	1	30	43.2	1.64	2.17	0.34		12.64	2.37	3.42	0.65	3.77	3.45
Gbimsi 2	DWVP137	Poubugou	1150590	743240	55	1.74	9	0.95	20	28.8	1.46	3.79	0.58		16.73	1.20	1.72	0.43	2.01	1.77
Guabulga 1	DWVP138	Poubugou	1151827	751945	45	1.65	9	0.95	80	115.2	2.06	3.77	0.58		4.7	17.02	24.51	1.41	23.06	23.31
Guabulga 2	DWVP139	Poubugou	1151783	752440	45	1.65	9	0.95	45	64.8	1.81	3.78	0.58			5.10	7.34	0.92	7.61	7.24
Guabulga 3	DWVP140	Poubugou	1151750	751934	44	1.64	6	0.78	15	21.6	1.33	2.17	0.34		33.86	0.44	0.64	0.21	0.81	0.68
Nayorko 1	DWVP146	Poubugou	1146656	744797	54	1.73	4	0.6	15	21.6	1.33	6.67	0.82		8.26	1.82	2.62	0.56	2.95	2.67
Nayorko 2	DWVP147	Poubugou	1147291	745686	72	1.86	3	0.48	20	28.8	1.46	5.91	0.77		10.96	1.82	2.63	0.56	2.96	2.67
Guabulga 4	DWVP159	Poubugou	1151651	751528	49	1.69	9	0.95	190	273.6	2.44	5.68	0.75		14.58	13.03	18.77	1.30	18.04	18.00
Gbimsi Woda-Fong	DWVP176	Poubugou	1149613	743302	34	1.53	10	1	10	14.4	1.16	7.29	0.86		12.21	0.82	1.18	0.34	1.42	1.23
Gbimsi Woda-Fong	DWVP177	Poubugou	1149613	743937	34	1.53	8	0.9	12	17.28	1.24	8.8	0.94		11.95	1.00	1.45	0.39	1.72	1.50
Gbimsi-Mugu	DWVP178	Poubugou	1149994	743048	31	1.49	6	0.78	15	21.6	1.33	4.15	0.62		8.02	1.87	2.69	0.57	3.03	2.73
Gaagbini	DWVP185	Poubogou	1146282	746151	43.8	1.64	3	0.48	45	64.8	1.81	4.69	0.67			4.48	6.45	0.87	6.76	6.39
Guabulga	DWVP187	Poubogou	1151836	752135	50	1.7	5	0.7	190	273.6	2.44	5.68	0.75			13.03	18.77	1.30	18.04	18.00
Manga	DWVP194	Poubogou	1155070	751786	61	1.79	6	0.78	10	14.4	1.16	7.3	0.86			0.47	0.67	0.22	0.84	0.71
Sandanfongu	DWVP204	Poubogou	1148826	742520	55.3	1.74	10	1	16	23.04	1.36	4.55	0.66			2.38	3.43	0.65	3.78	3.46
Sayoo	DWVP205	Poubpoou	1149270	742821	48	1.68	12	1.08	15	21.6	1.33	16.5	1.22			9.32	13.42	1.16	13.26	13.00
Guakudo Sch	DWVP141	Panabako sandstone	1132637	750921.8	50	1.70	8	0.90	10	14.4	1.158362	3.89	0.59			0.455581	0.66	0.21906989	1.14	0.70
Walewale-WA-01	DWVP233	Kodjari	1145528	739351	72	1.86	9	0.95	500	720	2.86	2.63	0.42		2.18	229.36	330.28	2.52	263.52	263.52
Walewale-WA-03	DWVP234	Kodjari	1145740	738955	55	1.74	9	0.95	250	360	2.56	6.35	0.8		5.75	43.48	62.61	1.80	70.84	70.84
Walewale-WA-02	DWVP235	Kodjari	1145713	738822	60	1.78	10	1	240	345.6	2.54	4.6	0.66		11.54	20.80	29.95	1.49	14.95	14.95

Community	BH ID	Formation	Northing	Easting	Depth (m)	LogD(m)	Thickness of Regolith	LogRegolith (m)	Discharge (l/min)	Discharge (m3/d)	LogYield (m3/d)	SWL (m)	LogSWL (m)	water strik	Drawdown (m) at 360mins	Specific Capacity (l/min/m)	Specific Capacity (m3/d/m)	LogSC(m3/d/m)	Transmissivity (m2/d)-sormation-specific	Transmissivity-Entire Nsia (m2/d)
Walewale 1-Norst	DWVP237	Kodjari	1145025	741256	80	1.9	5	0.7	400	576	2.76	0.64	-0.19		1.4	285.71	411.43	2.62	178.66	178.66
Walewale 2-Norst	DWVP238	Kodjari	1144920	741468	75	1.88	8	0.9	130	187.2	2.27	5.64	0.75		24.57	5.29	7.62	0.94	3.06	3.06
Walewale 3-Norst	DWVP239	Kodjari	1144602	741362	67	1.83	8	0.9	20	28.8	1.46	15.06	1.18		39.73	0.50	0.72	0.24	0.29	0.29
BUGYA PALA	WVB11	Kodjari	1137749	746795	56	1.75	19	1.28	9	12.96	1.11	7.26	0.86	30	0.3	30.00	43.20	1.65	42.30	40.40
BOAMASA_BH1	DWVP20	Kodjari	1137330	756709	42	1.62	10	1	50	72	1.86	2.56	0.41	20	7.32	6.83	9.84	1.04	9.75	9.62
BOAMASA_BH2	DWVP21	Kodjari	1137635	756753	42	1.62	10	1	30	43.2	1.64	3.01	0.48	20	9.31	3.22	4.64	0.75	4.62	4.64
BANAWA_BH1	DWVP30	Kodjari	1145281	744554	38	1.58	11	1.04	17	24.48	1.39	2.55	0.41	28	26.37	0.64	0.93	0.29	0.94	0.98
BANAWA_BH2	DWVP31	Kodjari	1145442	745076	45	1.65	9	0.95	34	48.96	1.69	2.98	0.47	36	11.26	3.02	4.35	0.73	4.34	4.36
SHELUVUYA	DWVP39	Kodjari	1137658	766388	51	1.71	10	1	10	14.4	1.16	6.89	0.84	18	32.41	0.31	0.44	0.16	0.45	0.47
Shevoya-chief palac	DWVP74	Kodjari	1137617	766798	49	1.69	6	0.78	45	64.8	1.81	2.7	0.43	20	17.63	2.55	3.68	0.67	3.67	3.71
Shelinvoya	DWVP81	Kodjari	1162601	764082	63	1.8	6	0.78	60	86.4	1.94	8.42	0.93	24	7.14	8.40	12.10	1.12	11.97	11.76
ZANGUM	DWVP86	Kodjari	1149885	737659	71	1.85	10	1	20	28.8	1.46	5.51	0.74	53	50.61	0.40	0.57	0.20	0.58	0.61
ZANGUM	DWVP87	Kodjari	1149817	737567	38	1.58	5	0.7	15	21.6	1.33	5.47	0.74	21	17.18	0.87	1.26	0.35	1.27	1.31
TAMPULUNGU	DWVP99	Kodjari	1146049	739640	72	1.86	3	0.48	10	14.4	1.16	7.7	0.89		37.21	0.27	0.39	0.14	0.40	0.42
TAMPULUNGU	DWVP100	Kodjari	1147119	739557	63	1.8	7	0.85	7	10.08	1	8.45	0.93		42.11	0.17	0.24	0.09	0.24	0.26
KPARIGU	DWVP104	Kodjari	1139273	758840	44	1.64	10	1	80	115.2	2.06	0.58	-0.24	21	4.23	18.91	27.23	1.45	26.76	25.82
BOAMASA	DWVP105	Kodjari	1137638	756758	42	1.62	9	0.95	65	93.6	1.97	1.49	0.17	23	11.8	5.51	7.93	0.95	7.87	7.80
BOAMASA	DWVP106	Kodjari	1137330	756710	42	1.62	9	0.95	45	64.8	1.81	3.23	0.51	23	11.6	3.88	5.59	0.82	5.56	5.56
GUAKUDO	DWVP107	Kodjari	1132622	750724	47	1.67	9	0.95	22	31.68	1.5	4.08	0.61	21	16.63	1.32	1.90	0.46	1.91	1.95
BUGYAKURA	DWVP109	Kodjari	1136335	747346	21	1.32	6	0.78	21	30.24	1.48	5.24	0.72	23	20.72	1.01	1.46	0.39	1.47	1.51
KPERIGA	DWVP110	Kodjari	1143666	741126	58	1.76	8	0.9	12	17.28	1.24	6.75	0.83		17	0.71	1.02	0.31	1.03	1.07
KPERIGA	DWVP111	Kodjari	1143646	741156	47	1.67	5	0.7	20	28.8	1.46	5.74	0.76	27	21.45	0.93	1.34	0.37	1.35	1.39
TAMPULUNGU	DWVP114	Kodjari	1145988	739659	53	1.72	6	0.78	15	21.6	1.33	9.34	0.97	32	15.08	0.99	1.43	0.39	1.44	1.48
TAKORAYIRI	DWVP115	Kodjari	1138125	750711	36	1.56	3	0.48	15	21.6	1.33	1.71	0.23	21	12.2	1.23	1.77	0.44	1.78	1.82
Tangbini	DWVP128	Kodjari	1147315	797489	52	1.72	5	0.7	12	17.28	1.24	1.98	0.3		13.42	0.89	1.29	0.36	1.30	1.34
Bugya PALA Bh1	DWVP133	Kodjari	1138104	746289	39	1.59	3	0.48	300	432	2.64	2.95	0.47		0.45	666.67	960.00	2.98	916.86	817.99
Bugya PALA Bh2	DWVP134	Kodjari	1138331	746288	45	1.65	7	0.85	50	72	1.86	1.46	0.16		9.72	5.14	7.41	0.92	7.36	7.31
Bugya PALA Bh3	DWVP135	Kodjari	1141971	738002	48	1.68	5	0.7	140	201.6	2.3	2.15	0.33		10.17	13.77	19.82	1.32	19.53	18.97
Guakudo Sch	DWVP141	Kodjari	1132637	750922	50	1.7	8	0.9	10	14.4	1.16	3.89	0.59			0.46	0.66	0.22	0.67	0.70
Shelinvoya 2	DWVP150	Kodjari	1138528	767149	49	1.69	3	0.48	20	28.8	1.46	8.2	0.91		7.5	2.67	3.84	0.68	3.83	3.86
shelinvoya 3	DWVP151	Kodjari	1137385	765371	39	1.59	2	0.3	38	54.72	1.74	7.55	0.88		8.02	4.74	6.82	0.89	6.78	6.74
Tampulungu 1	DWVP152	Kodjari	1146783	738955	72	1.86	10	1	15	21.6	1.33	10.82	1.03		30.05	0.50	0.72	0.24	0.73	0.76
Tampulungu 2	DWVP153	Kodjari	1147291	738320	63	1.8	15	1.18	15	21.6	1.33	11.76	1.07		18.98	0.79	1.14	0.33	1.15	1.19
Katigri	DWVP189	Kodjari	1148070	805834	50	1.7	2	0.3	17	24.48	1.39	12.8	1.11			2.26	3.26	0.63	3.26	3.29
Galabisi	DWVP219	Kodjari	1139059	782419	55.1	1.74	5	0.7	12	17.28	1.24	3.51	0.55			0.93	1.34	0.37	1.35	1.39
Gambaga SHS1	DWVP224	Panabako sandstone	1165331	780206.3	55	1.740363	6	0.78	10	14.4		10.18	24.14			0.287674	0.41	10.35	0.15	0.25
Gambaga SHS2	DWVP225	Panabako sandstone	1165736	780373.2	54	1.73	6	0.78	20	28.80	1.46	11.74	1.070		17.81	1.12	1.62	0.42	0.96	0.95
Gambaga SHS3	DWVP226	Panabako sandstone	1165546	780778.3	94	1.97	5	0.70	11	15.84	1.20	13.45	1.129		33.09	0.33	0.48	0.17	1.01	1.01
Gambaga SHS4	DWVP227	Panabako sandstone	1165927	780516.2	58	1.76	8	0.90	9	12.96	1.11	12.63	1.101		25	0.36	0.52	0.18	0.30	0.30
Gambaga BG-01	DWVP228	Panabako sandstone	1164902	780802.1	65	1.81	10	1.00	300	432.00	2.64	6.4	0.806		19.66	15.26	21.97	1.36	13.26	13.26
Nalerigu-NA-01	DWVP229	Panabako sandstone	1165069	787260.6	60	1.78	9	0.95	180	259.20	2.41	5.72	0.757		10.06	17.89	25.77	1.43	16.59	16.59
Wundua 1	DWVP240	Panabako sandstone	1143467	769873.8	55	1.74	10	1.00	200	288.00	2.46	2.92	0.465		3.22	62.11	89.44	1.96	65.88	65.88
Wundua 2	DWVP241	Panabako sandstone	1143298	770805.2	65	1.81	8	0.90	150	216.00	2.33	2.96	0.471		13.6	11.03	15.88	1.23	10.68	10.68
TAMBOKU	DWVP2	Panabako Sandstone	1144848	775912	100	2.00	12	1.08	132	190.08	2.28	9.55	0.980	37	5.76	22.92	33.00	1.53	13.48	13.48
NALERIGU SHS	HAP 11	Panabako Sandstone	1163361	785424.2	141	2.15	12	1.08	24	34.56	1.54	8.21	0.914	32	16.08	1.49	2.15	0.50	3.49	2.20
DAGBIBORE	DWVP1	Panabako Sandstone	1147263	778042	150	2.18	16	1.20	22	31.68	1.50	6.02	0.780	25	65.78	0.33	0.48	0.17	0.85	0.52
SAMENE	DWVP9	Panabako Sandstone	1157299	761494	100	2.00	16	1.20	4	5.76	0.76	7	0.845	18	47.48	0.08	0.12	0.05	0.23	0.14
MOATANKURA	DWVP19	Panabako Sandstone	1138624	755848	37	1.57	6	0.78	13	18.72	1.27	6.04	0.781	28	19.33	0.67	0.97	0.29	1.65	1.01
NABULUGU_BH1	DWVP22	Panabako Sandstone	1141502	755701.9	37	1.57	9	0.95	85	122.40	2.09	2.52	0.401	28	4.21	20.19	29.07	1.48	40.60	27.51
NABULUGU_BH2	DWVP23	Panabako Sandstone	1141893	755809	34	1.53	7	0.85	11	15.84	1.20	7.3	0.863	19	6.07	1.81	2.61	0.56	4.19	2.65
TAMBOKU_BH1	DWVP24	Panabako Sandstone	1144472	776445	31	1.49	10	1.00	60	86.40	1.94	1.87	0.272	28	9.29	6.46	9.30	1.01	13.88	9.11
TAMBOKU_BH2	DWVP25	Panabako Sandstone	1144025	776184.9	50	1.70	11	1.04	18	25.92	1.41	3.22	0.508	20	16.28	1.11	1.59	0.41	2.63	1.64
DAGBRIBOARI_BH1	DWVP26	Panabako Sandstone	1137635	756753	40	1.60	12	1.08	30	43.20	1.64	4.11	0.614	26	21.08	1.42	2.05	0.48	3.34	2.10
DAGBRIBOARI_BH2	DWVP27	Panabako Sandstone	1149487	777801	60	1.78	12	1.08	18	25.92	1.41	2.64	0.422	36	16.54	1.09	1.57	0.41	2.59	1.62
BURUGU	DWVP28	Panabako Sandstone	1148333	774050	50	1.70	13	1.11	60	86.40	1.94	5.2	0.716	36	15.27	3.93	5.66	0.82	8.69	5.62
KPARIGU	DWVP29	Panabako Sandstone	1139487	759089	34	1.53	10	1.00	35	50.40	1.70	14.03	1.147	19	18.37	1.91	2.74	0.57	4.39	2.79
LATARE	DWVP32	Panabako Sandstone	1154501	783293.8	40	1.60	10	1.00	55	79.20	1.90	4.77	0.679	20	12.11	4.54	6.54	0.88	9.96	6.47
TSICHIRIGA	DWVP33	Panabako Sandstone	1161725	796740.1	34	1.53	15	1.18	80	115.20	2.06	2.6	0.415	19	18.8	4.26	6.13	0.85	9.37	6.08
NANORI	DWVP34	Panabako Sandstone	1159614	780838	45	1.65	12	1.08	20	28.80	1.46	5.25	0.720	20	23.11	0.87	1.25	0.35	2.09	1.30

Community	BH ID	Formation	Northing	Easting	Depth (m)	LogD(m)	Thickness of Regolith	LogRegolith (m)	Discharge (l/min)	Discharge (m3/d)	LogYield (m3/d)	SWL (m)	LogSWL (m)	water strik	Drawdown (m) at 360mins	Specific Capacity (l/min/m)	Specific Capacity (m3/d/m)	LogSC(m3/d/m)	Transmissivity (m2/d)-sormation-specific	Transmissivity-Entire Nsia (m2/d)
NAGBOO	DWVP35	Panabako Sandstone	1106940	813190	78	1.89	10	1.00	60	86.40	1.94	13.12	1.118	20	20.84	2.88	4.15	0.71	6.48	4.16
TINGURI 1	DWVP37	Panabako Sandstone	1145240	750929.3	101	2.00	8	0.90	10	14.40	1.16	6.83	0.834	22	82.79	0.12	0.17	0.07	0.33	0.19
ZANGUGA	DWVP38	Panabako Sandstone	1150234	755785.8	92	1.96	9	0.95	10	14.40	1.16	8.46	0.927	16	52.91	0.19	0.27	0.10	0.50	0.30
GBANDABILA	DWVP54	Panabako Sandstone	1140414	801312.3	50	1.70	2	0.30	6	8.64	0.94	5.17	0.713		42.37	0.14	0.20	0.08	0.38	0.22
SILOMBOMA	DWVP55	Panabako Sandstone	1150871	797919.1	45	1.65	10	1.00	108	155.52	2.19	5.99	0.777	16	24.35	4.44	6.39	0.87	9.74	6.33
SAGADUGU	DWVP56	Panabako Sandstone	1146329	756743.6	80	1.90	15	1.18	24	34.56	1.54	9.66	0.985	24	17.19	1.40	2.01	0.48	3.28	2.06
SAKAGO	DWVP57	Panabako Sandstone	1171588	793854.2	60	1.78	10	1.00	35	50.40	1.70	6.43	0.808	35	12.68	2.76	3.97	0.70	6.23	3.99
JAWANI	DWVP58	Panabako Sandstone	1148166	787460.3	100	2.00	10	1.00	20	28.80	1.46	3.34	0.524	75	23.61	0.85	1.22	0.35	2.05	1.27
BUZULUNGU	DWVP66	Panabako Sandstone	1153095	762035	100	2.00	10	1.00	7	10.08	1.00	7.45	0.872	50	43.42	0.16	0.23	0.09	0.43	0.25
TAKORAYILI-A150	DWVP67	Panabako Sandstone	1138808	750499.1	50	1.70	9	0.95	10	14.40	1.16	4.13	0.616	18	37.74	0.26	0.38	0.14	0.69	0.41
KOLINVAR	DWVP68	Panabako Sandstone	1150873	795584.2	65	1.81	15	1.18	15	21.60	1.33	12.78	1.107	47	33.65	0.45	0.64	0.22	1.12	0.68
NAMANGU	DWVP69	Panabako Sandstone	1151614	771877.5	90	1.95	10	1.00	6	8.64	0.94	10.41	1.017	43	46.44	0.13	0.19	0.07	0.35	0.20
Tinguri 2	DWVP76	Panabako Sandstone	1145195	751951	42	1.62	10	1.00	70	100.80	2.00	1.6	0.204	10	11.76	5.95	8.57	0.98	12.85	8.41
Tinguri 3	DWVP77	Panabako Sandstone	1144754	752171	49	1.69	11	1.04	85	122.40	2.09	7.83	0.894	21	5.83	14.58	20.99	1.34	29.88	20.06
Gbinduri	DWVP80	Panabako Sandstone	1153796	754199.1	50	1.70	8	0.90	60	86.40	1.94	5.66	0.753	21	13.28	4.52	6.51	0.88	9.91	6.44
KPARIGU	DWVP84	Panabako Sandstone	1139387	758756.2	50	1.70	10	1.00	162	233.28	2.37	2.13	0.328	42	5.22	31.03	44.69	1.66	60.87	41.75
NABULUGA	DWVP94	Panabako Sandstone	1141509	755698.6	49	1.69	5	0.70	30	43.20	1.64	4.31	0.634	35	16.92	1.77	2.55	0.55	4.11	2.60
GBANI	DWVP101	Panabako Sandstone	1144522	752327.1	36	1.56	5	0.70	100	144.00	2.16	1.82	0.260	23	5.79	17.27	24.87	1.41	35.05	23.65
KPARIGU	DWVP104	Panabako Sandstone	1139273	758840.3	44	1.64	10	1.00	80	115.20	2.06	0.58	-0.237	21	4.23	18.91	27.23	1.45	38.18	25.82
GUAKUDO	DWVP107	Panabako Sandstone	1132622	750723.6	47	1.67	9	0.95	22	31.68	1.50	4.08	0.611	21	16.63	1.32	1.90	0.46	3.12	1.96
KPERIGA	DWVP111	Panabako Sandstone	1143646	741155.5	47	1.67	5	0.70	20	28.80	1.46	5.74	0.759	27	21.45	0.93	1.34	0.37	2.24	1.39
TAMPULUNGU	DWVP114	Panabako Sandstone	1145988	739659.3	53	1.72	6	0.78	15	21.60	1.33	9.34	0.970	32	15.08	0.99	1.43	0.39	2.38	1.48
TAKORAYIRI	DWVP115	Panabako Sandstone	1138125	750710.8	36	1.56	3	0.48	15	21.60	1.33	1.71	0.233	21	12.2	1.23	1.77	0.44	2.91	1.82
Dindane	DWVP125	Panabako Sandstone	1169646	800304	60	1.78	10	1.00	12	17.28	1.24	6.17	0.790		9.49	1.26	1.82	0.45	2.99	1.87
Bongbini	DWVP129	Panabako sandstone	1158152	773613	70	1.85	10	1.00	10	14.40	1.16	12.3	1.090		15.59	0.64	0.92	0.28	1.58	0.97
Kpikparigbini	DWVP130	Panabako sandstone	1158236	793848	52	1.72	10	1.00	25	36.00	1.56	12.56	1.099		14.56	1.72	2.47	0.54	3.98	2.52
Tenkpanga	DWVP131	Panabako sandstone	1153416	746636	46	1.66	5	0.70	15	21.60	1.33	6.7	0.826		1.92	7.81	11.25	1.09	16.60	10.95
Boiyini	DWVP132	Panabako sandstone	1145373	762934	44	1.64	5	0.70	42	60.48	1.78	2.1	0.322		8.71	4.82	6.94	0.90	10.54	6.86
Mimima 1	DWVP143	Panabako sandstone	1149069	761497.9	43	1.63	6	0.78	20	28.80	1.46	8	0.903		7.62	2.62	3.78	0.68	5.94	3.80
mimima 2	DWVP144	Panabako sandstone	1150593	761116.9	45	1.65	3	0.48	130	187.20	2.27	0.5	-0.301		5.89	22.07	31.78	1.52	44.16	30.00
Nayorko 1	DWVP146	Panabako sandstone	1146656	744797.3	54	1.73	4	0.60	15	21.60	1.33	6.67	0.824		8.26	1.82	2.62	0.56	4.20	2.66
Nayorko 2	DWVP147	Panabako sandstone	1147291	745686.3	72	1.86	3	0.48	20	28.80	1.46	5.91	0.772		10.96	1.82	2.63	0.56	4.22	2.67
Sagadugu #1	DWVP148	Panabako sandstone	1147418	757751.3	40	1.60	3	0.48	55	79.20	1.90	4.41	0.644		11.51	4.78	6.88	0.90	10.45	6.80
Sagadugu #2	DWVP149	Panabako sandstone	1147164	756227.3	44	1.64	5	0.70	47	67.68	1.83	11	1.041		16.16	2.91	4.19	0.72	6.54	4.20
Shelinvoya 2	DWVP150	Panabako sandstone	1138528	767149.4	49	1.69	3	0.48	20	28.80	1.46	8.2	0.914		7.5	2.67	3.84	0.68	6.03	3.86
shelinvoya 3	DWVP151	Panabako sandstone	1137385	765371.4	39	1.59	2	0.30	38	54.72	1.74	7.55	0.878		8.02	4.74	6.82	0.89	10.36	6.74
Tampulungu 1	DWVP152	Panabako sandstone	1146783	738955.3	72	1.86	10	1.00	15	21.60	1.33	10.82	1.034		30.05	0.50	0.72	0.24	1.24	0.76
Tampulungu 2	DWVP153	Panabako sandstone	1147291	738320.3	63	1.80	15	1.18	15	21.60	1.33	11.76	1.070		18.98	0.79	1.14	0.33	1.92	1.19
Nanori 2	DWVP162	Panabako sandstone	1160118	781775.6	43	1.63	9	0.95	14	20.16	1.30	9.63	0.984		17.93	0.78	1.12	0.33	1.90	1.17
Saamini BH	DWVP163	Panabako sandstone	1158149	760725.3	43	1.63	10	1.00	24	34.56	1.54	4.64	0.667		10.05	2.39	3.44	0.65	5.44	3.47
Langbinsi BHC	DWVP170	Panabako sandstone	1156598	765653.6	55	1.74	10	1.00	100	144.00	2.16	9.26	0.967		22.43	4.46	6.42	0.87	9.79	6.36
Sakogu BHC	DWVP171	Panabako sandstone	1171330	797784.7	46	1.66	6	0.78	70	100.80	2.00	12.7	1.104		16.91	4.14	5.96	0.84	9.13	5.92
SAKAGO BHD	DWVP172	Panabako sandstone	1171584	797530.7	44	1.64	6	0.78	160	230.40	2.36	8.33	0.921		14.39	11.12	16.01	1.23	23.15	15.43
Bantambari	DWVP183	Panabako sandstone	1159596	768179.7	50	1.70	3	0.48	10	14.40	1.16	11.3	1.053			0.51	0.74	0.24	1.28	0.78
Binduri	DWVP184	Panabako sandstone	1148914	754934.8	50	1.70	4	0.60	50	72.00	1.86	5.66	0.753			4.11	5.91	0.84	9.05	5.87
Moatani	DWVP195	Panabako Sandstone	1138341	756460.3	49.9	1.70	8	0.90	15	21.60	1.33	4.5	0.653			2.31	3.33	0.64	5.28	3.37
Moatani	DWVP196	Panabako Sandstone	1139217	756437.5	49.9	1.70	8	0.90	13.17	18.96	1.28	5.63	0.751			1.12	1.61	0.42	2.65	1.66
Nalerigu	DWVP197	Panabako Sandstone	1163497	785407.2	155	2.19	9	0.95	24	34.56	1.54	8.21	0.914			1.49	2.15	0.50	3.49	2.20
Namenyala	DWVP200	Panabako Sandstone	1156387	771747.8	43.4	1.64	9	0.95	13	18.72	1.27	9.76	0.989			0.49	0.70	0.23	1.21	0.74
Sagadugu No.2	DWVP202	Panabako Sandstone	1145609	758145.6	40.1	1.60	9	0.95	25	36.00	1.56	7	0.845			1.72	2.48	0.54	4.00	2.53
Sagadugu No.2	DWVP203	Panabako Sandstone	1146249	757413.4	44	1.64	15	1.18	47	67.68	1.83	11	1.041			2.91	4.19	0.72	6.54	4.20
Singbini	DWVP206	Panabako Sandstone	1143727	756762.4	34.9	1.54	10	1.00	150	216.00	2.33	3.27	0.515			2.21	3.18	0.62	5.04	3.21
Takoratinga	DWVP207	Panabako Sandstone	1163740	787114.8	37.8	1.58	10	1.00	18	25.92	1.41	15.92	1.202			3.33	4.80	0.76	7.44	4.79
Tintariga	DWVP208	Panabako Sandstone	1158623	802874.9	68.1	1.83	6	0.78	11.1	15.98	1.20	11.93	1.077			0.62	0.89	0.28	1.52	0.93
Tintariga	DWVP209	Panabako Sandstone	1158613	801638.1	68.16	1.83	6	0.78	11.13	16.03	1.20	12.29	1.090			0.63	0.91	0.28	1.55	0.95
Zambulugu	DWVP213	Panabako Sandstone	1161575	797371.1	31.2	1.49	10	1.00	100	144.00	2.16	4.54	0.657			4.21	6.07	0.85	9.28	6.02
Zigum	DWVP214	Panabako Sandstone	1155376	784647	49.5	1.69	8	0.90	154	221.76	2.35	2.61	0.417			8.38	12.07	1.12	17.73	11.72
Zojiligu	DWVP215	Panabako Sandstone	1165225	799157.5	68.2	1.83	6	0.78	10.5	15.12	1.18	6.58	0.818			1.85	2.66	0.56	4.27	2.71

APPENDIX 11- CROSS VALIDATION FOR GRAPHS FOR COKRIGING

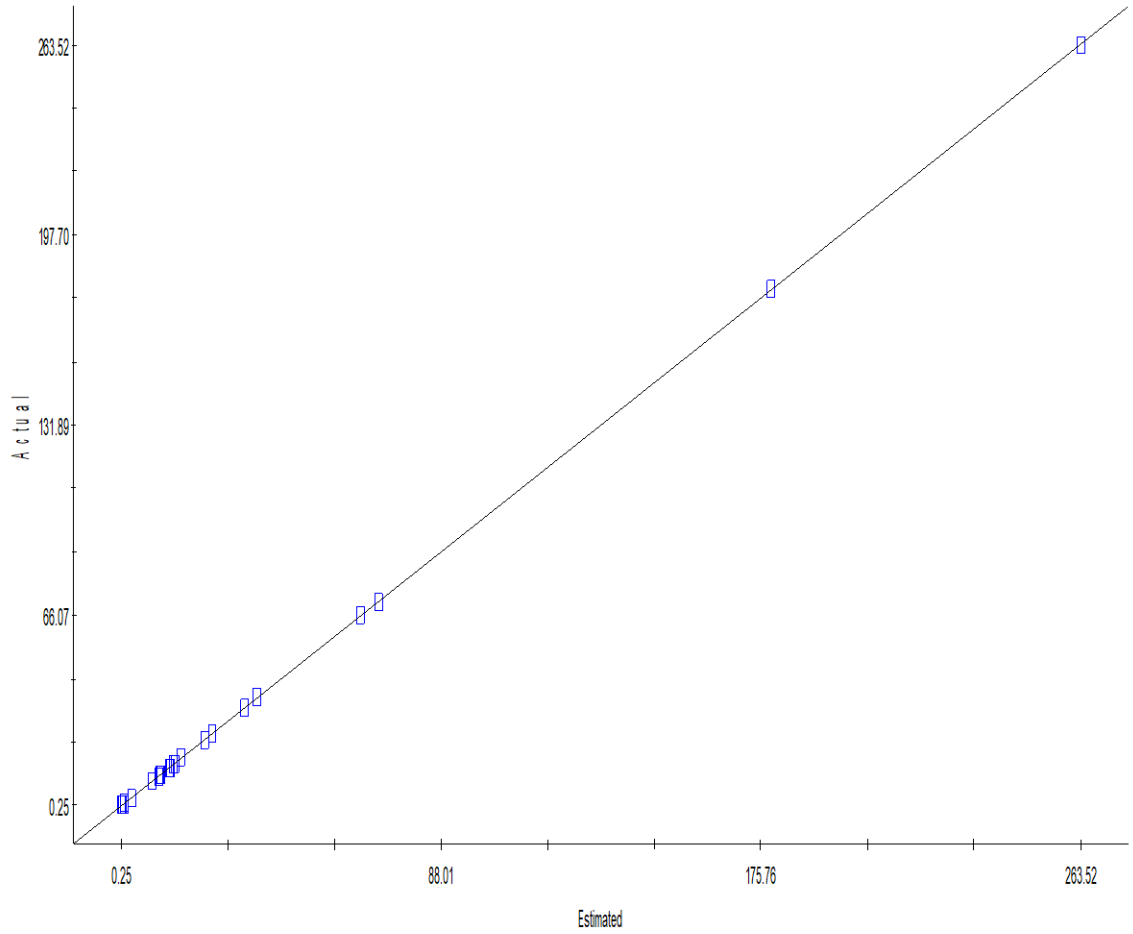

Regression coefficient = 1.000 (SE = 0.000 , r2 =1.000,
y intercept = 0.00, SE Prediction = 0.000, n = 26)

Cross validation of Transmissivity

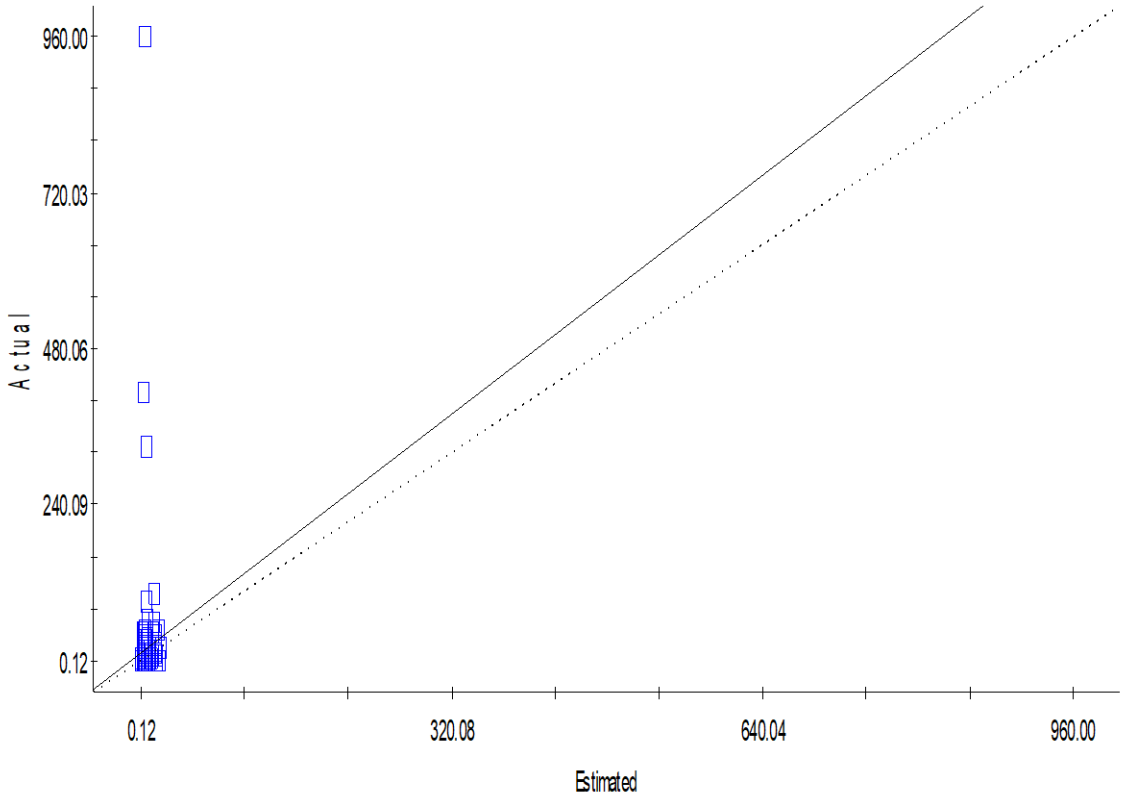

Regression coefficient = 1.150 (SE = 1.355 , r2 =0.003,
y intercept = 10.61, SE Prediction = 74.172, n = 219)

Cross validation of Specific Capacity model

APPENDIX 12- RECLASSIFICATION OF PARAMETERS FOR MULTI-CRITERIA ANALYSIS

Reclass of Lineament

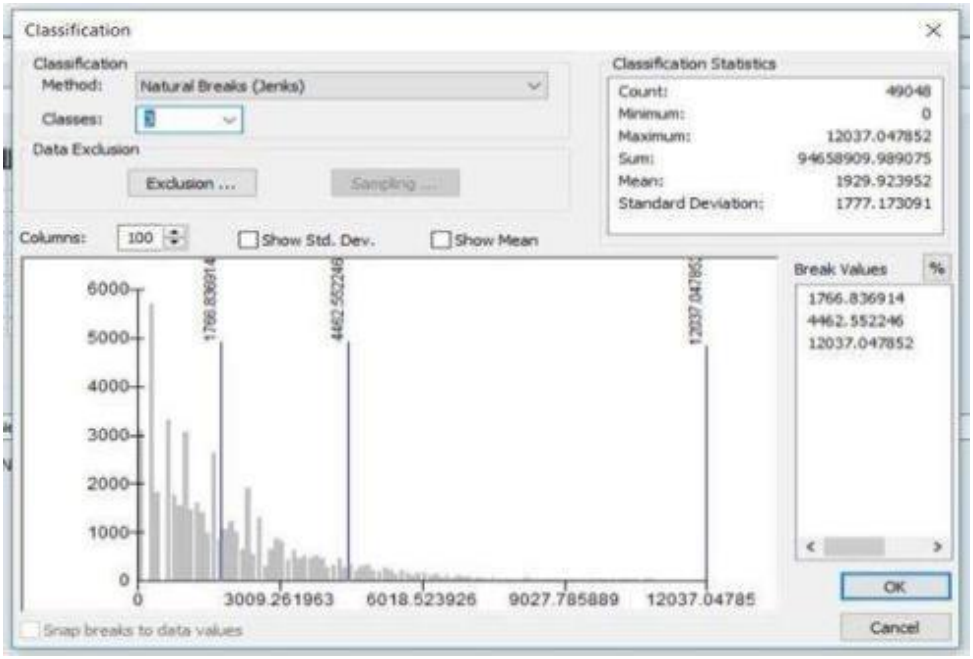

Reclass of recharge

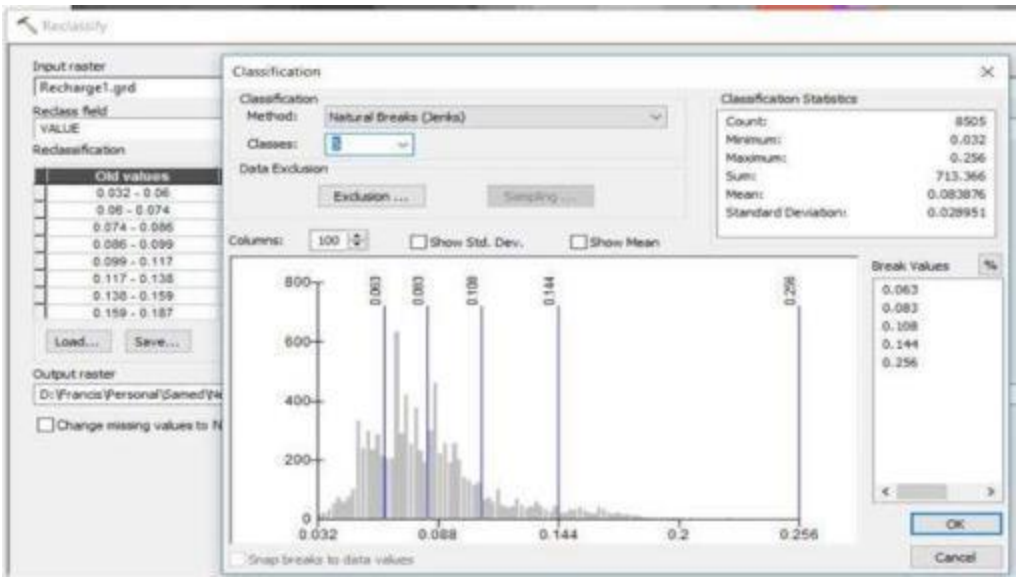

Reclass of Regolith

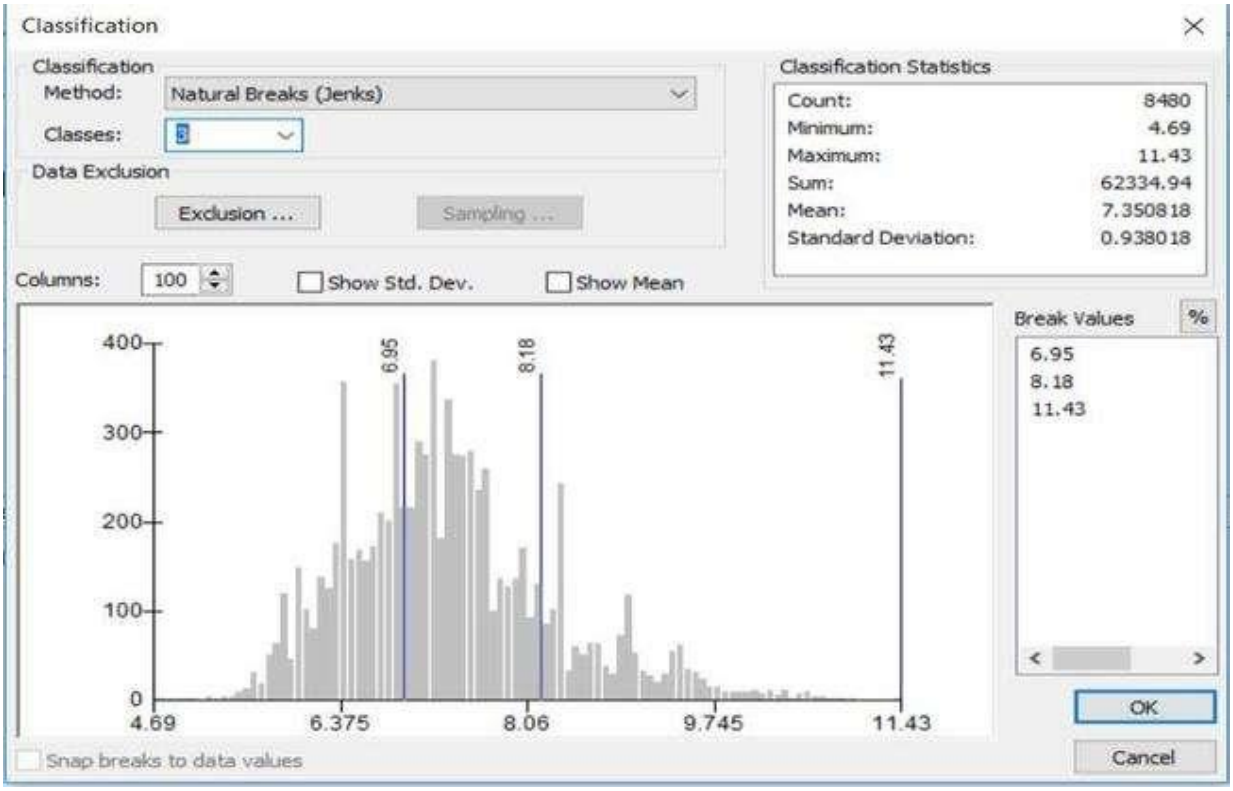

Drainage density

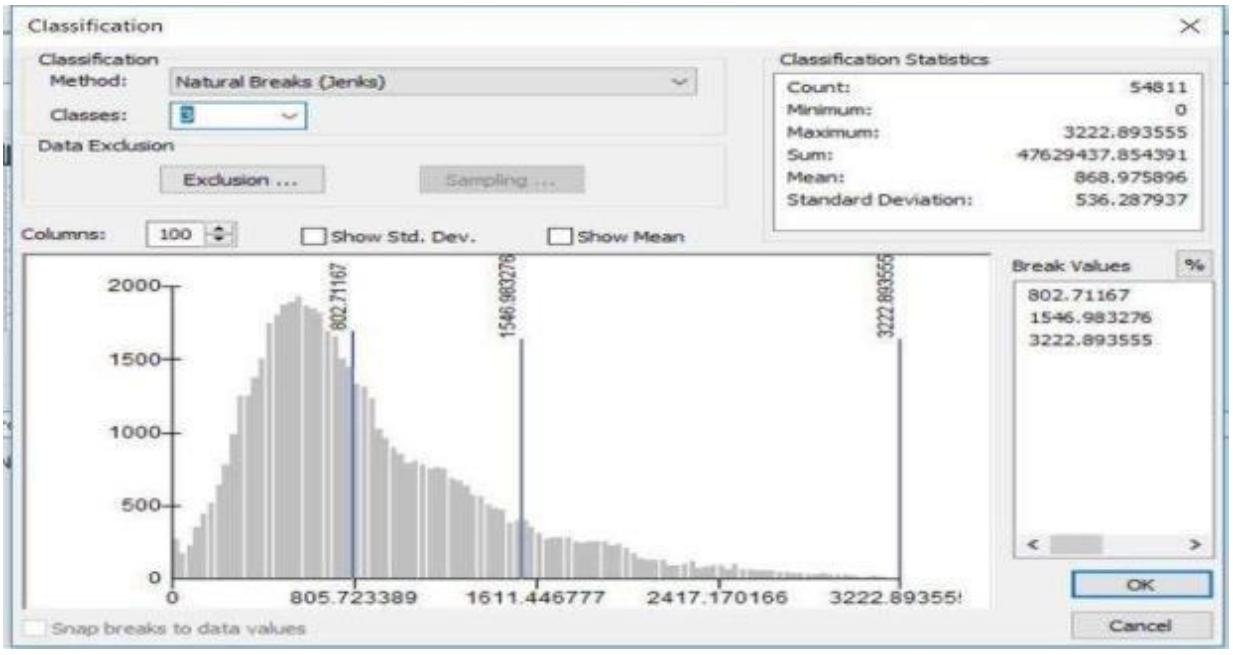

APPENDIX 13- RECLASSIFICATION MAPS OF PARAMETERS

DEPTH

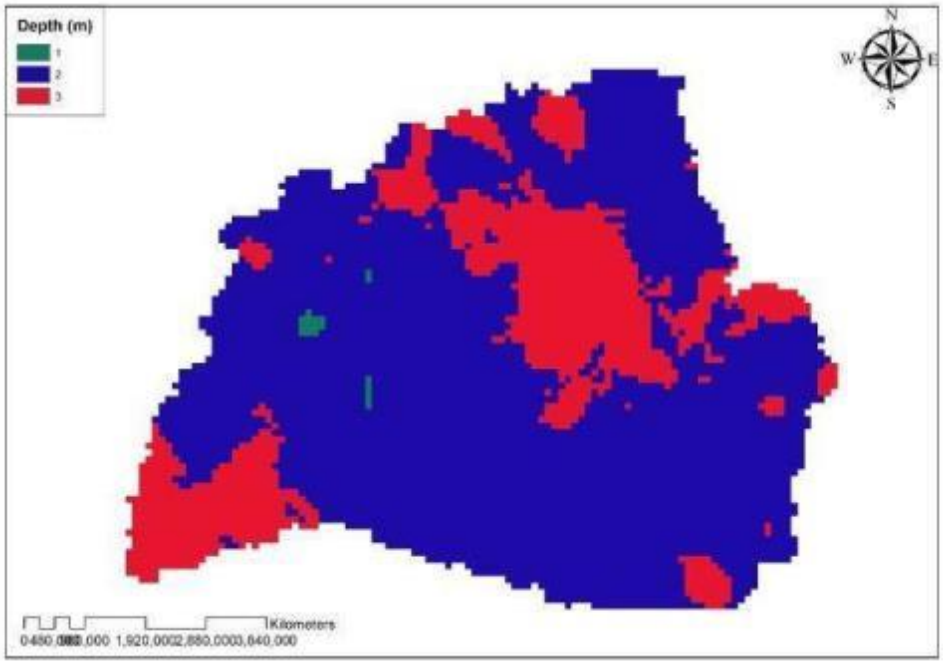

REGOLITH

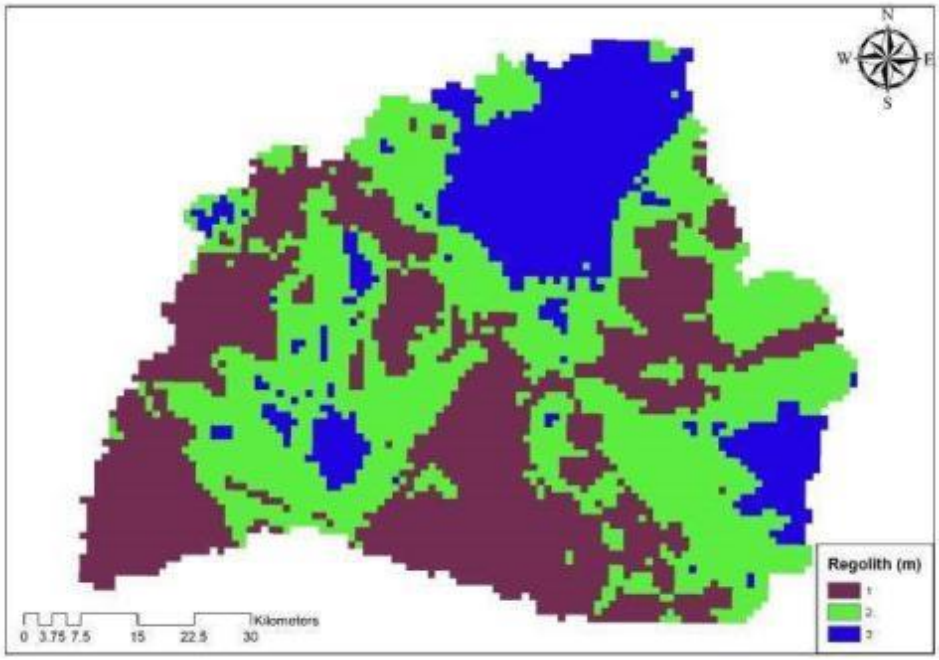

RECHARGE

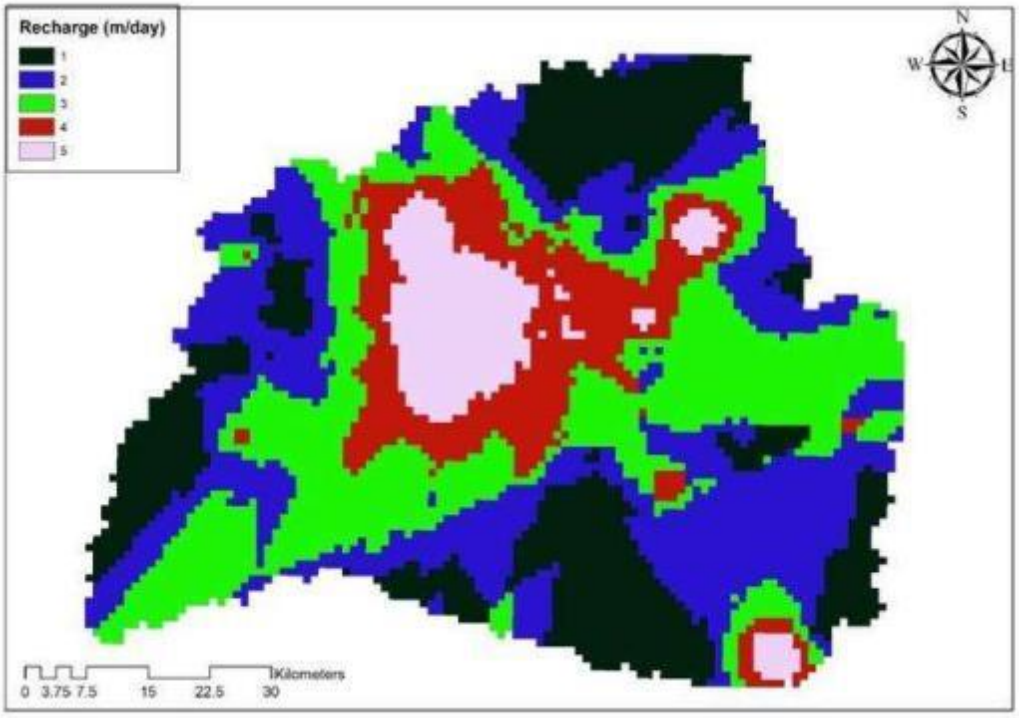

STATIC WATER LEVEL

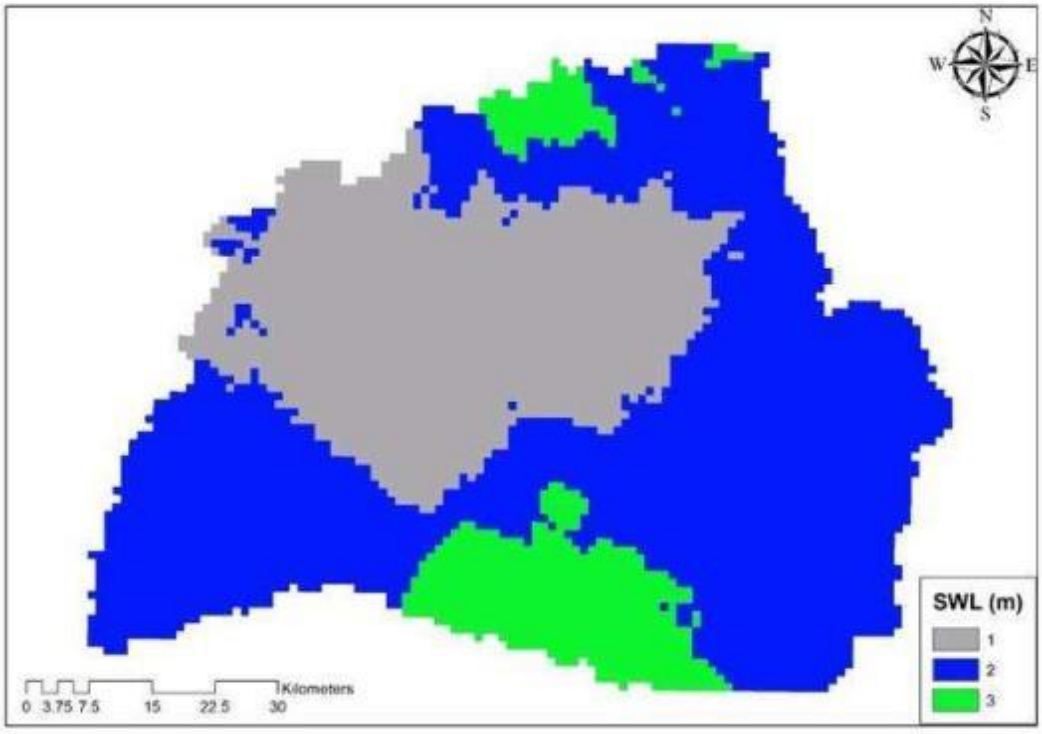

TRANSMISSIVITY

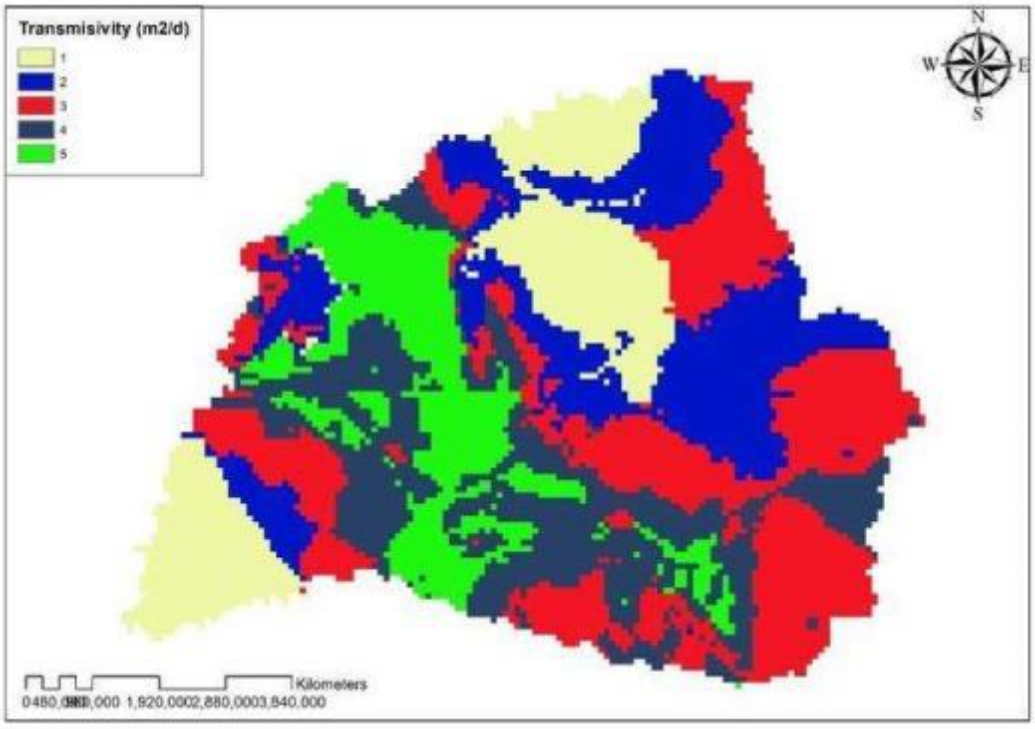

LINEAMENT

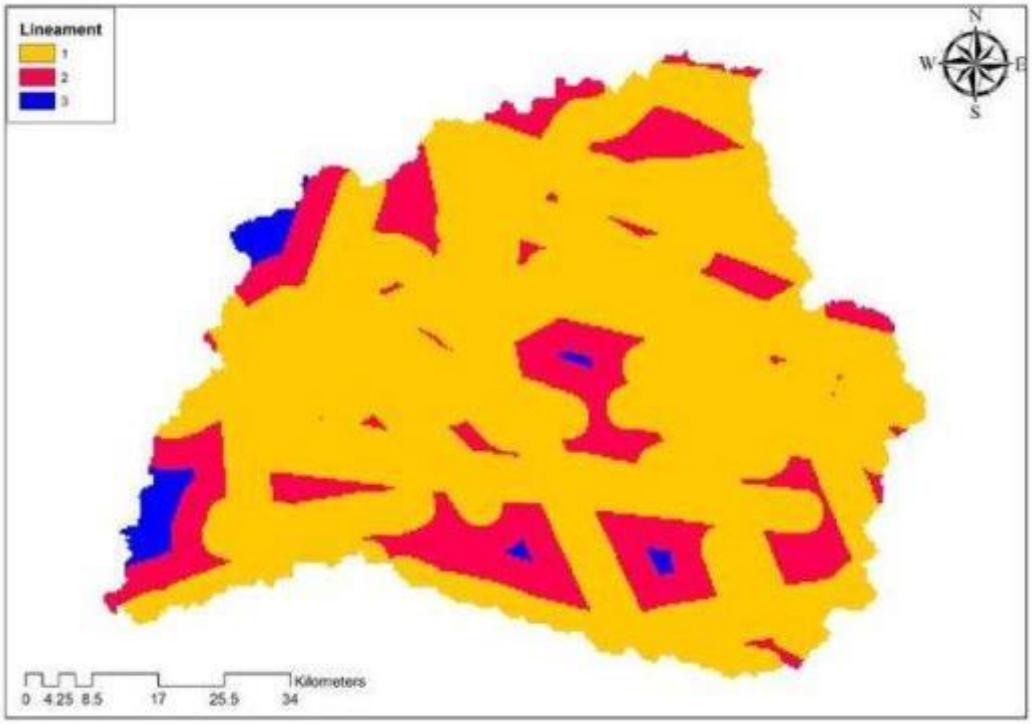

DRAINAGE NETWORK

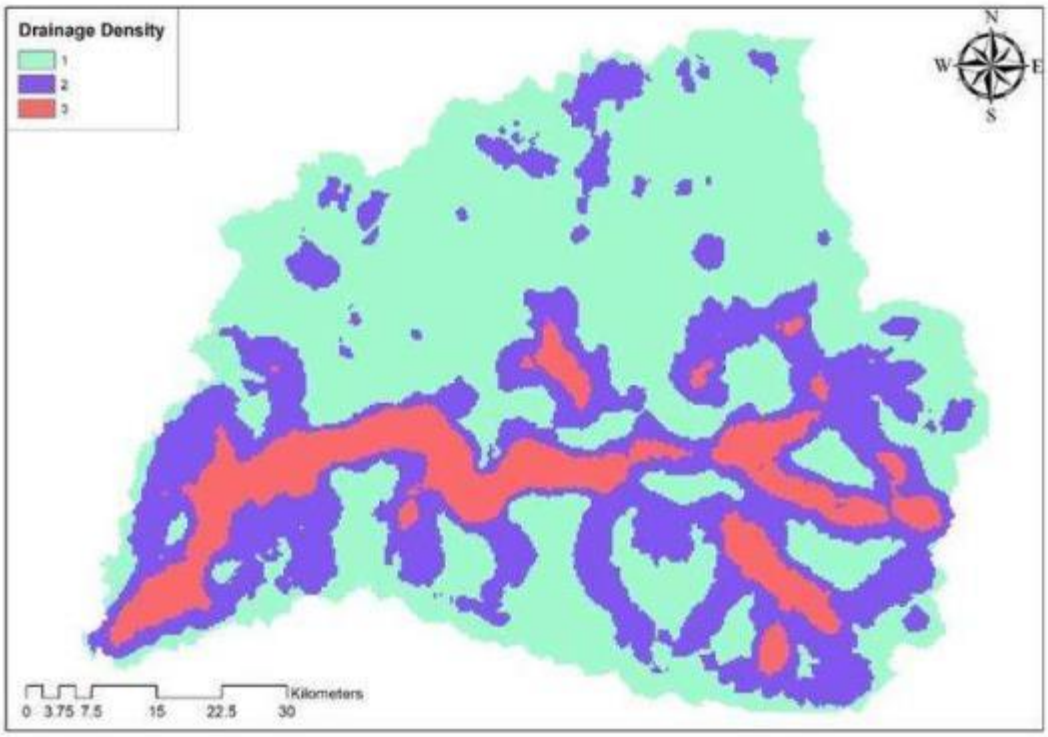

SLOPE

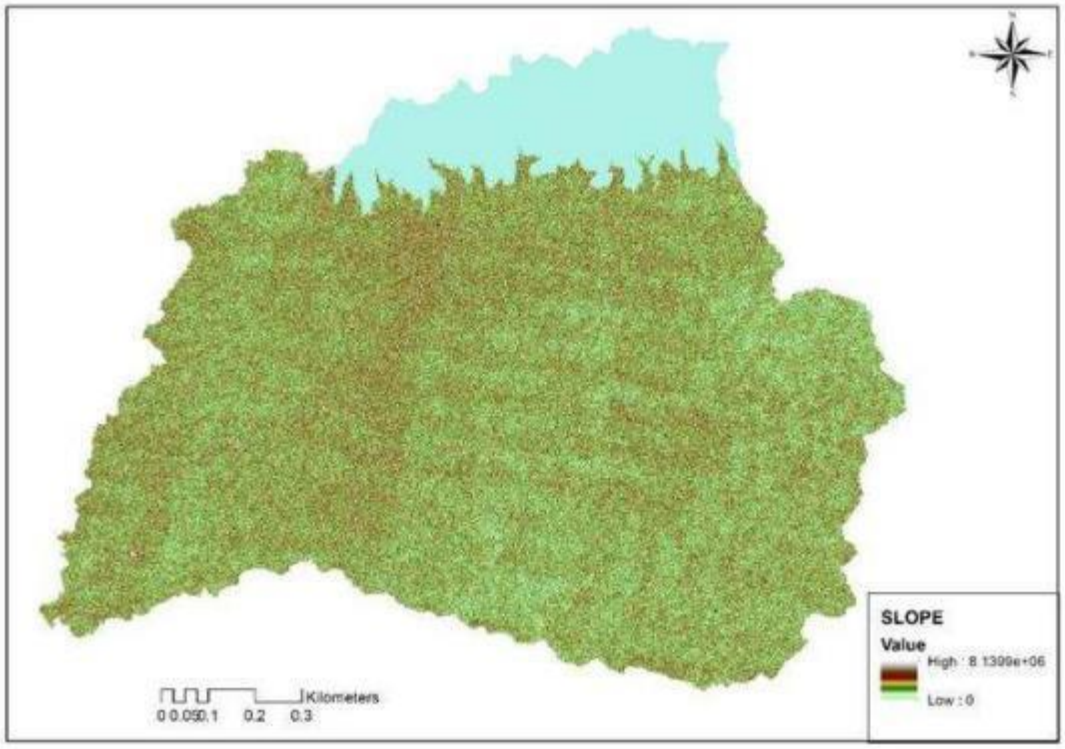

APPENDIX 14- SENSITIVITY ANALYSIS

GROUNDWATER POTENTIAL						SENSITIVITY 1	SENSITIVITY 2
Parameter	**Reclassified**	**Scale Value/Factor score**	**Potential of Score**	**Weight (% Influence)**		**Weight (% Influence)**	**Weight (% Influence)**
Depth	1	2	Low	5		5	5
	2	2	Low				
	3	2	Low				
Regolith	1	3	Moderate	5		5	5
	2	4	High				
	3	5	Very High				
Recharge	1	1	Very Low	10		10	10
	2	2	Low				
	3	3	Moderate				
	4	4	High				
	5	5	Very High				
SWL	1	5	Very High	10		10	10
	2	4	High				
	3	3	Moderate				
Aquifer Transmissivity	1	1	Very Low	25		**10**	**15**
	2	2	Low				

SENSITIVITY ANALYSIS

	3	3	Moderate				
	4	4	High				
	5	5	Very High				
Geological formation	Bimbilla	2	Low	10		**25**	10
	Poubogou	2	Low				
	Panabako Sandstone	3	Moderate				
	Kodjari	4	High				
Lineament	1	5	Very High	15		15	**25**
	2	4	High				
	3	3	Moderate				
Drainage Density	1	5	Very High	10		10	10
	2	4	High				
	3	3	Moderate				
Slope	1	5	Very High	10		10	5
	2	4	High				
	3	3	Moderate				
TOTAL SCORE				100		100	100